



**This electronic thesis or dissertation has been  
downloaded from Explore Bristol Research,  
<http://research-information.bristol.ac.uk>**

*Author:*

**Simon, Noriane**

*Title:*

**Involvement of circadian regulation and energy signalling in plant water use and development**

**General rights**

Access to the thesis is subject to the Creative Commons Attribution - NonCommercial-No Derivatives 4.0 International Public License. A copy of this may be found at <https://creativecommons.org/licenses/by-nc-nd/4.0/legalcode>. This license sets out your rights and the restrictions that apply to your access to the thesis so it is important you read this before proceeding.

**Take down policy**

Some pages of this thesis may have been removed for copyright restrictions prior to having it been deposited in Explore Bristol Research. However, if you have discovered material within the thesis that you consider to be unlawful e.g. breaches of copyright (either yours or that of a third party) or any other law, including but not limited to those relating to patent, trademark, confidentiality, data protection, obscenity, defamation, libel, then please contact [collections-metadata@bristol.ac.uk](mailto:collections-metadata@bristol.ac.uk) and include the following information in your message:

- Your contact details
- Bibliographic details for the item, including a URL
- An outline nature of the complaint

Your claim will be investigated and, where appropriate, the item in question will be removed from public view as soon as possible.

# INVOLVEMENT OF CIRCADIAN REGULATION AND ENERGY SIGNALLING IN PLANT WATER USE AND DEVELOPMENT

Noriane Margot Lea Simon

A dissertation submitted to the University of Bristol in accordance with  
the requirements for award of the degree of Doctor of Philosophy in  
the Faculty of Science.

School of Biological Sciences

August 2018



Word count: *circa* 43,000

# Abstract

Global food security represents a major challenge for modern agriculture, particularly within the context of climate change. In addition, pressure is increasing on available water resources, and reduced soil water availability often causes substantial decreases in crop biomass and yield. Therefore, it is a research priority to develop solutions for more sustainable use of water in agriculture. One possibility could involve targeting the signalling pathways involved in plant water use and development. Circadian rhythms regulate stomatal movements and increase water use efficiency (WUE) (Dodd et al. (2004, 2005)), and sucrose non-fermenting1-related kinase1 (SnRK1) is a central regulator of energy signalling, but the mechanisms underpinning these processes and their contributions to plant performance remain unclear. Using *Arabidopsis thaliana* (*Arabidopsis*) as my model system, I focused on elucidating roles of the circadian clock and SnRK1 signalling pathways in regulating WUE and physiology. I demonstrated that the circadian clock regulates whole plant WUE under diel conditions, and identified several circadian oscillator components that make key contributions to WUE. I generated and validated transgenic *Arabidopsis* with misregulated guard cell circadian clocks, then isolated guard cell-dependent and independent effects of the circadian clock upon whole plant physiology. In addition, I identified possible roles for other tissue-specific circadian clocks in regulating physiology, by comparing these transgenic genotypes with whole plant circadian clock gene overexpressors. Using a naturally-occurring population of *Arabidopsis halleri* subsp. *gemmifera*, I also detected rhythms of stomatal movement under field conditions, as well as a possible trade-off between stomatal and trichome development. Finally, I determined novel roles for SnRK1 in regulating WUE and sucrose-induced hypocotyl elongation. Overall, this thesis contributes to our understanding of the mechanisms underlying plant water use and development, and may inform future research and breeding efforts.

# Acknowledgements

The past four years of challenges, joys, exasperation and accomplishments would never have been possible without the financial help of the SWBioDTP, BBSRC, University of Bristol and Daiwa Anglo-Japanese Foundation. I would particularly like to thank my supervisor and mentor, Dr Antony Dodd, not least for reading this piece of work several times over and clinging to the hope that I could one day write good titles. Thank you for keeping me motivated and believing in me throughout, and for selflessly giving me your time and support for everything from a lab experiment to my future career. I would equally like to thank my co-supervisor Prof Alistair Hetherington, for his advice and help. I am also indebted to Dr Colin Lazarus, whose sound advice and scientific passion converted me to plant molecular biology and research in the first place, and without whom this adventure would never have even begun.

I cannot possibly come up with a full list of all the people who have helped me, but, if this PhD has taught me anything, it is to try the impossible. At times, I have felt that each and every member of the entire lab 324, the Grodome, and the wider LSB technical staff has either taught me a technique, given me advice, lent me equipment, or helped me in some other way. In particular, I need to thank the three other “Dodders” (Dr Kelly Atkins, Fiona Belbin, and Dora Cano-Ramirez), the Guard Cell Group (especially Dr Jean-Charles Isner, Dr Peng Sun, and Dr Deirdre McLachlan), and the Franklin Group (particularly Dr Ashutosh Sharma, Dr Bhavana Sharma, and Donald Fraser) for their support and willingness to answer my avalanche of questions. It was an absolute pleasure working with such friendly, intelligent, and frankly hilarious people. Outside of lab 324, I could not have been blessed with a better group of friends to share coffee and lunch with each and every day, and who helped me achieve that often sought-after work/life balance. To the “septuplets” and wider “bristolito fan group”, as well as to Jeremy Froidevaux, Mike Harrap, Dr Jeroen Maartens, Dr Luis Pablo-Rodriguez, Dr Matthew Jacobs, Trevor Hawke, Dr Bex Pike, and Tom Swift: thank you for the won-

derful memories, for helping me grow as a person, and for making me look forward to each Monday regardless of the state of my experimental work. You are incredible people and I am glad that we were able to share this experience together.

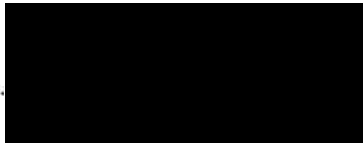
I am also fortunate enough to have both an amazingly supportive French family, as well as an incredibly encouraging adoptive English family. You have taken care of me and loved me fiercely on both sides of the Channel, and I truly appreciate you nodding and smiling at all the right times, despite not really understanding what I've been doing over the past four years nor what DNA is. For that, I am eternally grateful.

Lastly, but far from least, I would like to thank William Minchin. I may have performed the experiments and written this thesis, but he has experienced the rollercoaster of emotions with me and run alongside me throughout this marathon. Thank you for believing in me, for helping me gain a bit of perspective (you were right- the world did not end just because a few *E. coli* colonies wouldn't grow), for ensuring I didn't work late on week nights and kept my weekends free, and for generally keeping me mentally happy and physically healthy. I officially owe you.

## Author's declaration

I declare that the work in this dissertation was carried out in accordance with the requirements of the University's *Regulations and Code of Practice for Research Degree Programmes* and that it has not been submitted for any other academic award. Except where indicated by specific reference in the text, the work is the candidate's own work. Work done in collaboration with, or with assistance of, others, is indicated as such. Any views expressed in the dissertation are those of the author.

SIGNED:..



DATE: 03/11/18

# Contents

<b>Abstract</b>	<b>i</b>
<b>Acknowledgements</b>	<b>ii</b>
<b>Author's declaration</b>	<b>iv</b>
<b>List of Tables</b>	<b>xiv</b>
<b>List of Figures</b>	<b>xv</b>
<b>Abbreviations</b>	<b>xxii</b>
<b>1 Introduction</b>	<b>1</b>
1.1 The circadian clock . . . . .	1
1.1.1 Defining characteristics . . . . .	1
1.1.2 Impact and importance . . . . .	3
1.1.3 Molecular components and models of the Arabidopsis circadian clock . . . . .	5
1.1.4 Metabolism within the circadian clock . . . . .	8
1.1.5 Different circadian oscillators in different tissue types . . . . .	9

1.1.6	Circadian regulation under natural conditions . . . . .	10
1.1.7	Investigating and monitoring circadian rhythms . . . . .	12
1.2	Water use efficiency (WUE) . . . . .	13
1.2.1	Defining WUE . . . . .	13
1.2.2	Breeding for high WUE . . . . .	15
1.2.3	Stomatal guard cells: development, function, and manipulation	16
1.2.4	Targeting other tissue types to increase WUE . . . . .	27
1.3	The relationship between the circadian clock and WUE . . . . .	28
1.3.1	An accurate circadian clock increases WUE . . . . .	28
1.3.2	The bidirectional relationship between ABA and the circadian clock . . . . .	29
1.3.3	Circadian rhythms and abiotic stress . . . . .	31
1.3.4	Involvement of circadian regulation in C4 and CAM photosyn- thesis . . . . .	32
1.4	The SnRK1 energy signalling hub . . . . .	33
1.4.1	The sugar-sensing roles of T6P and KIN10/11 . . . . .	33
1.4.2	SnRK1/ T6P carbon signalling is linked to the circadian clock .	35
1.4.3	Interactions between sugar-sensing and ABA signalling pathways	36
1.5	Hypocotyl elongation as a model system . . . . .	37
1.6	Aims . . . . .	38
<b>2</b>	<b>Materials and methods</b>	<b>41</b>
2.1	Materials . . . . .	41



2.1.1	Chemical reagents . . . . .	41
2.1.2	Enzymes and commercially prepared kits . . . . .	42
2.1.3	Plasticware . . . . .	42
2.1.4	Machinery . . . . .	43
2.1.5	Software . . . . .	44
2.2	Common solutions . . . . .	45
2.3	Plant materials and growth conditions . . . . .	46
2.3.1	Plant materials and seed treatments . . . . .	46
2.3.2	Experimental plant growth conditions . . . . .	49
2.3.3	Seed bulking plant growth conditions . . . . .	49
2.4	Bacterial strains . . . . .	50
2.5	Molecular methods . . . . .	50
2.5.1	DNA extractions . . . . .	50
2.5.2	RNA extractions . . . . .	50
2.5.3	cDNA biosynthesis . . . . .	51
2.5.4	Polymerase Chain Reaction (PCR) . . . . .	51
2.5.5	Primers . . . . .	54
2.5.6	Gel electrophoresis . . . . .	60
2.5.7	Cloning protocols . . . . .	60
2.5.8	Stable Arabidopsis transformation . . . . .	65
2.5.9	Transient transformation . . . . .	67
2.6	Omoide-gawa field site . . . . .	68

2.7	Stomatal assays . . . . .	69
2.7.1	Stomatal density assay . . . . .	69
2.7.2	Stomatal density assay in the field . . . . .	70
2.7.3	Stomatal aperture assay in the field . . . . .	70
2.7.4	Detached leaf assay . . . . .	71
2.7.5	Stomatal aperture bioassay . . . . .	71
2.7.6	Gas exchange measurements . . . . .	72
2.7.7	Preparation of guard cell-enriched RNA . . . . .	72
2.8	WUE assay . . . . .	73
2.9	Flowering time assay . . . . .	74
2.10	Drought assays . . . . .	74
2.10.1	Dehydration assay on Petri dishes . . . . .	74
2.10.2	Drought assays on compost mix . . . . .	75
2.11	Hypocotyl elongation assay . . . . .	76
2.12	Confocal microscopy . . . . .	76
2.13	Luciferase bioluminescence imaging . . . . .	77
<b>3</b>	<b>The circadian clock and water use efficiency</b>	<b>79</b>
3.1	Introduction . . . . .	79
3.2	Hypothesis and aims . . . . .	80
3.3	Methods and methodology . . . . .	80
3.4	Results . . . . .	82

3.4.1	WUE assay: method optimisation . . . . .	82
3.4.2	The circadian clock affects WUE . . . . .	90
3.4.3	Testing candidate mutants for dehydration tolerance . . . . .	101
3.5	Discussion . . . . .	102
3.5.1	Development of WUE assay . . . . .	102
3.5.2	The circadian clock regulates WUE . . . . .	103
3.6	Conclusions . . . . .	111
<b>4</b>	<b>Generating, genotyping and validating transgenic Arabidopsis with misregulated guard cell circadian clocks</b>	<b>113</b>
4.1	Introduction . . . . .	113
4.2	Hypothesis and aims . . . . .	114
4.3	Methods and methodology . . . . .	114
4.4	Results . . . . .	117
4.4.1	Vector design . . . . .	117
4.4.2	Generation of expression cassettes . . . . .	118
4.4.3	Generation of transgenic Arabidopsis . . . . .	120
4.4.4	Verifying guard cell specificity of the promoters . . . . .	124
4.4.5	Confirming constant promoter activity . . . . .	126
4.4.6	Genotyping GCS-ox using expression data from whole seedlings	130
4.4.7	Genotyping GCS-ox using expression data from guard cells . .	131
4.5	Discussion . . . . .	134
4.6	Conclusions . . . . .	136

<b>5</b>	<b>Physiological examination and analysis of transgenic <i>Arabidopsis</i> with mis-regulated guard cell circadian clocks</b>	<b>139</b>
5.1	Introduction . . . . .	139
5.2	Hypothesis and aims . . . . .	140
5.3	Methods and methodology . . . . .	140
5.4	Results . . . . .	141
5.4.1	GCS-ox have unaltered hypocotyl elongation . . . . .	141
5.4.2	GCS-ox have late flowering time phenotypes under short photoperiods . . . . .	147
5.4.3	Drought response is unaltered in GCS-ox . . . . .	149
5.4.4	Overexpressing <i>CCA1</i> or <i>TOC1</i> in guard cells affects plant survival to dehydration . . . . .	159
5.4.5	GCS-ox have altered detached leaf water loss rates . . . . .	160
5.4.6	Stomatal density is unaffected in GCS-ox . . . . .	162
5.4.7	GCS-ox and <i>CCA1</i> -ox have unaltered stomatal closure responses to ABA . . . . .	163
5.4.8	Guard cell <i>CCA1</i> overexpressors have increased water use efficiency . . . . .	167
5.5	Discussion . . . . .	168
5.5.1	Hypocotyl elongation is unaltered in GCS-ox . . . . .	171
5.5.2	Misregulating the guard cell circadian clock may affect growth	171
5.5.3	Possible regulation of short-term drought responses by the guard cell circadian clock . . . . .	173
5.5.4	The guard cell circadian clock does not regulate stomatal development, but may affect stomatal responses to the environment	174

5.5.5	The guard cell circadian clock plays a role in regulating WUE . . . . .	176
5.6	Conclusions . . . . .	177
<b>6</b>	<b>Changes in stomatal aperture over time and stomatal density in naturally-occurring <i>Arabidopsis halleri</i> subsp. <i>gemmifera</i></b>	<b>179</b>
6.1	Introduction . . . . .	179
6.2	Hypothesis and aims . . . . .	180
6.3	Methods and methodology . . . . .	180
6.4	Results . . . . .	181
6.4.1	Circadian anticipation of dawn in stomatal aperture may occur in the field . . . . .	181
6.4.2	Stomatal density varies between two <i>A. halleri</i> trichome morphs	183
6.5	Discussion . . . . .	184
6.5.1	Circadian anticipation of dawn in stomatal aperture may occur under natural conditions . . . . .	184
6.5.2	Stomatal density varies between two <i>A. halleri</i> trichome morphs	186
6.6	Conclusions . . . . .	187
<b>7</b>	<b>The role of the energy-signalling hub SnRK1 in regulating sucrose-induced hypocotyl elongation</b>	<b>189</b>
7.1	Introduction . . . . .	189
7.2	Hypothesis and aims . . . . .	190
7.3	Methods and methodology . . . . .	191
7.4	Results . . . . .	193

7.4.1	<i>KIN10</i> and <i>TPS1</i> play a role in regulating sucrose-induced hypocotyl elongation under diel conditions . . . . .	193
7.4.2	Hexokinase is not required for sucrose-induced hypocotyl elongation . . . . .	197
7.4.3	The interplay between sucrose-induced hypocotyl elongation and photoperiod . . . . .	199
7.4.4	<i>CCA1</i> and <i>TOC1</i> do not regulate sucrose-induced hypocotyl elongation under 4 h photoperiods . . . . .	204
7.4.5	Phytohormone involvement in sucrose-induced hypocotyl elongation . . . . .	205
7.5	Discussion . . . . .	218
7.5.1	<i>KIN10</i> and <i>TPS1</i> play a role in regulating sucrose-induced hypocotyl elongation under diel conditions . . . . .	218
7.5.2	Sucrose-induced hypocotyl elongation is photoperiod-dependent	219
7.5.3	Phytohormone involvement in sucrose-induced hypocotyl elongation . . . . .	220
7.6	Conclusions . . . . .	222
<b>8</b>	<b>Discussion</b>	<b>225</b>
8.1	Involvement of circadian regulation and energy signalling in plant water use and development . . . . .	226
8.2	Novelty of research performed in this thesis . . . . .	229
8.3	Future work and possibilities . . . . .	229
8.4	Conclusions . . . . .	232
<b>9</b>	<b>Appendix</b>	<b>233</b>

9.1 The circadian clock and water use efficiency . . . . . 233

9.2 Generating, genotyping and validating transgenic Arabidopsis with mis-regulated guard cell circadian clocks . . . . . 237

9.3 Physiological examination and analysis of transgenic Arabidopsis with misregulated guard cell circadian clocks . . . . . 246

9.4 Changes in stomatal aperture over time and stomatal density in naturally-occurring *Arabidopsis halleri* subsp. *gemmifera* . . . . . 256

9.5 The role of the energy-signalling hub SnRK1 in regulating sucrose-induced hypocotyl elongation . . . . . 257

9.6 Published papers . . . . . 264

**References 283**

# List of Tables

1	List of abbreviations and meanings. . . . .	xxv
2.1	Manufacturers of specific chemicals. . . . .	42
2.2	Tools and machinery used in this thesis. . . . .	44
2.3	Arabidopsis genotypes used in this thesis. . . . .	48
2.4	Primers used for cloning. . . . .	55
2.5	Primers used for sequencing and verifying cloned plasmids. . . . .	56
2.6	Primers used for genotyping. . . . .	58
2.7	Primers used for qRT-PCR. . . . .	59
3.1	Arabidopsis genotypes screened for water use efficiency. . . . .	82
4.1	Genes examined by qRT-PCR in Chapter 4. . . . .	116
7.1	Arabidopsis genotypes examined in Chapter 7. . . . .	192
9.1	T <sub>0</sub> , T <sub>1</sub> and T <sub>2</sub> of each homozygous GCS-ox genotype and allele used in this study (Supplemental). . . . .	237



# List of Figures

1.1	Terms used to describe circadian oscillations. . . . .	2
1.2	Input and output pathways of the circadian oscillator. . . . .	3
1.3	The Arabidopsis circadian oscillator. . . . .	7
1.4	Sample collection of <i>Arabidopsis halleri</i> subsp. <i>gemmifera</i> for RNA extractions <i>in natura</i> . . . . .	11
1.5	Guard cell development in Arabidopsis. . . . .	18
1.6	Stomatal opening and closing mechanisms in Arabidopsis. . . . .	20
1.7	An increase in WUE could be achieved by targeting different plant tissues.	27
1.8	Interactions between the Arabidopsis circadian clock and ABA signalling pathway. . . . .	30
1.9	Links between environmental, metabolic and circadian clock regulation in Arabidopsis. . . . .	35
1.10	Several signalling pathways are integrated by PIFs to regulate hypocotyl elongation in Arabidopsis. . . . .	37
2.1	The Omoide-gawa field site. . . . .	69
2.2	<i>A. halleri</i> leaves with stomatal impression paste at the Omoide-gawa field site. . . . .	71

3.1	The optimised WUE assay used to screen circadian clock mutant and transgenic genotypes. . . . .	85
3.2	Minimal soil water evaporation occurred under these experimental conditions. . . . .	86
3.3	Four days at 60 °C is sufficient to obtain accurate dry weight measurements. . . . .	87
3.4	The method optimised to screen Arabidopsis for WUE is robust and reliable. . . . .	89
3.5	The circadian clock regulates whole plant WUE in Arabidopsis under light/dark conditions. . . . .	92
3.6	Analysis of raw WUE data. . . . .	94
3.7	Variations in WUE are not explained by phase of expression, altered period, or altered flowering time. . . . .	96
3.8	Altered circadian clocks can affect rosette architecture in Arabidopsis.	97
3.9	Rosette architecture affects WUE. . . . .	98
3.10	Variations in WUE are not fully explained by rosette leaf surface area.	100
3.11	<i>CCA1</i> , <i>ELF3</i> , <i>GI</i> , <i>TOC1</i> and <i>PRR9</i> regulate seedling response to dehydration under constant light conditions. . . . .	101
4.1	Map of the pGreenII 0229 plasmid. . . . .	117
4.2	Map of the pJET cloning vector. . . . .	119
4.3	Map of the pSOUP helper plasmid. . . . .	120
4.4	Screening <i>Agrobacterium</i> colonies for correct constructs. . . . .	122
4.5	Screening T <sub>1</sub> plants for positive transformants. . . . .	123
4.6	<i>GC1</i> and <i>MYB60</i> promoters have guard cell-specific activity. . . . .	125

4.7	<i>GC1</i> and <i>MYB60</i> promoters may have weakly rhythmic activity, as shown by luciferase bioluminescence data. . . . .	128
4.8	<i>GC1</i> and <i>MYB60</i> promoters have constant, arrhythmic activity, as shown by transcript abundance data. . . . .	129
4.9	Using whole seedlings to genotype GCS-ox. . . . .	131
4.10	Guard cell-enriched RNA sample produced using the “ice-blender” methodology. . . . .	132
4.11	Genotyping GCS-ox using RNA extracted from epidermal peels. . . . .	134
5.1	Overexpressing <i>CCA1</i> in guard cells does not affect hypocotyl elongation.	143
5.2	Overexpressing <i>TOC1</i> in guard cells does not affect hypocotyl elongation.	144
5.3	Overexpressing <i>CCA1</i> or <i>TOC1</i> in guard cells does not affect sucrose-induced hypocotyl elongation under short photoperiods. . . . .	146
5.4	Overexpressing <i>CCA1</i> or <i>TOC1</i> in guard cells affects flowering time under short photoperiods. . . . .	148
5.5	Overexpressing <i>CCA1</i> or <i>TOC1</i> in guard cells does not affect growth, green rosette leaf surface area or dry biomass under slow droughted or well-watered conditions. . . . .	151
5.6	Overexpressing <i>CCA1</i> or <i>TOC1</i> in guard cells does not affect growth, rosette leaf surface area or dry biomass under fast droughted or well-watered conditions. . . . .	153
5.7	Overexpressing <i>CCA1</i> or <i>TOC1</i> in guard cells does not affect rosette dry biomass or leaf surface area when watered at a fixed soil water capacity.	155
5.8	Overexpressing <i>CCA1</i> or <i>TOC1</i> in guard cells seems to cause earlier flowering under constant light conditions. . . . .	157
5.9	Overexpressing <i>CCA1</i> or <i>TOC1</i> in guard cells does not affect growth, rosette leaf surface area or dry biomass under well-watered or fast droughted conditions in constant light. . . . .	158

5.10	Overexpressing <i>CCA1</i> or <i>TOC1</i> in guard cells increases or decreases survival to dehydration under constant light conditions, respectively. . .	159
5.11	Overexpressing <i>CCA1</i> or <i>TOC1</i> in guard cells affects detached leaf water loss over time. . . . .	161
5.12	Overexpressing <i>CCA1</i> or <i>TOC1</i> in guard cells does not affect stomatal index nor stomatal density. . . . .	162
5.13	Overexpressing <i>CCA1</i> in guard cells does not affect ABA-induced stomatal closure. . . . .	164
5.14	Overexpressing <i>TOC1</i> in guard cells does not affect ABA-induced stomatal closure. . . . .	165
5.15	Overexpressing <i>CCA1</i> in the whole plant does not affect ABA-induced stomatal closure. . . . .	166
5.16	Overexpressing <i>CCA1</i> in guard cells seems to increase WUE. . . . .	167
5.17	Interpretive framework used to analyse the influence of the guard cell circadian clock and other tissue-specific circadian clocks upon whole plant physiology. . . . .	170
6.1	Stomatal aperture of <i>A. halleri</i> over time under natural conditions. . .	182
6.2	Glabrous <i>A. halleri</i> have higher stomatal index and stomatal density than hairy plants under field conditions. . . . .	184
7.1	<i>KIN10-ox</i> and <i>tps1</i> are fully or partially sucrose-insensitive under 8 h photoperiods, respectively. . . . .	194
7.2	Disrupting <i>KIN10</i> causes hypersensitivity of hypocotyls to sucrose supplementation. . . . .	195
7.3	<i>bzip63-1</i> has a greater magnitude of sucrose-induced increase in hypocotyl length than the wild type. . . . .	197

7.4	Hexokinase-induced glucose signalling does not regulate sucrose-induced hypocotyl elongation under diel conditions. . . . .	198
7.5	The magnitude of sucrose-induced hypocotyl elongation varies with photoperiod length. . . . .	200
7.6	Sucrose-induced hypocotyl elongation is affected by both photoperiod and daily integrated PAR. . . . .	203
7.7	Overexpressing <i>CCA1</i> or <i>TOC1</i> does not affect sucrose-induced hypocotyl elongation under short days. . . . .	205
7.8	NPA represses sucrose-induced hypocotyl elongation in a concentration-dependent manner. . . . .	207
7.9	<i>EXPA11</i> transcript abundance is regulated by KIN10. . . . .	209
7.10	Relative transcript abundance of several auxin biosynthesis and responsive genes were unaltered in presence of exogenous sucrose, due to fluctuating expression levels caused by the osmotic control. . . . .	211
7.11	GA signalling plays a role in regulating sucrose-induced hypocotyl elongation under short photoperiods. . . . .	214
7.12	GA partially affects sucrose-induced hypocotyl elongation through DELLA-induced signalling. . . . .	216
7.13	ABA signalling through PYR/PYL does not regulate sucrose-induced hypocotyl elongation under short photoperiods. . . . .	217
8.1	The whole plant circadian oscillator, composed of the guard cell circadian oscillator and other tissue-specific circadian oscillators, and SnRK1/T6P-based signalling pathways regulate WUE and development. . . . .	228
9.1	The circadian clock regulates whole plant WUE in Arabidopsis under light/dark conditions (Supplemental). . . . .	234
9.2	Variations in WUE are not fully explained by rosette leaf surface area (Supplemental). . . . .	235

9.3	<i>CCA1</i> , <i>ELF3</i> , <i>GI</i> , <i>TOC1</i> and <i>PRR9</i> regulate seedling response to dehydration under constant light conditions (Supplemental). . . . .	236
9.4	Map of the 2-Log DNA Ladder (0.1 kb - 10.0 kb) (Supplemental). . . . .	238
9.5	Relative transcript abundance of tissue-specific reporter genes to examine guard cell enrichment of epidermal peel samples (Supplemental). . . . .	239
9.6	<i>CCA1</i> and <i>TOC1</i> relative transcript abundance in epidermal peels (Supplemental). . . . .	240
9.7	Sequences of constructs used to generate (a) <i>GC</i> , (b) <i>GT</i> , (c) <i>MC</i> and (d) <i>MT</i> (Supplemental). . . . .	241
9.8	Overexpressing <i>CCA1</i> or <i>TOC1</i> in guard cells does not affect hypocotyl elongation (Supplemental). . . . .	247
9.9	Overexpressing <i>CCA1</i> or <i>TOC1</i> in guard cells affects flowering time under short photoperiods (Supplemental). . . . .	248
9.10	Overexpressing <i>CCA1</i> or <i>TOC1</i> in guard cells does not affect flowering time under long photoperiods (Supplemental). . . . .	249
9.11	Overexpressing <i>CCA1</i> or <i>TOC1</i> in guard cells does not affect growth, rosette leaf surface area or dry biomass under fast droughted or well-watered conditions (Supplemental). . . . .	250
9.12	Overexpressing <i>CCA1</i> or <i>TOC1</i> in guard cells does not affect growth, rosette leaf surface area or dry biomass under well-watered or fast droughted conditions in constant light (Supplemental). . . . .	251
9.13	Overexpressing <i>CCA1</i> or <i>TOC1</i> in guard cells increases or decreases survival to dehydration, respectively (Supplemental). . . . .	252
9.14	Overexpressing <i>CCA1</i> in the whole plant affects detached leaf water loss over time (Supplemental). . . . .	253
9.15	Overexpressing <i>CCA1</i> or <i>TOC1</i> in guard cells does not affect stomatal index nor stomatal density (Supplemental). . . . .	254

9.16	Overexpressing <i>CCA1</i> in guard cells seems to increase WUE (Supplemental). . . . .	255
9.17	Stomatal aperture of <i>A. halleri</i> subsp. <i>gemmifera</i> over time under field conditions, with statistical significance (Supplemental). . . . .	256
9.18	<i>bzip63-1</i> hypocotyls are hypersensitive to sucrose supplementation (Supplemental). . . . .	257
9.19	Hypocotyl length varies with photoperiod (Supplemental). . . . .	258
9.20	NPA abolishes sucrose-induced hypocotyl elongation at high concentrations (Supplemental). . . . .	259
9.21	Determining which <i>EXPA</i> genes are upregulated by conditions promoting hypocotyl elongation and downregulated by conditions suppressing hypocotyl elongation (Supplemental). . . . .	260
9.22	GA supplementation promotes hypocotyl elongation (Supplemental). . . . .	261
9.23	Effects of PAC and GA on sucrose-induced hypocotyl elongation are difficult to interpret for the <i>KIN10-ox</i> and <i>tps1</i> alleles (Supplemental). . . . .	262
9.24	GA signalling affects sucrose-induced hypocotyl elongation (Supplemental). . . . .	263

# Abbreviations

---

Abbreviation	Description
2PG	2-phosphoglycolate
<i>A. halleri</i>	<i>Arabidopsis halleri</i> subsp. <i>gemmifera</i>
ABA	abscisic acid
ABAR/ GUN5	GENOME UNCOUPLED 5
<i>Agrobacterium</i>	<i>Agrobacterium tumefaciens</i>
Arabidopsis	<i>Arabidopsis thaliana</i>
BBX32	Arabidopsis B-box domain gene
bHLH	basic helix-loop-helix
BR	brassinosteroid
$[Ca^{2+}]_{cyt}$	cytosolic free calcium concentration
cADPR	CYCLIC ADENOSINE DIPHOSPHATE RIBOSE
CAM	crassulacean acid metabolism
CCA1	CIRCADIAN CLOCK-ASSOCIATED1
CCR2/ GRP7	COLD- AND CIRCADIAN-REGULATED
CDF	CYCLING DOF FACTOR
CHE	CCA1 HIKING EXPEDITION
ChIP-seq	chromatin immunoprecipitation sequencing
CO	CONSTANS
COP1	CONSTITUTIVE PHOTOMORPHOGENIC 1
CRY1/2	CRYPTOCHROME 1/2
$\delta^{13}C$	carbon isotope discrimination
dH <sub>2</sub> O	deionised H <sub>2</sub> O
EC	evening complex
<i>E. coli</i>	<i>Escherichia coli</i>

---



---

**Continuation of Table 1**

---

<b>Abbreviation</b>	<b>Description</b>
ELF3/4	EARLY FLOWERING 3/4
EPC	epidermal protodermal cell
EPF1/2	EPIDERMAL PATTERNING FACTOR 1/2
EUW	effective use of water
EXPA4/8/11	EXPANSIN4/8/11
FFT-NLLS	fast fourier transform non-linear least squares
FKF1	FLAVIN BINDING, KELCH REPEAT, F-BOX
FT	FLOWERING LOCUS T
GA	gibberellin
GAI	GIBBERELIC ACID INSENSITIVE
GC	GC1::CCA1:nos
GCS-ox	guard cell circadian clock gene overexpressor
GT	GC1::TOC1:nos
GFP	GREEN FLUORESCENT PROTEIN
GI	GIGANTEA
GMC	guard mother cell
HXK1	HEXOKINASE1
IAA	indole-3-acetic acid
IRGA	infra-red gas analyser
KIN10/11	SNF1-RELATED PROTEIN KINASE 1.1/1.2
LHY	LATE ELONGATED HYPOCOTYL
LKP2	LOV KELCH PROTEIN 2
LUC	LUCIFERASE
LUX	LUX ARRHYTHMO
MC	MYB60::CCA1:nos
MESA	maximum entropy spectral analysis
MMC	meristemoid mother cell
MT	MYB60::TOC1:nos
NPA	<i>N</i> -1-naphthylphthalamic acid
PAC	paclobutrazol
PAR	photosynthetically active radiation

---

---

**Continuation of Table 1**

---

<b>Abbreviation</b>	<b>Description</b>
PCR	polymerase chain reaction
PEPC	PHOSPHOENOLPYRUVATE CARBOXYLASE
PhyB	PHYTOCHROME B
PIF	PHYTOCHROME INTERACTING FACTOR
PP2C	CLADE A TYPE 2C PROTEIN PHOSPHATASE
PPCK	PEPC kinase
PRR3/5/7/9	PSEUDO RESPONSE REGULATOR 3/5/7/9
PYL1/2/4	PYR1-LIKE1/2/4
PYR1	PYRABACTIN RESISTANCE1
QTL	quantitative trait locus
RAE	relative amplitude error
ROS	reactive oxygen species
RUBISCO	RIBULOSE-1,5-BISPHOSPHATE CARBOXYLASE/OXYGENASE
RVE4/6/8	REVEILLE 4/6/8
SCRM	SCREAM
SDD1	STOMATAL DENSITY AND DISTRIBUTION1
SGC	equivalent of GC produced by Hassidim et al. (2017)
SLAC1	SLOW ANION CHANNEL1
SLGC	stomatal-lineage ground cell
SNF1	SUCROSE NON-FERMENTING1
SnRK1	SNF1-RELATED KINASE1
SWC	soil water capacity
T <sub>0/1/2/3</sub>	Arabidopsis positive transformant, generation 0/1/2/3
T6P	trehalose-6-phosphate
TE	transpiration efficiency/ whole plant WUE
TIC	TIME FOR COFFEE
TILLING	targeted induced local lesions in genomes
TOC1	TIMING OF CAB2 EXPRESSION1
TOR	TARGET OF RAPAMYCIN
TPS1	TREHALOSE-6-PHOSPHATE SYNTHASE 1
TRE	trehalose

---

---

**Continuation of Table 1**

---

<b>Abbreviation</b>	<b>Description</b>
TTFL	transcription-translation feedback loop
WT	wild type
WNK1	WITH NO LYSINE KINASE 1
WUE	water use efficiency
WUE <sub>i</sub>	instantaneous WUE
ZTL	ZEITLUPE

---

Table 1: List of abbreviations and meanings.

# Chapter 1

## Introduction

### 1.1 The circadian clock

#### 1.1.1 Defining characteristics

Circadian clocks are endogenous cellular oscillators that generate a cellular measure of the time of day. This gives rise to 24-hour rhythms of gene expression, physiology, development, and biochemistry. The time necessary to complete one rhythmic cycle is defined as the period, while the time of day of an event, such as the highest or lowest point of the rhythm, is known as the phase (Fig. 1.1) (Hanano et al. (2006); Shor and Green (2016)). The amplitude of a rhythm refers strictly to the difference between the mid-point and peak or trough of the oscillation (Fig. 1.1) (McClung (2006); Hubbard and Dodd (2016)). However, it is often calculated as the maximal change observed in the oscillation, from peak to trough (Hanano et al. (2006); Shor and Green (2016)). Despite these different definitions, amplitude provides a useful measure of the magnitude of an oscillation (Kay and Remigereau (2016)).

These biological rhythms continue under constant environmental conditions and have a period of approximately (“*circa*”) 24 hours (“*diem*”). Persistence under constant conditions confirms that these rhythms are truly endogenous (McClung (2006)). Rhythms also persist with a period of about 24 h under a range of different temperatures, and this temperature compensation is thought to allow the circadian clock to function even during changes in cellular metabolism (McClung (2006)). The circadian oscillator

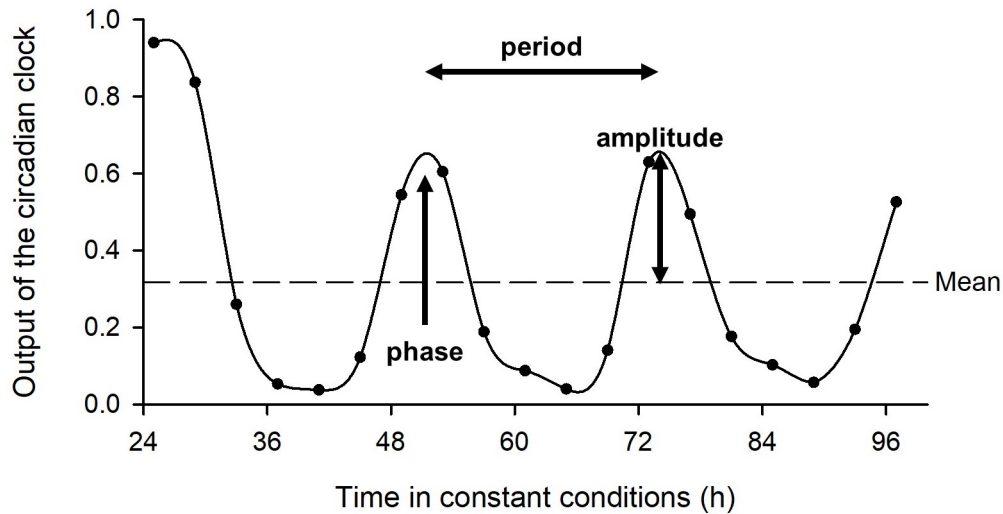


Figure 1.1: Terms used to describe circadian oscillations. Commonly measured outputs of the circadian clock include qRT-PCR, luciferase bioluminescence, or leaf movement. Commonly used constant conditions include constant light or constant darkness.

assimilates zeitgebers, or environmental time cues, through input pathways (Fig. 1.2) (Hsu and Harmer (2014)). Circadian rhythms gate their sensitivity to these environmental stimuli, meaning that the same zeitgeber given at different times of day will produce a different magnitude of entrainment response (Fig. 1.2) (McClung (2006)). In a similar fashion, gating can also occur for environmental signalling pathways: the circadian clock leads to temporal variation in the responsiveness of certain pathways to environmental stimuli (Fig. 1.2) (Hsu and Harmer (2014)).

These input pathways entrain the circadian clock to its external environment, thus ensuring that it has the correct phase relationship with its environment (Covington et al. (2008)), and the resulting outputs regulate a wide range of processes (Fig. 1.2) (Hsu and Harmer (2014)). This is thought to confer a competitive advantage to the organism, as circadian rhythms allow it to coordinate its metabolism, physiology and behaviour with its environment and so anticipate changes such as dawn and dusk.

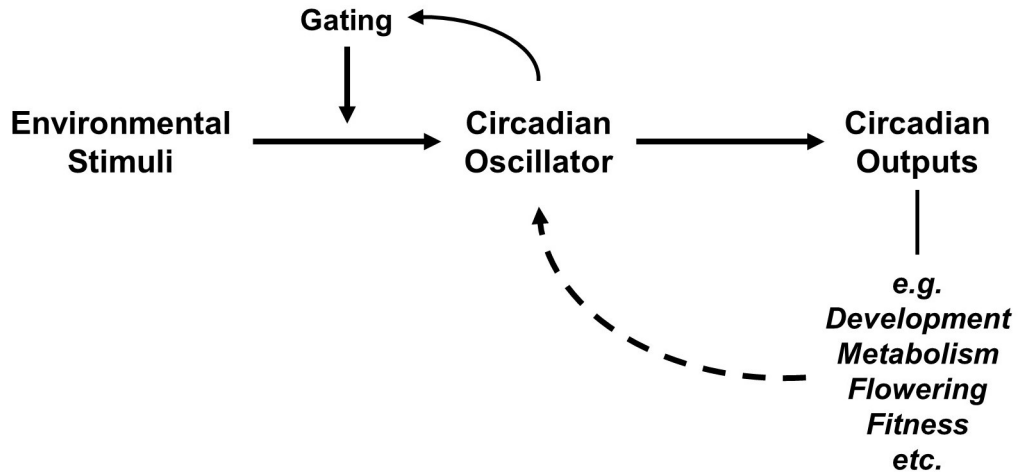


Figure 1.2: Input and output pathways of the circadian oscillator. The concept of circadian gating is also illustrated. Dotted arrows represent hypothetical feedback: although some outputs of the circadian clock are known to feed back into the clock, this may not be the case for all outputs. Additional information is provided in text.

### 1.1.2 Impact and importance

Circadian rhythms are thought to have evolved independently at least four times across different kingdoms (Young and Kay (2001)), suggesting that they confer a selective advantage. They are particularly crucial for sessile plants, which must continuously monitor and adapt to their ever-changing environment. For example, different *Arabidopsis* accessions not only have significantly different circadian clock amplitudes, periods and phases, but also have a correlation between photoperiod at their latitude of origin and length of their circadian period (Michael et al. (2003)). This illustrates the circadian oscillator role in synchronising the plant with its local environment (Michael et al. (2003)).

Up to one third of *Arabidopsis* transcripts are suggested to accumulate with a circadian rhythm, indicating that circadian regulation plays a vital role in most aspects of plant growth, development and metabolism (Covington et al. (2008); Graf et al. (2010)). Indeed, an accurate circadian clock increases plant fitness (Green et al. (2002); Dodd et al. (2005)), enabling an approximate doubling of productivity and a higher survival rate (Dodd et al. (2005)). The circadian oscillator also regulates flowering time, abiotic stress responses, defence, and hybrid vigour (Bendix et al. (2015)). Its impact on performance has been reported in key crop species, including *Hordeum vulgare* (barley), *Triticum aestivum* (wheat), *Oryza sativa* (rice), *Sorghum bicolor* (sorghum), *Zea mays* (maize), *Glycine max* (soybean), *Brassica rapa* (mustard), *Beta vulgaris* (sugar beet),

*Pisum sativum* (pea), and *Lens culinaris* (lentils) (Hsu and Harmer (2014); Bendix et al. (2015)).

Domestication has altered the circadian clock. Ancestral barley was fall-sown, required vernalisation and flowered rapidly under long days, whereas current spring barley varieties do not need vernalisation and have a diminished response to photoperiod (Turner et al. (2005)). Spring barleys, when grown at the higher latitudes of North America and Europe, have a longer period of vegetative growth, thus accumulate more biomass and produce higher yields in comparison with winter varieties (Turner et al. (2005)). Interestingly, this advantage was explained by a mutated allele which alters circadian expression of key photoperiod-sensing and flowering genes (Turner et al. (2005)). Müller et al. (2016) described how artificial selection slowed the tomato circadian clock as cultivars were transferred from the original Andean region to North America and Europe. They hypothesised that this decelerated circadian clock might optimise the rate of photosynthesis for the longer summer daylengths at these higher latitudes, thus increasing the tomato overall performance (Müller et al. (2016)). An additional mutation responsible for the deceleration of the tomato circadian clock was recently identified (Müller et al. (2018)). Interestingly, both mutations alter light input to the circadian clock, suggesting that the deceleration of the tomato circadian clock is light-dependent (Müller et al. (2018)). Evidence of artificial selection for circadian traits was also reported in different soybean cultivars (Greenham et al. (2017)), as well as for wheat, peas, lentils, rice, sorghum, maize and potatoes (Nakamichi (2015)).

Interestingly, orthologs of circadian clock components have been found within the genomes of most land plants, with several involved in photoperiod-dependent flowering time (Huang and Nusinow (2016)). In addition, altering circadian clock gene expression can improve crop production. Expressing Arabidopsis B-box domain gene (*BBX32*) in soybean significantly increased yield over several years (Preuss et al. (2012)). This may be caused by modifications in the abundance of several circadian clock transcripts, which in turn altered reproductive development (Preuss et al. (2012)). In contrast, overexpressing *CCA1* in maize decreased hybrid vigour (Ko et al. (2016)). Therefore, manipulating the circadian clock could become an effective tool for future breeding programs, particularly with regards to photoperiod-sensitive crops (Kay and Remigereau (2016); Shor and Green (2016)).

### 1.1.3 Molecular components and models of the Arabidopsis circadian clock

The plant circadian clock has been investigated extensively, with over twenty oscillator components identified in Arabidopsis (Hsu and Harmer (2014)). These participate in a series of interlocking transcription-translation feedback loops (TTFLs), and are active or expressed at specific times throughout the day-night cycle (Hsu and Harmer (2014)). One of the main transcriptional feedback loops involves two MYB-like transcription factors, known as CIRCADIAN CLOCK-ASSOCIATED1 (CCA1) and LATE ELONGATED HYPOCOTYL (LHY): these are highly abundant in the morning and repress the evening-phased element *TIMING OF CAB EXPRESSION1 (TOC1)*, which in turn inhibits CCA1 and LHY transcription through an interaction with CCA1 HIKING EXPEDITION (CHE) (Fig. 1.3) (Alabadí et al. (2001); Pruneda-Paz et al. (2009); Gendron et al. (2012); Huang et al. (2012); Hsu and Harmer (2014)).

Briefly, other key day-phased oscillator elements include *PSEUDO RESPONSE REGULATOR 9 (PRR9)*, *PRR7*, *PRR5*, and *PRR3*, which are sequentially expressed in that order throughout the day and repress CCA1 and LHY expression, and *REVEILLE 8 (RVE8)*, *RVE4* and *RVE6*, which induce the expression of hundreds of evening-phased genes (Fig. 1.3) (Hsu and Harmer (2014)). The so-called “evening complex” is composed of *LUX ARRHYTHMO (LUX)*, *EARLY FLOWERING 3 (ELF3)* and *ELF4*, which repress PRR9 and are repressed by CCA1 and LHY (Fig. 1.3) (Hsu and Harmer (2014)). The evening-phased *GIGANTEA (GI)* is also repressed by CCA1 and LHY, and positively regulates these two genes in another feedback loop (Fig. 1.3) (Hsu and Harmer (2014)).

Post-transcriptional regulation is equally important, complementing the TTFLs to sustain a rhythm of 24 h (Sanchez et al. (2011)). Known mechanisms include alternative splicing, protein degradation, and post-translational modifications such as protein phosphorylation (Hsu and Harmer (2014)). For example, alternative splicing has been described for CCA1, LHY, PRR9, PRR7, PRR5, PRR3, TOC1, RVE4 and RVE8 (Hsu and Harmer (2014)). ZEITLUPE (ZTL), combined with FLAVIN BINDING, KELCH REPEAT, F-BOX (FKF1) and LOV KELCH PROTEIN 2 (LKP2), targets TOC1 and PRR5 for protein degradation, while ELF3, GI, and CONSTITUTIVE PHOTOMORPHOGENIC 1 (COP1) interact to degrade GI (Fig. 1.3) (Hsu and Harmer (2014)). Finally, phosphorylation controls the stability of certain proteins, such as the PRRs (Hsu and Harmer (2014)), and promoter-binding activity, such as for CCA1 (Choudhary et al. (2015)). Circadian rhythms of protein



phosphorylation were also detected using phosphoproteomics (Choudhary et al. (2015)).

Many other genes are integrated within the circadian system, but their exact roles and interactions with the core circadian clock remain unclear. These include *TIME FOR COFFEE (TIC)*, an established regulator that resets the circadian clock at dawn (Sánchez-Villarreal et al. (2013)); *TEJ*, which affects circadian period length through post-translational poly(ADP-ribosylation) (Panda et al. (2002)); *WITH NO LYSINE KINASE 1 (WNK1)*, a regulator of circadian rhythms, vacuolar H<sup>+</sup>-ATPase, and flowering time (Wang et al. (2008)); and *COLD- AND CIRCADIAN-REGULATED (CCR2/GRP7)*, a marker for circadian clock output signals that autoregulates itself via alternative splicing (Fig. 1.3) (Heintzen et al. (1997); Staiger et al. (2003); Schöning et al. (2007)). Recently, the catalytic subunit of the energy signalling hub SnRK1, *KIN10*, was reported to genetically interact with *TIC* to regulate the circadian clock (Shin et al. (2017)).

Accurate time of day of expression and/or activity, as well as transcript and/or protein abundance, of circadian clock components are crucial for the correct functioning of the circadian oscillator. For example, photoperiod-dependent control of flowering time requires precise circadian regulation, as circadian clock mutants and overexpressors often have altered flowering time phenotypes (Schaffer et al. (1998); Fowler et al. (1999); Strayer et al. (2000); Doyle et al. (2002); Panda et al. (2002); Hayama and Coupland (2003); Yamamoto et al. (2003); Somers et al. (2004); Bendix et al. (2015)). This regulation has been investigated in depth elsewhere (Suárez-López et al. (2001); Yanovsky and Kay (2002); Hayama and Coupland (2003); Johansson and Staiger (2015)). Briefly, in *Arabidopsis*, *CONSTANS (CO)* expression is tightly controlled by the circadian clock with peak expression 8 h after dawn (Suárez-López et al. (2001); Yanovsky and Kay (2002)), and is repressed by CYCLING DOF FACTORS (CDFs) (Johansson and Staiger (2015)). Under long days, but not short days, GI and FKF1 protein accumulation is synchronised, enabling a light-dependent GI-FKF1 complex to form and target CDFs for degradation (Johansson and Staiger (2015)). In a similar fashion, CO protein is degraded in darkness by COP1, but stabilised in the light by FKF1 and other factors (Johansson and Staiger (2015)). Therefore, under long days, light-dependent CO accumulation occurs and induces *FLOWERING LOCUS T (FT)* expression, which then enables flowering (Fig. 1.3) (Suárez-López et al. (2001); Yanovsky and Kay (2002); Johansson and Staiger (2015)).

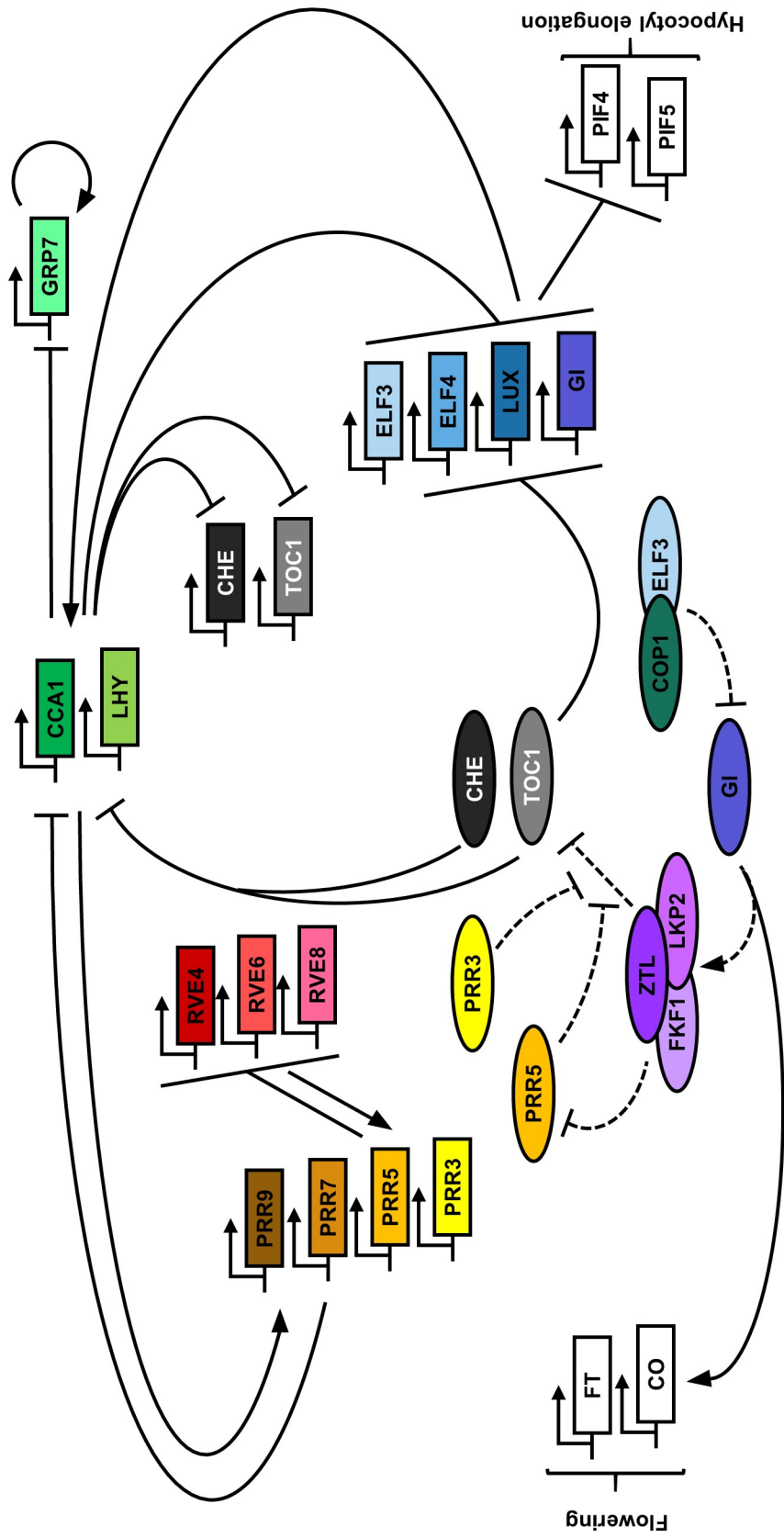


Figure 1.3: The Arabidopsis circadian oscillator. A few interactions between components investigated in this thesis are illustrated. Genes are represented by rectangles, proteins by circles, translational regulation by solid lines, transcriptional regulation by dotted lines, induction by arrows and suppression/degradation by bars. Identical colours are used to identify the gene and protein representations of the same component. Components *TEI*, *TIC*, *WNK1*, *KIN10*, and *TPS1* are not represented in this diagram, but full descriptions of their roles are provided in the text. Additional interactions are also described in the text. The roles of PHYTOCHROME INTERACTING FACTORS (PIFs) in hypocotyl elongation are further described in section 1.5. This figure was derived from the concept of Nagel and Kay (2012).

### 1.1.4 Metabolism within the circadian clock

The presence of circadian oscillations in intracellular calcium concentrations, intracellular magnesium concentrations, reactive oxygen species (ROS), adenosine triphosphate, and peroxiredoxin redox state among others suggests the existence of metabolic rhythms (Haydon et al. (2013a); Feeney et al. (2016)). Interestingly, there is increasing evidence that these metabolic rhythms interact with TTFLs. For example, sucrose feeds back into the circadian clock and regulates oscillator components (Haydon et al. (2013b)). The presence of metabolic rhythms across Kingdoms may give us more information regarding the evolution of circadian clocks (Haydon et al. (2013a)).

Several studies have focused on oscillations of cytosolic free calcium concentrations ( $[Ca^{2+}]_{cyt}$ ). By using calcium-sensitive aequorin as a luminescent reporter, Johnson et al. (1995) demonstrated that both tobacco and Arabidopsis have  $[Ca^{2+}]_{cyt}$  circadian oscillations. The characteristics of these oscillations, such as amplitude, phase and shape, incorporate both photoperiod and light intensity information (Love et al. (2004)). Red and blue light affect  $[Ca^{2+}]_{cyt}$  circadian oscillations through PHYTOCHROME B (PhyB) and through CRYPTOCHROME1 (CRY1) and CRY2 signalling pathways, respectively (Xu et al. (2007)). Several core circadian clock genes also regulate  $[Ca^{2+}]_{cyt}$  oscillations, including *CCA1*, *ELF3*, *LHY*, *TOC1* and *ZTL* (Xu et al. (2007)).

CYCLIC ADENOSINE DIPHOSPHATE RIBOSE (cADPR) induces  $Ca^{2+}$  release from internal stores, and oscillations in cADPR concentration are regulated by the circadian clock (Dodd et al. (2007); Robertson et al. (2009)). Interestingly, abolishing these rhythms also inhibits  $[Ca^{2+}]_{cyt}$  oscillations and increases the period of leaf movement and *CCA1*, *LHY* and *TOC1* transcript abundance (Dodd et al. (2007)). This feedback loop may enable interactions between the circadian clock and stress signalling, as both cADPR and  $[Ca^{2+}]_{cyt}$  are involved in stress signalling responses (Dodd et al. (2007); Robertson et al. (2009)).

Interestingly, there may be several, genetically independent circadian clocks present within Arabidopsis (Xu et al. (2007)). In *toc1-1*,  $[Ca^{2+}]_{cyt}$  rhythms have a 24 h period, whereas rhythms of stomatal aperture and closure have a 21 h period (Somers et al. (1998); Xu et al. (2007)). This uncoupling suggests that both rhythms are independent from one another (Robertson et al. (2009)). In addition, no  $[Ca^{2+}]_{cyt}$  rhythms were detected in *cca1-1* (Xu et al. (2007)). Therefore, these different circadian oscillators could be present within different tissue types in Arabidopsis (Xu et al. (2007)). Alternatively,

the uncoupling could be due to different behaviours of different cell types. Interestingly,  $[Ca^{2+}]_{cyt}$  signalling pathways are particularly known to affect stomatal behaviour (section 1.2.3.2).

### 1.1.5 Different circadian oscillators in different tissue types

The mammalian circadian system has a central oscillator located in the central suprachiasmatic nucleus of the hypothalamus, and this in turn tightly regulates circadian clocks located in other tissues (Mohawk et al. (2012)). However, this does not appear to be the case for the plant circadian clock. There is increasing evidence that distinctive circadian oscillators exist within different plant tissues and communicate with one another (James et al. (2008); Yakir et al. (2011); Wenden et al. (2012); Endo et al. (2014); Takahashi et al. (2015); Bordage et al. (2016); Kim et al. (2016); Hassidim et al. (2017)). Therefore, plants do not seem to have a central pacemaker, and plant circadian clocks appear to be largely uncoupled (Thain et al. (2000)).

Interestingly, cellular circadian clocks are weakly coupled to each other, with whole leaf synchronisation mainly achieved by cellular clocks' strong responses to environmental light-dark cycles (Wenden et al. (2012)). Therefore, circadian clocks of individual cells oscillate and respond independently to environmental stimuli, but this heterogeneity is rescued under day/night cycles to coordinate the plant as a whole (Muranaka and Oyama (2016); Gould et al. (2018)). This is also associated with age, as older leaves have a shorter period than younger leaves (Kim et al. (2016)). Shoot apex clocks have the highest synchrony which enable them to influence root circadian clocks (James et al. (2008); Bordage et al. (2016); Nimmo (2018)), thereby creating an overarching hierarchical circadian structure (Takahashi et al. (2015)).

This hierarchical organisation is also observed for different shoot circadian clocks. Endo et al. (2014) determined that vasculature and mesophyll circadian oscillators control each other in an asymmetric manner, with the vasculature clock regulating mesophyll gene expression and physiology. The circadian clock within vascular phloem companion cells controls the photoperiodic regulation of flowering, whereas the epidermal circadian clock was required for temperature-dependent hypocotyl and petiole cell elongation (Shimizu et al. (2015)).

Differences have been noted between clocks of guard cells and epidermal and meso-

phyll cells, with an 11 h period difference after seven days in constant conditions (Yakir et al. (2011)). Uncoupling was also reported in bean plants, where rhythms of leaflet movement had a 3 h period difference compared to those of stomatal opening and CO<sub>2</sub> assimilation (Hennessey and Field (1992)). As stomatal movements are under circadian control in *Arabidopsis* (Salomé et al. (2002); Dodd et al. (2004)) and mutations affecting the circadian clock can also alter stomatal aperture under constant light (Dodd et al. (2004)), an autonomous circadian oscillator may be present within and regulate each guard cell (Somers et al. (1998); Dodd et al. (2004)). This was confirmed by Hassidim et al. (2017), who report that altering the guard cell circadian clock affects stomatal aperture and drought tolerance. Therefore, it is important to understand circadian oscillators of single cell types, such as guard cells, to fully comprehend how they affect the plant as a whole (Hubbard and Webb (2011); Kinoshita and Hayashi (2011)).

### **1.1.6 Circadian regulation under natural conditions**

Studies conducted in the laboratory have been crucial to our understanding of plant circadian rhythms. However, artificial experimental conditions differ greatly from those under which plants have evolved. Under natural conditions, plants must respond accurately to a large number of environmental cues, which are continuously changing and interacting with one another. Therefore, it is valuable to also perform experiments in the natural habitat, *in natura*, to achieve a deeper understanding of gene and cell function (Fig. 1.4) (Kudoh (2016)).

Stomatal behaviour has been examined extensively under field conditions in maize (Turner (1973, 1974); Bunce (2004)), wheat (Bunce (2004)), sorghum (Turner (1973, 1974); Bunce (2004)), barley (Bunce (2004)), tobacco (Turner (1973, 1974)), soybean (Bunce (2004)), potato (Bunce (2004)), peach trees (Correia et al. (1997)), and a variety of other trees, shrubs, herbs and C4 plants (Hetherington and Woodward (2003)). Transcript abundance of genes related to drought stress (Merquiol et al. (2002)), flowering time (Aikawa et al. (2010); Kawagoe and Kudoh (2010)), and herbivory resistance (Kawagoe et al. (2011); Sato and Kudoh (2016, 2017)) was also reported for wild plants throughout the year.

The role of the circadian clock under natural conditions is also starting to be explored. Using field-grown rice leaves, Matsuzaki et al. (2015) developed a model for expression of circadian clock genes under fluctuating environmental conditions. The circadian



Figure 1.4: Sample collection of *Arabidopsis halleri* subsp. *gemmifera* for RNA extractions *in natura*. This photograph was taken at the Omoide-gawa field site described by Aikawa et al. (2010).

clock was found to be robust and punctual to 22 min, remaining unaffected by weather changes in the field (Matsuzaki et al. (2015)). A timecourse performed on a rice *gi* mutant grown under field conditions revealed that GI regulates 75% of transcripts, thereby generating robust diurnal rhythms in transcript abundance (Izawa et al. (2011)). In a similar fashion, Joo et al. (2017) grew transgenic tobacco with silenced *LHY* or *TOC1* under field conditions, and examined their photosynthetic performance. Interestingly, *LHY* was found to play a greater role than *TOC1* in enabling plants to anticipate dusk and suppress nocturnal photosynthesis (Joo et al. (2017)). Circadian regulation of stomatal conductance and carbon assimilation was also found to be significant in naturally lit glasshouses (Resco de Dios et al. (2016b)) and outdoor macrocosms (Resco de Dios et al. (2016a, 2017)). Work by Matthews et al. (2018) under different lighting regimes suggests that an internal signal accounts for 25% of the total diurnal stomatal conductance. However, an earlier model developed by Williams and Gorton (1998) suggests that circadian rhythms only account for 1% of carbon fixation in field-grown *Saurus cernuus* (lizard's tail). Therefore, it would be interesting to further investigate the contribution of the circadian clock to plant fitness under natural conditions.

### 1.1.7 Investigating and monitoring circadian rhythms

Circadian rhythms can be investigated using a variety of methods. To differentiate between diel rhythms and true circadian rhythms, plants are placed under constant environmental conditions for 24 h before the start of the experiment (Fig. 1.1). As the plant is deprived of external time cues, this eliminates rhythms that may be due to environmental conditions. Commonly used constant experimental conditions include constant light, darkness, or red light, and timecourses are often performed over several days.

Leaf movements were the first reported circadian rhythms (de Mairan (1729); Darwin (1880)), and are still used as a simple, easily observable output of the circadian clock (Schaffer et al. (1998); Salomé et al. (2002); Webb (2003); Greenham et al. (2017)). Circadian rhythms can also be investigated for other physiological processes, such as stomatal movements using infrared gas analysers (Dodd et al. (2004); Liu et al. (2013); Matthews et al. (2017)) and chlorophyll fluorescence using Pulse Amplitude Modulation equipment (Shimizu et al. (2015); Dakhiya et al. (2017)).

Development of luciferase reporter gene technology greatly accelerated Arabidopsis circadian clock research (Millar et al. (1992, 1995); Hall and Brown (2007)). It enabled screening of the first plant circadian mutants (Millar et al. (1995)) and remains widely used. Using ATP and O<sub>2</sub> as substrates, luciferase catalyses the oxidative decarboxylation of luciferin (Millar et al. (1992)). This releases a photon, which can be quantified using a sensitive camera. Split luciferase assays have also been developed to examine tissue-specific circadian rhythms (Endo et al. (2014)). This entails splitting the luciferase coding sequence into two complementing parts: one is under control of a circadian clock promoter, while the other is expressed by a tissue-specific promoter (Endo et al. (2014)). When both proteins are present in the same tissue at the same time, they join to form a functional luciferase enzyme, which emits luminescence in the presence of luciferin (Endo et al. (2014)).

Detection of transcript abundance using qRT-PCR has become a well-established technique to monitor circadian rhythms of gene expression. This often involves sampling plants at regular intervals under constant conditions. This can be performed for whole plants (Nozue et al. (2007); Niwa et al. (2009); Rawat et al. (2011); Noordally et al. (2013); Belbin et al. (2017)) and specific tissue types (Shimizu et al. (2015); Takahashi et al. (2015); Hassidim et al. (2017)). Transcriptome analysis datasets enable in-depth examination of the circadian clock at the transcriptional level (Covington et al. (2008);

Hayes et al. (2010); Gendron et al. (2012); Diurnal online resource by Mockler et al. (2007)). In a similar manner, circadian characteristics of protein abundance can be investigated using techniques such as immunodetection, yeast two-hybrid, immunoprecipitation, pull-down assays and phosphoproteomics (Más et al. (2003b); Kim et al. (2007); Fujiwara et al. (2008); Baudry et al. (2010); Choudhary et al. (2015)).

Several mathematical algorithms have been developed to enable subsequent analysis of these rhythmic datasets. Fast Fourier Transform Non-Linear Least Squares (FFT-NLLS) is based on curve-fitting and is the most commonly used algorithm to analyse circadian datasets obtained under constant conditions (Zielinski et al. (2014)). It is highly effective for noisy and relatively short datasets (Zielinski et al. (2014)). In addition, as it provides confidence levels for circadian period, phase and amplitude, a dataset for which no period can be identified is considered arrhythmic (Zielinski et al. (2014)). However, FFT-NLLS assumes the shape of the data's waveform to be sinusoidal, which limits its ability to fit a curve to certain datasets (Zielinski et al. (2014)). Maximum Entropy Spectral Analysis (MESA) overcomes this limitation by using a stochastic modelling approach, but does not produce a significance or confidence measure (Zielinski et al. (2014)). Other algorithms include Enright Periodogram, a simple algorithm that splits data into sections of a known period; mFourfit, a curve-fitting model; Lomb-Scargle periodogram, which generates a spectrum in which significance of each frequency is represented; Spectrum resampling, which refines period estimation for non-sinusoidal data; and HAYSTACK, which uses a pattern-matching approach to find genes with similar expression patterns (Mockler et al. (2007); Zielinski et al. (2014)). Online tools such as Biodare 2 (Zielinski et al. (2014)) have been made available for analysis of plant circadian rhythms.

## **1.2 Water use efficiency (WUE)**

### **1.2.1 Defining WUE**

Stomata are microscopic epidermal pores, and are crucial for CO<sub>2</sub> uptake for photosynthesis. However, this occurs at the expense of water loss (Fig. 1.6), with over 90% of available water being lost by higher plants through stomatal transpiration (Na and Metzger (2014)). As CO<sub>2</sub> enters the leaf through the substomatal cavity, it first encounters



resistance by the stomatal pores themselves, followed by “mesophyll resistance” consisting of aqueous and lipid boundaries located around mesophyll cells and chloroplasts (Lawson and Blatt (2014)). Water molecules leaving the leaf do not encounter this “mesophyll resistance”; thus their diffusion rate is 1.6 times greater than that of CO<sub>2</sub> (Lawson and Blatt (2014); Hetherington and Woodward (2003)). It has been estimated that as many as 400 water molecules are lost per CO<sub>2</sub> molecule assimilated (Ruggiero et al. (2017)).

Water use efficiency (WUE) is described as the ratio of carbon dioxide incorporated into photosynthetic reactions to the water lost via transpiration (Bacon (2009)). It has been investigated under a range of different scales, from individual leaves to an entire crop, and from a few days to the length of the growing season (The Royal Society (2009)). At the single leaf level, instantaneous, intrinsic WUE (WUE<sub>i</sub>) can be equated to net CO<sub>2</sub> assimilation per given unit of water transpired at a single time point (Violet-Chabrand et al. (2016); Ruggiero et al. (2017); Ferguson et al. (2018)):

$$WUE_i = \frac{\text{net CO}_2 \text{ assimilation}}{\text{stomatal conductance}} \quad (1.1)$$

Whole plant WUE is defined as total biomass produced per unit of water transpired (Violet-Chabrand et al. (2016); Ruggiero et al. (2017); Ferguson et al. (2018)):

$$WUE = \frac{\text{biomass}}{\text{water use}} \quad (1.2)$$

WUE can be measured using different techniques. Leaf gas exchange is commonly used to measure WUE<sub>i</sub> (Violet-Chabrand et al. (2016); Ferguson et al. (2018)). Both WUE<sub>i</sub> and whole plant WUE can be measured using carbon isotope discrimination ( $\delta^{13}\text{C}$ ) (Farquhar and Richards (1984)). Heavier <sup>13</sup>C is selected against during CO<sub>2</sub> diffusion and assimilation, causing a decreased <sup>13</sup>C/<sup>12</sup>C ratio within leaf tissues. This ratio varies with CO<sub>2</sub> diffusion into the leaf and photosynthetic demand, thereby reflecting the ratio of carbon assimilation to stomatal conductance (Morison et al. (2008)). Therefore, this ratio provides a measure for WUE<sub>i</sub> or whole plant WUE integrated over time (Farquhar and Richards (1984); Morison et al. (2008)). However,  $\delta^{13}\text{C}$  is unsuitable for C4 plants and unable to differentiate between alterations in CO<sub>2</sub> assimilation or stomatal conductance (Morison et al. (2008)). Whole plant WUE can also be obtained by measuring dry biomass and calculating the amount of water used (Violet-Chabrand et al. (2016); Li et al. (2017)). Finally, eddy covariance measures energy and gas fluxes between a

surface and the overlying atmosphere, enabling WUE estimations over entire agricultural ecosystems (Reichstein et al. (2012)).

Importantly, these techniques are not directly comparable. Different datasets yielded different WUE results depending on the method applied, highlighting the inconsistency and uncertainty between these techniques (Medlyn et al. (2017)). In addition,  $WUE_i$  measurements do not provide an accurate representation of TE over the plant lifetime (Condon et al. (2004); Tomás et al. (2014); Medrano et al. (2015); Ferguson et al. (2018)). This may be partially explained by effects of leaf position and dark respiration on WUE (Medrano et al. (2015)).

Finally, it is important to note that WUE is not a drought resistance trait (Blum (2009)). WUE varies across water regimes and tends to increase under drought conditions, as water loss decreases more than the rate of carbon fixation under water-limited conditions (Edwards et al. (2012)). In addition, drought-resistant plants tend to have low WUE, whereas plants with high WUE often have undesirable traits limiting water use such as smaller leaf area or earlier flowering time (Blum (2009); Ruggiero et al. (2017)). Therefore, some prefer to focus on the concept of Effective Use of Water (EUW), which indicates that maximising crop productivity under water-limited conditions requires both decreased water use and increased soil water capture (Blum (2009); Ferguson et al. (2018)).

## **1.2.2 Breeding for high WUE**

Demand for safe water has steadily increased as the world population grows exponentially, and, with it, demand in food requirements. The competition for freshwater is being exacerbated further by climate change (Ruggiero et al. (2017)). Global agriculture alone represents 4/5<sup>ths</sup> of worldwide freshwater consumption (Ruggiero et al. (2017)) and drought negatively affects both crop biomass accumulation and yield (Yoo et al. (2010); Hu and Xiong (2014)), with yield loss of over 50% in rice if drought stress occurs at the reproductive stage (Venuprasad et al. (2007)). In China alone, water deficit is estimated to cause over \$25 billion worth of damage per year (Hu and Xiong (2014)), while, in Europe, water shortage cost 100 billion euros between 1977 and 2007 (Grundy et al. (2015)). In addition, domesticated crops have been consistently bred for larger yields, but without considering water loss through transpiration (Lawson et al. (2012)).

As WUE combines both photosynthesis and transpiration, it is widely used as a tool to indicate vegetative performance (Medlyn et al. (2017)). Many breeding efforts focus on the plethora of existing drought resistance traits, such as a deep and dense root architecture (Hu and Xiong (2014)). Conventional breeding is already being used to develop hybrids with high drought tolerance and productivity, such as for maize at CIMMYT in Mexico (Xoconostle-Cázares et al. (2010)). Recently, a combination of conventional breeding approaches and marker-assisted selection is being used to obtain new varieties. This involves using drought-resistant varieties as QTL donors for introgression into drought-susceptible, high yielding genotypes (Ruggiero et al. (2017)). For example, the Shanghai Agrobiological Gene Center successfully produced water-efficient and drought-resistant rice varieties, but this process was very slow (Hu and Xiong (2014)). Recent advances in molecular genetics have made it possible to pinpoint genes responsible for desirable traits at the transcriptomic, proteomic, metabolomic and epigenetic levels (Hu and Xiong (2014)).

### **1.2.3 Stomatal guard cells: development, function, and manipulation**

#### **1.2.3.1 Guard cell development**

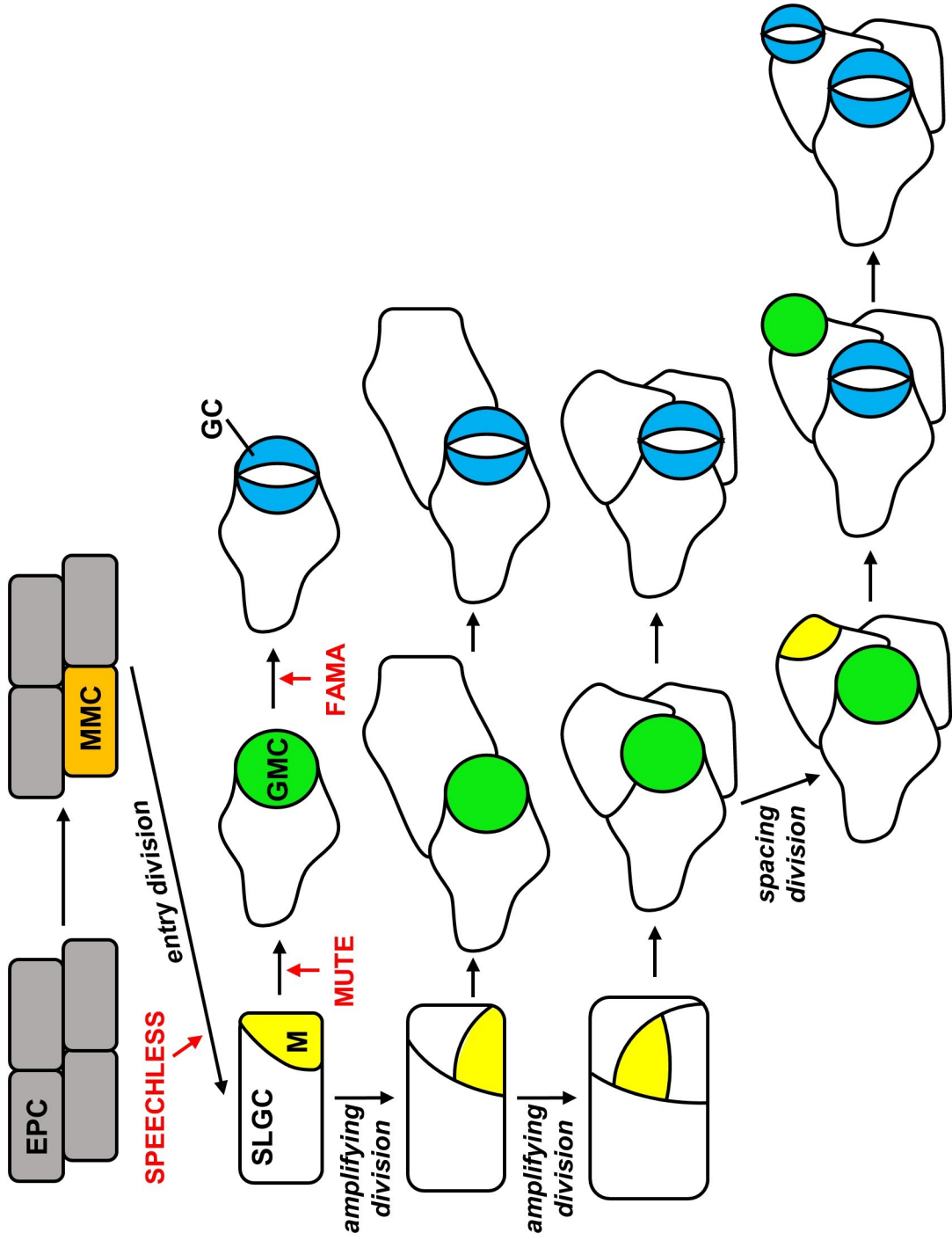
Stomata regulate both carbon dioxide uptake for photosynthesis and water loss through transpiration. Each stoma is surrounded by two guard cells, which adjust stomatal aperture through turgor pressure. In *Arabidopsis*, stomata are spatially separated by at least one cell, enabling efficient CO<sub>2</sub> diffusion and assimilation (Fig. 1.5) (Pillitteri and Dong (2013); Lawson and Blatt (2014)). *Arabidopsis* stomatal development and epidermal patterning involve a series of precise divisions regulated by a large number of genes (Fig. 1.5), and have been described in depth elsewhere (Nadeau and Sack (2002); Pillitteri and Dong (2013)).

Briefly, epidermal protodermal cells (EPCs) differentiate into meristemoid mother cells (MMCs) (Fig. 1.5) (Pillitteri and Dong (2013)). MMCs undergo an initial asymmetric “entry” division, which generates both a small meristemoid cell and a larger, stomatal-lineage ground cell (SLGC) (Fig. 1.5) (Pillitteri and Dong (2013)). This division is promoted by a basic helix-loop-helix (bHLH) protein called SPEECHLESS (Fig. 1.5) (Torii et al. (2007)). The meristemoid then divides asymmetrically up to four times in what are called “amplifying” divisions, thereby increasing the total number of SLGCs (Fig. 1.5)

(Pillitteri and Dong (2013)). SLGCs can become pavement cells or produce satellite meristemoids, which are separated by at least one cell from the existing stomatal precursor (Fig. 1.5) (Pillitteri and Dong (2013)). The bHLH MUTE protein directs terminal cell-fate transition from meristemoid to round-shaped guard mother cell (GMC) (Fig. 1.5) (Torii et al. (2007); Pillitteri and Dong (2013)). The bHLH FAMA protein then enables the GMC to divide symmetrically, generating two cells which will ultimately become guard cells (Fig. 1.5) (Torii et al. (2007); Pillitteri and Dong (2013)).

Many other genes are involved in this process, including *EPIDERMAL PATTERNING FACTOR1 (EPF1)*, *EPF2*, *SCREAM (SCRM)*, *SCRM2*, *FOUR LIPS*, *MYB88*, *STOMAGEN*, *ERECTA*, and *STOMATAL DENSITY AND DISTRIBUTION1 (SDD1)* (Pillitteri and Dong (2013)). Environmental factors, such as light and CO<sub>2</sub>, and hormones, such as brassinosteroids, also affect stomatal density (Pillitteri and Dong (2013)).

Figure 1.5: Guard cell development in Arabidopsis. An epidermal protodermal cell (EPC) is represented in grey, stomatal lineage ground cell (SLGC) or pavement cell in white, meristemoid mother cell (MMC) in orange, meristemoid (M) in yellow, guard mother cell (GMC) in green, guard cell (GC) in blue, enzymes in red, and division in *italics*. Additional information is provided in text. This figure was derived from the concept of Pillitteri and Dong (2013).



### 1.2.3.2 Stomatal movement

Stomatal aperture and closure mechanisms have been described in depth elsewhere (Schroeder et al. (2001); Hubbard and Webb (2011); Araújo et al. (2011); Chen et al. (2012); Kollist et al. (2014); Munemasa et al. (2015); Azoulay-Shemer et al. (2016)). Briefly, stomatal aperture is initiated when specific signals, such as blue light and circadian clock signals, activate a guard cell  $H^+$ -ATPase, which pumps protons out of guard cells and causes plasma membrane hyperpolarisation (Fig. 1.6) (Hubbard and Webb (2011)). This leads to an influx of potassium ions and accumulation of malate, potassium ions, and chloride ions within the guard cell vacuole (Fig. 1.6) (Hubbard and Webb (2011)). Water influx via osmosis then occurs, thereby increasing guard cell turgor and ultimately leading to stomatal aperture (Fig. 1.6) (Hubbard and Webb (2011)). For stomatal closure, signalling pathways inhibit  $H^+$ -ATPase and activate SLOW ANION CHANNEL1 (SLAC1), which promotes efflux of chloride ions (Fig. 1.6) (Hubbard and Webb (2011)). The subsequent depolarisation of the plasma membrane opens outwardly-rectifying  $K^+$  channels, leading to ion efflux (Fig. 1.6) (Hubbard and Webb (2011)). Water accordingly flows out of the guard cell, guard cell turgor decreases, and the stomatal pore closes (Fig. 1.6) (Hubbard and Webb (2011)).

Stomatal behaviour is regulated by many signalling pathways, including hormonal, light quality and quantity,  $CO_2$ , water availability and starch signalling pathways, and has been the focus of many studies and reviews (Schroeder et al. (2001); Hubbard and Webb (2011); Araújo et al. (2011); Chen et al. (2012); Kollist et al. (2014); Munemasa et al. (2015); Azoulay-Shemer et al. (2016)). Factors such as low  $CO_2$  concentrations, high humidity and high light intensity promote stomatal opening whereas high  $CO_2$  concentrations, drought, darkness and ABA induce stomatal closure (Fig. 1.6) (Araújo et al. (2011)). As guard cells do not have plasmodesmata, their responses are cell-autonomous (Sirichandra et al. (2009)).

The effect of light on stomatal aperture has been examined extensively (Chen et al. (2012)). For example, blue light induces stomatal aperture through both cryptochrome and phototropin signalling pathways (Chen et al. (2012)). Cryptochromes are particularly important for stomatal aperture at high fluence rates of blue light, whereas phototropins induce stomatal aperture over a range of fluence rates of blue light (Chen et al. (2012)). Stomatal aperture is also promoted by red light through PhyB signalling pathways (Chen et al. (2012)). Both PhyB and cryptochrome signalling pathways converge

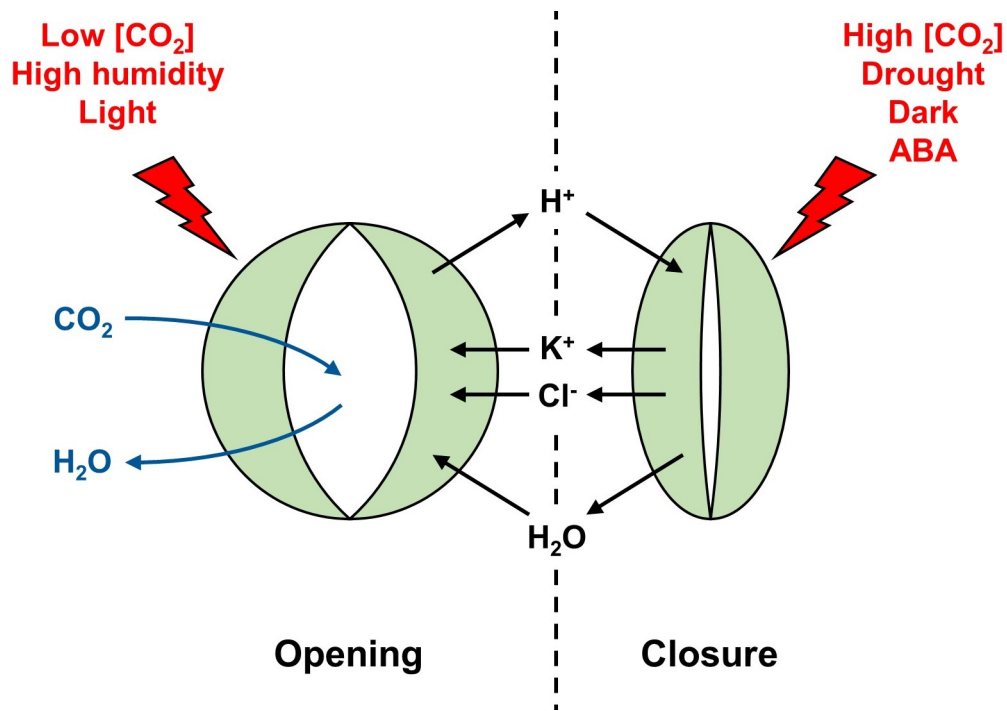


Figure 1.6: Stomatal opening and closing mechanisms in Arabidopsis. Examples of factors inducing stomatal opening or closure are represented in red; ion and water movements involved in stomatal opening or closure in black; and gas exchange in blue. Additional mechanisms and signalling pathways are provided in text.

upon the circadian clock component ELF3 (Chen et al. (2012)). Calcium signalling may link phototropins to guard cell  $H^+$ -ATPase activation (Chen et al. (2012)). MYB transcription factors are also involved in this mechanism, with MYB60 promoting stomatal aperture and MYB61 inducing stomatal closure (Chen et al. (2012)).

Many of these signal transduction pathways involve variations in  $[Ca^{2+}]_{cyt}$  (Schroeder et al. (2001)). For example, ABA-induced stomatal closure is dependent on increases in  $[Ca^{2+}]_{cyt}$  (Allen et al. (1999); Pei et al. (2000); Schroeder et al. (2001)). Increases in  $[Ca^{2+}]_{cyt}$  are also caused by elevated  $CO_2$ , cold shock, and  $H_2O_2$ , leading to stomatal closure (Webb et al. (1996); Pei et al. (2000); Schroeder et al. (2001); Young et al. (2006)). In addition, low temperature-mediated increases in  $[Ca^{2+}]_{cyt}$  are gated by the circadian clock (Dodd et al. (2006)). Specific  $[Ca^{2+}]_{cyt}$  oscillations occur in response to different stimuli, and these oscillations are required for stomatal closure (Allen et al. (2000); Schroeder et al. (2001)). Interestingly, signals promoting stomatal opening, such as auxin and blue light, can also increase  $[Ca^{2+}]_{cyt}$  (Schroeder et al. (2001)).

### 1.2.3.3 Guard cell metabolism and mesophyll photosynthesis affect stomatal conductance

The greater abundance of trehalose-related, sucrose transporter and hexose transporter transcripts within guard cells compared to other cell types suggests that sugars are particularly important for guard cell function (Van Houtte et al. (2013); Daloso et al. (2016)). Guard cells can produce sucrose through photosynthetic carbon fixation or starch breakdown in chloroplasts, but mesophyll photosynthesis is their main source of sucrose (Santelia and Lawson (2016)). This sucrose is transported via the apoplast to guard cells (Santelia and Lawson (2016)), where uptake might occur via H<sup>+</sup> symporters (Daloso et al. (2016)).

The photosynthetic capacity of guard cells remains disputed (Lawson et al. (2014)). Although guard cells possess functional chloroplasts and Calvin cycle enzymes, it has been suggested that their photosynthetic capacity is reduced compared with mesophyll cells, with fewer and smaller chloroplasts and a lower electron transport rate (Lawson et al. (2002, 2014)). Starch breakdown within guard cells also remains controversial. Tallman and Zeiger (1988) report that *Vicia* guard cells accumulate starch at night, while blue light induces starch degradation into sucrose during the day. In contrast, *Arabidopsis* guard cells do not contain starch around dawn (Stadler et al. (2003)). Therefore, starch catabolism within guard cells may be species-specific (Lawson et al. (2014)). An alternative energy source could include triacylglycerols, which are stored as lipid droplets within *Arabidopsis* guard cells and are crucial for light-induced stomatal opening (McLachlan et al. (2016)).

Guard cell sucrose might enable stomatal opening in the afternoon by acting as an osmotic regulator (Santelia and Lawson (2016)). Indeed, guard cell potassium ion concentration declines during the day, whereas sucrose concentration within guard cells increases (Santelia and Lawson (2016)). This suggests that sucrose replaces potassium as an osmoticum as the day progresses (Amodeo et al. (1996); Talbott and Zeiger (1998); Schroeder et al. (2001); Santelia and Lawson (2016)). In a similar fashion, sucrose accumulation in the extracellular apoplast causes stomatal closure via osmosis (Outlaw Jr. and De Vlieghere-He (2001); Santelia and Lawson (2016)). Sucrose also acts as a respiratory substrate, as sucrose breakdown and mitochondrial respiration provide energy required for stomatal opening (Daloso et al. (2015)).

It has also been hypothesised that sucrose could act as a messenger linking mesophyll



photosynthesis and stomatal conductance (Kelly et al. (2013); Santelia and Lawson (2016); Daloso et al. (2016)). Indeed, stomatal conductance and carbon assimilation are often tightly correlated (Hetherington and Woodward (2003)), suggesting that mesophyll cells and stomata are coordinated (Lawson et al. (2014)). This might occur through a mesophyll-driven signal, as several studies report that light and CO<sub>2</sub> affect stomatal aperture to a greater extent in intact leaves compared to isolated epidermal peels (Lee and Bowling (1992); Roelfsema et al. (2002); Young et al. (2006); Mott et al. (2008); Fujita et al. (2013); Lawson et al. (2014)). However, there is conflict over the nature of this “mesophyll signal”, with different reports arguing that it is a vapour phase (Sibbersen and Mott (2010); Mott et al. (2014)), aqueous apoplastic (Lee and Bowling (1992); Fujita et al. (2013)), metabolic (Wong et al. (1979)), redox state (Busch (2014)), intracellular CO<sub>2</sub> concentration (Roelfsema et al. (2002)), or sucrose signal (Kelly et al. (2013); Lawson et al. (2014)).

In the scenario in which sucrose is the messenger, photosynthetic saturation would produce an excess of sucrose, which would then be transported to the apoplast surrounding guard cells and induce stomatal closure (Kelly et al. (2013); Santelia and Lawson (2016)). However, stomatal closure is rarely induced by conditions resulting in an increase in photosynthesis, thereby an increase in sucrose concentrations (Lawson and Blatt (2014)). Therefore, it is unlikely that sucrose could coordinate mesophyll photosynthesis with stomatal behaviour in the short-term, but sucrose could still affect stomatal conductance in the long-term (Santelia and Lawson (2016); Daloso et al. (2016)). Interestingly, transgenic tobacco containing reduced RIBULOSE-1,5-BISPHOSPHATE CARBOXYLASE/OXYGENASE (RUBISCO), causing reduced photosynthesis and sucrose production, had no alterations in stomatal aperture or behaviour (Von Caemmerer et al. (2004)). This implies that mesophyll photosynthesis is not involved in connecting the mesophyll to guard cells (Daloso et al. (2016)).

#### **1.2.3.4 Guard cell manipulation to enhance WUE**

Given their pivotal role in regulating stomatal aperture and water loss, guard cells have become a clear target to improve water use (Fig. 1.7).

### ***Guard cell-specific promoters***

Guard cell-specific promoters could be a useful tool to engineer stomatal responses without affecting growth and productivity (Galbiati et al. (2008); Cominelli et al. (2011)). Several potential candidates have emerged. *MYB60* encodes an R2R3 MYB transcription factor involved in light-induced stomatal aperture (Cominelli et al. (2005, 2011)). The *MYB60* promoter is guard cell specific in dicots, and has been used to overexpress coding sequences in guard cells (Cominelli et al. (2005, 2011); Meyer et al. (2010); Rusconi et al. (2013); Nagy et al. (2009); Galbiati et al. (2008); Bauer et al. (2013)). However, it cannot be used in monocots, which limits its use for key crops such as wheat or rice. Truncated and chimeric versions of this promoter have been generated, but their activity is weaker and/or rapidly down-regulated by both dehydration and ABA (Francia et al. (2008); Cominelli et al. (2011); Rusconi et al. (2013)).

*GC1* is another strong candidate, coding for a 119 amino acid protein belonging to the gibberellic acid-stimulated family (Yang et al. (2008)). Its promoter has strong and relatively guard cell-specific reporter gene activity, with three and five to ten times higher expression than the *MYB60* and *KAT1* promoters, respectively (Yang et al. (2008)). It has been exploited successfully as an overexpressor for proteins in guard cells (Yang et al. (2008); Kinoshita et al. (2011); Wang et al. (2014)). Furthermore, its expression levels do not vary more than two-fold with drought, cold, light, ABA or gibberellin (Yang et al. (2008)), making it a useful tool for constant expression.

A partial segment of the potato *KST1* promoter was demonstrated to have constitutive, guard cell activity in both monocots and dicots, including *Arabidopsis* (Kelly et al. (2017)). The *CYP86A2* promoter was also reported to be guard cell-specific (Francia et al. (2008)). The *KAT1* promoter is guard cell-specific, but is too weak to drive guard cell-specific protein repression or overexpression (Nilson and Assmann (2007); Yang et al. (2008)).

### ***Altering stomatal density***

Genetic manipulation of stomatal density affects short- and long-term WUE (Fig. 1.7) (Yoo et al. (2010); Franks et al. (2015)). For example, the low stomatal density mutant *gt11* increases drought tolerance and WUE without affecting photosynthetic capacity

(Yoo et al. (2010)). However, manipulation of stomatal density was rarely shown to increase carbon assimilation and biomass (Lawson and Blatt (2014)). This was mainly reported by Tanaka et al. (2013), who overexpressed *STOMAGEN* in Arabidopsis. This resulted in higher stomatal density than the wild type, as well as a 30% increase in CO<sub>2</sub> assimilation (Tanaka et al. (2013)). However, these transgenic plants also transpired twice as much as the wild type and had a 50% decrease in WUE (Tanaka et al. (2013)).

### ***The effect of stomatal size***

Stomatal size can also impact WUE (Fig. 1.7) (Lawson and Blatt (2014)). A strong, negative correlation was reported between stomatal size and density when manipulating *EPF* genes: *epf1/epf2* double mutants had higher stomatal density and smaller stomata, whereas *EPF2-ox* had lower stomatal density and larger stomata (Doheny-Adams et al. (2012)). *EPF2-ox* had increased growth, WUE and drought tolerance, whereas *epf1/epf2* was inferior to the wild type (Doheny-Adams et al. (2012); Franks et al. (2015)). In addition, stomatal size influences speed of closure, with smaller stomata responding faster than larger stomata (Lawson and Blatt (2014)). Exceptions include ferns, which respond quickly due to passive hydraulic characteristics, and grasses, which have specialised subsidiary cells (Lawson and Blatt (2014)).

### ***Modifying guard cell signal transduction***

Manipulating guard cell signal transduction affects stomatal movement, which in turn can alter WUE and/or drought response (Fig. 1.7) (Pei et al. (1998); Hugouvieux et al. (2001); Schroeder et al. (2001)). For example, deleting the Arabidopsis *ERA1* farnesyltransferase gene increases sensitivity of stomatal closure to ABA, thereby reduces transpiration under water-limited conditions (Pei et al. (1998)). Merlot et al. (2002) isolated mutants with altered drought responses, and found that many had decreased ABA sensitivity in the guard cells, or were unable to synthesise or accumulate ABA.

Other stomatal genes affecting WUE in Arabidopsis include stomatal inward-rectifying K<sup>+</sup> channels like *KAT1* (Nilson and Assmann (2007)), guard cell-expressed ATP-binding cassette transporters such as *MRP4* and *MRP5* (Nilson and Assmann (2007)), the guard cell-expressed NO<sub>3</sub><sup>-</sup> transporter *CHL1* (Nilson and Assmann (2007)), and genes affecting

stomatal behaviour (*OST1*, *ABA2*) (Des Marais et al. (2014)).

### ***Natural variation in Arabidopsis WUE***

These effects can also be observed in different *Arabidopsis* accessions. The reduced stomatal conductance of C24 enables it to have a higher drought tolerance than Col-0 (Bechtold et al. (2010)). In contrast, an amino acid substitution in *MITOGEN-ACTIVATED PROTEIN KINASE 12* generates larger guard cells and stomata, altered ABA response, CO<sub>2</sub> insensitivity, and lower WUE in the CVI accession (Des Marais et al. (2014); Jakobson et al. (2016)). *L. er.*, with its mutated *erecta* gene, has altered stomatal density and decreased transpiration efficiency under both droughted and well-watered conditions (Masle et al. (2005)).

### ***Successfully increasing crop WUE based on knowledge acquired from plant model systems***

Knowledge gained from plant model systems has been successfully used to increase crop WUE. For example, an *Arabidopsis* gene known to repress ABA sensitivity in guard cells was transferred to canola as an RNAi construct, leading to an increase in drought resistance (Wang et al. (2009)). In cotton, overexpressing the *Arabidopsis* transcription factor *RAV1* improved WUE by affecting both stomatal density and aperture (Fiene et al. (2017)). In rice, overexpression of *Arabidopsis HARDY* decreased stomatal conductance and increased WUE, survivability, and photosynthesis (Karaba et al. (2007)). In a similar manner, overexpression of *SNAC1* in rice led to increased WUE and ABA sensitivity in guard cells, as well as enhanced drought resistance (Hu et al. (2006)). This also occurred when overexpressing *SNAC1* in wheat (Saad et al. (2013)).

### ***A future target to enhance WUE***

In future, it would be useful to target the temporal disconnect between stomatal conductance and photosynthetic carbon assimilation (Fig. 1.7). Indeed, the photosynthetic rate adjusts to new environmental conditions within seconds, whereas stomatal movement responses are an order of magnitude slower (Matthews et al. (2017); Lawson and

Blatt (2014)). This slower stomatal response constrains CO<sub>2</sub> uptake, thereby photosynthesis (Matthews et al. (2017); Lawson and Blatt (2014)). In addition, stomata will continue to open even if carbon assimilation has already achieved a steady state, resulting in unnecessary water loss compared to gain in CO<sub>2</sub> (Matthews et al. (2017); Lawson and Blatt (2014)).

Matthews et al. (2017) report a remarkable diversity of coordination between carbon assimilation and stomatal conductance in herbaceous crops. This implies that there is no strong evolutionary pressure on this coordination, which highlights a possible target for improvement of WUE (Matthews et al. (2017)). It is estimated that improving this synchrony between mesophyll CO<sub>2</sub> demands and stomatal aperture and closure responses could increase WUE by up to 22% (Fig. 1.7) (Lawson and Blatt (2014)). This could be achieved by targeting ion transport within guard cells, which includes guard cell vacuole, malate metabolism and transport, ion channel, and vesicle-trafficking proteins (Lawson and Blatt (2014)), or altering hydraulic conductance or leaf vein density (Matthews et al. (2017)).

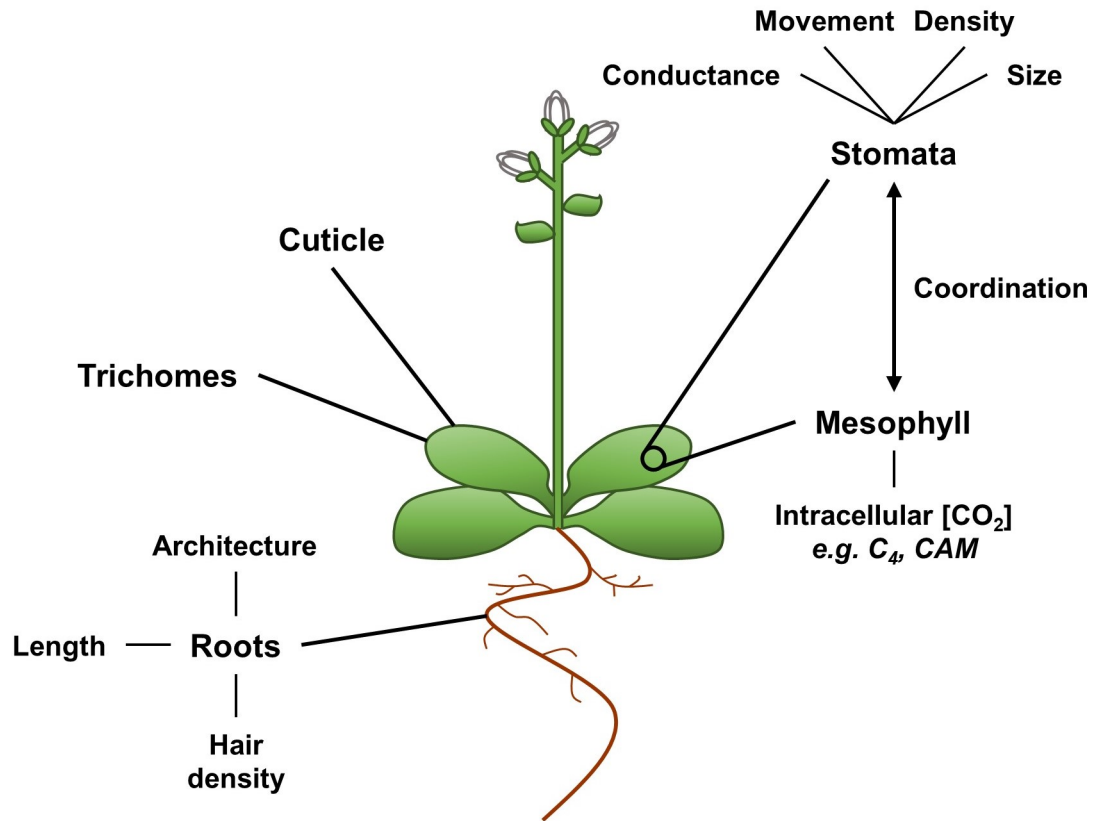


Figure 1.7: An increase in WUE could be achieved by targeting different plant tissues. This diagram summarises several possibilities for Arabidopsis discussed in the text. Additional targets are provided in text.

#### 1.2.4 Targeting other tissue types to increase WUE

Increasing WUE could also be achieved by targeting other plant tissues. Manipulation of root characteristics, such as architecture, length, and hair density, can enable a more efficient uptake of water (Fig. 1.7) (Kell (2011); Wasson et al. (2012); Paez-Garcia et al. (2015); Ruggiero et al. (2017)). Water loss can also be mitigated through alterations in the cuticle (Fig. 1.7) (Riederer and Schreiber (2001); Goodwin and Jenks (2005); Seo et al. (2011); Ruggiero et al. (2017)). Another plant strategy to increase drought tolerance involves accumulation of ROS scavengers, osmoprotectants, and antioxidants (Hu and Xiong (2014)). Efforts have also focused on introducing more water use efficient C<sub>4</sub> and Crassulacean Acid Metabolism (CAM) photosynthetic pathways into C<sub>3</sub> crops (Fig. 1.7) (Murchie et al. (2009); Borland et al. (2014)). Trichomes may represent another potential target (Fig. 1.7), as they increase drought stress tolerance (Dalin et al. (2008); Sletvold and Ågren (2012); Sato and Kudoh (2017)) as well as herbivore

resistance (Levin (1973); Mauricio and Rausher (1997); Handley et al. (2005); Sato and Kudoh (2016)).

In *Arabidopsis*, trichomes are large, three-branched, single celled hairs developing from the aerial epidermis (Hülkamp and Schnittger (1998); Dalin et al. (2008)). Their density and patterning on the leaf surface are mainly regulated by *GLABROUS1* and *TRANSPARENT TESTA GLABRA1* (Hülkamp and Schnittger (1998); Dalin et al. (2008)), and they develop before stomata (Larkin et al. (1996); Glover (2000)). Although trichomes are useful for plant defence and drought tolerance, they appear to be associated with a fitness cost. When natural herbivores were artificially removed, glabrous *Arabidopsis halleri* subsp. *gemmifera* plants had a 10% larger biomass than hairy plants (Sato and Kudoh (2016)). The fitness cost of trichome production was also observed for *A. lyrata* (Sletvold et al. (2010); Sletvold and Ågren (2012)) and *A. thaliana* populations (Mauricio and Rausher (1997); Mauricio (1998)). However, when natural herbivores were present, both morphs had similar fitness, enabling them to coexist within a population (Kawagoe et al. (2011)). It would be interesting to investigate whether trichome production could also be manipulated to increase WUE (Fig. 1.7).

## **1.3 The relationship between the circadian clock and WUE**

### **1.3.1 An accurate circadian clock increases WUE**

An accurate circadian clock increases WUE (Dodd et al. (2005)). Indeed, stomatal aperture, stomatal conductance and CO<sub>2</sub> assimilation are under circadian control in *Arabidopsis*, with these parameters peaking in the middle of the subjective day (Salomé et al. (2002); Dodd et al. (2004, 2005); Sanchez et al. (2011)). Furthermore, mutations affecting the circadian oscillator, such as *toc1-1* and *ztl-1*, affect the period of CO<sub>2</sub> assimilation and stomatal aperture in constant light (Dodd et al. (2004)). Even under light-dark cycles, abolishing the circadian clock in *CCA1-ox* prevents anticipation of dawn or dusk (Dodd et al. (2005)). This in turn causes stomata to remain open for the entire length of the photoperiod rather than closing at midday, leading to higher total transpiration compared to the wild type (Dodd et al. (2005)). Mutants with an altered circadian period were also unable to anticipate dawn and dusk (Dodd et al. (2014)). Interestingly, circadian period was significantly correlated with both stomatal

conductance and carbon assimilation (Edwards et al. (2012)).

This relationship between circadian regulation and WUE has been reported for a variety of species, including *Brassica rapa* (colza) (Edwards et al. (2012)), several *Populus* (poplar) species (Wilkins et al. (2009)), *Vicia faba* (broad bean) (Gorton et al. (1989)), *Phaseolus vulgaris* (red kidney bean) (Hennessey and Field (1991)), *Glycine max* (soybean) (Kerr et al. (1985)) and *Tradescantia virginiana* (virginia spiderwort) (Martin and Meidner (1971)). In bean and cotton at the canopy scale, the circadian oscillator contributes an estimated 70% to the regulation of diurnal rhythms in stomatal aperture, and 30% to that of carbon assimilation (Resco de Dios et al. (2017)). Circadian regulation of stomatal aperture was also found to play a crucial role in controlling the Crassulacean acid metabolism (CAM) cycle of two *Kalanchoe* species (von Caemmerer and Griffiths (2009)). Understanding the mechanisms underpinning circadian regulation of WUE could lead to breeding possibilities for enhanced WUE traits (McClung (2013)).

### **1.3.2 The bidirectional relationship between ABA and the circadian clock**

The stress hormone ABA may represent a possible link between the circadian clock and WUE. Interestingly, rhythmic stomatal movements are controlled by both the circadian clock, which enables stomata to anticipate dawn and dusk, and ABA, which induces stomatal closure (Lebaudy et al. (2008); Robertson et al. (2009)). In addition, transcript abundance of *CLA1*, *PSY*, *NCED3* and *ABA2* ABA biosynthesis genes, as well as over 40% of ABA-induced genes, are circadian-regulated (Dodd et al. (2007); Covington et al. (2008); Mizuno and Yamashino (2008)).

ABA response networks are also circadian-gated, with ABA being more effective at inducing stomatal closure in the afternoon (Legnaioli et al. (2009); Sanchez et al. (2011)). This enables stomatal opening and CO<sub>2</sub> uptake for moderately stressed plants in the cool of the morning, when evapotranspiration is low (Webb (1998); Robertson et al. (2009)). It also prevents excessive water loss in the afternoon, when temperatures are likely to be warmer (Webb (1998); Mizuno and Yamashino (2008); Legnaioli et al. (2009); Robertson et al. (2009)). Interestingly, this regulation between circadian signalling pathways and ABA is reciprocal, as treating plants with exogenous ABA lengthens circadian period by two hours under constant light conditions (Hanano et al. (2006);



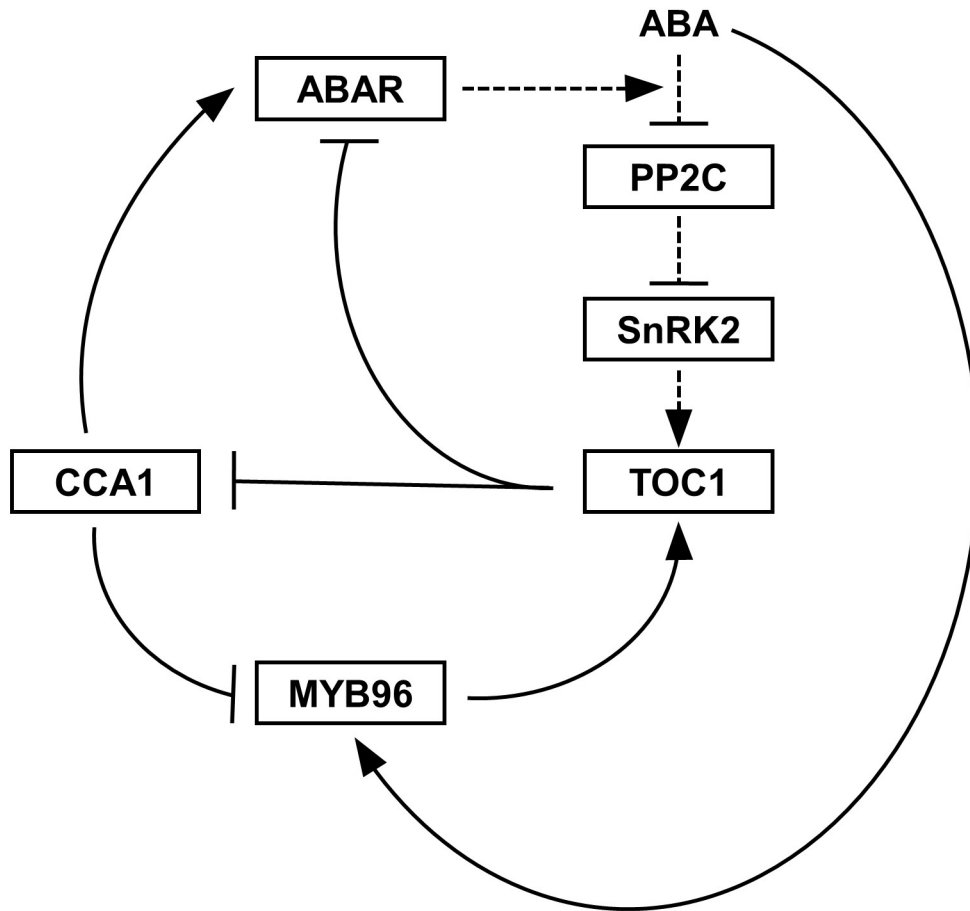


Figure 1.8: Interactions between the Arabidopsis circadian clock and ABA signalling pathway. Transcriptional regulation is represented by solid lines, translational regulation by dotted lines, induction by arrows and suppression/degradation by bars. Additional interactions are described in the text. The roles of clade A type 2C protein phosphatases (PP2Cs) and SnRKs are further described in section 1.4.3. This figure was derived from the concept of Pokhilko et al. (2013).

Legnaioli et al. (2009); Seung et al. (2012)).

Briefly, *TOC1* is induced by ABA under drought conditions and controls stomatal aperture by regulating *GENOME UNCOUPLED 5* (*ABAR/GUN5*), and ABA induction of *TOC1* requires *ABAR* (Fig. 1.8) (Legnaioli et al. (2009); Sanchez et al. (2011)). This negative feedback loop is strictly controlled by the circadian clock, with gating of ABA-mediated induction of *TOC1* (Legnaioli et al. (2009)). Accordingly, *toc1* mutants are more drought-tolerant than the wild type, whereas *TOC1* overexpressors are more drought-sensitive (Legnaioli et al. (2009)). Furthermore, the *ABAR* promoter contains two CCA1 binding sites, suggesting that CCA1/LHY could also regulate *ABAR* expression (Fig. 1.8) (Pokhilko

et al. (2013)).

The MYB96 transcription factor is also involved in gating of ABA signalling (Fig. 1.8) (Lee et al. (2016)). *MYB96* expression is regulated by the circadian clock and induced by ABA in a gated manner (Fig. 1.8) (Lee et al. (2016)). MYB96 then feeds back by inducing *TOC1* and enabling ABA-mediated induction of *TOC1* (Fig. 1.8) (Lee et al. (2016)). The relationship between transcription and signalling factors and oscillator components may enable very precise gating of stress responses (Lee et al. (2016)).

*PRR7* might also regulate WUE, as ABA upregulates 28% of *PRR7* targets and the *prp9 prr7 prr5* triple mutant has elevated ABA (Liu et al. (2013); Sanchez et al. (2011)). However, chromatin immunoprecipitation sequencing (ChIP-seq) analysis revealed that the three *PRRs* do not bind to promoters related to ABA biosynthesis, so their effect on ABA may be indirect (Grundy et al. (2015)). *GI* is another potential candidate, as *GI* and ABA interact to activate florigen genes and cause an early flowering drought escape response (Riboni et al. (2013)). *ELF3* may also be involved: wild type *Arabidopsis* has circadian rhythms of stomatal aperture under constant light conditions, whereas stomata of *elf3* mutants are constantly open and arrhythmic under the same conditions (Kinoshita et al. (2011)). In addition, *ELF3* negatively regulates stomatal opening in response to blue light signals (Kinoshita and Hayashi (2011); Chen et al. (2012)).

### 1.3.3 Circadian rhythms and abiotic stress

Responses to abiotic stress, such as cold, drought, nutrient availability and ROS, are often gated and regulated by the circadian clock (Sanchez et al. (2011); Greenham and McClung (2015); Grundy et al. (2015)). For example, the circadian clock gates transcription of several cold- and drought-responsive genes (Grundy et al. (2015)), and time of day strongly contributes to variations in transcript abundance (Wilkins et al. (2010); Greenham and McClung (2015)). In addition, altering the circadian clock affects abiotic stress responses. Both *LKP2-ox* and *prp5/prp7/prp9* triple mutant genotypes have increased drought tolerance (Nakamichi et al. (2009); Miyazaki et al. (2015)). Mutating *gi* affected both plant survival under water-limited conditions (Kim et al. (2013)) and the flowering drought escape response (Riboni et al. (2013)). Sensitivity to ROS was altered in *cca1*, *lhy*, *elf3*, *elf4*, *lux*, *prp5*, *prp7* and *prp9* mutants (Lai et al. (2012)). Therefore, circadian control might enable plants to fine-tune the balance between abiotic stress tolerance and productivity, and could be exploited to improve crop yield under

environmental stress conditions (Greenham and McClung (2015); Grundy et al. (2015)).

### **1.3.4 Involvement of circadian regulation in C4 and CAM photosynthesis**

Photosynthesis in C3 crops such as wheat, rice and potatoes is limited by both photorespiration and water loss. Indeed, RUBISCO has dual activity, catalysing either carboxylation or oxygenation reactions (Spreitzer and Salvucci (2002); Erb and Zarzycki (2018)). Although its carboxylase activity is crucial for carbon fixation, RUBISCO has low biochemical affinity for CO<sub>2</sub> and is a slow catalyst (Spreitzer and Salvucci (2002); Erb and Zarzycki (2018)). Its alternative oxygenase activity metabolises toxic 2-phosphoglycolate (2PG), which is then removed by photorespiration in an energy-demanding manner (Erb and Zarzycki (2018)). RUBISCO catalyses oxygenation especially under high temperature and/or low intracellular CO<sub>2</sub> conditions (Spreitzer and Salvucci (2002); Erb and Zarzycki (2018)), causing a decrease in carbon assimilation of up to 40% (Borland et al. (2014)).

Alternative photosynthetic pathways have evolved to overcome these limitations. In particular, C4 and CAM pathways concentrate CO<sub>2</sub> around RUBISCO to prevent oxygenation. C4 plants concentrate CO<sub>2</sub> using specialised bundle sheath cells and phosphoenolpyruvate carboxylase (PEPC), an additional carbon fixation enzyme (Murchie et al. (2009)). This ability to physically separate CO<sub>2</sub> fixation and the Calvin cycle improves photosynthetic efficiency of C4 plants under conditions of low CO<sub>2</sub> concentrations (Murchie et al. (2009)). In a similar fashion, CAM plants have evolved to temporally separate CO<sub>2</sub> fixation and the Calvin cycle, by shifting carbon dioxide uptake from day to night when temperatures are cooler and evapotranspiration rates smaller (Borland et al. (2014)). PEPC assimilates CO<sub>2</sub> into oxaloacetate that is stored as malate at night, and its activity is promoted by phosphorylation by PEPC kinase (PPCK) (Borland et al. (2014)). During the day, CO<sub>2</sub> is liberated then carboxylated by RUBISCO (Borland et al. (2014)). This different organisation of metabolic processes also enables CAM plants to maximise WUE (Sharma et al. (2017)).

Evidence suggests that circadian rhythms regulate C4 photosynthesis. In maize, Khan et al. (2010) report that 10% of all transcripts are rhythmic. This was further examined by Hayes et al. (2010) under field conditions for leaf (photosynthetic) and developing

ear (non-photosynthetic) maize tissues. Approximately 23% of leaf transcripts cycled, whereas few genes had rhythmic expression within the developing ear despite the presence of an intact circadian clock (Hayes et al. (2010)). In commercial sugarcane, the circadian clock is robust and controls both sense and anti-sense transcript abundance (Hotta et al. (2013)). In particular, transcripts associated with light energy harvesting and storage are abundant during the day, whereas those associated with nucleic acid and protein synthesis are dominant at night (Hotta et al. (2013)).

The circadian clock regulates CO<sub>2</sub> fixation in CAM plants, as well as the reversible phosphorylation of PEPC by PPCK (Borland et al. (2014)). Recently, Boxall et al. (2017) reported that transgenic *Kalanchoë fedtschenkoi* with reduced, arrhythmic *PPCK1* transcript abundance also had arrhythmic oscillations of several key circadian clock transcripts, including *TOC1* and *CCA1*. Therefore, circadian regulation of *PPCK1* not only optimises CO<sub>2</sub> fixation and production in *Kalanchoë fedtschenkoi*, but also improves the robustness of its circadian clock (Boxall et al. (2017)). In *Ananas comosus* (pineapple), Sharma et al. (2017) examined transcript abundance of transcription factors and coregulators, focusing on those that cycled in a tightly coupled manner in both non-photosynthetic and photosynthetic tissues. Interestingly, these were rich in homologs of Arabidopsis circadian clock genes (Sharma et al. (2017)). They found that *STOP1* in particular played an important role in regulating CAM photosynthesis in pineapple (Sharma et al. (2017)). von Caemmerer and Griffiths (2009) investigated the responsiveness of *Kalanchoe* stomata to different carbon dioxide concentrations, and found that circadian regulation of stomatal aperture was key to regulating the CAM cycle. Overall, these findings imply that the circadian clock is essential for high productivity resulting from CAM, and might represent an avenue for inserting CAM into C3 crops.

## **1.4 The SnRK1 energy signalling hub**

### **1.4.1 The sugar-sensing roles of T6P and KIN10/11**

Sugars are essential for plant growth and development (Gomez et al. (2010); Lastdrager et al. (2014)). Therefore, the ability to sense sugar abundance is key to plant survival (Lastdrager et al. (2014)), allowing it to coordinate its metabolic activities with carbohydrate availability. In Arabidopsis, the evolutionarily conserved energy sensor

SnRK1 was identified as one of the central regulators of the transcriptome (Fig. 1.9) (Baena-González et al. (2007)). SnRK1 is orthologous to mammalian AMP-activated kinase (AMPK) and yeast sucrose non-fermenting1 (SNF1) energy signalling kinases (Baena-González (2010); Ghillebert et al. (2011)). Its catalytic  $\alpha$ -subunit is composed of the sugar-sensing protein kinase KIN10 (known also as AKIN10/SnRK1.1) and KIN11 (Ghillebert et al. (2011)). Under low sugar conditions, SnRK1 regulates expression of 1021 genes (Fig. 1.9) (Baena-González et al. (2007); Lastdrager et al. (2014)), enabling the induction of both energy conservation and stress-induced processes (Ghillebert et al. (2011)). Targets include metabolic enzymes, such as sucrose phosphate synthase (Halford et al. (2003)), and transcription factors, such as S-group bZIP transcription factors (Baena-González (2010); Mair et al. (2015)). Activated targets include those involved in remobilisation of substitute energy sources, such as protein, lipid, starch and cell wall degradation, while repressed targets are involved in growth (Baena-González et al. (2007); Ghillebert et al. (2011)). KIN10 knockouts are lethal, indicating that SnRK1 function is indispensable (Baena-González et al. (2007)).

Trehalose-6-phosphate (T6P) represses SnRK1 activity and induces transcripts inhibited by SnRK1 (Fig. 1.9) (Zhang et al. (2009)). T6P and sucrose levels are positively correlated; thus, when sugar supplies are abundant, T6P accumulates and both represses transcripts involved in starvation responses and increases those involved in growth processes (Nunes et al. (2013)). T6P is synthesised from glucose-6-phosphate and uridine-diphosphate-glucose by T6P SYNTHASE1 (TPS1) (Lastdrager et al. (2014)). *TPS1* plays such a pivotal role in energy metabolism that *tps1* deletion mutants severely affect seedling development (Eastmond et al. (2002); Gómez et al. (2006); Gomez et al. (2010); Schluemann et al. (2012)).

Gomez et al. (2010) generated three weaker, non-lethal mutants via Targeted Induced Local Lesions in Genomes (TILLING), named *tps1-11*, *tps1-12* and *tps1-13*. This involved EMS chemical treatment followed by a screen using CEL1 endonucleases, gel electrophoresis and scanning (Colbert et al. (2001); Gomez et al. (2010)). Although these alleles enable embryo development, they have varying degrees of slow growth and delayed flowering, with *tps1-11* having the most altered growth phenotype and *tps1-13* the least (Gomez et al. (2010)).

Additional master glucose sensors and regulators include HEXOKINASE1 (HXK1) and TARGET OF RAPAMYCIN (TOR), which synchronise glucose signalling pathways with glucose-mediated development (Fig. 1.9) (Moore et al. (2003); Xiong and Sheen (2012);

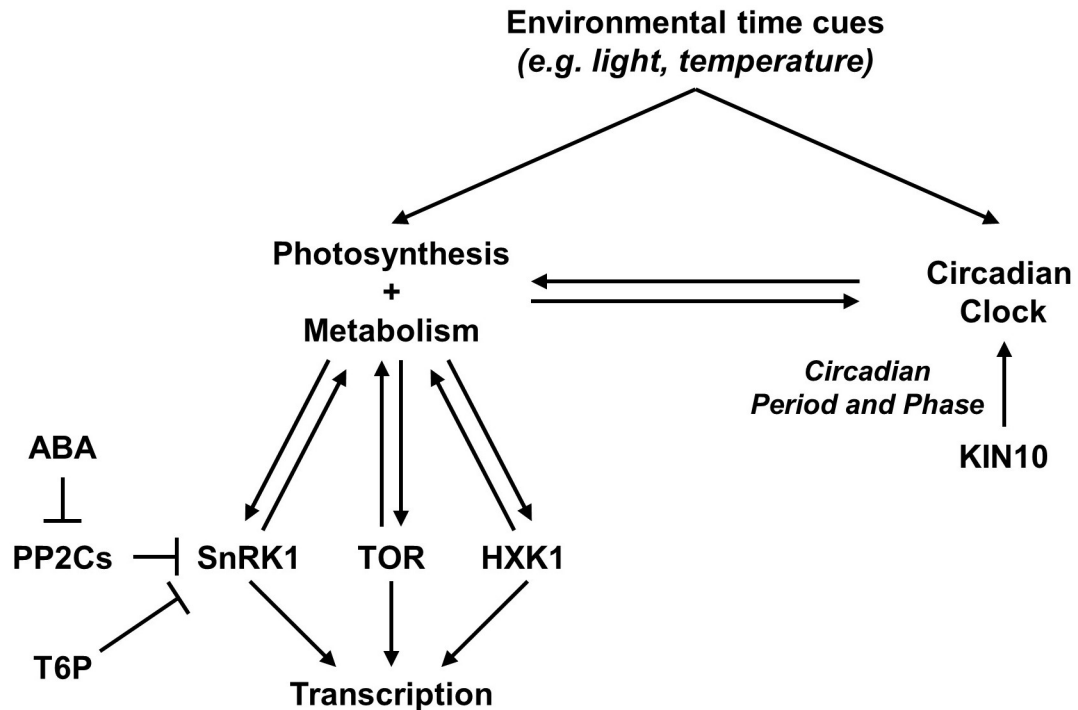


Figure 1.9: Links between environmental, metabolic and circadian clock regulation in Arabidopsis. Regulation is represented by arrows and suppression by bars. Roles of SnRK1/KIN10, TOR and HXK1 are further described in text, as well as regulation of SnRK1 by ABA, PP2Cs, and T6P. This figure was derived from the concept of Simon and Dodd (2017).

Sheen (2014)). HXK1 directly senses glucose abundance, and has independent glucose-sensing and -mediated metabolic functions (Moore et al. (2003); Sheen (2014)). In contrast to SnRK1, TOR senses high carbohydrate availability and is activated by glucose (Xiong and Sheen (2012); Sheen (2014)). SnRK1 and TOR activity have partially overlapping targets, but are mostly independent from HXK1 activity (Sheen (2014)).

#### 1.4.2 SnRK1/ T6P carbon signalling is linked to the circadian clock

Recent evidence suggests that the *KIN10/TPS1* signalling pathway contributes to circadian clock activity. Frank et al. (2018) demonstrated that bZIP63, KIN10 and TPS1 adjust the phase of the circadian clock in response to sucrose (Fig. 1.9). In addition, Shin et al. (2017) report that *KIN10* and *TIC* genetically interact to regulate the circadian clock under diel conditions (Fig. 1.9). However, although *KIN10* overexpression caused a peak delay of *G1* under diel conditions, transcript abundance of other circadian clock genes,

such as *CCA1*, *LHY*, *ELF4*, *PRR7* and *TOC1*, were unaltered (Shin et al. (2017)). These interactions between sugar-sensing pathways and the circadian clock might enable entrainment of the circadian clock by daily rhythms of carbohydrate availability (Sánchez-Villarreal et al. (2018); Frank et al. (2018)). Interestingly, this entrainment enables the circadian clock to detect sugar abundance (Haydon et al. (2013b); Seki et al. (2017)) and adjust the rate of nocturnal starch degradation accordingly (Seki et al. (2017)).

### **1.4.3 Interactions between sugar-sensing and ABA signalling pathways**

Glucose and ABA signalling pathways are connected, with both sharing signalling components such as GIN1-1/ABA2 (Cheng et al. (2002)). Interestingly, SnRK1 and ABA signalling pathways also appear to overlap and interact, with many transcripts induced by SnRK1 also being promoted by ABA (Rodrigues et al. (2013)). SnRK1 activity is inactivated by clade A type 2C protein phosphatases (PP2Cs), which in turn are repressed by ABA (Fig. 1.9) (Rodrigues et al. (2013)). Therefore, ABA indirectly promotes SnRK1 signalling through the PP2C hub (Rodrigues et al. (2013)). In addition, seedlings overexpressing *KIN10* are hypersensitive to ABA during germination and early development (Jossier et al. (2009)).

Altering T6P abundance slowed water loss and increased drought tolerance in rice transformed with *TPS*, tobacco transformed with *TPS1*, and potato transformed with yeast *TPS* (Lawlor and Paul (2014)). Trehalose (TRE) also affects ABA-mediated stomatal closure. TRE is a non-reducing disaccharide, and is produced from the breakdown of T6P (Lawlor and Paul (2014)). Arabidopsis *tre1* mutants with increased trehalose levels are drought sensitive and unable to close stomata in response to ABA (Van Houtte et al. (2013)). Overexpressors of *TRE1* display the opposite phenotype, with decreased trehalose abundance, guard cell hypersensitivity to ABA, and improved drought tolerance (Van Houtte et al. (2013)). In addition, altering TRE metabolism modifies stomatal development, density and conductance (Lawlor and Paul (2014)). Trehalose-related genes also have higher expression in guard cells than mesophyll cells (Van Houtte et al. (2013)). These observations may relate to T6P breakdown, or could be controlled by an independent TRE-producing process.

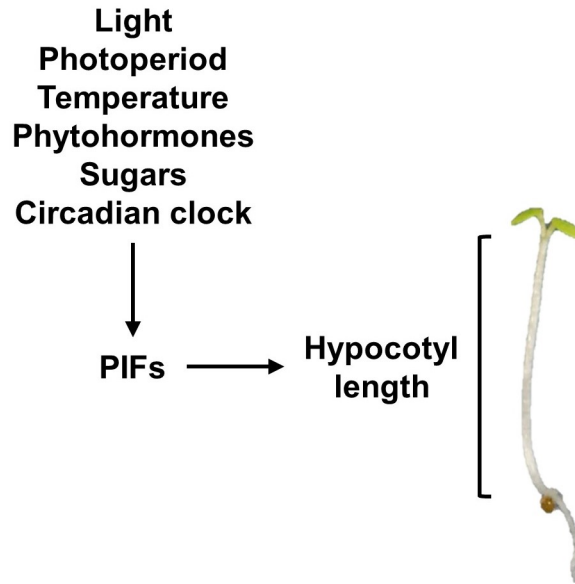


Figure 1.10: Several signalling pathways are integrated by PIFs to regulate hypocotyl elongation in Arabidopsis. Signalling pathways listed here are non-exhaustive. The hypocotyl is measured from the base of cotyledons to the top of the seedling root. Additional information is provided in text.

## 1.5 Hypocotyl elongation as a model system

Initial seedling growth occurs through expansion of cells within the hypocotyl. Hypocotyl elongation is tightly regulated by surrounding environmental conditions to optimise establishment of developing seedlings (Koini et al. (2009)). Therefore, several signalling pathways converge to control hypocotyl elongation, including light (Casal (2013); Hayes et al. (2014)), photoperiod (Niwa et al. (2009)), temperature (Koini et al. (2009); Mizuno et al. (2014)), phytohormones (Collett et al. (2000)), the circadian clock (Más et al. (2003a); Nusinow et al. (2011)) and sugars (Zhang et al. (2010); Liu et al. (2011); Stewart et al. (2011); Lilley et al. (2012); Zhang et al. (2015, 2016)) (Fig. 1.10). In Arabidopsis, these signals are integrated by PHYTOCHROME INTERACTING FACTORS (PIFs), a family of transcription factors that regulate seed germination and plant development by altering transcript abundance of over a thousand genes (Figs. 1.3, 1.10) (Leivar and Quail (2011)). Therefore, hypocotyl elongation in Arabidopsis is a useful experimental model to investigate regulation of plant development by signalling pathways.

Auxin and gibberellin (GA) are key phytohormones that regulate plant growth, development and environmental responses, including hypocotyl elongation (Jensen et al.



(1998); Cowling and Harberd (1999); Richards et al. (2001); Ogawa et al. (2003)). Auxin is mainly present in the indole-3-acetic acid (IAA) form (Sairanen et al. (2012)), and its function depends on its regulated transport via influx and efflux carriers (Jensen et al. (1998)). GA controls hypocotyl elongation by altering both the extent and rate of cell elongation (Cowling and Harberd (1999)). Evidence suggests that auxin and GA biosynthesis and ability to regulate growth are dependent on sucrose reserves (Sairanen et al. (2012); Paparelli et al. (2013)). In contrast, ABA suppresses hypocotyl elongation, possibly through deactivation of an H<sup>+</sup>-ATPase located in the plasma membrane (Gendreau et al. (1997); Gray et al. (1998); Hayashi et al. (2014)).

The addition of exogenous sucrose increases hypocotyl length (Fig. 1.10) (Kurata and Yamamoto (1998); Zhang et al. (2010); Liu et al. (2011); Stewart et al. (2011); Lilley et al. (2012); Zhang et al. (2015, 2016)). Different, light-dependent mechanisms are thought to underlie sucrose-induced hypocotyl elongation. Under constant darkness, as experienced by seedlings germinating in soil, sucrose-induced hypocotyl elongation is caused by brassinosteroid (BR) and GA signalling (Zhang et al. (2010, 2015)). TOR also regulates hypocotyl elongation in response to sucrose under constant darkness (Zhang et al. (2016)). However, under diel conditions, sucrose-induced hypocotyl elongation seems to be controlled by PIF-mediated auxin signalling (Stewart et al. (2011); Lilley et al. (2012)). Auxin signals are also implicated in developmental responses to glucose, and are integrated by the HXK1 glucose sensor signalling hub (Moore et al. (2003)).

Hypocotyl elongation is affected by photoperiod length and the circadian clock (Fig. 1.10) (Más et al. (2003a); Nozue et al. (2007); Niwa et al. (2009); Nusinow et al. (2011)). For example, overexpressing *CCA1* produces longer hypocotyls (Wang and Tobin (1998); Green et al. (2002); Dodd et al. (2005)) whereas overexpressing *TOC1* causes a decrease in hypocotyl length (Más et al. (2003a); Murakami et al. (2004)). In addition, a greater magnitude of hypocotyl elongation occurs under short photoperiods compared to long days, and this is regulated by the circadian clock (Niwa et al. (2009)).

## 1.6 Aims

I first focused on the importance of the circadian clock in determining whole plant WUE under diel conditions (Chapter 3). I then produced transgenic *Arabidopsis* with arrhythmic guard cell circadian clocks (Chapter 4) and investigated whether the guard

cell circadian clock modulates aspects of whole plant physiology, particularly those related to stomatal movement and water use (Chapter 5). I explored whether circadian regulation of stomatal opening might also occur under natural conditions in a naturally-occurring population of *A. halleri* subsp. *gemmifera* (Chapter 6). Finally, I examined the role of SnRK1 in regulating sucrose-induced hypocotyl elongation, as well as the signalling pathways underlying this process (Chapter 7).



# Chapter 2

## Materials and methods

### 2.1 Materials

#### 2.1.1 Chemical reagents

All common chemicals were purchased from Sigma-Aldrich, Fisher Scientific, or Melford. Manufacturers for specific chemicals are specified below.

<b>Manufacturer</b>	<b>Chemical</b>
Sigma-Aldrich	abscisic acid
Sigma-Aldrich	acetosyringone
Sigma-Aldrich	carbenicillin
Sigma-Aldrich	gibberellic acid (GA <sub>3</sub> form)
Melford	kanamycin
Melford	luciferin
Nippon Genetics	Midori Green Advance DNA Stain
Duchefa Biochemie	Murashige and Skoog basal salt nutrient mix
Chem Service	<i>N</i> -1-naphthylphthalamic acid
Duchefa Biochemie	paclobutrazol
Sigma-Aldrich	phosphinothricin
Melford	rifampicin

<b>Continuation of Table 2.1</b>	
<b>Manufacturer</b>	<b>Chemical</b>
De Sangosse	Silwet L-77
Sigma-Aldrich	tetracycline

Table 2.1: Manufacturers of specific chemicals.

### **2.1.2 Enzymes and commercially prepared kits**

Enzymes were purchased from Thermo Scientific or New England Biolabs. The following commercially prepared kits were used in this thesis:

- CloneJET PCR cloning kit (Thermo Scientific)
- High Capacity cDNA Reverse Transcription Kit with RNase inhibitor (Thermo Scientific)
- Macherey-Nagel NucleoSpin RNA extraction kit (Fisher Scientific)
- Macherey-Nagel Nucleospin gel and PCR clean-up kit (Fisher Scientific)
- Macherey-Nagel Nucleospin Plasmid kit (Fisher Scientific)
- RNeasy UCP Micro Kit (Qiagen)

### **2.1.3 Plasticware**

All plasticware was purchased from Greiner Bio-One or Sarstedt unless specified.

## 2.1.4 Machinery

Type	Manufacturer	Specification
Centrifuge	Starlabs	Microcentrifuge
Centrifuge	Eppendorf	MiniSpin Plus
Centrifuge	Eppendorf	Centrifuge 5415R
Centrifuge	Labnet	Mini Plate Spinner MPS1000
Centrifuge	Beckman Coulter	Allegra X-30R
Centrifuge	Beckman Coulter	Avanti J-30I
Dental Paste Distributor	Coltene	DS74 1:1/2:1
Digital camera	Nikon	D50
Electrophoresis	BioRad	Power Pac and (Wide) Mini-Sub Cell GT tank(s)
Electroporator	BioRad	MicroPulser
Gel imaging camera	Vilber Lourmat	Fusion Pulse
Incubator	Stuart	SI19
Incubator shaker	Stuart	Orbital Incubator SI500
Microscope	Zeiss	Epifluorescence HAL100 with Hamamatsu camera
Microscope	Leica	Confocal DMI6000 CS with TCS SP5 system
Microscope	Olympus	Upright Olympus BX50 with camera
Infra-red Gas Analyser	Walz	GFS-3000
Nanodrop	Thermo Scientific	ND-1000
Photon counting camera	Photek	HRPCS (high resolution photon counting system) 218 with DB2 dark box stage
Pipette	Gilson	Pipetman 0.2 µl–2 µl
Pipette	Gilson	Pipetman 2 µl–20 µl
Pipette	Gilson	Pipetman 20 µl–200 µl
Pipette	Gilson	Pipetman 100 µl–1000 µl
Pipette	Gilson	Pipetman 1000 µl–5000 µl
Pipette	Gilson	Electronic, adjustable volume Pipetman 200 µl

<b>Continuation of Table 2.2</b>		
<b>Type</b>	<b>Manufacturer</b>	<b>Specification</b>
Spectrophotometer	WPA	Biowave II
Temperature Bath	Clifton	Unstirred Bath
Temperature Block	VWR	Digital Heatblock
Thermal Cycler	Eppendorf	Mastercycler nexus gradient
Thermal Cycler	Agilent	Stratagene Mx3005P
Tissue Lyser	Qiagen	TissueLyser II
Upright drill press	Silverline	350W Drill Press
Vortex	Fisher Scientific	FB15013 TopMix

Table 2.2: Tools and machinery used in this thesis.

### **2.1.5 Software**

The following software was used in this thesis:

- Random numbers for randomised experimental designs were obtained using Random Sequence Generator (RANDOM.ORG, available from [www.random.org/](http://www.random.org/)).
- Hypocotyl elongation measurements, rosette leaf surface area measurements, and stomata and pavement cell counts were obtained using ImageJ 2 (Schindelin et al. (2015)) and FIJI (Schindelin et al. (2012)), which are both available from [www.imagej.net/Downloads](http://www.imagej.net/Downloads).
- Imaging was performed using Volocity (Perkin Elmer) for epifluorescence microscopy, LAS AF (Leica) for confocal microscopy, Motic Images Plus 2.0 (Motic) for stomatal bioassays, and Evolution-Capt (Vilber Lourmat) for agarose gel imaging.
- Luciferase bioluminescence set up and measurements were obtained using IMAGE32 (Photek).
- qRT-PCR set up and measurements were obtained using MxPro 4.10 (Agilent).

- Circadian time course data were analysed using BioDare 2, a platform for analysis of circadian datasets (Zielinski et al. (2014), available from [www.biodare2.ed.ac.uk](http://www.biodare2.ed.ac.uk)).
- Primer design was performed using TAIR BLAST 2.2.8 (TAIR, available from [www.arabidopsis.org/Blast/index.jsp](http://www.arabidopsis.org/Blast/index.jsp)), Tm Calculator (ThermoFisher, available from [www.thermofisher.com/uk/en/home/brands/thermo-scientific/molecular-biology/molecular-biology-learning-center/molecular-biology-resource-library/thermo-scientific-web-tools/tm-calculator.html](http://www.thermofisher.com/uk/en/home/brands/thermo-scientific/molecular-biology/molecular-biology-learning-center/molecular-biology-resource-library/thermo-scientific-web-tools/tm-calculator.html)), Multiple Primer Analyzer (ThermoFisher, available from [www.thermofisher.com/uk/en/home/brands/thermo-scientific/molecular-biology/molecular-biology-learning-center/molecular-biology-resource-library/thermo-scientific-web-tools/multiple-primer-analyzer.html](http://www.thermofisher.com/uk/en/home/brands/thermo-scientific/molecular-biology/molecular-biology-learning-center/molecular-biology-resource-library/thermo-scientific-web-tools/multiple-primer-analyzer.html)), and SALK T-DNA Primer Design (Salk Institute Genomic Analysis Laboratory, available from [signal.salk.edu/tdnaprimers.2.html](http://signal.salk.edu/tdnaprimers.2.html)).
- Sequence alignment was performed using Clustal Omega (Sievers et al. (2011), available from [www.ebi.ac.uk/Tools/msa/clustalo/](http://www.ebi.ac.uk/Tools/msa/clustalo/)).
- Statistical tests were performed using SPSS Statistics 23 (IBM) and Excel (Microsoft).
- Figures were generated using SigmaPlot 13.0 (Systat Software), SnapGene Viewer (GSL Biotech LLC) and Powerpoint (Microsoft).

## 2.2 Common solutions

Common solutions used in this thesis are listed below, with final concentrations of each reagent. All solutions and media were prepared in deionised water (dH<sub>2</sub>O) and autoclaved.

- MS: 0.5x Murashige and Skoog, 0.8% (w/v) agar
- LB broth: 1% (w/v) tryptone, 1% (w/v) NaCl, 0.5% (w/v) yeast extract
- LB agar: 1.5% (w/v) agar, 1% (w/v) tryptone, 1% (w/v) NaCl, 0.5% (w/v) yeast extract



- YEB media: 0.1% (w/v) yeast extract, 0.5% (w/v) beef extract, 0.5% (w/v) sucrose, 0.1% (w/v) peptone, 2 mM MgSO<sub>4</sub>
- YEBS media: 0.1% (w/v) yeast extract, 0.5% (w/v) beef extract, 0.5% (w/v) sucrose, 0.5% (w/v) bacto-peptone, 0.05% (w/v) MgSO<sub>4</sub>
- SOC recovery media: 2% (w/v) bactotryptone, 0.5% (w/v) yeast extract, 0.36% (w/v) glucose, 0.12% (w/v) MgSO<sub>4</sub>, 0.06% (w/v) NaCl, 0.02% (w/v) KCl, 0.01% (w/v) MgCl<sub>2</sub>
- 1x TAE buffer: 40 mM Tris acetate, 1 mM EDTA, pH 8.2-8.4
- Agarose gel: 1% (w/v) agarose, 1x TAE buffer, 0.6 µl L<sup>-1</sup> Midori Green

Antibiotics, herbicides, and plant growth regulators were filter-sterilised (0.22 µm syringe filters from Millex Millipore, 10 ml syringes from BD Plastipak) and added to media after autoclaving, with the following final concentrations and carriers:

- abscisic acid: 0.1 µM–10 µM (carrier: ethanol)
- carbenicillin: 10 mg L<sup>-1</sup> (carrier: dH<sub>2</sub>O)
- gibberellic acid: 100 µM (carrier: methanol)
- kanamycin: 50 mg L<sup>-1</sup> (carrier: dH<sub>2</sub>O)
- *N*-1-naphthylphthalamic acid: 1 µM–100 µM (carrier: DMSO)
- paclobutrazol: 20 µM (carrier: methanol)
- phosphinothricin: 10 mg L<sup>-1</sup> in media or 100 mg L<sup>-1</sup> in spray (carrier: dH<sub>2</sub>O)
- rifampicin: 50 mg L<sup>-1</sup> (carrier: DMSO)
- tetracycline: 5 mg L<sup>-1</sup> (carrier: ethanol)

## 2.3 Plant materials and growth conditions

### 2.3.1 Plant materials and seed treatments

Seeds from a variety of *Arabidopsis* genotypes were used in this thesis (Table 2.3). All lines were genotyped using PCR (described in section 2.5.4.1) or sequencing method-

ologies (described in section 2.5.7.8) by myself or another member of the Dodd laboratory. Primers used for genotyping are provided in Table 2.6.

Before use, seeds were surface-sterilised (1 min in 70% (v/v) ethanol, 10 min in 20% (v/v) sodium hypochlorite, two washes with autoclaved dH<sub>2</sub>O) and re-suspended in top agar (0.1% (w/v) agar).

AGI code	Gene	Genotype	Reference
AT5G28770	<i>bZIP63</i>	<i>bzip63-1</i>	Mair et al. (2015)
AT2G46830	<i>CCA1</i>	<i>cca1-11</i>	Hall et al. (2003)
AT2G46830	<i>CCA1</i>	CCA1-ox	Wang and Tobin (1998)
AT5G08330	<i>CHE</i>	<i>che-1</i> CCA1::LUC+	Pruneda-Paz et al. (2009)
AT5G08330	<i>CHE</i>	<i>che-2</i> CCA1::LUC+	Pruneda-Paz et al. (2009)
AT5G08330	<i>CHE</i>	CHE-ox CCA1::LUC+ 17	Pruneda-Paz et al. (2009)
AT5G08330	<i>CHE</i>	CHE-ox CCA1::LUC+ 6	Pruneda-Paz et al. (2009)
AT2G21660	<i>CCR2</i>	<i>grp7-1</i>	Streitner et al. (2008)
AT2G25930	<i>ELF3</i>	<i>elf3-1</i>	Zagotta et al. (1992)
AT2G40080	<i>ELF4</i>	<i>elf4-101</i>	Khanna et al. (2003)
AT1G68050	<i>FKF1</i>	<i>fkf1-2</i>	Imaizumi et al. (2003)
AT1G14920	<i>GAI</i>	<i>gai-1</i>	Koorneef et al. (1985)
AT1G14920, AT2G01570, AT1G66350, AT3G03450, AT5G17490	<i>GAI, RGA, RGL1, RGL2, RGL3</i>	<i>gai-t6 rga-t2 rgl1-1 rgl2-1 rgl3-4 (DELLA global)</i>	Koini et al. (2009)
AT1G22770	<i>GI</i>	<i>gi-11</i> CCA1:LUC	Ding et al. (2007b); Rédei (1962)
AT1G22770	<i>GI</i>	<i>gi-2</i>	Fowler et al. (1999)
AT4G29130	<i>HXK1</i>	<i>gin2-1</i>	Moore et al. (2003)
AT3G01090	<i>KIN10</i>	<i>akin10</i>	Mair et al. (2015)
AT3G01090	<i>KIN10</i>	<i>akin10-2</i>	Simon et al. (2018)
AT3G01090	<i>KIN10</i>	KIN10-ox 5.7	Baena-González et al. (2007)
AT3G01090	<i>KIN10</i>	KIN10-ox 6.5	Baena-González et al. (2007)
AT1G01060	<i>LHY</i>	LHY-ox	Schaffer et al. (1998)

Continuation of Table 2.3			
AGI code	Gene	Genotype	Reference
AT2G18915	<i>LKP2</i>	<i>lkp2-1</i>	Imaizumi et al. (2005)
AT3G46640	<i>LUX</i>	<i>lux-1</i>	Hazen et al. (2005)
Bacterial	<i>otsA</i>	<i>otsA-ox</i>	Schluepmann et al. (2003)
AT5G60100	<i>PRR3</i>	<i>prp3-1</i>	Alonso et al. (2003)
AT5G24470	<i>PRR5</i>	<i>prp5-3 TOC1::LUC</i>	Michael et al. (2003)
AT5G02810	<i>PRR7</i>	<i>prp7-11</i>	Yamamoto et al. (2003)
AT2G46790	<i>PRR9</i>	<i>prp9-1</i>	Eriksson et al. (2003)
AT4G17870, AT5G46790, AT2G26040, AT2G38310	<i>PYR1, PYL1, PYL2, PYL4</i>	<i>pyr1-1 pyl1-1 pyl2-1 pyl4-1 (ABA quad)</i>	Park et al. (2009)
AT5G02840	<i>RVE4</i>	<i>rve4-1</i>	Alonso et al. (2003)
AT3G09600	<i>RVE8</i>	<i>rve8-1</i>	Rawat et al. (2011)
AT2G31870	<i>TEJ</i>	<i>tej-1</i>	Panda et al. (2002)
AT3G22380	<i>TIC</i>	<i>tic-1</i>	Hall et al. (2003)
AT3G22380	<i>TIC</i>	<i>tic-2</i>	Ding et al. (2007b)
AT5G61380	<i>TOC1</i>	<i>toc1-1 CAB2::LUC</i>	Strayer et al. (2000)
AT5G61380	<i>TOC1</i>	<i>toc1-2 CAB2::LUC</i>	Strayer et al. (2000)
AT5G61380	<i>TOC1</i>	<i>toc1-21 CAB2::LUC</i>	Ding et al. (2007a)
AT5G61380	<i>TOC1</i>	<i>toc1-101</i>	Kikis et al. (2005)
AT5G61380	<i>TOC1</i>	<i>TOC1-ox</i>	Más et al. (2003)
AT1G78580	<i>TPS1</i>	<i>tps1-11</i>	Gomez et al. (2010)
AT1G78580	<i>TPS1</i>	<i>tps1-12</i>	Gomez et al. (2010)
AT1G78580	<i>TPS1</i>	<i>tps1-13</i>	Gomez et al. (2010)
AT3G04910	<i>WNK1</i>	<i>wnk1</i>	Alonso et al. (2003)
AT5G57360	<i>ZTL</i>	<i>ztl-1 CAB2::LUC</i>	Somers et al. (2000)

Table 2.3: Arabidopsis genotypes used in this thesis.

### **2.3.2 Experimental plant growth conditions**

Surface-sterilised seeds suspended in top agar (0.1% (w/v) agar) were transferred individually to Petri dishes containing MS, or MS supplemented with 87.6 mM sucrose, 87.6 mM sorbitol, herbicides and/or plant growth regulators according to experimental specification. Petri dishes were sealed with micropore tape (VWR), stratified in the dark at 4 °C for 2-3 days, and moved to MLR-352 growth chambers (Panasonic). Seedlings in Petri dishes were grown at a temperature of 19 °C and photon flux density of 120  $\mu\text{mol m}^{-2} \text{s}^{-1}$  from lateral lighting. Photoperiod was specific to each experiment.

Alternatively, surface-sterilised seeds suspended in top agar were directly stratified in the dark at 4 °C for 2-3 days. They were then transferred individually to moist compost mix, which consisted of a 3:1 ratio of coarsely sieved Levington Advance F2 seed and modular compost (Everris) and horticultural silver sand (Melcourt). Thiacloprid insecticide granules (Exemptor, Everris) were added at a concentration of 0.4 g L<sup>-1</sup>. Compost mix was added to individual plant inserts, which were arranged within trays. Unless specified otherwise, inserts were 5 cm (width) by 5 cm (length) by 5 cm (height), and placed in a 6x4 arrangement within a tray. For all experiments on compost mix, genotypes were mixed in a randomised experimental design, in which each plant was randomly associated with an insert number. Plants were kept under well-watered conditions by watering inserts from below every Tuesday and Friday with 500 ml of dH<sub>2</sub>O, except when performing drought assays. Plants on compost mix were grown in custom climatic chambers (Reftech) at 70% humidity, 20 °C, and a photon flux density of 100  $\mu\text{mol m}^{-2} \text{s}^{-1}$  from overhead lighting. Photoperiod was specific to each experiment.

Photon flux densities were measured regularly using a Spectrosense2 quantum sensor (Skye), and humidity and temperature with a HygroPalm (Rotronic).

### **2.3.3 Seed bulking plant growth conditions**

Seeds were sown on Petri dishes and grown under a 12 h photoperiod. After 2-3 weeks, seedlings were transferred to compost mix and grown in experimental glasshouses under a 16 h photoperiod (supplemented with LED lighting depending on the natural

photoperiod) at 20 °C. ARACONs (Arasystem) were used to isolate individual plants, thereby avoiding seed contamination. These consist of aracon bases, which are inverted cones placed on plants after inflorescence emergence, and aracon tubes, which guide falling seeds into the aracon base and isolate individual plants.

When plants began to senesce, water was withheld to allow plants to dry. Seeds were collected from individual plants using paper negative bags (Kenro), dried for at least 24 h at 37 °C, and separated from plant debris using a 150 mm mesh sieve (Wilko). Seeds were stored at 4 °C in 1.5 ml Eppendorf tubes.

## **2.4 Bacterial strains**

Electrocompetent *Escherichia coli* (*E. coli*) cells of the DH5 $\alpha$  strain and electrocompetent *Agrobacterium tumefaciens* (*Agrobacterium*) cells of the GV3101 strain were used.

## **2.5 Molecular methods**

### **2.5.1 DNA extractions**

DNA extractions were performed as described in Edwards et al. (1991), and concentrations determined using a nanodrop.

### **2.5.2 RNA extractions**

Sampling was performed under sterile conditions using RNaseZAP (Invitrogen). Samples were flash frozen in liquid nitrogen and conserved at –80 °C. Samples were homogenised using stainless steel beads (5 mm diameter, Qiagen) and a Tissue Lyser II. RNA was extracted from samples using the Macherey-Nagel NucleoSpin RNA extraction kit, according to manufacturer's instructions. RNA concentrations were measured using a nanodrop. RNA samples with a 260/280 ratio (ratio of absorbance at 260 nm and

280 nm) around 2.0 and a 260/230 ratio (ratio of absorbance at 260 nm and 230 nm) between 2.0 and 2.2 were considered pure, and could be used in subsequent reactions.

### **2.5.3 cDNA biosynthesis**

1.5 µg RNA or, in the case of low RNA yields (Chapter 7, Fig. 7.10), 0.5 µg RNA was added to the cDNA biosynthesis reaction. cDNA was generated using the High Capacity cDNA Reverse Transcription Kit with RNase inhibitor, according to the manufacturer's instructions.

### **2.5.4 Polymerase Chain Reaction (PCR)**

#### **2.5.4.1 DreamTaq PCR**

For each reaction, the following reagents were added: 2.5 µl template DNA, 1x DreamTaq Green Buffer (Thermo Scientific), 0.2 µM of each dNTP, 0.2 µM forward primer, 0.2 µM reverse primer, 1.25 U DreamTaq DNA Polymerase (Thermo Scientific), and nuclease-free water up to 50 µl. For negative controls, the equivalent volume of template DNA was replaced by nuclease-free water. Samples were briefly centrifuged to collect reagents at the bottom of the tube, then run using a Mastercycler nexus gradient. The cycling conditions were as follows: initial denaturation of 1 min at 94 °C, followed by 35 cycles of 30 sec at 94 °C (denaturing), 30 sec at 31 °C - 65 °C (annealing), and 2 min at 72 °C (extension), then a final extension of 7 min at 72 °C.

#### **2.5.4.2 Phusion PCR**

For reactions in which a correct amplified DNA sequence was required, Phusion DNA polymerase was used instead of DreamTaq DNA polymerase, as Phusion possesses 3' to 5' exonuclease (proofreading) activity in addition to its 5' to 3' polymerase activity. For each reaction, the following reagents were added: 2.5 µl template DNA, 1x Phusion HF Buffer (New England Biolabs), 0.2 µM of each dNTP, 0.5 µM forward primer, 0.5 µM reverse primer, 3% (v/v) DMSO, 1.0 U Phusion DNA Polymerase (New England Biolabs), and nuclease-free water up to 50 µl. For negative controls, the equivalent volume of

template DNA was replaced by nuclease-free water. Samples were briefly centrifuged, then run using a Mastercycler nexus gradient. The cycling conditions were as follows: initial denaturation of 30 sec at 98 °C, followed by 35 cycles of 10 sec at 98 °C (denaturing), 30 sec at 35 °C - 65 °C (annealing), and 1 min at 72 °C (extension), then a final extension of 5 min at 72 °C.

### **2.5.4.3 Colony PCR**

#### ***Colony PCR for E. coli***

For each reaction, the following reagents were added: 1x DreamTaq Green buffer, 0.1 µM of each dNTP, 0.2 µM of forward primer, 0.2 µM of reverse primer, 0.5 U of DreamTaq DNA polymerase and nuclease-free water up to 10 µl. Individual colonies were picked off using sterile pipette tips, swirled in the appropriate PCR tube, and streaked onto a Petri dish (LB agar, appropriate selection) to maintain the culture. Samples were briefly centrifuged, then run using a Mastercycler nexus gradient. The cycling conditions were as follows: initial denaturation of 3 min at 94 °C, followed by 35 cycles of 30 sec at 94 °C (denaturing), 2 min at 55 °C (annealing), and 1 min at 72 °C (extension), then a final extension of 10 min at 72 °C. Streaked Petri dishes were incubated at 37 °C overnight.

#### ***Colony PCR for Agrobacterium***

Colony PCR was performed as for *E. coli*, with the following modifications: picked individual colonies were first swirled in 10 µl aliquots of RNase-free dH<sub>2</sub>O, then 1 µl of this *Agrobacterium*/dH<sub>2</sub>O solution was added to 10 µl master mix. To maintain the culture, each colony was streaked onto a Petri dish (LB agar, appropriate selection), and incubated at 28 °C for 2 days.

### **2.5.4.4 RT-PCR**

Reactions were performed as for DreamTaq PCR (section 2.5.4.1), with the following modification: 2.5 µl template DNA was replaced with 2 µl cDNA.

#### 2.5.4.5 qRT-PCR

##### ***qRT-PCR using SYBR Green***

For each reaction, the following reagents were added: 5 µl cDNA, 1x Brilliant III Ultra-Fast SYBR Green QPCR master mix (Agilent), 0.5 µM forward primer, 0.5 µM reverse primer, 0.03 µM ROX reference dye (Agilent) and nuclease-free water up to 20 µl. Reactions were performed using non-skirted, 96-well plates (Agilent) closed with optical cap strips (Agilent) in a Mx3005 qPCR thermal cycler. The cycling conditions were as follows: initial activation of 3 min at 95 °C, followed by 40 cycles of 5 sec at 95 °C (denaturing) and 20 sec at 60 °C (annealing/extension). Two technical repeats were performed per reaction, and three biological repeats per experiment.

##### ***qRT-PCR using EvaGreen***

From April 2017, EvaGreen was used instead of SYBR Green. For each reaction, the following reagents were added: 5 µl cDNA, 1x HOT FIREPol EvaGreen qPCR Mix Plus (Solis Biodyne), 250 nM forward primer, 250 nM reverse primer and nuclease-free water up to 20 µl. For negative controls, the equivalent volume of template DNA was replaced by nuclease-free water. Reactions were performed using non-skirted, 96-well plates closed with optical cap strips in a Mx3005 qPCR thermal cycler. The cycling conditions were as follows: initial activation of 12 min at 95 °C, followed by 40 cycles of 15 sec at 95 °C (denaturing), 20 sec at 60 °C (annealing), and 20 sec at 72 °C (extension). Two technical repeats were performed per reaction, and three biological repeats per experiment.

##### ***qRT-PCR analysis***

qRT-PCR data were analysed using the MxPro QPCR Software. *PP2AA3* was used as a reference gene, except for Fig. 4.10 (Chapter 4) where *TIP41*-like was used. Threshold fluorescence was set to 0.280 for each assay. Data were analysed using the comparative CT method, also known as the  $2^{-\Delta\Delta CT}$  method (Schmittgen and Livak (2008)), in Excel.



## 2.5.5 Primers

### 2.5.5.1 Primer design and validation

Primers were obtained from Sigma-Aldrich, and added to reactions at 10  $\mu$ M. TAIR BLAST 2.2.8, Tm Calculator, and Multiple Primer Analyzer software were used for primer design. Primers were designed with the following rules: the annealing section consisted of 20-25 base pairs, the GC ratio was close to 50%, a terminal T base and GC clumps were avoided, the annealing temperature was compatible with the used enzyme, the difference in Tm within a primer pair did not exceed 2  $^{\circ}$ C, self- and cross-dimers were avoided, and primer specificity to target region was examined.

Primers used for cloning had the following specification: each primer consisted of 6 random base pairs, followed by the enzyme restriction site sequence and 20-24 base pairs of the target sequence.

Primers used for qRT-PCR were designed to amplify short amplicons (80-100 base pairs) and tested in the following manner: an additional dissociation/melt cycle was added at the end of the qRT-PCR run (1 min at 95  $^{\circ}$ C, 30 sec at 55  $^{\circ}$ C, 30 sec at 95  $^{\circ}$ C) and four cDNA dilutions (1:10, 1:100, 1:1 000, 1:10 000) were tested. Standard curve and dissociation curves were examined: acceptable primers had a standard curve R<sup>2</sup> over 0.980 and dissociation curves of different cDNA dilutions had a single, overlapping peak.

### 2.5.5.2 Primer sequences

AGI code	Target	Primer Sequences (5'-3')
At1g22690	<i>GC1</i> promoter sequence with 5' KpnI and 3' Apal	F: ATCGACGGTACCGAGTAAAGATTTCAGT AACCCGA R: AACTTAGGGCCCGTGATTTTGAAGTAG TGTGTGA
At1g22690	<i>GC1</i> promoter sequence with 5' PstI and 3' BamHI	F: ATCGACCTGCAGGAGTAAAGATTTCAGT AACCCGA R: AACTTAGGATCCGTGATTTTGAAGTAGT GTGTGA

**Continuation of Table 2.4**

AGI code	Target	Primer Sequences (5'-3')
At1g08810	<i>MYB60</i> promoter sequence with 5' KpnI and 3' ApaI	F: AATTAAGGTACCCACAAGGACACAAGG ACATA R: AATATTGGGCCCTCTTCTCTAGATCT CTCTGAG
At1g08810	<i>MYB60</i> promoter sequence with 5' PstI and 3' BamHI	F: AATTAAGGTACCCACAAGGACACAAGG ACATA R: AATATTGGATCCCTCTTCTCTAGATCTC TCTGAG
At2g46830	<i>CCA1</i> coding sequence with 5' XhoI and 3' XmaI	F: ATCGACCTCGAGATGGAGACAAATTCG TCTGG R: GTCAGACCCGGGAAAATAGAGTCTCAT GTGGAAGC
At5g61380	<i>TOC1</i> coding sequence with 5' XhoI and 3' XmaI	F: ATCGACCTCGAGATGGATTGAACGGT GAGTGTA R: AGGAAGCCCGGGTCAAGTTCCCAAAGC ATCATC
	<i>GFP</i> coding sequence with 5' XhoI and 3' XmaI	F: ATCAGACTCGAGATGAGTAAAGGAGAA GAACTTTTC R: ATCGAGCCCGGGTATTGTATAGTTCA TCCATGC
	<i>nos</i> terminator sequence with 5' SpeI and 3' NotI	F: ACTAGTGAATTTCCCGATCGTTC  R: GCGGCCGCTCTAGTAACATAGATG

Table 2.4: Primers used for cloning.

Location	Directionality	Sequence (5'-3')
510 bp downstream of 5' end of <i>GC1</i> promoter sequence	Forward	AAACTTTGGACGTGTAGGACAAAC
245 bp upstream of 3' end of <i>GC1</i> promoter sequence	Reverse	TTTCGGAGGATGCATGGAAG
128 bp upstream of 3' end of <i>GC1</i> promoter sequence	Forward	TTTATGTTTGGCTCCAGCGATG
411 bp downstream of 5' end of <i>MYB60</i> promoter sequence	Forward	CCCTTTCAAATTCACATCCTTCAC
167 bp upstream of 3' end of <i>MYB60</i> promoter sequence	Reverse	TTGGATCTGCCAAGCTCACG
112 bp upstream of 3' end of <i>MYB60</i> promoter sequence	Forward	GTTCTCCCTCTTCTTTAAGTCAC
395 bp downstream of 5' end of <i>CCA1</i> coding sequence	Forward	AAAGTGTCGCATCCTGAGATGG
89 bp upstream of 3' end of <i>CCA1</i> coding sequence	Reverse	GGATTCTACTTTCTTTGGCTTCC
430 bp downstream of 5' end of <i>TOC1</i> coding sequence	Forward	CATGCTAGGACTTGCTGAGAAG
118 bp upstream of 3' end of <i>TOC1</i> coding sequence	Reverse	ATTCACGCCGTTTCATCTTCC
200 bp downstream of 5' end of <i>LUC</i> coding sequence	Reverse	ATAGCTTCTGCCAACCGA
62 bp upstream of PCR product in pJET 2.1	Forward	CGACTCACTATAGGGAGAGCGGC
57 bp downstream of PCR product in pJET 2.1	Reverse	AAGAACATCGATTTTCCATGGCAG
60 bp upstream of M13F in pGreenII0229	Forward	CTCTTCGCTATTACGCCA

Table 2.5: Primers used for sequencing and verifying cloned plasmids.

Genotype	Genotyping Method	Sequences (5'-3')
T-DNA	T-DNA	LBb1 (LB): GCGTGGACCGCTTGCTGCAACT
T-DNA	T-DNA	LBb1.3 (LB): ATTTTGCCGATTTTCGGAAC
<i>bzip63-1</i>	T-DNA	LP: CCTCGAAAAATCCCTTTATGG RP: GAGTACCCTTTTCATGGCGAC
<i>cca1-11</i>	T-DNA	JL-202 (LB): CATTTTATAATAACGCTGCGGACAT CTAC LP: AAAGCTGAATCATCTCTTCAGCCACTAGT RP: AGTCAAATGTTACAGGAAGACTATGGACA
<i>elf3-1</i>	sequencing	F: CAGAGGATAAGCTGCGTGTAAG R: CTCATCGAGCAAGAGATCCG
<i>elf4-101</i>	T-DNA	LP: TTTGCTCCACGGATTATTC RP: TAGTTAGTGCCCAGGTTCCG
<i>gi-2</i>	sequencing	F: CATGCTTACTGATTTGGTGTAACC R: CCCATTACACCACTACACCTG
<i>gi-11</i>	PCR	F: GATCACCAACACAGCATGAAAG R: CAGTATGACACCAGCTCCATTAG
<i>gin2-1</i>	sequencing	F: TAAGGATATATTGGAGGTCCCTAC R: CGCCTTAGAACTTGGCTTAG
<i>grp7-1</i>	T-DNA	LP: CACCACCTCTTGAGGAGTAACC RP: TTTTCTGCCTCAATGGTTCAG
KIN10-ox	RT-PCR	F: TTGACAGAAACCACCTCATCGA R: GATAGTACGTCACAGTGCCATCATT
LHY-ox	RT-PCR	F: ACGGTCGGTACGGGATTTTCGCAT R: ACGCTTGATGAGAAGCTG
<i>lkp2-1</i>	T-DNA	LP: GGAGATCCATCTTTCCGAAAG RP: TGAAATGGAATCGAGCGAAG
<i>prp3-1</i>	T-DNA	LP: GGAGTCGGAGATGATTTCTCC RP: TCCTATTGCAAACTGTTGGG
<i>prp5-3</i>	T-DNA	LP: GACTAAAATATATGGCTGGCCG RP: TGCTTTAACCACCGTCACTTC
<i>prp7-11</i>	T-DNA	LP: AGCAAGGACATACACTTTGGC RP: TGAGAATTCGTCGTTCTTCAAC
<i>prp9-1</i>	T-DNA	LP: CCACCAATCAAATCCATTGTC

Continuation of Table 2.6

Genotype	Genotyping Method	Sequences (5'-3')
<i>prp9-1</i>	T-DNA	RP: AGTCTATGGGGGAGATTGTGG
<i>rve4-1</i>	T-DNA	LP: TGGAACATGTGCTAAAGTCCC RP: AATACCGGCGGAAACTTCTAC
<i>rve8-1</i>	T-DNA	LP: TTCAGCAAATCAGGAACACC RP: AGTTTGCTGCTGATTTCTGAG
<i>tic-1</i>	Sequencing	F: ATCGCCAGTGGCTGTACAAG R: TGATTACTGAACGGAACCTTGAC
<i>tic-2</i>	T-DNA	LP: GAAGAATAATTTCCGCCGAC RP: GTTGCTTTCTCTCGTCAGTGG
<i>tps1</i>	RT-PCR	F: GATCAGTGCTGGTGGTCTAGTCAGT R: CACATTA ACTCCAGCCCATCCT
<i>wnk1</i>	T-DNA	LP: AGACCTGACACGATCACATCC RP: GGATCAACTTCAACAACTCAGAG

Table 2.6: Primers used for genotyping. For genotyping of T-DNA lines, LB: left T-DNA border primer; LP: left genomic primer; RP: right genomic primer. For genotyping via sequencing, RT-PCR, or PCR, F: forward primer; R: reverse primer.

AGI code	Coding Sequence	Primer Sequences (5'-3')
At2g46830	<i>CCA1</i>	F: GCACTTTCCGCGAGTTCTTG R: TGACTCCTTTCTTACCCTGTTATTCTG
At5g54250	<i>CNGC4</i>	F: CATAGAGTGGTGGATGAAGAAG R: CATCTTTGCCGCTCATAG
At2g22330	<i>CYP79B3</i>	F: CCGTTGGCTACACGACAATAGA R: GAGATCGACTGGTTCAGAGTTC
At2g39700	<i>EXPA4</i>	F: CGGTAACCTATACAGCCAAG R: CAGGCTCCACA ACTCATA C
At2g40610	<i>EXPA8</i>	F: CCGAAGAGTACCATGTATGAAG R: GAGATCAGAACGAGGTTGAAG

Continuation of Table 2.7

AGI code	Coding Sequence	Primer Sequences (5'-3')
At1g20190	<i>EXPA11</i>	F: GGTTAGCCATGTCTCGTAAC R: GTGGTAATGGAGAAAGAGAGAG
At2g26250	<i>FDH</i>	F: TGTCACGAGCAAGATCAATAG R: CATTACAAGATGAGAGGGAACA
At1g22690	<i>GC1</i>	F: ACAGAGCCTGTGGAAGTTG R: ATACTGGCGTAGCAAGGACA
	<i>GFP</i>	F: CCATCTTCTTCAAGGACGAC R: CCTTAAGCTCGATCCTGTTG
At4g32280	<i>IAA29</i>	F: ATCACCATCATTGCCCGTAT R: ATTGCCACACCATCCATCT
At5g46540	<i>KAT1</i>	F: GACTTCCGACACTGCTCTAATG R: TTCCACTTTGGCTCTCTCTATC
At2g05100	<i>LHCB2.1</i>	F: GTCAAGTCTACTCCTCAAAGCA R: GGTTAGGTAGGACGGTGTATTC
At1g08810	<i>MYB60</i>	F: AGAACCGGACAAACAATTTTC R: CCTTTGCTATGACCCTCTTC
At1g13320	<i>PP2AA3</i>	F: TAACGTGGCCAAAATGATGC R: GTTCTCCACAACCGCTTGGT
At4g38850	<i>SAUR15</i>	F: GAATCATCGTCGACACCAAGAG R: TGTGAAACCGGCACCACATATC
At5g10180	<i>SULTR2;1</i>	F: CATGGTGTGAAGACAGTGAG R: GTCCGAGATGAGGAGTATTAAG
At4g34270	<i>TIP41-like</i>	F: GTGAAAACCTGTTGGAGAGAAGCAA R: TCAACTGGATACCCTTTTCGCA
At5g61380	<i>TOC1</i>	F: TCTTCGCAGAATCCCTGTGAT R: GCTGCACCTAGCTTCAAGCA
At4g28720	<i>YUCCA8</i>	F: ATCAACCCTAAGTTCAACGAGTG R: CTCCCGTAGCCACCACAAG
At1g04180	<i>YUCCA9</i>	F: GTCCCATTCGTTGTGGTTCG R: TTGCCACAGTGACGCTATGC

Table 2.7: Primers used for qRT-PCR.

## 2.5.6 Gel electrophoresis

PCR and restriction digest products were separated on agarose gels for 30 min at 90 V in either mini-sub cell GT tanks or wide mini-sub cell GT tanks with 1x TAE buffer. The 2-Log DNA ladder (New England Biolabs) was used as a fragment size reference (Sup. Fig. 9.4). Sample concentration was estimated from the ladder by finding the closest match in brightness between the sample band and a ladder band and using the following formula:

$$[\text{sample}] = \frac{\text{ladder band size (kb)}}{\text{sample band size (kb)}} \times \text{ladder band mass (ng)} \quad (2.1)$$

## 2.5.7 Cloning protocols

### 2.5.7.1 Restriction digest

#### *Restriction digest method from the Dodd laboratory*

This method was used for cloning of terminator and promoter sequences (Chapter 4). Restriction digests were performed with restriction enzymes (New England Biolabs) according to the recommendations of the manufacturer. For negative controls, the equivalent volume of template DNA was replaced by nuclease-free water.

#### *Restriction digest method from the Hetherington laboratory*

This method was used for cloning of coding sequences (Chapter 4). For each reaction, the following reagents were added: 1x CutSmart buffer (New England Biolabs), 20 U of each restriction enzyme (New England Biolabs), 1 µg of purified PCR product, and nuclease-free water up to 30 µl. Reactions were incubated at the appropriate, enzyme-dependent temperature for 3-4 h, then heat inactivated when possible.

### **2.5.7.2 PCR product clean-up**

#### ***PCR product clean-up using the Macherey-Nagel Nucleospin gel and PCR clean-up kit***

This method was used for cloning of terminator and promoter sequences (Chapter 4). PCR and restriction digest products were cleaned before use in subsequent reactions, meaning that DNA was purified via removal of reagents and enzymes. This was performed using the Macherey-Nagel Nucleospin gel and PCR clean-up kit according to manufacturer's instructions, with the following modifications: at step 5, the product was eluted in 30  $\mu$ l NE, incubated at room temperature for 5 min, incubated at 60 °C for 1 min, then centrifuged at 11,000 rpm for 1 min. Digested plasmids were cleaned using 33% NTI buffer.

#### ***PCR product clean-up using dialysis tubing***

This method was used for cloning of coding sequences (Chapter 4). A thick, 70 ml agarose gel with wide wells was cast. Gel electrophoresis was performed for PCR or restriction digest products for 20-25 min at 80 V. Desired bands were cut from the gel under blue light using a sterile scalpel, then placed at -20 °C for 1 h. Meanwhile, a piece of dialysis tubing (Sigma D9777) held between two clamps was soaked in 1x TAE buffer. One clamp was removed to add 300  $\mu$ l 1x TAE buffer and the frozen agarose gel fragment inside the dialysis tubing, then the membrane was securely clamped shut. This was run in the mini-sub cell GT electrophoresis tank at 70 V for 30 min. To detach DNA molecules from the sides of the dialysis tubing, electrodes were switched around and the membrane run for a further 5 min at 70 V. The solution was transferred from the dialysis tubing to a fresh Eppendorf tube, and cleaned using the Macherey-Nagel Nucleospin gel and PCR clean-up kit as described above.

#### ***PCR product clean-up by gel extraction***

This method was trialled for cloning of coding sequences, but resulted in lower concentrations of product (Chapter 4). Gel electrophoresis was performed as above using a thick, 70 ml agarose gel with wide wells. Desired bands were cut from the gel under blue light using a sterile scalpel, and incubated at 50 °C with NTI buffer. The solution



was vortexed every 2 min until complete dissolution of the gel slice, then cleaned using the Macherey-Nagel Nucleospin gel and PCR clean-up kit as described above.

### 2.5.7.3 Sub-cloning into the cloning vector pJET

This method was used for cloning of coding sequences (Chapter 4). Sub-cloning was performed using the CloneJET PCR cloning kit according to manufacturer's instructions, with the following modifications. The blunting reaction was set up on ice with the following reagents: 5  $\mu$ l 2x reaction buffer, 1  $\mu$ l DNA blunting enzyme, and 3  $\mu$ l purified PCR product. This was incubated at 70 °C for 5 min, then chilled on ice. To this reaction were added 0.5  $\mu$ l pJET1.2/blunt cloning vector (Chapter 4, Fig. 4.2) and 1  $\mu$ l T4 DNA Ligase. This was then incubated at room temperature for 30 min. *E. coli* transformation was performed as described elsewhere (section 2.5.7.5), using carbenicillin for selection.

### 2.5.7.4 Ligation

#### *Ligation method from the Dodd laboratory*

This method was used for cloning of terminator and promoter sequences (Chapter 4). For each reaction, the following reagents were added: 1x T4 DNA ligase buffer (New England Biolabs), 10 ng vector, a 6:1 molar ratio of insert:vector, 0.5  $\mu$ l T4 DNA ligase (New England Biolabs), and nuclease-free water up to 10  $\mu$ l. Insert and vector concentrations were estimated using the 2-Log DNA ladder as described previously (section 2.5.6). The mass of insert added to the reaction was calculated using the following formula:

$$\text{insert mass (ng)} = 6 \times \frac{\text{insert size (kb)}}{\text{vector size (kb)}} \times \text{vector mass (ng)} \quad (2.2)$$

The reaction was incubated at 4 °C overnight, then at 65 °C for 10 min. For the negative control, the volume of insert was replaced by nuclease-free water.

### ***Ligation method from the Hetherington laboratory***

This method was used for cloning of coding sequences (Chapter 4). Vectors and inserts digested using the Hetherington laboratory method (section 2.5.7.1) and cleaned using dialysis tubing (section 2.5.7.2) were ligated in this fashion. For each reaction, the following reagents were added: 1x T4 DNA ligase buffer, 1  $\mu$ l T4 DNA ligase, 3  $\mu$ l insert, 3  $\mu$ l vector, and nuclease-free water up to 10  $\mu$ l. The reaction was incubated at 16 °C overnight, then at 65 °C for 10 min. For the negative control, the volume of insert was replaced by nuclease-free water.

### **2.5.7.5 Bacterial transformation**

#### ***E. coli transformation via heat shock***

##### *E. coli transformation method from the Dodd laboratory*

This method was used for cloning of terminator and promoter sequences (Chapter 4). 1  $\mu$ l ligation reaction was added to a 50  $\mu$ l aliquot of *E. coli* cells. Cells were placed on ice for 30 min, incubated at 42 °C for exactly 35 sec, and immediately transferred onto ice. 1 ml of SOC recovery media was added. The mixture was then transferred to a 37 °C incubator shaker for 1 h. Aliquots of 50  $\mu$ l, 200  $\mu$ l and the rest were plated on Petri dishes (LB agar, appropriate selection), then incubated at 37 °C overnight.

##### *E. coli transformation method from the Hetherington laboratory*

This method was used for cloning of coding sequences (Chapter 4). *E. coli* were transformed as described above, with the following modifications: 5  $\mu$ l ligation reaction was added to a 50  $\mu$ l aliquot of *E. coli* cells; cells were incubated on ice for 30 min, heat-shocked at 42 °C for exactly 20 sec, and immediately transferred onto ice for 2 min; and 1 ml of SOC recovery media at 42 °C was added.

### ***Agrobacterium transformation via electroporation***

1  $\mu$ l plasmid and 1  $\mu$ l pSOUP replication helper plasmid (Chapter 4, Fig. 4.3) were added to a 50  $\mu$ l aliquot of *Agrobacterium* cells. This mixture was transferred into a chilled, sterile electroporation cuvette (Gene Pulser Cuvette, BioRad), and cells transformed by electroporation (pulse at 2.2 kV). 450  $\mu$ l SOC recovery media was added. Cells were incubated on ice for several minutes, then transferred to a 28 °C incubator shaker for 3 h. Aliquots of 50  $\mu$ l, 200  $\mu$ l and the rest were plated on Petri dishes (LB agar, appropriate selection), then incubated at 28 °C for two days. The negative control contained pSOUP only.

#### **2.5.7.6 Bacterial liquid cultures**

##### ***E. coli liquid cultures***

An individual *E. coli* colony was scraped off a Petri dish (LB agar, appropriate selection) and added to 10 ml of autoclaved LB broth with appropriate selection, then transferred to a 37 °C incubator shaker overnight.

##### ***Agrobacterium liquid cultures***

Glycerol stocks were streaked onto Petri dishes (LB agar, appropriate selection) and incubated at 28 °C for two days. An individual colony was scraped off and added to 6 ml of LB broth with appropriate selection, then transferred to a 28 °C incubator shaker for 2 days.

#### **2.5.7.7 Plasmid miniprep method**

Plasmids were extracted from bacterial liquid cultures using the Macherey-Nagel Nucleospin Plasmid kit, according to the manufacturer's instructions.

#### **2.5.7.8 Sequencing**

Premixed samples of template and primers were prepared according to the manufacturer's instructions, and sequenced by Eurofins. Sequences were checked and compared to expected sequences using Clustal Omega.

#### **2.5.7.9 Glycerol stocks**

200  $\mu$ l of 50% (v/v) glycerol was added to 800  $\mu$ l bacterial liquid culture. This was vortexed vigorously then stored at  $-80^{\circ}\text{C}$ .

### **2.5.8 Stable Arabidopsis transformation**

#### **2.5.8.1 Cultivation of Arabidopsis for floral dip**

Compost mix was mixed with water and packed into pots so as to create a domed surface. This was covered by muslin mesh (Yorkshire Purchasing Organisation) and abundantly sprayed with  $\text{dH}_2\text{O}$ . Wild type Col-0 seeds were sprinkled over the mesh. Plants were kept well-watered under a 16 h photoperiod. When inflorescences first started to appear, they were trimmed just above the first leaf. Plants were transformed by floral dip one week later.

#### **2.5.8.2 Floral dip**

Due to difficulties obtaining positive transformants, and as screening for positive transformants is time-consuming, three different floral dip methodologies- from the Dodd, Schumacher, and Franklin laboratories- were tested simultaneously for all plasmids (Chapter 4). All three methodologies yielded positive transformants (Chapter 4), which were then used in subsequent experiments (Chapter 5).

### ***Floral dip method from the Dodd laboratory***

An *Agrobacterium* liquid culture was inoculated and transferred to a 28 °C incubator shaker overnight. The starter culture was added to 400 ml of YEB media with appropriate selection, then transferred to a 28 °C incubator shaker for 2-3 days. The culture was centrifuged at 4,000 rpm for 15 min. The supernatant was discarded, and cells re-suspended in 1 L of 5% (w/v) sucrose with 500  $\mu\text{L L}^{-1}$  Silwet L-77. Plants were dipped, flowers facing downwards, into 200-250 ml fresh cell suspension. Four to five pots of plants were dipped for each construct. Dipped plants were kept in a low light, humid environment (closed floral bags, underneath a bench) for one day, then placed in normal growth conditions. This process was repeated one week later.

### ***Floral dip method from the Schumacher laboratory***

A 5 ml *Agrobacterium* liquid culture was grown for 2 days at 28 °C. 2 ml of this culture was centrifuged at 3,000 rpm for 10 min. The supernatant was discarded, and cells re-suspended in 2 ml of infiltration solution (0.5x MS, 0.05% (w/v) MES, pH 5.7 by KOH, 10% (w/v) sucrose, 500  $\mu\text{L L}^{-1}$  Silwet L-77). This was pipetted directly onto floral buds using 3 ml pastettes (Alpha Laboratories). Plants were kept in a low light, humid environment (closed floral bags, underneath a bench) for one day, then placed in normal growth conditions. This process was repeated one week later.

### ***Floral dip method from the Franklin laboratory***

An individual *Agrobacterium* colony was scraped off and added to 10 ml of YEBS media. The culture was grown for 2 days at 28 °C, added to 490 ml YEBS, and grown for a further 8-10 hours at 28 °C. 500 ml of 5% (w/v) sucrose and a final concentration of 200  $\mu\text{L L}^{-1}$  Silwet L-77 were added to the culture. Plants were dipped as described in the Dodd laboratory floral dip method.

### 2.5.8.3 Screening for positive transformants

T<sub>1</sub> seeds were collected from dipped T<sub>0</sub> plants, germinated and grown on compost mix for two weeks, then sprayed with phosphinothricin (100 mg L<sup>-1</sup>) on a weekly basis. After three sprays, DNA was extracted from surviving plants and PCR performed to verify the presence of the construct. Plants were left to grow until senescence, and their seed (T<sub>2</sub>) was collected.

50 T<sub>2</sub> seeds were sown on MS with 10 mg L<sup>-1</sup> phosphinothricin in large Petri dishes (145 mm diameter). After three weeks of growth, the ten healthiest T<sub>2</sub> survivors were transferred to compost mix and left to grow until senescence, and their seed (T<sub>3</sub>) was collected.

23 T<sub>3</sub> seeds were sown on MS with phosphinothricin in medium Petri dishes (90 mm diameter). After two to three weeks of growth, their survival rate was assessed to determine whether the T<sub>2</sub> parent plant was homozygous (100% of T<sub>3</sub> survive) or heterozygous (75% of T<sub>3</sub> survive, with visible variation in size and health). If no T<sub>2</sub> parent plant was homozygous, screening was repeated from the T<sub>2</sub> seed stage. Only homozygous seed was used for experiments.

## 2.5.9 Transient transformation

### 2.5.9.1 Infiltration of Arabidopsis seedlings with *Agrobacterium*

Arabidopsis were grown on Petri dishes for 2 weeks under a 12 h photoperiod. 20 ml of *Agrobacterium* YEB culture with appropriate selection was grown for 2 days at 28 °C, then centrifuged at 3,000 rpm for 10 min and re-suspended in dH<sub>2</sub>O with 200 µl L<sup>-1</sup> Silwet L-77. This solution was placed within a syringe (10 ml, BD Plastipak), and a seedling was added. A vacuum was created by blocking the syringe end and using the plunger. The vacuum-infiltrated seedling was transferred to a fresh Petri dish and examined 24 h later.

### 2.5.9.2 Infiltration of *Nicotiana benthamiana* (tobacco) with *Agrobacterium*

*Nicotiana benthamiana* were grown on compost mix in experimental glasshouses (16 h photoperiod, 20 °C) for 2 - 4 weeks by the staff of the experimental glasshouses. A 5 ml *Agrobacterium* liquid culture was grown overnight at 28 °C, then used to inoculate 25 ml of LB broth with appropriate selection. The 30 ml culture was grown for another day at 28 °C, then centrifuged at 3,000 rpm for 10 min at 4 °C. Cells were washed with 50 ml of 10 mM MgCl<sub>2</sub>, then centrifuged and washed once more. Cells were centrifuged, then re-suspended in an infiltration solution (10 mM MgCl<sub>2</sub>, 10 mM MES, 150 µg ml<sup>-1</sup> acetosyringone) and adjusted to an optical density at 600 nm of 1.0 using a spectrophotometer. This culture was incubated at room temperature for 5 h to induce *Agrobacterium* virulence genes. *Agrobacterium* were then infiltrated at the abaxial leaf surface using a 3 ml, needle-less syringe (BD Plastipak), and plants placed in a low light, humid environment (closed floral bags, underneath a bench) for 48 h.

## 2.6 Omoide-gawa field site

Fieldwork was conducted at the Omoide-gawa field site, near an abandoned mine in Hyogo prefecture, Japan (35°10'N, 134°93'E) (Fig. 2.1). This field site is described by Aikawa et al. (2010), and its naturally-occurring population of *Arabidopsis halleri* subsp. *gemmifera* (*A. halleri*) has been investigated previously (Aikawa et al. (2010); Kawagoe and Kudoh (2010); Kawagoe et al. (2011); Sato and Kudoh (2016, 2017)). The study population of *A. halleri* growing there contains two distinguishable morphs- with trichomes (hairy) and trichome-less (glabrous)- that coexist in a spatially intermingled manner.

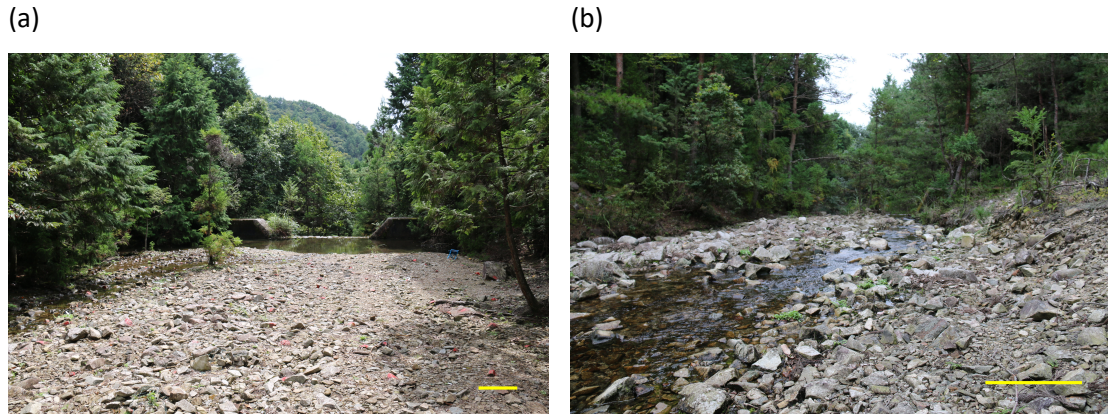


Figure 2.1: The Omoide-gawa field site. *Arabidopsis halleri* subsp. *gemmifera* plants used for the timecourse described in section 2.7.3 and density assays described in section 2.7.2 were collected from both (a) upriver and (b) downriver sites. Scale bar (yellow, bottom right) represents 5 m.

## 2.7 Stomatal assays

### 2.7.1 Stomatal density assay

Plants were grown on compost mix for 7-8 weeks under an 8 h photoperiod. Two fully developed leaves of similar size were sampled from each plant, and President Plus dental paste (Coltene) was applied to the abaxial side of each leaf to create a mould. Each mould was detached then painted with transparent nail varnish (60 seconds super shine, Rimmel), which was then peeled off using clear tape (Scotch Crystal) and taped to a 0.8-1.0 mm thick microscope slide. These were examined under an epifluorescence microscope, and photographs were taken at the centre of each leaf half at a 20x resolution using the Hamamatsu camera and Velocity software. Using FIJI software, stomata and pavement cells were counted in an 800  $\mu\text{m}$  x 800  $\mu\text{m}$  square to obtain stomatal index and density values. Stomatal index was calculated as follows:

$$\text{Stomatal Index} = \frac{\text{number of stomata}}{\text{number of stomata} + \text{number of pavement cells}} \times 100 \quad (2.3)$$



### 2.7.2 Stomatal density assay in the field

Eight plants of each trichome morph (hairy or glabrous) were selected at the Omoide-gawa field site, and 3-4 leaves were moulded per plant at midday using dental paste (Fig. 2.2a). These were transported to Bristol, where moulds were processed, imaged, and analysed as described above.

### 2.7.3 Stomatal aperture assay in the field

This experiment was conducted in September 2016 at the Omoide-gawa field site (described in section 2.6), when the photoperiod was approximately 12 h with dawn at 05:40 and dusk at 18:10. *Arabidopsis halleri* subsp. *gemmifera* (*A. halleri*) were sampled over a 40 h timecourse. Plants were chosen in advance, and marked by placing white tape on a nearby rock and aluminium foil near them, taking care not to disturb the plants. Selected plants were glabrous and located in non-shaded areas. Plants were selected from two areas of the Omoide-gawa field site, referred to as upriver (Fig. 2.1a) and downriver (Fig. 2.1b). Each was 25-30 m in length along the Omoide-gawa river, and separated by approximately 250 m. Samples were taken at 10 timepoints over three days: pre-dusk day 1 (upriver), post-dusk day 1 (upriver), midnight day 1 (upriver), pre-dawn day 2 (downriver), post-dawn day 2 (downriver), midday day 2 (upriver and downriver), pre-dusk day 2 (downriver), post-dusk day 2 (downriver), pre-dawn day 3 (upriver), and post-dawn day 3 (upriver). Sampling at night was performed using head-torches covered in green filters (Fig. 2.2b).

In a similar fashion to the stomatal density assay, dental paste was applied to the adaxial side of each leaf, still attached to the plant, to create a mould (Fig. 2.2). Eight plants were sampled per time point, with 3-4 leaves moulded per plant. Leaves moulded at pre-dawn timepoints were often covered in dew, making dental paste application slightly more difficult. As leaves could not be dried without affecting stomatal aperture, the dental paste itself was used to push dew drops off the leaf during moulding. Moulds were transported to Bristol, where they were each given a randomly generated number to conduct measurements in a blind fashion. Each mould was painted with transparent nail varnish, which was then peeled off using clear tape and taped to a microscope slide. These were examined under an epifluorescence microscope, and photographs were taken at a 40x resolution using a Hamamatsu camera and Volocity

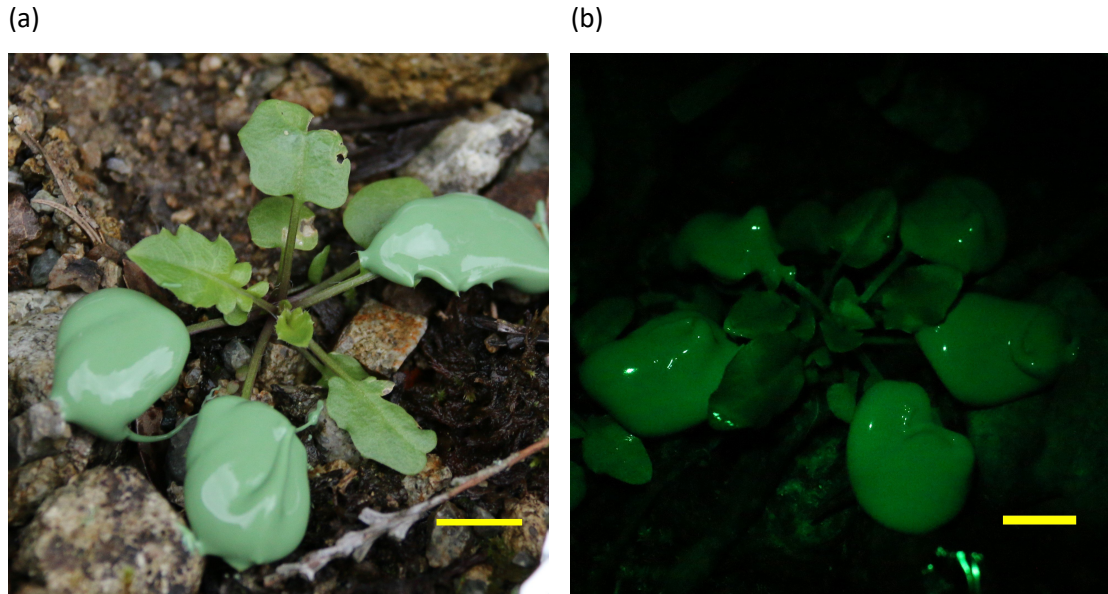


Figure 2.2: *A. halleri* leaves with stomatal impression paste at the Omoide-gawa field site. Photographs show leaves moulded (a) during the day and (b) at night using green light. Scale bar (yellow, bottom right) represents 1 cm.

software. Four photographs were taken per leaf and stomatal aperture was measured using Volocity.

#### 2.7.4 Detached leaf assay

Plants were grown on compost mix for 7-8 weeks under an 8 h photoperiod. One fully developed leaf was sampled for each plant, placed abaxial-side up in a weighing boat, and weighed immediately. Five plants were sampled per genotype, with each leaf weighed at a number of time points over three hours.

#### 2.7.5 Stomatal aperture bioassay

Plants were grown for 4-6 weeks on compost mix under a 16 h photoperiod. Leaf discs (5 mm diameter) were punched out from fully expanded leaves one hour after dawn, and incubated, abaxial-side down, in “opening buffer” (50 mM KCl, 10 mM MES, 6.15 pH) for 2 h in the growth chamber. This was to induce maximum stomatal aperture. Leaf discs were then transferred to “opening buffer” containing 0  $\mu\text{M}$ , 0.1  $\mu\text{M}$ ,

1  $\mu\text{M}$  or 10  $\mu\text{M}$  ABA, and incubated for a further 2 h under the same conditions. Leaf discs were then mounted on microscope slides, and stomatal aperture measurements were taken for ten stomata per leaf disc using an upright microscope with fitted camera and Motic Images Plus 2.0 software. One leaf disc was taken per plant, three leaf discs used per treatment, and each experiment repeated two to three times. Measurements were conducted blind to avoid experimenter bias.

## **2.7.6 Gas exchange measurements**

Plants were grown on compost mix for 5-7 weeks under an 8 h photoperiod. Stomatal conductance and  $\text{CO}_2$  assimilation were measured for a single leaf using a small leaf clamp (2  $\text{cm}^2$  area for the leaf) of a GFS-3000 infra-red gas analyser (Walz).

## **2.7.7 Preparation of guard cell-enriched RNA**

### **2.7.7.1 Ice-blender method**

This method was performed as described in Bauer et al. (2013).

### **2.7.7.2 Epidermal peel method**

This method was developed by Dr Ioanna Kostaki and performed by an undergraduate MSci student under my guidance. Plants were grown on compost mix in small inserts (4 cm (width) by 4 cm (length) by 5 cm (height)) for 5-6 weeks under a 10 h photoperiod. They were then moved to constant light and temperature conditions for 24 h before sampling.

Abaxial leaf epidermis was peeled using forceps, then incubated in 10 mM MES (6.15 pH, adjusted using 10 M KOH). Epidermal peels were obtained from five plants (4 leaves per plant, total of 20 leaves), collated, flash-frozen in liquid nitrogen, and stored at  $-80^\circ\text{C}$ . Three such samples were obtained for each genotype and time point. Peeling was performed around dawn (high *CCA1* transcript abundance) and dusk (high *TOC1* transcript abundance).

Guard cell RNA was extracted using the RNeasy UCP Micro Kit according to manufacturer's instructions, with the following modification: guard cell lysis was performed by adding glass beads (425  $\mu\text{m}$ –600  $\mu\text{m}$  diameter, acid washed, from Sigma-Aldrich) and 350  $\mu\text{l}$  RULT buffer to the sample, then vortexing for 5 min. RNA concentrations were determined using a nanodrop.

## 2.8 WUE assay

This assay to screen *Arabidopsis* for WUE was adapted from Wituszynska et al. (2013), and optimised in Chapter 3. Briefly, *Arabidopsis* were grown for 6 weeks in 50 ml falcon tubes (Corning) under an 8 h photoperiod at 70% humidity, 20 °C, and 100  $\mu\text{mol m}^{-2} \text{s}^{-1}$  of overhead lighting. A single 2 mm hole was drilled in the centre of each falcon tube lid using an upright pillar drill, then lids were spray-painted black with Bumper Black spraypaint (Hycote). Compost and perlite were mixed in a 1:1 ratio (1 ml of compost for 1 ml of perlite) and added to each falcon tube to 75% of its volume. 35 ml of Milli-Q water (Merck) was added, and the remaining volume filled with a 1:1 ratio of compost and Milli-Q water (1 ml of compost for 1 g of Milli-Q water). Drilled and painted lids were used to seal each falcon tube. The system was wrapped in aluminium foil. 10-15 surface-sterilised seeds were pipetted through the falcon tube lid hole.

Tubes were kept at 4 °C for three days, then transferred to the growth chamber. Tubes were placed within the chamber using a randomised experimental design, with each tube number randomly associated with a location number. One week later, seedlings were trimmed down to one per tube, and tube weight was recorded (initial falcon tube weight (g)). Data were collected from six week-old plants: photographs were taken from above to measure rosette leaf surface area, rosettes were removed and dried for 4 days at 60 °C to obtain dry weight measurements, and falcon tube weight without the rosette was recorded (final falcon tube weight (g)).

Negative controls consisted in falcon tube systems without plants, and were used to assess soil water evaporation through the lid's hole. 15 plants were measured per genotype, and this was repeated independently at least twice.

WUE was calculated as follows:

$$\text{WUE} = \frac{\text{rosette dry weight (mg)}}{\text{water used (ml)} - \text{soil water evaporation (g)}} \quad (2.4)$$

where

$$\text{water used (ml)} = \text{initial falcon tube weight (g)} - \text{final falcon tube weight (g)} \quad (2.5)$$

and

$$\text{soil water evaporation (g)} = 0.513 \quad (2.6)$$

## 2.9 Flowering time assay

Plants were grown on compost mix in large inserts (6.5 cm (width) by 6.5 cm (length) by 5 cm (height)), under either an 8 h photoperiod or a 16 h photoperiod. Plants with inflorescences measuring over 1 cm were sampled and stored in a paper negative bag. Flowering date was recorded, and number of leaves was counted and recorded.

## 2.10 Drought assays

### 2.10.1 Dehydration assay on Petri dishes

Dehydration assays on Petri dishes were performed as described in Legnaioli et al. (2009). Briefly, seeds were sown on MS containing 3% (w/v) sucrose at a density of 16 seeds per Petri dish, and grown for 14 days under an 8 h photoperiod. Seedlings were then transferred to a double layer of filter paper (QL100 filter paper, Fisher Scientific) in Petri dishes, and kept for 9 h under constant light conditions. Seedlings were watered by adding 4 ml of autoclaved dH<sub>2</sub>O per Petri dish, and kept under constant light conditions for a further 48 h before being scored for survival. Seedlings with a green apical meristematic region were counted as survivors. Two Petri dishes were used per experimental repeat (total of 32 seedlings per genotype), and each experiment repeated at least twice.

## **2.10.2 Drought assays on compost mix**

### **2.10.2.1 Slow drought assay on compost mix**

Plants were grown on compost mix in large inserts (6.5 cm (width) by 6.5 cm (length) by 5 cm (height)) under an 8 h photoperiod. The larger inserts meant that compost mix dried out slowly when water was withheld. After five weeks of growth, half of the trays were maintained in well-watered conditions, while water was withheld for remaining trays. Photographs were taken from above twice a week to measure rosette surface leaf area. Experiments ended when the majority of wild type plants died (defined as no longer having visible green tissue). Rosettes were dried for 4 days at 60 °C to obtain dry weight measurements.

### **2.10.2.2 Fast drought assay on compost mix**

This assay was performed as for the slow drought assay on compost mix, with the following modification: plants were grown on compost mix in small inserts (4 cm (width) by 4 cm (length) by 5 cm (height)). The smaller inserts meant that compost mix dried out rapidly when water was withheld.

### **2.10.2.3 Fixed drought assay on compost mix**

Compost mix was added to small inserts, and inserts were kept in individual plant saucers. Inserts were dried for 4 days at room temperature, then weighed to obtain the 0% soil water capacity (SWC) measurement. They were then watered from below with dH<sub>2</sub>O, and weighed several hours later to obtain 100% SWC measurements. Plants were grown in these inserts under a 16 h photoperiod. Well-watered conditions were maintained for one week, then individual inserts were maintained at 100%, 50% or 25% SWC by weighing each insert and adding dH<sub>2</sub>O with a 3 ml pastette (Alpha Laboratories) as required. At four weeks of growth, photographs were taken from above to measure rosette surface leaf area, and rosettes dried for 4 days at 60 °C to obtain dry weight measurements.

#### **2.10.2.4 Drought assay in constant light**

This assay was performed as for the fast drought assay on compost mix, with the following modification: seedlings were grown under a 16 h photoperiod and well-watered conditions for two weeks, then transferred to constant light conditions, with half of the trays maintained in well-watered conditions while water was withheld from remaining trays.

### **2.11 Hypocotyl elongation assay**

Seeds were sown in square Petri dishes (12 cm x 12 cm) on MS supplemented with 87.6 mM sucrose, 87.6 mM sorbitol, 20  $\mu$ M paclobutrazol, 100  $\mu$ M gibberellic acid, and/or up to 100  $\mu$ M *N*-1-naphthylphthalamic acid where indicated. After stratification, Petri dishes were placed at 45° angles within a Panasonic MLR-352 environmental growth chamber to prevent hypocotyl growth from being impeded by the Petri dish lid. Photoperiods varied from 4 h light/20 h dark to constant light conditions, depending on the experiment.

Seven-day old seedlings were positioned on 1% (w/v) agar, and photographs taken from above. Hypocotyl length was measured using ImageJ software.

### **2.12 Confocal microscopy**

Green fluorescent protein (GFP) bioluminescence of transgenic *Arabidopsis* expressing a promoter-GFP construct was examined using a confocal microscope and LAS AF software. Leaf discs (5 mm diameter) from seedlings or mature plants were obtained and mounted on slides. The following laser settings were used: argon laser at 20% capacity, 488 nm laser at 48% capacity, laser range of 505 nm–515 nm, gain of 1250, offset at 0.2%, 20x or 40x objective, zoom x1 to x4.

Guard cells are often found in a different vertical focus plane (*z*) than surrounding epidermal pavement cells, and GFP bioluminescence is only visible when a cell is in focus. To examine all different cell types equally for GFP bioluminescence, images were taken

over a range of different z planes, with a distance of 1  $\mu\text{m}$ –5  $\mu\text{m}$  between different z planes and 7-10 z planes imaged per area of focus.

WT Col-0 was used as a negative control. All images were processed equally using Fiji.

## 2.13 Luciferase bioluminescence imaging

Bioluminescence imaging of luciferase reporters was performed as described in Noordally et al. (2013). Briefly, transgenic seeds expressing a promoter-luciferase construct were sown within 1 cm long transparent rings (cut from medical grade PVC tubing, Fisher Scientific) on MS, with 10 seeds sown per ring. Seedlings were grown for 10 days under a 12 h photoperiod, then each ring was dosed with 100  $\mu\text{l}$  of 5 mM luciferin. Seedlings were kept under normal growing conditions for a further 24 h, then dosed once more with 50  $\mu\text{l}$  of 5 mM luciferin and transferred to constant light conditions (25  $\mu\text{mol m}^{-2} \text{s}^{-1}$  red light, 25  $\mu\text{mol m}^{-2} \text{s}^{-1}$  blue light).

Bioluminescence images were captured using a high resolution photon counting system (HRPCS 218, Photek) within a dark box (Photek) and IMAGE32 software every 2 h over 4 days, with an integration time of 10 min. The first 2 min of each integrated bioluminescence image were removed from analysis, due to signal contamination by delayed chlorophyll fluorescence. Rings containing non-bioluminescent, wild type seedlings were used as controls for background signal. Data were analysed using BioDare 2. Both the Fast Fourier Transform Non-Linear Least Squares (FFT-NLLS) and Maximum Entropy Spectral Analysis (MESA) algorithms were used: these produce estimates of circadian period and relative amplitude error (RAE: the ratio of amplitude error to the most probable amplitude estimate). RAE vary between 0 and 1, with lower values indicating a good rhythmic fit to the data. As FFT-NLLS and MESA are mathematically distinct approaches, using both analysis methods added confidence to my conclusions.





# Chapter 3

## The circadian clock and water use efficiency

### 3.1 Introduction

Over twenty oscillator components have been identified in *Arabidopsis*, and these form a series of interlocking transcription-translation feedback loops (Hsu and Harmer (2014)) (Fig. 1.3). Manipulating transcription and/or translation of these components can severely affect plant fitness, and often alters transcript and/or protein levels of other elements within the circadian system (Green et al. (2002); Dodd et al. (2005); Hsu and Harmer (2014)).

WUE has been widely used as a tool to indicate vegetative performance (Medlyn et al. (2017)), and has been examined under a range of different scales (The Royal Society (2009)). At the single leaf level, intrinsic, instantaneous WUE ( $WUE_i$ ) can be equated to the net amount of  $CO_2$  fixed per given unit of water transpired (equation 1.1) (Ruggiero et al. (2017); Ferguson et al. (2018)). Whole plant WUE is defined as the total biomass produced per unit of water transpired (equation 1.2) (Violet-Chabrand et al. (2016); Ruggiero et al. (2017); Ferguson et al. (2018)).

WUE appears to be regulated by the circadian clock. In *Arabidopsis*, stomatal aperture, stomatal conductance and  $CO_2$  assimilation are under circadian control (Salomé et al. (2002); Dodd et al. (2004, 2005)). In turn, altered circadian clocks can affect the pe-

riod of CO<sub>2</sub> assimilation and stomatal aperture in constant light (Dodd et al. (2004)). This link between the circadian oscillator and WUE has been observed in many species (Martin and Meidner (1971); Kerr et al. (1985); Gorton et al. (1989); Hennessey and Field (1991); Wilkins et al. (2009); Edwards et al. (2012); Resco de Dios et al. (2017)). Therefore, understanding the mechanisms underpinning the circadian regulation of WUE could lead to breeding possibilities for enhanced WUE traits (McClung (2013)).

## **3.2 Hypothesis and aims**

Based on previous reports (Salomé et al. (2002); Dodd et al. (2004, 2005)), we hypothesised that the circadian clock is an important determinant of whole plant WUE under diel conditions. In particular, as the circadian clock network is composed of interlocking transcriptional and translational feedback loops (Hsu and Harmer (2014)), we hypothesised that multiple circadian clock genes, rather than a single component, would be involved in regulating WUE.

We aimed to identify circadian clock genes that underlie this WUE phenotype. To achieve this, a simple and reliable WUE assay was developed, then used to screen single transgenic and/or mutant genotypes for each target gene.

## **3.3 Methods and methodology**

Seeds from a variety of *Arabidopsis* transgenic and mutant genotypes were used in this study (Table 3.1). These were genotyped by myself or another member of the Dodd laboratory using DreamTaq PCR (described in section 2.5.4.1) or sequencing (described in section 2.5.7.8) methodologies. Primers used for genotyping are provided in Chapter 2 (Table 2.6).

Plants were screened for WUE using a method adapted from Wituszynska et al. (2013). This method was optimised here (section 3.4.1), and a summarised version is provided in Chapter 2 (section 2.8).

Following this screen, genotypes of interest were further examined for survival under dehydration conditions. This dehydration assay was performed as described elsewhere

(Legnaioli et al. (2009)), and is provided in Chapter 2 (section 2.10.1).

<b>AGI code</b>	<b>Gene</b>	<b>Genotype</b>	<b>Reference</b>
AT2G46830	<i>CCA1</i>	<i>cca1-11</i>	Hall et al. (2003)
AT2G46830	<i>CCA1</i>	CCA1-ox	Wang and Tobin (1998)
AT5G08330	<i>CHE</i>	<i>che-1</i> CCA1::LUC+	Pruneda-Paz et al. (2009)
AT5G08330	<i>CHE</i>	<i>che-2</i> CCA1::LUC+	Pruneda-Paz et al. (2009)
AT5G08330	<i>CHE</i>	CHE-ox CCA1::LUC+ 17	Pruneda-Paz et al. (2009)
AT5G08330	<i>CHE</i>	CHE-ox CCA1::LUC+ 6	Pruneda-Paz et al. (2009)
AT2G25930	<i>ELF3</i>	<i>elf3-1</i>	Zagotta et al. (1992)
AT2G40080	<i>ELF4</i>	<i>elf4-101</i>	Khanna et al. (2003)
AT1G68050	<i>FKF1</i>	<i>fkf1-2</i>	Imaizumi et al. (2003)
AT1G22770	<i>GI</i>	<i>gi-11</i> CCA1:LUC	Ding et al. (2007b); Rédei (1962)
AT1G22770	<i>GI</i>	<i>gi-2</i>	Fowler et al. (1999)
AT2G21660	<i>CCR2</i>	<i>grp7-1</i>	Streitner et al. (2008)
AT3G01090	<i>KIN10</i>	KIN10-ox 5.7	Baena-González et al. (2007)
AT3G01090	<i>KIN10</i>	KIN10-ox 6.5	Baena-González et al. (2007)
AT1G01060	<i>LHY</i>	LHY-ox	Schaffer et al. (1998)
AT2G18915	<i>LKP2</i>	<i>lkp2-1</i>	Imaizumi et al. (2005)
AT3G46640	<i>LUX</i>	<i>lux-1</i>	Hazen et al. (2005a)
AT5G60100	<i>PRR3</i>	<i>prrr3-1</i>	Alonso et al. (2003)
AT5G24470	<i>PRR5</i>	<i>prrr5-3</i> TOC1::LUC	Michael et al. (2003)
AT5G02810	<i>PRR7</i>	<i>prrr7-11</i>	Yamamoto et al. (2003)
AT2G46790	<i>PRR9</i>	<i>prrr9-1</i>	Eriksson et al. (2003)
AT5G02840	<i>RVE4</i>	<i>rve4-1</i>	Alonso et al. (2003)
AT3G09600	<i>RVE8</i>	<i>rve8-1</i>	Rawat et al. (2011)
AT2G31870	<i>TEJ</i>	<i>tej-1</i>	Panda et al. (2002)
AT3G22380	<i>TIC</i>	<i>tic-1</i>	Hall et al. (2003)
AT3G22380	<i>TIC</i>	<i>tic-2</i>	Ding et al. (2007b)
AT5G61380	<i>TOC1</i>	<i>toc1-1</i> CAB2::LUC	Strayer et al. (2000)
AT5G61380	<i>TOC1</i>	<i>toc1-2</i> CAB2::LUC	Strayer et al. (2000)
AT5G61380	<i>TOC1</i>	<i>toc1-21</i> CAB2::LUC	Ding et al. (2007a)
AT5G61380	<i>TOC1</i>	<i>toc1-101</i>	Kikis et al. (2005)
AT5G61380	<i>TOC1</i>	TOC1-ox	Más et al. (2003a)

Continuation of Table 3.1			
AGI code	Gene	Genotype	Reference
AT1G78580	<i>TPS1</i>	<i>tps1-11</i>	Gomez et al. (2010)
AT1G78580	<i>TPS1</i>	<i>tps1-12</i>	Gomez et al. (2010)
AT1G78580	<i>TPS1</i>	<i>tps1-13</i>	Gomez et al. (2010)
AT3G04910	<i>WNK1</i>	<i>wnk1</i>	Alonso et al. (2003)
AT5G57360	<i>ZTL</i>	<i>ztl-1 CAB2::LUC</i>	Somers et al. (2000)

Table 3.1: Arabidopsis genotypes screened for water use efficiency.

## 3.4 Results

### 3.4.1 WUE assay: method optimisation

#### 3.4.1.1 Choosing an established methodology to measure WUE in Arabidopsis

In Arabidopsis, WUE can be measured using a variety of methods and experimental conditions. These include growing individual plants in wrapped containers (Nienhuis et al. (1994)), closed interlocking buckets (Sandoval et al. (2016)), plastic cuvettes (Easlon et al. (2014)), and falcon tubes (Wituszynska et al. (2013)); measuring WUE<sub>i</sub> through gas exchange measurements or whole plant WUE through final shoot dry biomass and total water loss; and using photoperiods ranging from 8 h to 16 h, relative humidity percentages from 40% to 90% and a variety of watering regimes (Nienhuis et al. (1994); Earley et al. (2009); Yoo et al. (2010); Xing et al. (2011); Sandoval et al. (2016); Wituszynska et al. (2013); Easlon et al. (2014); Kenney et al. (2014); Franks et al. (2015)).

The approach of Wituszynska et al. (2013) was used as a starting point. As it involved growing Arabidopsis in falcon tubes, a large number of plants could be screened within limited growth space. In addition, Wituszynska et al. (2013) used compost for plant growth, which is closer to the natural growing conditions of Arabidopsis.

In Wituszynska et al. (2013), WUE for each tube was calculated as follows:

$$\text{WUE} = \frac{\text{rosette dry weight (mg)}}{\text{water used (ml)}} \quad (3.1)$$

where

$$\text{water used (ml)} = \text{initial falcon tube weight (g)} - \text{final falcon tube weight (g)} \quad (3.2)$$

#### **3.4.1.2 Optimising falcon tube composition**

Circadian mutants and overexpressors often have alterations in growth, development and stress tolerance. Therefore, I conducted a WUE screen on these genotypes in the vegetative growth phase under well-watered conditions.

In other experiments performed in this thesis, plants are grown in a 3:1 ratio of compost and sand. However, sand was unsuitable for this procedure as it is heavy and dense. Perlite, as suggested by Wituszynska et al. (2013), was a better alternative as it kept compost porous and enabled homogeneous distribution of water. Therefore, each falcon tube was filled to 75% of its volume with a 1:1 ratio of compost and perlite.

MilliQ water was then added. The volume suggested by Wituszynska et al. (2013) was 35 ml: therefore, I tested the length of time wild type Col-0 could survive with this volume of water before exhibiting drought stress symptoms. Under our experimental conditions, Col-0 remained healthy for 12 weeks before the water supply was exhausted, which is double the length of experiment used.

It was important that all genotypes remain in a drought-free environment throughout the experiment. This was tested both informally, by verifying that falcon tubes still contained water at the end of the experiment, and systematically, by cross-examining water loss data to ensure that falcon tube weight loss remained below 35 g. Maximal weight loss during the experiment was 16 g (16 ml of water). Therefore, 35 ml of water is sufficient to maintain plants in well-watered conditions throughout the experiment.

Finally, a 1:1 ratio of compost and water was used to fill each falcon tube to capacity. This enabled germinating seedlings to reach the surface rapidly. In addition, the high

moisture content of this layer aided germination.

The falcon tube lid was used to close the system. A hole was drilled in the centre of each lid to allow seedling growth, and different hole diameters were trialled. It had to be sufficiently large to enable seedling growth, yet sufficiently small to minimise soil surface water evaporation. A 2 mm hole was determined to be the best diameter.

Unexpectedly, Col-0 grown in these falcon tube systems had curled leaves. This had also been reported by Sandoval et al. (2016) for Col-0 grown in closed pots with white lids, but not with black lids. They concluded that this curling leaf phenotype, similar to that of *Arabidopsis* grown under high light levels, was due to reflected light from the white lids (Sandoval et al. (2016)). In a similar fashion, I spray-painted the falcon tube lids black, and this abolished the curling leaf phenotype. Additional steps were taken to avoid paint chemicals affecting plant health.

#### **3.4.1.3 Homogenising seedling treatment**

For each genotype, screened plants were grown from seed collected from the same parent plant to ensure comparability between biological replicates. Seeds were surface sterilised to avoid bacterial or fungal contamination and aid germination. Seeds were then pipetted through the falcon tube lid hole. 10-15 seeds were added per tube to ensure survival of at least one seedling. This was a sufficiently low number of seeds to avoid overcrowding, which affects future growth by causing seedling competition and over-elongation.

The system was wrapped in foil to prevent growth of other photosynthetic organisms, and placed at 4 °C for 3 days to stratify. Tubes were subsequently placed in a growth chamber for six weeks. A randomised design was applied, with each falcon tube randomly assigned a number associated with a location, to avoid positional effects within the growth chamber from influencing the data.

An important step involved trimming seedlings down to one per tube and measuring tube weight. This needed to be performed early to obtain realistic “initial weight” measurements and avoid seedling competition. However, trimming young seedlings often caused damage or death, and slow-growing genotypes took longer to extend through the lid hole. Seven days of growth was found to be optimal for this procedure.

#### 3.4.1.4 Taking soil water evaporation into account

Data were collected from six week-old plants (Fig. 3.1b) and photographs taken from above to obtain rosette leaf surface area measurements (Fig. 3.1a). Each rosette was

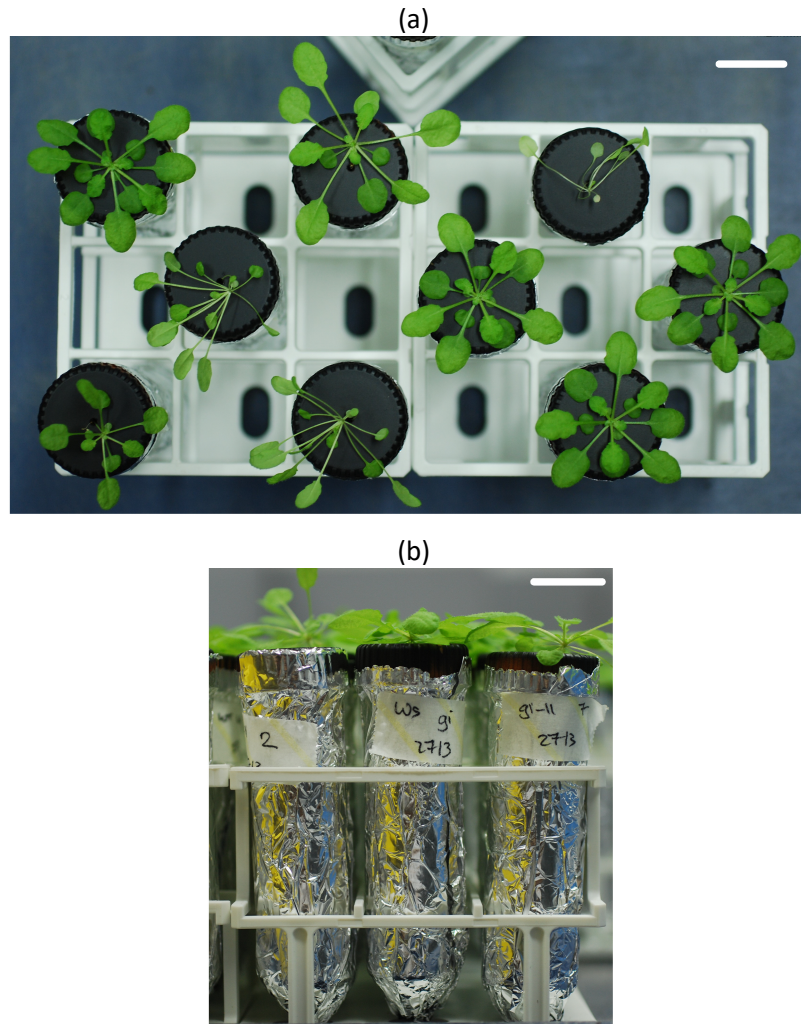


Figure 3.1: The optimised WUE assay used to screen circadian clock mutant and transgenic genotypes. Representative photographs of the falcon tube systems viewed from (a) above, separated to obtain accurate leaf area measurements and (b) the side. Scale bars (white, top right) represent 2 cm.

cut and dried to obtain dry weight measurements, and falcon tube weight without the rosette was recorded. The difference between initial and final falcon tube weight corresponded to plant water use. However, soil water evaporation could confound water use values. Therefore, negative controls (systems without plants) were placed in the chamber alongside each experimental repeat. Water loss by negative controls was



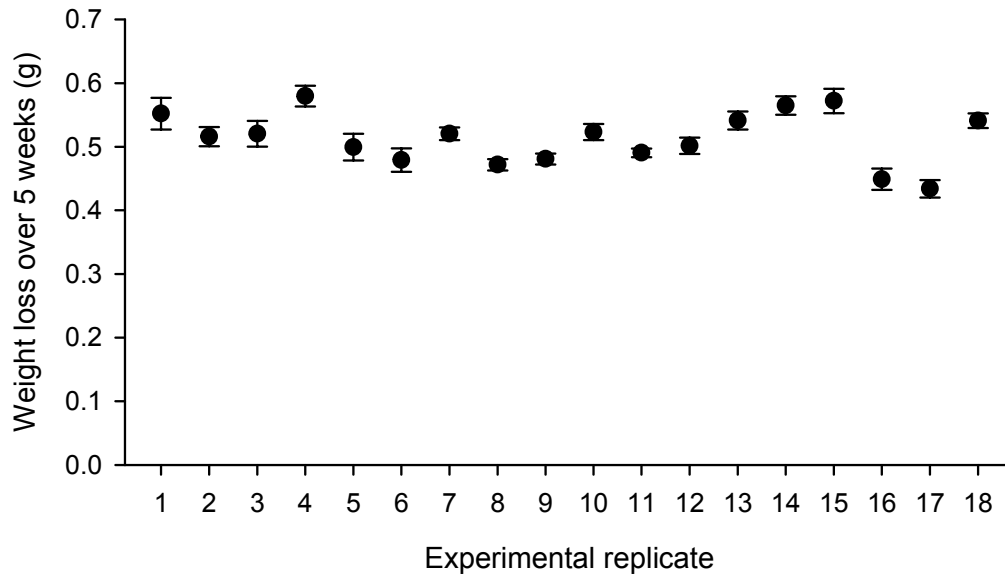


Figure 3.2: Minimal soil water evaporation occurred under these experimental conditions. Data show weight loss, hence water loss, throughout each experiment for negative controls in independent experimental repeats ( $n = 15$ ; mean  $\pm$  S.E.M.). Negative controls have little variation in soil water evaporation both within and between experimental repeats, with an overall mean weight loss of  $0.513 \pm 0.004$  g over five weeks.

small, corresponding to  $0.513$  g ( $\pm 0.004$  g) over 5 weeks (between week 1 and 6 of growth) (Fig. 3.2). This represents 13% of the mean weight loss. There was little variation in water lost by negative controls both within and between experimental replicates (Fig. 3.2).

Therefore, the equation applied to calculate WUE for each tube was modified in the following manner:

$$WUE = \frac{\text{rosette dry weight (mg)}}{[\text{weight}_{\text{initial}}(\text{g}) - \text{weight}_{\text{final}}(\text{g})] - \text{soil water evaporation (g)}} \quad (3.3)$$

where  $\text{weight}_{\text{initial}}$  and  $\text{weight}_{\text{final}}$  correspond to falcon tube weight at the start and end of the experiment, respectively. Water loss due to soil evaporation was normalised at  $0.513$  g for all falcon tubes.

#### 3.4.1.5 Standardising dry weight measurements

A pilot test was conducted in which three Col-0 rosettes (replicates A, B, C) were dried at  $90^\circ\text{C}$  or  $60^\circ\text{C}$  and weighed daily over 10 days. Under each of these temperature

conditions, weight decreased sharply from day 0 (fresh weight) to day 1, then remained stable for the remaining nine days (Fig. 3.3). Therefore, four days at 60 °C was sufficient to obtain accurate and comparable dry weight measurements.

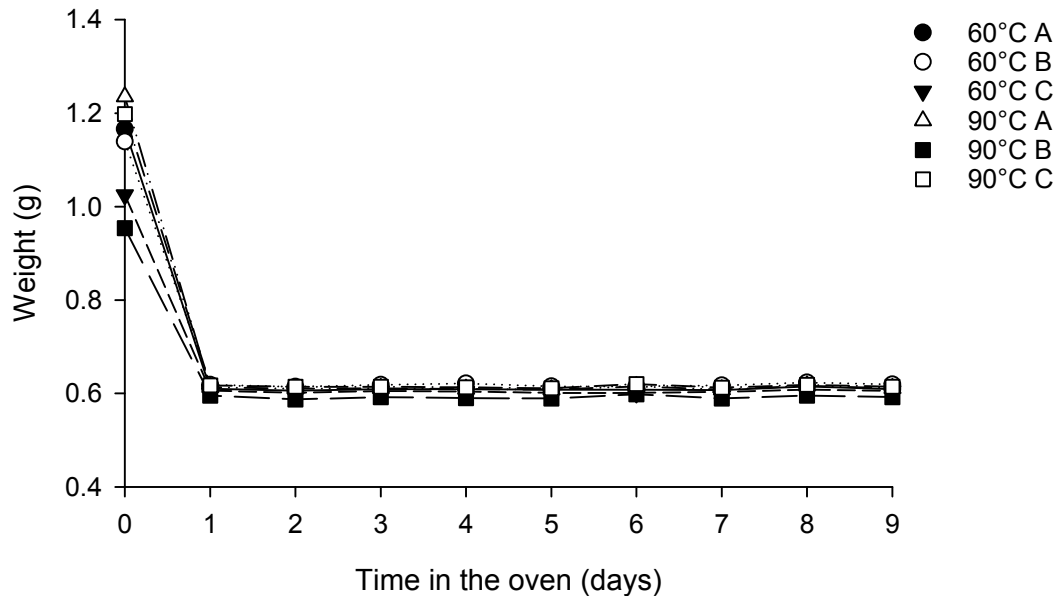


Figure 3.3: Four days at 60 °C is sufficient to obtain accurate dry weight measurements. In this pilot test, three Col-0 rosettes (replicates A-C) were dried at 60 °C or 90 °C and weighed daily over 10 days. Data show mean.

#### 3.4.1.6 Analysing robustness and precision of this WUE screen

The robustness of this WUE screen method was examined by comparing independent experimental repeats of wild types, and its precision was determined by comparing WUE between accessions. Within an experimental repeat, there was little variation in WUE: obtained standard error of the mean (S.E.M.) values varied between 0.03 and 0.10 for C24, 0.01 and 0.03 for Col-0, 0.02 and 0.03 for Ws, and 0.02 and 0.05 for *L. er.* (Fig. 3.4a). Each accession also had similar WUE across independent experimental repeats (overall S.E.M. of 0.07, 0.02, 0.06 and 0.04 for C24, Col-0, Ws and *L. er.*, respectively), confirming the robustness and usability of this method (Fig. 3.4a).

All four accessions had significantly different WUE ( $F_{3, 306} = 135.252$ ;  $p < 0.001$ ). C24 had the highest WUE (3.01), while *L. er.* had the lowest (1.60) (Fig. 3.4b). Col-0 was slightly more water use efficient than Ws (2.22 and 1.91, respectively) (Fig. 3.4b). These results are in line with previous studies (Nienhuis et al. (1994); Dodd et al. (2004);

Masle et al. (2005); Karaba et al. (2007); Ruggiero et al. (2017); Ferguson et al. (2018)), demonstrating that this method is accurate.

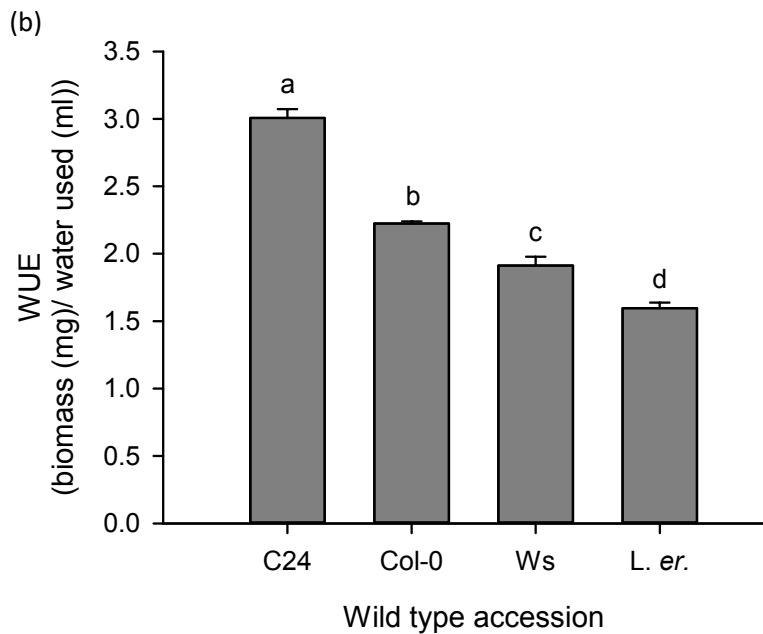
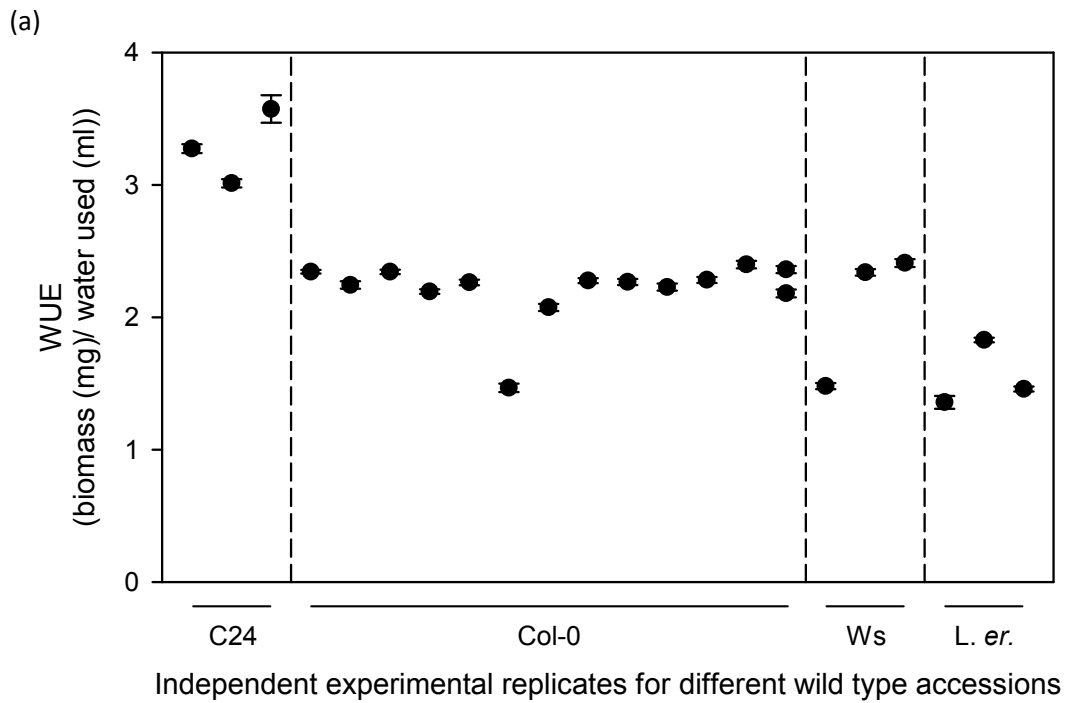


Figure 3.4: The method optimised to screen *Arabidopsis* for WUE is robust and reliable. (a) Wild type accessions have little variation in WUE both within and between experimental repeats. Data show WUE obtained for different experimental repeats ( $n = 6-15$ ; mean  $\pm$  S.E.M.). Vertical dotted lines separate different accessions. (b) Different accessions have distinct WUE. Data show mean WUE for all experimental repeats for each accession ( $n = 28-173$ ; mean  $\pm$  S.E.M.). Data were analysed with ANOVA and post-hoc Tukey tests. Different letters indicate statistically significant difference ( $p < 0.001$ ).

## 3.4.2 The circadian clock affects WUE

### 3.4.2.1 Screening single circadian clock mutants and overexpressors for WUE

The circadian clock is a complex, multilevel system, involving a large number of genes entwined in interlocking transcription-translation feedback loops. Following a literature search, 24 genes were selected as candidates to screen for effects upon WUE. These targets are either an integral part of the core circadian clock loops, or associated with core loop processes. *TREHALOSE-6-PHOSPHATE SYNTHASE 1 (TPS1)* was also examined in line with work performed in Chapter 7.

Well-known and characterised single mutant and/or overexpressor genotypes were obtained for each target gene, with several alleles acquired per genotype when possible (Table 3.1). These 36 genotypes and their backgrounds were screened for WUE using the method optimised previously (section 3.4.1).

Only two genotypes- *cop1-1* and *LHY-ox*- were unable to survive the screen due to morphological properties. Dark-grown *cop1* have a phenotype similar to light-grown wild type seedlings, with short hypocotyls and fully expanded cotyledons instead of long hypocotyls and an apical hook (Deng et al. (1991); Deng and Quail (1992)). Therefore, *cop1-1* expanded its cotyledons below the lid rather than first growing through the lid's hole. *LHY-ox* had the opposite problem: hypocotyls elongated to such an extent that they eventually fell and died. In addition, the few surviving *LHY-ox* had very small leaves, thus dry weight values were too small for accurate WUE measurements. Consequently, no WUE data were acquired for *COP1* and *LHY*.

For each genotype, mean WUE was expressed as a percentage of the background, with wild type (WT) WUE normalised to 100% (Fig. 3.5). This was necessary due to variation in WUE between accessions (Fig. 3.4b). At least two independent experimental repeats were performed per genotype. Data presented here are from one experimental replicate (Fig. 3.5); additional data are provided in the Appendix (Sup. Fig. 9.1).

Remarkably, nearly half of the genotypes had a significant difference in WUE compared to the WT (16/34 genotypes,  $p < 0.05$  for independent samples t-tests), representing half of the target genes (11/22 genes) (Fig. 3.5).

The *cca1-11*, *elf3-1*, *prr5-3*, *prr9-1*, *tps1-11*, *tps1-12*, and *ztl-1* mutants, as well as the

*TOC1*, *KIN10* 5.7 and 6.5 overexpressors, had significantly lower WUE than the WT, while *gi-2*, *gi-11*, *grp7-1*, *prp7-11* and *tej-1* had significantly higher WUE than the WT (Fig. 3.5). Therefore, *CCA1*, *ELF3*, *GI*, *GRP7*, *KIN10*, *PRR5*, *PRR7*, *PRR9*, *TEJ*, *TOC1*, *TPS1* and *ZTL* appear to regulate WUE under these experimental conditions.

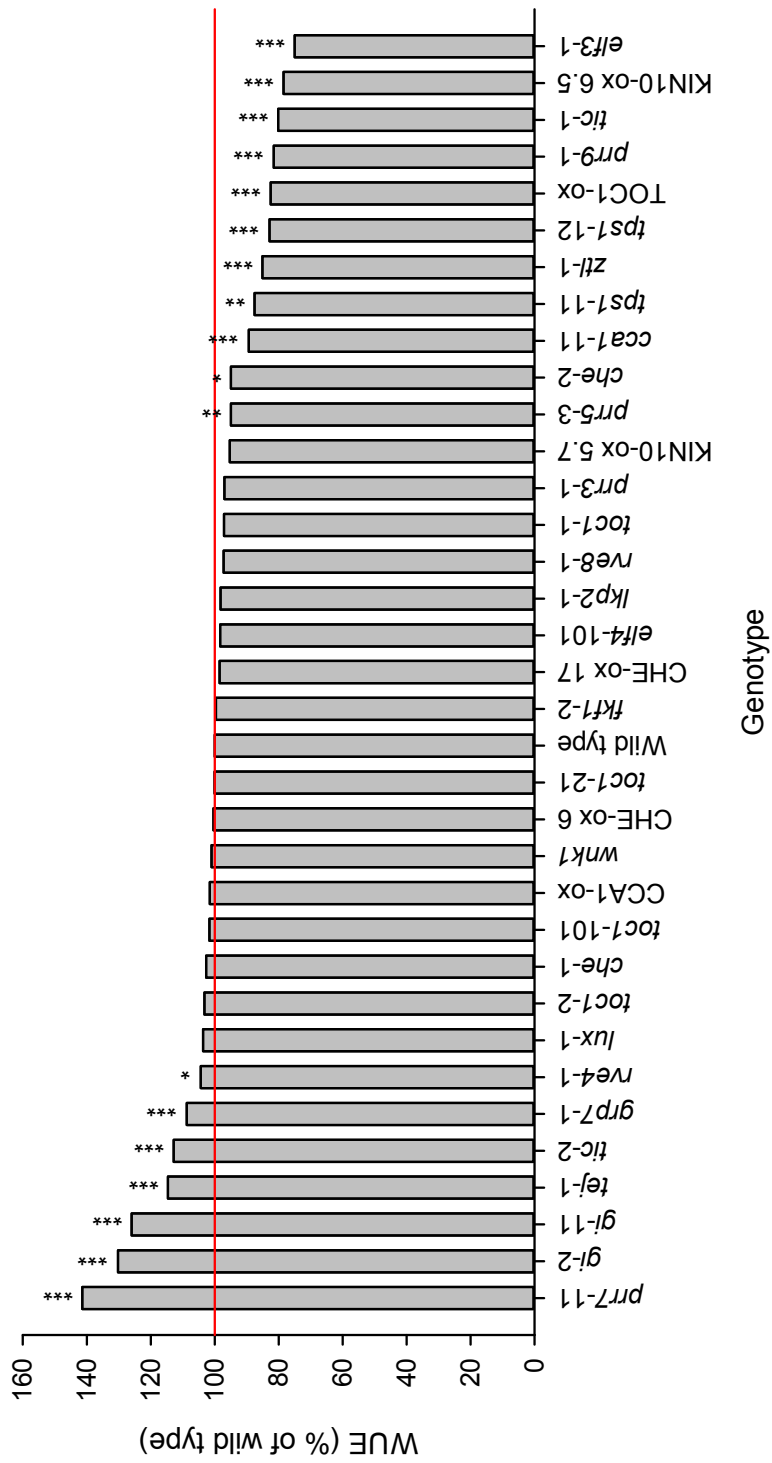


Figure 3.5: The circadian clock regulates whole plant WUE in Arabidopsis under light/dark conditions. Data show WUE of screened circadian clock mutants and overexpressors, which are expressed as a percentage of their respective wild type background (normalised to 100%, red reference line) due to variation between accessions ( $n = 5-15$ ; mean). Data were analysed using independent-samples t-tests, and statistical significance compared to the background is indicated using starrng (\* =  $p < 0.05$ ; \*\* =  $p < 0.01$ ; \*\*\* =  $p < 0.001$ ). One representative independent experimental repeat is represented here for each genotype. Additional experimental replicates are provided in the Appendix (Sup. Fig. 9.1).

### 3.4.2.2 Analysing raw water use and biomass production data

Data were further analysed to investigate whether genotypes with low WUE had this lower value due to higher water use or lower biomass production, and whether genotypes with high WUE had this higher value due to lower water use or higher biomass production. This analysis was inconclusive, because most screened genotypes had lower water use and final rosette biomass dry weight than their background (Fig. 3.6a, 3.6b). For example, *elf3-1* water use was 14.5% of WT water use (Fig. 3.6a), and *elf3-1* dry weight was 9.1% of WT dry weight (Fig. 3.6b).

The difference between dry weight percentage and water use percentage was then examined (Fig. 3.6c). As expected, this showed that genotypes with high WUE had a higher dry weight percentage compared to water used percentage, genotypes with low WUE had a lower dry weight percentage compared to water used percentage, and genotypes with similar WUE to the background had similar percentages of dry weight and water used (Fig. 3.6c).



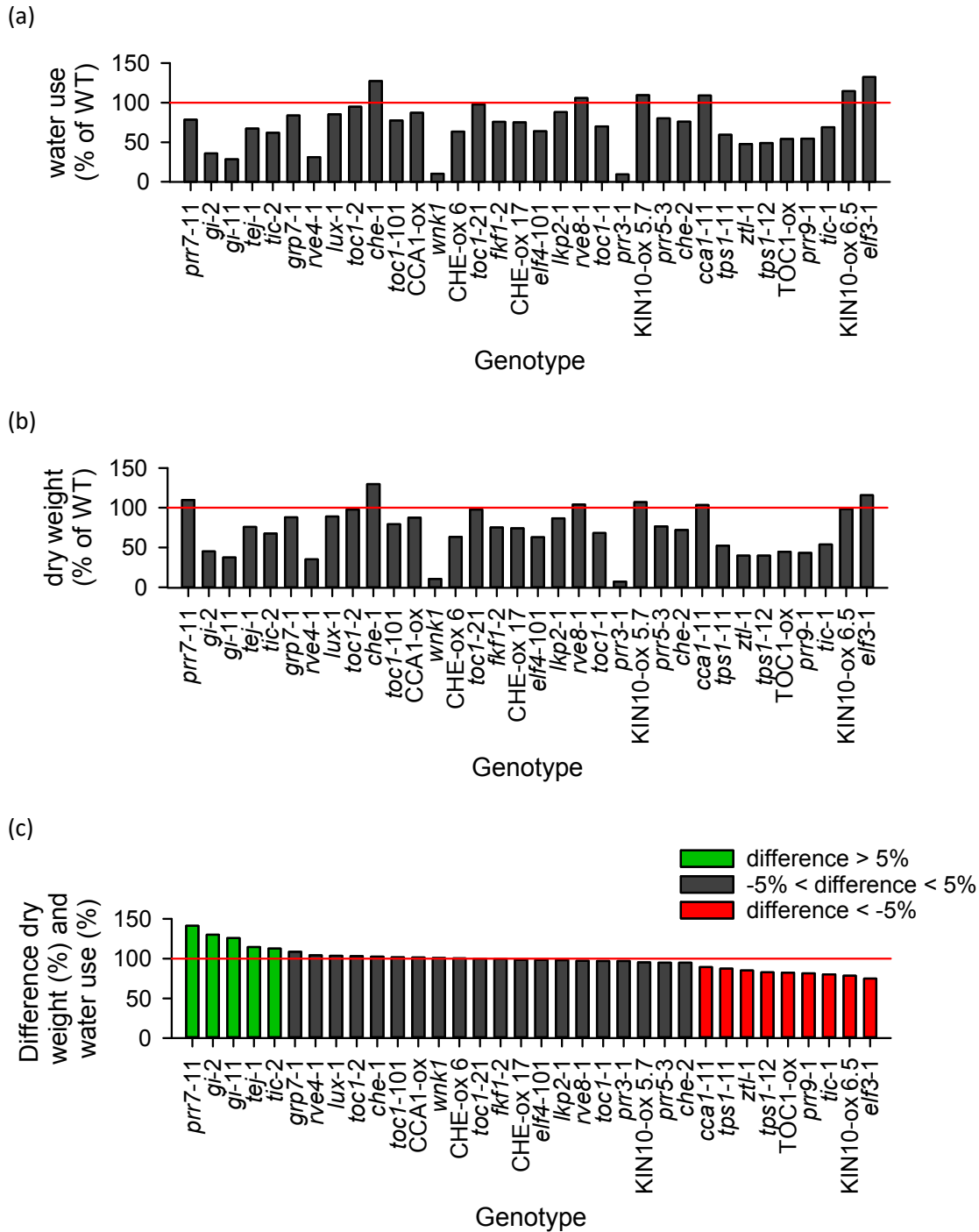


Figure 3.6: Analysis of raw WUE data used to draw Fig. 3.5. Data represent (a) mean water use and (b) mean dry weight of screened genotypes as a percentage of their respective wild type background (normalised to 100%, red reference line) ( $n = 5- 15$ ), and (c) difference between dry weight percentage and water use percentage. For ease of comparison, genotypes are presented in the same order as for Fig. 3.5. Colour-coding represents genotypes with a higher dry weight percentage (difference > 5%, green), a higher water use percentage (difference < -5%, red), or similar dry weight and water use percentages (difference between -5% and 5%, dark grey), using 5% as a cut-off point.

### 3.4.2.3 Alterations in WUE might not be due to alterations in circadian period, phase of expression, or flowering time

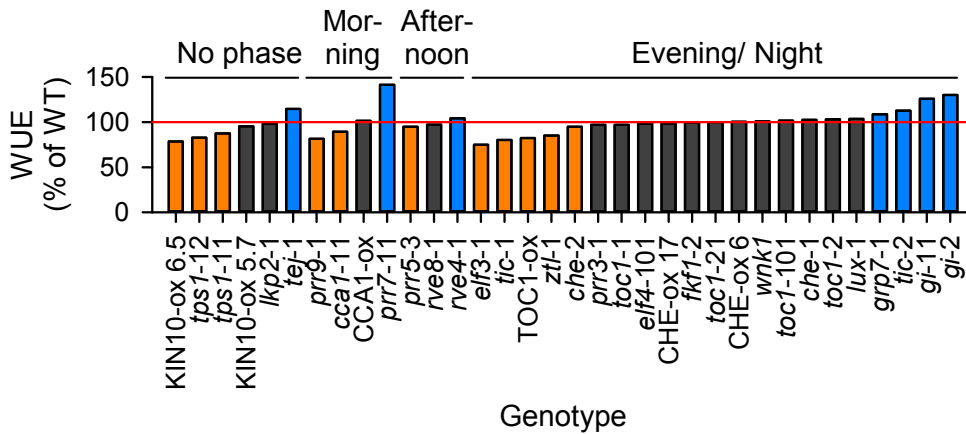
Variations in WUE were examined in the context of the phase of expression of target genes (Fig. 3.7a), the altered period of the circadian clock mutants and overexpressors (Fig. 3.7b), and the altered flowering time of these genotypes (Fig. 3.7c). Phase of expression, period and flowering time data were obtained from Fowler et al. (1999); Schultz et al. (2001); Doyle et al. (2002); Nakamichi et al. (2002); Yanovsky and Kay (2002); Imaizumi et al. (2003); Más et al. (2003b); Murakami et al. (2004); Farré et al. (2005); Hazen et al. (2005b); Baena-González et al. (2007); Streitner et al. (2008); Wang et al. (2008); Baudry et al. (2010); Nakamichi et al. (2010); Rawat et al. (2011); Wahl et al. (2013) and Hsu and Harmer (2014).

The time of peak expression of each mutated gene does not seem to explain alterations in WUE (Fig. 3.7a). For example, *CCA1* transcript abundance peaks at dawn whereas *ELF3* expression is evening-phased (Hsu and Harmer (2014)), but both *cca1-11* and *elf3-1* have significantly lower WUE than the WT (Fig. 3.5, 3.7a).

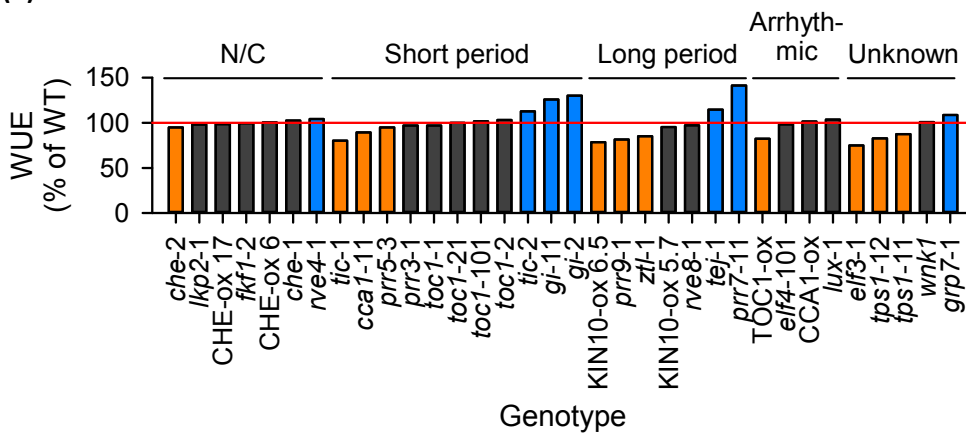
Alterations in circadian period do not appear to explain changes in WUE (Fig. 3.7b). For example, *prr7-11* and *ztl-1* are both long period mutants (Más et al. (2003b); Farré et al. (2005); Nakamichi et al. (2010); Baudry et al. (2010)), but *prr7-11* has significantly higher WUE whereas *ztl-1* has significantly lower WUE than the WT (Fig. 3.5, 3.7b).

As flowering time is controlled by the circadian clock (Yanovsky and Kay (2002); Hayama and Coupland (2003); Johansson and Staiger (2015)) and early flowering is a drought escape mechanism (Riboni et al. (2013)), the altered flowering time of circadian clock mutants and overexpressors was also analysed. No clear pattern was observed between altered flowering time and WUE (Fig. 3.7c). For example, although *elf3-1* has an early flowering response (Zagotta et al. (1992)) while *ztl-1* has a late flowering phenotype (Somers et al. (2000)), both have significantly lower WUE than the WT (Fig. 3.5, 3.7c).

**(a) Phase of expression**



**(b) Period**



**(c) Flowering time**

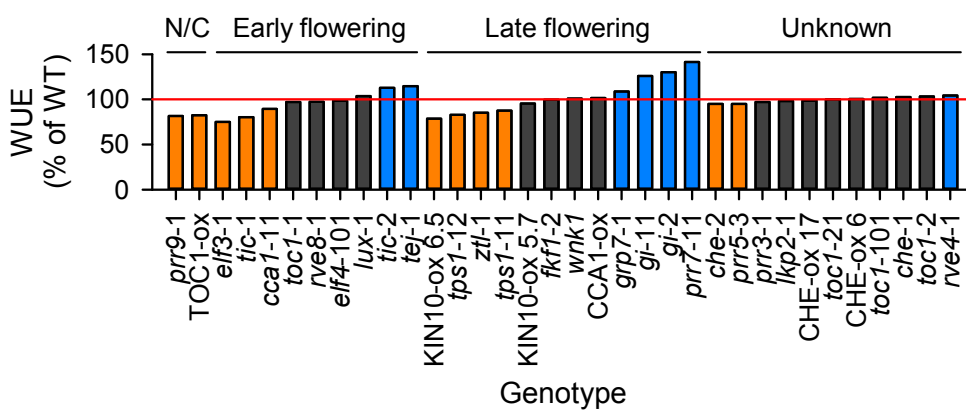


Figure 3.7: Variations in WUE are not explained by (a) phase of expression, (b) altered period, or (c) altered flowering time. Data are redrawn from Fig. 3.5 and represent mean WUE of screened circadian clock mutants and overexpressors expressed as a percentage of their respective WT background ( $n = 5-15$ ). The red reference line indicates WT WUE (100%). Genotypes reported to have no changes (N/C) in period or flowering time were included on the left of panels (b) and (c), while those for which period and/or flowering time are unknown were included on the right. Colour-coding highlights genotypes with significantly higher (blue) and lower (orange) WUE compared with the wild type (data taken from Fig. 3.5). References for phase of expression, period and flowering time data are provided in text.

#### 3.4.2.4 Rosette architecture affects WUE

In *Arabidopsis*, rosette structure and leaf morphology vary naturally between ecotypes (Alonso-Blanco and Koornneef (2000); Pérez-Pérez et al. (2002)). For example, C24 and *L. er.* have rounded leaves, whereas Col-0 and Ws have undulate and revolute leaf morphologies, respectively (Pérez-Pérez et al. (2002)). Changes in the circadian clock can affect rosette architecture substantially (Fig. 3.8) (Ruts et al. (2012); Rubin et al. (2018)). Therefore, the effect of rosette leaf surface area upon WUE was examined. Pearson

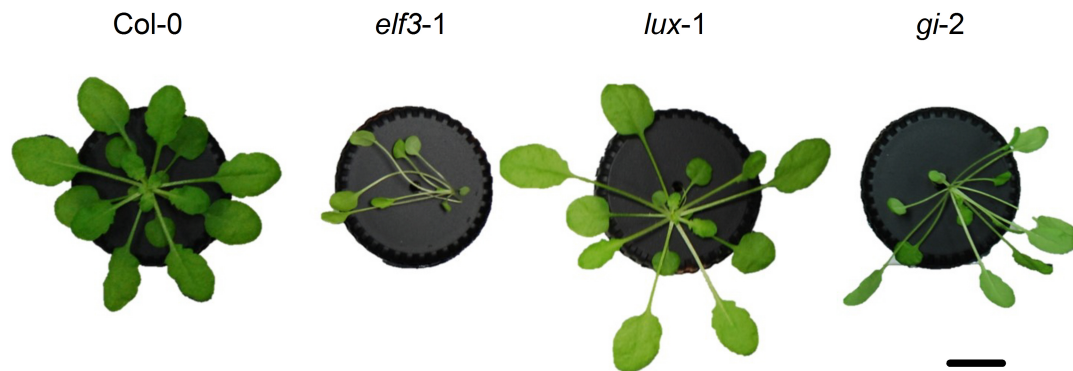


Figure 3.8: Altered circadian clocks can affect rosette architecture in *Arabidopsis*. Aerial photographs of *elf3-1*, *lux-1*, and *gi-2* circadian clock mutants in the Col-0 background illustrate this concept. Scale bar (black, bottom right) represents 1 cm.

correlation tests revealed a weak, positive correlation between rosette leaf surface area and WUE that was statistically significant ( $r=0.400$ ,  $r^2=0.160$ ,  $p<0.001$ ) (Fig. 3.9a). This analysis suggests that 16% of variability in WUE can be explained by rosette leaf surface area.

Rosette architecture is also characterised by rosette tightness, or leaf overlap. This might affect WUE by reducing the effective photosynthetic surface. Pearson correlation tests revealed that rosette leaf surface area and dry biomass were highly correlated, with rosette dry biomass predicting 73% of variability in rosette leaf surface area ( $r=0.857$ ,  $r^2=0.734$ ,  $p<0.001$ ) (Fig. 3.9b). This could suggest a small amount of leaf overlap, or changes in leaf thickness.

Finally, alterations in rosette architecture could also affect the number and/or density of stomata, which in turn could affect the amount of water used. Rosette leaf surface area explained 83% of water use (Pearson correlation test;  $r=0.912$ ,  $r^2=0.832$ ,  $p<0.001$ ) (Fig. 3.9c). As a larger leaf surface area can contain a greater number of stomata, this

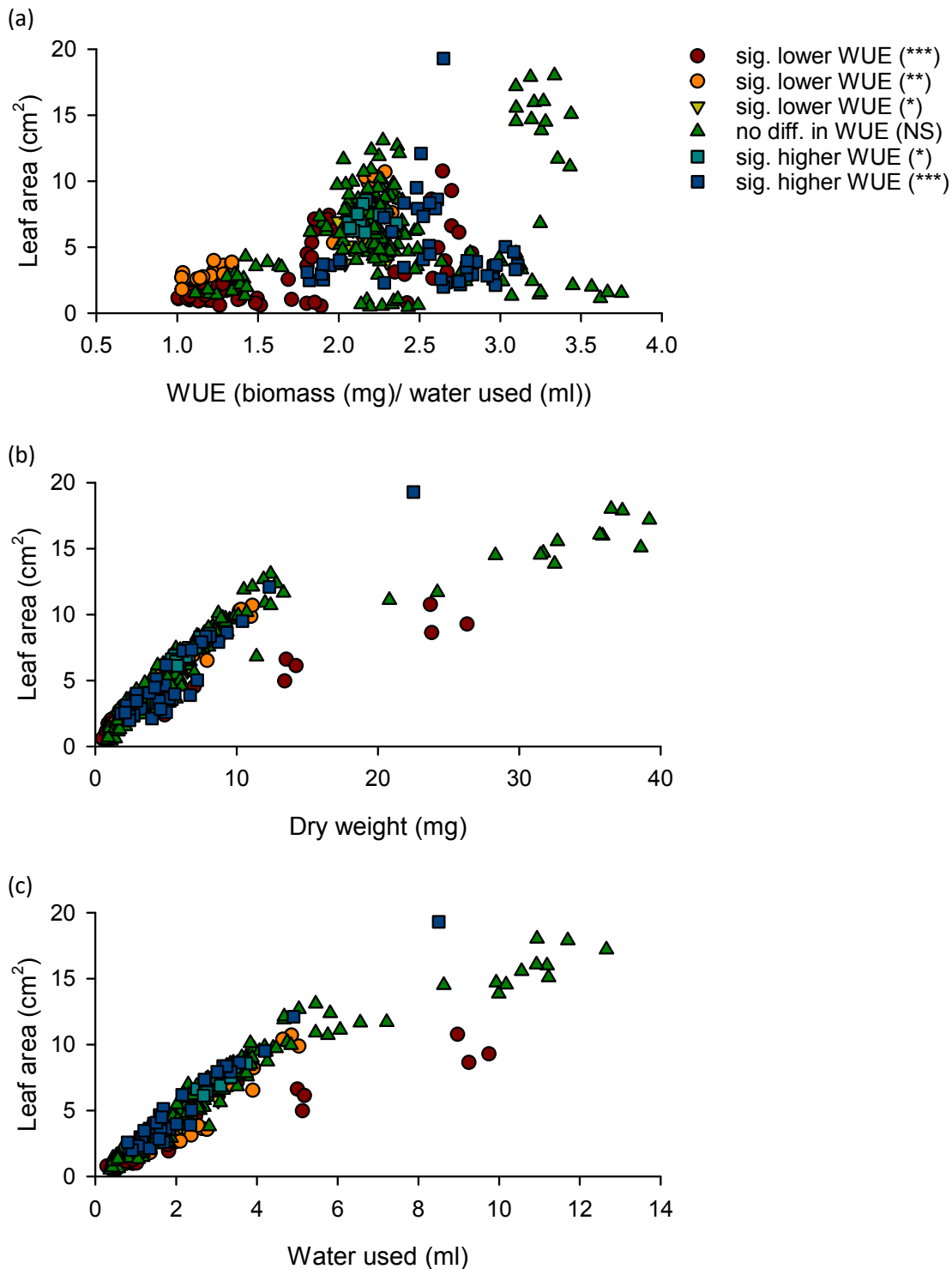


Figure 3.9: Rosette architecture affects WUE. Rosette leaf surface area explains (a) 16% of variability in WUE, (b) 73% of variability in rosette dry biomass, and (c) 83% of variability in plant water use. Data show rosette leaf surface area and (a) WUE, (b) dry weight and (c) water use of plants screened for WUE that are represented in Fig. 3.5 ( $n = 337$ ). Different coloured symbols mark genotypes that had significantly lower or higher WUE compared to their background WT, with statistical significance data taken from Fig. 3.5.

might imply that water use varies with the number and/or density of stomata.

As seen previously (Fig. 3.6), alterations in WUE do not appear to be explained by rosette leaf surface area alone (Fig. 3.9a), nor combinations of rosette leaf surface area with dry weight (Fig. 3.9b) or water use (Fig. 3.9c). For example, plants that had significantly lower ( $p < 0.001$ ; red circles) or significantly higher ( $p < 0.001$ ; blue squares) WUE compared to the WT had a full range of leaf area, dry weight, and water use values (Fig. 3.9). In addition, there did not appear to be a clear pattern relating alterations in WUE and alterations in rosette leaf surface area: for example, both *prr7-11* and *grp7-1* had significantly higher WUE than the WT, but *prr7-11* and *grp7-1* had a larger and smaller rosette leaf surface area compared with the WT, respectively (Fig. 3.10). In a similar fashion, no clear pattern was distinguished when mean rosette leaf area was examined instead (Sup. Fig. 9.2). Therefore, although rosette architecture has an effect upon WUE, it appears likely that other factors are also involved in the regulation of whole plant WUE.

Overall, these data demonstrate that the circadian clock regulates whole plant WUE in *Arabidopsis* under light/dark conditions. Specific circadian clock genes were identified as important determinants of WUE. WUE is partly affected by rosette architecture, but rosette structure in turn is modulated by the circadian clock.

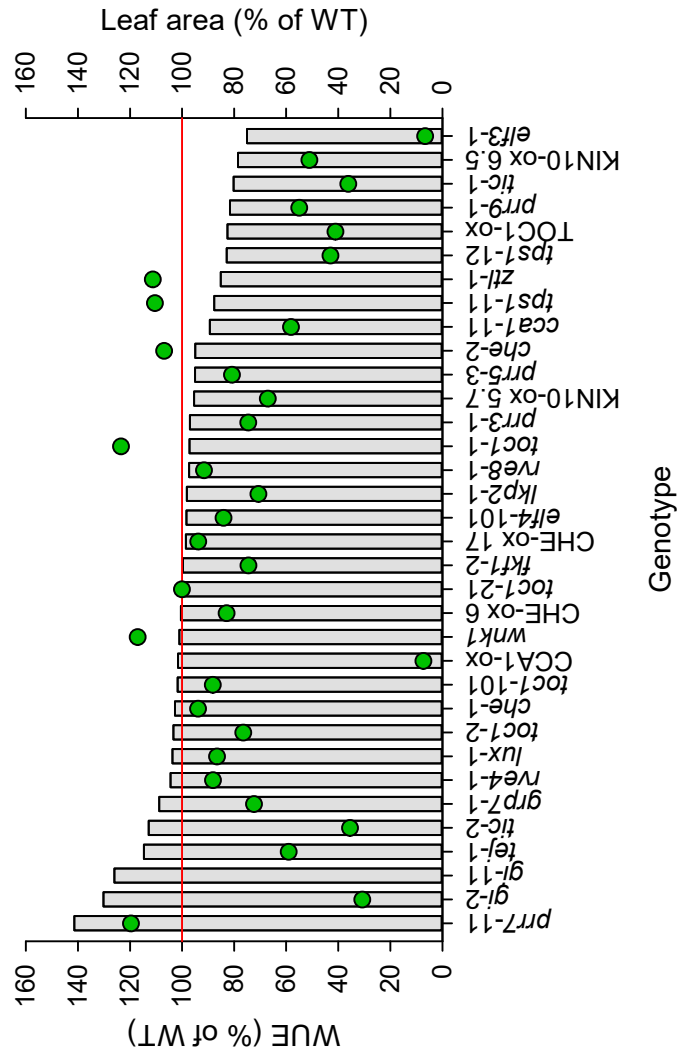


Figure 3.10: Variations in WUE are not fully explained by rosette leaf surface area. Data are redrawn from Fig. 3.5 and represent mean WUE of screened circadian clock mutants and overexpressors expressed as a percentage of their respective WT background ( $n = 5-15$ ). The red reference line indicates WT WUE (100%). Mean rosette leaf surface area for each genotype is also expressed as a percentage of the respective WT background (green;  $n = 5-15$ ). No leaf surface area data was obtained for *gl-11* due to experimental error. A supplemental figure showing mean rosette leaf surface area for each genotype is provided in the Appendix (Sup. Fig. 9.2).

### 3.4.3 Testing candidate mutants for dehydration tolerance

Genotypes with significantly higher or lower WUE than the WT were examined for their ability to survive dehydration. Although the ability to survive short-term dehydration is likely to be independent from whole plant WUE, it would be interesting to investigate both traits. Briefly, 2 week-old seedlings were dehydrated on filter paper for 9 h under constant light conditions, then re-watered and maintained under constant light conditions for a further 48 h (Legnaioli et al. (2009)). Seedling survival was normalised to the background, with seedlings having a green apical meristematic region counted as survivors. Two independent experimental repeats were performed per genotype. Data presented here are from one experimental repeat (Fig. 3.11); additional data are

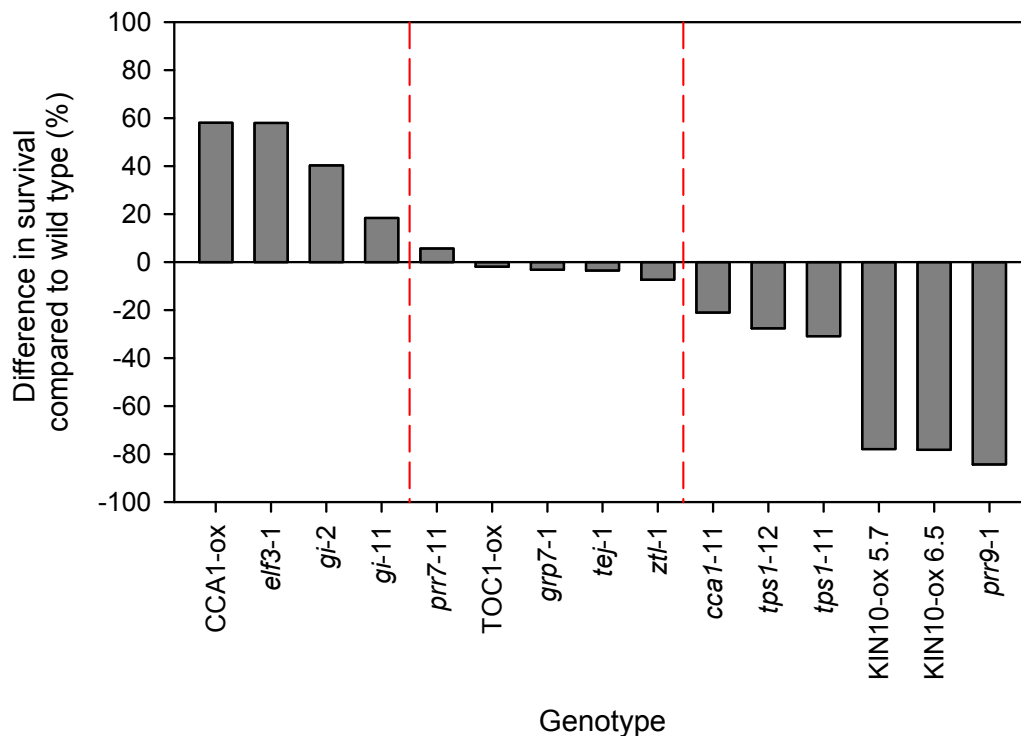


Figure 3.11: *CCA1*, *ELF3*, *GI*, *TOC1* and *PRR9* regulate seedling response to dehydration under constant light conditions. Data show percentage difference in dehydration survival of genotypes compared to their backgrounds ( $n = 32$ ). Red, dotted reference lines separate genotypes with a substantially higher, equal, or substantially lower survival rate to dehydration compared to the WT, using a difference of  $>10\%$  as cutoff. Data are from one representative experimental repeat; additional data are provided in the Appendix (Sup. Fig. 9.3).

provided in the Appendix (Sup. Fig. 9.3).



Interestingly, *cca1-11* survived less than the WT, whereas CCA1-ox responded better than the WT to dehydration conditions (Fig. 3.11). TOC1-ox and *prp9-1* survived less than the WT under these dehydration conditions, while mutations in *GI* and *ELF3* increased plant tolerance to water-deficit conditions (Fig. 3.11). Although KIN10-ox and *tps1* alleles had low survival to dehydration (Fig. 3.11), their poor growth on media supplemented with sucrose may confound results. Overall, these data imply that CCA1, ELF3, GI, TOC1 and PRR9 contribute to seedling responses to dehydration (Fig. 3.11; Sup. Fig. 9.3).

## 3.5 Discussion

### 3.5.1 Development of WUE assay

A method inspired by Wituszynska et al. (2013) was optimised to screen Arabidopsis circadian clock mutants and overexpressors for whole plant WUE. Our optimised screening method produced robust (Fig. 3.4a) and accurate (Fig. 3.4b) data in line with previous reports (Nienhuis et al. (1994); Dodd et al. (2004); Masle et al. (2005); Karaba et al. (2007); Ruggiero et al. (2017); Ferguson et al. (2018)).

WUE was affected by rosette architecture. Rosette leaf surface area explained 16% of variation observed in WUE (Fig. 3.9a), and leaf overlap, although representing a small proportion of rosette surface (Fig. 3.9b), may influence WUE by decreasing the effective photosynthetic surface. Leaf surface area might also affect water use by altering the number and/or density of stomata (Fig. 3.9c). Although the effect of rosette architecture upon WUE is non-negligible, the majority of variation observed in WUE remains unexplained (Fig. 3.10). One possibility may involve unstirred boundary layers around individual leaves, which affect transfer of gases and water vapour. For example, increasing boundary layer effects can improve WUE through decreased transpiration (Condon et al. (2002); Ruggiero et al. (2017)).

Alternatively, alteration in WUE might be caused by disruption of the circadian network, or the indirect repercussions of such a disruption. In addition, the circadian clock modulates rosette architecture (Ruts et al. (2012); Rubin et al. (2018)). Therefore, the circadian oscillator might indirectly affect WUE through modifications in rosette characteristics.

### 3.5.2 The circadian clock regulates WUE

These results suggest that the circadian clock regulates WUE in *Arabidopsis* under diel conditions. In particular, I found that *CCA1*, *ELF3*, *GI*, *GRP7*, *KIN10*, *PRR5*, *PRR7*, *PRR9*, *TEJ*, *TOC1*, *TPS1* and *ZTL* affect WUE under these experimental conditions, with *CCA1*, *ELF3*, *GI*, *PRR9* and *TOC1* also affecting survival to dehydration.

There was no obvious relationship between WUE under diel conditions and dehydration survival under constant conditions. For example, both *gi* alleles had higher resistance to dehydration and higher WUE than the WT, whereas *elf3-1* and *CCA1-ox* had high dehydration survival but low WUE (Figs. 3.5, 3.11). Although genotypes were normalised to their backgrounds, the accession might affect dehydration survival. *tej-1* and *ztl-1* had a nearly 100% survival, like their C24 background: therefore, the influence of the C24 accession may mask effects caused by the circadian mutation over the short (48 h) time frame of the dehydration assay. In addition, *KIN10-ox* and *tps1* alleles grew poorly on media supplemented with sucrose, which might have exacerbated their low dehydration survival. Finally, data from *prp5-3* were too variable to extrapolate a clear role for *PRR5* in dehydration survival. Therefore, although it is possible that *PRR5*, *TEJ*, *ZTL*, *KIN10* and *TPS1* regulate plant response to dehydration, our results do not allow clear conclusions for these genes.

The time of peak expression of each mutated gene, altered period, and altered flowering time did not seem to explain variations in WUE (Fig. 3.7). The diel conditions of the WUE screen may have partially rescued these circadian defects. As the circadian oscillator is reset at dawn, the misregulated circadian clocks of screened plants would be able to re-adjust to the environment every dawn. Therefore, differences between the free running period of circadian clock mutants and overexpressors and the period of the external environment would increase as the day continues, reaching a maximum prior to dawn (Dodd et al. (2014)). This in turn may affect stomatal closure and aperture in anticipation of dusk and dawn, respectively (Somers et al. (1998); Dodd et al. (2004, 2005); Resco de Dios et al. (2016); Joo et al. (2017); Hassidim et al. (2017)). For example, under diel conditions, an “internal signal” was found to play an important role in acclimating stomatal conductance to environmental light conditions, regulating up to 25% of the total diurnal stomatal conductance (Matthews et al. (2018)). This coordination between stomatal conductance and light signals could condition plant responses to future diurnal variations in light intensity and pattern, thereby enabling the

plant to maintain carbon fixation and water status (Matthews et al. (2018)). Therefore, although no grouping circadian period, phase of expression, and flowering time variables were found amongst the screened genotypes (Fig. 3.7), it is likely that they still affect stomatal behaviour and WUE.

Mutating or overexpressing a circadian clock component is likely to impact other circadian clock elements, and feedback loops further complicate analysis. Moreover, transcript and protein abundance data for circadian clock mutants are often obtained under constant conditions in the literature, with constant light, darkness or red light being the most common treatments. However, these data are not comparable to the light/dark conditions of my WUE screen, as light input affects the circadian clock. For example, *elf3-1* is arrhythmic under constant light conditions but has circadian rhythms under constant darkness (Wang and Tobin (1998)). Consequently, it is not possible to assume that a mutation affecting transcript and/or protein abundance of another gene under one light condition would regulate that same gene in a similar fashion under a different light condition. For example, under diel conditions, *Gl* and *TOC1* transcript abundance were unaltered in *tic-1* (Ding et al. (2007b)), whereas, under constant light conditions, *Gl* and *TOC1* expression decreased significantly in *tic-1* (Hall et al. (2003)).

With this in mind, I have first analysed each gene individually in the wider context of the literature, then hypothesised which interactions might be particularly important.

### **3.5.2.1 Core circadian clock genes *CCA1* and *TOC1* affect WUE**

*cca1-11* had decreased WUE compared to the WT (Fig. 3.5), while *CCA1-ox* varied between experimental repeats, with WUE being unaltered in one repeat (Fig. 3.5) and significantly decreased in the other (Sup. Fig. 9.1). This suggests that misregulating *CCA1* negatively impacts WUE. Indeed, overexpressing *CCA1* affects rhythms of stomatal opening and CO<sub>2</sub> fixation under constant conditions (Dodd et al. (2005)). Even under diel conditions, *CCA1-ox* cannot anticipate dawn or dusk, causing stomata to remain open throughout the light period rather than closing after midday and leading to a higher total transpiration (Dodd et al. (2005)). In addition, several links between *CCA1* and ABA have been established (Hanano et al. (2006); Grundy et al. (2015)).

Interestingly, the *CCA1* overexpressor and mutant had opposite phenotypes in the dehydration assay, with a higher and lower survival rate for *CCA1-ox* and *cca1-11*, respec-

tively (Fig. 3.11). This complements findings of Legnaioli et al. (2009), where TOC1-ox had decreased survival while *TOC1* RNAi survived better than the WT.

It would be interesting to investigate whether *CCA1* and *TOC1* affect survival to dehydration independently, or whether a single gene underlies this effect. Indeed, under constant light conditions, *CCA1*-ox has low, arrhythmic *TOC1* abundance (Alabadí et al. (2001); Matsushika et al. (2002)), whereas both *cca1-11* and *TOC1*-ox have lower *CCA1* expression than the WT (Makino et al. (2002); Más et al. (2003a); Hall et al. (2003); Ding et al. (2007a); Gendron et al. (2012)). Therefore, the low survival of *TOC1*-ox in this assay could be due to altered *CCA1* transcript abundance, or vice-versa. Alternatively, these phenotypes could be explained by other mechanisms involved in drought resistance, such as responses to reactive oxygen species (ROS). For example, *CCA1*-ox has higher expression of genes involved in ROS signalling and reacts better than the WT to ROS stress (Lai et al. (2012)). Perhaps further experimentation using double mutants would resolve this question.

Although overexpressing *TOC1* decreased both WUE and survival to dehydration, none of the screened *toc1* alleles had altered WUE (Fig. 3.5). It is likely that *TOC1* regulates WUE, as it modulates circadian rhythms of stomatal aperture (Somers et al. (1998)) and is involved in the bidirectional relationship between the circadian clock and ABA (Legnaioli et al. (2009); Sanchez et al. (2011)). In addition, *toc1-1* affects the period of CO<sub>2</sub> assimilation and stomatal aperture under constant light (Dodd et al. (2004)), and *TOC1* RNAi is drought-tolerant whereas *TOC1*-ox is drought sensitive compared to the WT (Legnaioli et al. (2009)).

There are at least two possible explanations for why *toc1-1*, *toc1-2*, *toc1-21* and *toc1-101* did not have altered WUE: either *toc1* effects upon WUE were overcome by the diel conditions of the screen, or *TOC1* overexpression had a stronger effect upon WUE than decreased *TOC1* transcript abundance. Interestingly, two mutants with high *TOC1* transcript and protein levels under light/dark conditions, *prr9-1* and *ztl-1*, also have low WUE (Fig. 3.5) (Farré et al. (2005); Más et al. (2003b)). *TOC1*-ox and *cca1-11* also have similar phenotypes, as both have low *CCA1* expression (Makino et al. (2002); Más et al. (2003a); Hall et al. (2003); Ding et al. (2007a); Gendron et al. (2012)) and significantly lower WUE (Fig. 3.5).

### 3.5.2.2 The evening complex may not regulate WUE

Our finding that *ELF3* is important for WUE is in line with previous evidence. Under constant light conditions, wild type *Arabidopsis* has circadian rhythms of stomatal aperture whereas *elf3* stomata are constantly open and arrhythmic (Kinoshita et al. (2011)). In addition, *ELF3* negatively regulates blue light-mediated stomatal opening (Kinoshita and Hayashi (2011); Chen et al. (2012)).

Interestingly, *ELF3* binds to the *PRR9* promoter and *elf3-1* has elevated *PRR9* transcript abundance (Thines and Harmon (2010); Dixon et al. (2011); Herrero et al. (2012)). The low WUE of *elf3-1* could be caused by altered *PRR9* expression, particularly as *PRR9* affects both WUE and survival to dehydration under our experimental conditions (Figs. 3.5, 3.11). In a similar fashion, *ELF3/ELF4* signalling represses *PRR7*, and *elf3-1* has elevated *PRR7* transcript abundance (Herrero et al. (2012)). Under diel conditions, *elf3-1* also has high, constitutive *GI* expression (Fowler et al. (1999)), and *elf3-1* and *gi* have opposite WUE phenotypes (Fig. 3.5). Therefore, the WUE phenotype observed in *elf3-1* might be caused by *ELF3* disruption, or alterations in *PRR7*, *PRR9* and/or *GI* transcript abundance.

Unexpectedly, mutating other core genes of the evening complex (EC), *ELF4* and *LUX*, did not affect WUE (Fig. 3.5). Indeed, these genes influence the circadian clock and plant physiology (Hsu and Harmer (2014); Huang and Nusinow (2016)), and nocturnal regulation of stomatal aperture impacts WUE (Costa et al. (2015); Coupel-Ledru et al. (2016)). One possibility is that *ELF3* is key to EC scaffolding, with *ELF3* functioning genetically downstream from *ELF4* and *LUX* circadian function requiring *ELF3* action (Herrero et al. (2012); Huang and Nusinow (2016)); thus the impact of *elf3* on WUE might be greater than that of *elf4* or *lux*.

Alternatively, *ELF4* seems to play a greater role in the vasculature tissue than in stomatal guard cells, with expression in the vasculature up to ten times higher than other tissues (Endo et al. (2014)). As *elf3-1* affects WUE differently than *elf4-101* and *lux-1*, it may also be possible that *ELF3* regulates WUE independently from *ELF4* and *LUX*. The reverse explanation is likely as well: as *ELF3* is the only EC gene to affect WUE, perhaps the EC is not involved in regulating WUE.

### 3.5.2.3 WUE is regulated by the PRRs

It is notable that three *PRRs* affect WUE (Fig. 3.5). These genes share partial redundancy (Hsu and Harmer (2014)). However, although *prp5-3* and *prp9-1* had lower WUE than the WT, *prp7-11* had higher WUE (Fig. 3.5). Furthermore, out of the *prp5*, *prp7* and *prp9* mutants examined, only *prp9-1* had a significantly different survival rate to dehydration under our experimental conditions (Fig. 3.11). As both *prp7-11* and *prp9-1* mutants have unaltered *PRR3* and *PRR5* expression under light/dark conditions (Farré et al. (2005)), it is likely that *PRR7* and *PRR9* affect WUE independently from *PRR3* and *PRR5*. Overall, these differences suggest that the *PRRs* might play distinct roles in regulating WUE.

*PRR7* seems linked to ABA, as *ABA1*, a gene involved in ABA biosynthesis, is a putative *PRR7* target and ABA upregulates 28% of *PRR7* targets (Liu et al. (2013)). In addition, *PRR7* targets many drought-responsive genes and affects leaf stomatal conductance (Liu et al. (2013)). Interestingly, *PRR7* directly represses *PRR9* expression, and *PRR7-ox* has reduced *PRR9* transcript abundance (Liu et al. (2013)). This might explain why mutations in *PRR7* and *PRR9* cause opposite WUE phenotypes. *prp3-1* did not have altered WUE, which is likely due to the vasculature-specific function of *PRR3* (Para et al. (2007)).

Finally, several other genotypes with significantly altered WUE are reported to have altered *PRR* expression under light/dark conditions (Fig. 3.5). For example, *cca1-1* has reduced *PRR9* expression while *CCA1-ox* has increased *PRR7* and *PRR9* transcript abundance (Farré et al. (2005)); *TOC1-ox* has decreased *PRR9* and unaltered *PRR3*, *PRR5* and *PRR7* transcript abundance (Makino et al. (2002)); and *PRR5* abundance was increased in a *ztl* mutant (Kiba et al. (2007)). Therefore, the altered WUE in these genotypes might be due to changes in *PRR* transcript abundance.

### 3.5.2.4 GI and other ZTL-mediated protein degradations might affect WUE

*GI* regulates both WUE and survival to dehydration stress, with two *gi* alleles having significantly higher WUE and survival to dehydration than the WT (Figs. 3.5, 3.11). Interestingly, *elf3-1* has high, constitutive *GI* expression under diel conditions (Fowler et al. (1999)) and the opposite WUE phenotype to *gi* (Fig. 3.5). In addition, *elf3-1* and *ztl-1* have high and low levels of *GI* (Fowler et al. (1999); Kim et al. (2007)), respectively, and low WUE (Fig. 3.5). These data suggest that *GI* transcript and/or protein abundance

are important determinants of WUE.

It is unsurprising that *ZTL* was identified as a regulator of WUE, as *ZTL* is part of the network regulating rhythms of stomatal conductance (Dodd et al. (2004)). Interestingly, *ZTL* is a key regulator of circadian clock protein degradation. *GI* and *ZTL* stabilise each other in a cooperative manner: *gi* mutants strongly diminish *ZTL* protein abundance, while *ztl* mutants have reduced *GI* protein abundance (Kim et al. (2007)). This suggests a conundrum in our results: based on previous literature, both *gi* and *ztl* mutants have reduced *GI* and *ZTL*, yet *gi-2* and *gi-11* are more water use efficient than the WT whereas *ztl-1* has reduced WUE (Fig. 3.5). This implies that protein interactions between *GI* and *ZTL* do not play a role in regulating WUE, but rather that *GI* and *ZTL* affect WUE independently.

*ZTL* targets *PRR5* for degradation, and *ztl* mutants have increased *PRR5* abundance (Kiba et al. (2007)). Both *prr5-3*, with decreased *PRR5* abundance (Michael et al. (2003)), and *ztl-1*, with elevated *PRR5* abundance (Kiba et al. (2007)), have low WUE (Fig. 3.5). This indicates that alterations in *PRR5* abundance negatively affect WUE. In addition, *PRR5* is required for correct *ZTL* circadian function (Kiba et al. (2007)), but it is unknown whether *ZTL* transcript and/or protein abundance are affected in *prr5-3* under light/dark conditions. If this was the case, it may indicate a role for *ZTL-PRR5* interactions in modulating WUE. It is also possible that *PRR5* and *ZTL* regulate WUE in an independent manner.

Unexpectedly, *lkp2-1* did not have altered WUE (Fig. 3.5). Overexpressing *LKP2* enhances drought tolerance by increasing expression of drought-responsive genes and reducing stomatal aperture (Miyazaki et al. (2015)). Although *LKP2* and *ZTL* are functionally homologous proteins, *LKP2* transcript abundance represents 4% of that of *ZTL* (Baudry et al. (2010)). In our screen, *ztl-1* had significantly lower WUE than the WT, while *lkp2-1* had a slight, albeit not statistically significant, decrease in WUE (Fig. 3.5). Therefore, it is possible that *lkp2-1* might be partly rescued by *ZTL*, thereby concealing any effect on WUE.

*FKF1* is redundant with *ZTL* and *LKP2* in flowering time signalling, and stabilises *TOC1* and *PRR5* as well (Imaizumi et al. (2003, 2005); Baudry et al. (2010)). It does not otherwise appear to be a core circadian clock regulator or affect processes other than flowering time, and *fkf1-2* did not alter WUE (Fig. 3.5).

### 3.5.2.5 *TEJ* and *GRP7* are likely to affect plant WUE indirectly

*TEJ* codes for a poly(ADP-ribose) glycohydrolase, which regulates protein poly(ADP-ribosylation) (Panda et al. (2002)). In Arabidopsis, *tej-1* increased amplitude and altered period length of over 450 clock-controlled genes by 4 - 8 h (Panda et al. (2002)). To our knowledge, *TEJ* does not affect water use or drought tolerance. Therefore, it is possible that the negative effect of *tej-1* upon WUE (Fig. 3.5) was indirectly caused by its effects on other circadian clock genes. Alternatively, *TEJ* might be affecting WUE through a mechanism independent of rhythmicity, such as by affecting transcription factor activity through poly(ADP-ribosylation) (Panda et al. (2002)).

In a similar fashion, *grp7-1* had low WUE (Fig. 3.5). *GRP7* autoregulates its transcriptional oscillations through alternative splicing and affects transcription of other circadian clock genes (Streitner et al. (2008)). However, few links have been made between *GRP7* and the core circadian clock network and none regarding water use. The negative effect of *grp7-1* upon WUE could be achieved via a clock-independent mechanism or unknown interactions with other circadian clock genes.

### 3.5.2.6 *TIC*, *CHE*, *RVE4*, *RVE8*, and *WNK1* do not seem to influence WUE

Two *tic* alleles did not have altered WUE (Fig. 3.5). *TIC* regulates osmotic and drought stress, carbohydrate metabolism, and ABA responses, and both *tic-1* and *tic-2* have growth and development defects (Shin et al. (2013); Sánchez-Villarreal et al. (2013)). Furthermore, *tic-2* alters expression of *ELF3*, *GI*, *TOC1*, *LHY*, *PRR3*, *PRR5*, and *PRR7* under light/dark conditions (Sánchez-Villarreal et al. (2013)). In contrast, under diel conditions, *tic-1* does not affect *ELF3*, *GI* and *TOC1* transcript abundance, and *TIC* expression was unaltered in several circadian clock mutants, including *toc1-21*, *gi-11*, *elf3-4* and *cca1-11* (Ding et al. (2007a)). Overall, our results suggest that *TIC* does not regulate WUE under our experimental conditions.

*CHE* modulates *CCA1* expression via interactions with *TOC1* (Hsu and Harmer (2014)). *CHE* does not regulate WUE, as two *CHE* overexpressors and two *che* mutants had similar WUE to the WT (Fig. 3.5). This was also the case for *RVE4* and *RVE8*, as neither *rve4-1* nor *rve8-1* had altered WUE (Fig. 3.5). Mutants with lower *RVE8* transcript abundance under diel conditions either did not have altered WUE, such as *toc1-1* or *lux-1*, or had pleiotropic effects, such as *CCA1-ox* (Fig. 3.5). This might be because *rve8-1* does not



affect transcription of several core clock genes, including *CCA1*, *LHY*, *PRR5*, *PRR7* and *TOC1* (Rawat et al. (2011); Hsu et al. (2013)).

*wnk1* did not have altered WUE (Fig. 3.5), suggesting that *WNK1* does not regulate WUE under our experimental conditions. This may seem surprising, as, in rice, *OsWNK1* is implicated in abiotic stress tolerance (Kumar et al. (2011)). In Arabidopsis, *WNK1* phosphorylates *PRR3* *in vitro* and *wnk1* has decreased *ELF4* and *TOC1* transcript abundance (Nakamichi et al. (2002); Wang et al. (2008)). However, mutations in *PRR3*, *ELF4* and *TOC1* also did not alter WUE under our conditions (Fig. 3.5).

### 3.5.2.7 The energy-sensing and WUE pathways may be interacting

*KIN10* is the catalytic subunit of the major energy-sensing and signalling hub *SnRK1*, which regulates expression of over 1000 genes under low sugar conditions (Baena-González et al. (2007)). Two *KIN10-ox* alleles had low WUE and survival to dehydration (Figs. 3.5, 3.11). *KIN10* genetically interacts with *TIC* to regulate the circadian clock under diel conditions (Shin et al. (2017)), but two *tic* alleles had unaltered WUE (Fig. 3.5). In addition, although overexpressing *KIN10* causes a peak delay of *GI* under diel conditions, expression of other core circadian clock genes, such as *LHY*, *CCA1*, *PRR7*, *TOC1* and *ELF4*, is unchanged (Shin et al. (2017)). Therefore, the effects of *KIN10-ox* upon WUE and survival to dehydration are unlikely to be caused by the relationship between *KIN10* and the circadian clock. Instead, it may be due to the impact of *KIN10* overexpression on metabolic and transcriptional signalling.

In a similar fashion, mutating *TPS1*, a central regulator of T6P carbon signalling, decreased WUE and survival to dehydration (Fig. 3.5). Although no link has been reported between *TPS1* and the circadian clock, *TPS1* is essential for induction of *FT*, a gene required for flowering, and flowering time is controlled by the circadian clock (Wahl et al. (2013)). However, *tps1-11* and *tps1-12* have slow growth and delayed flowering (Gomez et al. (2010)), which may affect WUE.

## 3.6 Conclusions

In this chapter, the WUE of a variety of circadian clock mutants and overexpressors was investigated, and the obtained results suggest the following:

- The circadian clock regulates whole plant WUE under diel conditions in *Arabidopsis*.
- Circadian control of WUE occurs partly through modifications in rosette architecture.
- Due to the interlocking nature of the circadian clock, it was not possible to identify specific effects of individual circadian clock genes upon WUE by using this experimental setup. However, several broad conclusions can still be reached:
  - *CCA1*, *TOC1*, *ELF3*, *GI*, *GRP7*, *PRR5*, *PRR7*, *PRR9*, *TEJ* and *ZTL* regulate WUE under these experimental conditions.
  - *KIN10* and *TPS1* also appear to regulate WUE, indicating a possible relationship between WUE and energy-sensing pathways under these experimental conditions.
  - *CHE*, *FKF1*, *LKP2*, *RVE4*, *RVE8*, *PRR3*, *ELF4*, *LUX*, *TIC* and *WNK1* do not appear to regulate WUE under our experimental conditions.

In future, it would be informative to further identify specific mechanisms by which the *CCA1*, *TOC1*, *ELF3*, *GI*, *GRP7*, *PRR5*, *PRR7*, *PRR9*, *TEJ* and *ZTL* circadian oscillator components contribute to WUE. It would also be interesting to distinguish whether the circadian clock within different plant tissues, such as stomatal guard cells, particularly affect WUE.



## Chapter 4

# Generating, genotyping and validating transgenic *Arabidopsis* with misregulated guard cell circadian clocks

### 4.1 Introduction

Low soil water availability represents a threat to contemporary agriculture, causing substantial decreases in crop yield and seed production throughout the world (Ruggiero et al. (2017)). Due to the large impact of stomata on transpiration (Na and Metzger (2014)), guard cells have become a clear target to improve water use.

There is increasing evidence that different circadian clocks exist within distinctive plant tissues and communicate with each other to create an overarching hierarchical circadian structure (James et al. (2008); Yakir et al. (2011); Wenden et al. (2012); Endo et al. (2014); Takahashi et al. (2015); Bordage et al. (2016); Kim et al. (2016); Hassidim et al. (2017)). Previous work suggests that the circadian clock is present within guard cells and regulates its activity (Somers et al. (1998); Dodd et al. (2004); Hassidim et al. (2017)). Therefore, it is important to understand the circadian clocks of single cell types, such as guard cells, to fully comprehend how they affect the plant as a whole (Hubbard and Webb (2011); Kinoshita et al. (2011); Hassidim et al. (2017)).

Previously, I showed that the circadian clock affects WUE (Chapter 3). To study this

further, I decided to manipulate the guard cell circadian clock to study the role of specifically the guard cell circadian clock in regulating WUE. Overexpressing key circadian clock components is an effective method to induce arrhythmicity in tissue-specific circadian clocks (Endo et al. (2014); Shimizu et al. (2015); Hassidim et al. (2017)). *CCA1* and *TOC1* participate in one of the core transcriptional feedback loops (Fig. 1.3) (Alabadí et al. (2001); Pruneda-Paz et al. (2009); Gendron et al. (2012); Huang et al. (2012); Hsu and Harmer (2014)). *GC1* and *MYB60* promoters are guard cell-specific with high expression levels and have been used previously to overexpress proteins within guard cells (Cominelli et al. (2005); Galbiati et al. (2008); Nagy et al. (2009); Cominelli et al. (2011); Meyer et al. (2010); Rusconi et al. (2013); Yang et al. (2008); Wang et al. (2014); Hassidim et al. (2017)).

## 4.2 Hypothesis and aims

This is essentially a methodological chapter, detailing the processes and verification steps used to produce transgenic *Arabidopsis* with arrhythmic guard cell circadian clocks for Chapter 5. We anticipate that using the strong, guard cell-specific *GC1* and *MYB60* promoters to overexpress the core circadian clock *CCA1* and *TOC1* genes will misregulate the guard cell circadian clock only. Due to the technical difficulties of extracting RNA from guard cells, a variety of control and proxy techniques were used to establish the correct functioning of these transgenic genotypes.

## 4.3 Methods and methodology

Several cloning and floral dipping protocols were tested and adopted to generate the transgenic *Arabidopsis*:

- For cloning of terminator and promoter sequences, the restriction digest method from the Dodd laboratory, PCR product clean-up method using the Macherey-Nagel Nucleospin gel and PCR clean-up kit, ligation method from the Dodd laboratory, and *E. coli* transformation method from the Dodd laboratory were used.
- For cloning of coding sequences, the restriction digest method from the Het-

herington laboratory, PCR product clean-up method using dialysis tubing, sub-cloning method into the cloning vector pJET, ligation method from the Hetherington laboratory, and *E. coli* transformation method from the Hetherington laboratory were used.

- Floral dip methods from the Dodd, Schumacher, and Franklin laboratories were tested simultaneously for all plasmids due to difficulties obtaining positive transformants, and as screening for positive transformants is time-consuming.

All used cloning protocols (section 2.5.7) and floral dipping protocols (section 2.5.8.2) are provided in Chapter 2. A single protocol was used to screen for positive transformants (Chapter 2, section 2.5.8.3).

Validating the transgenic genotypes involved several lines of work and methodologies, including:

- generation of stable control genotypes containing *GREEN FLUORESCENCE PROTEIN (GFP)* and *LUCIFERASE (LUC)* coding sequences
- transient transformation of *Arabidopsis* seedlings and *Nicotiana benthamiana* (protocols provided in Chapter 2, section 2.5.9)
- confocal microscopy (protocol provided in Chapter 2, section 2.12)
- luciferase bioluminescence imaging (protocol provided in Chapter 2, section 2.13)
- qRT-PCR (protocol provided in Chapter 2, section 2.5.4.5)
- guard cell RNA extractions using the “ice-blender” method adapted from Bauer et al. (2013) and the “epidermal peel” method developed by Dr Ioanna Kostaki (protocols provided in Chapter 2, section 2.7.7)

Genes examined by qRT-PCR in this chapter are provided in Table 4.1, below. Primer sequences used for cloning, sequencing and verification steps, and qRT-PCR are provided in Tables 2.4, 2.5, and 2.7, respectively (Chapter 2).

<b>AGI code</b>	<b>Gene</b>	<b>Tissue specificity</b>
AT2G46830	<i>CCA1</i>	
AT5G61380	<i>TOC1</i>	
AT1G22690	<i>GC1</i>	guard cells
AT1G08810	<i>MYB60</i>	guard cells
AT5G46240	<i>KAT1</i>	guard cells
AT2G05100	<i>LHCB2.1</i>	mesophyll
AT5G54250	<i>CNGC4</i>	mesophyll
AT2G26250	<i>FDH</i>	epidermis
AT5G10180	<i>SULTR2;1</i>	vasculature
	<i>GFP</i>	

Table 4.1: Genes examined by qRT-PCR in Chapter 4. Tissue-specificity is indicated for reporter genes. Genes were chosen based on previous studies (Yang et al. (2008); Endo et al. (2014); Bauer et al. (2013); Efremova et al. (2004); Kataoka et al. (2004); Takahashi et al. (2000)).

## 4.4 Results

### 4.4.1 Vector design

The *MYB60* and *GC1* promoters, *CCA1* and *TOC1* coding sequences (CDS) and CaMV *nos* terminator were selected to create expression cassettes within the pGreenII 0229 plasmid (Fig. 4.1) (Hellens et al. (2000)). Additional vectors containing *GC1* and *MYB60* promoters expressing *GFP* or *LUC* CDS were devised as controls to examine promoter activity.

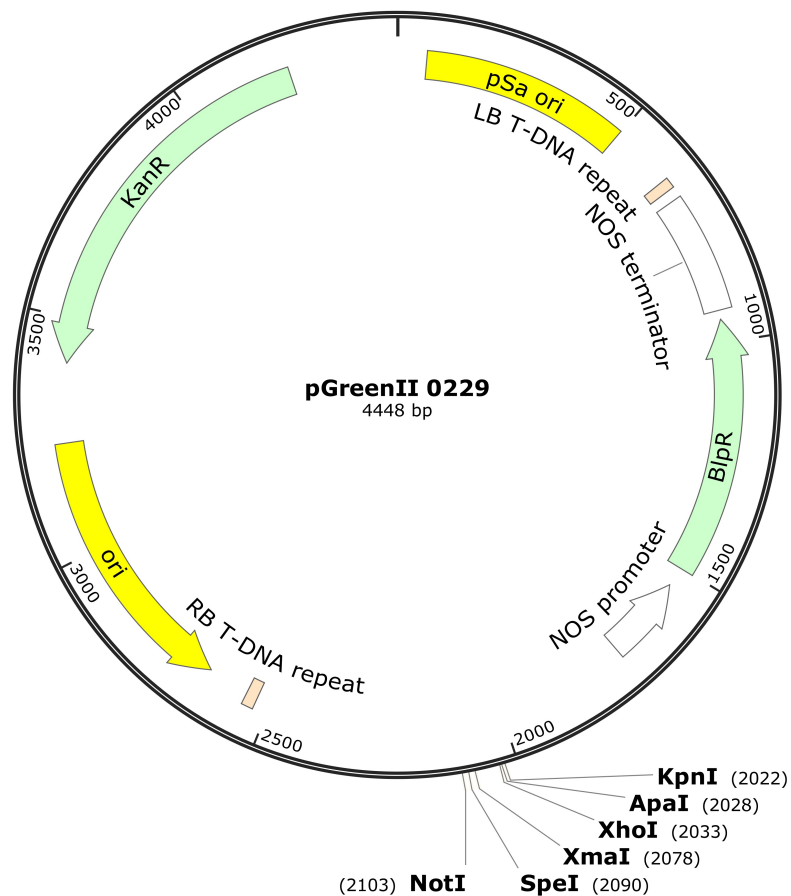


Figure 4.1: Map of the pGreenII 0229 plasmid. Elements used during cloning are represented: in green are resistance genes for kanamycin (*KanR*; for *E. coli* screening) and phosphinothricin (*BipR*; for screening of Arabidopsis transformants); in white is the *nos* expression cassette for correct expression of the phosphinothricin resistance CDS; in orange are the T-DNA borders; in yellow are the origins of replication; and relevant restriction sites are marked in bold. This plasmid was created by Hellens et al. (2000).



#### 4.4.2 Generation of expression cassettes

Expression cassettes were generated using pGreenII 0229 (Fig. 4.1). The CaMV *nos* terminator was inserted first using 5' *SpeI* and 3' *NotI* restriction sites. This plasmid was used as a base to insert *GC1* and *MYB60* promoter sequences between 5' *KpnI* and 3' *Apal* restriction sites. Finally, CDS with 5' *XhoI* and 3' *XmaI* restriction sites were inserted between the promoter and terminator sequences.

High fidelity copies of each sequence were acquired via Phusion PCR, cleaned, and verified by gel electrophoresis, then the purified product and pGreenII 0229 were digested. The Dodd laboratory restriction digest method was employed for insertion of the CaMV *nos* terminator and *GC1* and *MYB60* promoter sequences. This method did not always result in fully digested products, impeding future steps in the cloning process. The Hetherington laboratory method was tested, found to be more effective, and adopted to digest all CDS.

Digests were purified and ligated. As problems occurred repeatedly at this stage, several methods were trialled. Using the Macherey-Nagel Nucleospin gel and PCR clean-up kit alone yielded acceptable, but not optimal, results. Digested terminator and promoter sequences were purified in this fashion, but several attempts were required to achieve acceptable yields. Gel extractions resulted in even lower concentrations of product. An alternative methodology using dialysis tubing was more successful, so was used to purify digested CDS.

In a similar fashion, the Dodd laboratory ligation method was performed first for the terminator and promoter sequences. This involved estimating digest concentrations via gel electrophoresis and a molecular ladder, and calculating the required mass of insert and vector to add to the ligation reaction. Due to a large number of failed reactions, an alternative approach was used for the CDS. These were first sub-cloned into pJET (Fig. 4.2), using carbenicillin for selection. The CDS were isolated from pJET via restriction digest, then ligated into the digested and purified pGreenII 0229 vector by adding set volumes of insert and vector to the reaction. This alternative methodology, although slightly longer and less precise, was extremely efficient and successful. This is likely due to the use of pJET, which eliminated non- or partially-digested insert sequences from subsequent steps.

Ligated products were transformed into *E. coli* by heat shock, and transformants se-

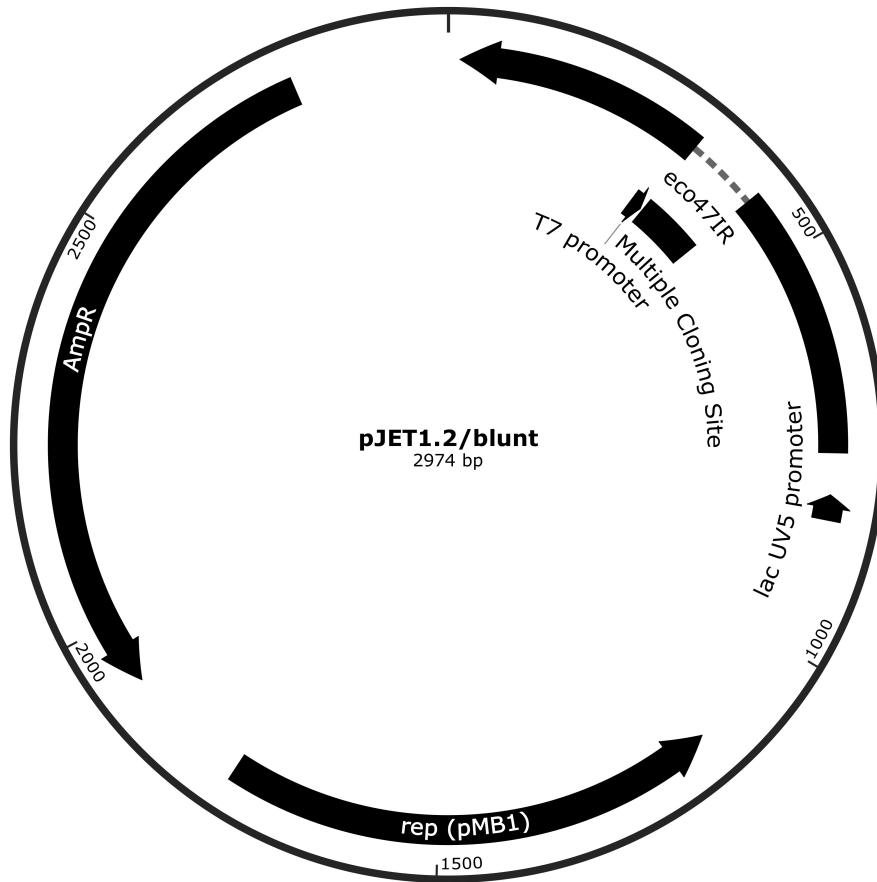


Figure 4.2: Map of the pJET cloning vector. The blunt-ended PCR product is inserted between 352 bp and 377 bp within the multiple cloning site. Ampicillin/carbenicillin resistance is provided by the *AmpR* CDS. This figure was derived from the concept of the CloneJET PCR Cloning Kit manual.

lected using kanamycin. The Dodd laboratory method was used for terminator and promoter sequences, while the Hetherington laboratory method was adopted for CDS. The Hetherington laboratory methodology yielded more positive colonies, which could either be due to the alternative heating and cooling approach employed during *E. coli* transformation, or the more successful digestion and ligation protocols used in previous steps.

Colony PCR screened colonies for the desired plasmid. Plasmids were sequenced to confirm correct sequence insertion and orientation, as well as absence of mutations (Sup. Fig. 9.7).

### 4.4.3 Generation of transgenic Arabidopsis

Each plasmid was co-transformed into *Agrobacterium* with pSOUP via electroporation (Fig. 4.3). A mixture of rifampicin, kanamycin and tetracycline was used to select for *Agrobacterium*, pGreenII 0229 and pSOUP, respectively. Surviving colonies were further screened by colony PCR (Fig. 4.4).

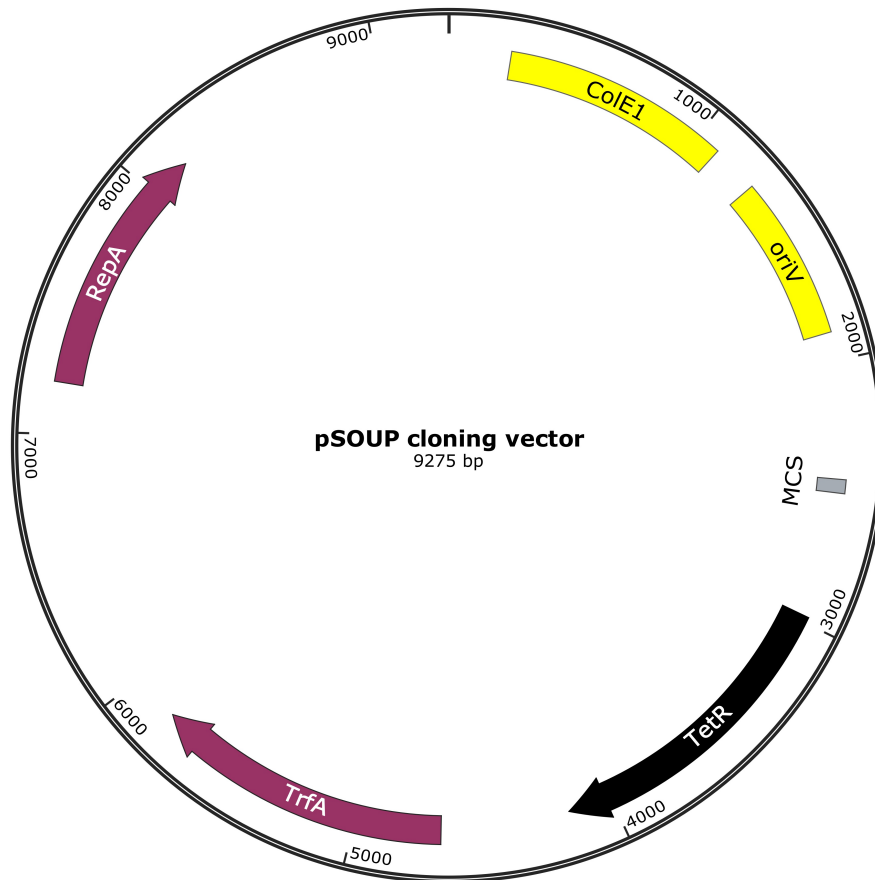


Figure 4.3: Map of the pSOUP helper plasmid. Tetracycline resistance is provided by the *TetR* CDS (black). In yellow are origins of replication; in purple are genes enabling replication; in grey is a multiple cloning site (MCS). pSOUP is required for pGreenII 0229 replication in *Agrobacterium* and was designed by Hellens et al. (2000).

WT Col-0 were transformed via floral dip, and the resulting seed was screened using phosphinothricin (Fig. 4.1). Problems occurred repeatedly at this stage, with few or no transformants obtained. To resolve this, floral dip was repeated several times for each plasmid. As screening for positive transformants is time-consuming, three different floral dip methodologies - from the Dodd, Schumacher and Franklin laboratories - were tested simultaneously for all plasmids. The Dodd laboratory method was the least

successful, requiring a large number of floral dips and high concentrations of *Agrobacterium* to obtain few transformants. The Schumacher laboratory methodology yielded slightly more positive transformants, but was extremely time-consuming as it involved pipetting suspended *Agrobacterium* culture onto individual floral buds. The Franklin laboratory approach was the most efficient, requiring the least preparatory work and generating the highest number of positive transformants.

T<sub>1</sub>, T<sub>2</sub> and T<sub>3</sub> seeds were screened using phosphinothricin. PCR was performed on T<sub>1</sub> DNA to confirm insertion of the desired construct (Fig. 4.5). Several independently transformed, homozygous alleles were obtained per construct.

For ease of understanding, independently transformed alleles were renamed as “1”, “2”, and such. In addition, different genotypes were abbreviated in the following manner:

- GC1::CCA1:nos as “GC”
- GC1::TOC1:nos as “GT”
- MYB60::CCA1:nos as “MC”
- MYB60::TOC1:nos as “MT”

Guard cell circadian clock gene overexpressors will also be referred to as “GCS-ox” from this point onwards. Details of each allele are provided in the Appendix (Table 9.1).

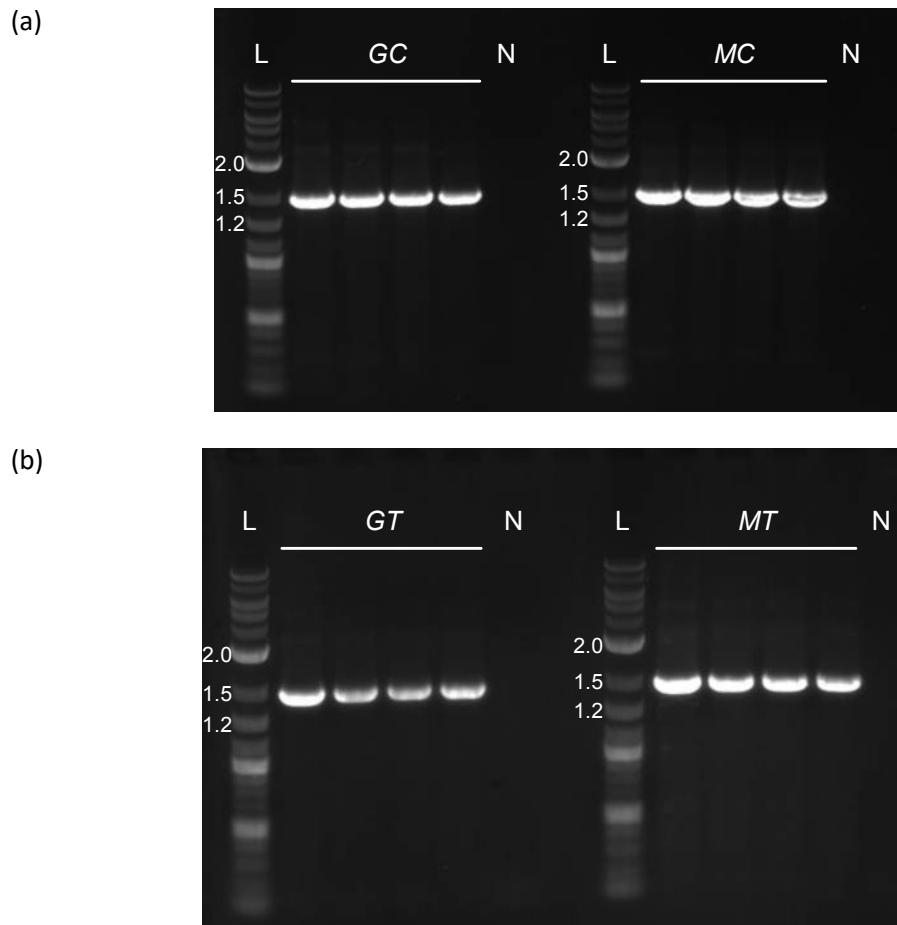


Figure 4.4: Screening *Agrobacterium* colonies for correct constructs. Gel electrophoresis showing results from *Agrobacterium* colony PCR for four colonies transformed with (a) GC1::CCA1:nos (*GC*, left) and MYB60::CCA1:nos (*MC*, right), and (b) GC1::TOC1:nos (*GT*, left) and MYB60::TOC1:nos (*MT*, right). The 2-Log DNA ladder (L) was used, with sizes of relevant reference bands marked (kb). A complete description of this ladder is provided in the Appendix (Sup. Fig. 9.4). Negative controls (N) contain dH<sub>2</sub>O instead of *Agrobacterium*. Forward primers are located on the promoter sequence; reverse primers are located on the CDS.

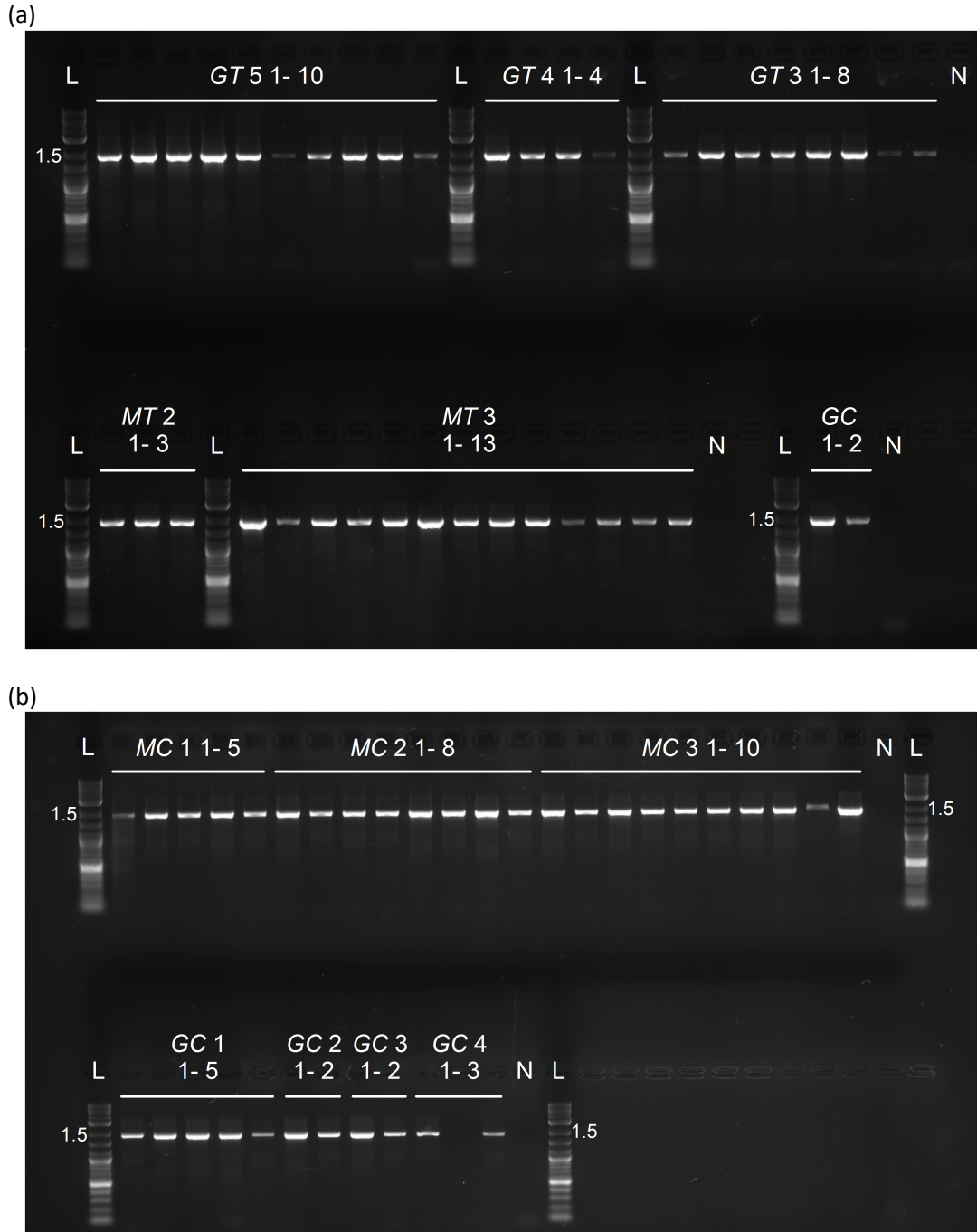


Figure 4.5: Screening  $T_1$  plants for positive transformants. Gel electrophoresis showing PCR results for  $T_1$  plants transformed with (a)  $GC1::TOC1:nos$  (*GT*, top),  $MYB60::TOC1:nos$  (*MT*) and  $GC1::CCA1:nos$  (*GC*) (bottom), and (b)  $MYB60::CCA1:nos$  (*MC*, top) and  $GC1::CCA1:nos$  (*GC*, bottom). Numbers correspond to  $T_0$  and  $T_1$  identity numbers for each construct. The 2-Log DNA ladder (L) was used, with sizes of relevant reference bands marked (kb). A full description of this ladder is provided in the Appendix (Sup. Fig. 9.4). Negative controls (N) contain  $dH_2O$  instead of DNA. Forward primers are located on the promoter sequence; reverse primers are located on the CDS.

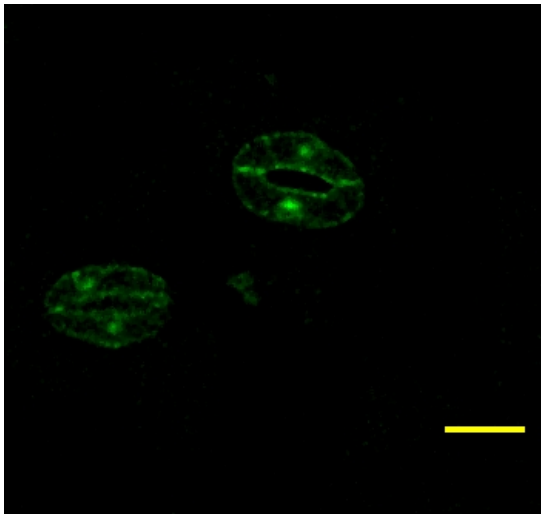
#### 4.4.4 Verifying guard cell specificity of the promoters

It was important to confirm that both *GC1* and *MYB60* promoters were guard cell-specific in my hands. Therefore, two control plasmids were created using the *GFP* CDS: *GC1::GFP:nos* and *MYB60::GFP:nos*. Insertion of *GFP* CDS into pGreenII 0229 was performed as for *CCA1* and *TOC1* CDS: *GFP* was inserted between 5' XhoI and 3' XmaI restriction sites in plasmids containing *GC1* and *MYB60* promoter sequences.

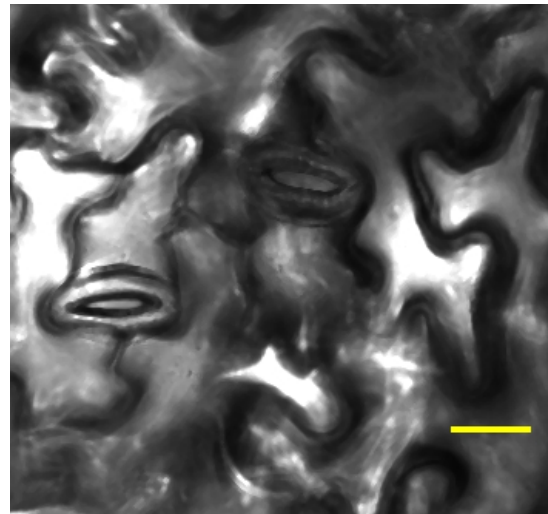
Two methods of transient expression were attempted. Col-0 seedlings were first transformed via vacuum infiltration, but this rendered GFP imaging impossible: the vacuum damaged cells and resulting chlorophyll fluorescence masked potential GFP signals. The second method involved transforming *Nicotiana tabacum* (tobacco) via a syringe, but the cellular damage caused by *Agrobacterium* also obscured possible GFP signals.

Consequently, stable *Arabidopsis* transformants were generated for the promoter-GFP constructs via floral dipping. Transformants were examined using confocal microscopy, with WT Col-0 as a negative control. GFP fluorescence was observed specifically within stomatal guard cells for both *GC1::GFP:nos* and *MYB60::GFP:nos* (Fig. 4.6).

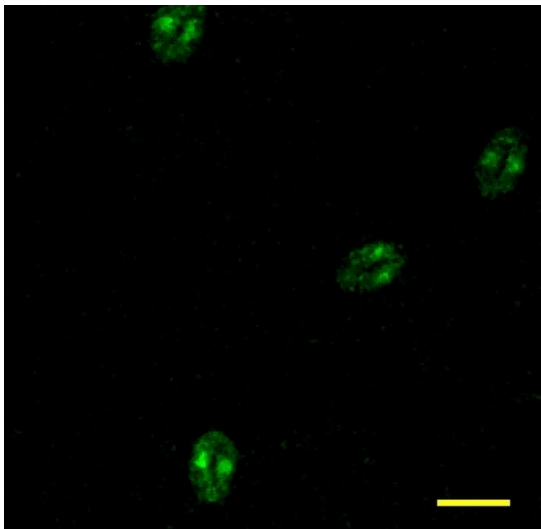
(a) GC1::GFP:nos, GFP



(b) GC1::GFP:nos, BF



(c) MYB60::GFP:nos, GFP



(d) MYB60::GFP:nos, BF

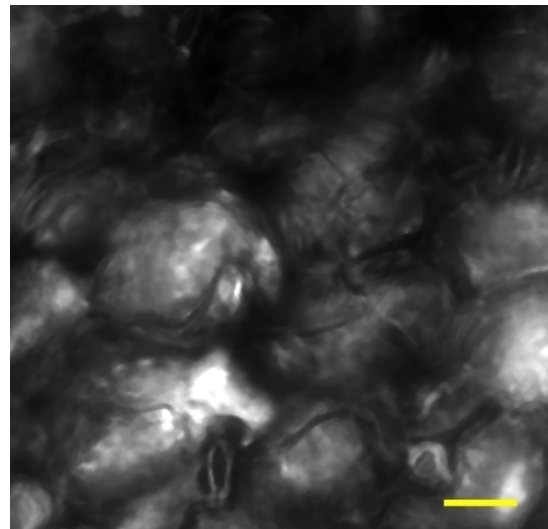


Figure 4.6: *GC1* and *MYB60* promoters have guard cell-specific activity. Photographs of GFP fluorescence were taken for (a) *GC1::GFP:nos* and (c) *MYB60::GFP:nos*, as well as of brightfield (BF) for (b) *GC1::GFP:nos* and (d) *MYB60::GFP:nos*. Photographs for *GC1::GFP:nos* were taken using a confocal microscope with the following settings: 40x objective, gain 1250, offset 0.2%, argon laser at 20% capacity, 488 nm laser at 48% capacity, laser range of 505-515 nm. Photographs for *MYB60::GFP:nos* were taken with the same settings, but at a 20x objective with 2x zoom. The focal plane is on guard cells, not pavement cells. All photographs were adjusted equally for brightness and contrast using Fiji. Scale bars (yellow, bottom right) represent 20  $\mu\text{m}$ .



#### 4.4.5 Confirming constant promoter activity

It was equally important to confirm that the *GC1* and *MYB60* promoters were not under circadian control. To examine *GC1* and *MYB60* promoter activity over time, two control plasmids were generated based on the *LUC* CDS: *GC1::LUC:nos* and *MYB60::LUC:nos*. Promoter sequences were inserted in a pGreenII 0229 plasmid containing the *LUC* CDS, using 5' PstI and 3' BamHI restriction sites. Stable Arabidopsis transformants were generated via floral dipping.

Homozygous seedlings were dosed with luciferin and monitored under a photon counting camera over four days (Fig. 4.7). Data were analysed using BioDare 2, a platform for analysis of circadian datasets (Zielinski et al. (2014)). Both FFT-NLLS and MESA algorithms were used. These generate estimates of circadian period via different statistical methods: FFT-NLLS is based on curve-fitting, while MESA uses a stochastic modelling approach. Both algorithms also generate relative amplitude error (RAE), which produces a measure of rhythmic robustness of the oscillation and varies between 0 and 1, with lower values indicating a good rhythmic fit to the data.

Panels 4.7e and 4.7f illustrate activity of a circadian clock promoter (*TOC1*) as detected through luciferase bioluminescence imaging. These data were redrawn from Noordally et al. (2013) for comparison with data obtained from *GC1::LUC:nos* and *MYB60::LUC:nos*. FFT-NLLS estimated a mean period of 25.6 and mean RAE of 0.12 for *TOC1::LUC* integrated luciferase bioluminescence (Fig. 4.7f).

In contrast, for *GC1::LUC:nos*, FFT-NLLS estimated a mean period of 25.2 h and mean RAE of 0.36, and MESA estimated a mean period of 25.2 h and mean RAE of 0.71 (Fig. 4.7b). In a similar manner, for *MYB60::LUC:nos*, FFT-NLLS estimated a mean period of 27.2 h and mean RAE of 0.49, and MESA estimated a mean period of 26.8 h and mean RAE of 0.76 (Fig. 4.7d). These data suggest that the *GC1* and *MYB60* promoters have weak rhythmicity.

To investigate this further, I examined transcripts accumulating from these promoters. *GC1::GFP:nos* and *MYB60::GFP:nos* seedlings were sampled every four hours over a three-day timecourse under constant light conditions, then probed for *GFP* and *CCA1* transcript abundance (Fig. 4.8). *GFP* relative transcript abundance reported activity of the *MYB60* and *GC1* promoters in guard cells. *CCA1* relative transcript abundance was used as a control for whole plant circadian rhythms and comparison with the

promoter-GFP reporters.

*CCA1* transcript abundance data were first analysed. For GC1::GFP:nos, FFT-NLLS estimated a mean period of 24 h and mean RAE of 0.47, and MESA estimated a mean period of 24.1 h and mean RAE of 0.50 (Fig. 4.8b). For MYB60::GFP:nos, FFT-NLLS estimated a mean period of 24.2 h and mean RAE of 0.58, and MESA estimated a mean period of 23.8 h and mean RAE of 0.56 (Fig. 4.8d). Therefore, *CCA1* transcript abundance is rhythmic in both genotypes.

In contrast, FFT-NLLS was unable to fit waves to *GFP* transcript abundance data for both GC1::GFP:nos and MYB60::GFP:nos, indicating arrhythmicity for *GFP* transcript abundance. MESA yielded period (GC1::GFP:nos : 27.2 h; MYB60::GFP:nos : 24.8 h) and RAE (GC1::GFP:nos : 0.80; MYB60::GFP:nos : 0.74) results. However, these period estimates were variable (S.E.M. of 3.5 and 1.9 for GC1::GFP:nos and MYB60::GFP:nos, respectively) and RAE very high, which we interpret to indicate arrhythmicity. Therefore, *GFP* transcript abundance was arrhythmic and constant throughout the timecourse for both promoters (Fig. 4.8).

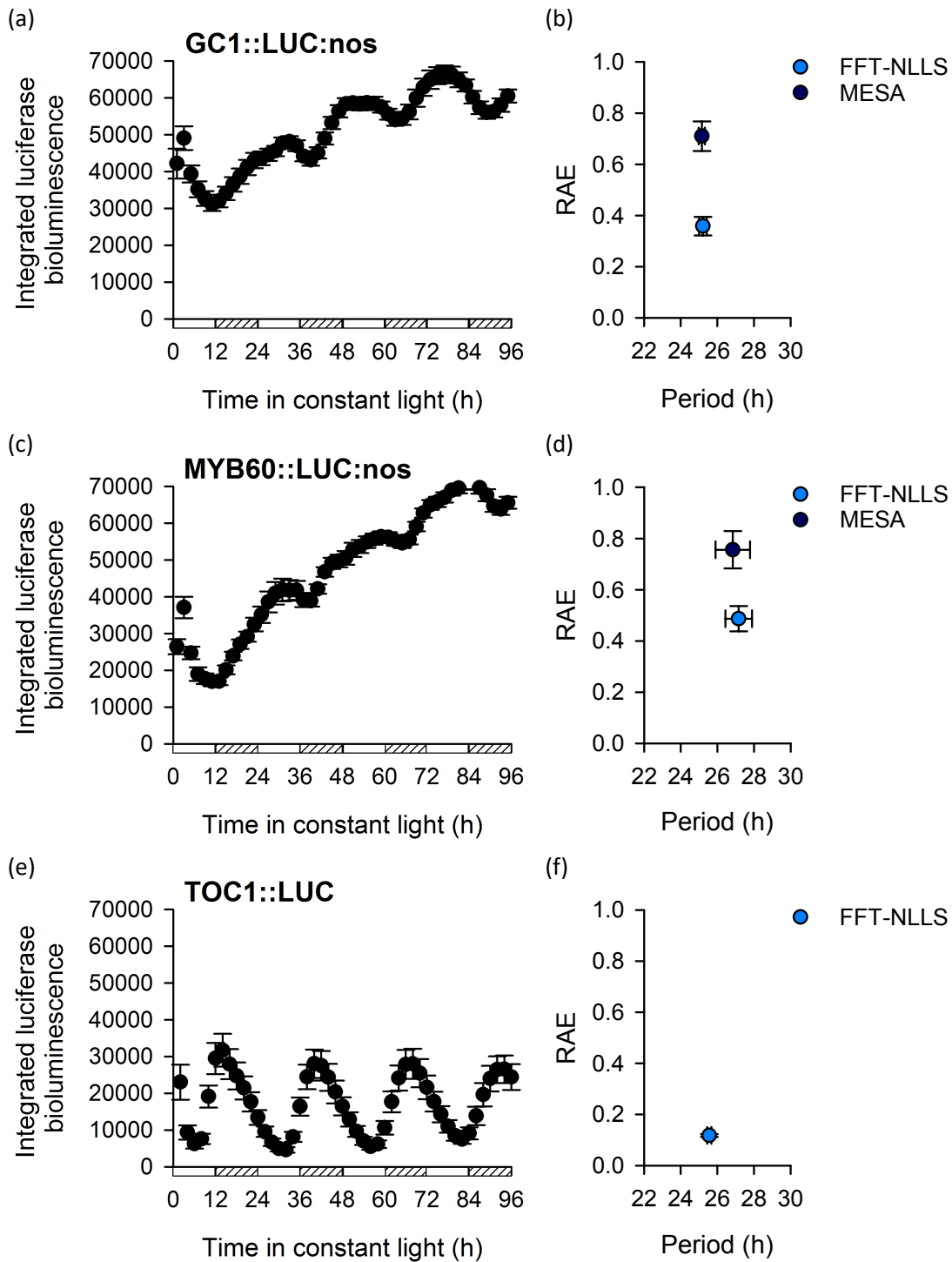


Figure 4.7: *GC1* and *MYB60* promoters may have weakly rhythmic activity, as shown by luciferase bioluminescence data. Integrated luciferase bioluminescence counts (counts in 480 s) in constant light for (a) *GC1::LUC:nos* and (c) *MYB60::LUC:nos* were analysed (b, d) using both FFT-NLLS and MESA algorithms ( $n = 8$ ; mean  $\pm$  S.E.M.). (e,f) Data are from Noordally et al. (2013) (counts in 750 s) and redrawn here for comparison with panels a-d. Boxes with and without hashed lines indicate subjective night and day, respectively.

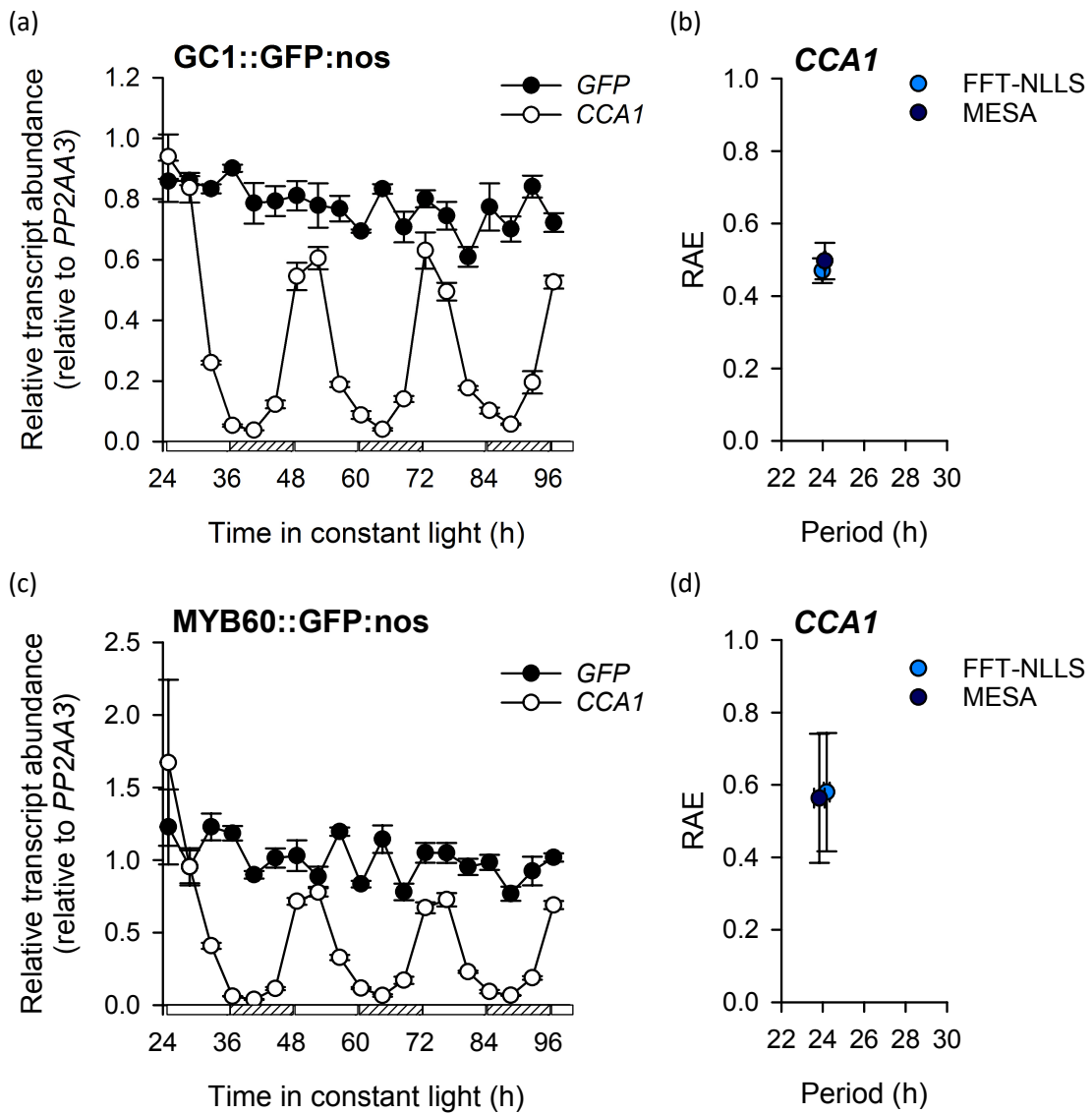


Figure 4.8: *GC1* and *MYB60* promoters have constant, arrhythmic activity, as shown by transcript abundance data. Data show *GFP* and *CCA1* relative transcript abundance over time in constant light for (a) *GC1::GFP:nos* and (c) *MYB60::GFP:nos* ( $n = 3$ ; mean  $\pm$  S.E.M.). Boxes with and without hashed lines indicate subjective night and day, respectively. *PP2AA3* was used as the reference gene. *CCA1* relative transcript abundance data were rhythmic in both (b) *GC1::GFP:nos* and (d) *MYB60::GFP:nos*, as analysed using both FFT-NLLS and MESA algorithms ( $n = 3$ ; mean  $\pm$  S.E.M.).

#### 4.4.6 Genotyping GCS-ox using expression data from whole seedlings

I then wished to explore further genotyping options in whole plants. One possibility would be to sample whole seedlings at timepoints when natural expression of *CCA1* and *TOC1* is low. This might reveal transgenic *CCA1* and *TOC1* transcript abundance caused by *GC1* and *MYB60* promoter activity within guard cells. Under control of their wild type promoters, *CCA1* transcript abundance peaks at dawn and troughs at dusk, while *TOC1* expression peaks at dusk and troughs at dawn (Hsu and Harmer (2014)). Therefore, *GC* and *MC* seedlings were sampled at dusk, when natural *CCA1* expression is the lowest, while *GT* and *MT* were sampled at dawn, when natural *TOC1* expression is the lowest (Fig. 4.9).

Guard cell *CCA1* and *TOC1* overexpressors were probed for *CCA1* and *TOC1* transcript abundance, respectively (Fig. 4.9). *GC* and *MC* had 5.5 and 6.5 times more *CCA1* at dusk than Col-0, respectively (Fig. 4.9a). In a similar fashion, *GT* and *MT* had 2.6 and 1.7 times more *TOC1* at dawn than Col-0, respectively (Fig. 4.9b).

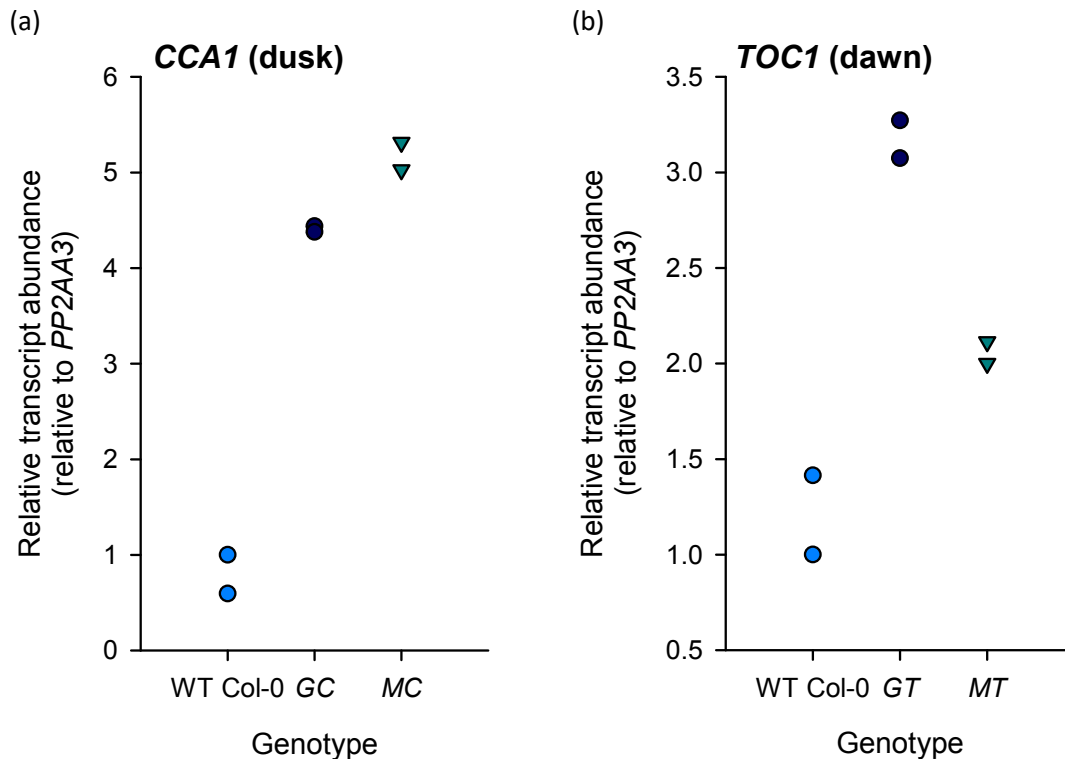


Figure 4.9: Using whole seedlings to genotype GCS-ox. RNA extracted from whole seedlings was probed for (a) *CCA1* relative transcript abundance at dusk for guard cell *CCA1* overexpressors and (b) *TOC1* relative transcript abundance at dawn for guard cell *TOC1* overexpressors ( $n = 2$ ). Different coloured symbols highlight the distinct genotypes. *PP2AA3* was used as the reference gene.

#### 4.4.7 Genotyping GCS-ox using expression data from guard cells

To further investigate guard cell-specific *CCA1* or *TOC1* overexpression in GCS-ox, I wished to obtain samples with enriched guard cell RNA.

##### 4.4.7.1 The “ice-blender” protocol

The “ice-blender” protocol from Bauer et al. (2013) was first attempted. This involved blending and sieving leaf material in ice-cold MilliQ water. I faced several issues with this protocol, including high material loss, impeded tissue homogenisation and low RNA yields. After optimisation, obtained samples were analysed using tissue-specific reporter genes (Table 4.1). A sample containing 2.7-fold enrichment of guard cell RNA was obtained (Fig. 4.10). Little mesophyll and epidermis tissue was left, but a substantial amount of vasculature tissue remained (Fig. 4.10). In addition, this technique was

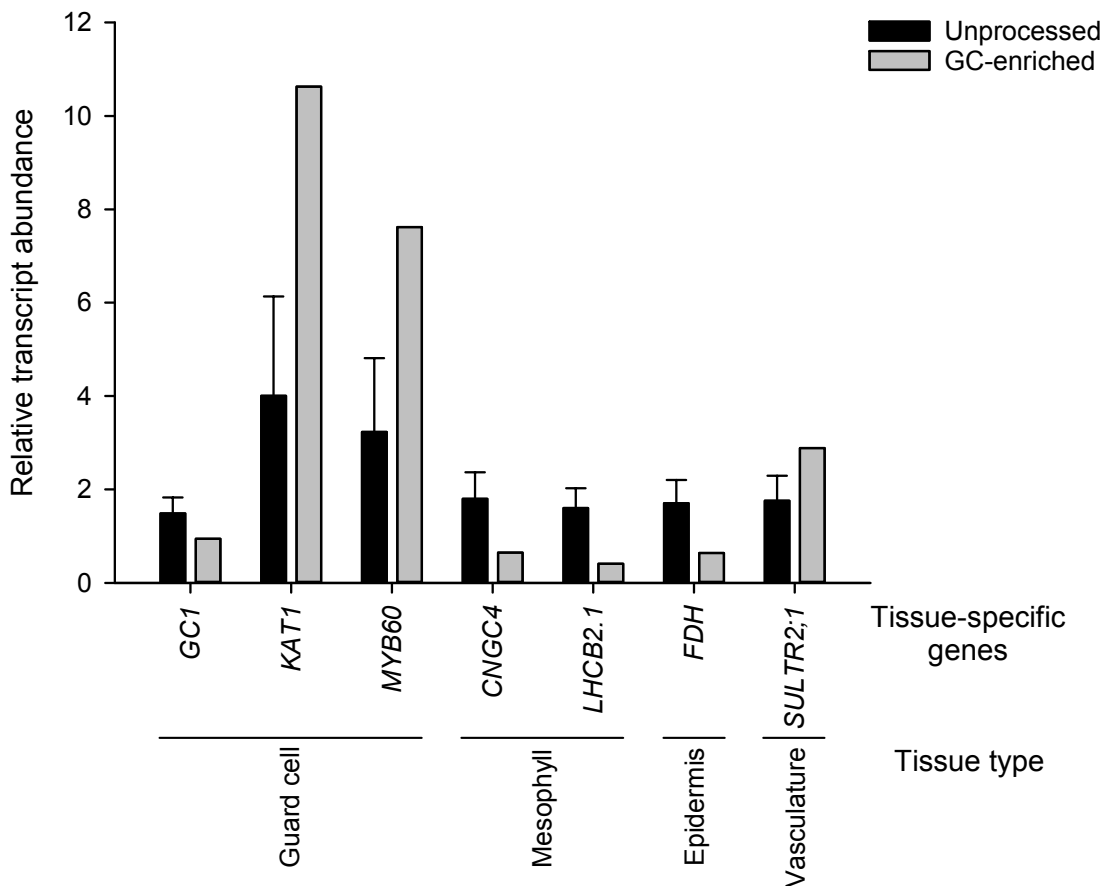


Figure 4.10: Guard cell-enriched RNA sample produced using the “ice-blender” methodology. Samples were probed for relative abundance of guard cell-specific (*GC1*, *KAT1*, *MYB60*), mesophyll-specific (*CNGC4*, *LHCB2.1*), epidermis-specific (*FDH*), and vasculature-specific (*SULTR2;1*) transcripts ( $n = 1-3$ ; mean  $\pm$  S.E.M.). RNA from unprocessed WT Col-0 samples was used as a control. *TIP41*-like was used as the reference gene.

difficult to repeat due to sample loss, was unsuitable for circadian time scales, and would cause plant cells considerable stress thereby could alter transcript abundance data.

#### 4.4.7.2 The “epidermal peel” protocol

Dr Ioanna Kostaki successfully probed guard cell transcripts by extracting RNA from epidermal peels. This is based on the assumption that the majority of epidermal and mesophyll cells burst during peeling, leaving only guard cells. Guard cells are able to survive in this state when incubated in buffer, allowing the sampling and compilation

of several epidermal peels. RNA can be extracted from this collated sample.

An undergraduate MSci student under my guidance applied this technique to isolate guard cell RNA from GCS-ox genotypes. Plants were placed under constant light conditions for 24 h, then samples collected at subjective dawn and dusk. The student also reverse-transcribed samples to cDNA. I performed subsequent qRT-PCR work and statistical analysis.

To verify guard cell enrichment of the samples, epidermal peels and leaf discs were probed for the above-mentioned tissue-specific transcripts (Table 4.1; Sup. Fig. 9.5). However, the data were inconclusive. This may be due to experimental error, as leaf discs were not sampled under the same experimental conditions and thus were not a comparable control for the epidermal peels. Nonetheless, microscopy determined that the epidermal peels solely contained guard cells, and previous work by Dr Ioanna Kostaki demonstrated that the technique produced guard cell-enriched samples (data not shown).

Transgenic epidermal peel samples were probed for *CCA1* and *TOC1* transcript abundance, using WT epidermal peels as a control (Fig. 4.11). As previously, I focused on *GC* and *MC* *CCA1* transcript abundance at dusk, when natural *CCA1* expression is low, and *GT* and *MT* *TOC1* transcript abundance at dawn, when natural *TOC1* expression is low. Overall, *GC* and *MC* had higher transcript abundance of guard cell *CCA1* than the WT at dusk (Fig. 4.11a) (*GC*:  $t_4 = -2.233$ ,  $p > 0.05$ ; *MC*:  $t_4 = -7.409$ ,  $p = 0.002$ ), while *GT* and *MT* had higher guard cell *TOC1* transcript abundance than the WT at dawn (Fig. 4.11b) (*GT*:  $t_4 = -6.636$ ,  $p = 0.003$ ; *MT*:  $t_4 = -2.736$ ,  $p = 0.050$ ).

Similar levels of *CCA1* were detected in *GC*, *MC* and Col-0 epidermal peels at dawn ( $F_{2, 6} = 2.796$ ,  $p > 0.05$ ), and of *TOC1* in *GT*, *MT* and Col-0 epidermal peels at dusk ( $F_{2, 6} = 1.142$ ,  $p > 0.05$ ) (Sup. Fig. 9.6). All epidermal peels had higher *CCA1* abundance at dawn than dusk, and higher *TOC1* abundance at dusk than dawn (Sup. Fig. 9.6).

Overall, these data suggest that *CCA1* is overexpressed in *GC* and *MC* guard cells, and *TOC1* is overexpressed in *GT* and *MT* guard cells.



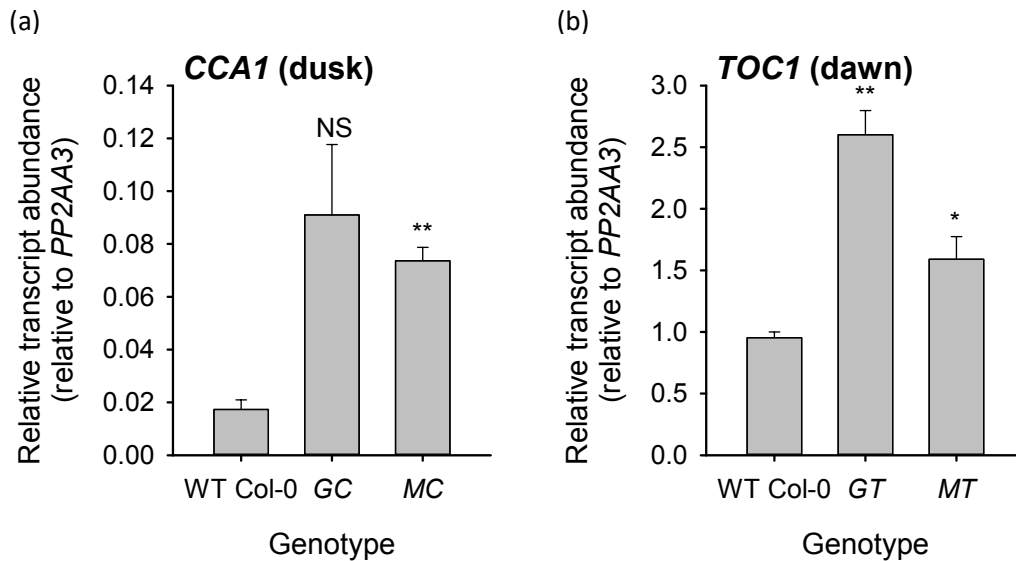


Figure 4.11: Genotyping GCS-ox using RNA extracted from epidermal peels. Epidermal peel RNA was probed for (a) *CCA1* relative transcript abundance at dusk for guard cell *CCA1* overexpressors and (b) *TOC1* relative transcript abundance at dawn for guard cell *TOC1* overexpressors ( $n = 3$ ; mean  $\pm$  S.E.M.). RNA from WT Col-0 epidermal peels was used as a control. *PP2AA3* was used as the reference gene. Sample collection, RNA extraction and cDNA biosynthesis were conducted by an MSci student under my guidance. Subsequent qRT-PCR work and statistical analysis was performed by myself. Data were analysed with independent samples t-tests, and statistical significance is indicated using starring (NS =  $p > 0.05$ ; \* =  $p < 0.05$ ; \*\* =  $p < 0.01$ ).

## 4.5 Discussion

Overexpressing key oscillator components is an effective tool to induce arrhythmicity (Schaffer et al. (1998); Wang and Tobin (1998); Más et al. (2003a); Somers et al. (2004); Dodd et al. (2005)). Oscillations in mRNA and protein abundance of core circadian clock genes are necessary for correct functioning of the circadian clock. Therefore, by forcing these levels to remain at a constant high abundance, the circadian oscillator becomes arrhythmic (McClung (2006)). This process has been validated for several circadian clock genes, including *TOC1* (Makino et al. (2002); Más et al. (2003a)) and *CCA1* (Wang and Tobin (1998); Dodd et al. (2005)), and tissue-specific circadian oscillators (Endo et al. (2014); Shimizu et al. (2015); Hassidim et al. (2017)). Therefore, I have used strong, guard cell-specific promoters to overexpress circadian clock coding sequences within guard cells.

*GC1* and *MYB60* promoter activity was analysed using GFP fluorescence and found to

be guard cell specific (Fig. 4.6). Indeed, both promoters have strong guard cell specificity in dicots and have been used previously to overexpress proteins in guard cells (Cominelli et al. (2005); Galbiati et al. (2008); Yang et al. (2008); Cominelli et al. (2011); Kinoshita et al. (2011); Rusconi et al. (2013); Wang et al. (2014); Hassidim et al. (2017)). Therefore, it is likely that these promoters have guard cell-specific activity in the GCS-ox genotypes.

Luciferase reporter genes enable the monitoring of circadian rhythms of promoter activity (Millar et al. (1992, 1995); Hall and Brown (2007)), so were employed to investigate *GC1* and *MYB60* promoter activity over time. However, the resulting luciferase bioluminescence data seemed weakly rhythmic (Figs. 4.7a, 4.7c). Several options were possible for subsequent data analysis. The FFT-NLLS algorithm is often used to analyse circadian timecourse data (Somers et al. (2000); Doyle et al. (2002); Más et al. (2003b); Ding et al. (2007); Thines and Harmon (2010); Yakir et al. (2011); Endo et al. (2014); Zielinski et al. (2014); Sánchez-Villarreal et al. (2018)) and is effective for noisy and relatively short datasets (Zielinski et al. (2014)). In contrast, the MESA algorithm is based on stochastic modelling, so does not assume the shape of the data's waveform and is more precise than methods based on Fourier transform methods (Zielinski et al. (2014)). However, MESA does not produce a measure of significance (Zielinski et al. (2014)). To avoid misinterpreting data, both methods were used.

Interpretation of RAE varies widely within the literature, even when using the same luciferase technique in Arabidopsis seedlings. For example, Müller et al. (2016) only considered seedlings with  $RAE < 0.25$  as rhythmic, while other studies used 0.6 as a cutoff point (Gendron et al. (2012); Shin et al. (2013, 2017)). Other reports interpret RAE values below 0.5 as rhythmic, or simply use the RAE of their control as the limit for rhythmicity (Noordally et al. (2013); McWatters et al. (2007); Rawat et al. (2011); Wang et al. (2011); Kolmos et al. (2009)). Therefore, the mean RAE estimated by MESA (*GC1::LUC:nos* : 0.71; *MYB60::LUC:nos* : 0.76) imply arrhythmicity, whereas that estimated by FFT-NLLS (*GC1::LUC:nos* : 0.36; *MYB60::LUC:nos* : 0.49) could be interpreted as rhythmic depending on the chosen cutoff point (Figs. 4.7b, 4.7d).

Performing qRT-PCR on plants sampled under constant conditions over time is a well-established technique to monitor circadian parameters of transcript abundance (Nozue et al. (2007); Niwa et al. (2009); Rawat et al. (2011); Sánchez-Villarreal et al. (2013); Takahashi et al. (2015); Noordally et al. (2013); Belbin et al. (2017); Hassidim et al. (2017)). Therefore, this was used to evaluate whether the *GC1* and *MYB60* promoters

were circadian regulated (Fig. 4.8). *GFP* transcript abundance under *GC1* and *MYB60* control was arrhythmic (Fig. 4.8).

The observed luciferase bioluminescence “pseudo-rhythms” may originate from diel variations in ATP availability under these conditions: as a larger leaf surface area is created and light levels are constantly maintained, higher levels of sugars and oxygen can be photosynthetically produced. However, Millar et al. (1992) established that wild type *CAB2::LUC* seedlings treated with or without a red flash of light had the same temporal pattern of luminescence, despite having different levels of endogenous ATP and O<sub>2</sub>. Nevertheless, as this was observed in the whole leaf (Millar et al. (1992)), it is still possible that guard cells are being influenced by surrounding tissues. These “pseudo-rhythms” could also be caused by plant growth over the timecourse: as leaves expand and new leaves are developed, more guard cells are formed thereby a stronger signal could be emitted. Overall, it seems that *GC1* and *MYB60* promoter activity leads to arrhythmic guard cell transcript accumulation.

Further steps were taken to genotype the GCS-ox in whole seedlings and guard cells only. As expected from previous studies, *MYB60* seemed to drive lower expression in guard cells than *GC1* (Yang et al. (2008)) (Fig. 4.11). Nevertheless, for both used promoters, guard cell *CCA1* overexpressors had higher *CCA1* abundance than the wild type at dusk and guard cell *TOC1* overexpressors had higher *TOC1* abundance at dawn, in both whole seedlings and guard cells only (Figs. 4.9, 4.11). This was also reported by Hassidim et al. (2017), who used transgenic *Arabidopsis* containing the *CCA1* CDS under control of the *GC1* promoter. Interestingly, Hassidim et al. (2017) report that overexpressing *CCA1* via the *GC1* promoter does not fully eradicate *LHY* rhythmic expression; thus it is possible that *GC* and *GT*, and perhaps *MC* and *MT*, retain partial rhythmicity of other oscillator components within guard cells.

## 4.6 Conclusions

Using a variety of different methodologies, a toolkit of transgenic *Arabidopsis* (*GC1::CCA1:nos*, *GC1::TOC1:nos*, *MYB60::CCA1:nos*, *MYB60::TOC1:nos*) was generated and genotyped.

Our results suggest that:

- *GC1* and *MYB60* promoters have guard cell-specific and constant activity.
- *CCA1* or *TOC1* are being overexpressed within guard cells of their respective GCS-ox genotypes.

GCS-ox were then examined physiologically in Chapter 5.



## Chapter 5

# Physiological examination and analysis of transgenic *Arabidopsis* with misregulated guard cell circadian clocks

### 5.1 Introduction

To tackle the challenge of food security in a rapidly changing climate, one possible solution involves improving crop WUE and drought resistance (Condon et al. (2004); Xoconostle-Cázares et al. (2010); Hu and Xiong (2014); Ruggiero et al. (2017)). Altering stomatal density, patterning, and behaviour could optimise the control of water loss (Pei et al. (1998); Hugouvieux et al. (2001); Schroeder et al. (2001); Wang et al. (2009); Yoo et al. (2010); Franks et al. (2015); Ruggiero et al. (2017)).

Plant circadian clocks seem to be uncoupled between cells and tissue types, with no centralised pacemaker (Thain et al. (2000)), and evidence suggests that an autonomous circadian oscillator is present within guard cells and controls its activity (Somers et al. (1998); Salomé et al. (2002); Dodd et al. (2004); Hassidim et al. (2017)). These tissue-specific circadian clocks appear to communicate with and regulate one another, creating a hierarchical circadian structure (James et al. (2008); Yakir et al. (2011); Endo et al. (2014); Takahashi et al. (2015); Bordage et al. (2016)).

## 5.2 Hypothesis and aims

The circadian clock present within guard cells may be autonomous and cell-specific (Somers et al. (1998); Salomé et al. (2002); Dodd et al. (2004); Hassidim et al. (2017)), and guard cells have been established as clear targets to control stomatal aperture and WUE (Lawson and Blatt (2014)). I hypothesised that the guard cell circadian clock modulates aspects of whole plant physiology, particularly those related to stomatal movement and water use. Previously, I generated, genotyped and validated transgenic *Arabidopsis* in which the circadian clock was misregulated within guard cells only (GCS-ox, Chapter 4). Here, a variety of physiological and developmental parameters were investigated in these genotypes to determine how the guard cell circadian clock affects whole plant physiology.

I was also interested in how the guard cell circadian clock interacts with other tissue-specific circadian oscillators. For example, it is possible that the guard cell circadian clock regulates stomatal movement, but that signals from other, tissue-specific circadian clocks override it for other physiological processes. Therefore, I analysed phenotypic differences between wild type plants, genotypes with an arrhythmic guard cell circadian clock, and genotypes in which the circadian clock is disrupted throughout the plant to try to determine interactions between the guard cell circadian clock and other tissue-specific circadian clocks.

## 5.3 Methods and methodology

Several independently transformed, homozygous alleles were used for each GCS-ox genotype (Chapter 4; GC1::CCA1:nos (*GC*), GC1::TOC1:nos (*GT*), MYB60::CCA1:nos (*MC*), MYB60::TOC1:nos (*MT*)). Details of each allele are provided in the Appendix (Table 9.1). The CCA1-ox (Wang and Tobin (1998)) and TOC1-ox (Más et al. (2003)) whole plant circadian clock gene overexpressors were used as controls, as well as the background Col-0.

A variety of physiological and developmental parameters were investigated in these genotypes, including:

- key physiological factors under circadian clock control
  - hypocotyl elongation assay (protocol provided in Chapter 2, section 2.11)
  - flowering time assay (protocol provided in Chapter 2, section 2.9)
- stomatal development and behaviour
  - stomatal density assay (protocol provided in Chapter 2, section 2.7.1)
  - stomatal aperture bioassay (protocol provided in Chapter 2, section 2.7.5)
- whole plant water use and drought stress resistance
  - detached leaf assay (protocol provided in Chapter 2, section 2.7.4)
  - slow, fast, fixed, and constant drought assays on compost mix (protocols provided in Chapter 2, section 2.10.2)
  - dehydration assay on Petri dishes (protocol provided in Chapter 2, section 2.10.1)
  - WUE assay (protocol provided in Chapter 2, section 2.8)

## **5.4 Results**

### **5.4.1 GCS-ox have unaltered hypocotyl elongation**

#### **5.4.1.1 The guard cell circadian clock does not influence hypocotyl elongation under different photoperiods**

Hypocotyl elongation is regulated by the circadian oscillator and photoperiod (Nozue et al. (2007); Niwa et al. (2009); Nusinow et al. (2011)). It occurs through cellular expansion of the hypocotyl, thus does not involve guard cells directly. However, if an altered guard cell circadian clock could influence or override another tissue-specific circadian clock, it may indirectly affect regulation of hypocotyl elongation. Therefore, hypocotyl elongation assays were performed on GCS-ox seedlings. They were grown



under 4 h, 8 h, 12 h, and 16 h photoperiods with WT Col-0 and CCA1-ox or TOC1-ox controls. Two independent repeats were performed per experiment: one is displayed here (Figs. 5.1, 5.2), while the other is provided in the Appendix (Sup. Fig. 9.8).

Guard cell *CCA1* overexpressors were examined first, with three alleles tested per genotype. CCA1-ox had a significantly longer hypocotyl than the WT under all photoperiods tested (Fig. 5.1) (Wang and Tobin (1998); Green et al. (2002); Dodd et al. (2005); Nozue et al. (2007)). CCA1-ox hypocotyl length was 2.3 times ( $F_{5, 114} = 27.969, p < 0.001$ ), 2.7 times ( $F_{5, 114} = 71.118, p < 0.001$ ), 3.2 times ( $F_{5, 114} = 198.992, p < 0.001$ ) and 2.4 times ( $F_{5, 114} = 108.150, p < 0.001$ ) the length of Col-0 hypocotyls under 16 h, 12 h, 8 h and 4 h photoperiods, respectively (Fig. 5.1). However, hypocotyl length was the same for all *GC* and *MC* alleles and Col-0 across all photoperiods tested ( $p > 0.05$ ) (Fig. 5.1).

As hypocotyl length was unaltered in guard cell *CCA1* overexpressors, only two alleles were examined for *GT* and *MT*. TOC1-ox had a significantly shorter hypocotyl than the WT under all photoperiods tested (Fig. 5.2). TOC1-ox hypocotyl length was 0.78 times ( $F_{5, 114} = 4.280, p = 0.025$ ), 0.69 times ( $F_{5, 114} = 12.715, p < 0.001$ ), 0.61 times ( $F_{5, 114} = 27.779, p < 0.001$ ) and 0.48 times ( $F_{5, 114} = 32.365, p < 0.001$ ) the length of Col-0 hypocotyls under 16 h, 12 h, 8 h and 4 h photoperiods, respectively (Fig. 5.2). Hypocotyl length was the same for most *GT* and *MT* alleles and Col-0 ( $p > 0.05$ ) across all photoperiods tested (Fig. 5.2). The sole exception was *GT-2* under a 4 h photoperiod, which had significantly longer hypocotyls than Col-0 (Fig. 5.2d) ( $F_{5, 114} = 32.365, p = 0.033$ ).

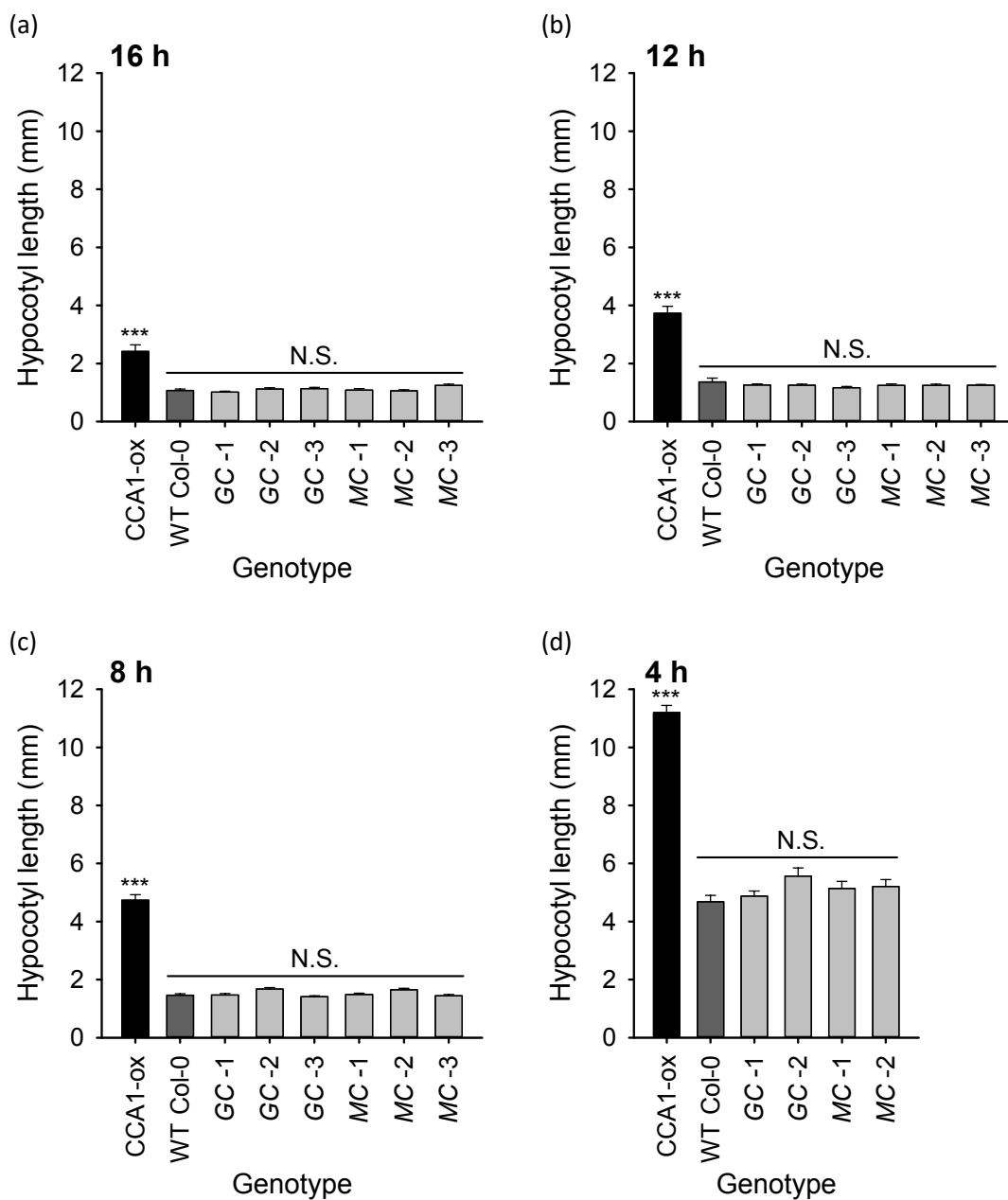


Figure 5.1: Overexpressing *CCA1* in guard cells does not affect hypocotyl elongation. Hypocotyl lengths were measured for seedlings grown under (a) 16 h, (b) 12 h, (c) 8 h or (d) 4 h photoperiods ( $n = 20$ ; mean  $\pm$  S.E.M.). Photoperiods are indicated above graphs. Colour-coding highlights the whole plant overexpressor control (black), wild type control (dark grey), and GCS-ox genotypes (light grey). Data were analysed with ANOVA and Tukey's post hoc tests, and statistical significance compared to Col-0 is indicated using starring (N.S. =  $p > 0.05$ ; \*\*\* =  $p < 0.001$ ).

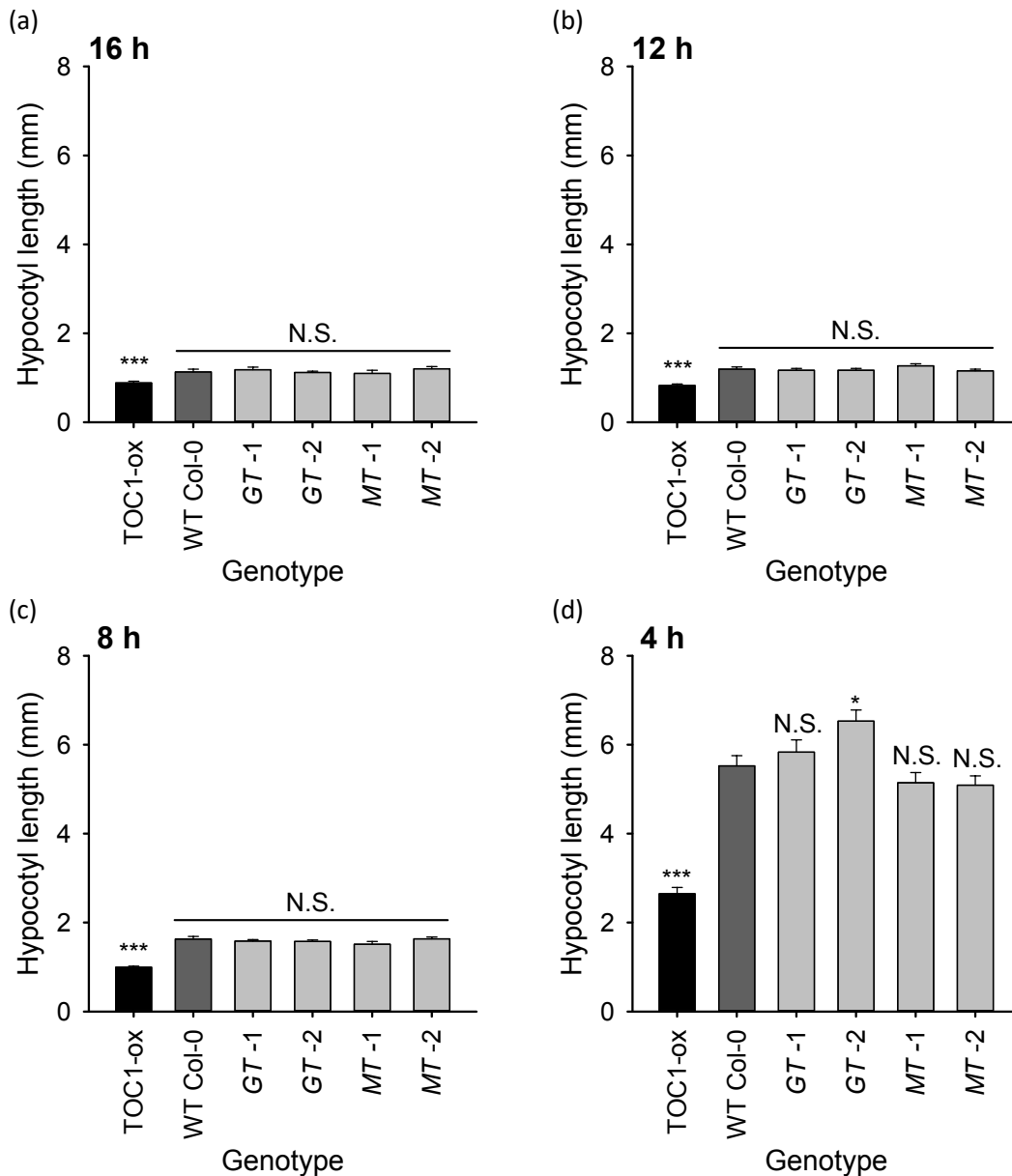


Figure 5.2: Overexpressing *TOC1* in guard cells does not affect hypocotyl elongation. Hypocotyl lengths were measured for seedlings grown under (a) 16 h, (b) 12 h, (c) 8 h or (d) 4 h photoperiods ( $n = 20$ ; mean  $\pm$  S.E.M.). Photoperiods are indicated above graphs. Colour-coding highlights the whole plant overexpressor control (black), wild type control (dark grey), and GCS-ox genotypes (light grey). Data were analysed with ANOVA and Tukey's post hoc tests, and statistical significance compared to Col-0 is indicated using starring (N.S. =  $p > 0.05$ ; \* =  $p < 0.05$ ; \*\*\* =  $p < 0.001$ ).

#### 5.4.1.2 Sucrose-induced hypocotyl elongation is not affected by the guard cell circadian clock

Supplementing media with exogenous sucrose increases hypocotyl length under shorter photoperiods or lower light conditions (Stewart et al. (2011); Lilley et al. (2012); Simon et al. (2018a,b)). This may be due to the low endogenous sugar levels present in seedlings grown under these conditions (Simon et al. (2018a)). Although the whole plant circadian oscillator does not participate in sucrose-induced hypocotyl elongation (Chapter 7; Simon et al. (2018a)), it is possible that the guard cell circadian clock could affect the photosynthetic apparatus thus endogenous sugar levels. Therefore, hypocotyl elongation was investigated for GCS-ox grown under 4 h photoperiods in MS (0.5 MS, 0.8% (w/v) agar) supplemented with 3% sucrose (Suc) or equimolar sorbitol (osmotic control, Sor) (Fig. 5.3).

Guard cell *CCA1* overexpressors were first examined (Fig. 5.3a). There was a significant increase in hypocotyl length between seedlings grown on Sor and those on Suc, for all alleles tested ( $F_{17, 342} = 81.212, p < 0.001$ ). *CCA1*-ox had significantly longer hypocotyls than Col-0 when grown on MS, Sor or Suc ( $p < 0.001$ ), but hypocotyl length was the same for Col-0 and guard cell *CCA1* overexpressors for all media types ( $p > 0.05$ ).

This assay was then performed on guard cell *TOC1* overexpressors (Fig. 5.3b). There was a significant increase in hypocotyl length between seedlings grown on Sor and those on Suc, for all alleles tested ( $F_{17, 342} = 93.896, p < 0.001$ ). *TOC1*-ox had significantly shorter hypocotyls than Col-0 when grown on MS, Sor or Suc ( $p < 0.001$ ). Hypocotyl length was the same for Col-0 and guard cell *TOC1* overexpressors when grown on MS or Sor ( $p > 0.05$ ). When grown on Suc, there was no significant difference in hypocotyl length between Col-0, *GT-2* and *MT-1*, but *GT-1* and *MT-2* had significantly longer hypocotyls than Col-0 ( $p = 0.001$  and  $p = 0.018$ , respectively).

Overall, the guard cell circadian clock does not seem involved in the regulation of sucrose-induced hypocotyl elongation.

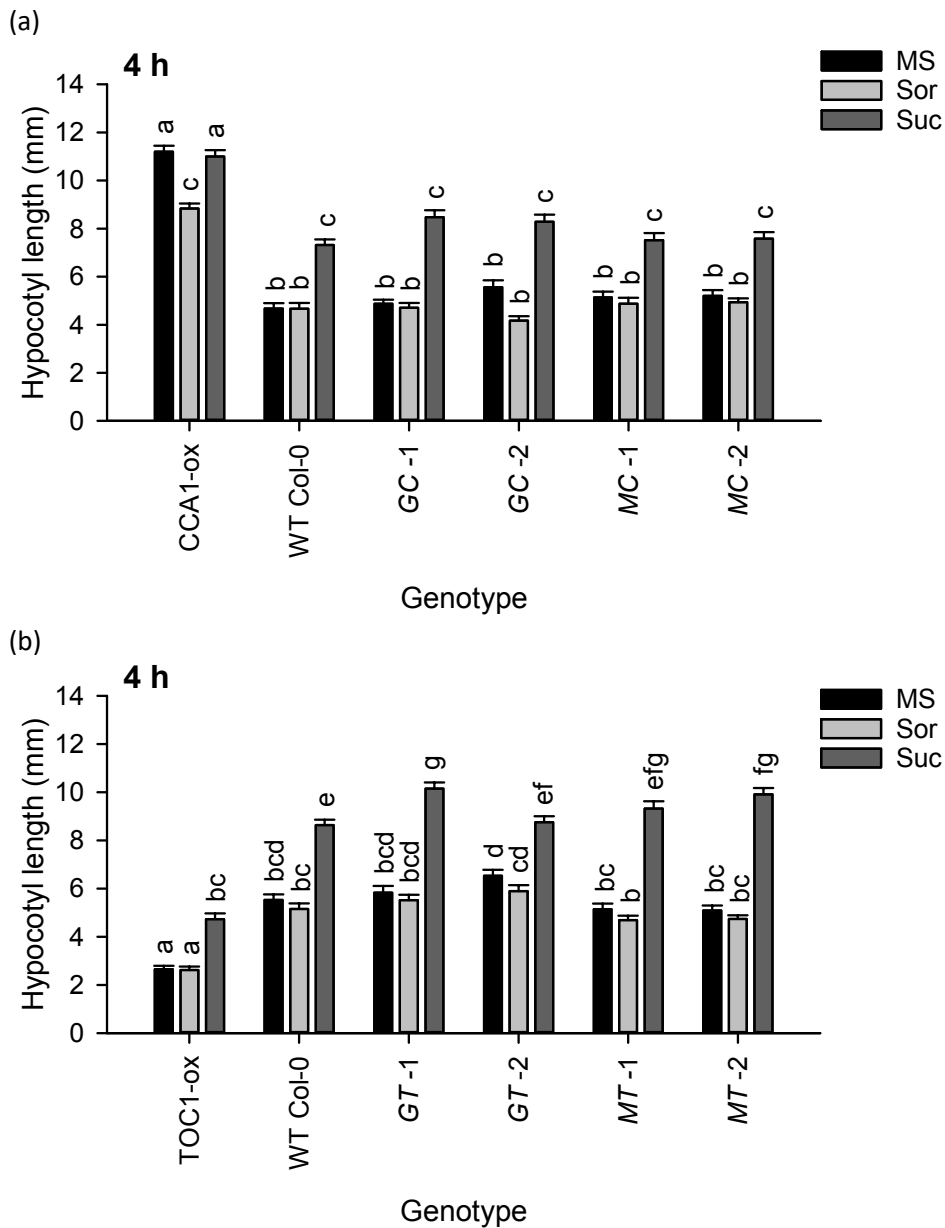


Figure 5.3: Overexpressing *CCA1* or *TOC1* in guard cells does not affect sucrose-induced hypocotyl elongation under short photoperiods. Hypocotyl lengths were measured for (a) guard cell *CCA1* overexpressors and (b) guard cell *TOC1* overexpressors grown on MS supplemented with 3% sucrose (Suc) or equimolar sorbitol (Sor) under a 4 h photoperiod ( $n = 20$ ; mean  $\pm$  S.E.M.). Whole plant overexpressor and WT controls are indicated on the left of each panel. Data were analysed with ANOVA and Tukey's post hoc tests. Different letters indicate statistically significant difference between means ( $p < 0.05$ ).

## 5.4.2 GCS-ox have late flowering time phenotypes under short photoperiods

The circadian clock regulates flowering time in *Arabidopsis*, and circadian clock mutants often have altered flowering time phenotypes (Schaffer et al. (1998); Fowler et al. (1999); Strayer et al. (2000); Doyle et al. (2002); Panda et al. (2002); Hayama and Coupland (2003); Yamamoto et al. (2003); Somers et al. (2004); Bendix et al. (2015)). Flowering time affects plant fitness and reproductive success, and coordinates many genes across different cell types (Yanovsky and Kay (2002); Johansson and Staiger (2015)). As guard cells play a role in carbon assimilation and photosynthesis, it is possible that the guard cell circadian clock could also influence flowering time.

Flowering time was examined for GCS-ox genotypes, under both 8 h and 16 h photoperiods. Flowering time was noted and leaves counted for each plant. Only one allele was examined per genotype due to space and time constraints. Experiments were repeated three times per photoperiod. Data examined here were obtained from one experimental repeat per photoperiodic condition; data from other experimental repeats are provided in the Appendix (Sup. Figs. 9.9, 9.10).

Under an 8 h photoperiod, all GCS-ox flowered significantly later than Col-0 (Fig. 5.4a) ( $F_{4, 66} = 28.204, p < 0.001$ ). *GC*, *GT*, *MC* and *MT* flowered on average 7, 6, 11 and 8 days after Col-0, respectively (Fig. 5.4a). However, Col-0 and GCS-ox possessed the same number of vegetative leaves at flowering under these conditions ( $F_{4, 66} = 2.371, p > 0.05$ ) (Fig. 5.4b).

Under a 16 h photoperiod, *MC* flowered three days later than Col-0 ( $F_{5, 83} = 410.677, p < 0.001$ ) (Fig. 5.4c), but the other three GCS-ox genotypes flowered at the same time as Col-0 ( $p > 0.05$ ) (Fig. 5.4c). As observed under an 8 h photoperiod, there was no significant difference in number of vegetative leaves at flowering between Col-0 and GCS-ox under a 16 h photoperiod ( $F_{5, 83} = 54.762, p > 0.05$ ) (Fig. 5.4d).

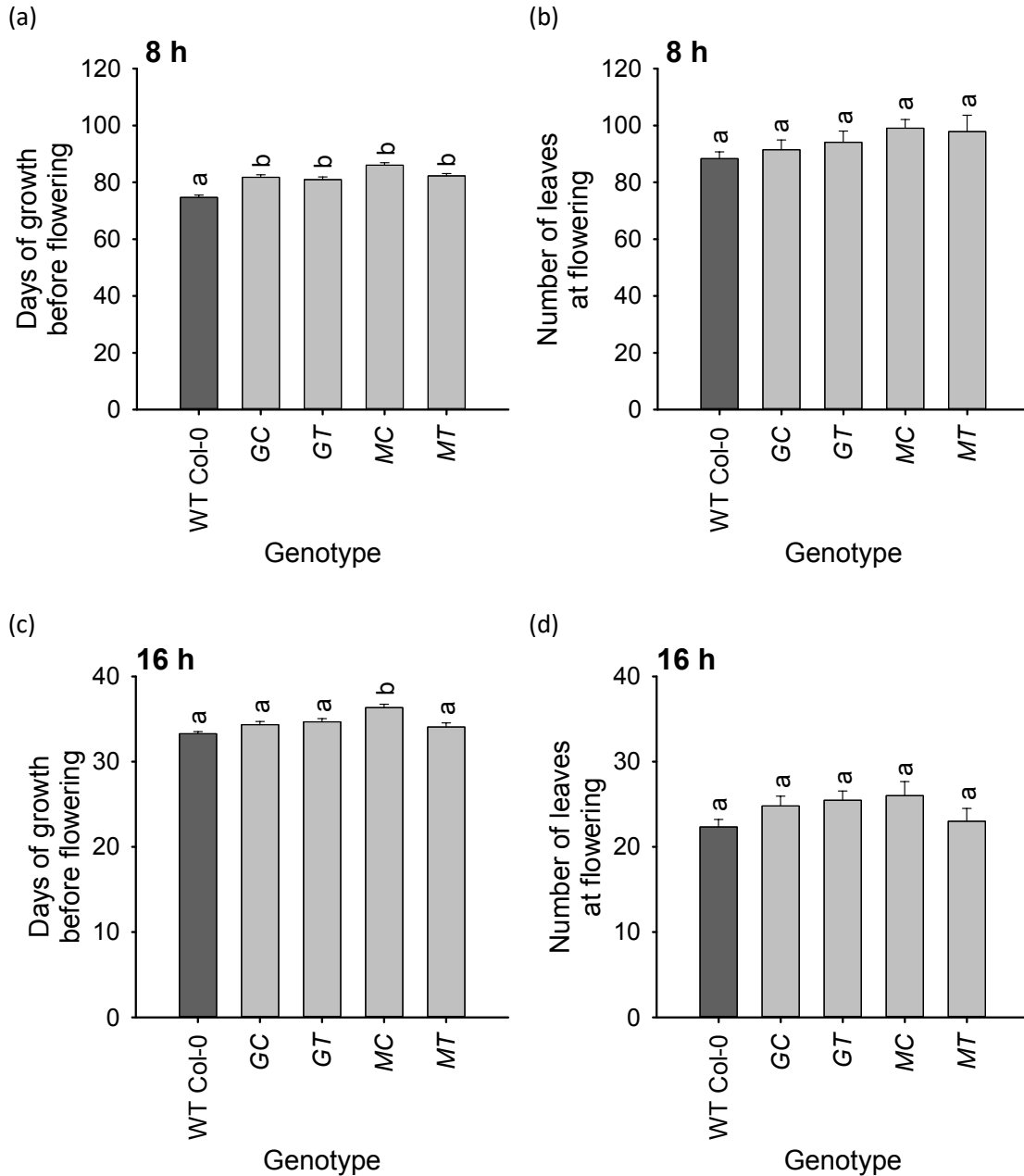


Figure 5.4: Overexpressing *CCA1* or *TOC1* in guard cells affects flowering time under short photoperiods. Data show number of days of vegetative growth before flowering time under (a) 8 h and (c) 16 h photoperiods, and number of vegetative leaves at flowering time under (b) 8 h and (d) 16 h photoperiods ( $n = 13-15$ ; mean  $\pm$  S.E.M.). Panels (a) and (b), and (c) and (d), show data from one experimental replicate. Supplemental experimental data are provided in the Appendix (Sup. Figs. 9.9 and 9.10). Photoperiods are indicated above graphs. Colour-coding highlights the WT control (dark grey) and GCS-ox genotypes (light grey). Data were analysed with ANOVA and Tukey's post hoc tests. Different letters indicate statistically significant difference between means ( $p < 0.05$ ).

### 5.4.3 Drought response is unaltered in GCS-ox

There is a strong link between the circadian clock and abiotic stress, and the nature of this complex relationship is still being established (Legnaioli et al. (2009); Grundy et al. (2015)). It would be interesting to examine whether misregulating the guard cell circadian clock would affect the ability to resist drought stress. Drought tolerance can be investigated in a variety of ways. For example, water can be fully withheld, or soil water capacity (SWC) can be maintained at a certain level. Pot size determines how quickly compost dries, thereby the amount of time the plant has to adapt to these new conditions, and influences root system architecture, thereby its ability to extract water from compost. With this in mind, three different drought assays on compost mix were performed for each GCS-ox genotype, using Col-0 and CCA1-ox as controls:

- the slow drought assay, with large inserts and water fully withheld. The larger inserts meant that compost dried out slowly when water was withheld.
- the fast drought assay, with small inserts and water fully withheld. The smaller inserts meant that compost dried out rapidly when water was withheld.
- the fixed drought assay, with inserts individually maintained at 100%, 50% or 25% SWC.

Each experiment ended when the majority of WT Col-0 plants died. A dead plant was defined as no longer having visible green tissue. Photographs were taken twice weekly from the start of the drought to the end of the experiment for both slow and fast drought assays. These were used to measure the rosette leaf surface area that remained green (alive) over time, which provided a proxy for growth under well-watered or droughted conditions. Rosettes were dried and weighed at the end of each experiment. Data were analysed as green rosette leaf surface area over time and final rosette dry biomass (Figs. 5.5, 5.6, 5.7; Sup. Fig. 9.11).

#### 5.4.3.1 GCS-ox did not have an altered response to the slow drought assay

There was no statistically significant difference in green rosette leaf area between GCS-ox and Col-0 when grown under slow droughted conditions ( $F_{5, 54} = 11.775, 13.883, 14.760, 5.643, 1.038, 1.101, \text{ or } 2.173$  at days 0, 4, 7, 11, 14, 18 and 21 post-drought,



respectively;  $p > 0.05$ ) (Fig. 5.5b). This was also observed for plants grown under well-watered conditions ( $F_{5, 54} = 16.358, 11.787, 12.475, 11.049, 11.946, 12.904, \text{ or } 7.920$  at days 0, 4, 7, 11, 14, 18 and 21 post-drought, respectively;  $p > 0.05$ ) (Fig. 5.5a). Although CCA1-ox had significantly smaller leaf area than Col-0 at all time points and under all watering conditions ( $p < 0.05$ ), their growth rates followed a similar pattern (Figs. 5.5a, 5.5b).

All plants had significantly smaller rosette dry biomass under slow droughted conditions than under well-watered conditions ( $p < 0.001$ ) (Fig. 5.5c). Rosette dry biomass was the same for Col-0 and GCS-ox grown under both well-watered ( $F_{5, 54} = 10.358, p > 0.05$ ) and slow droughted conditions ( $F_{5, 54} = 5.704, p > 0.05$ ) (Fig. 5.5c). CCA1-ox dry biomass was significantly smaller than Col-0 dry biomass under both well-watered ( $p < 0.001$ ) and slow droughted ( $p = 0.009$ ) conditions. However, the relative decrease in biomass between well-watered and slow droughted conditions was the same (68% and 70% for CCA1-ox and Col-0, respectively) (Fig. 5.5c).

Overall, overexpressing *CCA1* or *TOC1* in guard cells did not alter growth, rosette dry biomass or green leaf surface area under slow droughted conditions (Fig. 5.5).

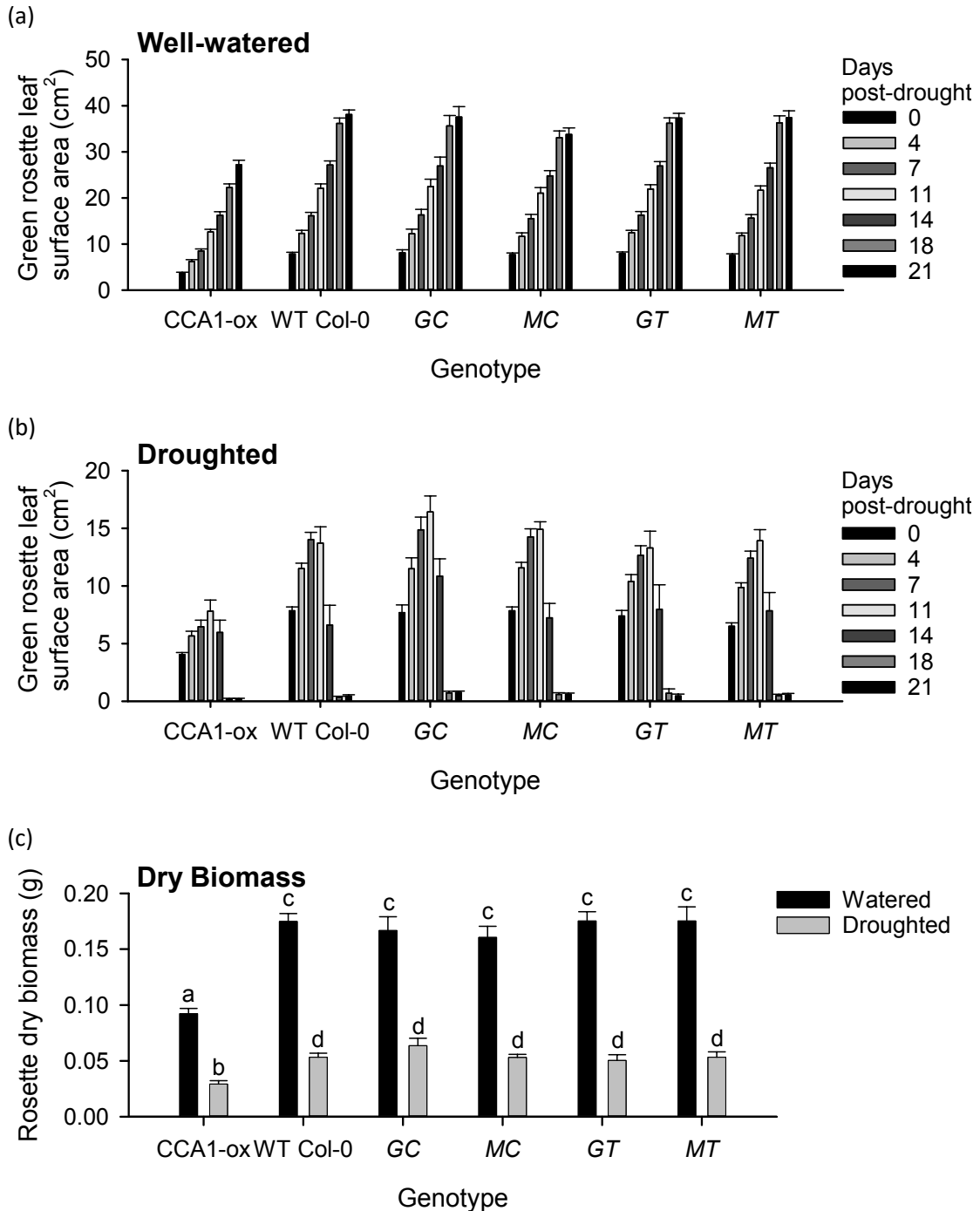


Figure 5.5: Overexpressing *CCA1* or *TOC1* in guard cells does not affect growth, green rosette leaf surface area or dry biomass under slow droughted or well-watered conditions. Plants were grown in large inserts under an 8 h photoperiod, with drought imposed after 36 days of growth. Green rosette leaf surface area measurements were taken at 0, 4, 7, 11, 14, 18 and 21 days post-drought for (a) well-watered and (b) slow droughted plants, and (c) final rosette dry biomass was measured ( $n = 10$ ; mean  $\pm$  S.E.M.). Whole plant overexpressor and WT controls are indicated on the left of each panel. Data were analysed with ANOVA and Tukey's post hoc tests. Different letters indicate statistically significant difference between means ( $p < 0.05$ ).

#### 5.4.3.2 GCS-ox did not have an altered response to the fast drought assay

A similar pattern occurred for plants subjected to the fast drought assay. There was no statistically significant difference in green rosette leaf area between GCS-ox and Col-0 when grown under fast droughted conditions (Fig. 5.6b) ( $F_{5, 52} = 7.762, 7.385, 5.587, 2.917, \text{ or } 2.362$  at days 1, 3, 7, 10 and 13 post-drought, respectively;  $p > 0.05$ ). This was also observed for plants grown under well-watered conditions ( $F_{5, 53} = 17.889, 18.866, 16.819, 22.153, \text{ or } 14.107$  at days 1, 3, 7, 10 and 13 post-drought, respectively;  $p > 0.05$ ) (Fig. 5.6a).

All plants had significantly smaller rosette dry biomass under fast droughted conditions than under well-watered conditions (Fig. 5.6c) ( $p < 0.001$ ). Rosette dry biomass was the same between Col-0 and GCS-ox grown under both well-watered ( $F_{5, 53} = 8.150, p > 0.05$ ) and fast droughted conditions ( $F_{5, 53} = 5.496, p > 0.05$ ) (Fig. 5.6c). CCA1-ox had a significantly smaller leaf area than Col-0 at all time points and under all watering conditions ( $p < 0.05$ ), as well as a significantly smaller biomass under both well-watered ( $p < 0.001$ ) and fast droughted ( $p = 0.005$ ) conditions. Nonetheless, CCA1-ox growth followed a similar pattern to that of Col-0 (Figs. 5.6a, 5.6b), and the relative decrease in biomass between well-watered and fast droughted conditions was the same (47% and 52% for CCA1-ox and Col-0, respectively) (Fig. 5.6c). Additional alleles were examined in this manner (*GC-3*, *GT-2*, *MC-3*, *MT-3*), and similar results obtained (Sup. Fig. 9.11).

Overall, overexpressing *CCA1* or *TOC1* in guard cells did not alter growth, rosette dry biomass or green leaf surface area under fast droughted conditions (Fig. 5.6).

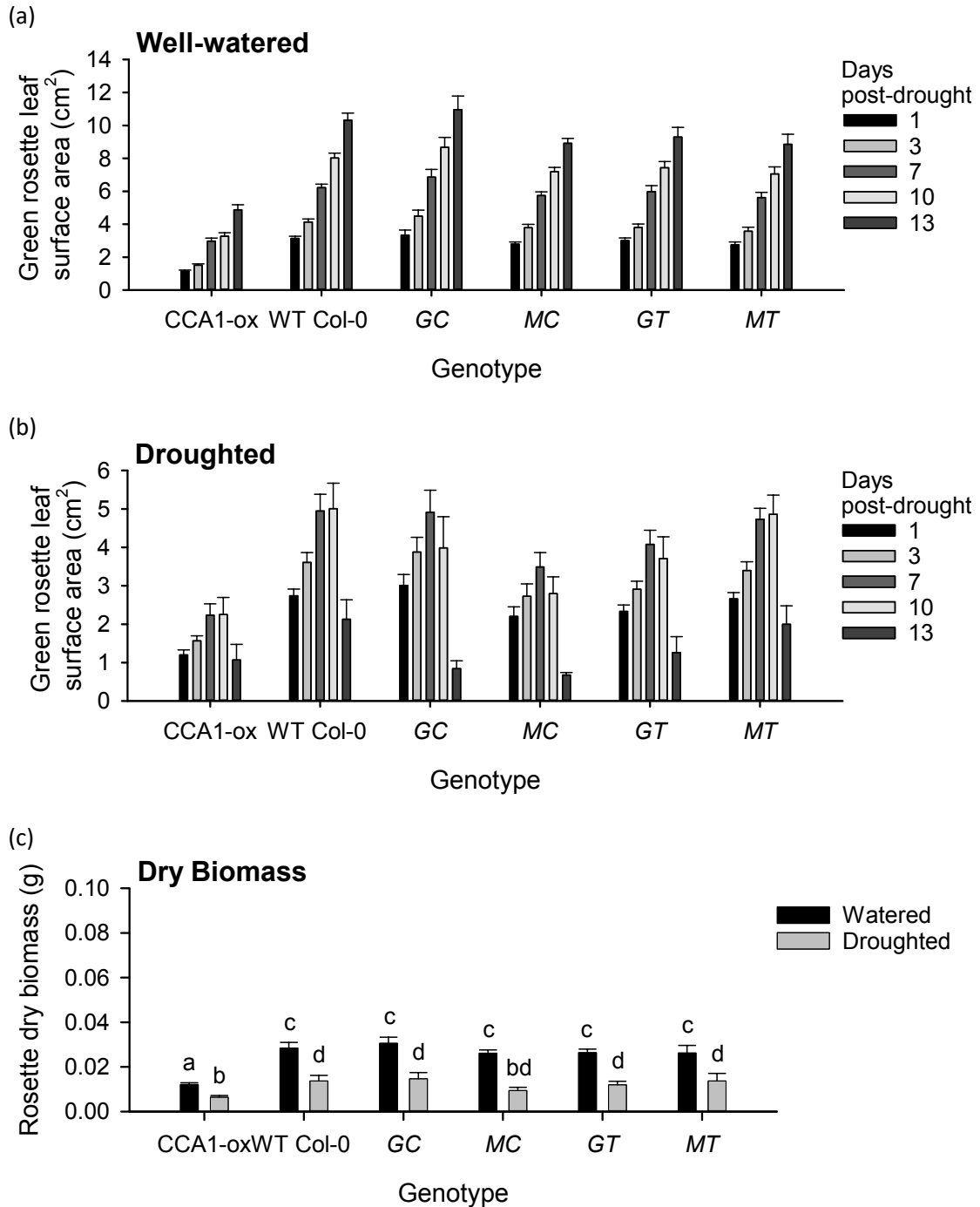


Figure 5.6: Overexpressing *CCA1* or *TOC1* in guard cells does not affect growth, rosette leaf surface area or dry biomass under fast droughted or well-watered conditions. Plants were grown in small inserts under an 8 h photoperiod, with drought imposed after 28 days of growth. Green rosette leaf area measurements were taken at 1, 3, 7, 10 and 13 days post-drought for (a) well-watered and (b) fast droughted plants, and (c) final rosette dry biomass was measured ( $n = 10$ ; mean  $\pm$  S.E.M.). Whole plant over-expressor and WT controls are indicated on the left of each panel. Data were analysed with ANOVA and Tukey's post hoc tests. Different letters indicate statistically significant difference between means ( $p < 0.05$ ).

### 5.4.3.3 GCS-ox did not have an altered response to the fixed drought assay

The fixed drought assay was then performed, with plants individually watered at a constant soil water capacity (SWC) of 100%, 50% or 25% (Fig. 5.7). Due to time constraints, this assay was not repeated for all GCS-ox genotypes. The first experimental repeat was performed on *GT* and *MC* (Figs. 5.7a, 5.7b), the second on *GC* and *GT* (Figs. 5.7c, 5.7d), and the third on *MC* and *MT* (Figs. 5.7e, 5.7f). Rosette leaf surface area and dry weight were measured at the end of each experiment. During the second experimental repeat, several plants flowered, and plants with inflorescences were removed from analysis. To prevent this from reoccurring, data were harvested from the third experimental repeat a few days earlier than for previous experimental repeats.

Mean rosette leaf surface area and dry weight decreased as SWC decreased. Rosette dry weight was the same between Col-0 and GCS-ox for each SWC ( $F_{8, 72} = 13.252$ ,  $F_{8, 53} = 3.841$ , and  $F_{8, 75} = 5.564$  for each experimental repeat, respectively;  $p > 0.050$ ) (Figs. 5.7a, 5.7c, 5.7e). Rosette leaf surface area was also the same between Col-0 and GCS-ox for each SWC ( $F_{8, 72} = 15.046$ ,  $F_{8, 53} = 2.880$ , and  $F_{8, 75} = 5.061$  for each experimental repeat, respectively;  $p > 0.05$ ) (Figs. 5.7b, 5.7d, 5.7f).

Overall, overexpressing *CCA1* or *TOC1* in guard cells did not alter growth, rosette dry biomass or green leaf surface area under fixed droughted conditions (Fig. 5.7).

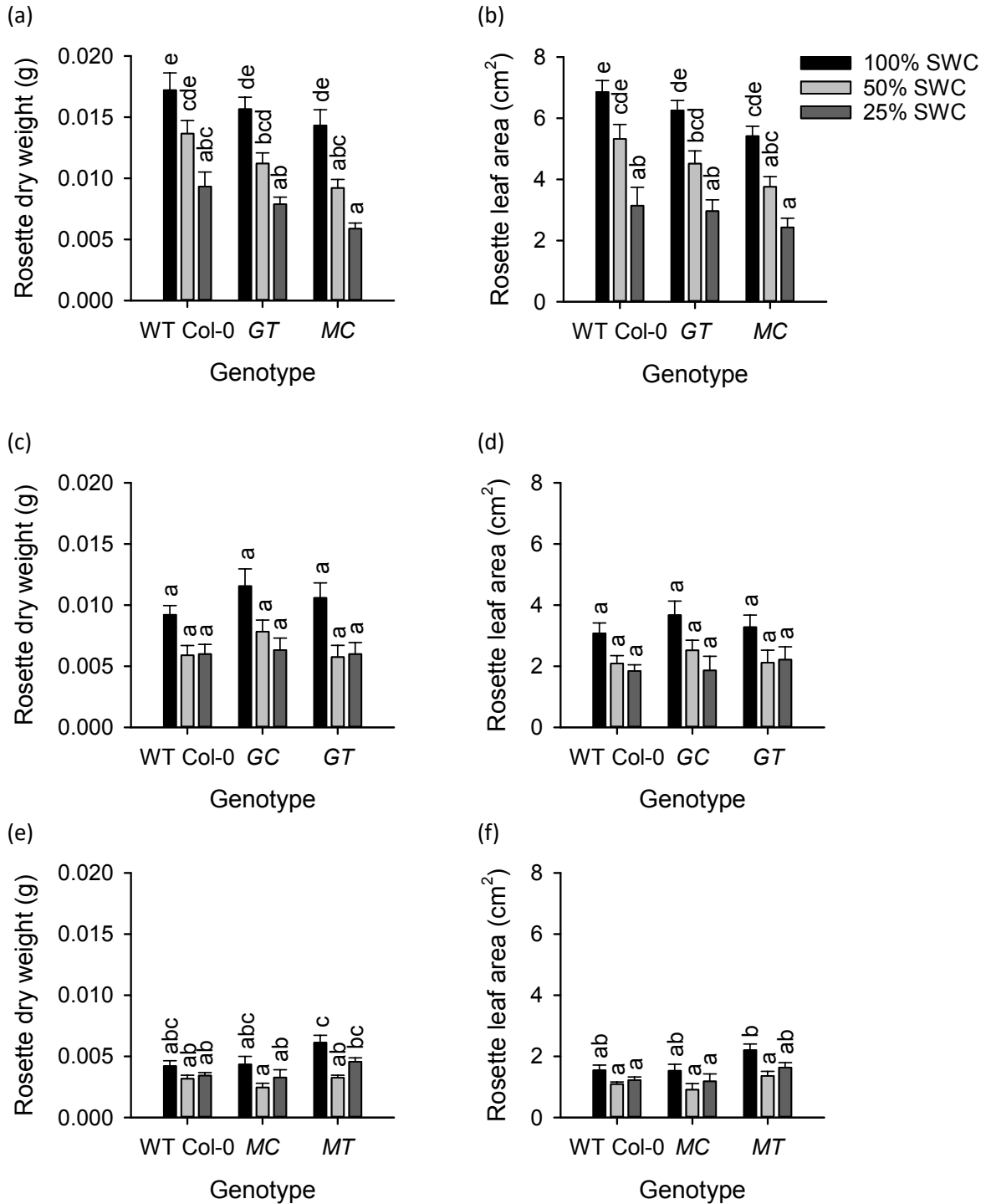


Figure 5.7: Overexpressing *CCA1* or *TOC1* in guard cells does not affect rosette dry biomass or leaf surface area when watered at a fixed soil water capacity. Plants were grown in small inserts under a 16 h photoperiod, with a soil water capacity (SWC) of 100%, 50% or 25% imposed from 7 days of growth. Data show rosette (a, c, e) dry biomass and (b, d, f) leaf area from three independent experimental repeats ( $n = 3-10$ ; mean  $\pm$  S.E.M.). Data were analysed with ANOVA and Tukey's post hoc tests. Different letters indicate statistically significant difference between means ( $p < 0.05$ ).

#### 5.4.3.4 GCS-ox did not have an altered response to the fast drought assay under conditions of constant light

Potential effects of an altered guard cell circadian clock upon drought resistance might be masked by the light/dark experimental conditions, which would reset the circadian clock at dawn each day. To remove this possible confounding factor, the fast drought assay was repeated under conditions of constant light. After 14 days of growth, water was withheld and plants placed under constant light conditions for a further 14 days. Droughted plants did not survive past 7 days under these conditions (Fig. 5.9b).

Under well-watered conditions, there was no statistically significant difference in green rosette leaf surface area between *GT*, *MC*, *MT* and Col-0 (Fig. 5.9a) ( $F_{5, 54} = 4.487, 3.226, 3.390, 1.918, \text{ or } 0.780$  at days 0, 4, 7, 11, and 14 post-drought, respectively;  $p > 0.05$ ). Under well-watered conditions, *GC* had a significantly larger green leaf surface area than Col-0 at days 4 ( $p = 0.019$ ) and 7 ( $p = 0.007$ ) post-drought, but otherwise had the same leaf surface area as Col-0 (Fig. 5.9a) ( $p > 0.05$ ). In a similar manner, GCS-ox had the same green rosette leaf surface area as Col-0 under droughted conditions (Fig. 5.9b) ( $F_{5, 53} = 2.363, 1.150, \text{ or } 1.317$  at days 0, 4, and 7 post-drought, respectively;  $p > 0.05$ ). CCA1-ox had the same green rosette leaf surface area as Col-0 under both well-watered ( $p > 0.05$ ) and droughted ( $p > 0.05$ ) conditions (Figs. 5.9a, 5.9b).

All genotypes had significantly smaller rosette dry biomass under droughted conditions than under well-watered conditions (Fig. 5.9c) ( $p < 0.001$ ). Rosette dry biomass was the same for Col-0, GCS-ox and CCA1-ox grown under both well-watered ( $F_{5, 54} = 1.713, p > 0.05$ ) and droughted conditions ( $F_{5, 52} = 2.261, p > 0.05$ ) (Fig. 5.9c). Additional alleles were tested in this manner (*GC-2*, *GT-2*, *MC-2*, *MT-2*), and similar results obtained (Sup. Fig. 9.12).

Overall, overexpressing *CCA1* or *TOC1* in guard cells did not alter growth, rosette dry biomass or green leaf surface area under conditions of fast drought in constant light (Fig. 5.9).

Under constant light conditions, several well-watered plants flowered. For the second experimental repeat, it was noted which well-watered plants had an inflorescence, and the length of this inflorescence was measured. No CCA1-ox flowered, and only a single Col-0 had beginning inflorescence emergence. However, 50-100% of plants within each GCS-ox genotype had an inflorescence (Fig. 5.8). This does not appear consistent with

data obtained from the flowering time assay, where GCS-ox flowered later than Col-0 under short photoperiods (Fig. 5.4). However, earlier flowering may also be caused by stress.

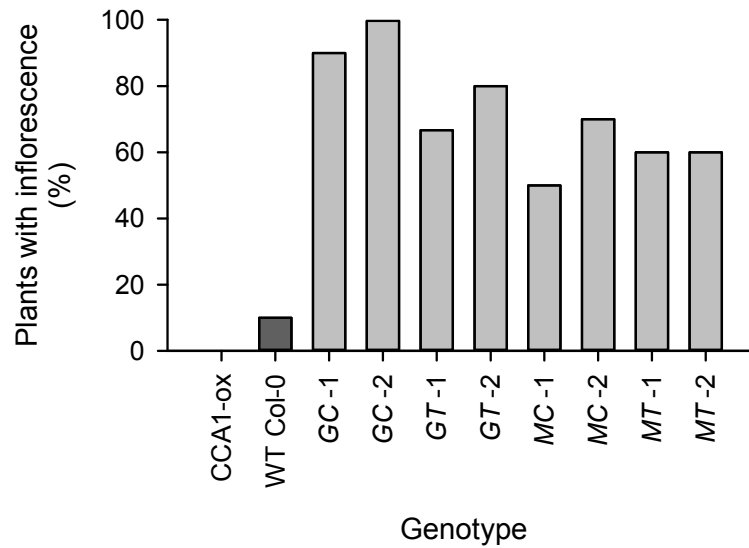


Figure 5.8: Overexpressing *CCA1* or *TOC1* in guard cells seems to cause earlier flowering under constant light conditions. Data show percentage of flowering plants after two weeks under constant light and well-watered conditions ( $n = 10$ ). Colour-coding highlights the whole plant overexpressor control (black), wild type control (dark grey), and GCS-ox genotypes (light grey). Data derive from a single experimental repeat, thus should be treated with caution.



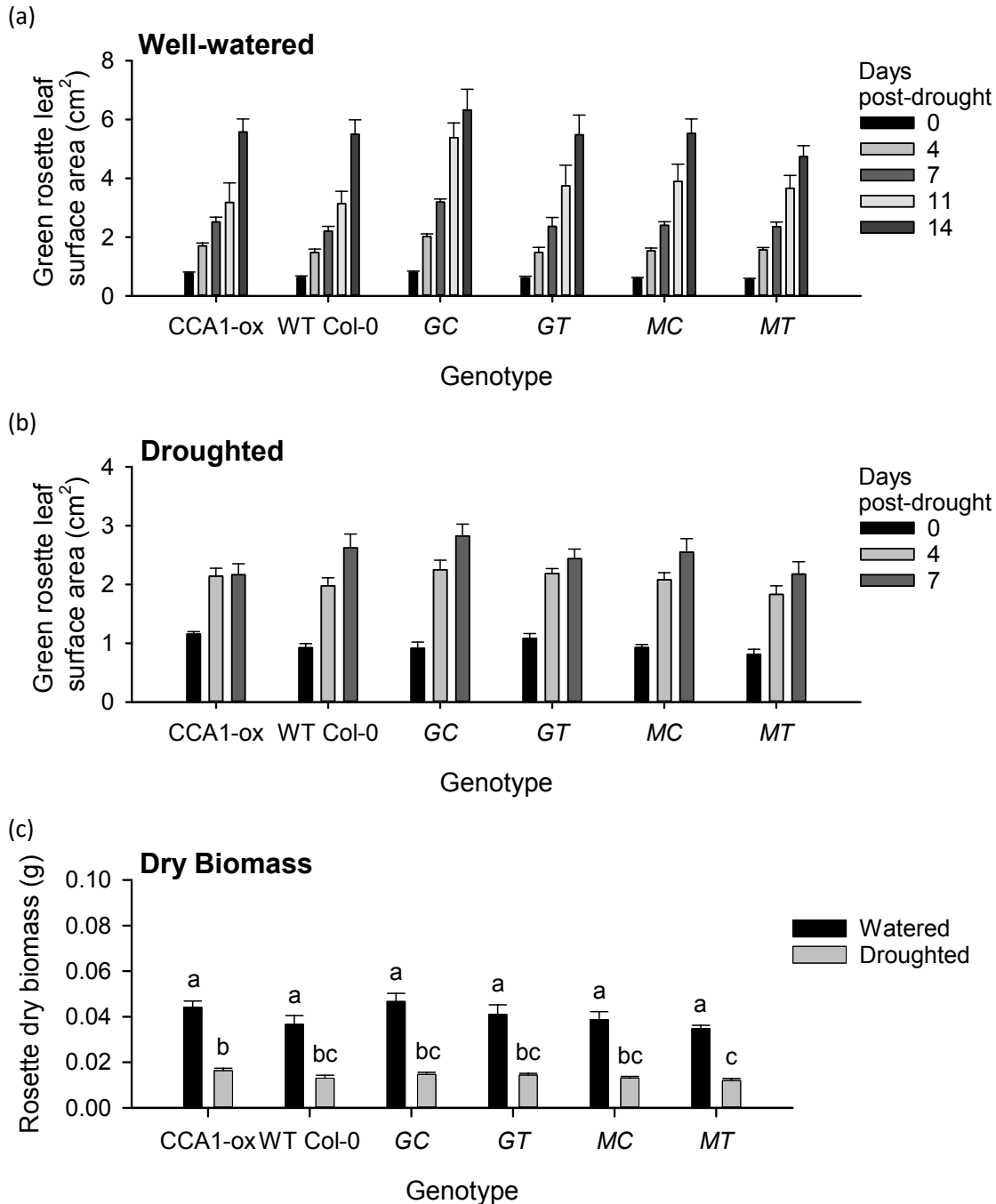


Figure 5.9: Overexpressing *CCA1* or *TOC1* in guard cells does not affect growth, rosette leaf surface area or dry biomass under well-watered or fast droughted conditions in constant light. Plants were grown in small inserts under a 16 h photoperiod for the first 14 days of growth, then drought was imposed and plants moved to constant light conditions. Green rosette leaf area measurements were taken at 0, 4, 7, 11 and 14 days post-drought for (a) well-watered and (b) droughted plants, and (c) final rosette dry biomass was measured ( $n = 10$ ; mean  $\pm$  S.E.M.). Whole plant overexpressor and WT controls are indicated on the left of each panel. Data were analysed with ANOVA and Tukey's post hoc tests. Different letters indicate statistically significant difference between means ( $p < 0.05$ ).

#### 5.4.4 Overexpressing *CCA1* or *TOC1* in guard cells affects plant survival to dehydration

A dehydration assay was also performed on GCS-ox. Briefly, 2 week-old seedlings were dehydrated on filter paper for 9 h under constant light conditions, then re-watered and maintained under constant light conditions for a further 48 h (Legnaioli et al. (2009)). Seedling survival was analysed, with seedlings having a green apical meristematic region counted as survivors.

*CCA1*-ox, two *MC* alleles and two *GC* alleles had higher survival to dehydration than Col-0, whereas one *GT* allele and two *MT* alleles survived less than Col-0 (Fig. 5.10). *TOC1*-ox also survived slightly less than Col-0. However, phenotypes observed for guard

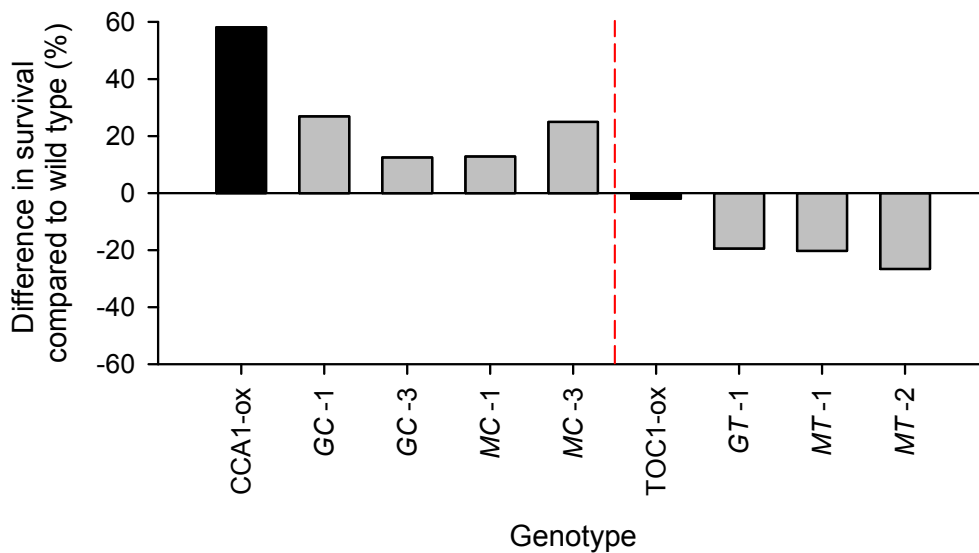


Figure 5.10: Overexpressing *CCA1* or *TOC1* in guard cells increases or decreases survival to dehydration under constant light conditions, respectively. Data show percentage difference in survival of GCS-ox genotypes and alleles compared to WT Col-0 in the dehydration assay. Colour-coding highlights whole plant overexpressor controls (black) and GCS-ox genotypes (light grey). Data were obtained from two or three experimental repeats (mean;  $n = 32$  per independent experimental repeat). Supplemental data with additional alleles are provided in the Appendix (Sup. Fig. 9.13).

cell *TOC1* overexpressors were more extreme, with a ten times lower survival than *TOC1*-ox (Fig. 5.10).

Only one *GT* allele is shown here, as data obtained from other *GT* alleles were too vari-

able. Data varied excessively between experimental repeats for some alleles, and a few additional alleles were examined with only a single experimental repeat. These supplemental data are provided in the Appendix (Sup. Fig. 9.13). Despite the poorer quality of these supplemental data, the overall pattern of survival to dehydration remains the same: the majority of guard cell *CCA1* overexpressors survived more than Col-0, whereas guard cell *TOC1* overexpressors had lower survival than Col-0 (Sup. Fig. 9.13).

#### 5.4.5 GCS-ox have altered detached leaf water loss rates

Stomatal pores close to minimise water loss as a short term solution to drought stress (Sirichandra et al. (2009); Pantin et al. (2013)). To determine whether misregulating the guard cell circadian clock affects stomatal response to drought stress, detached leaf assays were performed. This involves detaching leaves and weighing them over time. When stomata are open, more water is lost, thereby more weight is lost (Verslues et al. (2006)). Four experimental repeats were performed per GCS-ox genotype, and data were averaged between experimental repeats.

GCS-ox detached leaves lost weight at a similar rate to Col-0 detached leaves for the first 60 min, then lost more water than Col-0 detached leaves for the remainder of the experiment (Fig. 5.11). *GC* detached leaves lost significantly more water than Col-0 detached leaves at 150 min ( $t_{38}=2.268$ ,  $p=0.029$ ) and 180 min ( $t_{32}=2.188$ ,  $p=0.036$ ) after being detached (Fig. 5.11a). *GT* detached leaves lost significantly more water than Col-0 detached leaves at 120 min ( $t_{38}=2.264$ ,  $p=0.029$ ), 150 min ( $t_{33}=2.724$ ,  $p=0.01$ ) and 180 min ( $t_{31}=3.301$ ,  $p=0.002$ ) post-detachment (Fig. 5.11b). Detached *MT* leaves lost significantly more water than Col-0 leaves from 90 min post-detachment onwards (90 min:  $t_{38}=2.333$ ,  $p=0.025$ ; 120 min:  $t_{32}=2.826$ ,  $p=0.008$ ; 150 min:  $t_{27}=2.958$ ,  $p=0.006$ ; 180 min:  $t_{25}=3.154$ ,  $p=0.004$ ) (Fig. 5.11d). There was no statistically significant difference in percentage weight loss between *MC* and Col-0 detached leaves, but a similar trend occurred (Fig. 5.11c). Interestingly, a nearly opposite phenotype was observed for *CCA1*-ox: detached leaves lost significantly less weight than Col-0 leaves during the first 60 min, then rapidly lost weight to reach the same values as Col-0 (Sup. Fig. 9.14).

Overall, overexpressing *CCA1* or *TOC1* in guard cells caused detached leaves to lose more water than Col-0 (Fig. 5.11).

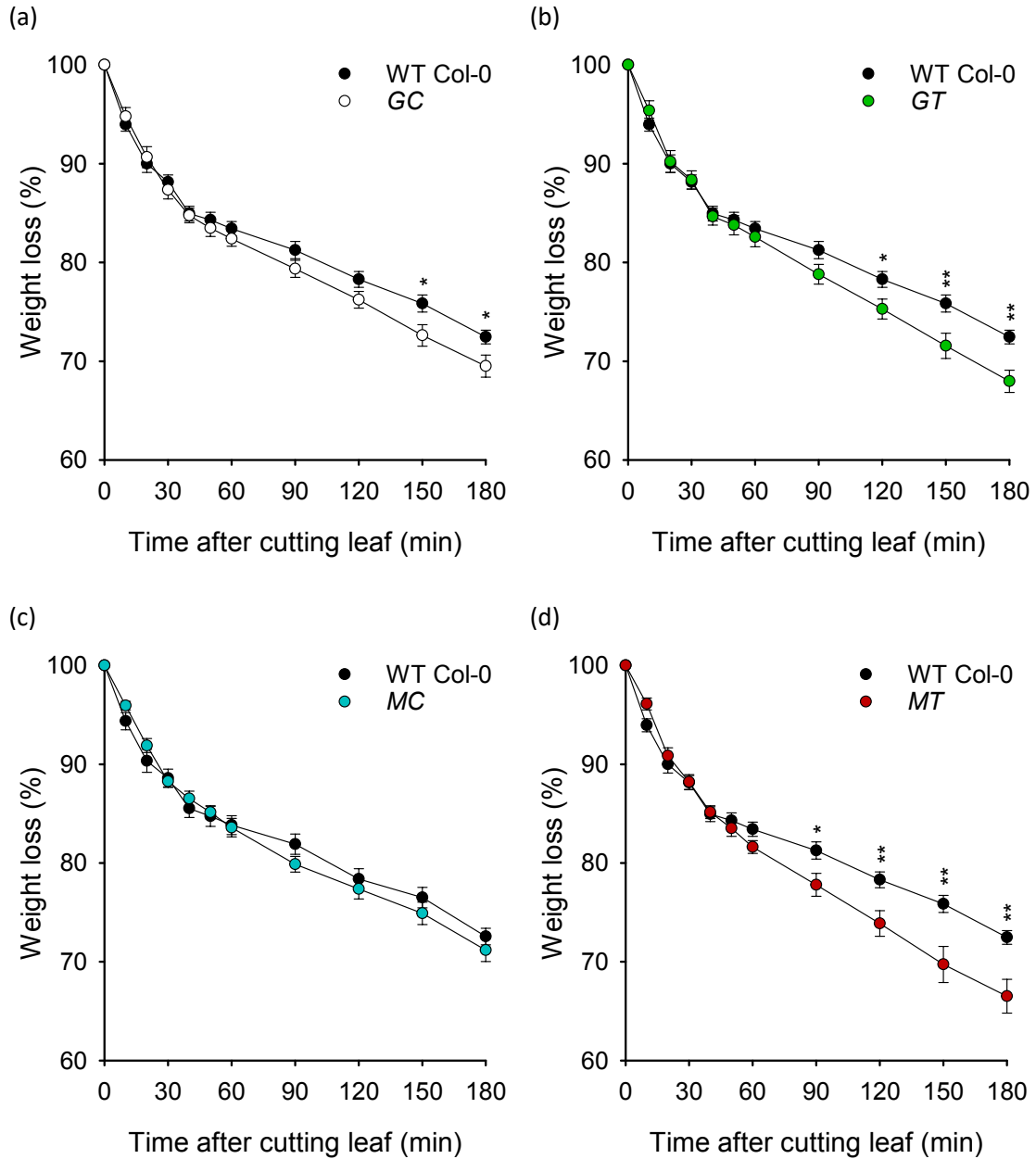


Figure 5.11: Overexpressing *CCA1* or *TOC1* in guard cells affects detached leaf water loss over time. Data show percentage of weight loss over time from three or four experimental repeats for (a) *GC1::CCA1:nos* (*GC*), (b), *GC1::TOC1:nos* (*GT*), (c) *MYB60::CCA1:nos* (*MC*) and (d) *MYB60::TOC1:nos* (*MT*) ( $n = 15-20$  total; mean  $\pm$  S.E.M.). Data were analysed with independent samples t-tests, and statistical significance compared to Col-0 at the same timepoint is indicated using starring (\* =  $p < 0.05$ ; \*\* =  $p < 0.01$ ; \*\*\* =  $p < 0.001$ ).

### 5.4.6 Stomatal density is unaffected in GCS-ox

Stomatal water loss is also affected by stomatal density (Lawson and Blatt (2014)). Therefore, stomatal density was measured for each GCS-ox genotype, as well as for Col-0 and CCA1-ox. Stomatal density and index were obtained for two sites per leaf, two fully developed leaves were sampled per plant, and eight plants were sampled per genotype.

GCS-ox and CCA1-ox had the same stomatal density ( $F_{5, 159} = 1.640, p > 0.05$ ) and stomatal index ( $F_{5, 159} = 2.080, p > 0.05$ ) as Col-0 (Fig. 5.12). An experimental repeat produced identical results (Sup. Fig. 9.15) (stomatal density:  $F_{5, 163} = 0.959, p > 0.05$ ; stomatal index:  $F_{5, 163} = 4.487, p > 0.05$ ).

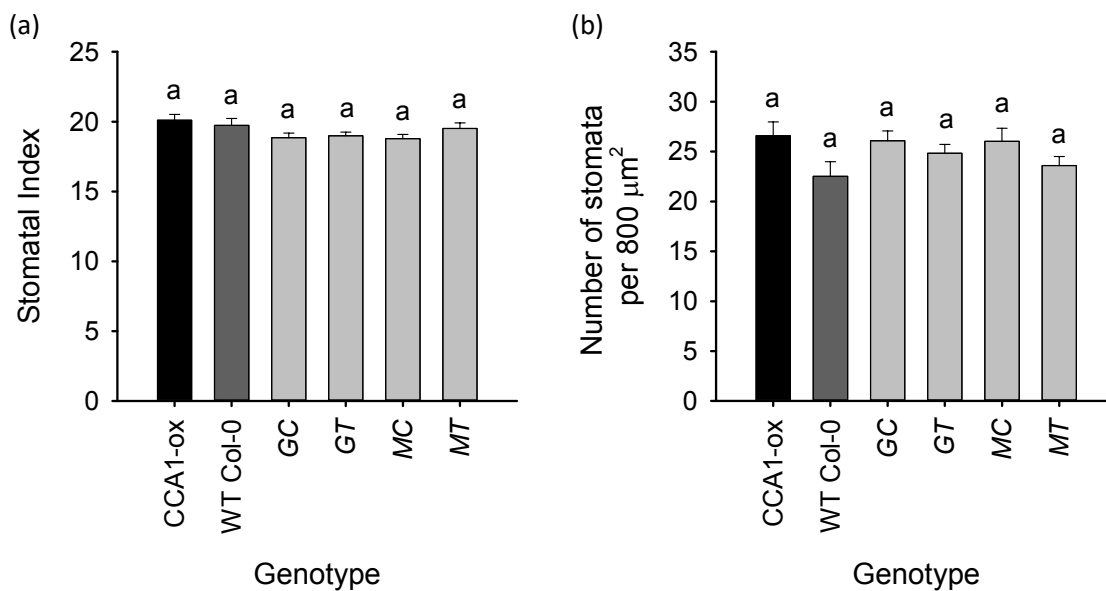


Figure 5.12: Overexpressing *CCA1* or *TOC1* in guard cells does not affect (a) stomatal index nor (b) stomatal density. Data were collected from one experimental repeat ( $n = 19-32$ ; mean  $\pm$  S.E.M.); data from an additional experimental repeat are provided in the Appendix (Sup. Fig. 9.15). Colour-coding highlights the whole plant overexpressor control (black), wild type control (dark grey), and GCS-ox genotypes (light grey). Data were analysed with ANOVA and Tukey's post hoc tests. Different letters indicate statistically significant difference between means ( $p < 0.05$ ).

#### **5.4.7 GCS-ox and CCA1-ox have unaltered stomatal closure responses to ABA**

The bidirectional relationship between the circadian clock and ABA is very complex and not yet fully understood. ABA is sensed by guard cells and promotes stomatal closure, and this is regulated by *TOC1* (Legnaioli et al. (2009)). Therefore, involvement of the guard cell circadian clock in ABA-induced stomatal closure was examined. Leaf discs were incubated in buffer containing 0  $\mu\text{M}$ , 0.1  $\mu\text{M}$ , 1  $\mu\text{M}$  or 10  $\mu\text{M}$  ABA, and stomatal aperture was measured.

Data varied substantially between experimental repeats, so data from several experimental repeats are provided here for clarity. ABA induced stomatal closure for all genotypes, with GCS-ox and CCA1-ox stomata responding in a similar manner to Col-0 stomata (Figs. 5.13, 5.14, 5.15). The variability between experimental repeats does not allow me to reach any conclusions on the role of the guard cell circadian clock in ABA-mediated stomatal closure.

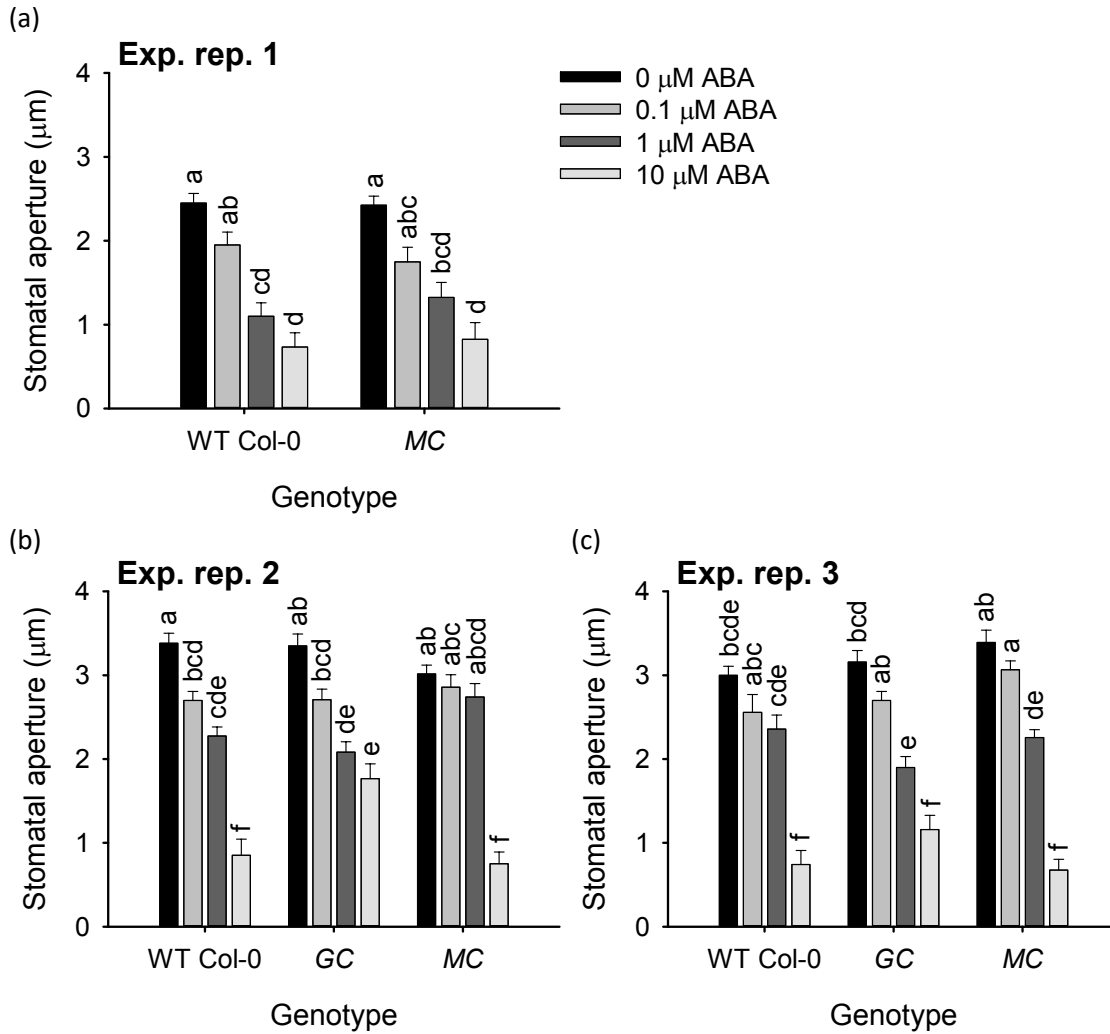


Figure 5.13: Overexpressing *CCA1* in guard cells does not affect ABA-induced stomatal closure. Stomatal aperture was measured in leaf discs incubated in 0 µM, 0.1 µM, 1 µM or 10 µM ABA ( $n = 30$ ; mean  $\pm$  S.E.M.). Each panel represents an independent experimental repeat (Exp. rep.), as data varied substantially between experimental repeats. Data were analysed with ANOVA and Tukey's post hoc tests. Different letters indicate statistically significant difference between means ( $p < 0.05$ ).

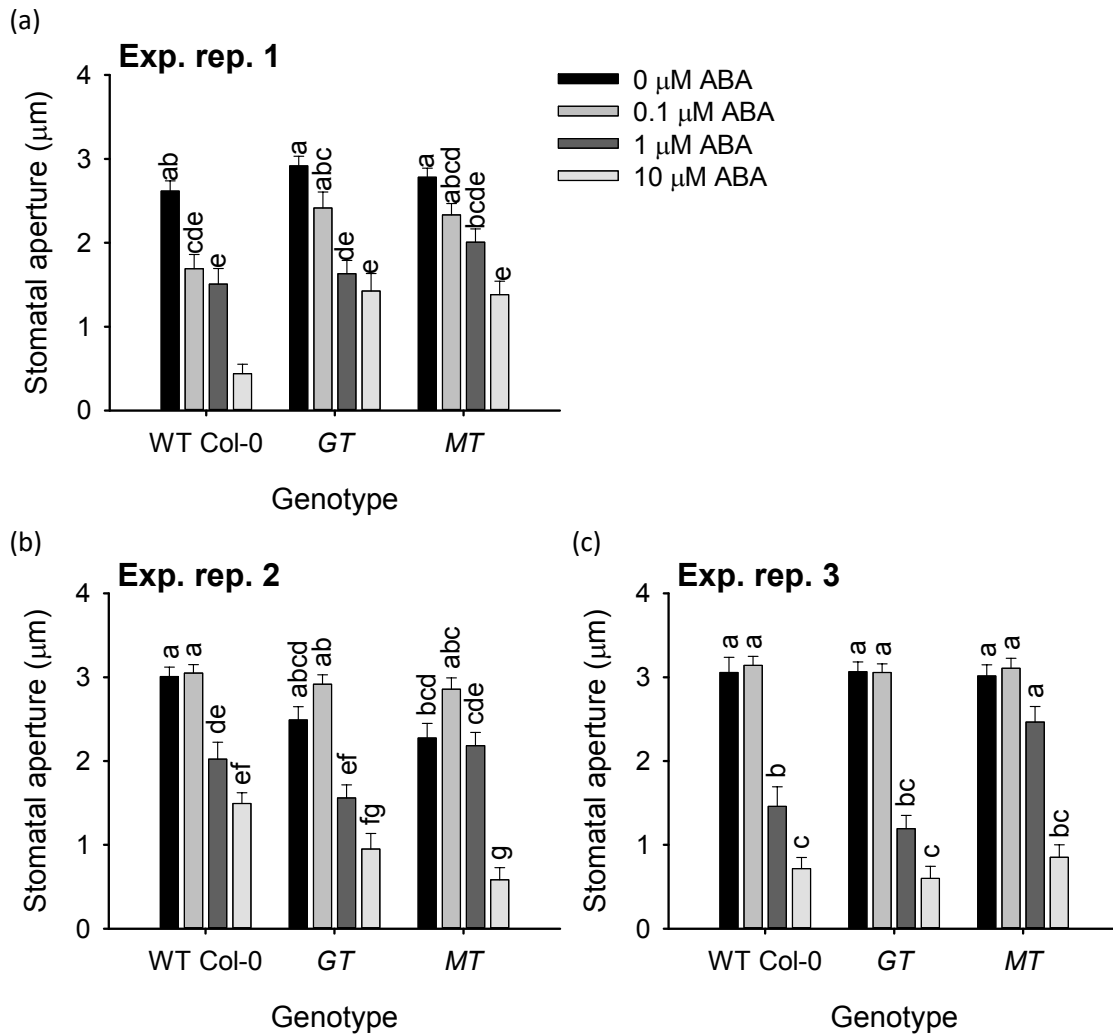


Figure 5.14: Overexpressing *TOC1* in guard cells does not affect ABA-induced stomatal closure. Stomatal aperture was measured in leaf discs incubated in 0  $\mu\text{M}$ , 0.1  $\mu\text{M}$ , 1  $\mu\text{M}$  or 10  $\mu\text{M}$  ABA ( $n = 30$ ; mean  $\pm$  S.E.M.). Each panel represents an independent experimental repeat (Exp. rep.), as data varied substantially between experimental repeats. Data were analysed with ANOVA and Tukey's post hoc tests. Different letters indicate statistically significant difference between means ( $p < 0.05$ ).



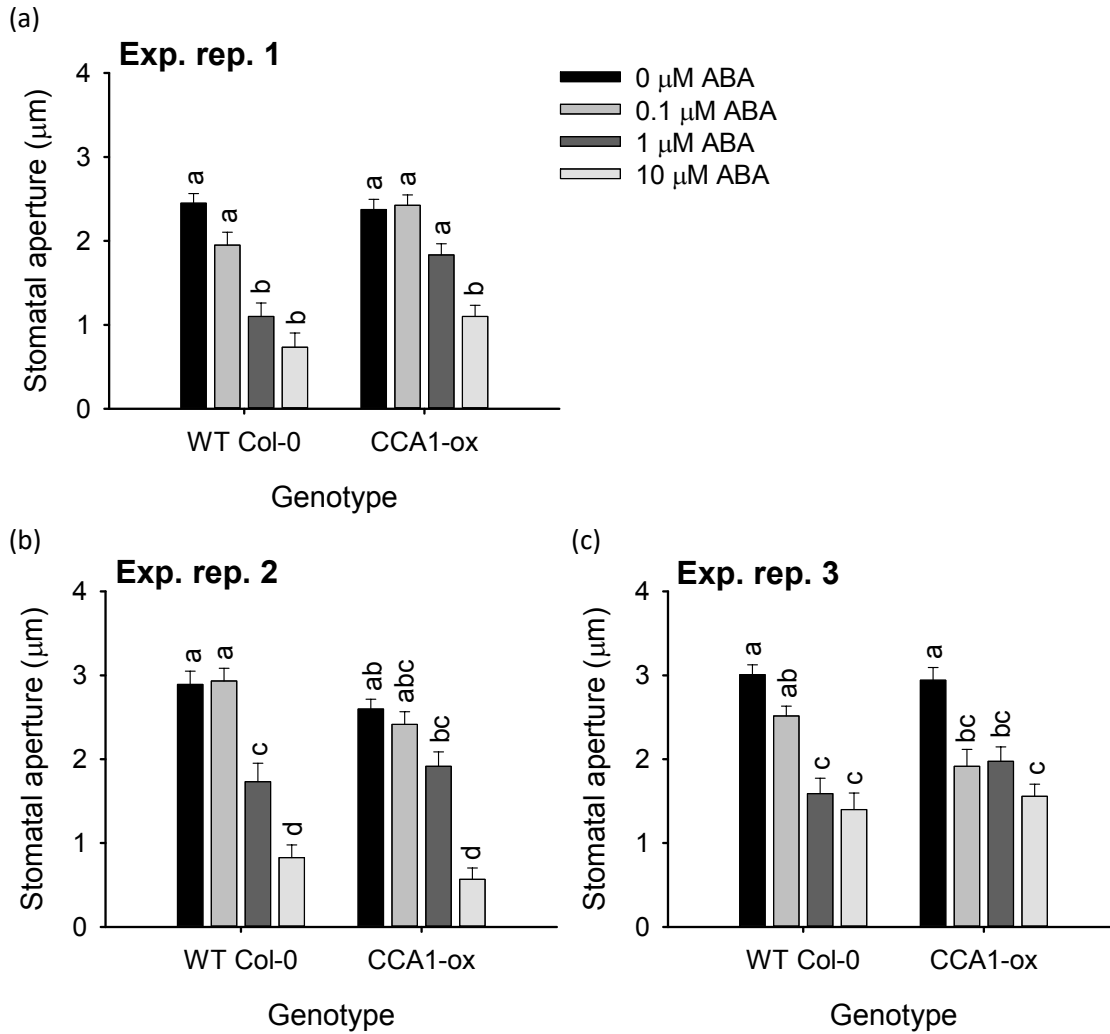


Figure 5.15: Overexpressing *CCA1* in the whole plant does not affect ABA-induced stomatal closure. Stomatal aperture was measured in leaf discs incubated in 0  $\mu\text{M}$ , 0.1  $\mu\text{M}$ , 1  $\mu\text{M}$  or 10  $\mu\text{M}$  ABA ( $n = 30$ ; mean  $\pm$  S.E.M.). Each panel represents an independent experimental repeat (Exp. rep.), as data varied substantially between experimental repeats. Data were analysed with ANOVA and Tukey's post hoc tests. Different letters indicate statistically significant difference between means ( $p < 0.05$ ).

### 5.4.8 Guard cell *CCA1* overexpressors have increased water use efficiency

I previously demonstrated that circadian clock components influence WUE (Chapter 3). Here, WUE was analysed in two alleles for each GCS-ox genotype.

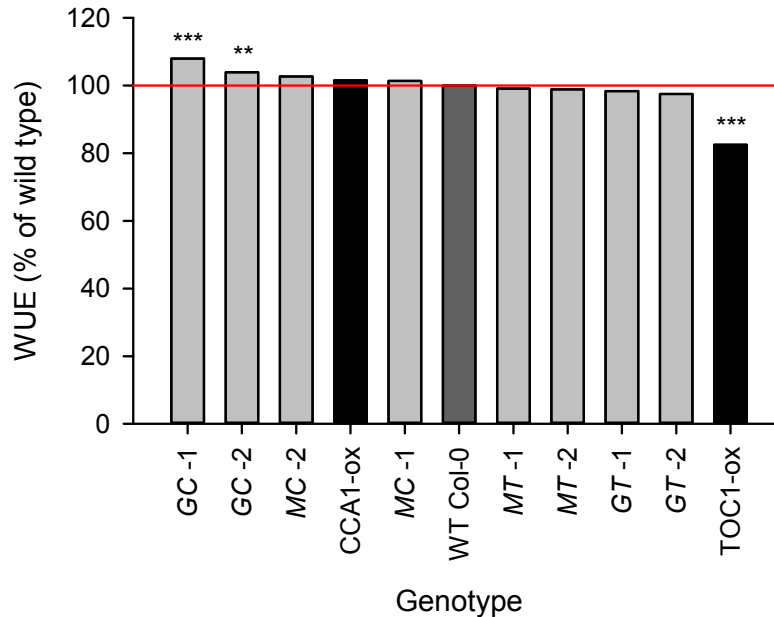


Figure 5.16: Overexpressing *CCA1* in guard cells seems to increase WUE. Data are WUE as a percentage of the wild type (WT), with WUE of WT Col-0 normalised to 100%. One experimental repeat is provided here for each allele ( $n=5-15$ ); additional experimental replicates are in the Appendix (Sup. Fig. 9.16). Data for *CCA1-ox* and *TOC1-ox* are from Chapter 3 and redrawn here for comparison with their respective GCS-ox genotypes. Colour-coding highlights whole plant overexpressor controls (black), WT control (dark grey), and GCS-ox genotypes (light grey). Data were analysed with independent samples t-tests, and statistical significance compared to Col-0 is indicated using starring (\*\* =  $p < 0.01$ ; \*\*\* =  $p < 0.001$ ).

Both *GC* alleles were significantly more water use efficient than Col-0 (*GC-1*:  $p < 0.001$ ; *GC-2*:  $p = 0.002$ ), with *GC-1* being 8% more water use efficient than Col-0 (Fig. 5.16). *MC* alleles also had slightly higher WUE than Col-0, but this was not statistically significant for the majority of experimental replicates ( $p > 0.05$ ) (Fig. 5.16; Sup. Fig. 9.16).

In contrast, guard cell *TOC1* overexpressors had slightly lower WUE than Col-0, with values up to 5% lower than Col-0, but these were not statistically significant ( $p > 0.05$ )

(Fig. 5.16; Sup. Fig. 9.16). Interestingly, WUE was unaltered or decreased in CCA1-ox, and significantly decreased in TOC1-ox (data from Chapter 3).

Overall, these data suggest that guard cell *CCA1* overexpressors are significantly more water use efficient than the WT, whereas overexpressing *TOC1* in guard cells does not alter WUE (Fig. 5.16; Sup. Fig. 9.16).

## 5.5 Discussion

The relationship between the guard cell circadian clock and the circadian clocks in other tissues, such as vasculature, mesophyll or epidermis, is complex. To understand this, one could compare the phenotypes of a WT plant (*e.g.* Col-0), a plant in which the guard cell circadian clock is disrupted (*e.g.* GCS-ox), and a plant in which the circadian clock is disrupted throughout all tissues (*e.g.* CCA1-ox, TOC1-ox) for a given physiological experiment (Fig. 5.17). The following interpretive framework can then be envisaged (Fig. 5.17).

Firstly, let us examine the scenario in which the GCS-ox and whole plant circadian clock gene overexpressor have the same phenotype, and that this phenotype is different to that of the WT (Fig. 5.17a). One interpretation is that signals from the guard cell circadian clock are overriding signals from the circadian clocks of surrounding tissues for this physiological response (Fig. 5.17a). Alternatively, the guard cell circadian clock alone is regulating the observable physiological response, with no or little input from other circadian clocks.

An alternative scenario would be that the GCS-ox and WT have the same phenotype, and that this phenotype is different to that of the whole plant circadian clock gene overexpressor (Fig. 5.17b). In this case, it is likely that circadian clocks from other tissues are regulating the guard cell circadian clock and/or this particular physiological response (Fig. 5.17b).

An additional scenario would be if all three genotypes (WT, GCS-ox, whole plant circadian clock gene overexpressor) have distinct phenotypes (Fig. 5.17c). One possible interpretation is that the examined phenotype is controlled partly by the guard cell circadian clock and partly by the circadian clocks of other tissues (Fig. 5.17c). Alternatively, these phenotypes may indicate that the guard cell circadian clock is only partly

regulated by the circadian clocks of other tissues, or vice-versa.

Finally, if no differences are observed between the GCS-ox, WT, and whole plant circadian clock gene overexpressor, then it is likely that this physiological response is not regulated by the circadian clock (Fig. 5.17d).

This interpretive framework will be used throughout this section to analyse the influence of the guard cell circadian clock and other tissue-specific circadian clocks upon whole plant physiology (Fig. 5.17).

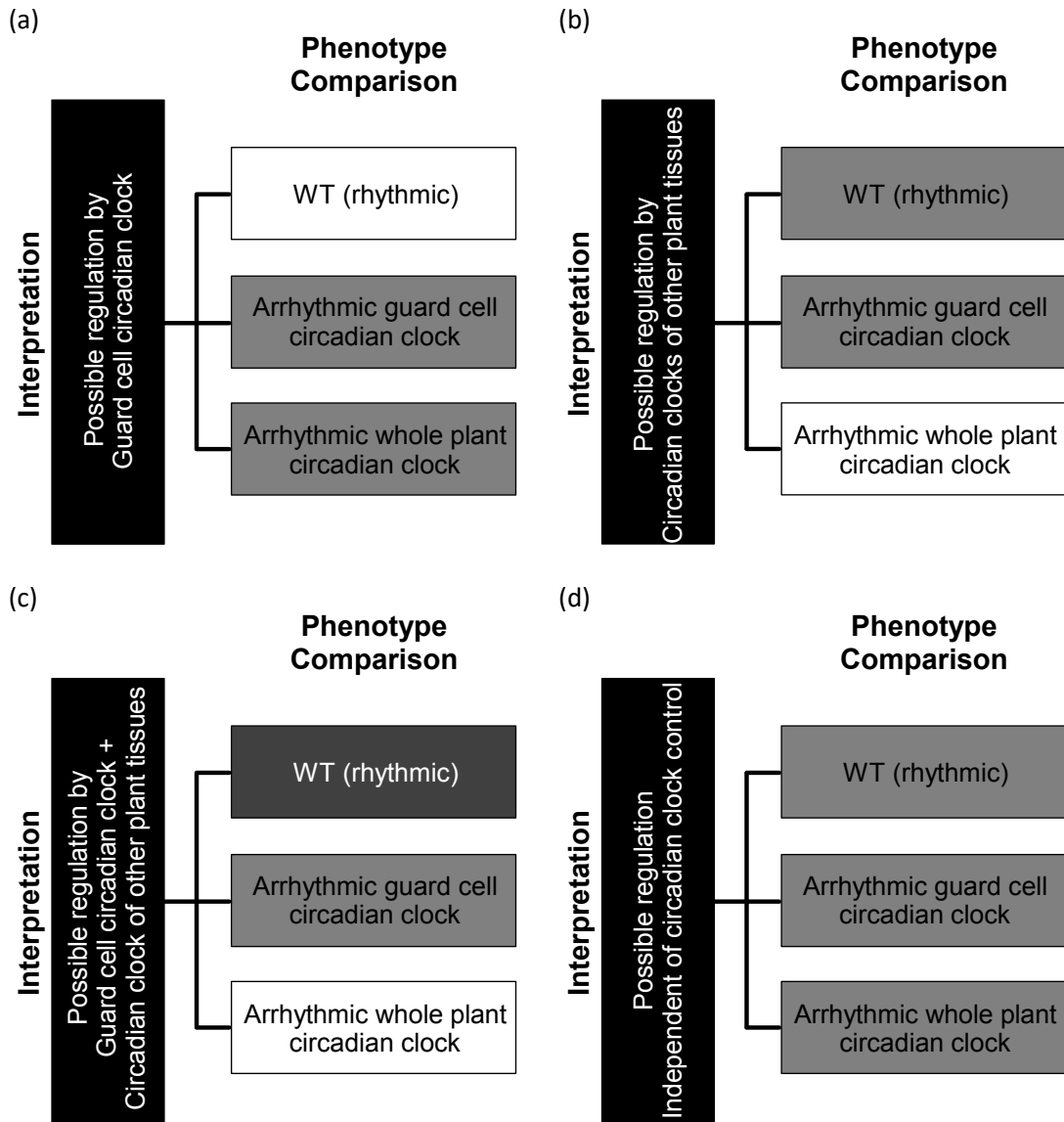


Figure 5.17: Interpretive framework used to analyse the influence of the guard cell circadian clock and other tissue-specific circadian clocks upon whole plant physiology. The phenotype of each genotype (wild type, plant with an arrhythmic guard cell circadian clock, plant with an arrhythmic circadian clock in all plant tissues) is represented by an individual box. The colour of the box represents the comparison between phenotypes: different phenotypes are represented by boxes of different colours (white, grey, dark grey), whereas identical phenotypes are represented by boxes of identical colour. Each possible combination of phenotype comparisons may be interpreted in the following manner (represented vertically within black boxes): the physiological process is (a) regulated by the guard cell circadian clock, (b) regulated by the circadian clock(s) of (an)other plant tissue(s), (c) regulated by both the guard cell circadian clock and the circadian clock(s) of (an)other plant tissue(s), or (d) not regulated by the circadian clock.

### 5.5.1 Hypocotyl elongation is unaltered in GCS-ox

Overexpressing *CCA1* or *TOC1* in guard cells did not alter hypocotyl elongation under a range of photoperiods, whereas, consistent with previous reports, overexpressing these genes throughout the plant produced taller and shorter hypocotyls, respectively (Figs. 5.1, 5.2) (Wang and Tobin (1998); Green et al. (2002); Más et al. (2003); Murakami et al. (2004); Dodd et al. (2005); Nozue et al. (2007); Nusinow et al. (2011); Hassidim et al. (2017)). Following our interpretative framework, this implies that hypocotyl elongation is not regulated by the guard cell circadian clock, but rather by other tissue-specific circadian clocks (Fig. 5.17b).

Indeed, the epidermal circadian clock was shown to regulate hypocotyl length through cell elongation but not proliferation mechanisms (Shimizu et al. (2015)). As the epidermal circadian clock is arrhythmic in *CCA1-ox* and *TOC1-ox*, but not in *GCS-ox*, this may explain the different hypocotyl lengths observed between *CCA1-ox/TOC1-ox* and *GCS-ox* (Figs. 5.1, 5.2). However, *CCA1-ox* and *TOC1-ox* hypocotyl length varied with day length, confirming the existence of an additional clock-independent, photoperiod-dependent pathway involved in hypocotyl cell elongation (Shimizu et al. (2015)).

The magnitude of sucrose-induced hypocotyl elongation under 4 h photoperiods was unaltered in *CCA1-ox*, *TOC1-ox* and *GCS-ox* (Fig. 5.3). This indicates that the circadian clock is not involved in sucrose-induced hypocotyl elongation under short photoperiods (Fig. 5.17d), as was observed previously (Appendix, Simon et al. (2018a)).

### 5.5.2 Misregulating the guard cell circadian clock may affect growth

Misregulating the circadian clock often produces altered flowering time phenotypes (Schaffer et al. (1998); Fowler et al. (1999); Strayer et al. (2000); Doyle et al. (2002); Panda et al. (2002); Hayama and Coupland (2003); Yamamoto et al. (2003); Somers et al. (2004); Bendix et al. (2015); Johansson and Staiger (2015)). Under short days, misregulating the guard cell circadian clock caused plants to flower significantly later than the WT, yet with the same number of leaves at flowering time (Figs. 5.4a, 5.4b). Under long days, there were no differences between flowering time or number of leaves at flowering for Col-0 and *GCS-ox* (Figs. 5.4c, 5.4d). Similar results were obtained by Hassidim et al. (2017): plants in which *CCA1* was overexpressed in guard

cells only (named *SGC*) had a similar number of leaves to the WT at flowering, with a photoperiod-sensitive flowering time. However, growth time prior to flowering was not indicated in Hassidim et al. (2017), so it is unknown whether *SGC* had the same late flowering phenotype under short days as I observed in *GCS-ox*.

Leaf number can be used as a proxy for developmental stage. Our data suggest that *GCS-ox* required more days than *Col-0* to achieve the same developmental stage. However, this was only observed when plants were grown under 8 h photoperiods (Fig. 5.4). This difference between short and long photoperiods may be caused by the different lengths of time spent in the vegetative state under each photoperiod. Under long photoperiods, the duration of vegetative growth is relatively short (33 days  $\pm$  0.3), while, under short photoperiods, it is over twice the length (75 days  $\pm$  0.8) (Fig. 5.4). With a short photoperiod and long vegetative lifespan, a small difference in growth rate would accumulate and become significant, whereas under a long photoperiod and short vegetative lifespan, this lag could be masked and not cause a significant difference. A similar disparity between photoperiods was reported by Ferguson et al. (2018): flowering time and WUE were correlated under a 16 h photoperiod due to the shorter vegetative lifespan, whereas WUE was no longer a predictor of flowering time under short days. This interpretation implies that misregulating the guard cell circadian clock causes a small change in development and growth.

Interestingly, guard cell *CCA1* overexpressors have an identical flowering time phenotype to guard cell *TOC1* overexpressors (Fig. 5.4), despite these genes playing distinct roles in regulating flowering time. For example, *CCA1-ox* has photoperiod-insensitive, delayed flowering compared to the WT (Wang and Tobin (1998); Green et al. (2002)). However, *TOC1-ox* does not have a marked flowering time phenotype (Makino et al. (2002)), and *TOC1* may affect flowering time independently from its role in the circadian clock (Hayama and Coupland (2003)). In contrast, *toc1-1* flowers early and the photoperiod-dependent control of flowering time was affected both in *toc1-1* and *TOC1* RNAi (Somers et al. (1998); Strayer et al. (2000); Más et al. (2003)). These findings reinforce the interpretation that misregulating the guard cell circadian clock in this fashion does not cause a “true” circadian flowering defect, but instead alters development by impacting growth.

Well-watered *GCS-ox* appeared to flower earlier than *Col-0* after two weeks under constant light, whereas *CCA1-ox* did not flower at all (Fig. 5.8). This early flowering phenotype under constant light differs from the late flowering time phenotype of *GCS-ox*

under 8 h photoperiods (Fig. 5.4). One possible interpretation is that constant light conditions induced stress in GCS-ox plants, thus causing them to flower earlier as an escape response. This would imply that constant light conditions have a larger impact on plants in which the guard cell circadian clock is misregulated.

Finally, overexpressing *CCA1* throughout the plant caused a decrease in rosette dry biomass under well-watered, light/dark conditions (Figs. 5.5, 5.6), as reported previously (Dodd et al. (2005); Ko et al. (2016)), whereas *SGC* plants had the opposite biomass phenotype (Hassidim et al. (2017)). The different biomass phenotypes observed for WT, *CCA1*-ox and *SGC* plants imply that growth is influenced by both the guard cell circadian clock and circadian clocks of other tissues (Fig. 5.17c), and perhaps by additional, circadian clock-independent factors as well.

### **5.5.3 Possible regulation of short-term drought responses by the guard cell circadian clock**

Overexpressing *CCA1* or *TOC1* in guard cells did not alter growth, rosette dry biomass or green leaf surface area under well-watered and slow, fast and fixed drought conditions, as well as under conditions of constant light (Figs. 5.5, 5.6, 5.7, 5.9). This disagrees with the findings of Hassidim et al. (2017), who reported that *SGC* plants had significantly larger leaf areas, rosette fresh weights and dry weights than the WT under both well-watered and mild drought conditions. However, *SGC* did not outperform the WT under severe drought stress (Hassidim et al. (2017)).

This discrepancy in results is difficult to explain, as both their *SGC* and my *GC* genotypes were generated using the *GC1* promoter to overexpress *CCA1* in guard cells in the Col-0 background (Chapter 4; Hassidim et al. (2017)). In addition, the experimental conditions of their drought experiment are similar to those of our fixed drought experiment (Hassidim et al. (2017)). However, the WT behaved differently in our fixed drought experiment: although not always statistically different, Col-0 rosette dry weight and leaf area decreased with the decrease in soil water capacity (Fig. 5.7), whereas no difference in WT rosette dry weight was observed between 100% and 50% soil water capacity conditions in Hassidim et al. (2017). Therefore, it is likely that some experimental conditions differed, such as compost type used.

When subjected to the dehydration assay, guard cell *CCA1* overexpressors survived



better than Col-0, but did not survive as well as CCA1-ox (Fig. 5.10). In contrast, guard cell *TOC1* overexpressors had lower survival than both Col-0 and *TOC1*-ox (Fig. 5.10). As similar results were obtained for whole plant and guard cell-specific circadian clock gene overexpression, the dehydration phenotypes observed in CCA1-ox and *TOC1*-ox may be at least partly caused specifically by the guard cell circadian clock (Fig. 5.17a) (Legnaioli et al. (2009)).

Interestingly, more CCA1-ox survived than the WT whereas *TOC1*-ox had slightly reduced dehydration survival (Fig. 5.10). This confirms previous work, as Legnaioli et al. (2009) demonstrated that *TOC1*-ox had lower survival to dehydration than the WT. In addition, *TOC1* RNAi had higher survival to dehydration than the WT (Legnaioli et al. (2009)). As CCA1-ox has constant, low *TOC1* levels under constant light conditions (Alabadí et al. (2001)), the similar survival phenotypes observed for CCA1-ox and *TOC1* RNAi may be due to decreases in *TOC1* expression. In a similar fashion, it is likely that overexpressing *CCA1* in guard cells causes lower *TOC1* transcript abundance levels in guard cells. This may explain the similar results obtained for *TOC1* RNAi (Legnaioli et al. (2009)) and guard cell *CCA1* overexpressor seedlings (Fig. 5.10).

Collectively, these dehydration and drought studies suggest that the guard cell circadian clock is more involved in short-term responses than in the long-term response to drought stress. Indeed, misregulating the guard cell circadian clock affected plant dehydration survival over 60 hours, but not response to drought on compost mix over several weeks. In addition, the detached leaf assay demonstrated that GCS-ox detached leaves lost more water than Col-0 leaves over 3 h (Fig. 5.11). Further experimentation would be necessary to confirm this hypothesis, using specialised assays to specifically target short-term and long-term responses to drought stress.

#### **5.5.4 The guard cell circadian clock does not regulate stomatal development, but may affect stomatal responses to the environment**

Stomatal density was unaffected by misregulation of the guard cell circadian clock, nor did it change when the whole plant circadian clock was disrupted in CCA1-ox. Hassidim et al. (2017) reported similar phenotypes for *SGC*. This suggests that the circadian clock does not control stomatal development (Fig. 5.17d). Additional circadian clock genes would need to be examined before concluding this.

Overexpressing *CCA1* or *TOC1* in guard cells caused detached leaves to lose more water over time than WT leaves (Fig. 5.11). As GCS-ox have the same stomatal density and index as Col-0, this result may be due to two aspects of stomatal behaviour: either their stomata closed more slowly, and/or they did not close as much as those of the WT. Detached leaves from GCS-ox lost weight at a similar rate to Col-0 detached leaves during the first hour (Fig. 5.11); thus GCS-ox did not appear to have a slower closure response. However, the percentage of water loss then increased for GCS-ox compared to the WT, resulting in a lower final water loss percentage. This suggests that GCS-ox stomata remained more open than Col-0 stomata, leading to greater water loss. Attempts were made to examine this using an infra-red gas analyser (IRGA), but data were inconclusive (data not shown). Further work should be performed with the IRGA to confirm this.

It is of note that overexpressing *CCA1* or *TOC1* in guard cells caused a similar water loss phenotype as for *TOC1*-ox, with detached leaves losing a higher percentage of water than WT detached leaves (Legnaioli et al. (2009)). This may imply that the detached leaf phenotype observed for *TOC1*-ox is specifically due, at least in part, to the guard cell circadian clock (Fig. 5.17a).

The effect of ABA upon stomatal closure was difficult to analyse due to high variability between experimental repeats. Overall, ABA-induced stomatal closure appeared to be the same for Col-0, *CCA1*-ox and GCS-ox after treatment with different ABA concentrations (Figs. 5.13, 5.14, 5.15). This was also observed by Hassidim et al. (2017) for WT, *CCA1*-ox and *SGC* genotypes when treated with stomatal opening solution or ABA.

In contrast, Legnaioli et al. (2009) demonstrated that *TOC1*-ox stomata were less responsive to ABA, whereas *TOC1* RNAi and *toc1-2* ABA-mediated stomatal closure was more effective than the WT. Therefore, although both *CCA1*-ox and *TOC1* RNAi have low *TOC1* levels, their stomata do not seem to respond in a similar fashion to ABA (Alabadí et al. (2001); Legnaioli et al. (2009); Hassidim et al. (2017)). In addition, overexpressing *TOC1* in guard cells does not appear to affect ABA-mediated stomatal closure under our experimental conditions, whereas overexpressing *TOC1* in the whole plant decreases ABA sensitivity (Legnaioli et al. (2009)). Another potential difference is that *CCA1*-ox detached leaves behaved in a similar fashion to *TOC1* RNAi detached leaves for the first hour after detachment, with detached leaves from both genotypes initially losing less water than the WT (Legnaioli et al. (2009)) (Sup. Fig. 9.14). This in itself is perplexing, as *CCA1*-ox and guard cell *CCA1* overexpressors have nearly opposite de-

tached leaf phenotypes (Fig. 5.11; Sup. Fig. 9.14). It is equally intriguing that GCS-ox have a clear water loss phenotype in detached leaves, but not an altered response to ABA in both our dataset and results obtained by Hassidim et al. (2017).

One possible explanation for these discrepancies is that *TOC1* plays a greater role than *CCA1* in ABA-mediated stomatal closure, which would resolve differences observed between *TOC1*-ox and *CCA1*-ox (Legnaioli et al. (2009); Hassidim et al. (2017)). Alternatively, *CCA1*-ox and *TOC1*-ox affect transcription of many genes other than *CCA1* and *TOC1*, thus could affect stomatal behaviour independently and/or indirectly. This may explain why similar data were obtained in detached leaves and stomatal aperture assays for guard cell *CCA1* overexpressors and guard cell *TOC1* overexpressors (Figs. 5.11, 5.13, 5.14). Furthermore, Hassidim et al. (2017) report that overexpressing *CCA1* using the *GC1* promoter does not fully eradicate *LHY* rhythmic expression; thus it is possible that *MC* and *GC* retain partial rhythmicity of other circadian oscillator genes in guard cells. This may elucidate why *CCA1*-ox and guard cell *CCA1* overexpressors have nearly opposite detached leaf phenotypes (Fig. 5.11). These differences between GCS-ox and whole plant circadian clock gene overexpressors may also point towards a role of other tissue-specific circadian clocks in sensing and responding to these abiotic stresses (Figs. 5.17b, 5.17c). Finally, these differences could simply be due to experimental error, as our results for ABA-mediated stomatal responses are variable and data for *CCA1*-ox detached leaves were produced from only two independent experimental repeats.

### 5.5.5 The guard cell circadian clock plays a role in regulating WUE

The investigation of WUE in GCS-ox produced a similar pattern of results as for the dehydration assay. Guard cell *CCA1* overexpressors were significantly more water use efficient, whereas guard cell *TOC1* overexpressors had slightly lower WUE than the WT (Fig. 5.16). Data from Chapter 3 revealed that WUE was unaltered or decreased in *CCA1*-ox, whereas overexpressing *TOC1* significantly lowered WUE (Fig. 5.16). Altogether, these results demonstrate that *CCA1* and *TOC1* play important, yet different, roles in regulating WUE.

GCS-ox had significantly altered WUE (Fig. 5.16), demonstrating that the guard cell circadian clock regulates WUE. It is also likely that circadian clocks from other tissues are involved, as *CCA1*-ox and *TOC1*-ox have different WUE phenotypes to their respec-

tive GCS-ox genotypes (Figs. 5.16, 5.17c). Indeed, overexpressing *CCA1* in guard cells increases WUE, but overexpressing *CCA1* in other tissues might decrease WUE. This means that, in *CCA1-ox*, *CCA1* overexpression in other tissue types may counteract any positive effects that *CCA1* overexpression in guard cells has on WUE. The opposite might be occurring for *TOC1-ox*, which has a more severe WUE phenotype than the guard cell *TOC1* overexpressors. In this case, the small decrease in WUE caused by *TOC1* overexpression in guard cells may be combining with other negative effects caused by overexpressing *TOC1* in other tissues, thereby leading to a much lower WUE overall. Therefore, the interplay between the guard cell and other tissue-specific circadian clocks might be causing the different WUE phenotypes observed in *CCA1-ox* and *TOC1-ox*.

Interestingly, *CCA1-ox* and *TOC1-ox* plants have noticeably different rosette structures than the GCS-ox genotypes. As rosette architecture affects WUE (Chapter 3), this may be one mechanism by which other tissue-specific circadian clocks influence WUE.

## 5.6 Conclusions

Misregulating specifically the guard cell circadian clock has allowed me to isolate the influence of the guard cell circadian clock upon whole plant physiology:

- The circadian clock seems to have guard cell-specific effects upon WUE and short-term responses to drought.
- Misregulating the guard cell circadian clock might also influence growth rate.
- The circadian clock has guard cell-independent effects upon hypocotyl elongation.

Following comparisons with whole plant circadian clock gene overexpressors, it is likely that other tissue-specific circadian clocks play a role in regulating:

- Survival to dehydration
- WUE
- Stomatal responses to ABA

- Leaf detachment

It is likely that additional, clock-independent mechanisms are also involved in these processes.

In future, it would be interesting to further disentangle the relationships between different tissue-specific circadian clocks. It would also be fascinating to gain a deeper understanding of the clock under natural conditions, particularly in relation to stomatal behaviour, water loss and carbon assimilation.

## Chapter 6

# Changes in stomatal aperture over time and stomatal density in naturally-occurring *Arabidopsis halleri* subsp. *gemmifera*

### 6.1 Introduction

Although laboratory studies have been crucial in advancing our knowledge of plant biological rhythms, these experimental conditions are far removed from the conditions under which plants evolved, where abiotic and biotic cues are continuously changing and interacting with each other. Therefore, it is informative to also perform experiments in the species' natural habitat, *in natura*, to obtain a deeper understanding of gene and cell function (Kudoh (2016)).

An increasing number of studies have adopted this approach. For example, studies on a wild population of *Arabidopsis halleri* subsp. *gemmifera* (*A. halleri*) have provided information on how flowering time and herbivory resistance pathways operate under natural conditions (Aikawa et al. (2010); Kawagoe and Kudoh (2010); Kawagoe et al. (2011); Sato and Kudoh (2016, 2017)). The population of *A. halleri* used for these studies has a genetic dimorphism, such that approximately half of plants are trichome-producing, while the remaining half lack trichomes (Kawagoe et al. (2011)).

In *Arabidopsis*, trichomes play important roles in both defense and tolerance to abiotic stress (Levin (1973); Mauricio and Rausher (1997); Handley et al. (2005); Dalin et al. (2008); Sletvold et al. (2010); Sletvold and Ågren (2012); Sato and Kudoh (2016)), but this trait imposes a fitness cost on growth and reproduction (Mauricio (1998); Sletvold et al. (2010); Kawagoe et al. (2011); Sletvold and Ågren (2012); Sato and Kudoh (2016)). Trichome formation occurs prior to stomatal meristemoid development (Larkin et al. (1996); Glover (2000)), and patterning of both cell types is linked (Bean et al. (2002)). Therefore, there may be a trade-off between trichome and stomatal development (Glover et al. (1998)).

## 6.2 Hypothesis and aims

As it is informative to study plants in their natural habitat, I examined stomatal aperture over time in a naturally-occurring population of *A. halleri*. I hypothesised that circadian regulation of stomatal opening might occur *in natura* in *A. halleri*. I investigated whether anticipation of dawn by stomatal opening, which might be assigned to circadian regulation, was detectable under natural conditions.

As this population of *A. halleri* has a genetic trichome dimorphism (Kawagoe et al. (2011); Sato and Kudoh (2016, 2017)), we hypothesised that these morphs might have different stomatal patterns, thus trichome development would affect stomatal patterning *in natura*. To examine this possibility, I measured stomatal density and index for both *A. halleri* trichome morphs.

## 6.3 Methods and methodology

Fieldwork was conducted at the Omoide-gawa field site, near an abandoned mine in Hyogo prefecture, Japan. This field site is described by Aikawa et al. (2010) and its naturally-occurring population of *A. halleri* has been investigated previously (Aikawa et al. (2010); Kawagoe and Kudoh (2010); Kawagoe et al. (2011); Sato and Kudoh (2016, 2017)). Further description of this field site is provided in Chapter 2 (section 2.6). Experiments were conducted in September 2016, when the photoperiod was approximately 12 h with dawn at 05:40 and dusk at 18:10.

Stomatal aperture was measured for glabrous *A. halleri* plants at 10 timepoints over three days: pre-dusk day 1, post-dusk day 1, midnight day 1, pre-dawn day 2, post-dawn day 2, midday day 2, pre-dusk day 2, post-dusk day 2, pre-dawn day 3, and post-dawn day 3. Adaxial leaf surfaces were moulded with dental paste in the field. Moulds were processed subsequently in the laboratory. Photon irradiance was measured every five minutes for 30 h between timepoints 15:43 and 45:03, using a spectroradiometer set up by Dora L. Cano-Ramirez. Protocols are provided in Chapter 2 (section 2.7.3).

Stomatal density was measured for glabrous and hairy *A. halleri* morphs. Samples were taken at the Omoide-gawa field site by myself, then processed at the University of Bristol by two BSci students under my direction (George Tunna, Sverre Tunstad). I analysed the data. Protocols are provided in Chapter 2 (section 2.7.2).

## 6.4 Results

### 6.4.1 Circadian anticipation of dawn in stomatal aperture may occur in the field

Involvement of circadian regulation in stomatal movements was explored in a naturally-occurring population of *A. halleri* at the Omoide-gawa field site. A 40 h timecourse was performed in the field, using dental paste to create adaxial leaf surface imprints (3-4 leaves per plant, 8 plants per timepoint) (Fig. 6.1). To test whether anticipation of dawn in stomatal opening was detectable under field conditions, samples were taken just before and after dawn on two consecutive days. With a similar reasoning in mind, samples were taken before and after dusk to examine changes in aperture at dusk. Finally, aperture was measured once at midday and once at midnight to obtain approximate measures of maximal and minimal stomatal aperture, respectively. Photon irradiance levels were measured continuously at the field site between timepoints 15:43 and 45:03 (Fig. 6.1).

Light intensity was significantly correlated with stomatal aperture (Pearson correlation analysis:  $r_{3980} = 0.373$ ;  $r^2 = 0.139$ ;  $p < 0.001$ ). Light intensity explained 14% of variation in stomatal aperture for the first eight timepoints.

Independent samples t-tests compared stomatal aperture at pre-dusk and post-dusk,



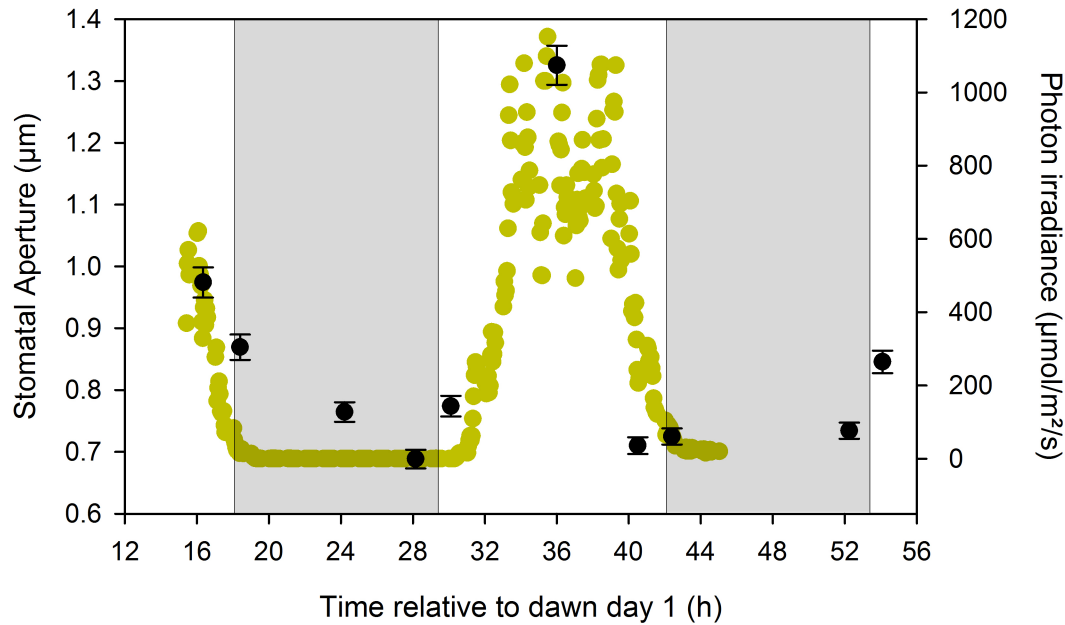


Figure 6.1: Stomatal aperture of *A. halleri* over time under natural conditions. Stomatal aperture (black symbols) is represented on the left y axis ( $n = 373\text{-}616$  stomata measured per timepoint; mean  $\pm$  S.E.M.). Photon irradiance at the field site (yellow symbols) is represented on the right y axis (point measurements every 5 min). Shading represents night.

and at pre-dawn and post-dawn, for each light-dark and dark-light transition. Stomatal aperture decreased significantly after dusk for the first day-to-night shift (timepoints 16:35 and 18:40;  $t_{982} = 3.303$ ;  $p < 0.001$ ), whereas no change in stomatal aperture occurred during the second dusk period (timepoints 40:50 and 42:40;  $t_{1178} = -0.785$ ;  $p > 0.05$ ) (Fig. 6.1). In contrast, stomatal aperture increased significantly by  $0.09 \mu\text{m}$  and  $0.11 \mu\text{m}$  for dawn day 2 and dawn day 3, respectively (dawn day 2, timepoints 28:15 and 30:10:  $t_{750.388} = -3.798$ ,  $p < 0.001$ ; dawn day 3, timepoints 52:25 and 54:10:  $t_{926.109} = -4.961$ ,  $p < 0.001$ ) (Fig. 6.1). Statistically significant differences between all timepoints were also identified using ANOVA and post hoc Tukey tests ( $F_{9, 4958} = 97.313$ ) and provided in the Appendix (Sup. Fig. 9.17).

Interestingly, on day 2, stomatal aperture post-dawn (timepoint 30:10) is significantly larger than stomatal aperture pre-dusk (timepoint 40:50) ( $t_{947} = 2.962$ ;  $p = 0.003$ ), despite light levels being over 2 000 times higher at pre-dusk (40:50;  $224.6 \mu\text{mol m}^{-2} \text{s}^{-1}$ ) than at post-dawn (30:10;  $0.11 \mu\text{mol m}^{-2} \text{s}^{-1}$ ) (Fig. 6.1; Sup. Fig. 9.17). In addition, there is no significant difference between stomatal apertures at timepoints 24:20 (midnight), 28:20 (pre-dawn day 2), 40:50 (pre-dusk day 2), 42:40 (post-dusk day 2) and 52:30 (pre-dawn day 3) ( $F_{9, 4958} = 97.313$ ;  $p > 0.05$ ) (Sup. Fig. 9.17). These data imply

that circadian anticipation of dawn in stomatal aperture is detectable under field conditions.

#### **6.4.2 Stomatal density varies between two *A. halleri* trichome morphs**

To investigate whether trichome development might affect stomatal development *in natura*, stomatal patterning was explored for hairy and glabrous *A. halleri* morphs at the Omoide-gawa field site. As previously, leaf surface imprints were created using dental paste (3-4 leaves per plant, 8 plants sampled per morph). Two BSci students under my guidance processed these moulds and counted the number of stomata and pavement cells. I analysed these data to obtain measures of stomatal index (Fig. 6.2a) and density (Fig. 6.2b).

Glabrous plants had significantly higher stomatal density ( $F_{1, 118} = 15.798$ ;  $p < 0.001$ ) and index ( $F_{1, 118} = 10.552$ ;  $p = 0.002$ ) than hairy plants. Both morphs had the same density of pavement cells ( $F_{1, 118} = 3.527$ ;  $p > 0.05$ ) (data not shown).

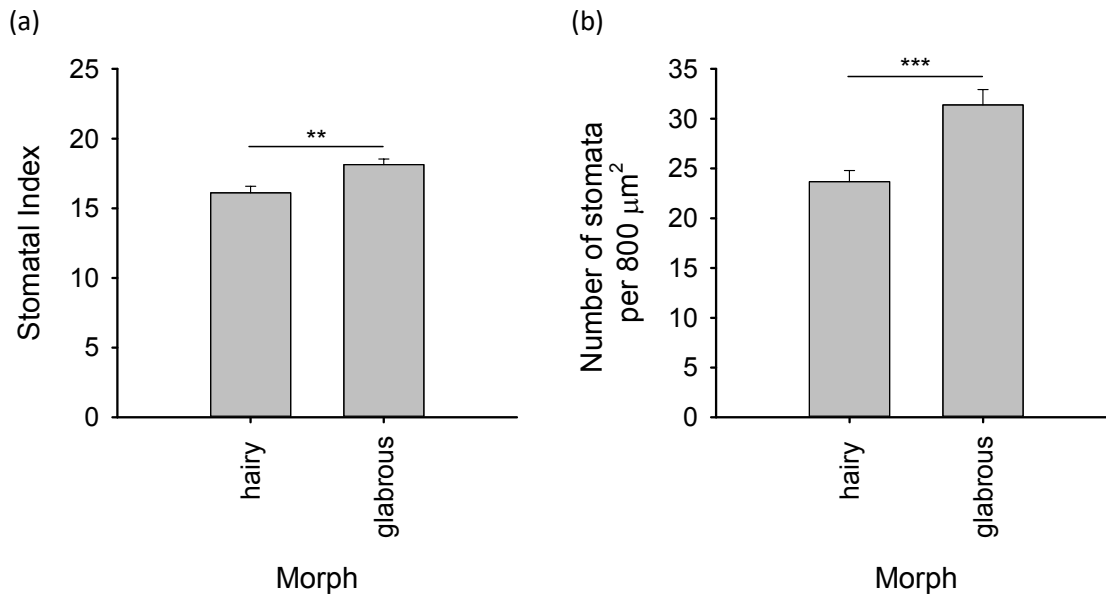


Figure 6.2: Glabrous *A. halleri* have higher stomatal index and stomatal density than hairy plants under field conditions. Samples were collected in the field at midday, day 2. Data represent (a) stomatal index and (b) stomatal density ( $n = 58-62$ ; mean  $\pm$  S.E.M.). Samples were collected at the field site by myself; leaf surface imprints were processed and number of stomata and pavement cells counted by two BSci students under my guidance; data analysis was performed by myself. Data were analysed using ANOVA and statistical significance is indicated using starring (\*\* =  $p < 0.01$ ; \*\*\* =  $p < 0.001$ ).

## 6.5 Discussion

### 6.5.1 Circadian anticipation of dawn in stomatal aperture may occur under natural conditions

Stomatal circadian rhythms have long been reported under laboratory conditions (Darwin (1898); Snaith and Mansfield (1986); Gorton et al. (1989); Wilkins (1992); Gorton et al. (1993); Correia et al. (1995)), and several circadian clock genes have been identified as regulators of stomatal aperture in *Arabidopsis* (Somers et al. (1998); Dodd et al. (2004, 2005); Kinoshita et al. (2011)). Therefore, we were interested in whether circadian regulation of stomatal aperture is detectable *in natura*.

Light intensity explained 14% of variation in stomatal aperture for the first eight time points (Fig. 6.1). The remaining 86% might be explained by additional abiotic factors

that were not measured, such as humidity and CO<sub>2</sub> levels, which affect stomatal aperture (Turner (1991); Schroeder et al. (2001a,b); Kim et al. (2010); Azoulay-Shemer et al. (2016)). Stress levels caused by abiotic factors such as dehydration or biotic factors such as herbivory might also have affected stomatal aperture (Cominelli et al. (2005); Seung et al. (2012)). Although care was taken to sample plants throughout the field site, it is equally possible that stomatal aperture was influenced by spatial heterogeneity at the field site.

Although light appears to override endogenous circadian signals, it is of note that stomatal aperture increased rapidly and significantly at dawn despite very low light levels (Fig. 6.1). This is unlikely to be caused by simple correlation between light intensity and stomatal aperture. For example, stomatal aperture post-dawn (timepoint 30:10) is significantly larger than stomatal aperture pre-dusk of the same day (timepoint 40:50), despite light levels being 2 000 times higher at 40:50 compared to 30:10 (Fig. 6.1; Sup. Fig. 9.17). This might be due to circadian gating of stomatal aperture.

Previous work has demonstrated that stomatal responses to light vary with time of day (Martin and Meidner (1971); Webb (2003)). Sensitivity to light peaks between dawn and midday, whereas sensitivity to dark is maximal at night (Martin and Meidner (1971); Webb (2003)). In a similar manner, ABA is more effective at inducing stomatal closure after midday (Correia et al. (1995)). This gating of ABA sensitivity may enable stomatal aperture, thereby photosynthesis, to occur in the morning even under conditions of abiotic stress, as well as promote stomatal closure in the afternoon to reduce water loss (Webb (2003)). This phenomenon was reported for peach trees under field conditions (Correia et al. (1997)). Therefore, gating of light and ABA sensitivity could explain our *A. halleri* stomatal aperture data, with a near-immediate response to light at dawn and decreased stomatal aperture prior to dusk (Fig. 6.1).

It is difficult to determine whether circadian regulation of stomatal opening is occurring *in natura* solely based on the data I obtained, particularly as previous studies report conflicting results. For example, modelling by Williams and Gorton (1998) suggested that circadian rhythms enable only 1% of daily carbon uptake under natural conditions, whereas other reports suggest that 15% to 35% of diel oscillations in CO<sub>2</sub> assimilation and stomatal movement are under circadian clock control in field-grown bean and cotton (Resco de Dios et al. (2016, 2017); Resco de Dios and Gessler (2018)). Joo et al. (2017) also report that a functioning circadian clock significantly enhances photosynthetic performance in the field.

To further understand the role of stomatal circadian rhythms *in natura*, one possibility could involve measuring stomatal conductance directly in the field over a longer time period using a non-invasive method, and monitoring abiotic data in a more complete manner. This may require development of new techniques and/or technology, as it is quite challenging to do this reliably under natural conditions for a long period of time. This could possibly be achieved using eddy flux measurements, which estimate carbon assimilation and evapotranspiration at the ecosystem level (Medlyn et al. (2017)). However, eddy flux data are noisy, as it is not possible to distinguish between water vapour fluxes due to evapotranspiration and those caused by soil and canopy evaporation (Medlyn et al. (2017)).

An alternative approach could be to create transgenic plants with misregulated guard cell circadian clocks in a variety of *Arabidopsis* backgrounds, then grow them under naturally fluctuating conditions. This would allow us to pinpoint the role of the guard cell circadian clock in regulating stomatal aperture *in natura*, as well as its overall effect on fitness under natural conditions.

### **6.5.2 Stomatal density varies between two *A. halleri* trichome morphs**

Approximately half of the *A. halleri* population at the Omoide-gawa field site is glabrous, while remaining plants have trichomes (Kawagoe et al. (2011)). As trichome initiation occurs prior to stomatal meristemoid formation (Larkin et al. (1996); Glover (2000)), it is likely that trichome and stomatal patterning are linked (Bean et al. (2002)). Therefore, stomatal patterning of hairy and glabrous *A. halleri* was explored *in natura*.

Glabrous plants had a significantly higher stomatal density and index compared to hairy plants (Fig. 6.2). As density of surrounding pavement cells did not vary between morphs, these differences in stomatal density and index are due to a greater number of stomata on glabrous plants. This is consistent with a previous report in which transgenic *Antirrhinum* with an excess of trichomes had significant reduction in stomatal density (Glover et al. (1998)). A study comparing trichome number and leaf traits for the Col-0, C24, *L. er* and *Ws A. thaliana* accessions also found a significant negative correlation between trichome and stomatal densities (Tunna and Tunstad (2017), laboratory project). This suggests that there is a tradeoff between trichome and stomatal development.

Interestingly, trichome production comes at a fitness cost. This was examined by artificially removing herbivory, thus creating an environment in which herbivory resistance strategies no longer produce an advantage. For example, glabrous *A. halleri* have a 10% greater biomass than hairy plants in absence of herbivores (Sato and Kudoh (2016)). This cost of resistance was also reported for glabrous and hairy *A. lyrata* (Løe et al. (2007); Sletvold et al. (2010)) and *A. thaliana* (Mauricio and Rausher (1997); Mauricio (1998)) in absence of herbivores.

The fitness advantage of glabrous plants over hairy plants may be due to the cost of trichome production, as explored in previous studies (Mauricio and Rausher (1997); Mauricio (1998); Sletvold et al. (2010); Kawagoe et al. (2011); Sletvold and Ågren (2012); Sato and Kudoh (2016)). However, it might also be caused by the higher number of stomata in glabrous plants. Indeed, it has often been hypothesised that increasing the number of stomata could increase carbon assimilation (Lawson and Blatt (2014)). For example, *Arabidopsis* overexpressing *STOMAGEN* have a higher stomatal density and 30% increase in carbon assimilation compared with the wild type; however, they also have a high transpiration rate and consequently a lower WUE (Tanaka et al. (2013)).

In addition, optimal stomatal density is important to achieve high photosynthetic rates. A low stomatal density restricts CO<sub>2</sub> vertical diffusion and reduces photosynthetic rates, whereas high density stomatal clustering diminishes CO<sub>2</sub> diffusion and causes low carbon assimilation (Lawson and Blatt (2014)). Both examined *A. halleri* morphs are likely to be in this optimal range of stomatal density, having evolved and survived in the natural environment. However, higher stomatal density in the glabrous morph might contribute to its faster growth in absence of herbivory (Sato and Kudoh (2017)). It would be interesting to explore this further by measuring the assimilation rate of these trichome morphs under both laboratory and field conditions.

## 6.6 Conclusions

Brief studies on naturally-occurring populations of *A. halleri* were conducted in the Omoide-gawa field site:

- Rhythms of stomatal aperture and closure were detected *in natura*, and it is likely that the rapid and significant increase of stomatal aperture at dawn is due to

circadian gating of light and ABA sensitivity.

- Glabrous plants were found to have a higher stomatal density and index than the hairy morph, which might contribute to the reported fitness advantage of glabrous plants over hairy plants in absence of herbivores.

It would be interesting to explore these hypotheses further both *in natura* and under laboratory conditions. It would also be informative to investigate the role of the guard cell circadian clock under field conditions. This would enable us to explore the impact of the guard cell circadian clock on whole plant physiology *in natura*. Understanding this might help with crop breeding, as crops also grow under natural fluctuating conditions.

## Chapter 7

# The role of the energy-signalling hub SnRK1 in regulating sucrose-induced hypocotyl elongation

### 7.1 Introduction

Sugars play a pivotal role in plant growth and development by supplying the energy and carbon necessary for RNA and protein biosynthesis (Gomez et al. (2010); Lastdrager et al. (2014)). This is particularly important for emerging seedlings, which must synchronize growth with their environment to establish successfully (Koini et al. (2009)). Seedling growth occurs initially through cellular expansion within the hypocotyl, and is tightly regulated by several signalling pathways including light (Casal (2013); Hayes et al. (2014)), photoperiod (Niwa et al. (2009)), phytohormones (Collett et al. (2000)), the circadian clock (Más et al. (2003); Nusinow et al. (2011)) and sugars (Zhang et al. (2010); Liu et al. (2011); Stewart et al. (2011); Lilley et al. (2012); Zhang et al. (2015b, 2016)). Arabidopsis coordinates its metabolic and developmental responses with carbohydrate availability via several sugar-signalling mechanisms, including SUCROSE NON-FERMENTING1 (SNF1)-RELATED KINASE1 (SnRK1) (Baena-González et al. (2007)) and HEXOKINASE1 (HXK1) (Moore et al. (2003)) signalling pathways.

SnRK1 has been established as a central energy-signalling hub (Baena-González et al. (2007); Baena-González (2010); Ghillebert et al. (2011)). It controls expression of over



1000 genes under low sugar conditions (Baena-González et al. (2007); Lastdrager et al. (2014)), enabling the plant to trigger both energy-conserving and stress-induced processes (Ghillebert et al. (2011)). Its catalytic  $\alpha$ -subunit is composed of SNF1-RELATED PROTEIN KINASE1.1 (KIN10/ AKIN10/ SnRK1.1) and KIN11 (Ghillebert et al. (2011)).

SnRK1 activity is repressed by trehalose-6-phosphate (T6P) (Zhang et al. (2009)), and T6P levels are positively correlated with sucrose (Nunes et al. (2013)). T6P is synthesised by T6P SYNTHASE1 (TPS1) (Lastdrager et al. (2014)) and TPS1 deletion mutants severely affect seedling development (Eastmond et al. (2002); Gómez et al. (2006); Schluepmann et al. (2012)), indicating that TPS1 activity is indispensable for development and survival (Schluepmann et al. (2012)). The KIN10/T6P-based signalling pathway has also been linked to the circadian clock (Shin et al. (2017); Sánchez-Villarreal et al. (2018); Frank et al. (2018)), phytohormone signalling (Cheng et al. (2002); Zhang et al. (2008); Jossier et al. (2009); Paul et al. (2010); Coello et al. (2012); Li et al. (2014)), and water use efficiency (Lawlor and Paul (2014)).

## 7.2 Hypothesis and aims

In *Arabidopsis*, SnRK1 and T6P-based energy-signalling pathways enable plants to adjust development and metabolism in response to carbohydrate availability (Schluepmann et al. (2003); Gómez et al. (2006); Baena-González et al. (2007); Nunes et al. (2013)), and hypocotyls elongate in response to exogenous sucrose (Kurata and Yamamoto (1998); Zhang et al. (2010); Liu et al. (2011); Stewart et al. (2011); Lilley et al. (2012); Zhang et al. (2016)). Therefore, we hypothesised that KIN10 and TPS1 regulate sucrose-induced hypocotyl elongation under diel conditions, and aimed to identify their roles in this pathway using hypocotyl elongation as a model.

Phytohormones are also involved in sucrose-induced hypocotyl elongation (Zhang et al. (2010); Lilley et al. (2012)), and the SnRK1/T6P-based signalling pathway has been linked to gibberellin, auxin, and ABA signalling (Jossier et al. (2009); Paul et al. (2010); Li et al. (2014)). We investigated whether SnRK1 interacts with these phytohormone signalling pathways to enable sucrose-induced hypocotyl elongation.

In a similar fashion, we reasoned that the hexokinase energy-signalling pathway and circadian clock might be involved in sucrose-induced hypocotyl elongation as well. We

also explored the interplay between sucrose-induced hypocotyl elongation, photoperiod, and light input.

The majority of data presented here has been published in Simon et al. (2018a) and Simon et al. (2018b), which are provided in the Appendix. Dr Jelena Kusakina contributed equally to work published in Simon et al. (2018a). For clarity, a few experiments performed by Dr Jelena Kusakina are included in this chapter and labelled as such.

### **7.3 Methods and methodology**

*Arabidopsis* seedlings were grown on MS (0.5 MS, 0.8% (w/v) agar), or on MS supplemented with 3% (w/v) (87.6 mM) sucrose (Suc) or equimolar (87.6 mM) sorbitol as an osmotic control (Sor). According to the experiment, media was further supplemented with 20  $\mu$ M paclobutrazol (PAC) and/or 100  $\mu$ M GA with a methanol carrier, or with up to 100  $\mu$ M *N*-1-naphthylphthalamic acid (NPA) with a DMSO carrier. Carrier controls were supplemented with either 0.12% (v/v) methanol or 0.1% (v/v) DMSO, as appropriate. Further details are provided in Chapter 2 (section 2.2).

Genotypes used here are provided in Table 7.1. Protocols for hypocotyl elongation assays (section 2.11), RNA extractions (section 2.5.2), cDNA biosynthesis (section 2.5.3) and qRT-PCR (section 2.5.4.5) are described in Chapter 2. Depending on the nature of the data, statistical analysis was performed using independent samples t-tests, ANOVA followed by post hoc Tukey tests, or independent-samples Kruskal-Wallis test followed by Dunn's pairwise tests with Bonferroni correction.

AGI code	Gene	Genotype	Reference
AT3G01090	<i>KIN10</i>	KIN10-ox 5.7	Baena-González et al. (2007)
AT3G01090	<i>KIN10</i>	KIN10-ox 6.5	Baena-González et al. (2007)
AT3G01090	<i>KIN10</i>	<i>akin10</i>	Mair et al. (2015)
AT3G01090	<i>KIN10</i>	<i>akin10-2</i>	Simon et al. (2018b)
AT1G78580	<i>TPS1</i>	<i>tps1-11</i>	Gomez et al. (2010)
AT1G78580	<i>TPS1</i>	<i>tps1-12</i>	Gomez et al. (2010)
AT1G78580	<i>TPS1</i>	<i>tps1-13</i>	Gomez et al. (2010)
Bacterial	<i>otsA</i>	otsA-ox	Schluepmann et al. (2003)
AT5G28770	<i>bZIP63</i>	<i>bzip63-1</i>	Mair et al. (2015)
AT4G29130	<i>HXK1</i>	<i>gin2-1</i>	Moore et al. (2003)
AT2G46830	<i>CCA1</i>	CCA1-ox	Wang and Tobin (1998)
AT5G61380	<i>TOC1</i>	TOC1-ox	Más et al. (2003)
AT1G14920	<i>GAI</i>	<i>gai-1</i>	Koorneef et al. (1985)
AT1G14920, AT2G01570, AT1G66350, AT3G03450, AT5G17490	<i>GAI, RGA, RGL1, RGL2, RGL3</i>	<i>gai-t6 rga-t2 rgl1-1 rgl2-1 rgl3-4 (DELLA global)</i>	Koini et al. (2009)
AT4G17870, AT5G46790, AT2G26040, AT2G38310	<i>PYR1, PYL1, PYL2, PYL4</i>	<i>pyr1-1 pyl1-1 pyl2-1 pyl4-1 (ABA quad)</i>	Park et al. (2009)

Table 7.1: Arabidopsis genotypes examined in Chapter 7.

## 7.4 Results

### 7.4.1 *KIN10* and *TPS1* play a role in regulating sucrose-induced hypocotyl elongation under diel conditions

#### 7.4.1.1 *KIN10* overexpressors and *tps1* TILLING mutants are conditionally sucrose-insensitive

As *KIN10* and *TPS1* regulate growth under light/dark conditions (Schluepmann et al. (2003); Gómez et al. (2006); Baena-González et al. (2007); Nunes et al. (2013)), they may also be implicated in sucrose-induced hypocotyl elongation. We explored this possibility using two *KIN10* overexpressors (Baena-González et al. (2007)) and three *tps1* Targeted Induced Local Lesions In Genomes (TILLING) mutants with reduced *TPS1* expression (Gomez et al. (2010)). Overexpressing *KIN10* affects expression of genes involved in energy responses (Baena-González et al. (2007)). Fully disrupting *TPS1* affects embryo development (Eastmond et al. (2002); Gómez et al. (2006)), making it preferable to work with weaker TILLING alleles. The *tps1* TILLING alleles were generated using EMS chemical treatment and screened by incubating amplification products with CEL1 endonucleases, followed by gel electrophoresis and scanning (Colbert et al. (2001); Gomez et al. (2010)). These genotypes are predominantly in the *L. er.* background (Baena-González et al. (2007); Gómez et al. (2006)).

Hypocotyl elongation assays were performed on these genotypes grown on MS, or MS supplemented with either 3% (w/v) sucrose (Suc) or equimolar sorbitol as an osmotic control (Sor), under different photoperiods. Dr Jelena Kusakina demonstrated that sucrose supplementation significantly increased WT hypocotyl length compared to the osmotic control under 4 h and 8 h photoperiods (Simon et al. (2018a), Appendix). However, hypocotyl lengths of both *KIN10*-ox alleles were unaltered by the presence of sucrose under a 4 h photoperiod (Simon et al. (2018a), Appendix). In a similar fashion, under a 4 h photoperiod, exogenous sucrose did not alter *tps1*-11 hypocotyl length, but a small yet significant increase occurred for *tps1*-12 (Simon et al. (2018a), Appendix).

I repeated this experiment under an 8 h photoperiod, with *KIN10*-ox 5.7 and *tps1*-11 grown on MS, Sor or Suc (Fig. 7.1). As previously, *L. er.* had significantly longer hypocotyls when grown on Suc compared to Sor ( $F_{8, 164} = 85.773$ ;  $p < 0.001$ ) (Fig. 7.1). However,

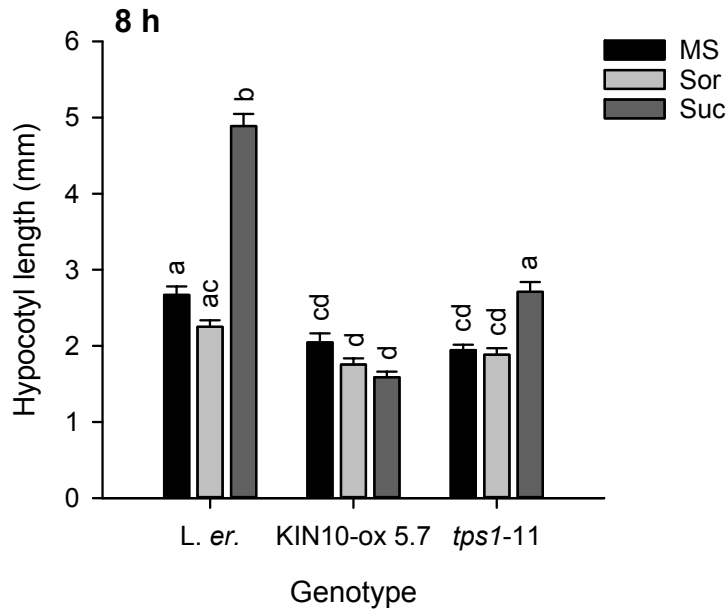


Figure 7.1: *KIN10-ox* and *tps1* are fully or partially sucrose-insensitive under 8 h photoperiods, respectively. Hypocotyl lengths were measured for 7 day-old seedlings grown on MS supplemented with 3% sucrose (Suc) or equimolar sorbitol (Sor) under an 8 h photoperiod ( $n = 20$ ; mean  $\pm$  S.E.M.). Data were analysed with ANOVA and Tukey's post hoc tests. Different letters indicate statistically significant difference between means ( $p < 0.05$ ).

*KIN10-ox 5.7* hypocotyl length was unaltered in presence of sucrose ( $p > 0.05$ ). *tps1-11* hypocotyls were significantly longer on Suc ( $p < 0.001$ ), but the magnitude of this sucrose-induced hypocotyl elongation (0.83 mm longer, 44% increase) was smaller than for *L. er.* (2.64 mm longer, 117% increase).

Therefore, under short photoperiods, overexpressing *KIN10* or mutating *TPS1* prevents or strongly attenuates sucrose-induced hypocotyl elongation, respectively.

#### 7.4.1.2 Disrupting *KIN10* expression amplifies sucrose-induced hypocotyl elongation

Sucrose-induced hypocotyl elongation was then measured in two T-DNA insertion mutants of *KIN10* in the Col-0 background, referred to as *akin10* and *akin10-2* (Mair et al. (2015); Simon et al. (2018b), Appendix). Under a 4 h photoperiod, *akin10* and *akin10-2* hypocotyls were significantly shorter than Col-0 hypocotyls when grown on MS (*akin10*:  $t_{38} = 9.594$ ,  $p < 0.001$ ; *akin10-2*:  $t_{38} = 8.144$ ,  $p < 0.001$ ) (Fig. 7.2a). However, all genotypes

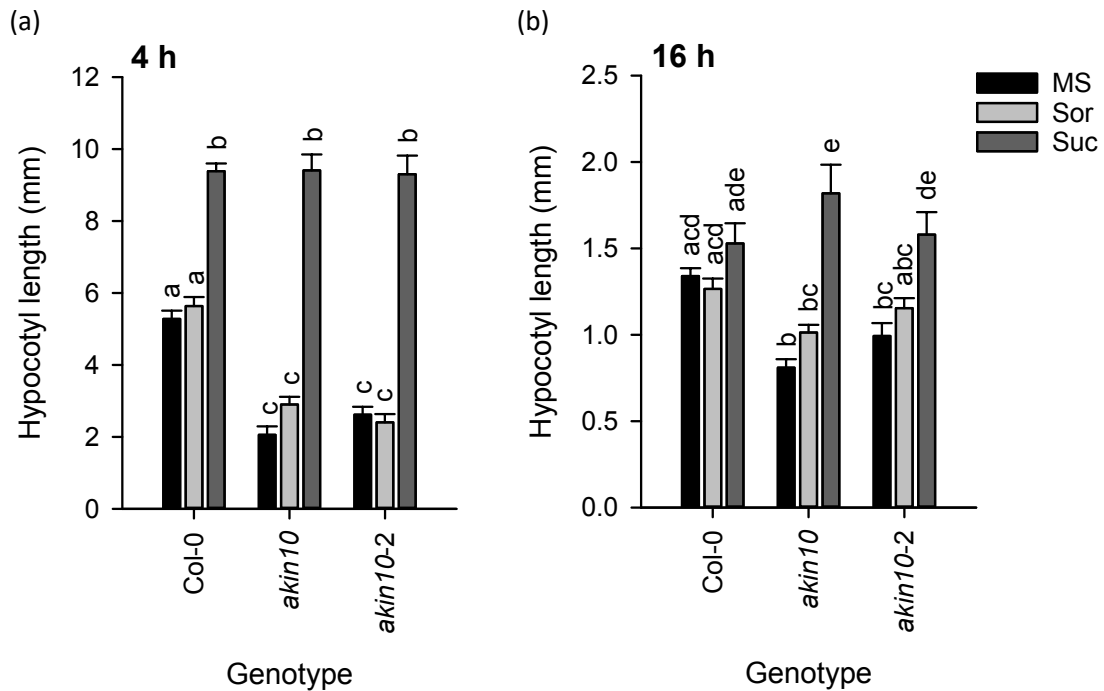


Figure 7.2: Disrupting *KIN10* causes hypersensitivity of hypocotyls to sucrose supplementation. Hypocotyl lengths were measured for 7 day-old seedlings grown on MS supplemented with 3% sucrose (Suc) or equimolar sorbitol (Sor) under a (a) 4 h photoperiod or (b) 16 h photoperiod ( $n = 20$ ; mean  $\pm$  S.E.M.). Data were analysed with ANOVA and Tukey's post hoc tests. Different letters indicate statistically significant difference between means ( $p < 0.05$ ). Data were published in Simon et al. (2018b) (Appendix).

had the same hypocotyl length when grown on Suc ( $F_{8, 171} = 105.468$ ,  $p > 0.05$ ) (Fig. 7.2a). Consequently, exogenous sucrose caused a greater magnitude of hypocotyl elongation in *akin10* (6.51 mm longer, 224% increase) and *akin10-2* (6.90 mm longer, 286% increase) compared with Col-0 (3.75 mm longer, 67% increase).

A similar pattern occurred for seedlings grown under a 16 h photoperiod: *akin10* and *akin10-2* hypocotyls were significantly shorter than Col-0 hypocotyls when grown on MS (*akin10*:  $t_{38} = 7.728$ ,  $p < 0.001$ ; *akin10-2*:  $t_{31.474} = 3.866$ ,  $p = 0.001$ ) and the same length as Col-0 when grown on Suc ( $F_{8, 170} = 11.779$ ;  $p > 0.05$  for both *akin10* alleles) (Fig. 7.2b). Sucrose-induced hypocotyl elongation occurred for *akin10* ( $p < 0.001$ ) and *akin10-2* ( $p = 0.039$ ), but not for Col-0 ( $p > 0.05$ ). However, the magnitude of this sucrose-induced increase in hypocotyl length under a 16 h photoperiod (*akin10*: 79%; *akin10-2*: 37%) was smaller than under a 4 h photoperiod (*akin10*: 224%; *akin10-2*: 286%) (Fig. 7.2).

Therefore, disrupting *KIN10* causes hypocotyl length to be hypersensitive to sucrose supplementation, and this response varies with photoperiod.

#### **7.4.1.3 Experimentation with inducible TPS overexpressors**

In a similar fashion, I wished to examine seedlings with high T6P concentrations, as these would have the opposite phenotype to the *tps1* alleles. This can be achieved by overexpressing the bacterial gene *otsA*, which encodes TPS (Schluepmann et al. (2003)). Therefore, Arabidopsis in which *otsA* was under the control of the ethanol-inducible AlcR/AlcA promoter system (Caddick et al. (1998); Martins et al. (2013)) were obtained. However, exposing seeds and young seedlings to ethanol severely affected growth and development and promoter induction was unsuccessful (data not shown), so no further experiments were performed on this genotype.

#### **7.4.1.4 *KIN10* acts at least partially through bZIP63 to regulate sucrose-induced hypocotyl elongation**

SnRK1 phosphorylates and thereby increases activity of bZIP63, a key transcription factor which regulates response to starvation (Mair et al. (2015); Frank et al. (2018)). To determine whether SnRK1 regulation of sucrose-induced hypocotyl elongation involves bZIP63, I investigated hypocotyl elongation responses to sucrose in *bzip63-1* and its Col-0 background.

Under a 4 h photoperiod, *bzip63-1* hypocotyls were significantly longer in the presence of exogenous sucrose compared with the osmotic control ( $F_{5, 114} = 101.639$ ,  $p < 0.001$ ) (Fig. 7.3a). However, the magnitude of this sucrose-induced increase in hypocotyl length (4.5 mm longer, 121% increase) was double that observed in Col-0 (2.8 mm longer, 60% increase). An independent experimental repeat confirmed this result, with sucrose supplementation causing a greater proportional sucrose-induced hypocotyl elongation in *bzip63-1* (5.9 mm, 138%) compared to Col-0 (4.0 mm, 77%) (Sup. Fig. 9.18a).

Under a 16 h photoperiod, no sucrose-induced hypocotyl elongation occurred in Col-0 ( $F_{5, 114} = 10.390$ ,  $p > 0.05$ ) (Fig. 7.3b). In contrast, sucrose supplementation caused a small but significant increase in *bzip63-1* hypocotyl length ( $p = 0.010$ , 0.4 mm longer, 35% increase). Finally, under constant light conditions, exogenous sucrose had no ef-

fect upon hypocotyl elongation for both Col-0 and *bzip63-1* ( $F_{5, 114} = 6.446$ ,  $p > 0.05$ ) (Sup. Fig. 9.18b).

Therefore, disrupting *bZIP63* caused a greater magnitude of sucrose-induced hypocotyl elongation compared to the WT, and this response varies with photoperiod. Interestingly, *bzip63-1* hypocotyl elongation responses to sucrose are similar to those of the *akin10* alleles (Fig. 7.2).

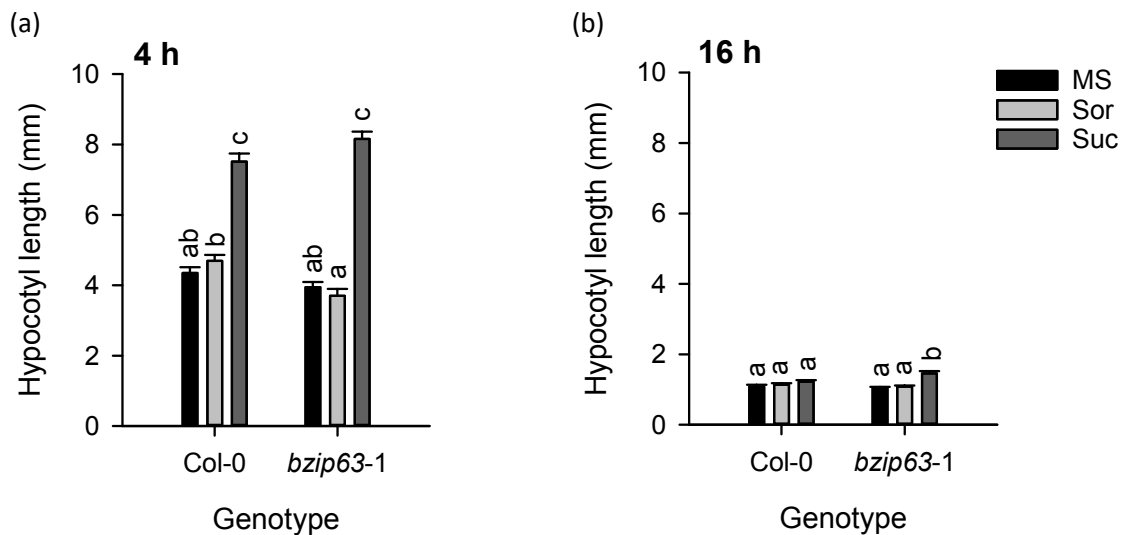


Figure 7.3: *bzip63-1* has a greater magnitude of sucrose-induced increase in hypocotyl length than the wild type. Hypocotyl lengths were measured for 7 day-old seedlings grown on MS supplemented with 3% sucrose (Suc) or equimolar sorbitol (Sor) under a (a) 4 h photoperiod or (b) 16 h photoperiod ( $n = 20$ ; mean  $\pm$  S.E.M.). Data were analysed with ANOVA and Tukey's post hoc tests. Different letters indicate statistically significant difference between means ( $p < 0.05$ ). Additional experimental repeats are provided in the Appendix (Sup. Fig. 9.18).

#### 7.4.2 Hexokinase is not required for sucrose-induced hypocotyl elongation

Sucrose may be converted to glucose, and HXK1 can sense changes in glucose concentration and regulate development accordingly (Moore et al. (2003)). Therefore, we hypothesised that hexokinase-based glucose signalling might regulate sucrose-induced hypocotyl elongation under diel conditions. This was tested using the *gin2-1* mutant



in the *L. er.* background, which has reduced *HXK1* transcript abundance (Moore et al. (2003)).

Under a 4 h photoperiod, sucrose supplementation significantly increased hypocotyl length for both *gin2-1* ( $F_{5, 114} = 96.377, p < 0.001$ ) and *L. er.* ( $p < 0.001$ ) (Fig. 7.4a). *gin2-1* hypocotyls were significantly shorter than *L. er.* hypocotyls on all growth media conditions ( $p < 0.001$ ), but the proportional hypocotyl elongation in response to sucrose was the same (64.1% and 64.4% increase between Sor and Suc for *L. er.* and *gin2-1*, respectively). Under constant light conditions, sucrose supplementation did not alter *L. er.* and *gin2-1* hypocotyl lengths ( $F_{5, 114} = 15.790; p > 0.05$ ) (Fig. 7.4b).

Therefore, disrupting hexokinase-induced glucose signalling in *gin2-1* does not affect sucrose-induced hypocotyl elongation.

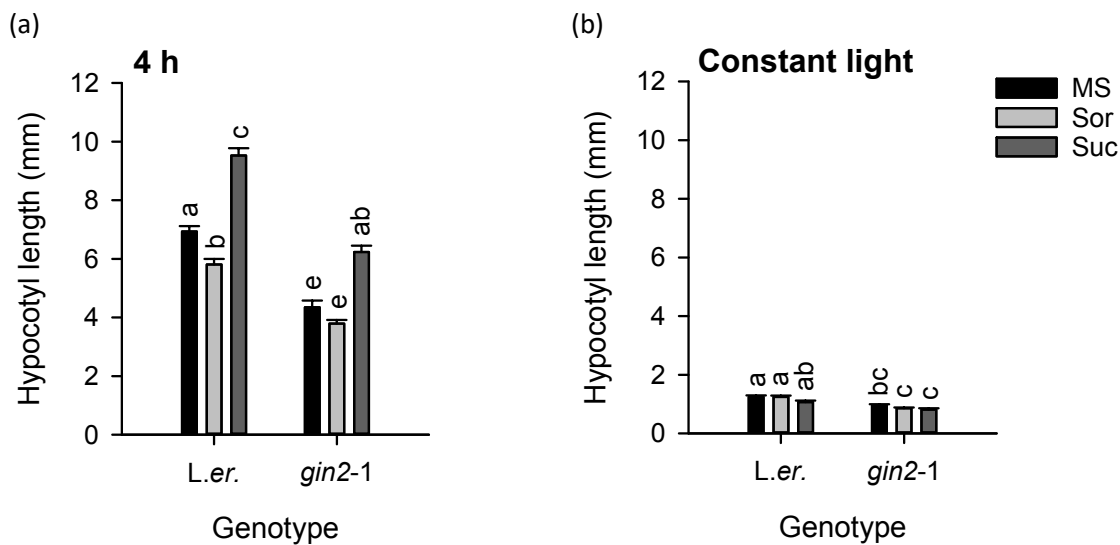


Figure 7.4: Hexokinase-induced glucose signalling does not regulate sucrose-induced hypocotyl elongation under diel conditions. Hypocotyl lengths were measured for 7 day-old seedlings grown on MS supplemented with 3% sucrose (Suc) or equimolar sorbitol (Sor) under (a) a 4 h photoperiod or (b) constant light conditions ( $n = 20$ ; mean  $\pm$  S.E.M.). Data were analysed with ANOVA and Tukey's post hoc tests. Different letters indicate statistically significant difference between means ( $p < 0.05$ ). Data were published in Simon et al. (2018a) (Appendix).

### 7.4.3 The interplay between sucrose-induced hypocotyl elongation and photoperiod

#### 7.4.3.1 Sucrose-induced hypocotyl elongation is photoperiod-dependent

Hypocotyl elongation is photoperiod-dependent, with hypocotyl length increasing as day length decreases (Sup. Fig. 9.19) (Niwa et al. (2009)). We examined whether sucrose-induced hypocotyl elongation is regulated by photoperiod (Fig. 7.5). Under short photoperiods (4 h, 8 h), Col-0 and *L. er.* hypocotyl length significantly increased in response to exogenous sucrose ( $p < 0.001$  for all; Col-0 4 h:  $F_{2, 57} = 157.739$ ; *L. er.* 4 h:  $F_{2, 57} = 86.526$ ; Col-0 8 h:  $F_{2, 57} = 226.966$ ; *L. er.* 8 h:  $F_{2, 57} = 129.094$ ). However, under long photoperiods (16 h, 24 h), sucrose supplementation was without effect on hypocotyl length ( $p > 0.05$  for all; Col-0 16 h:  $F_{2, 57} = 2.257$ ; *L. er.* 16 h:  $F_{2, 57} = 0.082$ ; Col-0 24 h:  $F_{2, 57} = 5.123$ ) or caused a small decrease (*L. er.* 24 h:  $F_{2, 57} = 4.227$ ,  $p = 0.039$ ). Similar data were obtained by Dr Jelena Kusakina (Simon et al. (2018a), Appendix).

Therefore, the magnitude of sucrose-induced hypocotyl elongation varies with photoperiod length.

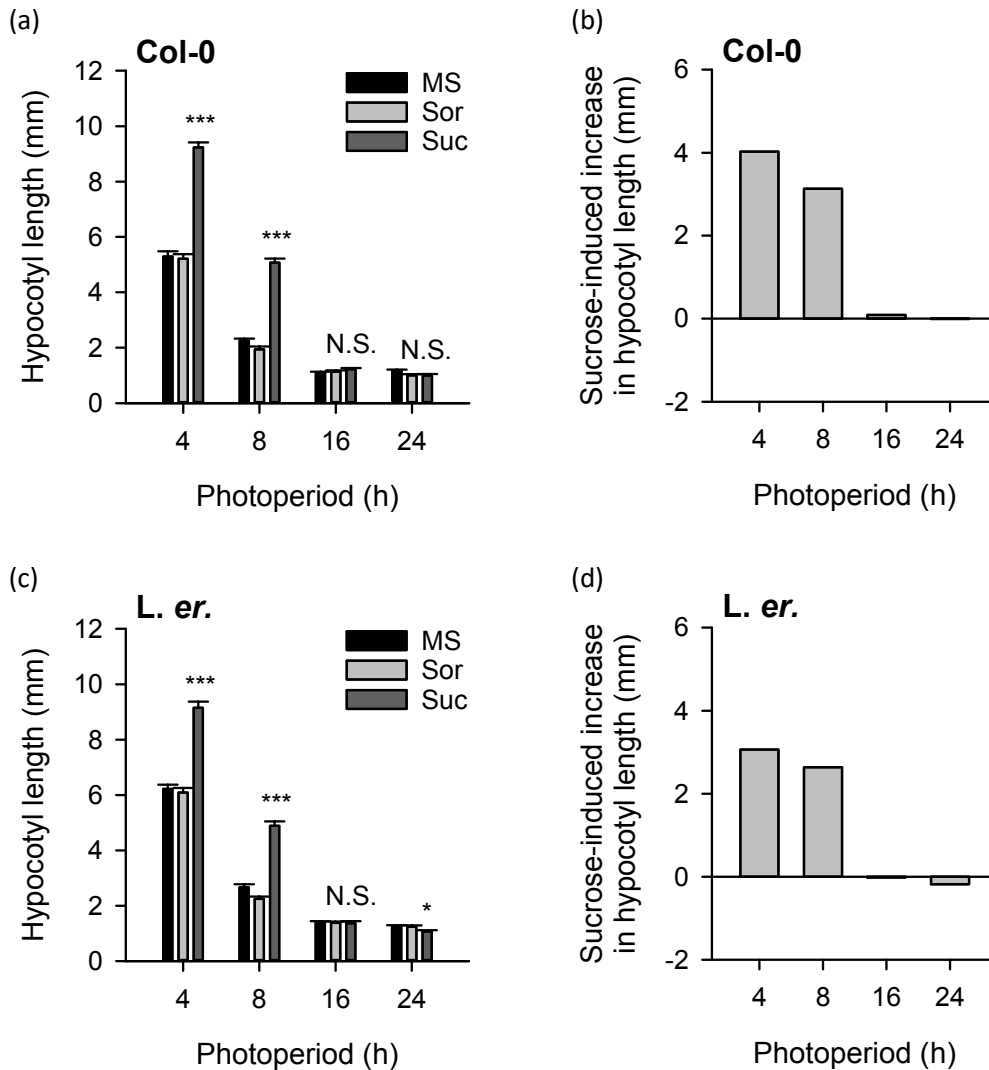


Figure 7.5: The magnitude of sucrose-induced hypocotyl elongation varies with photoperiod length. Hypocotyl lengths were measured for 7 day-old (a, b) *Col-0* and (c, d) *L. er.* grown on MS supplemented with 3% sucrose (Suc) or equimolar sorbitol (Sor) under different photoperiods ( $n = 20$ ; mean  $\pm$  S.E.M.). Data show (a, c) seedling hypocotyl length, as well as (b, d) the increase in hypocotyl length caused by sucrose supplementation relative to the sorbitol control. Data were compiled from several experiments in which *Col-0* and/or *L. er.* were used as controls. Data were analysed with ANOVA and Tukey's post hoc tests, and statistical significance compared to the respective Sor control is indicated using starring (N.S. =  $p > 0.05$ ; \* =  $p < 0.05$ ; \*\* =  $p < 0.01$ ; \*\*\* =  $p < 0.001$ ).

#### 7.4.3.2 Both the absolute photoperiod and daily integrated PAR determine the photoperiod-sensitivity of sucrose-induced hypocotyl elongation

This variation in sucrose-induced hypocotyl elongation could derive from photoperiod sensing. Alternatively, this may be due to the differences in total daily integrated photosynthetically active radiation (PAR) under the different photoperiods. To test this, sucrose-induced hypocotyl elongation was examined for Col-0 and *L. er.* grown under two different photoperiods, but receiving the same total daily integrated PAR.

The greatest difference in the magnitude of sucrose-induced hypocotyl elongation was observed between 8 h and 16 h photoperiods (Figs. 7.5b, 7.5d). Therefore, I grew seedlings under either an 8 h photoperiod with a PAR of  $80 \mu\text{mol m}^{-2} \text{s}^{-1}$  or a 16 h photoperiod with a PAR of  $40 \mu\text{mol m}^{-2} \text{s}^{-1}$ , so that seedlings would receive the same daily integrated PAR of  $640 \mu\text{mol m}^{-2} \text{s}^{-1}$ .

Sucrose supplementation significantly increased hypocotyl length for Col-0 and *L. er.* grown under a 16 h photoperiod with a PAR of  $40 \mu\text{mol m}^{-2} \text{s}^{-1}$  (Col-0:  $F_{5, 114} = 46.258$ ,  $p = 0.027$ ; *L. er.*:  $F_{5, 114} = 78.792$ ,  $p < 0.001$ ) (Fig. 7.6). In contrast, sucrose supplementation did not alter hypocotyl length when seedlings were grown under a 16 h photoperiod with a PAR of  $120 \mu\text{mol m}^{-2} \text{s}^{-1}$  (Fig. 7.5). These results imply that daily integrated PAR affects hypocotyl elongation in response to sucrose.

Sucrose-induced hypocotyl elongation occurred in seedlings grown under an 8 h photoperiod with a PAR of  $80 \mu\text{mol m}^{-2} \text{s}^{-1}$  ( $p < 0.001$  for both Col-0 and *L. er.*) (Fig. 7.6). However, sucrose supplementation under an 8 h photoperiod caused a greater proportional increase in hypocotyl length (Col-0: 110%; *L. er.*: 111%) than under the 16 h photoperiod with the same daily integrated PAR (Col-0: 43%; *L. er.*: 64%) (Figs. 7.6b, 7.6d). These data demonstrate that photoperiod length also determines the magnitude of sucrose-induced hypocotyl elongation (Figs. 7.6b, 7.6d).

In a similar fashion, Dr Jelena Kusakina examined sucrose-induced hypocotyl elongation for *L. er.* grown under 8 h or 4 h photoperiods with the same total daily integrated PAR (Simon et al. (2018a), Appendix). Interestingly, no differences were observed in the magnitude of sucrose-induced hypocotyl elongation between these two conditions. This further demonstrates the role of daily integrated PAR in regulating sucrose-induced hypocotyl elongation.

Therefore, both photoperiod length and daily integrated PAR determine the photoperiod-sensitivity of hypocotyl elongation in response to exogenous sucrose.

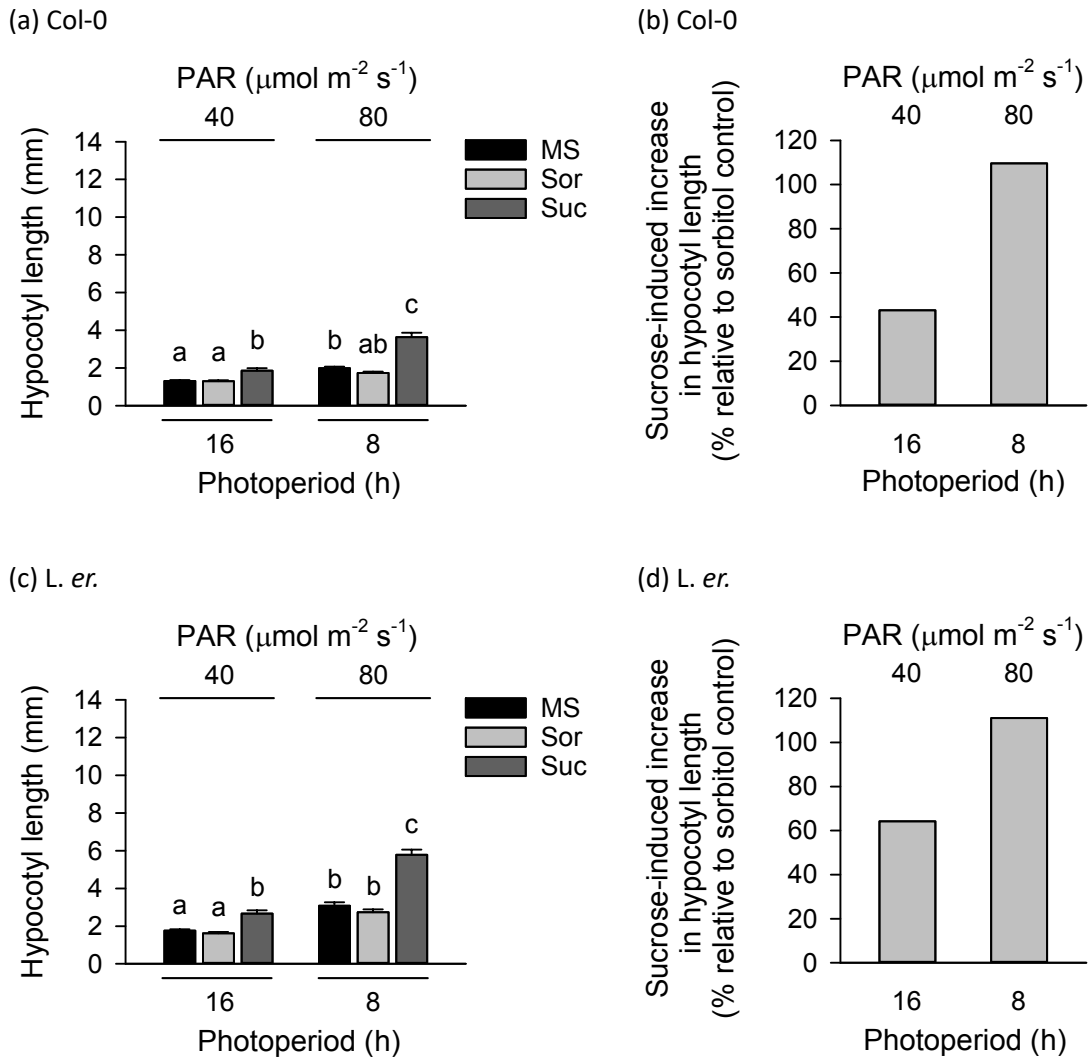


Figure 7.6: Sucrose-induced hypocotyl elongation is affected by both photoperiod and daily integrated PAR. Hypocotyl lengths were measured for 7 day-old (a, b) Col-0 and (c, d) *L. er.* grown on MS supplemented with 3% sucrose (Suc) or equimolar sorbitol (Sor), under either a 16 h photoperiod with a PAR of  $40 \mu\text{mol m}^{-2} \text{s}^{-1}$  or an 8 h photoperiod with a PAR of  $80 \mu\text{mol m}^{-2} \text{s}^{-1}$  ( $n = 20$ ; mean  $\pm$  S.E.M.). Data show (a, c) seedling hypocotyl length, as well as (b, d) the increase in hypocotyl length caused by sucrose supplementation relative to the sorbitol control. Data were analysed with ANOVA and Tukey's post hoc tests. Different letters indicate statistically significant difference between means ( $p < 0.05$ ). Data from panels (c) and (d) were published in Simon et al. (2018a) (Appendix).

#### 7.4.4 *CCA1* and *TOC1* do not regulate sucrose-induced hypocotyl elongation under 4 h photoperiods

As the circadian clock affects hypocotyl elongation (Más et al. (2003); Nozue et al. (2007); Nusinow et al. (2011)) and is altered by sugar signals and KIN10 (Haydon et al. (2013); Shin et al. (2017); Sánchez-Villarreal et al. (2018); Frank et al. (2018)), we reasoned that the circadian clock might regulate hypocotyl elongation in presence of sucrose.

Using the *gi-11*, *prr7-11* and *cca1-11 lhy-21 toc1-21* mutants, Dr Jelena Kusakina demonstrated that the circadian oscillator components *GI*, *PRR7*, *CCA1*, *LHY* and *TOC1* do not contribute to sucrose-induced hypocotyl elongation under short photoperiods (Simon et al. (2018a), Appendix). In Chapter 5, I measured the hypocotyl lengths of *CCA1-ox* and *TOC1-ox* grown on MS, Sor, or Suc under a 4 h photoperiod. Data are redrawn here for clarity (Fig. 7.7).

Exogenous sucrose significantly increased *CCA1-ox* and *TOC1-ox* hypocotyl length under a 4 h photoperiod (*CCA1-ox*:  $F_{5, 114} = 143.348$ ,  $p < 0.001$ ; *TOC1-ox*:  $F_{5, 114} = 110.295$ ,  $p < 0.001$ ) (Fig. 7.7). Sucrose supplementation caused a similar proportional increase in hypocotyl length for *TOC1-ox* (2.11 mm, 81%) and Col-0 (3.48 mm, 68%) (Fig. 7.7b). In contrast, sucrose supplementation caused a higher proportional increase in hypocotyl length in Col-0 (56.8%) than *CCA1-ox* (24.5%), but the physical increases were similar (Col-0: 2.7 mm; *CCA1-ox*: 2.2 mm) (Fig. 7.7a). As *CCA1-ox* have very elongated hypocotyls (Hassidim et al. (2017); Wang and Tobin (1998); Green et al. (2002); Dodd et al. (2005); Nozue et al. (2007); Nusinow et al. (2011)), it is possible that the addition of exogenous sucrose caused cell expansion to reach a physical limit, thereby preventing hypocotyls from elongating further.

Overall, these results confirm that *CCA1* and *TOC1* do not regulate sucrose-induced hypocotyl elongation under our experimental conditions.

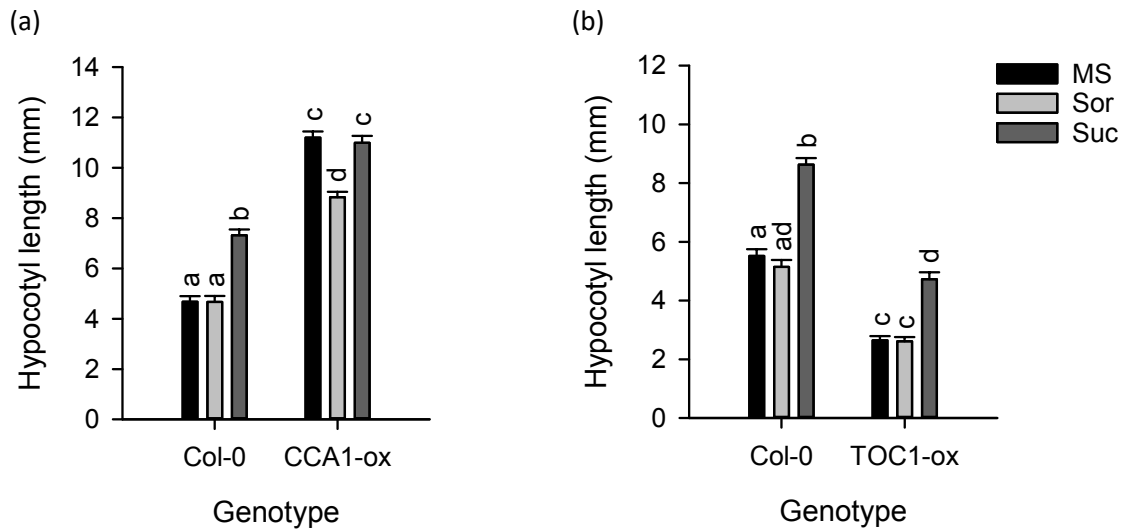


Figure 7.7: Overexpressing *CCA1* or *TOC1* does not affect sucrose-induced hypocotyl elongation under short days. Hypocotyl lengths were measured for 7 day-old (a) *CCA1-ox* and (b) *TOC1-ox* grown on MS supplemented with 3% sucrose (Suc) or equimolar sorbitol (Sor) under a 4 h photoperiod ( $n = 20$ ; mean  $\pm$  S.E.M.). Data were taken from Chapter 5 and redrawn here for clarity. Data were analysed with ANOVA and Tukey's post hoc tests. Different letters indicate statistically significant difference between means ( $p < 0.05$ ).

#### 7.4.5 Phytohormone involvement in sucrose-induced hypocotyl elongation

Sucrose-induced hypocotyl elongation involves phytohormone signalling (Zhang et al. (2010); Lilley et al. (2012)). Therefore, I examined the roles of the hormones auxin, GA and ABA in regulating hypocotyl length in response to exogenous sucrose under short photoperiods.

##### 7.4.5.1 Auxin

##### *The polar auxin transport inhibitor NPA represses sucrose-induced hypocotyl elongation in a concentration-dependent fashion*

Hypocotyl elongation in response to exogenous sucrose requires auxin signalling (Lilley et al. (2012)). I wished to determine whether this was also the case under my experi-



mental conditions. I performed hypocotyl elongation assays on Col-0 and *L. er* grown on MS, Sor, or Suc further supplemented with different concentrations of the polar auxin transport inhibitor NPA (Rubery (1990)) (Fig. 7.8).

Col-0 hypocotyl length significantly increased in response to exogenous sucrose supplemented with 0  $\mu\text{M}$ , 1  $\mu\text{M}$  and 5  $\mu\text{M}$  NPA ( $F_{11, 228} = 55.570$ ;  $p < 0.001$ ). However, sucrose supplementation was without effect when seedlings were grown on 10  $\mu\text{M}$  NPA ( $p > 0.05$ ) (Fig. 7.8a). Similar results were obtained for *L. er*. (0  $\mu\text{M}$  NPA:  $F_{11, 228} = 56.264$ ,  $p < 0.001$ ; 1  $\mu\text{M}$  NPA:  $p < 0.001$ ; 5  $\mu\text{M}$  NPA:  $p = 0.012$ ; 10  $\mu\text{M}$  NPA:  $p > 0.05$ ) (Fig. 7.8c). Addition of 50  $\mu\text{M}$  and 100  $\mu\text{M}$  NPA also fully abolished sucrose-induced hypocotyl elongation (Col-0:  $F_{8, 252} = 135.455$ ,  $p > 0.05$ ; *L. er*:  $F_{8, 218} = 111.941$ ,  $p > 0.05$ ) (Sup. Fig. 9.20). In addition, the proportional sucrose-induced increase in hypocotyl length steadily decreased as NPA concentration increased (Figs. 7.8b, 7.8d).

Therefore, polar auxin transport is required for sucrose-induced hypocotyl elongation in *L. er* and Col-0.

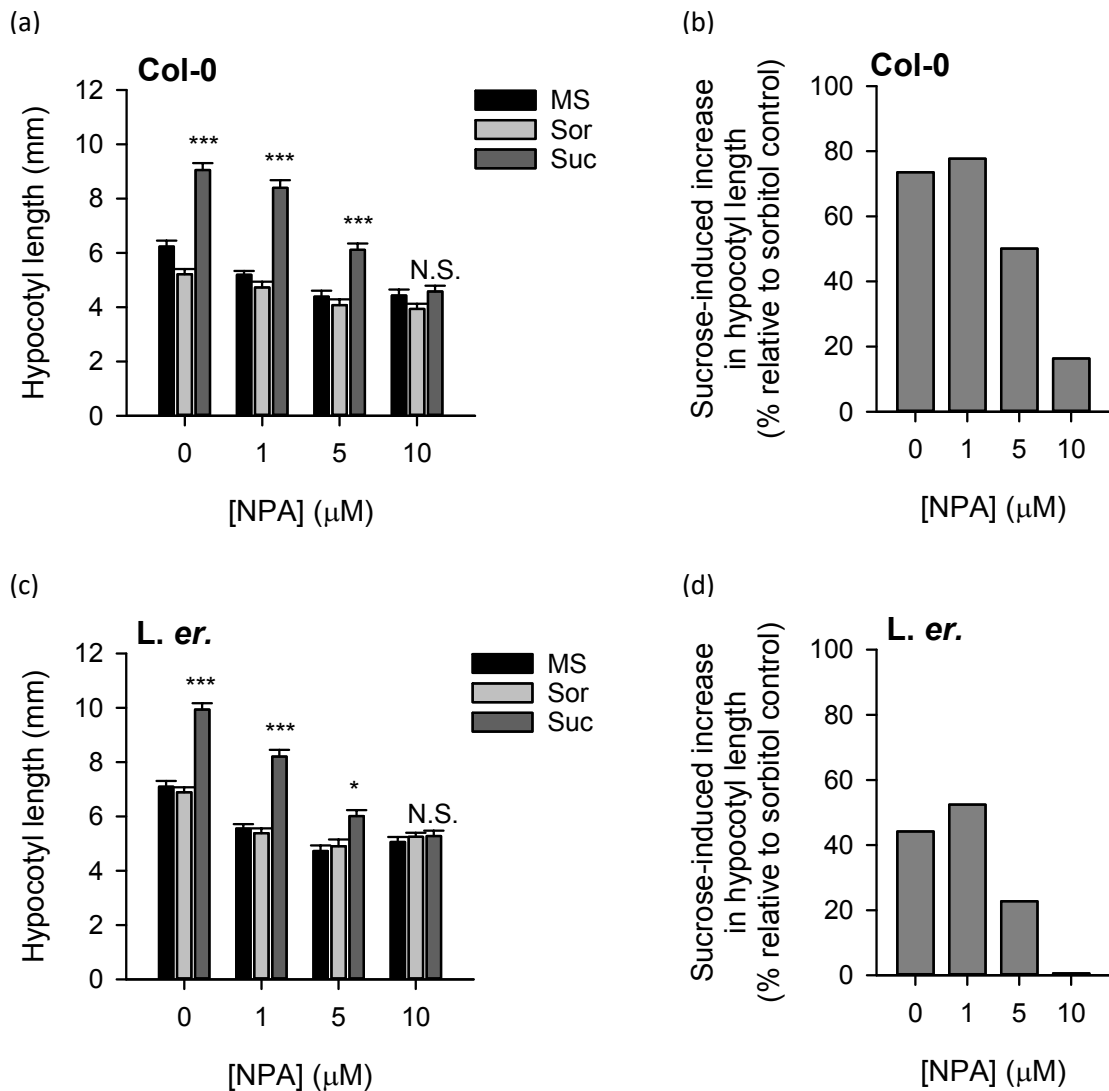


Figure 7.8: NPA represses sucrose-induced hypocotyl elongation in a concentration-dependent manner. Hypocotyl lengths were measured for 7 day-old (a, b) *Col-0* and (c, d) *L. er.* grown on MS supplemented with 3% sucrose (Suc) or equimolar sorbitol (Sor) under a 4 h photoperiod, with these growth media being further supplemented with the carrier control (0.1% (v/v) DMSO), 1  $\mu\text{M}$  NPA, 5  $\mu\text{M}$  NPA or 10  $\mu\text{M}$  NPA ( $n = 20$ ; mean  $\pm$  S.E.M.). Data show (a, c) seedling hypocotyl length, as well as (b, d) the increase in hypocotyl length caused by sucrose supplementation relative to the sorbitol control. Data were analysed with ANOVA and Tukey's post hoc tests, and statistical significance compared to the respective Sor control is indicated using starring (N.S. =  $p > 0.05$ ; \* =  $p < 0.05$ ; \*\* =  $p < 0.01$ ; \*\*\* =  $p < 0.001$ ). Data from panel (c) were published in Simon et al. (2018a) (Appendix). Data for additional NPA concentrations are provided in the Appendix (Sup. Fig. 9.20).

### ***EXPA11 transcript abundance is regulated by KIN10***

Expansins are cell wall modifying enzymes that enable turgor-driven cell expansion (Li et al. (2002)). During hypocotyl elongation, auxin induces expression of several expansin genes in a PIF-dependent manner (Li et al. (2002)). Transcripts encoding *EXPANSIN4* (*EXPA4*), *EXPA8* and *EXPA11* are up-regulated by auxin in seedlings (Goda (2004); Esmon et al. (2006); Lee et al. (2009)), so were chosen for further analysis in this study.

I particularly wished to examine expansin genes that were induced by conditions promoting hypocotyl elongation and repressed by conditions suppressing it. Constant darkness increases hypocotyl elongation (Boylan and Quail (1991)) while addition of 10  $\mu\text{M}$  NPA causes the opposing phenotype (Lilley et al. (2012)). Therefore, *EXPA4*, *EXPA8* and *EXPA11* transcript abundance were analysed in seedlings grown under constant darkness or with 10  $\mu\text{M}$  NPA (Sup. Fig. 9.21). *EXPA8* and *EXPA11* expression significantly increased in constant darkness ( $F_{5, 12} = 40.661$ ; *EXPA8*:  $p < 0.001$ ; *EXPA11*:  $p = 0.009$ ), and decreased in response to 10  $\mu\text{M}$  NPA ( $F_{5, 12} = 51.779$ ; *EXPA8*:  $p < 0.001$ ; *EXPA11*:  $p = 0.009$ ). *EXPA4* transcript abundance was unaltered under both conditions ( $p > 0.05$ ), so was excluded from subsequent experiments.

*EXPA8* and *EXPA11* transcript abundance was monitored in *L. er.*, two *tps1* alleles and two KIN10-ox alleles grown in MS, Sor and Suc (Fig. 7.9). In *L. er.*, addition of exogenous sucrose significantly upregulated *EXPA11* ( $t_4 = -11.299$ ,  $p < 0.001$ ). This was also detected for *tps1-11* ( $t_4 = -3.417$ ,  $p = 0.027$ ) and *tps1-12* ( $t_4 = -3.842$ ,  $p = 0.018$ ). However, sucrose supplementation did not alter *EXPA11* transcript abundance for KIN10-ox 5.7 ( $t_4 = 0.644$ ;  $p > 0.05$ ) or KIN10-ox 6.5 ( $t_4 = 0.456$ ,  $p > 0.05$ ). As sucrose supplementation did not alter *EXPA8* in the wild type, interpretation of these data for other alleles is difficult in this context.

Overall, KIN10 appears to regulate *EXPA11* transcript abundance in response to exogenous sucrose.

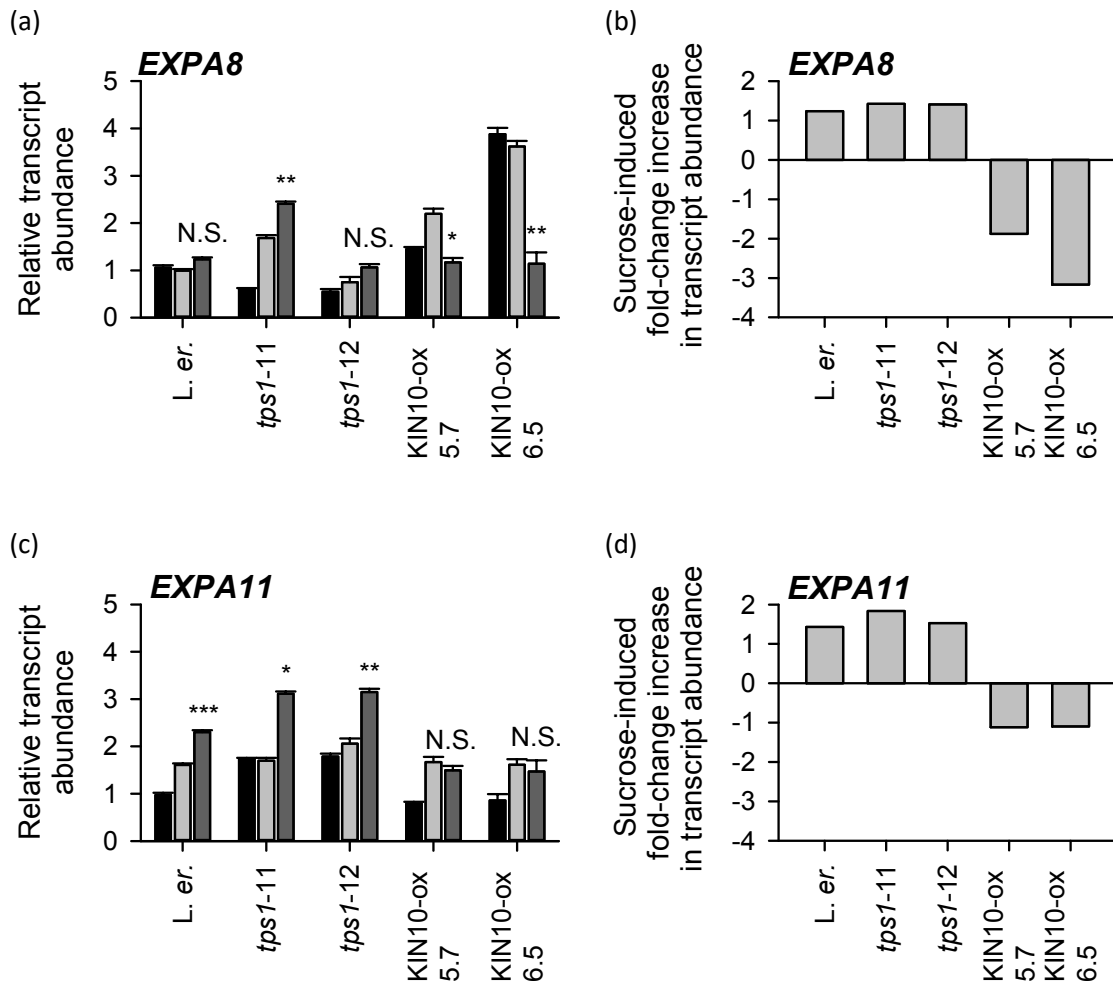


Figure 7.9: *EXPA11* transcript abundance is regulated by KIN10. (a, b) *EXPA8* and (c, d) *EXPA11* relative transcript abundance was measured for seedlings grown on MS supplemented with 3% sucrose (Suc) or equimolar sorbitol (Sor) under a 4 h photoperiod ( $n = 3$ ; mean  $\pm$  S.E.M.). *PP2AA3* was used as the reference gene. Data show (a, c) relative transcript abundance levels, as well as (b, d) fold-change in transcript abundance caused by sucrose supplementation relative to sorbitol. Data were analysed with ANOVA and Tukey's post hoc tests, and statistical significance compared to the respective Sor control is indicated using starring (N.S. =  $p > 0.05$ ; \* =  $p < 0.05$ ; \*\* =  $p < 0.01$ ; \*\*\* =  $p < 0.001$ ). Data were published in Simon et al. (2018a) (Appendix).

***Sucrose supplementation did not cause detectable accumulation of several auxin biosynthesis and response transcripts***

Seedlings undergo auxin-induced, rapid hypocotyl elongation between days three and seven of growth after germination (Gendreau et al. (1997)). Transcript abundance of three auxin biosynthesis genes (*YUCCA8*, *YUCCA9*, *CYP79B3*) and two auxin-responsive genes (*IAA29*, *SAUR15*) were examined in 4- and 7-day old seedlings grown on MS, Sor or Suc under a 4 h photoperiod (Fig. 7.10).

Transcript abundance was substantially altered in response to the osmotic control. This sorbitol-induced response masked any potential effect of sucrose: no significant alteration in *YUCCA8*, *YUCCA9*, *CYP79B3*, *IAA29* and *SAUR15* transcript abundance occurred between samples grown on Sor and Suc for each genotype and sampling day ( $p > 0.05$  for all; *YUCCA8*:  $F_{2, 24} = 0.849$ ; *YUCCA9*:  $F_{2, 24} = 0.618$ ; *CYP79B3*:  $F_{2, 24} = 0.724$ ; *IAA29*:  $F_{2, 24} = 0.742$ ; *SAUR15*:  $F_{2, 24} = 0.737$ ) (Fig. 7.10).

Overall, relative transcript abundance levels of several auxin biosynthesis and responsive genes were unaltered in presence of sucrose, but this is likely due to fluctuating expression levels caused by the osmotic control.

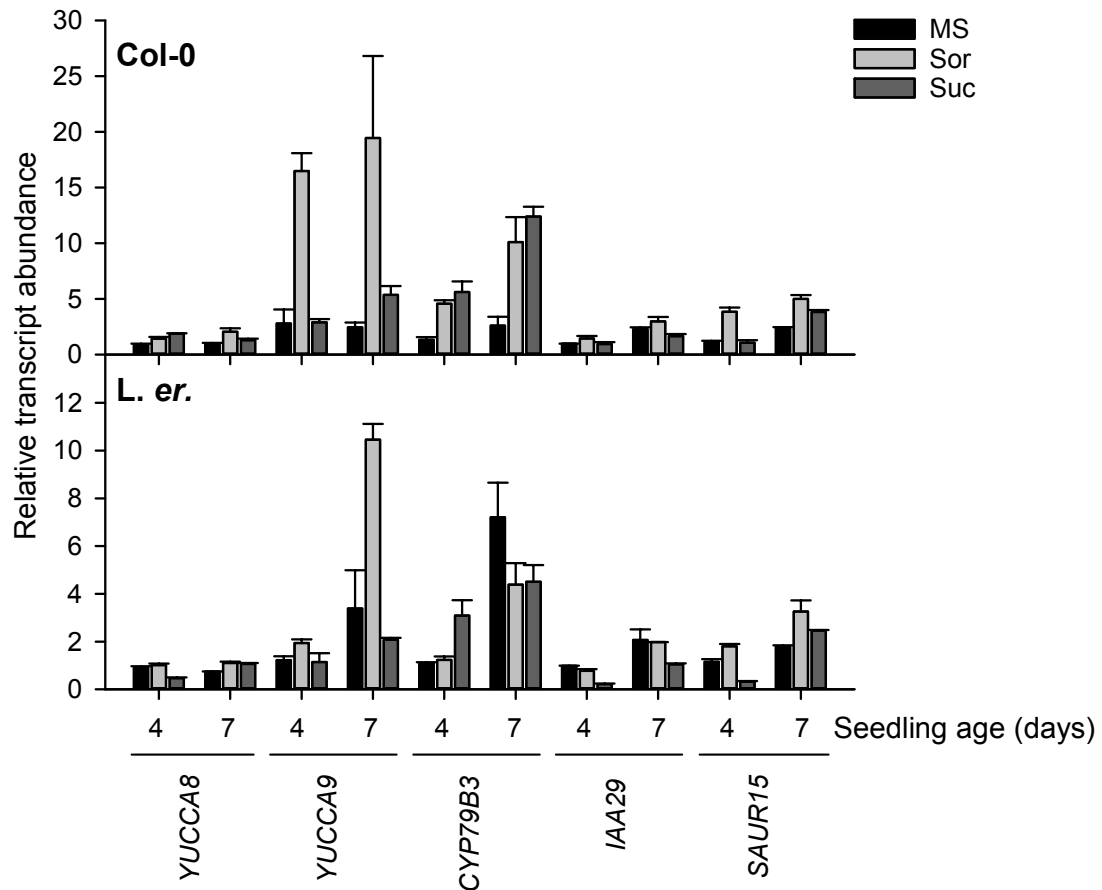


Figure 7.10: Relative transcript abundance of several auxin biosynthesis and responsive genes were unaltered in presence of exogenous sucrose, due to fluctuating expression levels caused by the osmotic control. Relative transcript abundance of three auxin biosynthesis (*YUCCA8*, *YUCCA9*, *CYP79B3*) and two auxin responsive (*IAA29*, *SAUR15*) genes was measured for Col-0 (top) and *L. er.* (bottom) grown on MS supplemented with 3% sucrose (Suc) or equimolar sorbitol (Sor) under a 4 h photoperiod ( $n = 3$ ; mean  $\pm$  S.E.M.). *PP2AA3* was used as the reference gene. Data were analysed with ANOVA and Tukey's post hoc tests, and comparisons between Sor and Suc were found to be non-significant ( $p > 0.05$ ). Data were published in Simon et al. (2018a) (Appendix).

#### 7.4.5.2 Gibberellin (GA)

##### ***Manipulating GA signalling***

Addition of exogenous GA increases hypocotyl elongation due to cellular elongation (Cowling and Harberd (1999)). To confirm this was the case under our experimental conditions, *L. er.* and Col-0 were grown on MS supplemented with GA under 4 h and 16 h photoperiods (Sup. Fig. 9.22). GA significantly increased hypocotyl length for both *L. er.* (4 h:  $t_{38} = -4.375$ ,  $p < 0.001$ ; 16 h:  $t_{38} = -7.246$ ,  $p < 0.001$ ) and Col-0 (4 h:  $t_{38} = -8.065$ ,  $p < 0.001$ ; 16 h:  $t_{27.09} = -6.674$ ,  $p < 0.001$ ) (Sup. Fig. 9.22).

I wished to investigate whether GA signalling contributes to sucrose-induced hypocotyl elongation under short photoperiods. Pilots were first performed to optimise manipulation of GA signalling. Col-0, *L. er.*, KIN10-ox 5.7 and *tps1-11* seedlings were grown on MS supplemented with combinations of exogenous GA, the GA biosynthesis inhibitor PAC (Offringa and Hooykaas (1999); MacGregor et al. (2015)), or the carrier control (methanol). The carrier control alone significantly decreased hypocotyl length ( $F_{1, 252} = 37.3$ ;  $p < 0.001$ ), but affected all genotypes equally ( $F_{3, 252} = 1.52$ ;  $p > 0.05$ ) (data not included). No seeds germinated on media supplemented with PAC alone. All hypocotyls were significantly shorter when grown on media containing both PAC and GA compared to the carrier control alone ( $F_{1, 304} = 1298.65$ ,  $p < 0.001$ ) (data not included).

Following these initial experiments, hypocotyl length was measured for Col-0, *L. er.*, KIN10-ox 5.7, *tps1-11*, *tps1-12* and *tps1-13* grown on MS, Sor or Suc supplemented with PAC and GA, or the carrier control (Sup. Fig. 9.23). However, sucrose supplementation caused unaltered or slightly decreased hypocotyl length for KIN10-ox 5.7 and the three *tps1* alleles. Consequently, data arising from the addition of PAC and GA were difficult to interpret further for these genotypes (Sup. Fig. 9.23). Subsequent experiments were performed with Col-0 and *L. er.* only.

##### ***GA signalling regulates sucrose-induced hypocotyl elongation***

Col-0 and *L. er.* were grown on MS, Sor or Suc supplemented with PAC and GA or the carrier control (Fig. 7.11). For Col-0, sucrose caused a 112% increase in hypocotyl length

in presence of the carrier control but only a 51% increase when PAC and GA were added (Fig. 7.11a), whereas *L. er.* sucrose-induced hypocotyl elongation went from 98% to 64% in presence of PAC and GA (Fig. 7.11b). An experimental repeat yielded similar results (Sup. Fig. 9.24).

As PAC prevents seed germination, it was not possible to directly explore the effect of PAC only on sucrose-induced hypocotyl elongation with my experimental design. Therefore, Dr Jelena Kusakina first germinated seedlings on MS, then transferred three day-old seedlings to MS, Sor or Suc supplemented with the carrier control, PAC alone, GA alone, or both PAC and GA (Fig. 7.11c, redrawn from Simon et al. (2018a)). PAC abolished hypocotyl elongation in response to exogenous sucrose, and the addition of GA slightly rescued this effect.

Overall, these data indicate that GA signalling regulates sucrose-induced hypocotyl elongation.



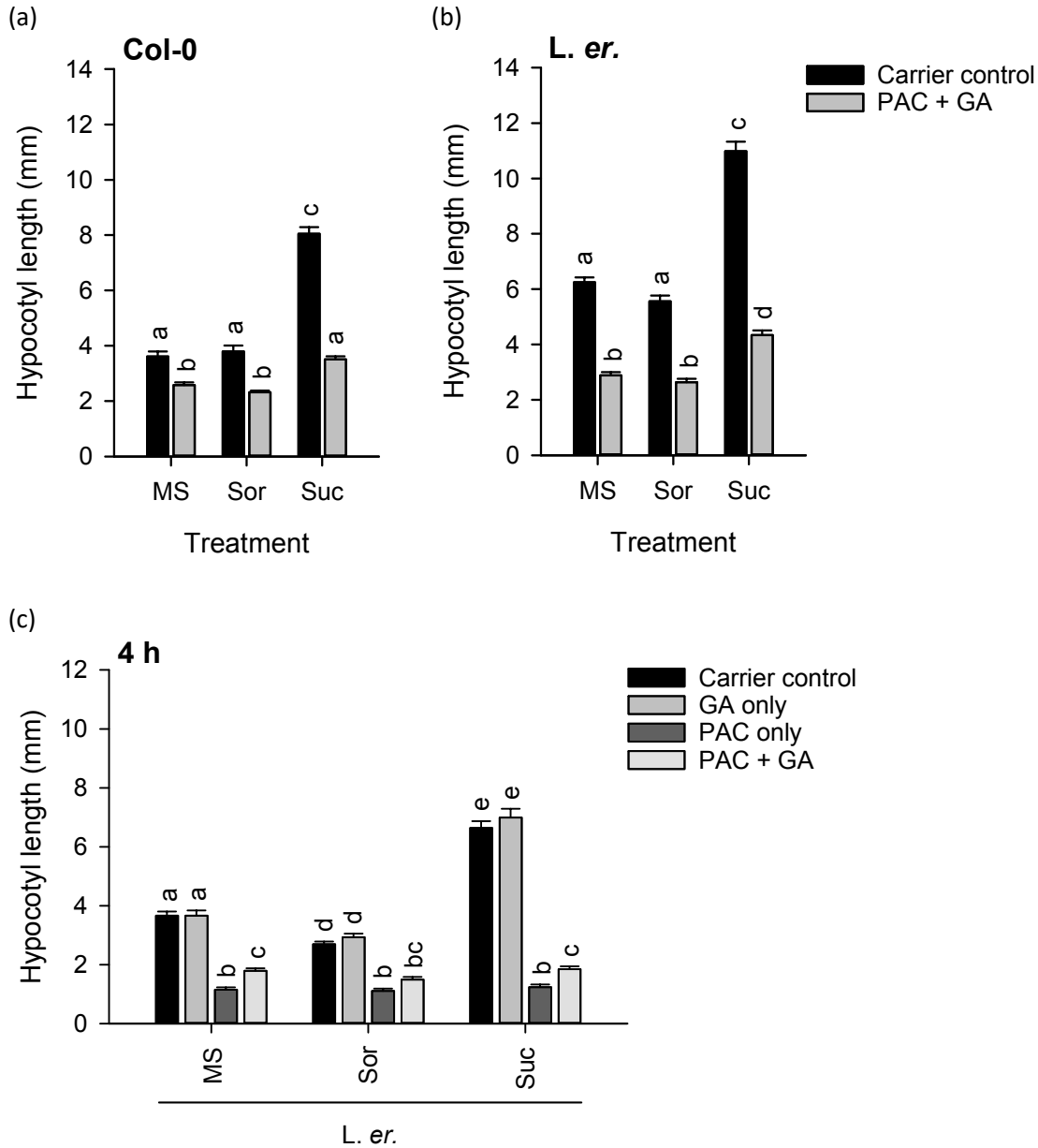


Figure 7.11: GA signalling plays a role in regulating sucrose-induced hypocotyl elongation under short photoperiods. Hypocotyl lengths were measured for 7 day-old (a) *Col-0* and (b) *L. er.* grown on MS supplemented with 3% sucrose (Suc) or equimolar sorbitol (Sor) under a 4 h photoperiod, with these growth media being further supplemented with the carrier control (0.12% (v/v) methanol) or 20  $\mu$ M PAC and 100  $\mu$ M GA ( $n = 20$ ; mean  $\pm$  S.E.M.). Data presented in (c) were obtained by Dr Jelena Kusakina: seedlings were germinated on MS, then transferred to MS, Suc or Sor further supplemented with the carrier control, 100  $\mu$ M GA, 20  $\mu$ M PAC, or both PAC and GA ( $n = 20$ ; mean  $\pm$  S.E.M.). Data were analysed with ANOVA and Tukey's post hoc tests. Different letters indicate statistically significant difference between means ( $p > 0.05$ ). Data from panel (c) were published in Simon et al. (2018a) (Appendix).

### ***The effect of GA on sucrose-induced hypocotyl elongation occurs partially through DELLA-induced signalling***

GA increases hypocotyl length through degradation of DELLA growth repressor proteins and other, DELLA-independent processes (Peng et al. (1997); Fu et al. (2002); Cheng et al. (2004); Cao et al. (2006)). Experiments were performed to elucidate the mechanism through which GA affects sucrose-induced hypocotyl elongation. *GIBBERELIC ACID INSENSITIVE (GAI)* encodes a DELLA protein, and mutating *GAI* reduces the response to GA as GA is no longer able to degrade GAI (Peng et al. (1997)). Therefore, *gai-1* in the *L. er.* background was grown on MS, Sor or Suc under 4 h or 16 h photoperiods (Figs. 7.12a, 7.12b).

Under a 4 h photoperiod, sucrose supplementation significantly increased hypocotyl length for both *gai-1* ( $F_{5, 114} = 190.708$ ,  $p = 0.005$ ) and *L. er.* ( $p < 0.001$ ) (Fig. 7.12a). However, the magnitude of sucrose-induced hypocotyl elongation was reduced in *gai-1* (37%) compared with *L. er.* (59%). Under a 16 h photoperiod, hypocotyl length was unaltered by sucrose supplementation ( $F_{5, 114} = 12.122$ ,  $p > 0.05$ ) (Fig. 7.12b).

This was repeated for a mutant lacking all five known DELLA proteins in the *L. er.* background (Koini et al. (2009)), named *DELLA global* here. Under a 4 h photoperiod, sucrose supplementation significantly increased hypocotyl length for both *DELLA global* ( $F_{5, 114} = 83.130$ ;  $p < 0.001$ ) and *L. er.* ( $p < 0.001$ ) (Fig. 7.12c). The proportional sucrose-induced increases in hypocotyl length were identical (*DELLA global*: 49%; *L. er.*: 50%) (Fig. 7.12c). Under a 16 h photoperiod, sucrose supplementation significantly increased hypocotyl length for *DELLA global* ( $F_{5, 114} = 22.677$ ;  $p = 0.003$ ), but not for *L. er.* ( $p > 0.05$ ) (Fig. 7.12d).

Overall, these data indicate that GA partially regulates sucrose-induced hypocotyl elongation through DELLA-induced signalling.

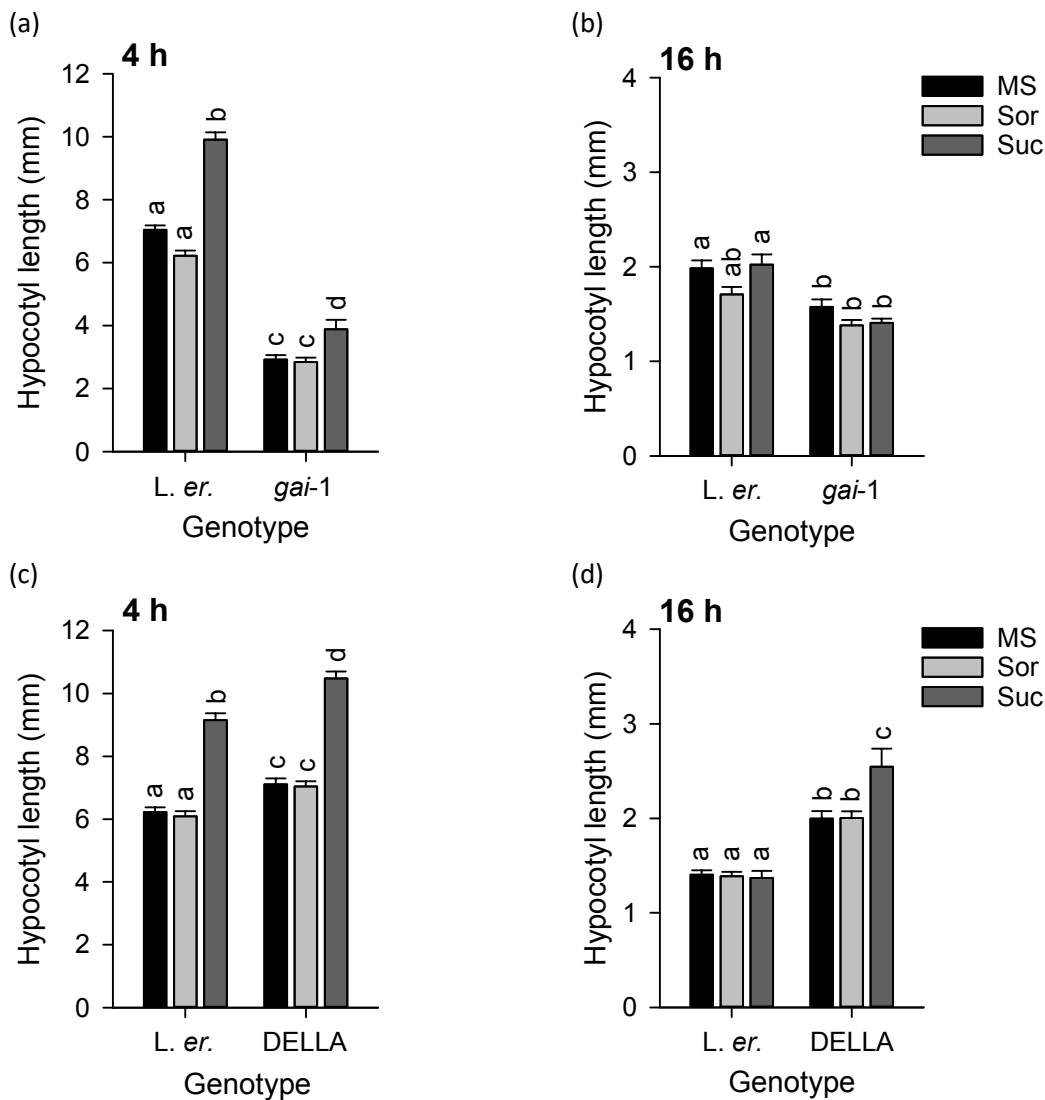


Figure 7.12: GA partially affects sucrose-induced hypocotyl elongation through DELLA-induced signalling. Hypocotyl lengths were measured for 7 day-old (a-b) *gai-1* and (c-d) *DELLA* global grown on MS supplemented with 3% sucrose (Suc) or equimolar sorbitol (Sor) under a (a, c) 4 h photoperiod or (b, d) 16 h photoperiod ( $n = 20$ ; mean  $\pm$  S.E.M.). Photoperiods are indicated over each figure. Data were analysed with ANOVA and Tukey's posthoc tests. Different letters indicate statistically significant difference between means ( $p < 0.05$ ). Data were published in Simon et al. (2018a) (Appendix).

### 7.4.5.3 Abscisic Acid (ABA)

Links have been reported between ABA signalling and T6P (Schluepmann et al. (2003); Avonce et al. (2004); Ramon et al. (2007); Gomez et al. (2010); Debast et al. (2011)). To examine whether ABA regulates sucrose-induced hypocotyl elongation under short photoperiods, *ABA quad* was used (Park et al. (2009)). This mutant harbours defects in four ABA receptors (*PYRABACTIN RESISTANCE1* (*PYR1*), *PYR1-LIKE1* (*PYL1*), *PYL2* and *PYL4*), and is insensitive to ABA signalling (Park et al. (2009)). It incorporates Col-0 and *L. er.* backgrounds, so both accessions were included as controls.

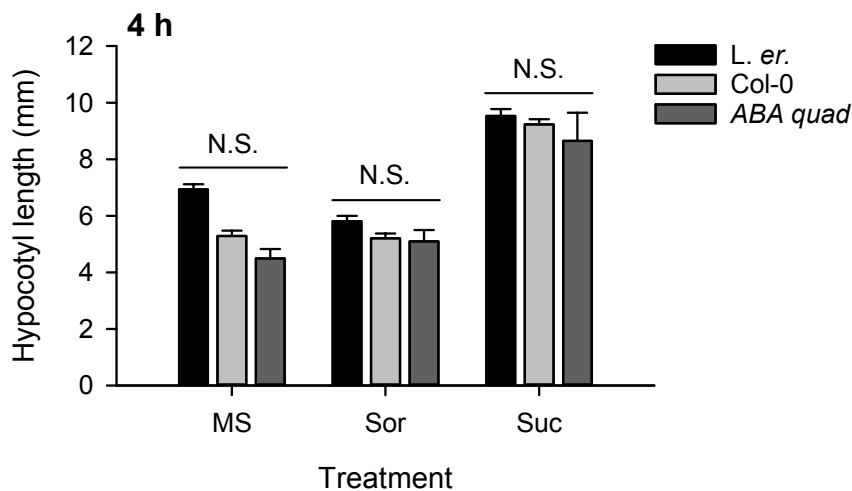


Figure 7.13: ABA signalling through PYR/PYL does not regulate sucrose-induced hypocotyl elongation under short photoperiods. Hypocotyl lengths were measured for 7 day-old *ABA quad* grown on MS supplemented with 3% sucrose (Suc) or equimolar sorbitol (Sor) under a 4 h photoperiod. Both Col-0 and *L. er.* accessions were included as controls, as *ABA quad* incorporates both backgrounds (Park et al. (2009)) ( $n = 20$ ; mean  $\pm$  S.E.M.). *ABA quad* had low germination rates, most likely due to poor seed quality ( $n = 3-9$ ; mean  $\pm$  S.E.M.). Data were analysed using Kruskal-Wallis and Dunn's pairwise tests with Bonferroni correction (N.S. =  $p > 0.05$ ). Data were published in Simon et al. (2018a) (Appendix).

Seedlings were grown on MS, Sor or Suc under a 4 h photoperiod (Fig. 7.13). *ABA quad* had low germination, most likely due to poor seed quality. Due to the low number of seedlings, an independent-samples Kruskal-Wallis test was performed, followed by Dunn's pairwise tests. Sucrose supplementation significantly increased hypocotyl length for all three genotypes ( $\chi^2_8 = 94.213$ ,  $p < 0.001$ , adjusted using the Bonferroni correction). Within each media type, there was no difference in hypocotyl length between *ABA quad* and the two backgrounds ( $p > 0.05$ , adjusted using the Bonferroni

correction).

Therefore, ABA does not regulate sucrose-induced hypocotyl elongation under short photoperiods through PYR/PYL signalling.

## 7.5 Discussion

### 7.5.1 *KIN10* and *TPS1* play a role in regulating sucrose-induced hypocotyl elongation under diel conditions

Here, we demonstrated that the SnRK1 and T6P-based energy-signalling pathways regulate sucrose-induced hypocotyl elongation under light/dark conditions. Overexpressing *KIN10* diminished hypocotyl response to exogenous sucrose (Fig. 7.1; Simon et al. (2018a), Appendix), whereas *KIN10* mutants had increased hypocotyl sensitivity to sucrose supplementation (Fig. 7.2; Simon et al. (2018b), Appendix). This implies that *KIN10* activity inhibits sucrose-induced hypocotyl elongation. Interestingly, abolishing *KIN10* expression alone was sufficient to confer hypocotyl hypersensitivity to sucrose supplementation, despite evidence that both *KIN10* and *KIN11* control SnRK1 kinase activity (Baena-González et al. (2007); Mair et al. (2015)). This suggests that *KIN10* and *KIN11* are not completely redundant within the mechanisms underlying sucrose-induced hypocotyl elongation.

Similar to the *akin10* alleles, sucrose supplementation caused a greater proportional increase in hypocotyl length for *bzip63-1* than the WT (Fig. 7.3). *KIN10* phosphorylation of bZIP63 increases bZIP63 activity levels, and *akin10* has very low levels of phosphorylated bZIP63 (Mair et al. (2015)). Therefore, it is likely that *KIN10* phosphorylation of bZIP63 at least partially regulates sucrose-induced hypocotyl elongation under short photoperiods.

Overexpressing *KIN10* induces genes involved with energy starvation and represses genes involved with energy storage (Baena-González et al. (2007)). This may explain why, under our experimental conditions, *KIN10*-ox seedlings were unable to take advantage of the additional energy provided by sucrose supplementation and accordingly did not grow longer (Fig. 7.1; Simon et al. (2018a), Appendix).

Under short photoperiods, decreasing T6P concentrations in the *tps1* mutants reduced or eliminated sucrose-induced hypocotyl elongation (Fig. 7.1; Simon et al. (2018a), Appendix). Similar results were reported for transgenic *Arabidopsis* overexpressing bacterial *otsA* (*TPS*) and *otsB* (*T6P phosphatase*) genes (Schluepmann et al. (2003); Zhang et al. (2009); Paul et al. (2010); Martins et al. (2013)). In presence of exogenous sucrose, *otsA* overexpressors accumulate higher concentrations of T6P and have improved growth compared with the WT (Schluepmann et al. (2003); Paul et al. (2010); Martins et al. (2013)), whereas *otsB* overexpressors have low T6P levels and accumulate less biomass (Schluepmann et al. (2003)). Therefore, T6P metabolism plays a critical role in regulating sucrose-induced growth responses.

## 7.5.2 Sucrose-induced hypocotyl elongation is photoperiod-dependent

We found that sucrose-induced hypocotyl elongation varied with photoperiod length, with elongation occurring in response to sucrose under 8 h photoperiods or shorter (Fig. 7.5). This may explain disparities between previous studies, where hypocotyl elongation was found to be either promoted by or insensitive to sucrose. Under conditions of continuous light, Zhang et al. (2010) found hypocotyl elongation to be unaltered in presence of sucrose, as was likewise observed in our experiments (Fig. 7.4b; Sup. Fig. 9.18; Simon et al. (2018a), Appendix). In contrast, Stewart et al. (2011) and Lilley et al. (2012) reported that exogenous sucrose promoted hypocotyl elongation under 8 h photoperiods, where we also detected sucrose-induced hypocotyl elongation (Fig. 7.5; Simon et al. (2018a), Appendix). Therefore, these opposing results in sucrose-sensitivity could be reconciled through these variations in photoperiod (Simon et al. (2018a)).

Both absolute photoperiod and daily integrated PAR regulate the photoperiod-sensitivity of sucrose-induced hypocotyl elongation (Fig. 7.6). Under low light levels and short photoperiods, cells have low concentrations of sugars, whereas, under high light levels and long photoperiods, endogenous sugar levels are high (Sulpice et al. (2014)). Consequently, the addition of exogenous sucrose would have a greater impact on sugar-starved seedlings compared to sugar-saturated seedlings.

Alternatively, PIFs might convey photoperiod information. T6P modulates PIF expression levels (Paul et al. (2010)), and PIFs regulate sucrose-induced hypocotyl elongation (Stewart et al. (2011); Lilley et al. (2012)). Therefore, PIFs might merge light and sugar

signalling pathways to enable elongating hypocotyls to respond appropriately to exogenous sucrose.

Although *bzip63-1*, *akin10* and *akin10-2* elongated in response to sucrose under both 4 h and 16 h photoperiods, the magnitude of sucrose-induced hypocotyl elongation was reduced under a 16 h photoperiod compared with a 4 h photoperiod (Figs. 7.2, 7.3). In addition, sucrose supplementation significantly increased KIN10-ox 5.7 and KIN10-ox 6.5 hypocotyls under an 8 h photoperiod, but not under a 4 h photoperiod (Simon et al. (2018a)). As the KIN10-ox response to sucrose supplementation appears to vary with photoperiod, signals conveying photoperiod and daily integrated PAR to hypocotyl elongation may be independent from KIN10 activity within SnRK1. Alternative mechanisms may include other energy-sensing mechanisms, such as the TOR signalling pathway (Schepetilnikov and Ryabova (2018)), or photoperiod-sensing mechanisms, such as the circadian clock (Johansson and Staiger (2015)). In future, it would be interesting to further decipher the links between these various signalling pathways.

### **7.5.3 Phytohormone involvement in sucrose-induced hypocotyl elongation**

Our experiments indicate that both auxin and GA signalling contribute to sucrose-induced hypocotyl elongation under short photoperiods (Figs. 7.8, 7.9, 7.11; Simon et al. (2018a), Appendix). These data are consistent with previous studies reporting roles for auxin and GA in sucrose-induced hypocotyl elongation (De Lucas et al. (2008); Zhang et al. (2010); Liu et al. (2011); Stewart et al. (2011); Lilley et al. (2012)). Addition of the auxin transport inhibitor NPA at concentrations over 10  $\mu$ M suppressed sucrose-induced hypocotyl elongation (Fig. 7.8; Sup. Fig. 9.20), as also reported by Lilley et al. (2012).

To further explore the role of auxin in regulating sucrose-induced hypocotyl elongation, the abundance of several auxin-upregulated expansin transcripts was analysed (Fig. 7.9; Simon et al. (2018a), Appendix). *EXPA4* transcript abundance did not vary under conditions promoting or inhibiting hypocotyl elongation (Sup. Fig. 9.21; Simon et al. (2018a), Appendix), and sucrose supplementation did not alter wild type *EXPA8* expression levels (Fig. 7.9; Simon et al. (2018a), Appendix). Therefore, *EXPA4* and *EXPA8* were considered unsuitable reporters and not pursued.

*EXPA11* was upregulated in response to exogenous sucrose in *L. er.* and two *tps1* alleles, but downregulated in both *KIN10* overexpressors (Fig. 7.9; Simon et al. (2018a), Appendix). This suggests that *KIN10* affects expansin gene expression during sucrose-induced hypocotyl elongation. *tps1* mutants did not have the same effect on *EXPA11* transcript abundance as *KIN10*-ox. This could be due to the nature of the TILLING mutants, which are hypomorphic because they only partially reduce T6P concentrations (Gomez et al. (2010)). Indeed, sucrose-induced hypocotyl elongation, although reduced, still occurred in the *tps1-11* and *tps1-12* alleles (Fig. 7.1; Simon et al. (2018a), Appendix). Alternatively, the effect of *KIN10* upon sucrose-induced hypocotyl elongation may be partially independent from that of *TPS1*. In this speculative scenario, each pathway might regulate sucrose-induced hypocotyl elongation through independent signalling and metabolic processes. For example, SnRK1 targets transcription factors involved in anabolism and catabolism (Baena-González et al. (2007)), while *TPS1* regulates starch and sucrose degradation (Gómez et al. (2006)).

Several auxin biosynthesis and response transcripts were examined in the presence of exogenous sucrose, but no alterations in transcript abundance were observed (Fig. 7.10; Simon et al. (2018a), Appendix). This differs from the findings of Lilley et al. (2012), who reported upregulation of *YUCCA8*, *IAA29* and *SAUR15* in response to sucrose. However, Lilley et al. (2012) compared transcript abundance between seedlings grown on sucrose and those grown without treatment, and did not report such data for seedlings grown on an osmotic control. Sucrose is also known to affect auxin distribution and sensitivity (Stokes et al. (2013)). In addition, a genome-wide analysis of *Arabidopsis* under anoxic conditions revealed that the addition of exogenous sucrose mitigated repression of auxin responsive genes (Loreti et al. (2005)). Therefore, under our experimental conditions, it is likely that the osmotic control masked possible effects of sucrose supplementation on transcript abundance of auxin biosynthesis and response genes (Fig. 7.10; Simon et al. (2018a), Appendix).

The GA biosynthesis inhibitor PAC abolished hypocotyl elongation in response to exogenous sucrose (Fig. 7.11c; Simon et al. (2018a), Appendix). In contrast, *gai-1* only partially abolished sucrose-induced hypocotyl elongation under a 4 h photoperiod, and a small yet significant sucrose-induced hypocotyl elongation was detected for *DELLA global* under a 16 h photoperiod (Fig. 7.12; Simon et al. (2018a), Appendix). As 40% to 60% of GA-regulated transcripts are controlled by DELLA proteins (Cao et al. (2006)), these discrepancies may be explained by the contribution of DELLA-independent signalling pathways to sucrose-induced hypocotyl elongation. PAC may also have ectopic



or off-target effects on hypocotyl elongation, because the addition of exogenous GA does not fully rescue the effect of PAC upon sucrose-induced hypocotyl elongation (Fig. 7.11; Simon et al. (2018a), Appendix).

Mechanisms other than auxin and GA signalling might also regulate sucrose-induced hypocotyl elongation. Under conditions of darkness, hypocotyl elongation in response to sucrose supplementation involves brassinosteroid (BR) and/or TOR signalling (Zhang et al. (2015a, 2016)). Therefore, the same sucrose-induced hypocotyl elongation phenotype occurs under constant darkness and light/dark conditions. It would be interesting to investigate whether these diel, SnRK1-induced pathways and dark, TOR- and/or BR-regulated pathways interact with each other.

## 7.6 Conclusions

Using Arabidopsis hypocotyl elongation as a model system:

- We isolated a novel role for the KIN10 subunit of the energy signalling hub SnRK1 in regulating sucrose-induced hypocotyl elongation under short photoperiods. This is likely to occur through bZIP63 phosphorylation (Mair et al. (2015)) and interactions with auxin and GA phytohormone signalling pathways (Liu et al. (2011); Stewart et al. (2011); Lilley et al. (2012)).
- We identified TPS1 as necessary for sucrose-induced hypocotyl elongation under short photoperiods. Interestingly, this effect might be partially independent from that of KIN10.
- We showed that day length and light intensity signals affect sucrose-induced hypocotyl elongation via KIN10- and TPS1-independent mechanisms. This resolved discrepancies reported by previous studies (Zhang et al. (2010); Stewart et al. (2011); Lilley et al. (2012)).
- Although our data suggest that the circadian oscillator does not contribute to sucrose-induced hypocotyl elongation, it might play an indirect role through photoperiod sensing (Johansson and Staiger (2015)).
- Hexokinase-induced glucose signalling and ABA signalling through PYR/PYL are

not involved in regulating sucrose-induced hypocotyl elongation under diel conditions.

These identified mechanisms deepen our understanding of seedling development in response to carbohydrate availability. Interestingly, manipulating the SnRK1 and T6P signalling pathways can significantly increase yields and/or drought tolerance of key crops (Nuccio et al. (2015); Griffiths et al. (2016)). In future, it would be interesting to investigate whether these signalling pathways could also be used to optimise seedling establishment under difficult environmental conditions.



# Chapter 8

## Discussion

Global food security represents a major challenge for modern society, particularly within the context of climate change (Rosegrant and Cline (2003); Schmidhuber and Tubiello (2007); Lobell et al. (2008)). Pressure is increasing on available freshwater resources, and water-limited conditions can cause substantial decreases in crop biomass and yield, leading to socio-economic consequences (Hu and Xiong (2014); Underwood (2015); Ruggiero et al. (2017)). Therefore, it is crucial to adapt crops to these rapidly changing environmental conditions, which can include heavy flooding (Schmidhuber and Tubiello (2007)) and drought (Underwood (2015)). Increasing the latitudinal range over which certain crops are grown must also be considered, as well as adjustments to new growth practices such as vertical farming (Benke and Tomkins (2017)).

Scientists and breeders are currently trying to increase crop yield and drought tolerance (Xoconostle-Cázares et al. (2010); Hu and Xiong (2014); Ruggiero et al. (2017)). Technological advances in molecular genetics have enabled a more rapid and targeted approach to obtain desirable traits (Hu and Xiong (2014); Ruggiero et al. (2017)). However, crops are becoming increasingly homogeneous (Khoury et al. (2014)), and the genetic diversity necessary to adapt crops to new and changing environments is rapidly decreasing (Esquinas-Alcázar (2005)). In addition, public opinion remains divided around new biotechnology, which then has repercussions on governmental policies. For example, this led to a ban on genetically modified foods and crops in Europe (Malyska et al. (2016); McFadden (2016); Valente and Chaves (2018)), which hinders the use of this technology in addressing food security.

Despite these challenges, it remains important to continue researching the molecular mechanisms underlying desirable crop traits. Indeed, the complex, interacting signalling pathways involved in plant water use and development could represent future breeding targets. Therefore, this thesis has focused on trying to elucidate roles of circadian clock and SnRK1/T6P-based signalling pathways in regulating WUE and physiology.

## 8.1 Involvement of circadian regulation and energy signalling in plant water use and development

The research in this thesis demonstrated that, in *Arabidopsis*, whole plant WUE under diel conditions is regulated by the guard cell-specific (Chapter 5) and whole plant circadian clocks (Chapter 3), as well as by the SnRK1/T6P-based energy signalling pathways (Chapter 3) (Fig. 8.1). The circadian clock may partially control WUE through alterations in rosette architecture, such as rosette leaf surface area and leaf overlap, and possible effects on boundary layers (Chapter 3). Circadian clock components *CCA1*, *TOC1*, *ELF3*, *GI*, *GRP7*, *PRR5*, *PRR7*, *PRR9*, *TEJ* and *ZTL* were found to regulate WUE (Chapter 3). However, due to the complex, interlocking nature of the circadian system, it was difficult to distinguish whether roles of circadian clock components were independent, overlapping, or indirect via effects on transcript and/or protein abundance of other circadian clock elements (Chapter 3). Therefore, it is possible that these circadian oscillator components are acting through the same mechanisms, or alternatively having distinct effects upon WUE. SnRK1/T6P-based regulation of WUE is likely to be independent of the circadian clock (Chapter 3), as manipulating *KIN10* and *TPS1* expression severely impacts development and metabolism (Eastmond et al. (2002); Baena-González et al. (2007); Baena-González (2010); Gomez et al. (2010)).

This thesis also reinforces the growing hypothesis that distinct circadian oscillators exist within different plant tissues and control specific aspects of plant physiology (Chapter 5; James et al. (2008); Endo et al. (2014); Shimizu et al. (2015); Takahashi et al. (2015); Hassidim et al. (2017)). By misregulating specifically the guard cell circadian clock (Chapter 4), I identified guard-cell specific roles of the circadian clock in regulating WUE, short-term responses to drought, and possibly growth (Chapter 5) (Fig. 8.1). Comparisons with whole plant circadian clock gene overexpressors also established

guard cell-independent roles of the circadian clock, such as the regulation of hypocotyl elongation (Chapter 5) (Fig. 8.1).

Brief studies on naturally-occurring populations of *A. halleri* subsp. *gemmaifera* confirmed that rhythms of stomatal aperture and closure were also detectable under field conditions (Chapter 6). Interestingly, stomatal density was found to differ between glabrous and hairy morphs (Chapter 6). This may indicate that, in the absence of herbivores, the higher stomatal density of glabrous plants contributes to their fitness advantage over hairy plants (Chapter 6).

In addition to regulating WUE, the SnRK1/T6P-based energy signalling pathways also mediate sucrose-induced hypocotyl elongation under short photoperiods (Chapter 7) (Fig. 8.1). Mechanisms underlying this control of sucrose-induced hypocotyl elongation are likely to include bZIP63 phosphorylation (Mair et al. (2015)), interactions with auxin and GA phytohormone signalling pathways (Liu et al. (2011); Stewart et al. (2011); Lilley et al. (2012)), and interactions with photoperiod and light intensity signals (Chapter 7). Although the circadian clock does not control sucrose-induced hypocotyl elongation under our experimental conditions, it may play an indirect role through photoperiod sensing (Johansson and Staiger (2015)).

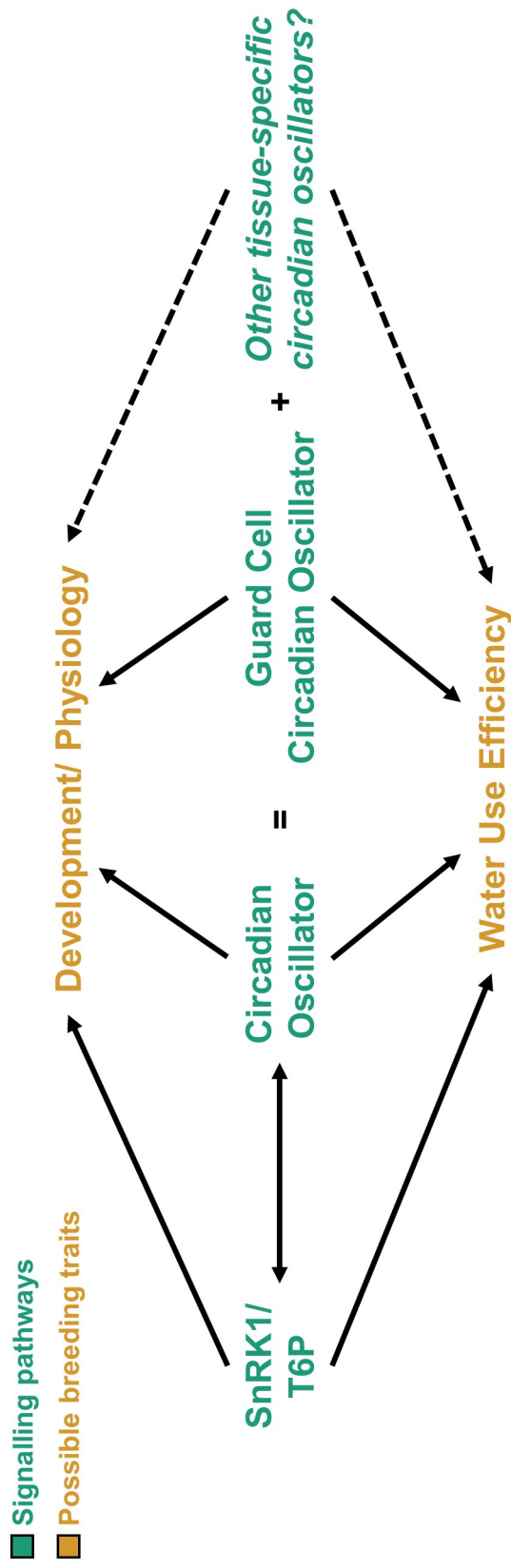


Figure 8.1: The whole plant circadian oscillator, composed of the guard cell circadian oscillator and other tissue-specific circadian oscillators, and SnRK1/T6P-based signalling pathways regulate WUE and development. Interactions between signalling pathways are obtained from previous reports (Shin et al. (2017); Sánchez-Villarreal et al. (2018); Frank et al. (2018)). Possible breeding traits are represented by orange text, signalling pathways by green text, regulation by arrows, interactions by double arrows or mathematical symbols, and hypothetical regulation by italicised text and dotted arrows.

## 8.2 Novelty of research performed in this thesis

The research in this thesis further expands scientific knowledge in the following ways:

- I optimised a high-throughput screening technique to measure WUE in *Arabidopsis*, and demonstrated that the circadian clock regulates whole plant WUE under diel conditions (Chapter 3). In particular, I identified ten circadian clock genes involved in the regulation of WUE (Chapter 3).
- I generated a toolkit of transgenic *Arabidopsis* in which the guard cell circadian clock is arrhythmic (Chapter 4). This toolkit may be of use to future research.
- I isolated guard cell-dependent and independent effects of the circadian clock upon whole plant physiology (Chapter 5). I also determined possible roles for other tissue-specific circadian clocks in regulating physiology (Chapter 5).
- Using naturally-occurring populations of *A. halleri* subsp. *gemmifera*, I detected rhythms of stomatal aperture and closure under field conditions (Chapter 6). In addition, I established that the hairy morph had a lower stomatal density and index than the glabrous morph (Chapter 6).
- I demonstrated novel roles for the SnRK1/T6P-based energy signalling pathways in regulating WUE (Chapter 3) and sucrose-induced hypocotyl elongation (Chapter 7; Simon et al. (2018a,b)).

## 8.3 Future work and possibilities

Circadian traits were artificially selected during domestication of key crops, including barley (Turner et al. (2005)), tomato (Müller et al. (2016, 2018)), soybean (Greenham et al. (2017)), wheat, rice, maize and potatoes (Nakamichi (2015)). Consequently, the circadian clock could be exploited as a possible breeding avenue for crops (Kay and Remigereau (2016); Shor and Green (2016)). For example, the circadian clock could be used to adapt photoperiod-sensitive crops to new geographic areas (Huang and Nusinow (2016); Shor and Green (2016)). Circadian regulation of C4 and CAM metabolism may also be important for the transfer of these photosynthetic pathways to C3 crops



(Khan et al. (2010); Hayes et al. (2010); Boxall et al. (2017); Sharma et al. (2017)). The results obtained in this thesis suggest that the circadian clock could be used to achieve other targets as well.

The research in this thesis highlights the role of the circadian clock in regulating WUE (Chapter 3). As several genotypes with altered circadian clocks had increased WUE (Chapter 3), circadian clock manipulation could be used as a tool to breed for more water use efficient crops. However, breeding for high WUE can select for plants with undesirable traits limiting water use, including smaller leaf areas or earlier flowering times (Blum (2009); Ruggiero et al. (2017); Ferguson et al. (2018)). In addition, plants with high WUE under water-limited conditions can be penalised under more favourable growth conditions, with lower yields and slower growth rates (Condon et al. (2002)). WUE can also vary with environmental conditions, with genotypes having high WUE under droughted conditions and low WUE under favourable conditions (Edwards et al. (2012)). Therefore, it would be useful to exploit WUE manipulation not as a tool in isolation, but rather as a component of a much larger toolkit. By combining WUE with other vegetative and reproductive physiological data, such as leaf area, flowering time, and yield data, a much more realistic overview of crop performance can be obtained. It would be equally informative to collate data acquired under both favourable growth conditions and conditions of abiotic and/or biotic stress.

As crops are grown under naturally fluctuating conditions, it is important to further investigate the role of the circadian clock *in natura*. In particular, it would be interesting to explore mechanisms underlying the rhythms of stomatal aperture detected in this thesis (Chapter 6) and previous studies (Resco de Dios et al. (2016a,b, 2017)). This could then be exploited to manipulate circadian gating of environmental signalling in guard cells. One possibility could involve restricting or expanding the length of time stomata remain open, depending on environmental conditions. For example, under droughted conditions, limiting stomatal opening to early morning could prevent excessive water loss, whereas, under well-watered conditions, postponing stomatal closure could enable greater carbon assimilation and growth. This mechanism could also be used to synchronise mesophyll CO<sub>2</sub> demands with stomatal aperture and closure responses, as photosynthesis is under circadian regulation as well (Dodd et al. (2005, 2015)). This target has great potential, as reducing the temporal disconnect between stomatal conductance and photosynthetic carbon assimilation could increase WUE by up to 22% (Chapter 1; Lawson and Blatt (2014)).

Although altering the circadian clock can increase yields (Preuss et al. (2012)), it is equally possible for it to negatively affect plant physiology and fitness (Green et al. (2002); Dodd et al. (2005); Bendix et al. (2015)). Similar issues were also reported when manipulating stomatal characteristics to breed for higher WUE. For example, in *Arabidopsis*, a higher stomatal density increased carbon assimilation, but decreased WUE (Tanaka et al. (2013)). To avoid this, guard cell-specific promoters can be used to engineer stomatal responses without impacting plant growth and productivity (Galbiati et al. (2008); Cominelli et al. (2011)).

In a similar fashion, it might be possible to achieve precise breeding goals by exploiting tissue-specific circadian clocks via tissue-specific promoters. For example, guard cell *CCA1* overexpressors have increased WUE and survival to dehydration stress, yet hypocotyl elongation, flowering time under long days, and rosette architecture are unaltered (Chapter 5). In contrast, *CCA1-ox* has metabolic and developmental defects, as well as unaltered or decreased WUE (Chapter 5; Wang and Tobin (1998); Green et al. (2002); Dodd et al. (2005); Matsushika et al. (2002)). Therefore, breeders could potentially use tissue-specific circadian oscillators as tools to insert desirable traits into crops. It may even be conceivable to manipulate several tissue-specific circadian clocks simultaneously to achieve the best possible combinations of yield, WUE, desired flowering time, and abiotic and biotic stress tolerance, as these traits are all under circadian regulation (Dodd et al. (2005); Sanchez et al. (2011); Moghaddam and Van Den Ende (2013); Hsu and Harmer (2014); Grundy et al. (2015); Johansson and Staiger (2015)). Further work would be necessary to understand the distinct roles of each tissue-specific circadian clock, and their interactions within the hierarchical circadian system.

Manipulation of signalling messengers may represent an alternative breeding strategy. Indeed, sucrose affects SnRK1/T6P-based energy signalling (Chapter 7; Halford et al. (2003); Schluempmann et al. (2003); Baena-González et al. (2007); Baena-González (2010); Ghillebert et al. (2011)), circadian clock signalling (Haydon et al. (2013a,b); Frank et al. (2018)), and guard cell signalling (Kelly et al. (2013); Daloso et al. (2016); Santelia and Lawson (2016)). In a similar fashion, cytosolic free calcium concentrations ( $[Ca^{2+}]_{cyt}$ ) are connected with the circadian clock (Love et al. (2004); Dodd et al. (2007); Xu et al. (2007); Robertson et al. (2009)), guard cell signal transduction (Allen et al. (2000); Pei et al. (2000); Schroeder et al. (2001); Young et al. (2006)) and SnRK signalling pathways (Coello et al. (2011)). As these various signalling pathways converge upon the same messengers, it would be useful to further elucidate how sucrose and  $Ca^{2+}_{cyt}$  concentrations can encode different messages. Previous reports have ex-

plored how sucrose signalling (Paul et al. (2001); Coello et al. (2011); Hammond and White (2011); Patrick et al. (2013); Braun et al. (2014); Lastdrager et al. (2014); Griffiths et al. (2016); Li and Sheen (2016)) and calcium signalling (Knight et al. (1997); Kiegle et al. (2000); Wood et al. (2000); Allen et al. (2001); Evans et al. (2001); McAinsh et al. (2002); Gomez et al. (2004); Siegel et al. (2009); Hubbard et al. (2012); Brandt et al. (2015); Aldon et al. (2018)) encode information. In this fashion, breeders might be able to manipulate different signalling pathways simultaneously to obtain desirable traits. Indeed, messenger manipulation is already being explored for both sucrose (Micallef et al. (1995); Fukushima et al. (2001); Park et al. (2008); Braun et al. (2014)) and calcium (Saijo et al. (2000, 2001); Persson et al. (2001); Wyatt et al. (2002); Pittman and Hirschi (2003)). It would also be interesting to investigate whether messenger concentrations could be modified in an external fashion, such as watering. This would enable breeders to regulate signalling pathways without generating transgenic plants, and to coordinate this regulation with environmental conditions.

## **8.4 Conclusions**

The mechanisms underlying plant water use and development are very complex, involving a large number of elaborate, interlocking signalling pathways. These signalling pathways represent a largely untapped potential for crop improvement. Overall, the research in this thesis has contributed to our understanding of how circadian and energy signalling regulate water use efficiency and physiology. However, future work is necessary to enable effective breeding efforts. This includes research to further comprehend interactions between circadian clock genes, relationships between tissue-specific circadian clocks, and connections between various signalling pathways.

# **Chapter 9**

## **Appendix**

### **9.1 The circadian clock and water use efficiency**

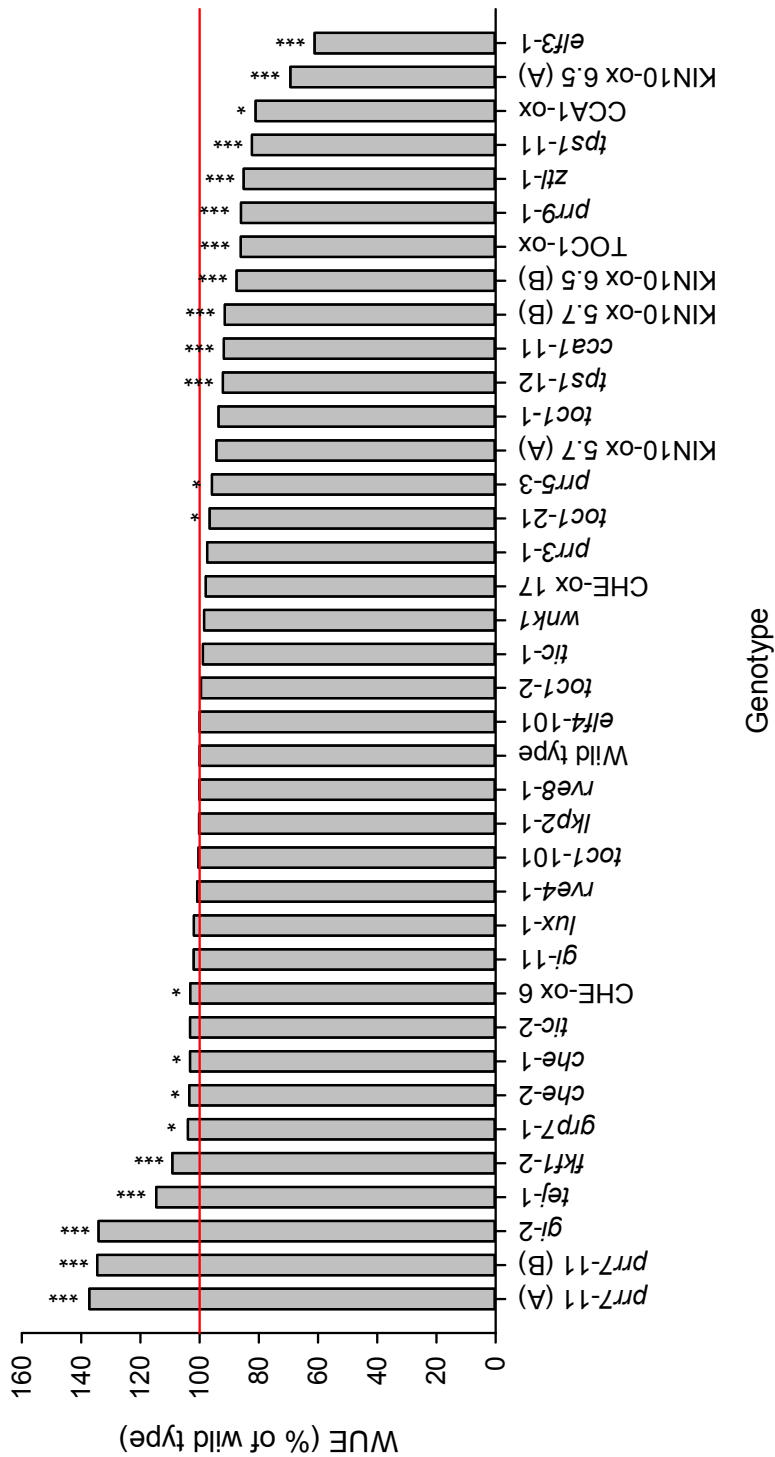


Figure 9.1: The circadian clock regulates whole plant WUE in Arabidopsis under light/dark conditions. Data were collected from additional experimental repeats of Fig. 3.5. Data show WUE of screened circadian clock mutants and overexpressors, which are expressed as a percentage of their respective wild type background (normalised to 100%, red reference line) due to variation between accessions ( $n = 5-15$ ; mean). Data were analysed using independent-samples t-tests, and statistical significance is indicated using starring (\* =  $p < 0.05$ ; \*\* =  $p < 0.01$ ; \*\*\* =  $p < 0.001$ ). Supplemental independent experimental repeats are shown here for each genotype, and genotypes with more than one additional experimental repeat are further marked with (A) and (B) to separate these repeats.

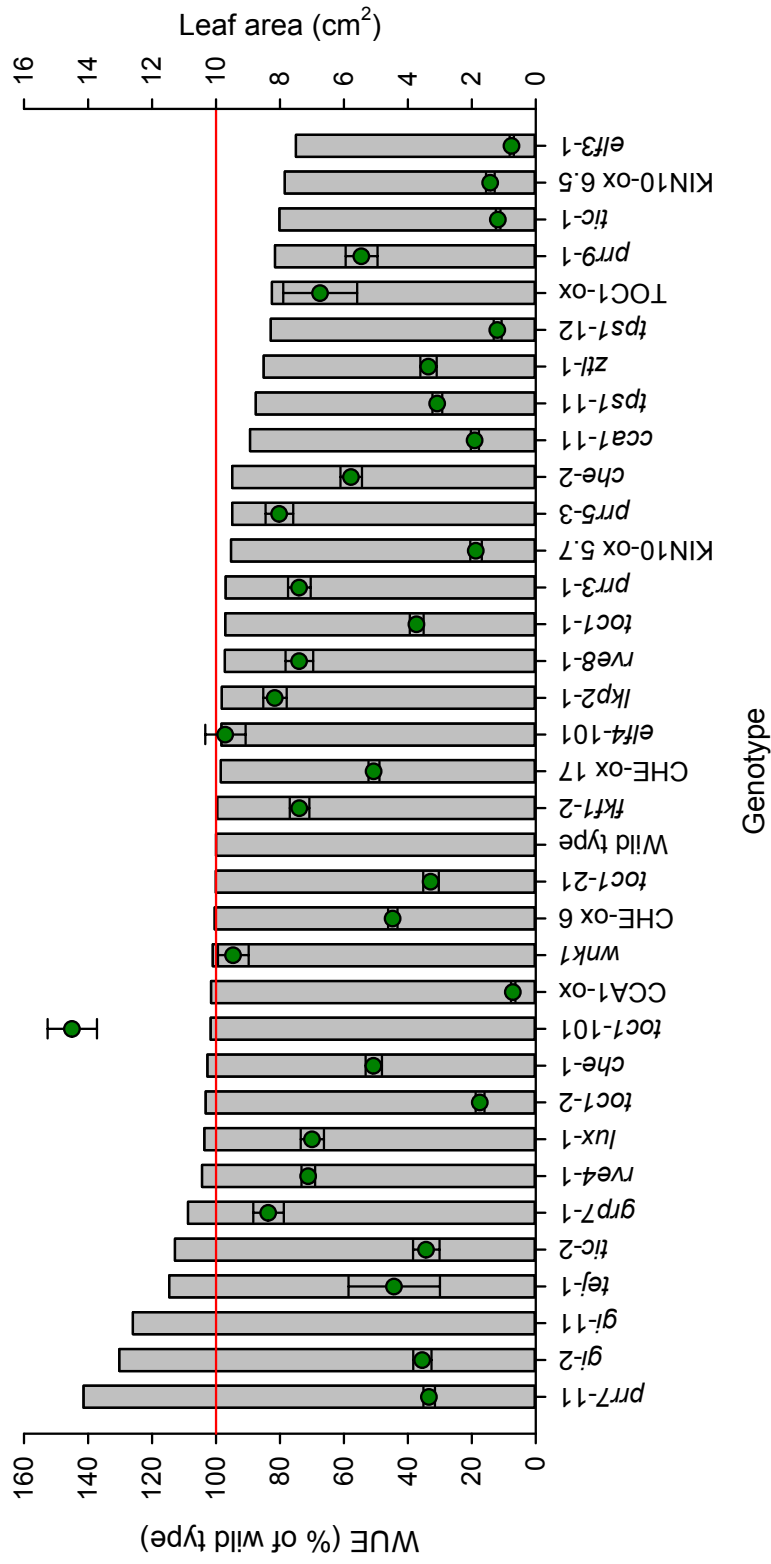


Figure 9.2: Variations in WUE are not fully explained by rosette leaf surface area. Data are redrawn from Fig. 3.5 and represent mean WUE of screened circadian clock mutants and overexpressors expressed as a percentage of their respective WT background ( $n = 5-15$ ). The red reference line indicates WT WUE (100%). Mean rosette leaf surface area is included for each genotype (green;  $n = 5-15$ ; mean  $\pm$  S.E.M.). No leaf surface area data was obtained for *gi-11* due to experimental error. A figure showing mean rosette leaf surface area expressed as a percentage of the WT is provided in the main text (Fig. 3.10).

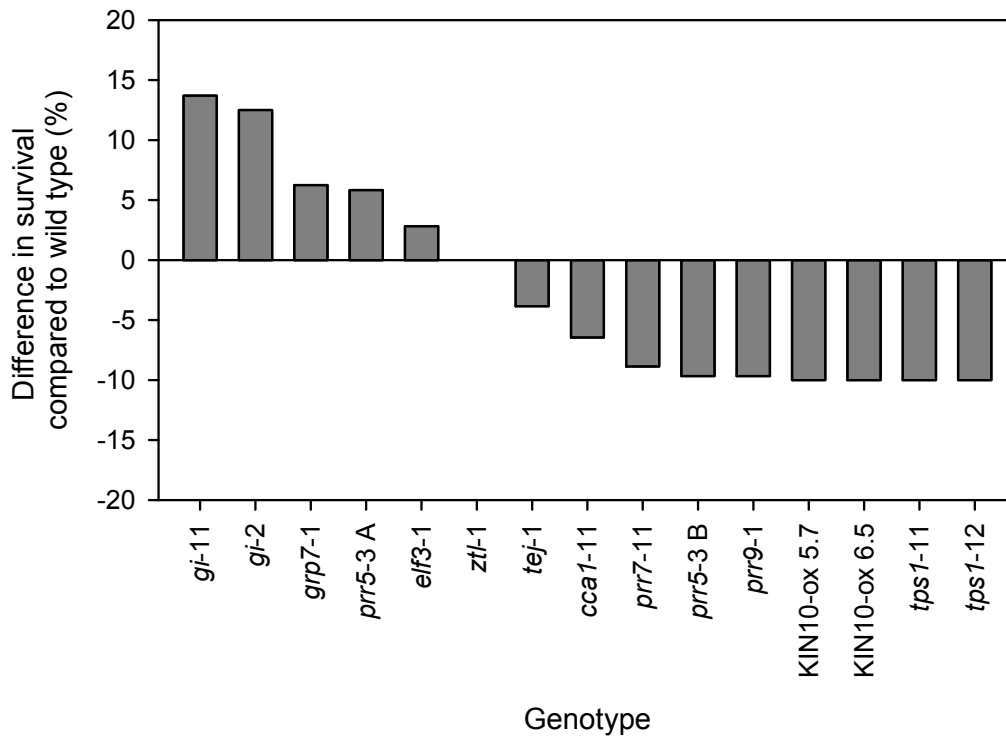


Figure 9.3: *CCA1*, *ELF3*, *GI*, *TOC1* and *PRR9* regulate seedling response to dehydration under constant light conditions. Data were collected from additional experimental repeats of Fig. 3.11. Data show percentage difference in survival to dehydration of the circadian clock mutants and overexpressors compared to their backgrounds ( $n = 32$ ). Supplemental independent experimental repeats are shown here for each genotype, and genotypes with more than one additional experimental repeat are further marked with (A) and (B) to separate these repeats.

## 9.2 Generating, genotyping and validating transgenic Arabidopsis with misregulated guard cell circadian clocks

<i>Genotype-allele</i>	<b>Construct</b>	<b>T<sub>0</sub> ID</b>	<b>T<sub>1</sub> ID</b>	<b>T<sub>2</sub> ID</b>
<i>GC-1</i>	GC1::CCA1:nos	5	m1-1	1
<i>GC-2</i>	GC1::CCA1:nos	5	m1-2	10
<i>GC-3</i>	GC1::CCA1:nos	5	m2	2
<i>GC-4</i>	GC1::CCA1:nos	9	m1-1	8
<i>GC-5</i>	GC1::CCA1:nos	5	m3	6
<i>MC-1</i>	MYB60::CCA1:nos	1	1A	10
<i>MC-2</i>	MYB60::CCA1:nos	1	1B	7
<i>MC-3</i>	MYB60::CCA1:nos	5	m2-2	1
<i>MC-4</i>	MYB60::CCA1:nos	5	m2-1	9
<i>MC-5</i>	MYB60::CCA1:nos	5	m.m2-1	7
<i>GT-1</i>	GC1::TOC1:nos	1	B	4
<i>GT-2</i>	GC1::TOC1:nos	1	D	8
<i>GT-3</i>	GC1::TOC1:nos	7	m3-3	9
<i>MT-1</i>	MYB60::TOC1:nos	1	1	1
<i>MT-2</i>	MYB60::TOC1:nos	1	2	10
<i>MT-3</i>	MYB60::TOC1:nos	6	m1p1	1

Table 9.1: T<sub>0</sub>, T<sub>1</sub> and T<sub>2</sub> of each homozygous GCS-ox genotype and allele used in this study.



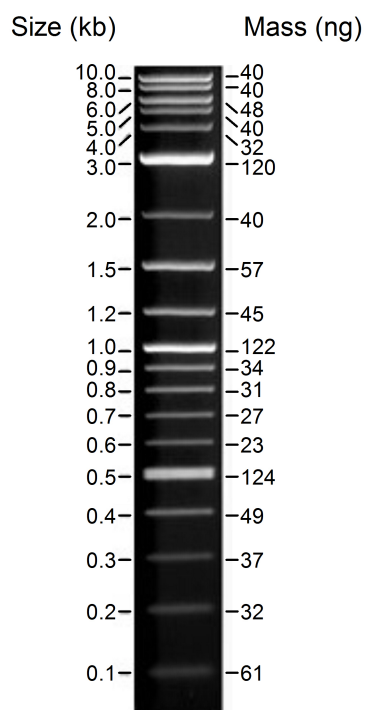


Figure 9.4: Map of the 2-Log DNA Ladder (0.1 kb - 10.0 kb), based on the map provided by NEB. Mass (ng) and size (kb) are indicated for each ladder band.

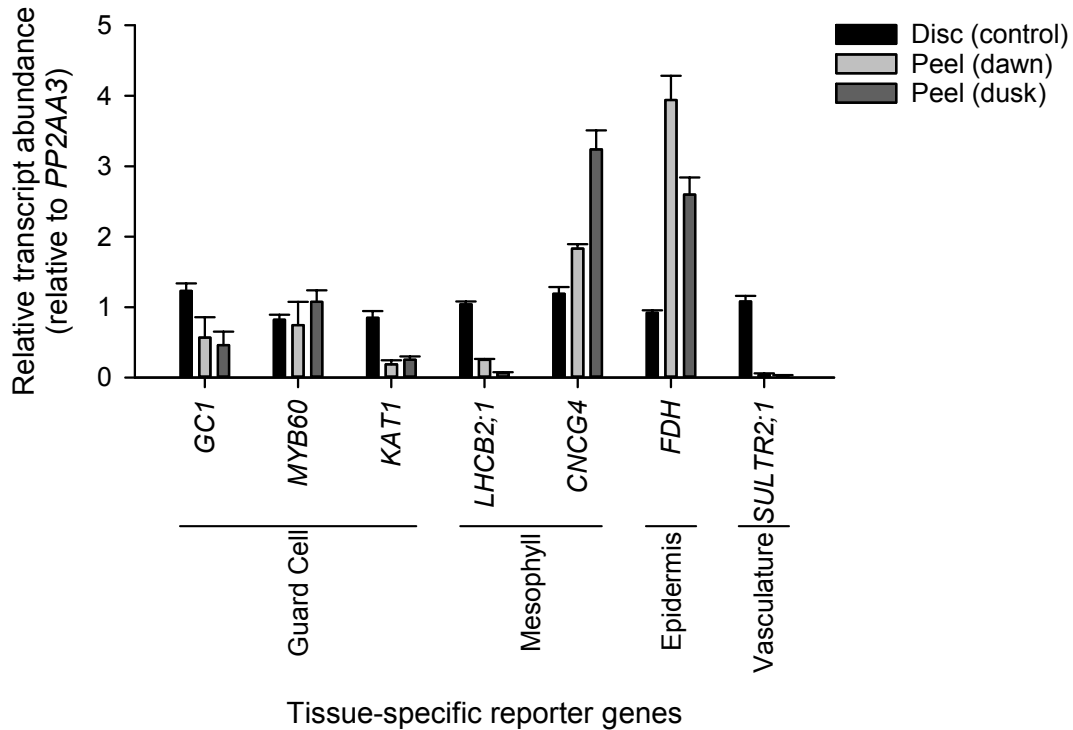


Figure 9.5: Relative transcript abundance of tissue-specific reporter genes to examine guard cell enrichment of epidermal peel samples. RNA from Col-0 leaf discs and epidermal peels sampled at dawn and dusk were probed for guard cell, mesophyll, epidermal and vasculature reporter gene transcripts ( $n = 3$ ; mean  $\pm$  S.E.M.). *PP2AA3* was used as the reference gene. Sample collection, RNA extraction and cDNA biosynthesis were conducted by an MSci student under my guidance. qRT-PCR and statistical analysis were performed by myself. Experimental error rendered leaf discs unsuitable as controls.

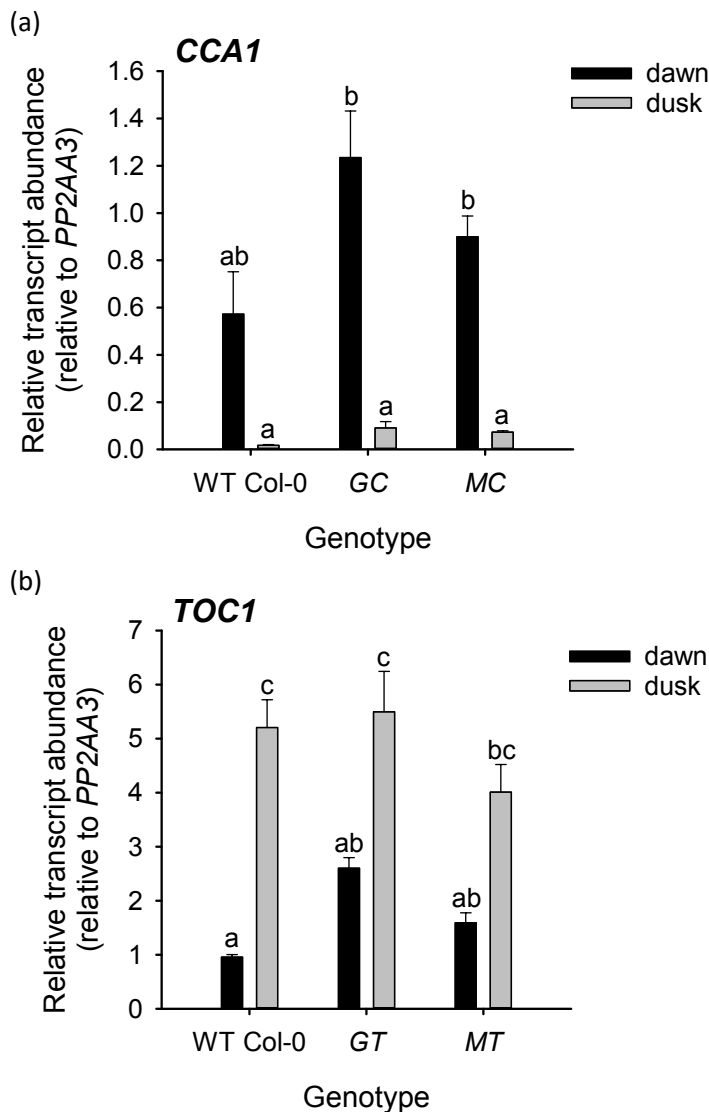


Figure 9.6: *CCA1* and *TOC1* relative transcript abundance in epidermal peels. Epidermal peel RNA was probed for (a) *CCA1* transcript abundance in guard cell *CCA1* overexpressors and (b) *TOC1* transcript abundance for guard cell *TOC1* overexpressors ( $n = 3$ ; mean  $\pm$  S.E.M.). RNA from Col-0 epidermal peels was used as a control. Epidermal peels were sampled both at dawn and dusk. *PP2AA3* was used as the reference gene. Sample collection, RNA extraction and cDNA biosynthesis were conducted by an undergraduate MSci student under my guidance. qRT-PCR and subsequent data analysis were performed by myself. Data were analysed with ANOVA and Tukey's post hoc tests. Different letters indicate statistically significant difference between means ( $p < 0.05$ ). Data for guard cell *CCA1* overexpressors at dusk and guard cell *TOC1* overexpressors at dawn come from Fig. 4.11.

Figure 9.7: Sequences of constructs used to generate (a) *GC*, (b) *GT*, (c) *MC* and (d) *MT*. In red are restriction enzyme sites used for insertion into pGreenII 0229; underlined are promoter sequences; in bold are coding sequences; in italics is the *nos* terminator sequence. These sequences were compiled from several sequencing reactions, aiming to cover each portion of DNA at least twice in independent reactions. The Clustral Omega multiple sequence alignment tool was used to confirm correct orientation and lack of mutations.

(a) GC1::CCA1:nos

**GGTACC**GAGTAAAGATTTCAGTAACCCGATGCTCCTGCTCTTCCCTCAAGACCTTCCTTGAT  
TCGCCGCCGGTATGTTCTCCGTCTGTGGTAGCGCCTTTGGAACACTCTACCAACGCCGCC  
ATGAAAGGATCTCTCATGGCCGAGGGGACGTGTTCTTCTTACATCTGGTGTAGGGCTA  
TGGTACTCCAGTGAGGAGGGAGAGGCAAGAGGTTGCTTAATGATTCGTTTTCCGGTGA  
TACGAGAACTCTTAGGTTTACCGGGAAGCTTTTCCCATGAAATGGGATGCCAAGTGGG  
TGGAGAGGAGTTGCCGGAGAGTTGCCGGAGAATAGGAGGGAATGGAGGAGGAGGAAGAG  
AGTGATCGCCGGTTGAAATGTTAACCGTCGAGGAGAATTTGACCGAGTTGGATCGTCTA  
GTAGGTACAATTCGGGTCTTGGCGAAGTATCCATTCAAAATAGTGTGTTAGTTTTGGACT  
TGAGAACTTGTGTCTCTTTGATCTCTTTATATAAACTTTGGACGTGTAGGACAACT  
TGTC AACATAAGAAACAAAATGGTTGCAACAGAGAGGATGAATTTATAAGTTTTCAACAC  
CGCTTTCTTATTAGACGGACAACAATCTATAGTGGAGTAAATTTTTATTTTTGGTAA  
TGTTAGTGAATCAAATATCTAAATTTGTGACTCACTAACATTAACAAATATGCATAA  
GACATAAAAAAAGAAAGATAAATTTCTATGAAACAAGAAAAAACCTATACAATCAAT  
CTTAGGAATTGACGATGTAGAATTGTAGATGATAAATTTTCTCAAATATAGATGGGCCT  
AATGAAGGGTGCCGCTTATGGATCTGACCCATTTGAGGACATTAATATTTTCATTGGT  
TATAAGCCTTTAATCAAATTTGTCATTAATTTGATGTCTCCCTCTCGGGTCATTTTCCCT  
TTCTCCCTCACAATTAATGTAGACTTTAGCAATTTGCACGCTGTGCTTTGTCTTTATATT  
TAGTAACACAAAATTTGACTTGTCTTGTAGAGTTTTTCTCTTTTATTTTTCTATCCAA  
TATGAAAACATAAAAGTGTCTCGTATACATATATTAATAATTAAGAAACCTATGAAAACA  
CCAAATACAAATGCGATATGTTTTTCAGTTTCGACGTTTCATGTTTGTAGAAAATTTCTAA  
TGACGTTTGTATAAAATAGACAATTAACGCCAAACACTACATCTGTGTTTTCGAACAA  
ATTGCGTCTGCGTTTTCTTCATCTATCTCTCAGTGTCACAATGTCTGAACTAAGAGAC  
AGCTGTAACATATCATTAAAGACATAAACTACCAAAGTATCAAGCTAATGTAAAAATTA  
CTCATTTCCACGTAACAAAATGAGTTAGCTTAAGATATTAGTGAACACTAGGTTTGAATTT  
TCTTCTTCTTCTCCATGCATCCTCCGAAAAAAGGGAACCAATCAAACCTGTTTGCATAT  
CAAACCTCAACACTTTACAGCAAATGCAATCTATAATCTGTGATTTATCCAATAAAACC  
TGTGATTTATGTTGGCTCCAGCGATGAAAGTCTATGCATGTGATCTCTATCCAACATGA  
GTAATTTGTTGAGAAAATAAAAAGTAGCTGAAATGTATCTATAAAAGAAATCATCCACAAG  
TACTATTTTACACACTACTTCAAATCACGGGCCCTTCGAGATGGAGACAAATTCG  
TCTGGAGAAGATCTGGTTATTAAGACTCGGAAGCCATATACGATAACAAAGCAACGTGAA  
AGGTGGACTGAGGAAGAACATAATAGATTTCATTGAAGCTTTGAGGCTTTATGGTAGAGCA  
TGGCAGAAGATTGAAGAACATGTAGCAACAAAACACTGCTGTCCAGATAAGAAGTCACGCT  
CAGAAAATTTTTCTCAAGGTAGAGAAAAGAGGCTGAAGCTAAAGGTGTAGCTATGGGTCAA  
GCGCTAGACATAGCTATTTCTCCTCCACGGCCTAAGCGTAAACCAAACAATCCTTATCCT  
CGAAAGACGGGAAGTGGAACGATCCTTATGTCAAACCGGGTGTGAATGATGGAAAAGAG  
TCCCTTGGATCAGAAAAGTGTGCGATCCTGAGATGGCCAATGAAGATCGACAACAATCA  
AAGCCTGAAGAGAAAACCTGCAGGAAGACAACCTGTTTCAGATTGTTTCACTCATCAGTAT  
CTCTCTGCTGCATCCTCCATGAATAAAAGTTGTATAGAGACATCAAACGCAAGCACTTTC  
CGCGAGTTCTTGCCTTACGCGGAAGAGGGAAGTCAAGATAACAGGGTAAGAAAGGAGTCA  
AACTCAGATTTGAATGCAAAATCTCTGGAAAACGGTAATGAGCAAGGACCTCAGACTCAT  
CCGATGCATATCCTGTGCTAGTGCCATTTGGGGAGCTCAATAACAAGTTCTCTATCCAT  
CCTCCTTTCAGAGCCAGATAGTTCATCCCCACACAGTTGCAGGAGATTATCAGTCTGTTTCT  
AATCATATAATGTCAACCCTTTTACAAAACACCGGCTCTTTATACTGCCGCAACTTTCCGCC  
TCATCATTTTTGGCCTCCCGATTCTAGTGGTGGCTCACCTGTTCCAGGGAACCTCACCTCCG  
AATCTGGCTGCCATGGCCGAGCCACTGTTGCAGCTGCTAGTCTTGGTGGGCTGCCAAT  
GGATTATTACCTTTATGTCTCCTCTTAGTTTCAGGTGGTTTTCACTAGTCACTCCTCCATCT  
ACTTTTGGACCATCATGTGATGTAGTACACAAAAGCAAGCACTTTACAACATGGTTCT  
GTGCAGAGCCGAGAGCAAGAACTCCGAGGCATCAAAGGCTCGATCTTCACTGGACTCA  
GAGGATGTTGAAAATAAGAGTAAACCAGTTTGTCAATGAGCAGCCTTCTGCAACACCTGAG  
AGTGATGCAAAGGGTTTCAGATGGAGCAGGAGACAGAAAACAAGTTGACCGGTCTCTCGTGT  
GGCTCAAACACTCCGTCGAGTAGTGATGATGTTGAGGCGGATGCATCAGAAAAGGCAAGAG  
GATGGCACCAATGGTGAAGTGAAGAAAACGAATGAAGCACTAATAAACCTCAAACCTCA  
GAGTCCAATGCACGCGCAGTAGAATCAGCTCCAATATAACCGATCCATGGAAGCTGTG  
TCTGACGAGGGTCAATGTCCTTCCAAGCTCTCTTCTCCAGAGAGGTATTGCCGCAAAGT  
TTTACATATCGAGAAGAACAAGAGAGGAAGAACAACAACAAGAACAAGATATCCA  
ATGGCACTTGATCTTAACCTTACAGCTCAGTTAACACCAGTTGATGATCAAGAGGAGAG  
AGAAAACACAGGATTTCTTGGAAATCGGATTAGATGCTTCAAAGCTAATGAGTAGAGGAAGA  
ACAGGTTTTAAACCATACAAAAGATGTTCCATGGAAAGCAAGAAAGATGAAATCCTCAAC  
AACAACTCTATCATTATGTTGGAACAGAAAGATCCCAAACGGATGCGGTTGGAAACTCAA  
GCTTCCACATGAGACTCTATTTTTCCCGGGGATCCACTAGTGAATTTCCCGATCGTTCA  
AACATTTGGCAATAAAGTTTCTTAAGATTGAATCCTGTTGCCGGTCTTGGCATGATTATC  
ATATAATTTCTGTTGAATTACGTTAAGCATGTAATAATTAACATGTAATGCATGACGTTA  
TTTATGAGATGGGTTTTTATGATTAGAGTCCCGCAATTAACATTTAATACGCGATAGAA  
AACAAAATATAGCGCGCAAACTAGGATAAATATCGCGCGGTTGTCATCTATGTTACTA  
GAGCGGCCGC

(b) GC1::TOC1:nos

GGTACC GAGTAAAGATT CAGTAACCCGATGCTCCTGCTCTTCCCTCAAGACCTTCCTTGAT  
TCGCCGCCGGTATGTTCTCCGTCTGTGGTAGCGCCTTTGGAACACTCTACCAACGCCGCC  
ATGAAAGGATCTCTCATGGCCGAGGGGACGTGTTCTTCTTACATCTGGTGTAGGGCTA  
TGGTACTCCAGTGAGGAGGGAGAGGCAAGAGGTTGCTTAATGATTCGTTTTCCGGTGA  
TACGAGAACTCTTAGGTTTACCGGGAAGCTTTTCCCATGAAAATGGGATGCCAAGTGA  
TGGAGAGGAGTTGCCGGAGAGTTGCCGGAGAATAGGAGGGAATGGAGGAGGAGGAAGAG  
AGTGATCGCCGGTTGAAATGTTAACCGTCGAGGAGAATTTGACCGAGTTGGATCGTCTA  
GTAGGTACAATTCGGGTCTTGGCGAAGTATCCATTCAAAATAGTGTGTTAGTTTTGGACT  
TGAGAACTTGTGTCTCTTTGATCTCTTTATATAAACTTTGGACGTGTAGGACAACT  
TGTC AACATAAGAAACAAAATGGTTGCAACAGAGAGGATGAATTTATAAGTTTTCAACAC  
CGCTTTCTTATTAGACGGACAACAATCTATAGTGGAGTAAATTTTTATTTTTGGTAAA  
TGGT TAGTGAATCAAATATCTAAATTTGTGACTCACTAACATTAACAAATATGCATAA  
GACATAAAAAAAGAAAGATAAATTTCTATGAAACAAGAAAAAAACCTATACAATCAAT  
CTTAGGAATTGACGATGTAGAATTGTAGATGATAAAATTTTCTCAAATATAGATGGGCCT  
AATGAAGGGTGCCGCTTATGGATCTGACCCATTTGAGGACATTAATATTTTCATTGGT  
TATAAGCCTTTAATCAAATTTGTCATTAATTTGATGTCTCCCTCTCGGGTCATTTTTCT  
TTCTCCCTCACAATTAATGTAGACTTTAGCAATTTGCACGCTGTGCTTTGTCTTTATATT  
TAGTAACACAAAATTTGACTTGTCTTGTAGAGTTTTTCTCTTTTATTTTTCTATCCAA  
TATGAAAACATAAAAGTGTCTCGTATACATATATTAATAATTAAGAAACCTATGAAAACA  
CCAAATACAAATGCGATATGTTTTTCAGTTTCGACGTTTCATGTTTGTAGAAAATTTCTAA  
TGACGTTTGTATAAAATAGACAATTAACGCCAAACACTACATCTGTGTTTTCGAACAA  
ATTGCGTCTGCGTTTTCTTCATCTATCTCTCAGTGTCAAAATGTCTGAACTAAGAGAC  
AGCTGTAACATATCATTAAAGACATAAACTACCAAAGTATCAAGCTAATGTAAAAATTA  
CTCATTTCCACGTAACAAAATGAGTTAGCTTAAGATATTAGTGAACACTAGGTTTGAATTT  
TCTTCTTCTTCTCCATGCATCCTCCGAAAAAAGGGAACCAATCAAACCTGTTTGCATAT  
CAAACCTCAACACTTTACAGCAAATGCAATCTATAATCTGTGATTTATCCAATAAAACC  
TGTGATTTATGTTTGGCTCCAGCGATGAAAGTCTATGCATGTGATCTCTATCCAACATGA  
GTAATTTGTTGAGAAAATAAAAAGTAGCTGAAATGTATCTATAAAAGAAATCATCCACAAG  
TACTATTTTACACACTACTTCAAATCACGGGCCCTTCGAGATGGATTTGAACGGT  
GAGTGTAAAGGAGGAGATGGGTTTTATTGATAGAAGCAGAGTCAGGATTTTGCCTTTGTGAC  
AATGATTCACGAGTTTGGGAGAGGTTTTTACTCTCCTTTTCAGAGTGTCTTATCAAGTG  
ACTGCAGTGAAATCAGCAAGGCAGGTGATTGATGCACCTAATGCAGAGGGACCTGATATC  
GATATAATAC TGGCGGAAATGATCTCCAATGGCTAAGGGTATGAAGATGCTGAGGTAC  
ATCACACGAGACAAAGATCTTCGCAGAATCCCTGTGATAATGATGTGAGGCAAGACGAA  
GTCCCTGTCTGTTGTAAGTGCTTGAAGCTAGGTGCAGCTGACTACCTTGTGAAGCCTCTT  
CGCACCAACGAGCTTCTGAACTTGTGGACACACATGTGGAGAAGAAGACGCGATGAGGA  
CTTGCTGAGAAGAATATGTTGAGCTATGATTTTGTGATCTTGTGGGATCTGATCAAAGTGA  
CCAAACACAAATAGTACCAACCTGTTCTCTGACGACACAGATGATAGAAGTCTTAGGTCC  
ACCAACCACAGAGAGGAAATTTAAGTACCAGGAAAATGAGTGGTCTGTTGCTACTGCT  
CCTGTTTATGCTCGTGATGGTGGTCTTGGTGTGATGGAACAGCCACTTCTTCTTGTGCT  
GTTACTGCTATAGAGCCTCCATTGGATCATCTTGTGCTGGGCTCACCATGAGCCAAATGAA  
AGAAATAGTAAATCCAGCGCAATTTTCTTTCAGCACCGAAGAAAAGTAGATTGAAGATCGGA  
GAGTCTCTGCTTTCTTTACATATGTCAAATCTACTGTCTTGAACACTAACGGTCAGGAT  
CCTCCTCTTGTGATGGAATGGCTCACTTCATCTTCATCGGGGTTTGGCGGAGAAGTTT  
CAAGTGGTGGCTAGTGAAGGGATCAACAACACCAAAACAAGCACGAGAGCAACCAAAA  
TCTACTGTCTTAGAACTAACGGTCAGGATCCTCCTCTTGTCAATGGAATGGCTCACAT  
CATCTTCATCGGGGTGCGCGGAAAAGTTTCAAGTGGTGGCTAGTGAAGGATCAACAAC  
ACCAACAAGCACACAGAAGTAGAGGGACCGAGCAATACCATTCTCAAGGAGAGACCTTG  
CAGAATGGCGCCAGCTATCCACATTCCTTGGAGCGGTACGCGACGCTTCCCACATCAATG  
GAATCTCATGTTAGGAATACCAAGAGGGCAATATGAATATTCCTCAAGTTGCTATGAAC  
AGAAGTAAAGATTCGCTCAAGTTGATGGATCGGGTTTTCTCTGCACCAATGCCTATCCT  
TACTATATGCATGGGTCATGAACCAAGTTATGATGCAATCAGCAGCCATGATGCCTCAA  
TATGGTTCATCAAATTCCTCATTGCCAACCAAAATCATCCGAATGGAATGACGGGATATCCT  
TACTACCACCACCAATGAACACATCTTTCAGCAGATAGTCAAGTGTCTTTACAGAATGGT  
CAGATGTCTATGGTTCATCATTCTTGGTACCAGGAGGAAATCCGCTTCTAATGAGGTG  
AGGTTAAATAAACTTACAGAAAGAGAGGAAAGCTCTGCTGAAATTCAGACGTTAAAAGGAA  
CAACGTTGTTTTGATAAGAAGATTAGGTATGTGAATAGGAAACGCCTTGTGAGAGGAGA  
CCCCGCTTAAAGGTCAGTTTGTAGGAAGATGAACGGCCTGATGTTGATTTAAATGGA  
CAGCCTGACTCTGCTGACTATGATGACGAGGAAGAGGGAAGAAGAAGAAGAAGAGGAG  
AACCGGGATTCATCTCCTCAGGATGATGCTTTGGGAACTTGA CCGGGGGATCCACTAGT  
GAATTTCCCGATCGTTCAAACATTTGGCAATAAAGTTTCTTAAAGATTGAATCCTGTTGC  
CGGTCTTCCGATGATTATCATATAATTTCTGTTGAATTACGTTAAGCATGTAATAATTAA  
CATGTAATGCATGACGTTATTTATGAGATGGGTTTTTATGATTAGAGTCCCGCAATTATA  
CATTTAATACGCGATAGAAAACAAAATATAGCGCGAAAACCTAGGATAAATATCGCGCGC  
GGTGTATCTATGTTACTAGACGGCCGC

(c) MYB60::CCA1:nos

GGTACC CACAAGGACACAAGGACATATGGTATGATGATATGCTTTGTTTCTCTGCTTCTC  
TTACTAATTTGAAGCTGTTGGATTGATTTGTCTCTTCTTACGTTCCCTTCTTTTTTTTTT  
CGTTTTCTTTTGTGCGTATAGACCAGGCAGGGGCTAGGGCCTAGTGATGGGTATTGGCCCA  
ATACTATTGGGTATTTGCCTGGTTTATATTTTCGATTTTAGGTTAATTCATTTTAAGA  
ATACGTAGATTTGTTGGTTAGTTTGGTTTGGTTGCACCTAAGTTCGGTTTTACATAAAT  
AGAATCTAACACTACTAATTTGTATACGTAATAACAACAATAACAGATTTTTCGTT  
TCAATTTTCGTTTAAAGGGGTAGACATTTTGGTTTGGTTTGGTTCATTTTTTTTTTCCCT  
TTCAAATTCACATCCTTTCAGTAGATGACAAAATAAAGAAAAACATGAATGAAAGTTGTA  
ACTTGTAAAGCATCAACATGGAAATCATATCACAAGAACACAAATCTAACTAATGGGTCT  
TTTCACATATTGGTATAAATATAAGTTGTAAGAAATATTAGTTAAACAGAGGCAACGAGAG  
ATGCGTGATATATGAAAAGTTGAAAACAAAAGACATGGATCTAAAGAGTCAAGCAAAATG  
TAATATCTTTTTTCTTCTAAACTTGAGGATGTCCAAGTTGCAGTGAATGATTCCTTTA  
ATCATGGAGAAATTCATGAAATAAATTTGTGTTTCTCCACACTTTATCTTTATTTATTT  
TCTTACCACAATTACAACATTTATCACAATAATGTAAGTAACATAGCTTGTGACTCTTCT  
TCCATTTATGAGTTGATTATCACTATATTTATAAGTAATTACCAACGAATGTCCAAAT  
AAGCAAAATATGTAATCGATACACTATGTATTCTACATCTACAATATGTTAAGGAGCTCCT  
TTATGGAAATATTCGATTGAAAAACATTTGATGGATCGTTCACTAAATAAATAATCCA  
GTAACGTTTTCTAAGGGAGATATACATATTCGTGTGGAGATCAACATATCTCGTTAAT  
TGACTACGCAAAATAGTTAATGGAAAAGGCAGAGTGACTCGTGAGCTTGGCAGATCCAAA  
AGAGGTTGTCAAGAAAAGCAGATTTAAAAGTTCTTCCCTCTCTTAAAGTCACCCATTA  
ATTTACATATATGTACATACATGTTGCATTTAACTCATATACATACATATCTCACATC  
TATAAAGAGAGCATAAGACTCAGAGAGATCTAGAGGAAGAGGGGCCCCCTCGAGATGG  
AGACAAATTCGCTGGAGAAGATCTGGTTATTAAGACTCGGAAGCCATATACGATAACAA  
AGCAACGTGAAAGGTGGACTGAGGAAGAACATAATAGATTCATTGAAGCTTTGAGGCTT  
ATGGTAGAGCATGGCAGAAGATTGAAGAACATGTAGCAACAAAACTGCTGTCCAGATAA  
GAAGTCACGCTCAGAAATTTTTCTCCAAGGTAGAGAAAGAGGCTGAAGCTAAAGGTGTAG  
CTATGGGTCAAGCGCTAGACATAGCTATTCCTCCTCCACGGCTAAGCGTAAACCAACA  
ATCCTTATCCTCGAAAGACGGGAAGTGAACGATCCTTATGTCAAAAACGGGTGTGAATG  
ATGAAAAGAGTCCCTTGGATCAGAAAAGTGTGCGATCCTGAGATGGCCAATGAAGATC  
GACAAACATCAAAGCCTGAAGAGAAAACCTCTGCAGGAAGACAACCTGTTTCAGATTGTTCA  
CTCATCAGTATCTCTGCTGCATCCTCCATGAATAAAAAGTTGTATAGAGACATCAAACG  
CAAGCACTTTCGCGAGTTCTTGCCTTACGGGAAGAGGGAAGTCAGAATAACAGGGTAA  
GAAAGGAGTCAAACCTCAGATTTGAATGCAAAATCTCTGAAAACGGTAATGAGCAAGGAC  
CTCAGACTTATCCGATGCATATCCCTGTGCTAGTGCCATTGGGGAGCTCAATAACAAGTT  
CTCATACATCCTCCTTACAGCCAGATAGTCACTCCACACAGTTGCAGGAGATTATC  
AGTCGTTTTCCATATATAATGTCAACCCTTTTACAAAACACCGGCTCTTTATACATTGCCG  
CACTTTCGCCTCATCATTTTGGCCTCCCGATTCTAGTGGTGGCTCACCTGTTCCAGGGA  
ACTCACCTCCGAATCTGGCTGCCATGGCCGAGCCACTGTTGCAGCTGCTAGTGCTTGGT  
GGGCTGCCAATGGATTATTACCTTTATGTGCTCCTTAGTTAGGTTGAGGTTTCACTAGTC  
ATCCTCCATCTACTTTTGGACCATCATGTGATGTAGAGTACACAAAAGCAAGCACTTTAC  
AACATGGTTCTGTGCAGAGCCGAGAGCAAGAACACTCCGAGGCATCAAAGGCTCGATTTCT  
CACTGGACTCAGAGGATGTTGAAAATAAGAGTAAACCAGTTTGTATGAGCAGCCTTCTG  
CAACACCTGAGAGTGATGCAAAGGTTTCAAGTGGAGCAGGAGACAGAAAACAAGTTGACC  
GGTCTCGTGTGGCTCAAACACTCCGTCGAGTAGTGATGATGTTGAGGCGGATGCATCAG  
AAAGGCAAGAGGATGGCACCATGGTGAAGTGAAGAAAACGAATGAAGACACTAATAAAC  
CTCAAACCTCAGAGTCCAATGCACGCCGAGTAGAATCAGTCCAATATAACCGATCCAT  
GGAAGTCTGTGCTGACGAGGGTCAATGTCCTTCCAAGCTCTTCTTCCAGAGAGGTAT  
TGCCGCAAAGTTTTACATATCGAGAAGAACACAGAGAGGAAGAACAACAACAAGAAC  
AAAGATATCCAATGGCCTTGTATCTTAACTTACAGCTCAGTTAACACCAGTTGATGATC  
AAGAGGAGAAGAGAAACACAGGATTTCTTGAATCGGATTAGATGCTTCAAAGCTAATGA  
GTAGAGGAAGAACAGGTTTTAAACCATACAAAAGATGTTCCATGGAAGCCAAAGAAAGTA  
GAATCCTCAACAACAATCCTATCATTGTTGGAACAGAAAGATCCCAAACGGATGCGGT  
TGGAAAACCAAGCTTCCACATGAGACTCTATTTTCCCGGGGATCCACTAGTGAATTTCC  
CCGATCGTTCAAACATTTGGCAATAAAGTTTCTTAAAGATTGAATCCTGTTGCCGGTCTTG  
CGATGATTATCATATAATTTCTGTTGAATTACGTTAAGCATGTAATAATTAACATGTAAT  
GCATGACGTTATTTATGAGATGGGTTTTATGATTAGAGTCCCGCAATTATACATTTAAT  
ACGGATAGAAAACAAAATATAGCGCGCAAACCTAGGATAAATATCGCGCGGGTGTCAAT  
CTATGTTACTAGAGCGGCCCGC

(d) MYB60::TOC1:nos

GGTACCACAAGGACACAAGGACATATGGTATGATGATATGCTTTGTTTCTCTGCTTCTC  
TTACTAATTTGAAGCTGTTGGATTGATTTGTCTCTCTTACGTTCCCTTCTTTTTTTTTT  
CGTTTTCTTTTGTCTATAGACCAGGCAGGGGCTAGGGCCTAGTGATGGGTATTGGCCCA  
ATACTATTGGGTATTTGCCTGGTTTATATTTTCGATTTTAGGTTAATTCATTTTAAGA  
ATACGTAGATTTGTTGGTTAGTTTGGTTTGGTTGCACCTAAGTTCGGTTTTACATAAAT  
AGAATCTAACACTACTAATTTGTATACGTAATAACAACAATAACAGATTTTTCGTT  
TCAATTTTCGTTTAAAGGGTAGACATTTTGGTTTGGTTTGGTTCATTTTTTTTTTCCCT  
TTCAAATTCACATCCTTTCAGTAGATGACAAAATAAAGAAAAACATGAATGAAAGTTGTA  
ACTTGTAAAGCATCAACATGGAAATCATATCACAAAGAACACAAATCTAACTAATGGGTCT  
TTTCACATATTGGTATAAATATAAGTTGTAAGAAATATTAGTTAAACAGAGGCAACGAGAG  
ATGCGTGATATATGAAAAGTTGAAAACAAAAGACATGGATCTAAAGAGTCAAGCAAAATG  
TAATATCTTTTTTCTTCTAAACTTGAGGATGTCCAAGTTGCAGTGAATGATTCCTTTA  
ATCATGGAGAATTCATGAAATAATTTGTGTTTCTCCACACTTTATCTTTATTTATTT  
TCTTACCACAATTACAACATTTATCACAAAAATGTAAGTAACATAGCTTGTGACTCTTCT  
TCCATTTATGAGTTGATTATCACTATATTTATAAGTAATTACCAACGAATGTCCAAAT  
AAGCAAAATATGTAATCGATACACTATGTATTCATCTACAATATGTTAACGAGCTCCTT  
TTATGGAAATATTCGATTGAAAAACATTTGATGGATCGTTCACTAAATAAATAATCCA  
GTAACGTTTTCTTAAAGGGAGATACATATTCGTGTGGAGATCAACATATCTCGTTAAT  
TGACTACGCAAAATAGTTAATGGAAAAGGCAGAGTGACTCGTGAGCTTGGCAGATCCAAA  
AGAGGTTGTCAAGAAAAGCAGATTTAAAAGTTCCTCCCTCTCTTAAAGTCAACCCATTA  
ATTTACATATATGTACATACATGTTGCATTTAACTCATATACATACATATCTCACATC  
TATAAAGAGAGCATAAGACTCAGAGAGATCTAGAGGAAGAGGGGCCCCCTCGAGATGG  
ATTTGAACGGTGAGTGTAAAGGAGGAGATGGGTTTATTGATAGAAGCAGAGTCAGGATTT  
TGCTTTGTGACAATGATTCACGAGTTTGGGAGAGGTTTTTACTCTCTCTTCAGAGTGT  
CTTATCAAGTGACTGCAGTGAATCAGCAAGGCAGGTGATTGATGCACCTAATGCAGAGG  
GACCTGATATCGATATAATACTGGCGGAAATGATCTCCCAATGGCTAAGGGTATGAAGA  
TGCTGAGGTACATCACACGAGACAAAGATCTTCGAGAATCCCTGTGATAATGATGTGCA  
GGCAAGACGAAGTCCCTGTCTGTTAAAGTGTGAAAGTGTGAGGTCAGCTGACTACCTTG  
TGAAGCCTCTTCGCACCAACGAGCTTCTGAACTTGTGGACACACATGTGGAGAAGAAGAC  
GCATGTAGGACTTGCTGAGAAGAATATGTTGAGCTATGATTTTGTATCTTGTGGATCTG  
ATCAAAGTGATCCAAACCAAAATAGTACCAACCTGTTCTCTGACGACACAGATGATAGAA  
GTCTTAGGTCCACCAACCCACAGAGAGGAAATTTAAGTACCAGGAAATGAGTGGTCTG  
TTGCTACTGCTCCTGTTTCTGCTCGTATGGTGGTCTTGGTGTGATGGAACAGCCACTT  
CTTCTCTGCTGTTACTGCTATAGAGCCTCCATTTGGATCATCTTGTCTGGGCTCACCATG  
AGCCAATGAAAAGAAATAGTAATCCAGCGCAATTTCTTCAGCACCGAAGAAAAGTAGAT  
TGAAGATCGGAGAGTCCCTCTGCTTTTACATATGTCAAATCTACTGTCTTAGAACTA  
ACGGTCAGGATCCTCCTCTTGTGATGGAAATGGCTCACTTCACTTCACTCGGGTTTTGG  
CGGAGAAGTTCAAGTGGTGGCTAGTGAAGGATCAACAACACCAACAAGCACGCAGAG  
CAACACCAAAATCTACTGTCTTAGAACTAACGGTCAGGATCCTCCTCTTGTCAATGGAA  
ATGGCTCACATCATCTTCACTCGGGGTGCGGCGGAAAAGTTCAAGTGGTGGCTAGTGAAG  
GGATCAACAACACCAACCAAGCACACAGAAGTAGAGGGACCGAGCAATACCATTCTCAAG  
GAGAGACCTTGCAGAATGGCGCCAGCTATCCACATTCCTTGGCGGTCACGCACGCTTC  
CCACATCAATGGAATCTCATGGTAGGAACACCAAGAGGGCAATATGAATATCCCCAAG  
TTGCTATGAACAGAAGTAAAGATTCGTCTCAAGTTGATGGATCGGGTTTTCTGACCCAA  
ATGCCTATCCTTACTATATGCATGGGGTCATGAACCAAGTTATGATGCAATCAGCAGCCA  
TGATGCCTCAATATGGTCAATCAATTCCTCATTTGCCAACCAATCATCCGAATGGAATGA  
CGGGATATCCTTACTACCACCACCAATGAACACATCTTTGCAGCATAGTCAGATGTCTT  
TACAGAATGGTCAGATGTCTATGGTTCACTTCTTGGTCAACCGGCAGGAAATCCGCCCTT  
CTAATGAGGTGAGGGTAAATAAACTTGACAGAAGAGAGGAAGCTCTGCTGAAATTCAGAC  
GTAAAAGGAACCAACGTTGTTTTGATAAGAAGATTAGGTATGTGAATAGGAAACGCCCTG  
CTGAGAGGAGACCCCGGTTAAGGGTCAGTTTGTAGGAAGATGAACGGCGTGAATGTTG  
ATTTAAATGGACAGCCTGACTCTGCTGACTATGATGACGAGGAAGAGGAGGAAGAAG  
AAGAAAGAGGAGAACCAGGATTCATCTCCTCAGGATGATGCTTTGGGAACCTGACCCGGG  
GATCCACTAGTGAATTTCCCGGATCGTTCAAACATTTGGCAATAAAGTTTCTTAAAGATTG  
AATCCTGTTGCCGCTTGGGATGATTATCATATAATTTCTGTTGAATTACGTTAAGCAT  
GTAATAATTAACATGTAATGCATGACGTTATTTATGAGATGGGTTTTTATGATTAGAGTC  
CCGCAATTATACATTTAATACGCGATAGAAAACAAAATATAGCGCGCAAACCTAGGATAAA  
TTATCGCGCGGGTGTCTATCTATGTTACTAGAGCGGCCCG



### **9.3 Physiological examination and analysis of transgenic *Arabidopsis* with misregulated guard cell circadian clocks**

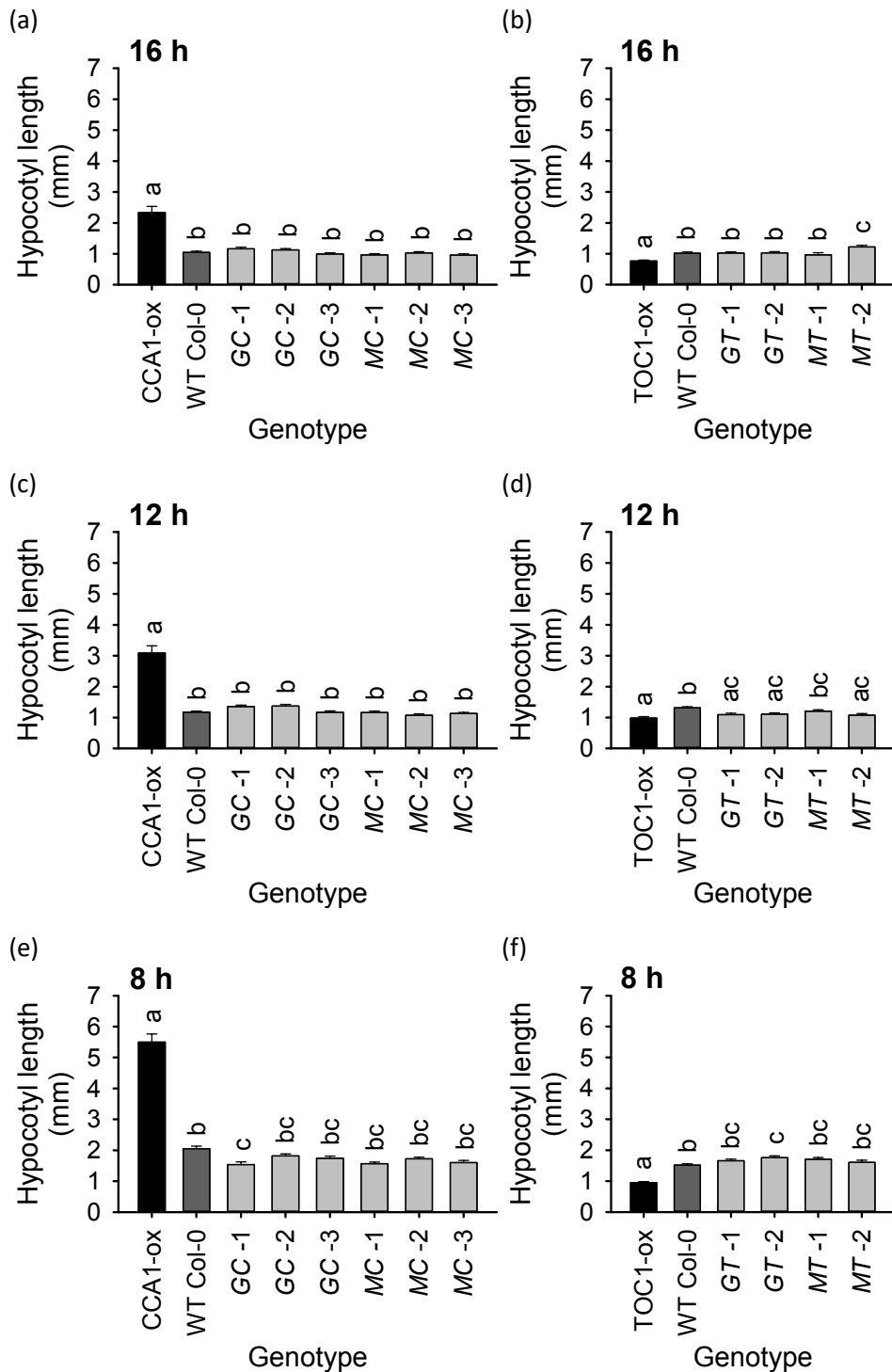


Figure 9.8: Overexpressing *CCA1* or *TOC1* in guard cells does not affect hypocotyl elongation. Data were collected from additional experimental repeats of Figs. 5.1 and 5.2. Hypocotyl lengths were measured for seedlings grown under (a, b) 16 h, (c, d) 12 h or (e, f) 8 h photoperiods ( $n = 13-20$ ; mean  $\pm$  S.E.M.). Colour-coding highlights the whole plant overexpressor control (black), wild type control (dark grey), and GCS-ox genotypes (light grey). Data were analysed with ANOVA and Tukey's post hoc tests. Different letters indicate statistically significant difference between means ( $p < 0.05$ ). Germination was poor for panels d, e and f.

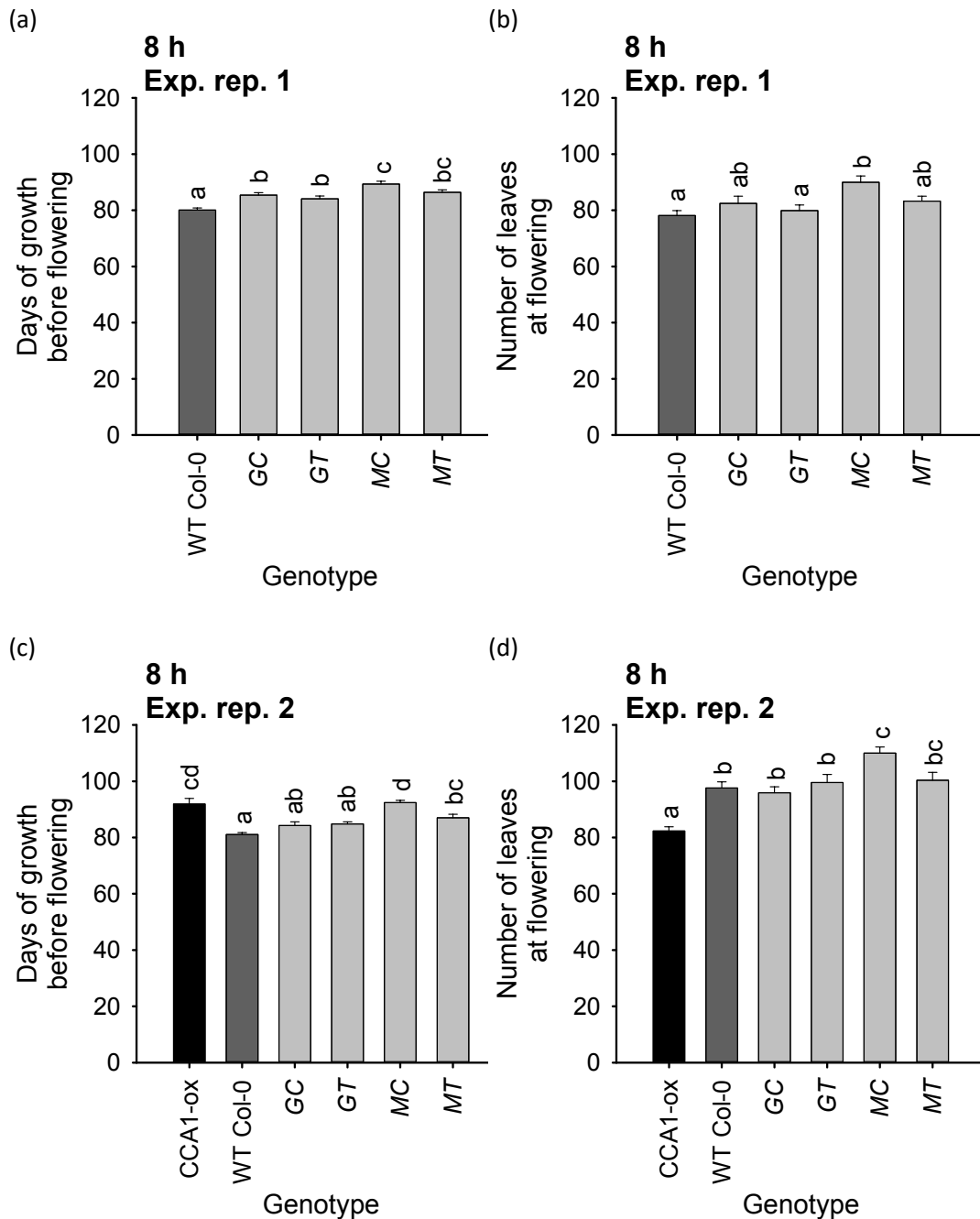


Figure 9.9: Overexpressing *CCA1* or *TOC1* in guard cells affects flowering time under short photoperiods. Panels (a) and (b), and (c) and (d), show data from two additional experimental replicates under an 8 h photoperiod ( $n = 13-15$ ; mean  $\pm$  S.E.M.), performed as for Fig. 5.4. Panels show number of (a, c) days of vegetative growth before flowering and (b, d) vegetative leaves at flowering. Photoperiod and experimental replicate (Exp. rep.) number are indicated above each graph. Colour-coding highlights the whole plant overexpressor control (black), wild type control (dark grey), and GCS-ox genotypes (light grey). Data were analysed with ANOVA and Tukey's post hoc tests. Different letters indicate statistically significant difference between means ( $p < 0.05$ ).

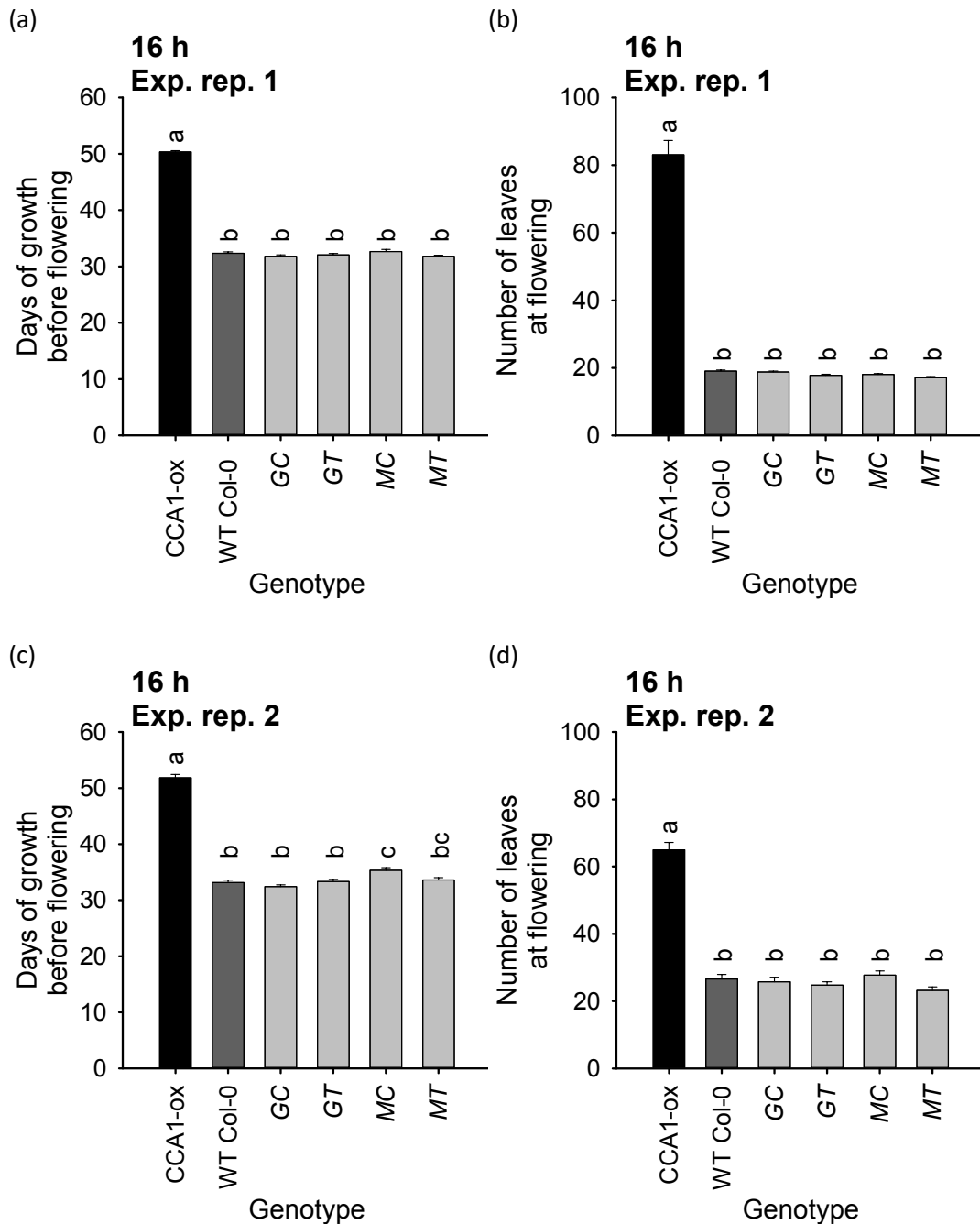


Figure 9.10: Overexpressing *CCA1* or *TOC1* in guard cells does not affect flowering time under long photoperiods. Panels (a) and (b), and (c) and (d), show data from two additional experimental replicates under a 16 h photoperiod ( $n = 13-15$ ; mean  $\pm$  S.E.M.), performed as for Fig. 5.4. Panels show number of (a, c) days of vegetative growth before flowering and (b, d) leaves at flowering. Photoperiod and experimental replicate (Exp. rep.) number are indicated above each graph. Colour-coding highlights the whole plant overexpressor control (black), wild type control (dark grey), and GCS-ox genotypes (light grey). Data were analysed with ANOVA and Tukey's post hoc tests. Different letters indicate statistically significant difference between means ( $p < 0.05$ ).

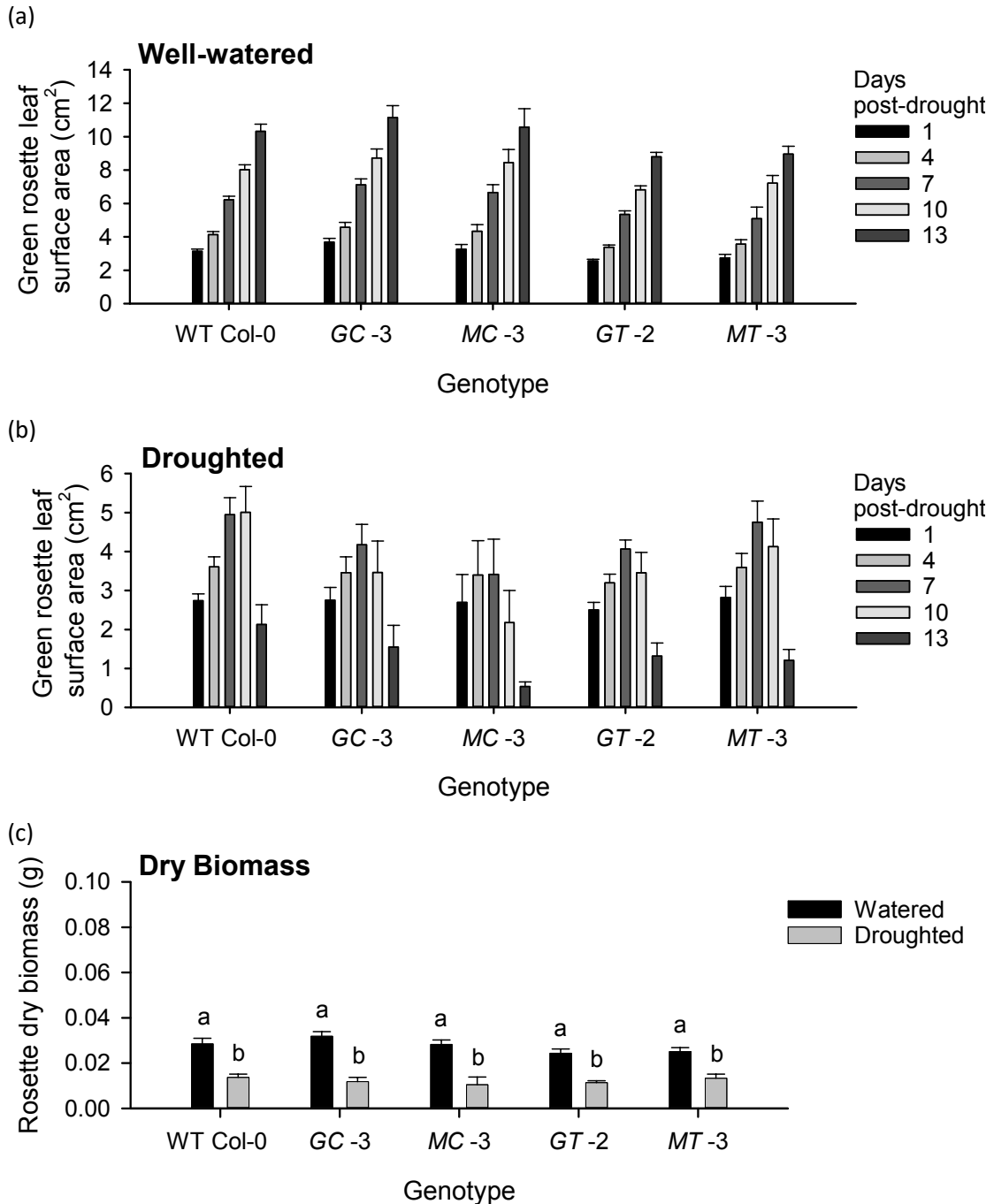


Figure 9.11: Overexpressing *CCA1* or *TOC1* in guard cells does not affect growth, rosette leaf surface area or dry biomass under fast droughted or well-watered conditions. Additional alleles were grown in small inserts under an 8 h photoperiod, with drought imposed after 28 days of growth. Green rosette leaf area measurements were taken at 1, 3, 7, 10 and 13 days post-drought for (a) well-watered and (b) fast droughted plants, and (c) final rosette dry biomass was measured ( $n = 10$ ; mean  $\pm$  S.E.M.). Data were analysed with ANOVA and Tukey's post hoc tests. Different letters indicate statistically significant difference between means ( $p < 0.05$ ).

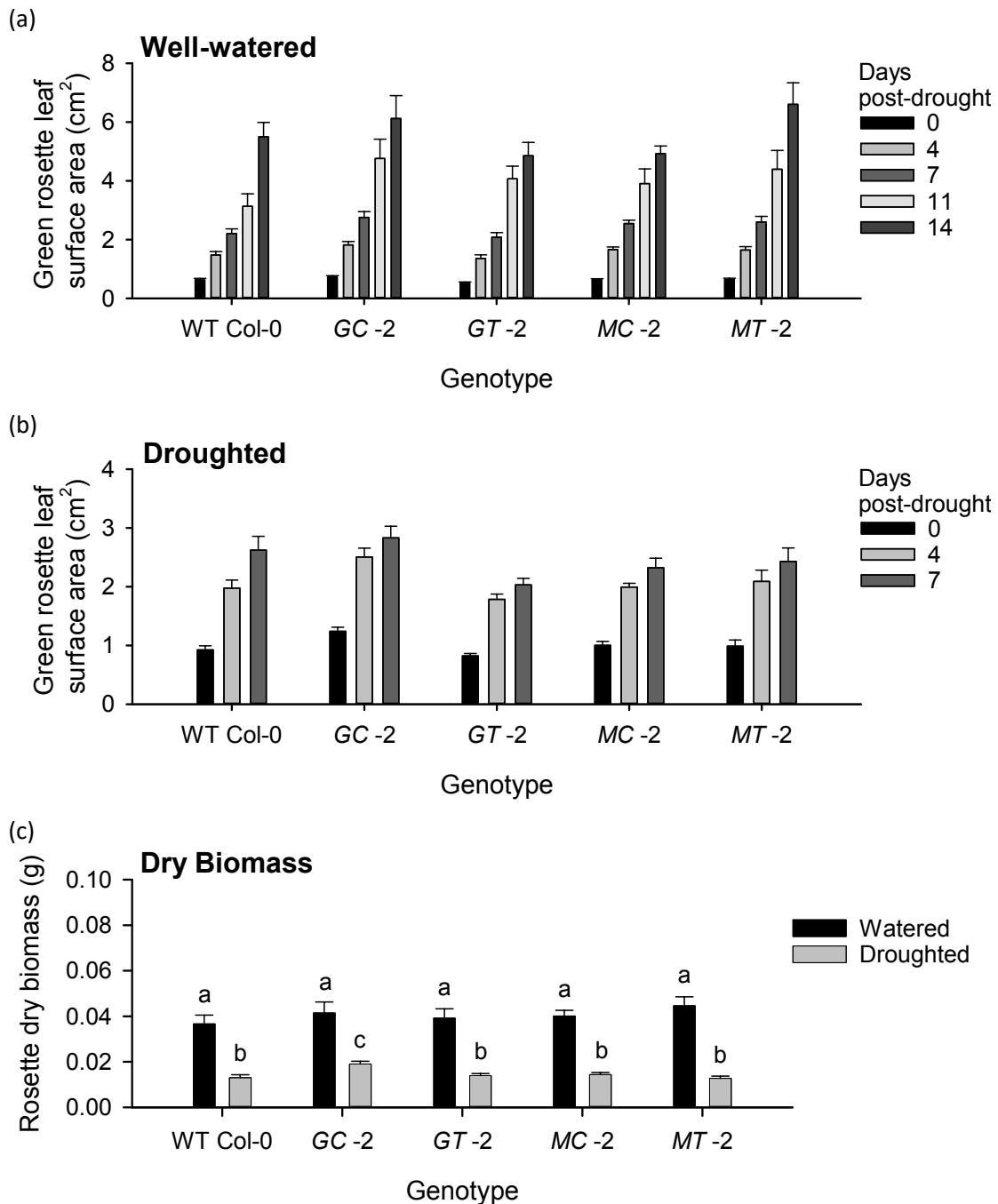


Figure 9.12: Overexpressing *CCA1* or *TOC1* in guard cells does not affect growth, rosette leaf surface area or dry biomass under well-watered or fast droughted conditions in constant light. Additional alleles were grown in small inserts under a 16 h photoperiod for the first 14 days of growth, then drought was imposed and plants moved to constant light conditions. Green rosette leaf area measurements were taken at 0, 4, 7, 11 and 14 days post-drought for (a) well-watered and (b) droughted plants, and (c) final rosette dry biomass was measured ( $n = 10$ ; mean  $\pm$  S.E.M.). Data were analysed with ANOVA and Tukey's post hoc tests. Different letters indicate statistically significant difference between means ( $p < 0.05$ ).

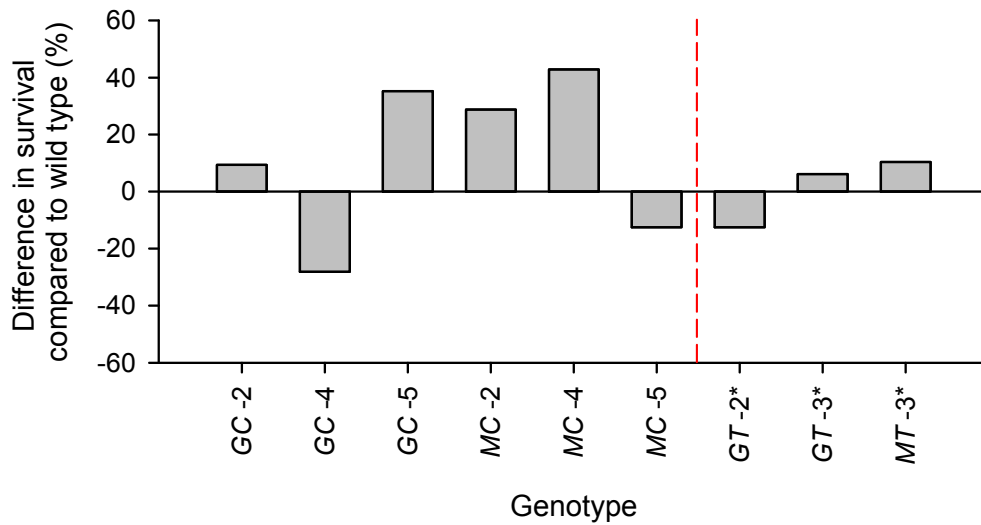


Figure 9.13: Overexpressing *CCA1* or *TOC1* in guard cells increases or decreases survival to dehydration, respectively. Data show percentage difference in survival to dehydration compared to the wild type for additional alleles ( $n = 32$ ). Alleles marked with “\*” indicate variable data between two experimental repeats, while other data were obtained from a single experimental repeat.

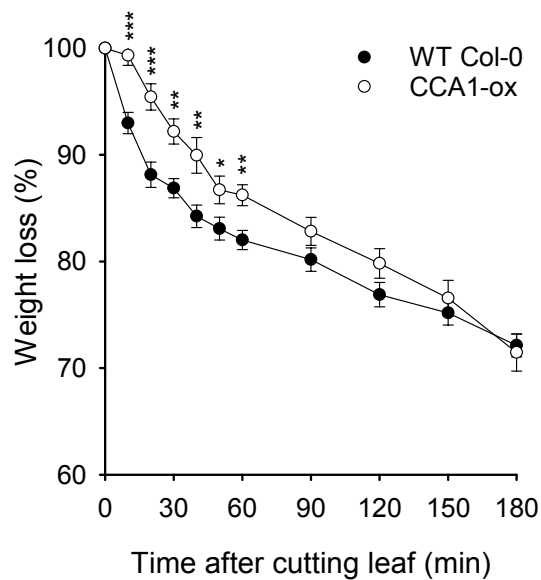


Figure 9.14: Overexpressing *CCA1* in the whole plant affects detached leaf water loss over time. Data show percentage of weight loss over time from two experimental repeats for CCA1-ox ( $n = 10$  total; mean  $\pm$  S.E.M.). Data were analysed with independent samples t-tests, and statistical significance compared to Col-0 for each time point is indicated using starring (\* =  $p < 0.05$ ; \*\* =  $p < 0.01$ ; \*\*\* =  $p < 0.001$ ).



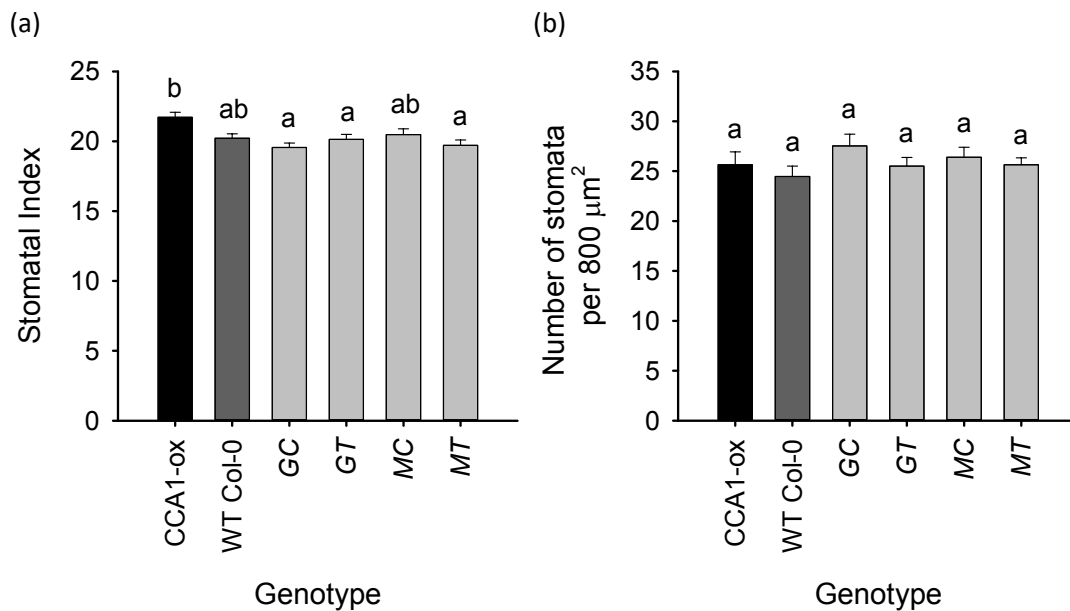


Figure 9.15: Overexpressing *CCA1* or *TOC1* in guard cells does not affect (a) stomatal index nor (b) stomatal density. Data were collected from an additional experimental repeat of Fig. 5.12 ( $n = 20-22$ ; mean  $\pm$  S.E.M.). Colour-coding highlights the whole plant overexpressor control (black), wild type control (dark grey), and GCS-ox genotypes (light grey). Data were analysed with ANOVA and Tukey's post hoc tests. Different letters indicate statistically significant difference between means ( $p < 0.05$ ).

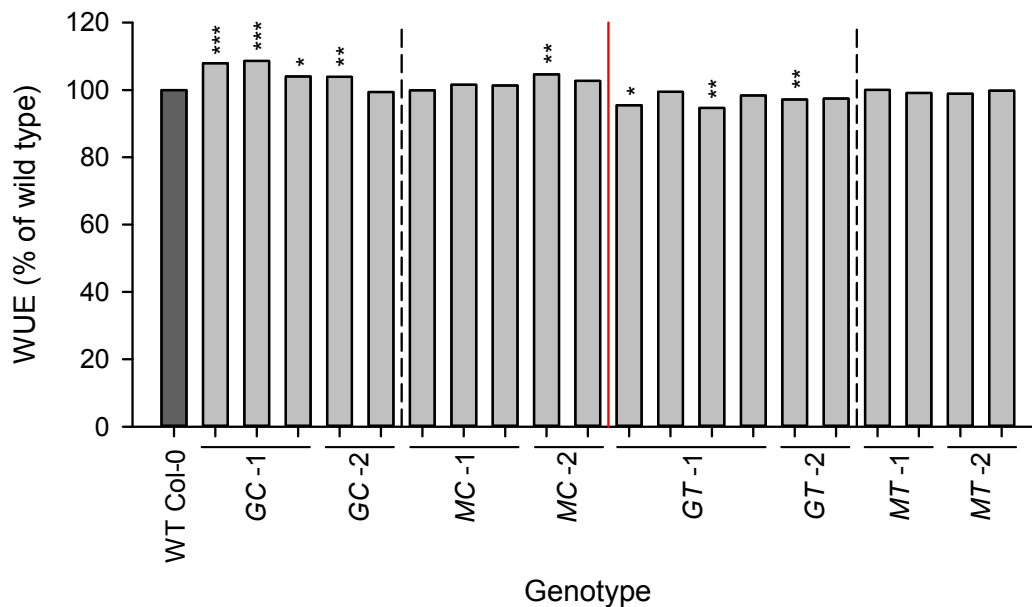


Figure 9.16: Overexpressing *CCA1* in guard cells seems to increase WUE. Data are WUE as a percentage of the wild type, with WUE of WT Col-0 normalised to 100%. All experimental repeats are represented here for each allele ( $n= 5-15$ ), including those represented in Fig. 5.16. For clarity, vertical dotted reference lines mark separations between data from different genotypes, and the vertical red reference line marks the separation between data from guard cell *CCA1* overexpressors and guard cell *TOC1* overexpressors. Colour-coding highlights the wild type control (dark grey) and GCS-ox genotypes (light grey). Data were analysed with independent samples t-tests, and statistical significance compared to Col-0 is indicated using starring (\* =  $p < 0.05$ ; \*\* =  $p < 0.01$ ; \*\*\* =  $p < 0.001$ ).

## 9.4 Changes in stomatal aperture over time and stomatal density in naturally-occurring *Arabidopsis halleri* subsp. *gemmaifera*

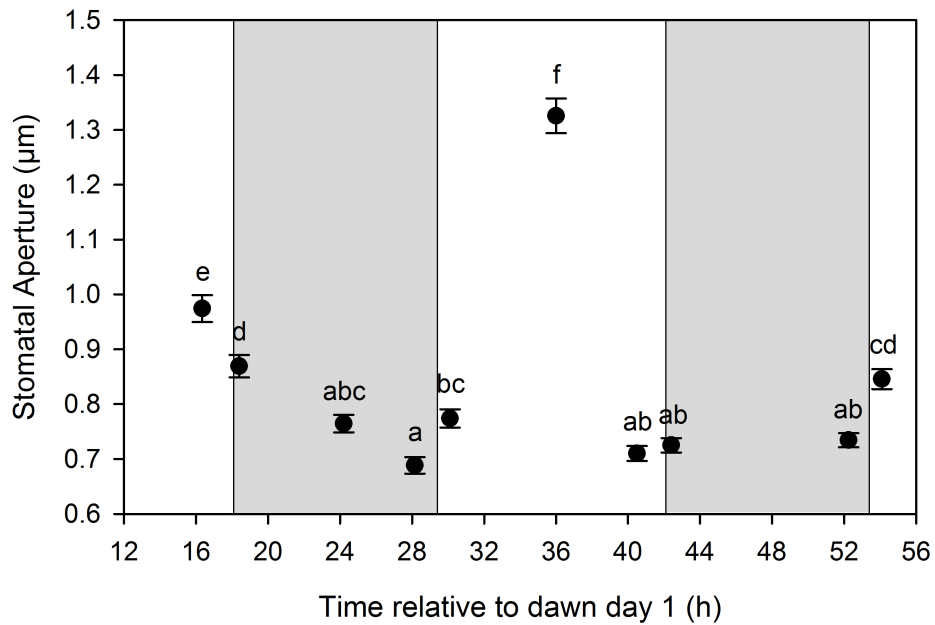


Figure 9.17: Stomatal aperture of *A. halleri* subsp. *gemmaifera* over time under field conditions. Shading represents night. Data are from Fig. 6.1 and redrawn here with statistical data obtained from ANOVA and post hoc Tukey tests ( $n = 373-616$  stomata measured per timepoint; mean  $\pm$  S.E.M.). Different letters represent statistically significant differences between means ( $p < 0.05$ ).

## 9.5 The role of the energy-signalling hub SnRK1 in regulating sucrose-induced hypocotyl elongation

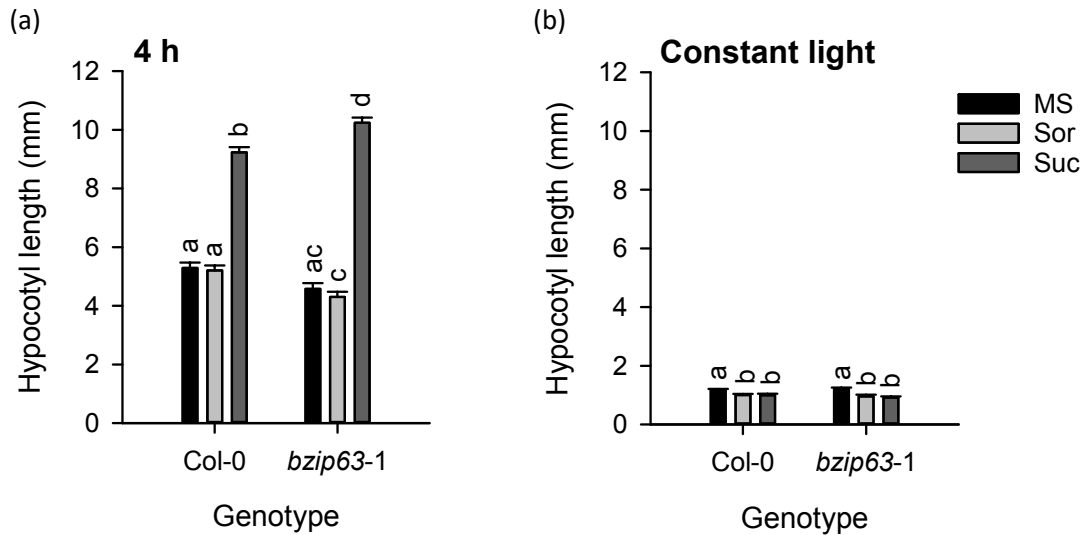


Figure 9.18: *bzip63-1* hypocotyls are hypersensitive to sucrose supplementation. Hypocotyl lengths were measured for 7 day-old seedlings grown on MS supplemented with 3% sucrose (Suc) or equimolar sorbitol (Sor) under (a) a 4 h photoperiod or (b) constant light conditions ( $n = 20$ ; mean  $\pm$  S.E.M.). Data were collected from an additional experimental repeat of Fig. 7.3. Data were analysed with ANOVA and Tukey's post hoc tests. Different letters indicate statistically significant difference between means ( $p < 0.05$ ).

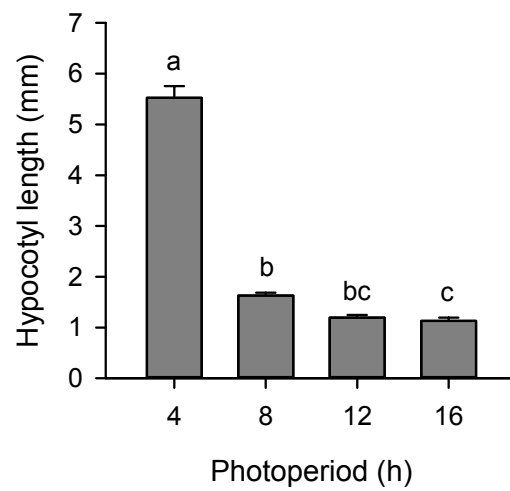


Figure 9.19: Hypocotyl length varies with photoperiod. Hypocotyl lengths were measured for 7 day-old Col-0 grown on MS under photoperiods of 4 h, 8 h, 12 h and 16 h ( $n = 20$ ; mean  $\pm$  S.E.M.). Data were taken from Chapter 5 and re-drawn here for clarity. Data were analysed with ANOVA and Tukey's post hoc tests. Different letters indicate statistically significant difference between means ( $p < 0.05$ ).

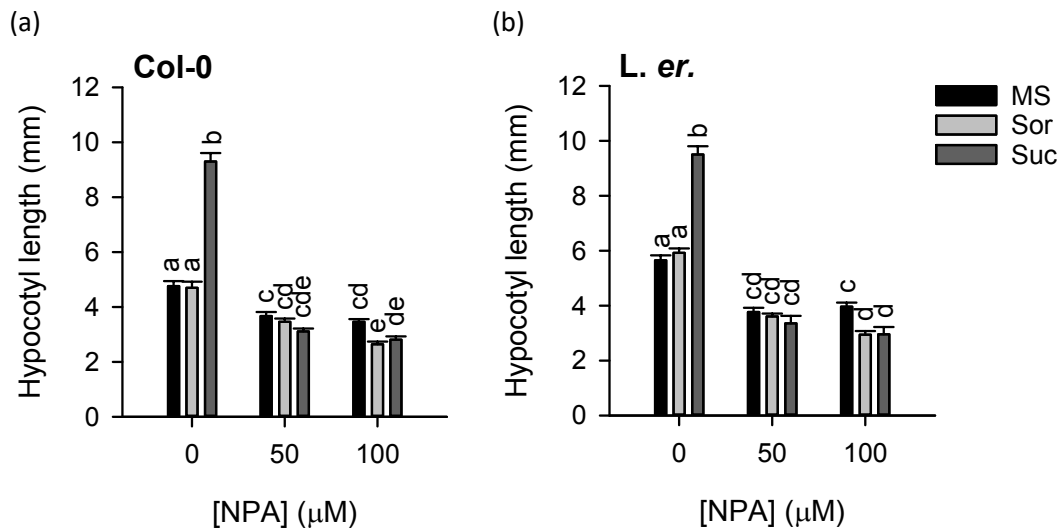


Figure 9.20: NPA abolishes sucrose-induced hypocotyl elongation at high concentrations. Hypocotyl lengths were measured for 7 day-old (a) *Col-0* and (b) *L. er.* grown on MS supplemented with 3% sucrose (Suc) or equimolar sorbitol (Sor) under a 4 h photoperiod, with these growth media being further supplemented with the carrier control (0.1% (v/v) DMSO), 50 μM NPA, or 100 μM NPA ( $n = 20$ ; mean  $\pm$  S.E.M.). Data were analysed with ANOVA and Tukey's post hoc tests. Different letters indicate statistically significant difference between means ( $p < 0.05$ ).

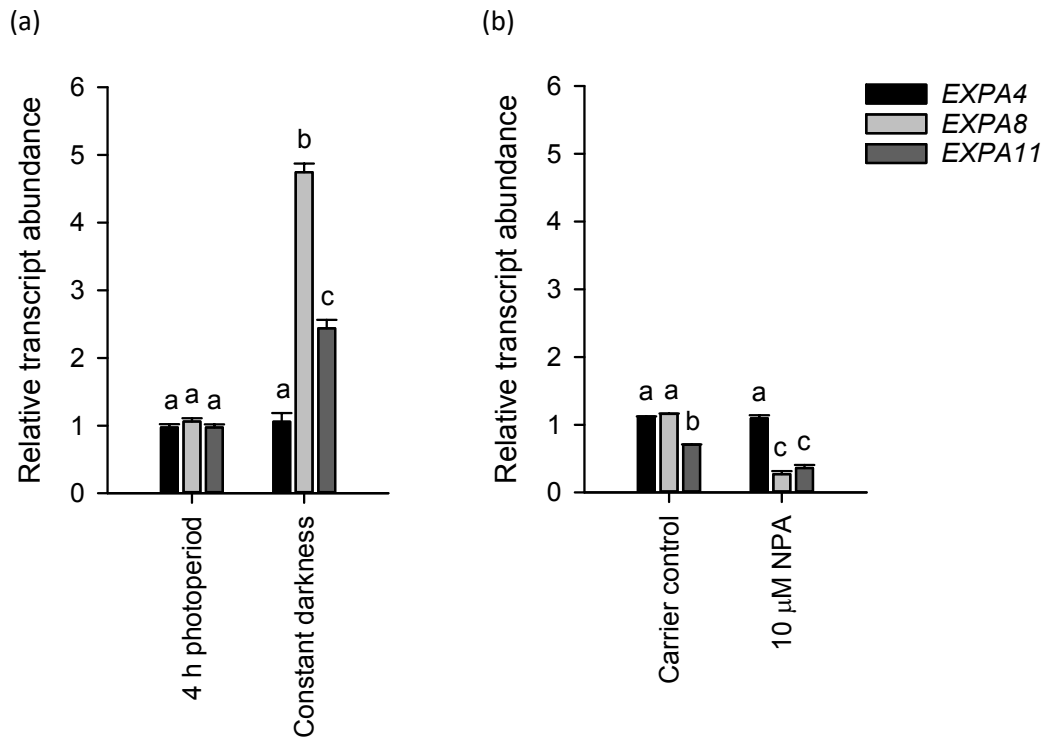


Figure 9.21: Determining which *EXPA* genes are upregulated by conditions promoting hypocotyl elongation and downregulated by conditions suppressing hypocotyl elongation. Relative transcript abundance of *EXPA4*, *EXPA8* and *EXPA11* were measured in 7 day-old *L. er.* grown on MS (a) under constant darkness, a condition promoting hypocotyl elongation or (b) supplemented with 10 μM NPA, a condition suppressing hypocotyl elongation ( $n = 3$ ; mean  $\pm$  S.E.M.). Seedlings in panel (b) were grown under a 4 h photoperiod, and 0.12% (v/v) methanol was used as the carrier control. *PP2AA3* was used as the reference gene. Data were analysed with ANOVA and Tukey's post hoc tests. Different letters indicate statistically significant difference between means ( $p < 0.05$ ). Data were published in Simon et al. (2018a) (Appendix).

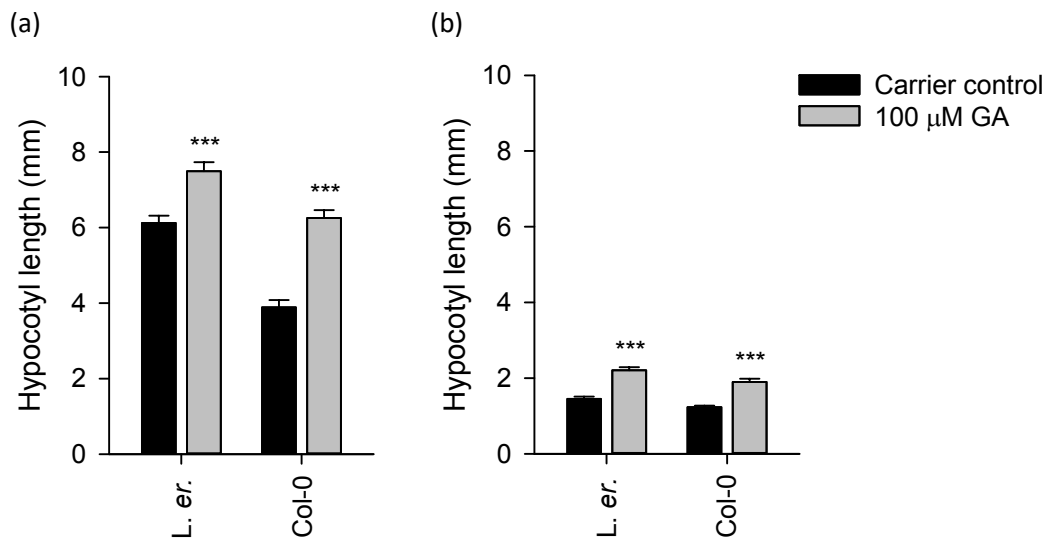


Figure 9.22: GA supplementation promotes hypocotyl elongation. Hypocotyl length was measured for 7 day-old *L. er.* and *Col-0* grown on MS supplemented with the carrier control (0.1% (v/v) DMSO) or 100 μM GA under a (a) 4 h photoperiod or (b) 16 h photoperiod ( $n = 20$ ; mean  $\pm$  S.E.M.). Data were analysed with ANOVA and Tukey's post hoc tests, and statistical significance compared to the respective carrier control is indicated by starring (\*\*\*) =  $p < 0.001$ ). Data were published in Simon et al. (2018a) (Appendix).



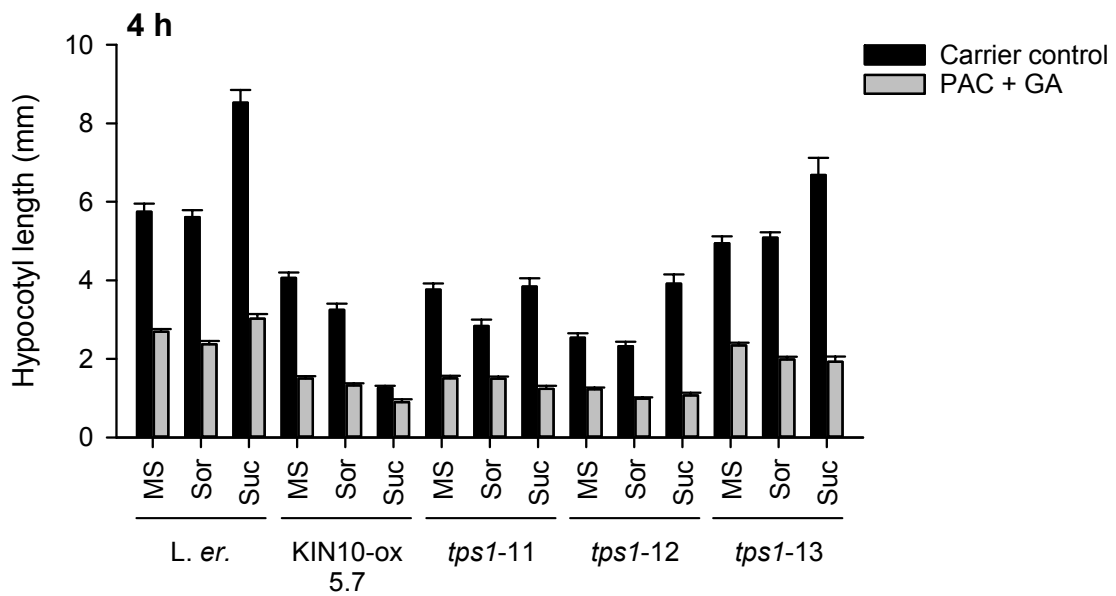


Figure 9.23: Effects of PAC and GA on sucrose-induced hypocotyl elongation are difficult to interpret for the KIN10-ox and *tps1* alleles. Hypocotyl length was measured for 7 day-old seedlings grown on MS supplemented with 3% sucrose (Suc) or equimolar sorbitol (Sor) under a 4 h photoperiod, with these growth media being further supplemented with the carrier control (0.12% (v/v) methanol) or 20  $\mu$ M PAC and 100  $\mu$ M GA ( $n = 20$ ; mean  $\pm$  S.E.M.). Data were analysed with independent-samples t-tests, ANOVA and Tukey's post hoc tests. Effects of sucrose supplementation on KIN10-ox and *tps1* hypocotyl length masked the additional potential effects of PAC and GA supplementation.

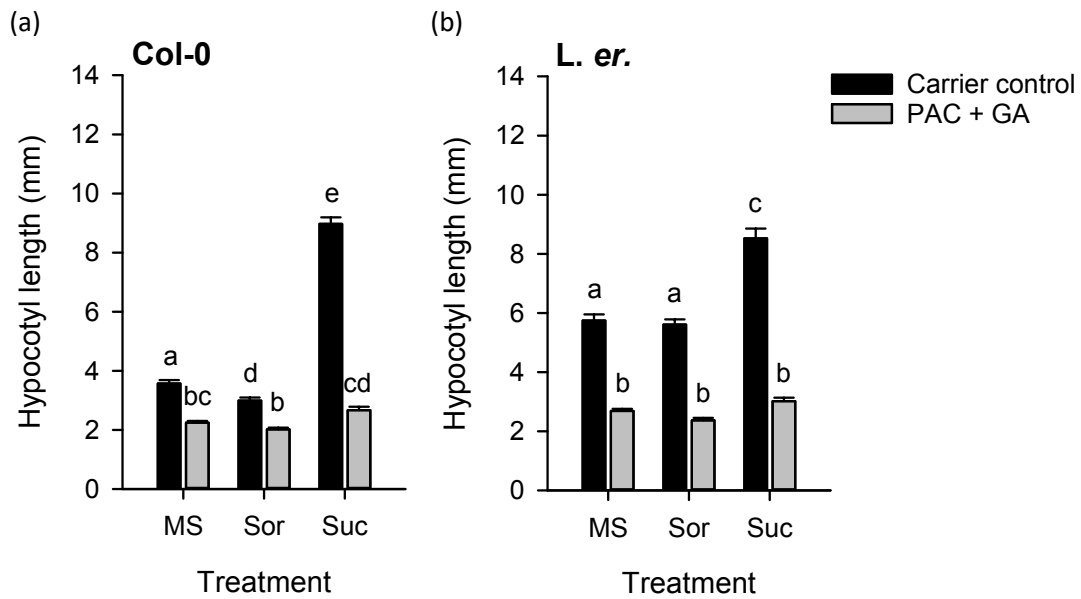


Figure 9.24: GA signalling affects sucrose-induced hypocotyl elongation. Hypocotyl length was measured in 7 day-old seedlings grown on MS supplemented with 3% sucrose (Suc) or equimolar sorbitol (Sor) under a 4 h photoperiod, with these growth media being further supplemented with the carrier control (0.12% (v/v) methanol) or 20  $\mu\text{M}$  PAC and 100  $\mu\text{M}$  GA ( $n = 20$ ; mean  $\pm$  S.E.M.). Data were collected from an additional experimental repeat of Fig. 7.11. Data were analysed with ANOVA and Tukey's post hoc tests. Different letters indicate statistically significant difference between means ( $p < 0.05$ ).

## **9.6 Published papers**

- 1) Simon et al. (2018a): pages 256-267
- 2) Simon et al. (2018b): pages 268-270
- 3) Simon and Dodd (2017): pages 271-272

# The Energy-Signaling Hub SnRK1 Is Important for Sucrose-Induced Hypocotyl Elongation<sup>1</sup>[CC-BY]

Noriane M. L. Simon,<sup>a,2</sup> Jelena Kusakina,<sup>b,2,3</sup> Ángela Fernández-López,<sup>a</sup> Anupama Chembath,<sup>4</sup> Fiona E. Belbin,<sup>a</sup> and Antony N. Dodd<sup>a,b,5</sup>

<sup>a</sup>School of Biological Sciences, University of Bristol, Life Sciences Building, Bristol BS8 1TQ, United Kingdom

<sup>b</sup>Cabot Institute, University of Bristol, Bristol BS8 1UJ, United Kingdom

ORCID ID: 0000-0001-6859-0105 (A.N.D.).

Emerging seedlings respond to environmental conditions such as light and temperature to optimize their establishment. Seedlings grow initially through elongation of the hypocotyl, which is regulated by signaling pathways that integrate environmental information to regulate seedling development. The hypocotyls of *Arabidopsis* (*Arabidopsis thaliana*) also elongate in response to sucrose. Here, we investigated the role of cellular sugar-sensing mechanisms in the elongation of hypocotyls in response to Suc. We focused upon the role of SnRK1, which is a sugar-signaling hub that regulates metabolism and transcription in response to cellular energy status. We also investigated the role of TPS1, which synthesizes the signaling sugar trehalose-6-P that is proposed to regulate SnRK1 activity. Under light/dark cycles, we found that Suc-induced hypocotyl elongation did not occur in *tps1* mutants and overexpressors of KIN10 (AKIN10/SnRK1.1), a catalytic subunit of SnRK1. We demonstrate that the magnitude of Suc-induced hypocotyl elongation depends on the day length and light intensity. We identified roles for auxin and gibberellin signaling in Suc-induced hypocotyl elongation under short photoperiods. We found that Suc-induced hypocotyl elongation under light/dark cycles does not involve another proposed sugar sensor, HEXOKINASE1, or the circadian oscillator. Our study identifies novel roles for KIN10 and TPS1 in mediating a signal that underlies Suc-induced hypocotyl elongation in light/dark cycles.

Emerging seedlings monitor the environment to optimize their establishment and out-compete neighboring plants (Salter et al., 2003; Weinig et al., 2007; Koini et al., 2009; Keuskamp et al., 2010; Crawford et al., 2012). Seedlings grow initially through cell expansion within the hypocotyl, which elongates rapidly to optimize light capture by the cotyledons. Hypocotyl elongation is controlled by several signaling pathways that

converge upon phytohormones to regulate cell expansion (Lincoln et al., 1990; Collett et al., 2000). Examples of signals that adjust hypocotyl elongation include phytochrome-mediated signals concerning the ratio of red to far red light (Casal, 2013), blue light (Liscum and Hangarter, 1991), UV-B light (Kim et al., 1998; Hayes et al., 2014), temperature (Koini et al., 2009; Wigge, 2013; Mizuno et al., 2014), photoperiod and the circadian oscillator (Dowson-Day and Millar, 1999; Más et al., 2003; Nusinow et al., 2011). These signals are integrated by the PHYTOCHROME INTERACTING FACTOR (PIF) family of basic helix-loop-helix transcription factors. The PIFs are signaling hubs that control plant development through genomewide transcriptional alterations. One outcome of these PIF-mediated transcriptional changes is the alteration in phytohormone signaling that regulates hypocotyl elongation (Lorrain et al., 2008; Leivar and Quail, 2011).

Hypocotyl length is also increased by exogenous and endogenous sugars (Kurata and Yamamoto, 1998; Takahashi et al., 2003; Zhang et al., 2010, 2015, 2016; Liu et al., 2011; Stewart et al., 2011; Lilley et al., 2012). Under light/dark cycles, exogenous sugars are proposed to cause hypocotyl elongation by inducing auxin signals through the PIF-mediated gene regulation (Stewart et al., 2011; Lilley et al., 2012). Under extended darkness, brassinosteroid and gibberellin (GA) phytohormones are involved in sugar-induced hypocotyl elongation, which may also involve the target of rapamycin (TOR) kinase regulator of energy- and nutrient-responses (Zhang et al., 2010, 2015, 2016; Dobrenel et al., 2011). This elongation phenotype in darkness is thought to form a response to the starvation

<sup>1</sup> This research was funded by the Biotechnology and Biological Sciences Research Council (BBSRC grant BB/I005811/2; South-West Doctoral Training Partnership BB/J014400/1), the Lady Emily Smyth Agricultural Research Station (Bristol), the Wolfson Foundation and The Royal Society. A.N.D. is grateful to Kyoto University for awarding a Guest Professorship (Joint Usage/Research Program of the Center for Ecological Research, Kyoto University) and to The Royal Society for awarding a University Research Fellowship.

<sup>2</sup> These authors contributed equally to this article.

<sup>3</sup> Present address: Centre for Plant Sciences, Faculty of Biological Sciences, University of Leeds, Leeds LS2 9JT United Kingdom.

<sup>4</sup> Present address: Institute for Cell and Molecular Biosciences, Faculty of Medical Sciences, Newcastle University, Framlington Place, Newcastle upon Tyne NE2 4HH, United Kingdom.

<sup>5</sup> Address correspondence to antony.dodd@bristol.ac.uk.

The author responsible for distribution of materials integral to the findings presented in this article in accordance with the policy described in the Instructions for Authors ([www.plantphysiol.org](http://www.plantphysiol.org)) is: Antony N. Dodd ([antony.dodd@bristol.ac.uk](mailto:antony.dodd@bristol.ac.uk)).

A.D. and J.K. conceived the study; N.S., J.K., A.F.L., F.B., and A.C. performed experiments; N.S., J.K., A.F.L., and A.D. analyzed data; N.S., J.K., and A.D. interpreted data and wrote the paper.

[CC-BY] Article free via Creative Commons CC-BY 4.0 license.

[www.plantphysiol.org/cgi/doi/10.1104/pp.17.01395](http://www.plantphysiol.org/cgi/doi/10.1104/pp.17.01395)

conditions that arise when plants are cultivated under periods of darkness exceeding the length of the daily light/dark cycle (Graf et al., 2010; Zhang et al., 2016). In comparison to these known roles for phytohormones and transcriptional regulators, the contribution of sugar sensing mechanisms to sucrose-induced hypocotyl elongation remains unknown.

Several sugar- or energy-signaling mechanisms underlie the metabolic and developmental responses of plants to sugars. One mechanism involves the sucrose nonfermenting1 (Snf1)-related protein kinase SnRK1 (Baena-González et al., 2007; Baena-González and Sheen, 2008), and another involves HEXOKINASE1 (Jang et al., 1997; Moore et al., 2003). SnRK1 controls metabolic enzymes directly by protein phosphorylation (Baena-González and Sheen, 2008). It also regulates greater than 1000 transcripts in response to carbohydrate availability, for example by adjusting bZIP transcription factor activity (Baena-González et al., 2007; Smeekens et al., 2010; Delatte et al., 2011; Mantioli et al., 2011; Mair et al., 2015). Both SnRK1- and hexokinase-mediated sugar signaling involve specific sugars functioning as signaling molecules that provide cellular information concerning sugar availability. For example, SnRK1 activity is thought to be regulated by trehalose-6-P (Tre6P), whose concentration tracks the cellular concentration of Suc (Lunn et al., 2006; Zhang et al., 2009; Nunes et al., 2013a, 2013b; Yadav et al., 2014). Tre6P is synthesized from UDP Glc and Glc-6-P, which are derived from mobilized and transported Suc, and also directly from photosynthesis. In *Arabidopsis thaliana*, Tre6P is synthesized by trehalose-6-P synthase (TPS). Of 11 TPS homologs encoded by the *Arabidopsis* genome, TREHALOSE-6-PHOSPHATE SYNTHASE1 (TPS1) synthesizes Tre6P in plants (Gómez et al., 2010; Vandesteene et al., 2010), and TPS2 and TPS4 are catalytically active in yeast complementation assays (Delorge et al., 2015). Tre6P is believed to regulate SnRK1-mediated signaling by suppressing the activity of SNF1-RELATED PROTEIN KINASE1.1 (KIN10/AKIN10/SnRK1.1), which is a catalytic subunit of SnRK1 that is fundamental to the signaling role of SnRK1 (Baena-González et al., 2007; Zhang et al., 2009; Nunes et al., 2013a, 2013b).

Manipulation of Tre6P metabolism in plants alters developmental phenotypes. For example, *tps1* knockout mutants undergo seedling developmental arrest (Gómez et al., 2006), expression of bacterial Tre6P synthase (*otsA*) or phosphatase (*otsB*) affects leaf senescence (Wingler et al., 2012), and Tre6P and KIN10 act within a photoperiod-response pathway that controls the induction of flowering (Baena-González et al., 2007; Gómez et al., 2010; Wahl et al., 2013). Signaling by Tre6P and KIN10 is also important for the regulation of growth rates. Growth is increased by Suc in the presence of Tre6P (Schluepmann et al., 2003; Paul et al., 2010), but the lack of a quantitative (correlative) relationship between relative growth rates and [Tre6P] suggests that a threshold [Tre6P] is required for growth to occur (Nunes et al., 2013a, 2013b). Therefore, it has been suggested that

control of KIN10/11 by [Tre6P] may prime the regulation of growth-related genes to capitalize upon increased energy availability, rather than by inducing growth directly (Nunes et al., 2013a, 2013b). Remarkably, the impact of this pathway is sufficiently global that its manipulation can increase maize (*Zea mays*) yields by almost 50% (Nuccio et al., 2015) and increase the yield and drought tolerance of wheat (*Triticum aestivum*; Griffiths et al., 2016).

Given the importance of Tre6P metabolism and SnRK1 for growth regulation under cycles of light and dark, we wished to determine whether this energy-signaling mechanism is important for the regulation of Suc-induced hypocotyl elongation. Moreover, because Tre6P signaling is reported to act upon GA and auxin signaling genes (Paul et al., 2010; Li et al., 2014) and these phytohormones are involved in Suc-induced hypocotyl elongation (Zhang et al., 2010; Lilley et al., 2012), we reasoned that SnRK1 might act upon these phytohormones to regulate Suc-induced hypocotyl elongation.

Here, we identified a novel role for Tre6P and KIN10 in the mechanisms that cause Suc-induced hypocotyl elongation. We focused upon light/dark cycles rather than conditions of extended darkness (Zhang et al., 2010, 2015, 2016), because we wished to identify mechanisms that regulate growth and development under regimes more representative of real-world growing conditions that do not elicit prolonged starvation. We found that the sensitivity of hypocotyl elongation to sugars depends on the photoperiod and light intensity. We identified that KIN10 is important for expression of transcripts encoding auxin-induced expansins. Our data reveal a new mechanistic link among carbohydrate supply, energy sensing, and phytohormone signaling during seedling emergence.

## RESULTS

### KIN10 and TPS1 Are Required for Suc-Induced Hypocotyl Elongation in Light/Dark Cycles

We investigated whether KIN10 and TPS1 contribute to Suc-induced hypocotyl elongation under light/dark cycles (Kurata and Yamamoto, 1998; Takahashi et al., 2003; Stewart et al., 2011; Lilley et al., 2012). We studied hypocotyl elongation in transgenic *Arabidopsis* where KIN10 activity was manipulated by overexpressing the catalytic subunit of KIN10 (KIN10-ox; Baena-González et al., 2007). Although KIN10 activity is regulated posttranslationally by Tre6P (Zhang et al., 2009), KIN10 overexpression alone alters the abundance of energy-response transcripts in protoplasts (Baena-González et al., 2007). We used KIN10 overexpression rather than knockouts, because KIN10/11 double knockouts disrupt pollen production and are lethal (Zhang et al., 2001; Baena-González et al., 2007). We also used hypomorphic Targeted Induced Local Lesions In Genomes (TILLING) mutants with reduced TPS1 activity (*tps1-11*, *tps1-12*; Gómez et al., 2006, 2010), which is preferable to *tps1* loss-of-function mutants that cause seedling developmental arrest (Gómez et al., 2006).

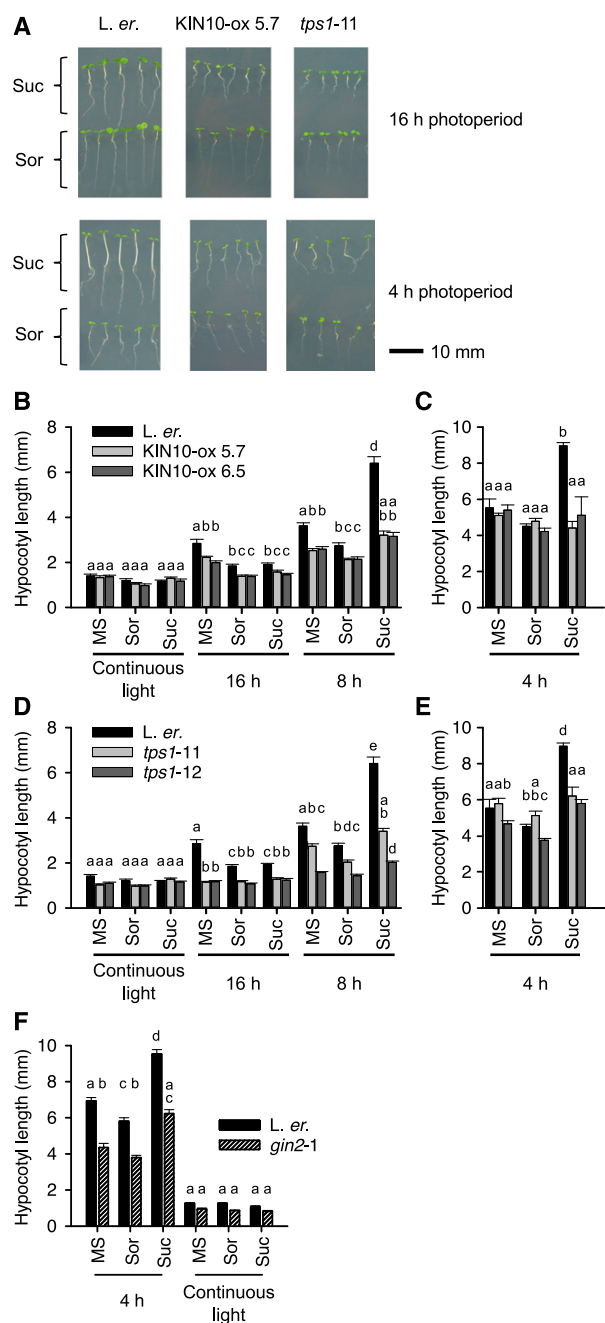


**Figure 1.** KIN10 and TPS1 participate in Suc-induced hypocotyl elongation. A, Representative images of *L. er.* wild-type, KIN10-ox, and *tps1* seedlings cultivated under a variety of photoperiods, with and without supplementation with 3% (w/v) Suc. All panels scaled identically. Images are a subset of seedlings used to generate data in (B) to (E). B to E, Lengths of hypocotyls of seedlings grown under (B and D) constant light, 16-h and 8-h photoperiods and (C and E) 4-h photoperiods. Photoperiods are indicated underneath graphs. F, Effect of Suc supplementation upon *gin2-1* hypocotyl length. SEM is small under continuous light (0.03 mm to 0.05 mm), so is not visible on graphs. Data were analyzed with ANOVA and Tukey's posthoc tests ( $n = 10$  (B to E) or  $n = 20$  (F) seedlings in three independent experiments; mean  $\pm$  se). Different

First, we investigated the effect of exogenous Suc upon hypocotyl elongation in a variety of photoperiods (Fig. 1). Under 4-h and 8-h photoperiods, Suc supplementation of wild-type seedlings caused a significant increase in hypocotyl length relative to the sorbitol control (2.1-fold and 2.3-fold relative to sorbitol controls, under 4-h and 8-h photoperiods, respectively; Fig. 1, A to E). In comparison, under 16-h photoperiods and constant light conditions, exogenous Suc did not promote hypocotyl elongation (Fig. 1, A to E).

Next, we investigated roles of KIN10 in Suc-induced hypocotyl elongation under light/dark cycles. Under 8-h photoperiods, the hypocotyls of two KIN10-ox lines (Baena-González et al., 2007) did not elongate significantly in response to exogenous Suc relative to the MS control (Fig. 1B). Both KIN10-ox lines elongated 1.5-fold in response to Suc relative to the sorbitol control (Fig. 1B). Exogenous Suc caused no significant increase in the hypocotyl length of KIN10-ox seedlings under 4-h photoperiods (Fig. 1C). Hypocotyls of the *L. er.* background and KIN10-ox appeared shorter when supplemented with exogenous Suc in constant light and 16-h photoperiods. However, this could be an osmotic effect rather than a Suc response because hypocotyl elongation responded identically to Suc and the sorbitol control (Fig. 1B).

Because KIN10 activity is thought to be regulated by Tre6P (Zhang et al., 2009), we investigated the role of the Tre6P biosynthetic enzyme TPS1 in Suc-induced hypocotyl elongation under light/dark cycles. In two *tps1* TILLING mutants under 8-h photoperiods, Suc supplementation caused a significant 2.3-fold increase in hypocotyl length in the wild type relative to the sorbitol control, compared with 1.6-fold and 1.3-fold increases in hypocotyl length in *tps1-11* and *tps1-12*, respectively (Fig. 1D). Under 4-h photoperiods, Suc caused a significant 2-fold increase in hypocotyl length of the wild type relative to the sorbitol control, compared with no significant increase in length in *tps1-11* but a significant 1.5-fold increase in hypocotyl length in *tps1-12* (Fig. 1E). Together, these experiments with KIN10 overexpressors and *tps1* mutants indicate that TPS1 and KIN10 are involved in one or more mechanisms that increase hypocotyl length in response to exogenous Suc. This suggests that SnRK1-mediated energy signaling regulates hypocotyl elongation in response to Suc supplementation.

#### HEXOKINASE1 Is Not Required for Suc-Induced Hypocotyl Elongation under Light/Dark Cycles

Hexokinase is thought to function as a sugar sensor that regulates development in response to the concentration of Glc (Jang et al., 1997; Moore et al., 2003), so we

letters indicate statistically significant differences between means, specifically within each light condition ( $P < 0.05$ ). B to E, MS is half-strength MS media, and Suc and Sor are 0.5 MS supplemented with 3% (w/v) Suc or equimolar sorbitol (87.6 mM osmotic control), respectively.

investigated whether hexokinase-based signaling also contributes to Suc-induced hypocotyl elongation. For this, we measured the elongation of hypocotyls in response to exogenous Suc in the *glucose insensitive2* (*gin2-1*) mutant of *HEXOKINASE1*. Overall, *gin2-1* hypocotyls were slightly shorter than the wild type under all conditions tested (Fig. 1F). Exogenous Suc caused a significant increase in hypocotyl length of wild-type and *gin2-1* seedlings, producing hypocotyls 63% and 67% longer than the osmotic control in the wild type and *gin2-1*, respectively (Fig. 1F). Therefore, Suc caused a similar magnitude of hypocotyl elongation in *gin2-1* and the wild type. This suggests that interconversion of Suc to Glc, and therefore hexokinase-based Glc signaling, does not contribute to Suc-induced hypocotyl elongation in short photoperiods.

### Relationship among Day-Length, Light Intensity, and Suc-Induced Hypocotyl Elongation

Our data suggest that the magnitude of the Suc-induced increase in hypocotyl length depends upon the photoperiod or the quantity of light received. In the wild type, Suc increased hypocotyl length under short (4 h or 8 h) but not long (16 h or constant light) photoperiods under photosynthetically active radiation (PAR) of  $100 \mu\text{mol m}^{-2} \text{s}^{-1}$  (Figs. 1, B to E and 2A). In addition, Suc caused significantly greater hypocotyl elongation under 4-h photoperiods compared with 8-h photoperiods of  $100 \mu\text{mol m}^{-2} \text{s}^{-1}$  (Fig. 2A). We reasoned that these varying responses to Suc might arise from differences in total daily PAR received under each of these conditions, or alternatively from the sensing of photoperiod length. To investigate this, we compared the magnitude of Suc-induced hypocotyl elongation under the same total daily integrated PAR, under longer photoperiods (16 h at  $40 \mu\text{mol m}^{-2} \text{s}^{-1}$  and 8 h at  $80 \mu\text{mol m}^{-2} \text{s}^{-1}$ ) and under shorter photoperiods (8 h at  $40 \mu\text{mol m}^{-2} \text{s}^{-1}$  and 4 h at  $80 \mu\text{mol m}^{-2} \text{s}^{-1}$ ). Under a 16-h photoperiod at  $40 \mu\text{mol m}^{-2} \text{s}^{-1}$ , Suc caused a significant increase in hypocotyl length (Fig. 2, B and C). This contrasts a 16-h photoperiod at  $100 \mu\text{mol m}^{-2} \text{s}^{-1}$ , where Suc did not promote hypocotyl elongation (Figs. 1 and 2A). This suggests that the quantity of light received influences the sensitivity of hypocotyl elongation to Suc. Under 8-h photoperiods, Suc caused greater hypocotyl elongation under  $40 \mu\text{mol m}^{-2} \text{s}^{-1}$  (mean 4.1 mm increase) than under  $80 \mu\text{mol m}^{-2} \text{s}^{-1}$  (mean 3.3 mm increase), which also suggests that hypocotyl elongation is more responsive to Suc under lower light conditions (Fig. 2, B and D). When daily integrated PAR was the same under 4-h and 8-h photoperiods, there was no difference in the increase in hypocotyl length caused by Suc (Fig. 2, D and E). These responses suggest that daily integrated PAR influences the magnitude of Suc-induced hypocotyl elongation. However, the magnitude of Suc-induced hypocotyl elongation was significantly less under 16-h photoperiods at  $40 \mu\text{mol m}^{-2} \text{s}^{-1}$  than 8-h photoperiods at

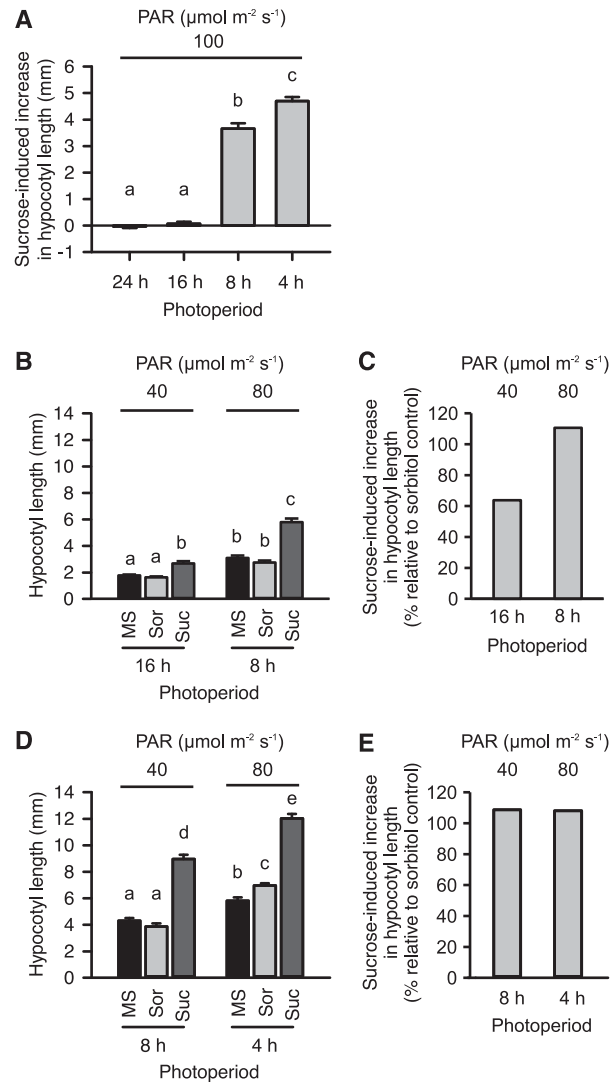


**Figure 2.** Day-length dependency of Suc-induced hypocotyl elongation in wild-type seedlings. A, Increase in hypocotyl length caused by Suc under range of photoperiods (data derived from Fig. 1, plotted relative to sorbitol control). B to E, Comparison of (B) and (D) absolute hypocotyl length and (C) and (E) proportional increase in hypocotyl length caused by Suc supplementation under specified PAR and photoperiod. Mean  $\pm$  SE (A, C to E),  $n = 10$  seedlings in two independent experiments; (B)  $n = 20$  seedlings. Data analyzed using ANOVA followed by posthoc Tukey test. Different letters indicate statistically significant differences between means ( $P < 0.05$ ).

$80 \mu\text{mol m}^{-2} \text{s}^{-1}$  (Fig. 2, B and C), suggesting that under long photoperiods, the magnitude of Suc-induced hypocotyl elongation could be also determined by a photoperiod-response mechanism acting independently from daily integrated PAR. These data provide the insight that the photoperiod-sensitivity of Suc-induced hypocotyl elongation is determined by both the absolute photoperiod and the amount of light received.

### Interaction between Hypocotyl Elongation by Exogenous Suc and the Circadian Oscillator

The circadian oscillator regulates hypocotyl elongation because the accumulation of PIF proteins is restricted to the end of the night (Nozue et al., 2007; Nusinow et al., 2011). Because the circadian oscillator responds to exogenous and endogenous sugars (Dalchau et al., 2011; Haydon et al., 2013) and KIN10 overexpression can lengthen circadian period (Shin et al., 2017), we investigated whether Suc-induced increases in hypocotyl length under short photoperiods involve the circadian oscillator. First, we tested whether the circadian oscillator components CIRCADIAN CLOCK ASSOCIATED1 (CCA1), LATE ELONGATED HYPOCOTYL (LHY), and TIMING OF CAB2 EXPRESSION1 (TOC1) are required for Suc-induced hypocotyl elongation using the *cca1-11 lhy-21 toc1-21* triple mutant (Ding et al., 2007). *cca1-11 lhy-21 toc1-21* causes circadian arrhythmia under constant light and temperature, and disrupts rhythms of oscillator transcripts, including evening complex components that regulate hypocotyl elongation (Ding et al., 2007). Under 4-h photoperiods, the magnitude of the Suc-induced increase in hypocotyl length was unaltered in *cca1-11 lhy-21 toc1-21* (Fig. 3A; Supplemental Fig. S1). Under 40-h photoperiods, the hypocotyls of *cca1-11 lhy-21 toc1-21* were of similar length to the wild type (Fig. 3A), whereas under 8-h photoperiods, *cca1-11 lhy-21 toc1-21* has longer hypocotyls than the wild type (Ding et al., 2007).

We also investigated whether two proteins that confer sugar sensitivity to the circadian oscillator, GIGANTEA (GI) and PSEUDO-RESPONSE REGULATOR7 (PRR7; Dalchau et al., 2011; Haydon et al., 2013), contribute to Suc-induced hypocotyl elongation under short photoperiods. We tested this because the *prp7-11* mutation renders the oscillator insensitive to sugar signals that entrain the oscillator (Haydon et al., 2013), and the *gi-11* mutation alters oscillator responses to long-term exposure to exogenous Suc (Dalchau et al., 2011). In all cases, *gi-11* had longer hypocotyls than the wild type (Fig. 3B), but the magnitude of the Suc-induced increase in hypocotyl length was unaltered in *gi-11* relative to the wild type (Fig. 3D). Likewise, the *prp7-11* mutant also did not alter the magnitude of Suc-induced increases in hypocotyl length (Fig. 3, C and D).

These experiments indicate that two mechanisms providing sugar inputs to the circadian oscillator (Dalchau et al., 2011; Haydon et al., 2013) and three core oscillator components do not contribute to Suc-induced increases in hypocotyl length under short photoperiods.

### Phytohormone Signaling and Suc-Induced Hypocotyl Elongation under Light/Dark Cycles: Auxin

Suc-induced hypocotyl elongation in the light involves auxin and GA signaling (Zhang et al., 2010; Lilley et al., 2012). We investigated the involvement of phytohormones in Suc-induced hypocotyl elongation under light/dark cycles, and their relationship

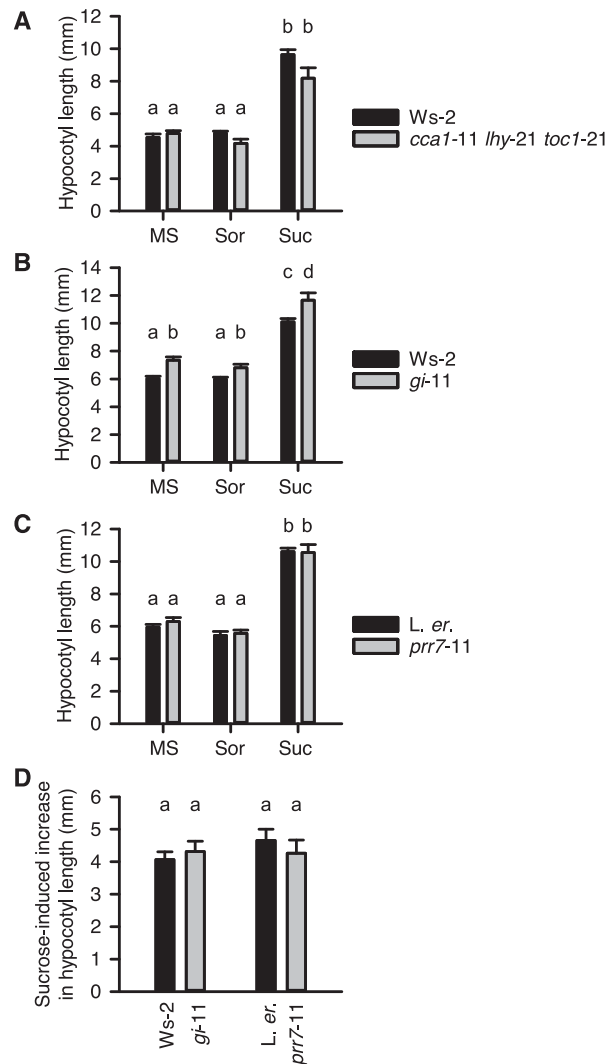


**Figure 3.** The circadian oscillator does not participate in Suc-induced hypocotyl elongation under short photoperiods. Suc-induced change in hypocotyl length of (A) a circadian oscillator triple mutant (*cca1-11 lhy-21 toc1-21*, background *Ws-2*) and (B and C) two oscillator components participating in Suc regulation of the circadian oscillator. D, Change in hypocotyl length caused by Suc supplementation in *gi-11* and *prp7-11*, expressed relative to 0.5 MS control. MS is 0.5 MS media, and Suc and Sor are 0.5 MS supplemented with 3% (w/v) Suc and sorbitol (87.6 mM, osmotic control), respectively. Data are mean  $\pm$  se ( $n = 10 - 16$ ), analyzed with (A to C) ANOVA and posthoc Tukey tests and (D) two-sample *t* test comparing mutant with wild type for each treatment. Data show one of three independent repeats of the experiment, conducted under 4-h photoperiods. Different letters indicate statistically significant differences between means ( $P < 0.05$ ).

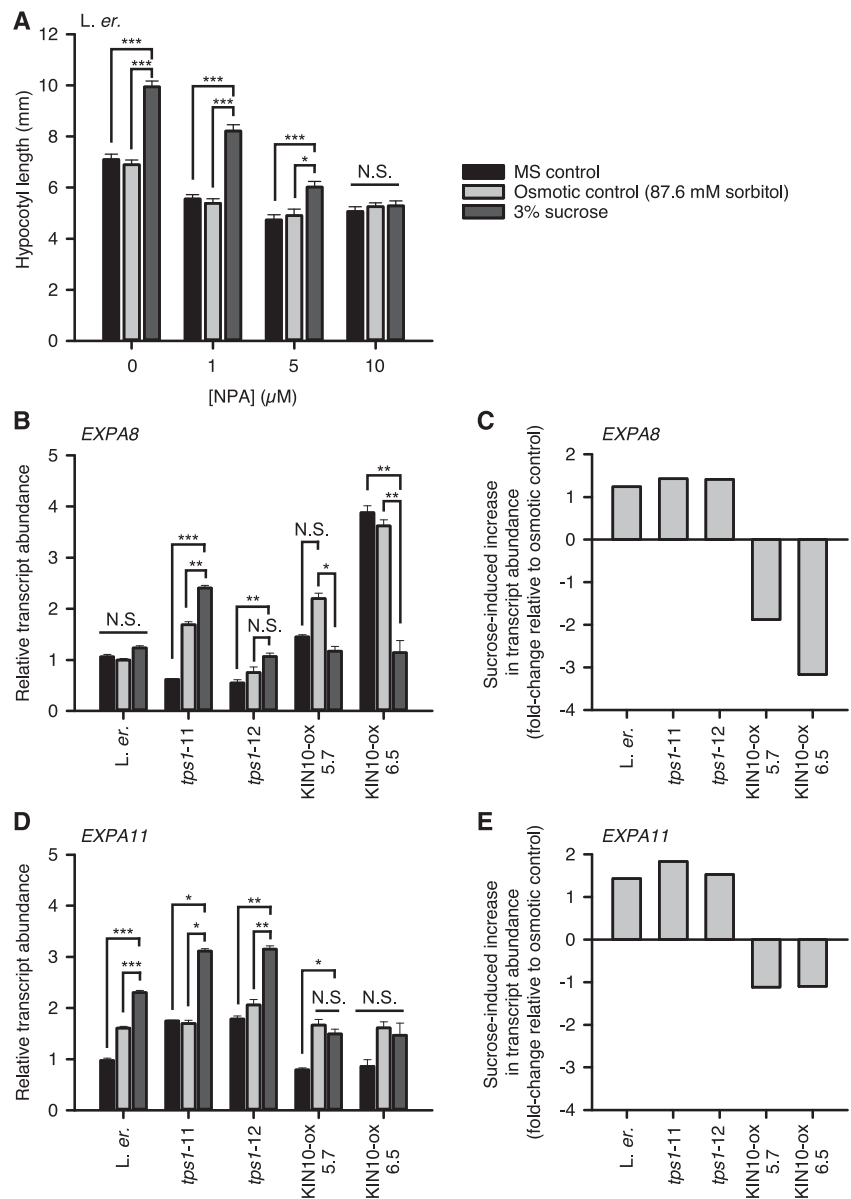
with SnRK1-mediated signaling. First, we examined the effect of the inhibitor of polar auxin transport 1-N-naphthylphthalamic acid (NPA) upon Suc-induced hypocotyl elongation. NPA inhibited Suc-induced hypocotyl elongation in a concentration-dependent manner,



such that 10  $\mu\text{M}$  NPA completely abolished Suc-induced elongation (Fig. 4A). Consistent with previous work (Lilley et al., 2012), this indicates that under light/dark cycles Suc-induced hypocotyl elongation is auxin-dependent. Next, we examined the responses of auxin- and PIF-dependent expansin transcripts to Suc. Expansins are a large family of cell wall modifying enzymes that allow turgor-driven cell expansion, and some expansin transcripts are up-regulated by auxins in a PIF-dependent manner during hypocotyl elongation (Li et al., 2002; Miyazaki et al., 2016; Gangappa and Kumar, 2017). We examined *EXPANSIN A4* (*EXPA4*), *EXPA8*, and *EXPA11* transcripts, which are auxin-induced in seedlings (Goda et al., 2004; Esmon et al.,

2006; Winter et al., 2007; Lee et al., 2009). *EXPA8* and *EXPA11* transcripts were up-regulated by conditions of constant darkness, which also increases hypocotyl elongation (Supplemental Fig. S2A; Boylan and Quail, 1991), and down-regulated by 10  $\mu\text{M}$  NPA, which suppresses hypocotyl elongation (Supplemental Fig. S2B; Lilley et al., 2012). *EXPA4* was unaltered by these conditions (Supplemental Fig. S2). Therefore, *EXPA8* and *EXPA11* transcript abundance was increased by conditions that promote hypocotyl elongation, and reduced by conditions that suppress hypocotyl elongation. Next, we monitored the change in abundance of these two expansin transcripts in response to Suc under 4-h photoperiods. In the wild type, *EXPA11* transcripts

**Figure 4.** Auxin signaling underlies Suc-induced hypocotyl elongation and KIN10 regulates expansin gene expression. A, Hypocotyl length of seedlings cultivated with a range of concentrations of the inhibitor of polar auxin transport NPA, under 4-h photoperiods (mean  $\pm$  SE;  $n = 20$ ). B to E, Suc-induced changes in expansin transcript abundance in elongating wild-type, *tps1*, and KIN10-ox seedlings under 4-h photoperiods. B and D, *EXPA8* and *EXPA11* transcript abundance relative to *PP2AA3* (mean  $\pm$  SE;  $n = 3$ ). C and E, The magnitude of Suc-induced change in transcript abundance in each genotype relative to the osmotic control. Data analyzed with ANOVA and posthoc Tukey tests, and with statistical significance indicated using starring ( $P > 0.05$ ; \* =  $P < 0.05$ ; \*\* =  $P < 0.01$ ; \*\*\* =  $P < 0.001$ ).



were up-regulated by 3% (w/v) Suc, whereas *EXPA8* transcripts were not up-regulated by Suc relative to the controls (Fig. 4, B to E). In KIN10-ox, where Suc does not promote hypocotyl elongation under light/dark cycles, *EXPA8* and *EXPA11* transcripts were not increased by Suc (Fig. 4, B to E). *EXPA8* was Suc-induced relative to the controls in *tps1-11*, but not in *tps1-12* (Fig. 4, B and C). *EXPA11* transcripts were Suc-induced in both *tps1-11* and *tps1-12* (Fig. 4, D and E). The induction of these two expansin transcripts by Suc in *tps1* mutants was unexpected, because both KIN10-ox and *tps* mutants suppress Suc-induced hypocotyl elongation under short photoperiods (Fig. 1). We also examined several other transcripts associated with auxin biosynthesis or responses, but the osmotic controls caused substantial alterations in transcript abundance that prevented interpretation of their regulation by Suc (Supplemental Fig. S3).

#### Phytohormone Signaling and Suc-Induced Hypocotyl Elongation under Light/Dark Cycles: Gibberellins

We tested whether GA signaling also contributes to Suc-induced hypocotyl elongation under short photoperiods. After germination, wild-type seedlings were transferred to media containing 3% (w/v) Suc or an osmotic control, supplemented with combinations of the GA biosynthesis inhibitor paclobutrazol (PAC), GA, or a carrier control. Consistent with previous studies, wild-type seedlings grown on media supplemented with PAC or PAC and GA had significantly shorter hypocotyls than controls (Fig. 5A; Cowling and Harberd, 1999; Liu et al., 2011). PAC abolished Suc-induced hypocotyl elongation, with a small hypocotyl length rescue occurring when GA was supplied in combination with PAC (Fig. 5A). We confirmed that the GA was active by demonstrating that, consistent with previous reports (Cowling and Harberd, 1999), hypocotyl length is increased by GA supplementation (Supplemental Fig. S4).

GA increases growth by causing degradation of DELLA growth repressor proteins, and also through DELLA-independent mechanisms (Peng et al., 1997; Fu et al., 2002; Cheng et al., 2004; Cao et al., 2006). Therefore, we investigated the involvement of DELLA proteins in Suc-induced hypocotyl elongation under light/dark cycles. The *gai-1* mutant harbors a deletion within the DELLA domain of *GIBBERELLIC ACID INSENSITIVE* (*GAI*), which prevents GA-induced proteasomal degradation of *GAI* (Peng et al., 1997; Fu et al., 2002). Under 4-h photoperiods, Suc supplementation increased hypocotyl length in *gai-1*, but the magnitude of Suc-induced elongation in *gai-1* was reduced compared with the wild type (hypocotyls became 36.5% longer in *gai-1* in response to Suc, compared with 59.2% longer in the wild type; Fig. 5B). Under 16-h photoperiods, Suc did not induce hypocotyl elongation in the wild type or *gai-1* (Fig. 5B), which is consistent with Figure 1, B and C. We also examined the effect of a mutant lacking all

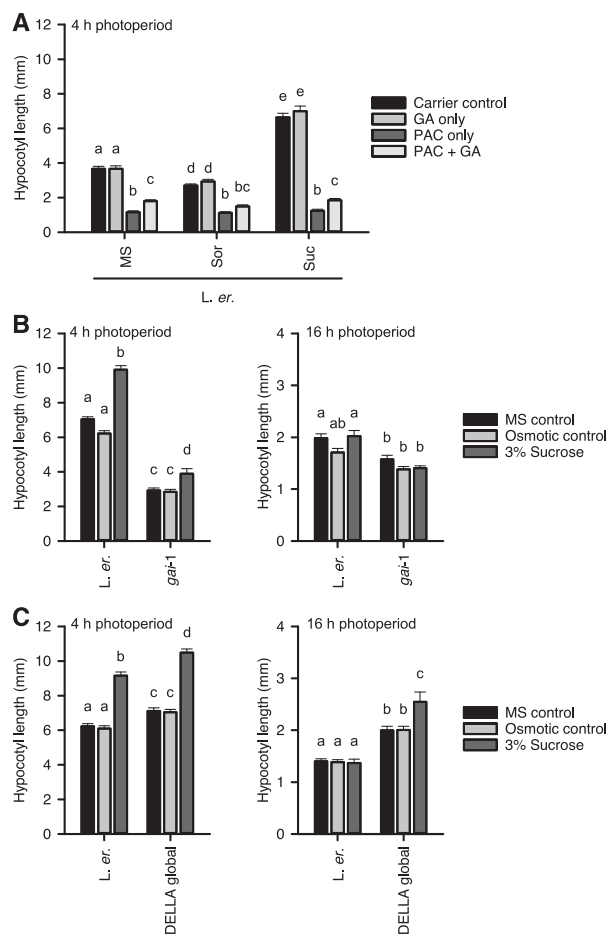


**Figure 5.** Gibberellin signals contribute to Suc-induced hypocotyl elongation under short photoperiods. A, The GA biosynthesis inhibitor PAC at 20  $\mu\text{M}$  inhibits Suc-induced hypocotyl elongation. Seedlings were germinated on MS agar and transferred to treatment media after germination; carrier control was 0.12% (v/v) methanol. B, Suc-induced hypocotyl elongation was attenuated in *gai-1* mutant seedlings. C, Suc-induced hypocotyl elongation was unaltered in a DELLA global knockout mutant. Experiments performed under 4-h photoperiods. Data are mean  $\pm$  SE ( $n = 20$ ) from one of two independent repeats, analyzed with ANOVA and posthoc Tukey tests. Different letters indicate statistically significant differences between means ( $P < 0.05$ ). Osmotic control was 87.6 mM sorbitol.

five DELLA proteins upon Suc-induced hypocotyl elongation under light/dark cycles (Koini et al., 2009). Under short photoperiods, Suc-induced hypocotyl elongation was unaltered in this mutant (Fig. 5C). Interestingly, under long photoperiods Suc promoted hypocotyl elongation in the DELLA global mutant, whereas Suc was without effect upon wild-type hypocotyls (Fig. 5C). The partial attenuation of Suc-induced hypocotyl elongation in *gai-1* (Fig. 5B) combined with the derepression of Suc-induced hypocotyl elongation under long photoperiods in the DELLA global mutant (Fig. 5C) suggests that DELLA-mediated GA signaling

contributes to, but does not exclusively control, Suc-induced hypocotyl elongation.

#### Phytohormone Signaling and Suc-Induced Hypocotyl Elongation under Light/Dark Cycles: Abscisic Acid

ABA suppresses seedling development (Belin et al., 2009) and several studies have linked Tre6P and abscisic acid (ABA) signaling (Avonce et al., 2004; Ramon et al., 2007; Gómez et al., 2010; Debast et al., 2011). Therefore, we investigated whether ABA signaling contributes to Suc-induced hypocotyl elongation under light/dark cycles. Suc-induced hypocotyl elongation was unaffected by the ABA receptor quadruple mutant *pyr1-1 pyl1-1 pyl2-1 pyl4-1*, which is highly ABA-insensitive (Park et al., 2009; Supplemental Fig. S5). This suggests that PYR/PYL-mediated ABA signaling does not participate in the mechanisms underlying Suc-induced hypocotyl elongation under light/dark cycles.

## DISCUSSION

#### KIN10 and TPS1 Contribute to Sugar-Induced Hypocotyl Elongation under Light/Dark Cycles

Here, we make the new finding that a mechanism involving KIN10 activity and Tre6P metabolism regulates Suc-induced hypocotyl elongation under light/dark cycles. Although hypocotyl elongation arises from cell expansion rather than growth through increases in cell number (Gendreau et al., 1997), our data are consistent with studies demonstrating that Tre6P metabolism is a crucial regulator of growth responses to Suc. For example, *Arabidopsis* seedlings overexpressing the bacterial Tre6P phosphatase *otsB*, which reduces [Tre6P], accumulate less biomass compared with the wild type when supplemented with Suc (Schluepmann et al., 2003). The converse is also true; *otsA* (TPS) overexpressors, in which [Tre6P] is increased, accumulate more biomass than the wild type when supplemented with Suc (Schluepmann et al., 2003). Therefore, our data using *tps1* mutants as a proxy for altered Tre6P metabolism provide new evidence to support the notion that Tre6P promotes growth under conditions of increased Suc availability (Schluepmann et al., 2003; Zhang et al., 2009).

Overexpression in *Arabidopsis* of the bacterial Tre6P synthase *otsA* has been reported to produce seedlings having shorter hypocotyls than the wild type (Paul et al., 2010). The Suc-insensitivity of hypocotyl elongation in *tps1* mutants (Fig. 1) and the shorter hypocotyls in seedlings with increased [Tre6P] (*otsA-ox*) may appear to conflict with each other (Paul et al., 2010). However, the experiments are not directly comparable. We found that exogenous Suc only caused hypocotyl elongation under short photoperiods or lower light conditions (Fig. 2). In comparison, the *otsA-ox* experiments involved 16-h photoperiods at

higher PAR ( $150 \mu\text{mol m}^{-2} \text{s}^{-1}$ ) and shaking liquid culture (Zhang et al., 2009), both of which could mask the hypocotyl elongation response that we investigated.

Our experiments suggest that increased KIN10 activity might attenuate the elongation response of hypocotyls to exogenous Suc under light/dark cycles. The KIN10-ox lines that we used overexpress the catalytic subunit of SnRK1 (Baena-González et al., 2007). KIN10 overexpression down-regulates transcripts associated with anabolic processes and up-regulates transcripts associated with energy starvation (Baena-González et al., 2007). Therefore, in our experiments KIN10 overexpression may have stopped seedlings from taking advantage of the greater energy availability caused by Suc supplementation, thereby preventing Suc-induced hypocotyl elongation in KIN10-ox (Fig. 1).

#### Photoperiod-Dependency of Sugar-Induced Hypocotyl Elongation

We made the new finding that under relatively high light, exogenous Suc increases hypocotyl length in photoperiods of 8 h and shorter, but not under long photoperiods or constant light (Figs. 1 and 2). These data reconcile differences between previous studies of Suc-induced hypocotyl elongation. Previous studies reporting Suc-insensitivity of hypocotyl elongation in the light were conducted in continuous light (Zhang et al., 2010), in which we also found Suc to be without effect upon hypocotyls (Figs. 1B and 2A). In comparison, studies reporting that Suc does promote hypocotyl elongation in the light were conducted under 8-h photoperiods (Stewart et al., 2011; Lilley et al., 2012), where we likewise found that Suc causes hypocotyl elongation (Figs. 1B and 2). Therefore, the sensitivity of hypocotyls to Suc-induced elongation depends upon the photoperiod or the amount of light received each day.

One explanation for this response could be that the daily quantity of light determines the magnitude of Suc-induced hypocotyl elongation through the accumulation of photosynthetic metabolites. Our experiments indicate that under shorter photoperiods, the sensitivity of hypocotyl elongation to Suc depends upon the total amount of daily light (Fig. 2, A, D, and E). Furthermore, Suc-induced hypocotyl elongation under long photoperiods only occurred when the seedlings were under lower light conditions (Fig. 2, A to C). One interpretation is that under long photoperiods and higher light, cells are replete with sugars (Sulpice et al., 2014), therefore supplementation with exogenous Suc has a relatively small effect upon the hypocotyl length of already sugar-rich seedlings. In contrast, under short photoperiods or lower light, the background level of endogenous sugar is lower (Sulpice et al., 2014), so supplementation with exogenous Suc has a greater effect upon hypocotyl length.

An alternative interpretation is that PIFs integrate light signals derived from photoreceptors with

SnRK1-mediated sugar signals to modulate the sensitivity of elongating hypocotyls to Suc, because PIFs are required for Suc-induced hypocotyl elongation (Stewart et al., 2011; Lilley et al., 2012). This might explain the PAR-independent reduction in Suc-induced hypocotyl elongation that occurred under long photoperiods (Fig. 2C). In the future, it will be informative to resolve the relative contributions of these mechanisms to Suc-induced hypocotyl elongation, given that Tre6P can regulate expression of both PIFs and auxin signaling genes (Paul et al., 2010). This could provide insights into the nature of the coupling of SnRK1-mediated sugar signaling and growth regulation by PIFs (Paul et al., 2010; Stewart et al., 2011; Lilley et al., 2012).

### Involvement of Phytohormone Signals in Suc-Induced Hypocotyl Elongation under Light/Dark Cycles

Auxin, GA, and brassinosteroids are reported to mediate Suc-induced hypocotyl elongation, with a role for auxin identified under light/dark cycles and roles for GA and brassinosteroids identified under extended darkness (de Lucas et al., 2008; Zhang et al., 2010, 2015, 2016; Liu et al., 2011; Stewart et al., 2011; Lilley et al., 2012;). Consistent with this, our data indicate that auxin signaling has a major role in Suc-induced hypocotyl elongation under light/dark cycles (Fig. 4A), with GA signaling also contributing to this process (Fig. 5, B and C). We suggest two possible reasons why paclobutrazol completely abolished Suc-induced hypocotyl elongation (Fig. 5A), whereas the *gai-1* mutant only led to partial inhibition of this phenotype (Fig. 5B). One possibility is that DELLA-independent GA signaling contributes to Suc-induced hypocotyl elongation, because DELLA proteins control approximately 40% to 60% of GA-regulated transcripts (Cao et al., 2006). An alternative possibility is that these were off-target or ectopic effects of paclobutrazol, because the paclobutrazol-induced attenuation of hypocotyl elongation was not rescued fully by GA supplementation (Fig. 5A).

Auxin-induced expansins that are up-regulated during hypocotyl elongation were also induced by Suc supplementation (Fig. 4, B to E; Supplemental Fig. S2). Although *EXPA11* was induced strongly by Suc, the small response of *EXPA8* to Suc in the wild type makes it difficult to interpret the responses of *EXPA8* to Suc in KIN10-ox and the *tps1* mutants (Fig. 4, B and C). Interestingly, Suc induction of *EXPA11* was abolished in KIN10-ox, suggesting a role for KIN10 in expansin gene expression within elongating hypocotyls. In comparison, these expansins were Suc-inducible in *tps1-11* and *tps1-12* (Fig. 4, B to E). One possible explanation is that KIN10-ox causes a much greater level of SnRK1 activity compared with the *tps* mutants, which are hypomorphic alleles that harbor reduced Tre6P concentrations (Gómez et al., 2010) and are not completely deficient in Suc-induced hypocotyl elongation (Fig. 1, D and E).

An alternative and speculative explanation for the different behavior of expansin transcripts in KIN10-ox

and *tps* mutants could relate to Tre6P-KIN10 regulating growth through two broad processes—first, through direct signaling effects upon growth (e.g. by regulating auxin signals), and second, through metabolic effects, such as growth constraints due to altered nocturnal catabolism. This could point to TPS1 and SnRK1 making independent contributions to Suc-induced hypocotyl elongation under light/dark cycles, potentially through separate signaling and metabolic effects, rather than acting in series. Our data suggest that Suc-induced hypocotyl elongation under light/dark cycles includes a signaling effect, previously proposed to occur through PIF-regulated auxin signals (Stewart et al., 2011; Lilley et al., 2012). On the other hand, the unexpected behavior of expansin transcripts in *tps1* mutants (Fig. 1, D and E) suggests that mechanisms additional to auxin/GA signaling might contribute to Suc-induced hypocotyl elongation under light/dark cycles. These additional mechanisms could involve brassinosteroid and/or TOR signaling, which are required for Suc-induced increases in hypocotyl length under extended darkness (Zhang et al., 2015, 2016). It would be informative in future to investigate the cross talk between SnRK1 and TOR energy signaling during hypocotyl elongation, to gain insights into the relative importance of these energy management pathways to the below-ground (darkness) and above-ground (light/dark cycles) stages of seedling establishment.

### CONCLUSIONS

We identified a novel role for the SnRK1 energy signaling hub in the regulation of Suc-induced hypocotyl elongation under light/dark cycles. We propose that KIN10 could be positioned upstream from the auxin and GA signals that lead to Suc-induced hypocotyl elongation in the light (Liu et al., 2011; Stewart et al., 2011; Lilley et al., 2012). A question for future investigation concerns the functional organization of this pathway. In one scenario, KIN10-mediated energy signaling regulates hypocotyl elongation by acting upon phytohormone signaling, potentially through PIFs (Lilley et al., 2012). In a different and nonexclusive scenario, SnRK1-mediated alterations in metabolic enzyme activity and growth-related transcripts prime the hypocotyls to capitalize upon increased Suc availability (Nunes et al., 2013a). This is an interesting question in the case of hypocotyl elongation, which arises from cell expansion rather than growth through cell division and biomass accumulation per se (Gendreau et al., 1997). These two possibilities are nonexclusive, because the phenotypic differences that we report between KIN10-ox lines and *tps1* mutants (e.g. expansin transcript accumulation; Fig. 4) could implicate more than one mechanism in Suc-induced hypocotyl elongation.

A further question for future investigation is of the nature of the interplay among KIN10/Tre6P, TOR, and brassinosteroids in the regulation of hypocotyl elongation in response to sugars. One speculative

hypothesis is that under conditions of starvation, such as when a developing below-ground seedling is exhausting its seed-based energy store, brassinosteroid signaling produces a strong elongation cue to drive seedling emergence into the light (Zhang et al., 2015, 2016). Then, once the seedling has emerged into the daily cycles of light and dark, KIN10/Tre6P adjusts the elongation of hypocotyls to allow optimal seedling establishment under local light conditions (Figs. 1 and 2). It is possible that increased SnRK1 activity under conditions of transiently low light, for example due to unpredictable changes in the weather, operates alongside phototransduction pathways to prevent inappropriate etiolation after seedling emergence. Therefore, one potential function of the mechanism that we identified might be to adapt the rate of seedling development to optimize the use of seed and photosynthetic resources under fluctuating light environments.

## MATERIALS AND METHODS

### Plant Material and Growth Conditions

*Arabidopsis* (*Arabidopsis thaliana* (L.) Heynh.) seeds were surface-sterilized and sown on half-strength Murashige & Skoog (MS) basal salt mixture (0.5 MS; Duchefa) with 0.8% (w/v) agar (Noordally et al., 2013). Seeds were then stratified (3 d at 4°C) and germinated and grown for 7 d under 100  $\mu\text{mol m}^{-2} \text{s}^{-1}$  of white light at 19°C, except Figure 2, B to E, where PAR was reduced. Media was supplemented with either 3% (w/v) Suc (87.6 mM) or 87.6 mM sorbitol as an osmotic control, according to the experiment. For experiments investigating gibberellin signaling, media was supplemented with 20  $\mu\text{M}$  paclobutrazol (PAC) and 100  $\mu\text{M}$  gibberellic acid (GA<sub>3</sub> form, both Sigma-Aldrich) with a methanol carrier. Paclobutrazol is effective for studies of GA signaling during development at the concentration of 20  $\mu\text{M}$  (Penfield et al., 2004; MacGregor et al., 2015). For experiments investigating auxin signaling, media was supplemented with *N*-1-naphthylphthalamic acid (NPA) (Sigma-Aldrich) at up to 10  $\mu\text{M}$  with a DMSO carrier. Controls were supplemented with the appropriate carrier at the same concentration as treatment media (0.1% (v/v) DMSO for NPA; 0.12% (v/v) methanol for PAC and GA).

To transfer growing seedlings to media containing GA or PAC, surface-sterilized and stratified seeds were pipetted onto 1- $\mu\text{m}$ -pore-diameter nylon mesh (Normesh), on top of 0.5 MS 0.8% (w/v) agar, and allowed to germinate for 3 d. Seedlings were then transferred to 0.5 MS supplemented with either 3% (w/v) Suc (87.6 mM) or 87.6 mM sorbitol, plus 20  $\mu\text{M}$  PAC, 100  $\mu\text{M}$  GA, or both PAC and GA. Hypocotyls were measured after 5-d growth on treatment plates. For experiments with circadian oscillator mutants, we did not use arrhythmic CCA1-ox plants because overexpression of CCA1 causes very long hypocotyls (Wang and Tobin, 1998), which would confound investigation of the role of sugars in hypocotyl elongation.

Genotypes used were *tps1* TILLING mutants (Gómez et al., 2010), KIN10-ox (Baena-González et al., 2007), *gin2-1* (Moore et al., 2003), *gai-1* (Koorneef et al., 1985), DELLA global mutant (Koini et al., 2009), *pyr1 pyl1 pyl2 pyl4* (Park et al., 2009), *cca1-11 lhy-21 toc1-21* (Ding et al., 2007), *gi-11* (Richardson et al., 1998), and *prr7-11* (Yamamoto et al., 2003; Nakamichi et al., 2005). In the KIN10-ox lines, KIN10 transcript abundance was 17-fold greater than the wild type in elongating hypocotyls (Supplemental Fig. S6A). In the *tps1-11* and *tps1-12* alleles, *TPS1* transcript abundance was unchanged (*tps1-11*) or slightly increased (*tps1-12*) compared with the wild type (Supplemental Fig. S6B). This result for the *tps1* alleles was unsurprising, because these are mis-sense mutants rather than insertion mutants (Gómez et al., 2010).

### Hypocotyl Measurement

Seedlings were grown on square petri dishes within temperature-controlled growth chambers (MLR-352; Panasonic). Plates were angled at approximately 45 degrees to allow hypocotyls to elongate without touching lids. Hypocotyls were measured by positioning 7-d-old seedlings on the surface of 1% (w/v) agar

for photography (D50; Nikon) and subsequent measurement using the ImageJ software (<https://imagej.nih.gov/ij/>).

### RNA Extraction and qRT-PCR

RNA was extracted according to Noordally et al. (2013), using the Machery-Nagel Nucleospin II plant RNA extraction kit incorporating DNase I treatment (Thermo Fisher Scientific), except approximately 60 seedlings were used per RNA sample. cDNA was synthesized using the High Capacity cDNA Reverse Transcription Kit with RNase Inhibitor (Applied Biosystems), according to manufacturer's instructions. cDNA was analyzed using an MXPro 3005 real time PCR system (Agilent) with Brilliant III Ultra-Fast SYBR qPCR mastermix (Agilent; primers are given in Supplemental Table S1). At least two technical repeats were performed for each qRT-PCR reaction. Data were analyzed using the  $\Delta\Delta\text{Ct}$  method, with *PROTEIN PHOSPHATASE 2A SUBUNIT A3* (*PP2AA3*) as a reference transcript.

### Accession Numbers

*Arabidopsis* Genome Initiative identifiers for the genes mentioned in this study are: KIN10 (At3g01090), *TPS1* (At1g78580), *HEXOKINASE1* (At4g29130), *CCA1* (At2g46830), *LHY* (At1g01060), *TOC1* (At5g61380), *GI* (At1g22770), *PRR7* (At5g02810), *EXPA4* (At2g39700), *EXPA8* (At2g40610), *EXPA11* (At1g20190), *YUCCA8* (At4g28720), *YUCCA9* (At1g04180), *CYP79B3* (At2g22330), *IAA29* (At4g32280), and *SAUR15* (At4g38850).

### Supplemental Data

The following supplemental materials are available.

**Supplemental Figure S1.** The *cca1-11 lhy-21 toc1-21* triple mutant does not alter Suc-induced hypocotyl elongation (direct repeat of Fig. 3A).

**Supplemental Figure S2.** Selection of expansin transcripts for experimentation.

**Supplemental Figure S3.** Suc supplementation of growth media did not alter abundance of auxin biosynthesis transcripts or auxin-responsive transcripts relative to osmotic controls.

**Supplemental Figure S4.** Efficacy of GA<sub>3</sub> used for study.

**Supplemental Figure S5.** ABA signaling is not required for Suc-induced hypocotyl elongation under short photoperiods.

**Supplemental Figure S6.** KIN10 and *TPS1* transcript abundance in KIN10-ox and *tps1* TILLING mutants.

**Supplemental Table S1.** qRT-PCR primer sequences.

### ACKNOWLEDGMENTS

We thank Ian Graham (York), Filip Rolland (KU Leuven), Kerry Franklin (Bristol), Jean-Charles Isner (Bristol), Nicholas Harberd (Oxford), and Alex Webb (Cambridge) for seed donation, and Ian Graham for the discussion and encouragement that led to this work. We thank Kerry Franklin and Brendan Davies (Leeds) for critical feedback.

Received October 3, 2017; accepted November 5, 2017; published November 7, 2017.

### LITERATURE CITED

- Avonce N, Leyman B, Mascorro-Gallardo JO, van Dijk P, Thevelein JM, Iturriaga G (2004) The *Arabidopsis* trehalose-6-P synthase *AtTPS1* gene is a regulator of glucose, abscisic acid, and stress signaling. *Plant Physiol* **136**: 3649–3659
- Baena-González E, Rolland F, Thevelein JM, Sheen J (2007) A central integrator of transcription networks in plant stress and energy signaling. *Nature* **448**: 938–942
- Baena-González E, Sheen J (2008) Convergent energy and stress signaling. *Trends Plant Sci* **13**: 474–482
- Belin C, Megies C, Hauserová E, Lopez-Molina L (2009) Abscisic acid represses growth of the *Arabidopsis* embryonic axis after germination by enhancing auxin signaling. *Plant Cell* **21**: 2253–2268

- Boylan MT, Quail PH (1991) Phytochrome a overexpression inhibits hypocotyl elongation in transgenic Arabidopsis. *Proc Natl Acad Sci USA* **88**: 10806–10810
- Cao D, Cheng H, Wu W, Soo HM, Peng J (2006) Gibberellin mobilizes distinct DELLA-dependent transcriptomes to regulate seed germination and floral development in Arabidopsis. *Plant Physiol* **142**: 509–525
- Casal JJ (2013) Photoreceptor signaling networks in plant responses to shade. *Annu Rev Plant Biol* **64**: 403–427
- Cheng H, Qin L, Lee S, Fu X, Richards DE, Cao D, Luo D, Harberd NP, Peng J (2004) Gibberellin regulates Arabidopsis floral development via suppression of DELLA protein function. *Development* **131**: 1055–1064
- Collett CE, Harberd NP, Leyser O (2000) Hormonal interactions in the control of Arabidopsis hypocotyl elongation. *Plant Physiol* **124**: 553–562
- Cowling RJ, Harberd NP (1999) Gibberellins control Arabidopsis hypocotyl growth via regulation of cellular elongation. *J Exp Bot* **50**: 1351–1357
- Crawford AJ, McLachlan DH, Hetherington AM, Franklin KA (2012) High temperature exposure increases plant cooling capacity. *Curr Biol* **22**: R396–R397
- Dalchau N, Baek SJ, Briggs HM, Robertson FC, Dodd AN, Gardner MJ, Stancombe MA, Haydon MJ, Stan G-B, Gonçalves JM, Webb AAR (2011) The circadian oscillator gene GIGANTEA mediates a long-term response of the *Arabidopsis thaliana* circadian clock to sucrose. *Proc Natl Acad Sci USA* **108**: 5104–5109
- Debast S, Nunes-Nesi A, Hajirezaei MR, Hofmann J, Sonnewald U, Fernie AR, Börnke F (2011) Altering trehalose-6-phosphate content in transgenic potato tubers affects tuber growth and alters responsiveness to hormones during sprouting. *Plant Physiol* **156**: 1754–1771
- Delatte TL, Sedijani P, Kondou Y, Matsui M, de Jong GJ, Somsen GW, Wiese-Klinkenberg A, Primavesi LF, Paul MJ, Schlupepmann H (2011) Growth arrest by trehalose-6-phosphate: an astonishing case of primary metabolite control over growth by way of the SnRK1 signaling pathway. *Plant Physiol* **157**: 160–174
- Delorge I, Figueroa CM, Feil R, Lunn JE, van Dijk P (2015) Trehalose-6-phosphate synthase 1 is not the only active TPS in *Arabidopsis thaliana*. *Biochem J* **466**: 283–290
- de Lucas M, Davière JM, Rodríguez-Falcón M, Pontin M, Iglesias-Pedraz JM, Lorrain S, Fankhauser C, Blázquez MA, Titarenko E, Prat S (2008) A molecular framework for light and gibberellin control of cell elongation. *Nature* **451**: 480–484
- Ding Z, Doyle MR, Amasino RM, Davis SJ (2007) A complex genetic interaction between *Arabidopsis thaliana* TOC1 and CCA1/LHY in driving the circadian clock and in output regulation. *Genetics* **176**: 1501–1510
- Dobrenel T, Marchive C, Sormani R, Moreau M, Mozzo M, Montané M-H, Menand B, Robaglia C, Meyer C (2011) Regulation of plant growth and metabolism by the TOR kinase. *Biochem Soc Trans* **39**: 477–481
- Dowson-Day MJ, Millar AJ (1999) Circadian dysfunction causes aberrant hypocotyl elongation patterns in Arabidopsis. *Plant J* **17**: 63–71
- Esmon CA, Tinsley AG, Ljung K, Sandberg G, Hearne LB, Liscum E (2006) A gradient of auxin and auxin-dependent transcription precedes tropic growth responses. *Proc Natl Acad Sci USA* **103**: 236–241
- Fu X, Richards DE, Ait-Ali T, Hynes LW, Ougham H, Peng J, Harberd NP (2002) Gibberellin-mediated proteasome-dependent degradation of the barley DELLA protein SLN1 repressor. *Plant Cell* **14**: 3191–3200
- Gangappa SN, Kumar SV (2017) DET1 and HY5 control PIF4-mediated thermosensory elongation growth through distinct mechanisms. *Cell Reports* **18**: 344–351
- Gendreau E, Traas J, Desnos T, Grandjean O, Caboche M, Höfte H (1997) Cellular basis of hypocotyl growth in *Arabidopsis thaliana*. *Plant Physiol* **114**: 295–305
- Goda H, Sawa S, Asami T, Fujioka S, Shimada Y, Yoshida S (2004) Comprehensive comparison of auxin-regulated and brassinosteroid-regulated genes in Arabidopsis. *Plant Physiol* **134**: 1555–1573
- Gómez LD, Baud S, Gilday A, Li Y, Graham IA (2006) Delayed embryo development in the ARABIDOPSIS TREHALOSE-6-PHOSPHATE SYNTHASE 1 mutant is associated with altered cell wall structure, decreased cell division and starch accumulation. *Plant J* **46**: 69–84
- Gómez LD, Gilday A, Feil R, Lunn JE, Graham IA (2010) AtTPS1-mediated trehalose 6-phosphate synthesis is essential for embryogenic and vegetative growth and responsiveness to ABA in germinating seeds and stomatal guard cells. *Plant J* **64**: 1–13
- Graf A, Schlereth A, Stitt M, Smith AM (2010) Circadian control of carbohydrate availability for growth in Arabidopsis plants at night. *Proc Natl Acad Sci USA* **107**: 9458–9463
- Griffiths CA, Sagar R, Geng Y, Primavesi LF, Patel MK, Passarelli MK, Gilmore IS, Steven RT, Bunch J, Paul MJ, Davis BG (2016) Chemical intervention in plant sugar signalling increases yield and resilience. *Nature* **540**: 574–578
- Haydon MJ, Mielczarek O, Robertson FC, Hubbard KE, Webb AAR (2013) Photosynthetic entrainment of the *Arabidopsis thaliana* circadian clock. *Nature* **502**: 689–692
- Hayes S, Velanis CN, Jenkins GI, Franklin KA (2014) UV-B detected by the UVR8 photoreceptor antagonizes auxin signaling and plant shade avoidance. *Proc Natl Acad Sci USA* **111**: 11894–11899
- Jang JC, León P, Zhou L, Sheen J (1997) Hexokinase as a sugar sensor in higher plants. *Plant Cell* **9**: 5–19
- Keuskamp DH, Pollmann S, Voeselek LACJ, Peeters AJM, Pierik R (2010) Auxin transport through PIN-FORMED 3 (PIN3) controls shade avoidance and fitness during competition. *Proc Natl Acad Sci USA* **107**: 22740–22744
- Kim BC, Tennessen DJ, Last RL (1998) UV-B-induced photomorphogenesis in *Arabidopsis thaliana*. *Plant J* **15**: 667–674
- Koini MA, Alvey L, Allen T, Tilley CA, Harberd NP, Whitelam GC, Franklin KA (2009) High temperature-mediated adaptations in plant architecture require the bHLH transcription factor PIF4. *Curr Biol* **19**: 408–413
- Koorneef M, Elgersma A, Hanhart CJ, van Loenen-Martinet EP, van Rijn L, Zeevaert JAD (1985) A gibberellin insensitive mutant of *Arabidopsis thaliana*. *Physiol Plant* **65**: 33–39
- Kurata T, Yamamoto KT (1998) *petit1*, a conditional growth mutant of Arabidopsis defective in sucrose-dependent elongation growth. *Plant Physiol* **118**: 793–801
- Lee DJ, Park JW, Lee HW, Kim J (2009) Genome-wide analysis of the auxin-responsive transcriptome downstream of *iaa1* and its expression analysis reveal the diversity and complexity of auxin-regulated gene expression. *J Exp Bot* **60**: 3935–3957
- Leivar P, Quail PH (2011) PIFs: pivotal components in a cellular signaling hub. *Trends Plant Sci* **16**: 19–28
- Li Y, Darley CP, Ongaro V, Fleming A, Schipper O, Baldauf SL, McQueen-Mason SJ (2002) Plant expansins are a complex multigene family with an ancient evolutionary origin. *Plant Physiol* **128**: 854–864
- Li Y, van den Ende W, Rolland F (2014) Sucrose induction of anthocyanin biosynthesis is mediated by DELLA. *Mol Plant* **7**: 570–572
- Lilley JL, Gee CW, Sairanen I, Ljung K, Nemhauser JL (2012) An endogenous carbon-sensing pathway triggers increased auxin flux and hypocotyl elongation. *Plant Physiol* **160**: 2261–2270
- Lincoln C, Britton JH, Estelle M (1990) Growth and development of the *axr1* mutants of Arabidopsis. *Plant Cell* **2**: 1071–1080
- Liscum E, Hangarter RP (1991) Arabidopsis mutants lacking blue light-dependent inhibition of hypocotyl elongation. *Plant Cell* **3**: 685–694
- Liu Z, Zhang Y, Liu R, Hao H, Wang Z, Bi Y (2011) Phytochrome interacting factors (PIFs) are essential regulators for sucrose-induced hypocotyl elongation in Arabidopsis. *J Plant Physiol* **168**: 1771–1779
- Lorrain S, Allen T, Duek PD, Whitelam GC, Fankhauser C (2008) Phytochrome-mediated inhibition of shade avoidance involves degradation of growth-promoting bHLH transcription factors. *Plant J* **53**: 312–323
- Lunn JE, Feil R, Hendriks JHM, Gibon Y, Morcuende R, Osuna D, Scheible WR, Carillo P, Hajirezaei MR, Stitt M (2006) Sugar-induced increases in trehalose 6-phosphate are correlated with redox activation of ADP-glucose pyrophosphorylase and higher rates of starch synthesis in *Arabidopsis thaliana*. *Biochem J* **397**: 139–148
- MacGregor DR, Kendall SL, Florance H, Fedi F, Moore K, Paszkiewicz K, Smirnov N, Penfield S (2015) Seed production temperature regulation of primary dormancy occurs through control of seed coat phenylpropanoid metabolism. *New Phytol* **205**: 642–652
- Mair A, Pedrotti L, Wurzinger B, Anrather D, Simeunovic A, Weiste C, Valerio C, Dietrich K, Kirchlner T, Nägele T, Vicente Carbajosa J, Hanson J, et al (2015) SnRK1-triggered switch of bZIP63 dimerization mediates the low-energy response in plants. *eLife* **4**: 10.7554/eLife.05828
- Más P, Alabadi D, Yanovsky MJ, Oyama T, Kay SA (2003) Dual role of TOC1 in the control of circadian and photomorphogenic responses in Arabidopsis. *Plant Cell* **15**: 223–236
- Mattioli CC, Tomaz JP, Duarte GT, Prado FM, Del Bem LEV, Silveira AB, Gauer L, Corrêa LGG, Drummond RD, Viana AJC, Di Mascio P, Meyer C, et al (2011) The Arabidopsis bZIP gene AtbZIP63 is a sensitive

- integrator of transient abscisic acid and glucose signals. *Plant Physiol* 157: 692–705
- Miyazaki Y, Jikumaru Y, Takase T, Saitoh A, Sugitani A, Kamiya Y, Kiyosue T (2016) Enhancement of hypocotyl elongation by LOV KELCH PROTEIN2 production is mediated by auxin and phytochrome-interacting factors in *Arabidopsis thaliana*. *Plant Cell Rep* 35: 455–467
- Mizuno T, Nomoto Y, Oka H, Kitayama M, Takeuchi A, Tsubouchi M, Yamashino T (2014) Ambient temperature signal feeds into the circadian clock transcriptional circuitry through the EC night-time repressor in *Arabidopsis thaliana*. *Plant Cell Physiol* 55: 958–976
- Moore B, Zhou L, Rolland F, Hall Q, Cheng W-H, Liu Y-X, Hwang I, Jones T, Sheen J (2003) Role of the *Arabidopsis* glucose sensor HXK1 in nutrient, light, and hormonal signaling. *Science* 300: 332–336
- Nakamichi N, Kita M, Ito S, Yamashino T, Mizuno T (2005) PSEUDO-RESPONSE REGULATORS, PRR9, PRR7 and PRR5, together play essential roles close to the circadian clock of *Arabidopsis thaliana*. *Plant Cell Physiol* 46: 686–698
- Noordally ZB, Ishii K, Atkins KA, Wetherill SJ, Kusakina J, Walton EJ, Kato M, Azuma M, Tanaka K, Hanaoka M, Dodd AN (2013) Circadian control of chloroplast transcription by a nuclear-encoded timing signal. *Science* 339: 1316–1319
- Nozue K, Covington MF, Duek PD, Lorrain S, Fankhauser C, Harmer SL, Maloof JN (2007) Rhythmic growth explained by coincidence between internal and external cues. *Nature* 448: 358–361
- Nuccio ML, Wu J, Mowers R, Zhou H-P, Meghji M, Primavesi LF, Paul MJ, Chen X, Gao Y, Haque E, Basu SS, Lagrimini LM (2015) Expression of trehalose-6-phosphate phosphatase in maize ears improves yield in well-watered and drought conditions. *Nat Biotechnol* 33: 862–869
- Nunes C, O'Hara LE, Primavesi LF, Delatte TL, Schluepmann H, Somsen GW, Silva AB, Feveteiro PS, Wingler A, Paul MJ (2013a) The trehalose 6-phosphate/SnRK1 signaling pathway primes growth recovery following relief of sink limitation. *Plant Physiol* 162: 1720–1732
- Nunes C, Primavesi LF, Patel MK, Martinez-Barajas E, Powers SJ, Sagar R, Feveteiro PS, Davis BG, Paul MJ (2013b) Inhibition of SnRK1 by metabolites: tissue-dependent effects and cooperative inhibition by glucose 1-phosphate in combination with trehalose 6-phosphate. *Plant Physiol Biochem* 63: 89–98
- Nusinow DA, Helfer A, Hamilton EE, King JJ, Imaizumi T, Schultz TF, Farré EM, Kay SA (2011) The ELF4-ELF3-LUX complex links the circadian clock to diurnal control of hypocotyl growth. *Nature* 475: 398–402
- Park S, Fung P, Nishimura N, Jensen DR, Fujii H, Zhao Y, Lumba S, Santiago J, Rodrigues A, Chow TF, Alfred SE, Bonetta D, et al (2009) Abscisic acid inhibits PP2Cs via the PYR/PYL family of ABA-binding START proteins. *Science* 324: 1068–1071
- Paul MJ, Jhurreea D, Zhang Y, Primavesi LF, Delatte T, Schluepmann H, Wingler A (2010) Upregulation of biosynthetic processes associated with growth by trehalose 6-phosphate. *Plant Signal Behav* 5: 386–392
- Penfield S, Rylott EL, Gilday AD, Graham S, Larson TR, Graham IA (2004) Reserve mobilization in the *Arabidopsis* endosperm fuels hypocotyl elongation in the dark, is independent of abscisic acid, and requires PHOSPHOENOLPYRUVATE CARBOXYKINASE1. *Plant Cell* 16: 2705–2718
- Peng J, Carol P, Richards DE, King KE, Cowling RJ, Murphy GP, Harberd NP (1997) The *Arabidopsis* *GAI* gene defines a signaling pathway that negatively regulates gibberellin responses. *Genes Dev* 11: 3194–3205
- Ramon M, Rolland F, Thevelein JM, van Dijck P, Leyman B (2007) ABI4 mediates the effects of exogenous trehalose on *Arabidopsis* growth and starch breakdown. *Plant Mol Biol* 63: 195–206
- Richardson K, Fowler S, Pullen C, Skelton C, Morris B, Putterill J (1998) T-DNA tagging of a flowering-time gene and improved gene transfer by *in planta* transformation of *Arabidopsis*. *Funct Plant Biol* 25: 125–130
- Salter MG, Franklin KA, Whitelam GC (2003) Gating of the rapid shade-avoidance response by the circadian clock in plants. *Nature* 426: 680–683
- Schluepmann H, Pellny T, van Dijck A, Smeeckens S, Paul M (2003) Trehalose 6-phosphate is indispensable for carbohydrate utilization and growth in *Arabidopsis thaliana*. *Proc Natl Acad Sci USA* 100: 6849–6854
- Shin J, Sánchez-Villarreal A, Davis AM, Du SX, Berendzen KW, Koncz C, Ding Z, Li C, Davis SJ (2017) The metabolic sensor AKIN10 modulates the *Arabidopsis* circadian clock in a light-dependent manner. *Plant Cell Environ* 40: 997–1008
- Smeeckens S, Ma J, Hanson J, Rolland F (2010) Sugar signals and molecular networks controlling plant growth. *Curr Opin Plant Biol* 13: 274–279
- Stewart JL, Maloof JN, Nemhauser JL (2011) PIF genes mediate the effect of sucrose on seedling growth dynamics. *PLoS One* 6: e19894
- Sulpice R, Flis A, Ivakov AA, Apelt F, Krohn N, Encke B, Abel C, Feil R, Lunn JE, Stitt M (2014) *Arabidopsis* coordinates the diurnal regulation of carbon allocation and growth across a wide range of photoperiods. *Mol Plant* 7: 137–155
- Takahashi F, Sato-Nara K, Kobayashi K, Suzuki M, Suzuki H (2003) Sugar-induced adventitious roots in *Arabidopsis* seedlings. *J Plant Res* 116: 83–91
- Vandesteene L, Ramon M, Le Roy K, van Dijck P, Rolland F (2010) A single active trehalose-6-P synthase (TPS) and a family of putative regulatory TPS-like proteins in *Arabidopsis*. *Mol Plant* 3: 406–419
- Wahl V, Ponnu J, Schlereth A, Arrivault S, Langenecker T, Franke A, Feil R, Lunn JE, Stitt M, Schmid M (2013) Regulation of flowering by trehalose-6-phosphate signaling in *Arabidopsis thaliana*. *Science* 339: 704–707
- Wang Z-Y, Tobin EM (1998) Constitutive expression of the *CIRCADIAN CLOCK ASSOCIATED1* (*CCA1*) gene disrupts circadian rhythms and suppresses its own expression. *Cell* 93: 1207–1217
- Weinig C, Johnston JA, Willis CG, Maloof JN (2007) Antagonistic multi-level selection on size and architecture in variable density settings. *Evolution* 61: 58–67
- Wigge PA (2013) Ambient temperature signalling in plants. *Curr Opin Plant Biol* 16: 661–666
- Wingler A, Delatte TL, O'Hara LE, Primavesi LF, Jhurreea D, Paul MJ, Schluepmann H (2012) Trehalose 6-phosphate is required for the onset of leaf senescence associated with high carbon availability. *Plant Physiol* 158: 1241–1251
- Winter D, Vinegar B, Nahal H, Ammar R, Wilson GV, Provart NJ (2007) An “Electronic Fluorescent Pictograph” browser for exploring and analyzing large-scale biological data sets. *PLoS One* 2: e718
- Yadav UP, Ivakov A, Feil R, Duan GY, Walther D, Gialalisco P, Piques M, Carillo P, Hubberten H-M, Stitt M, Lunn JE (2014) The sucrose-trehalose 6-phosphate (Tre6P) nexus: specificity and mechanisms of sucrose signalling by Tre6P. *J Exp Bot* 65: 1051–1068
- Yamamoto Y, Sato E, Shimizu T, Nakamichi N, Sato S, Kato T, Tabata S, Nagatani A, Yamashino T, Mizuno T (2003) Comparative genetic studies on the *APRR5* and *APRR7* genes belonging to the *APRR1/TOC1* quintet implicated in circadian rhythm, control of flowering time, and early photomorphogenesis. *Plant Cell Physiol* 44: 1119–1130
- Zhang Y, Liu Z, Wang J, Chen Y, Bi Y, He J (2015) Brassinosteroid is required for sugar promotion of hypocotyl elongation in *Arabidopsis* in darkness. *Planta* 242: 881–893
- Zhang Y, Liu Z, Wang L, Zheng S, Xie J, Bi Y (2010) Sucrose-induced hypocotyl elongation of *Arabidopsis* seedlings in darkness depends on the presence of gibberellins. *J Plant Physiol* 167: 1130–1136
- Zhang Y, Primavesi LF, Jhurreea D, Andralojc PJ, Mitchell RAC, Powers SJ, Schluepmann H, Delatte T, Wingler A, Paul MJ (2009) Inhibition of SNF1-related protein kinase1 activity and regulation of metabolic pathways by trehalose-6-phosphate. *Plant Physiol* 149: 1860–1871
- Zhang Y, Shewry PR, Jones H, Barcelo P, Lazzeri PA, Halford NG (2001) Expression of antisense SnRK1 protein kinase sequence causes abnormal pollen development and male sterility in transgenic barley. *Plant J* 28: 431–441
- Zhang Z, Zhu J-Y, Roh J, Marchive C, Kim S-K, Meyer C, Sun Y, Wang W, Wang Z-Y (2016) TOR signaling promotes accumulation of BZR1 to balance growth with carbon availability in *Arabidopsis*. *Curr Biol* 26: 1854–1860

SHORT COMMUNICATION

OPEN ACCESS



## Involvement of the SnRK1 subunit KIN10 in sucrose-induced hypocotyl elongation

Noriane M. L. Simon, Ellie Sawkins, and Antony N. Dodd 

School of Biological Sciences, University of Bristol, Life Sciences Building, 24 Tyndall Avenue, Bristol BS8 1TQ, U.K.

### ABSTRACT

A mechanism participating in energy sensing and signalling in plants involves the regulation of sucrose non-fermenting1 (Snf1)-related protein kinase 1 (SnRK1) activity in response to sugar availability. SnRK1 is thought to regulate the activity of both metabolic enzymes and transcription factors in response to changes in energy availability, with trehalose-6-phosphate functioning as a signalling sugar that suppresses SnRK1 activity under sugar-replete conditions. Sucrose supplementation increases the elongation of hypocotyls of developing Arabidopsis seedlings, and this response to sucrose involves both the SnRK1 subunit KIN10 and also TREHALOSE-6-PHOSPHATE SYNTHASE1 (TPS1). Here, we measured sucrose-induced hypocotyl elongation in two insertional mutants of KIN10 (*akin10* and *akin10-2*). Under short photoperiods, sucrose supplementation caused great proportional hypocotyl elongation in these KIN10 mutants compared with the wild type, and these mutants had shorter hypocotyls than the wild type in the absence of sucrose supplementation. One interpretation is that SnRK1 activity might suppress hypocotyl elongation in the presence of sucrose, because KIN10 overexpression inhibits sucrose-induced hypocotyl elongation and *akin10* mutants enhance sucrose-induced hypocotyl elongation.

### ARTICLE HISTORY

Received 22 February 2018  
Revised 20 March 2018  
Accepted 21 March 2018

### KEYWORDS



Arabidopsis; signal transduction; metabolism; development


We reported recently the involvement of a sugar-signalling mechanism in a pathway that causes hypocotyl elongation in response to sucrose.<sup>1</sup> Hypocotyl elongation in *Arabidopsis thaliana* (Arabidopsis) seedlings is caused by cell expansion within the elongating hypocotyl and represents an informative experimental model to study signalling processes that regulate development. In Arabidopsis, hypocotyl length is increased by supplementation of the growth media with sucrose.<sup>2-9</sup> We identified that the sugar- and energy-sensing kinase sucrose non-fermenting1 (Snf1)-related protein kinase 1 (SnRK1) regulates sucrose-induced hypocotyl elongation.<sup>1</sup> Under short photoperiods, hypocotyls did not elongate in response to exogenous sucrose in seedlings overexpressing the catalytic alpha subunit of SnRK1, termed SNF1-RELATED PROTEIN KINASE1.1 (KIN10/AKIN10/SnRK1.1).<sup>1</sup> We also found that TREHALOSE-6-PHOSPHATE SYNTHASE1 (TPS1) is required for sucrose-induced hypocotyl elongation under short photoperiods.<sup>1</sup> TPS1 synthesizes the sugar trehalose-6-phosphate (Tre6P), which is a potent inhibitor of SnRK1 activity.<sup>10</sup> Tre6P is thought to function as a signalling sugar that provides information about cellular energy availability.<sup>10,11</sup>

Hypocotyl elongation in response to sucrose might be suppressed in overexpressors of KIN10 (KIN10-ox) because SnRK1 activity is thought to inhibit growth and catabolism under conditions of starvation,<sup>12-14</sup> preventing seedlings from taking advantage of the additional sugars.<sup>1</sup> We reasoned that the converse might be true when SnRK1 activity is low, as occurs under sugar-

replete conditions.<sup>10</sup> To investigate this, we measured the elongation of hypocotyls in response to sucrose in two T-DNA mutants of the KIN10 catalytic subunit of SnRK1 (GABI\_579E09 or *akin10*<sup>15</sup>, and SALKseq\_093965, a new allele named here *akin10-2* for consistency) (Fig S1A). The full-length KIN10 transcript is absent in these *akin10* and *akin10-2* T-DNA lines (Fig. S1B). In the *akin10* mutant, there is a partial loss of phosphorylation of the SnRK1 target bZIP63, most likely due to reduced SnRK1 activity.<sup>15</sup> The remaining phosphorylation of bZIP63 in *akin10* is likely due to KIN11 activity.<sup>15</sup>

Supplementation of wild type seedlings with 3% (w/v) sucrose increased the hypocotyl length under short photoperiods but not under long photoperiods (Fig. 1A, B), as we reported previously.<sup>1</sup> Sucrose supplementation also increased the hypocotyl length of two *akin10* mutants under both short and long photoperiods (Fig. 1A, B). Under short photoperiods, sucrose caused a greater increase in hypocotyl length in *akin10* (6.51 mm longer, 224% increase) and *akin10-2* (6.90 mm longer, 286% increase) compared with the wild type (3.75 mm longer, 67% increase) (Fig. 1A). This greater fold-change in hypocotyl length in the *akin10* mutants under these conditions is because the mutants had significantly shorter hypocotyls than the wild type in the absence of sucrose (Fig. 1A). Under long photoperiods, sucrose supplementation induced hypocotyl elongation in *akin10* mutants, which contrasted the wild type in which sucrose supplementation did not increase hypocotyl length (Fig. 1B). We found previously that sucrose supplementation can decrease the

**CONTACT** Antony N. Dodd  [antony.dodd@bristol.ac.uk](mailto:antony.dodd@bristol.ac.uk)  School of Biological Sciences, University of Bristol, Life Sciences Building, 24 Tyndall Avenue, Bristol BS8 1TQ, U.K.

 Supplemental data for this article can be accessed on the publisher's website.

© 2018 Noriane M. L. Simon, Ellie Sawkins, and Antony N. Dodd. Published with license by Taylor & Francis Group, LLC

This is an Open Access article distributed under the terms of the Creative Commons Attribution-NonCommercial-NoDerivatives License (<http://creativecommons.org/licenses/by-nc-nd/4.0/>), which permits non-commercial re-use, distribution, and reproduction in any medium, provided the original work is properly cited, and is not altered, transformed, or built upon in any way.



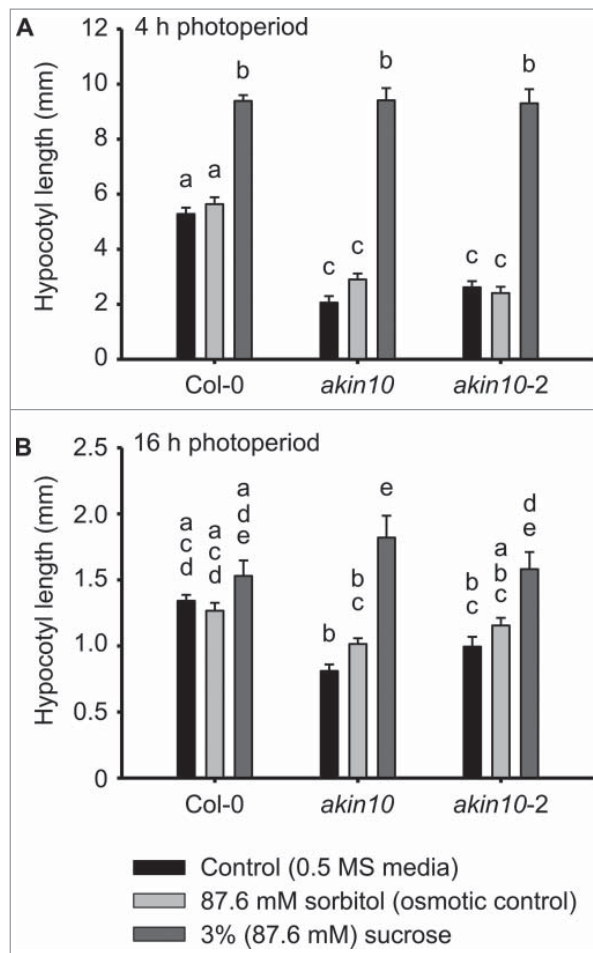


**Figure 1.** Sucrose-induced hypocotyl elongation in wild type and *akin10* seedlings measured under (A) 4 h and (B) 16 h photoperiods. Seedlings were cultivated on control media (half strength Murashige and Skoog medium with 0.8% (w/v) agar; 0.5 MS), an equimolar osmotic control (sorbitol), or 3% (w/v) sucrose. Measurement of hypocotyl elongation was conducted as described by Simon et al. 2018. Statistical significance indicated for comparison between seedlings supplemented with 3% (w/v) sucrose and 87.6 mM sorbitol (osmotic control); analysis by univariate ANOVA followed by post-hoc Tukey analysis. Different letters indicate statistically-significant differences between means ( $p < 0.05$ );  $n = 20 \pm$  s.e.m.

hypocotyl length of the Landsberg *erecta* background under long photoperiods,<sup>1</sup> but this did not occur in the Col-0 background used here (Fig. 1B), suggesting that there is some variation between accessions in this developmental response to sucrose.

Hypocotyls of *akin10* and *akin10-2* mutants were significantly shorter than the wild type when cultivated in the absence of sucrose on 0.5MS media (4 h photoperiods, *akin10*  $p < 0.001$ ; *akin10-2*  $p < 0.001$ ; 16 h photoperiods, *akin10*  $p < 0.006$ ; *akin10-2*  $p < 0.001$ ). In addition to changes in phytohormone signalling, the reduced hypocotyl elongation of *akin10* mutations might derive from altered seed quality,<sup>16</sup> attenuated seedling development as occurs in *tps1* knockouts,<sup>17</sup> altered circadian regulation,<sup>18</sup> or altered carbohydrate utilization.<sup>12,19</sup>

The greater proportional increase in hypocotyl length that was caused by sucrose in *akin10* mutants compared with the wild type suggests that SnRK1 activity might contribute to suppression of hypocotyl elongation in response to sucrose. This is because

KIN10 forms a catalytic subunit of SnRK1, and in the absence of this catalytic subunit there was an increase in the magnitude of sucrose-induced hypocotyl elongation. Although KIN10 and KIN11 are thought to confer kinase activity to the SnRK1 complex,<sup>12,15</sup> *akin10* single mutants change the response of elongating hypocotyls to sucrose (Fig. 1). This indicates that KIN11 cannot completely replace KIN10 within the mechanisms underlying sucrose-induced hypocotyl elongation. This is consistent with the loss of SnRK1 kinase activity in the *akin10* single mutant.<sup>15</sup> An alternative interpretation is that there is some suppression of hypocotyl elongation in the *akin10* mutants in the absence of sucrose, and that this phenotype is lost in the presence of sucrose supplementation (Fig. 1A). Under long photoperiods, sucrose does not cause hypocotyl elongation in the wild type (Fig. 1B), which appears to be due to a combination of photoperiod and daily light input.<sup>1</sup> In comparison, there was sucrose-induced hypocotyl elongation in two *akin10* mutants under long photoperiods. However, under 16 h photoperiods sucrose induced a smaller increase in hypocotyl length in the *akin10* mutants than in *akin10-2* mutants under 4 h photoperiods. Therefore, as with the wild type,<sup>1</sup> photoperiod and/or daily light input influence the magnitude of sucrose-induced hypocotyl elongation in *akin10* mutants. This suggests that mechanisms additional to KIN10 activity within SnRK1 contribute to the photoperiod/daily light input within the response of elongating hypocotyls to sucrose. Such additional mechanisms could include the circadian oscillator, phototransduction pathways, and additional energy-sensing mechanisms.

## Disclosure of potential conflicts of interest

The authors declare no potential conflicts of interest.

## Acknowledgments

We thank BBSRC (UK) for funding (South-West Doctoral Training Partnership grant BB/J014400/1). We thank Prof. Alistair Hetherington for donating *akin10* mutants and Dr. Jean-Charles Isner for discussion about reference transcripts.

## Funding

This work was supported by the Biotechnology and Biological Sciences Research Council (grant BB/J014400/1).

## ORCID

Antony N. Dodd  <http://orcid.org/0000-0001-6859-0105>

## References

- Simon NML, Kusakina J, Fernandez-Lopez A, Chembath A, Belbin FE, Dodd AN. The energy-signaling hub SnRK1 is important for sucrose-induced hypocotyl elongation. *Plant Physiol.* 2018;176:1299–310. doi:10.1104/pp.17.01395.
- Kurata T, Yamamoto KT. *petit1*, a conditional growth mutant of Arabidopsis defective in sucrose-dependent elongation growth. *Plant Physiol.* 1998;118:793. doi:10.1104/pp.118.3.793.
- Takahashi F, Sato-Nara K, Kobayashi K, Suzuki M, Suzuki H. Sugar-induced adventitious roots in Arabidopsis seedlings. *J Plant Res.* 2003;116:83–91.

4. Zhang Y, Liu Z, Wang L, Zheng S, Xie J, Bi Y. Sucrose-induced hypocotyl elongation of Arabidopsis seedlings in darkness depends on the presence of gibberellins. *J Plant Physiol.* **2010**;167:1130–6. doi:10.1016/j.jplph.2010.03.007.
5. Liu Z, Zhang Y, Liu R, Hao H, Wang Z, Bi Y. Phytochrome interacting factors (PIFs) are essential regulators for sucrose-induced hypocotyl elongation in Arabidopsis. *J Plant Physiol.* **2011**; 168:1771–9. doi:10.1016/j.jplph.2011.04.009.
6. Stewart JL, Maloof JN, Nemhauser JL. PIF genes mediate the effect of sucrose on seedling growth dynamics. *PLoS One.* **2011**;6:e19894. doi:10.1371/journal.pone.0019894.
7. Stewart Lilley JL, Gee CW, Sairanen I, Ljung K, Nemhauser JL. An endogenous carbon-sensing pathway triggers increased auxin flux and hypocotyl elongation. *Plant Physiol.* **2012**;160:2261–70. doi:10.1104/pp.112.205575.
8. Zhang Z, Zhu J-Y, Roh J, Marchive C, Kim S-K, Meyer C, Sun Y, Wang W, Wang ZY. TOR signaling promotes accumulation of BZR1 to balance growth with carbon availability in *Arabidopsis*. *Curr Biol.* **2016**;26:1854–60. doi:10.1016/j.cub.2016.05.005.
9. Zhang Y, Liu Z, Wang J, Chen Y, Bi Y, He J. Brassinosteroid is required for sugar promotion of hypocotyl elongation in Arabidopsis in darkness. *Planta.* **2015**;242:881–93. doi:10.1007/s00425-015-2328-y.
10. Zhang Y, Primavesi LF, Jhurrea D, Andralojc PJ, Mitchell RAC, Powers SJ, Schlupepmann H, Delatte T, Winger A, Paul MJ. Inhibition of SNF1-related protein kinase 1 activity and regulation of metabolic pathways by trehalose-6-phosphate. *Plant Physiol.* **2009**;149:1860–71. doi:10.1104/pp.108.133934.
11. Yadav UP, Ivakov A, Feil R, Duan GY, Walther D, Gialvalisco P, Piques M, Carillo P, Hubberten HM, Stitt M, et al. The sucrose-trehalose 6-phosphate (Tre6P) nexus: specificity and mechanisms of sucrose signalling by Tre6P. *J Exp Bot.* **2014**;65:1051–68. doi:10.1093/jxb/ert457.
12. Baena-González E, Rolland F, Thevelein JM, Sheen J. A central integrator of transcription networks in plant stress and energy signalling. *Nature.* **2007**;448:938–42. doi:10.1038/nature06069.
13. Baena-González E, Sheen J. Convergent energy and stress signaling. *Trends Plant Sci.* **2008**;13:474–82. doi:10.1016/j.tplants.2008.06.006.
14. Delatte TL, Sedjani P, Kondou Y, Matsui M, de Jong GJ, Somsen GW, Wiese-Klinkenberg A, Primavesi LF, Paul MJ, Schlupepmann H. Growth arrest by trehalose-6-phosphate: An astonishing case of primary metabolite control over growth by way of the SnRK1 signaling pathway. *Plant Physiol.* **2011**;157:160. doi:10.1104/pp.111.180422.
15. Mair A, Pedrotti L, Wurzinger B, Anrather D, Simeunovic A, Weiste C, Valerio C, Dietrich K, Kirchlner T, Nägele T, et al. SnRK1-triggered switch of bZIP63 dimerization mediates the low-energy response in plants. *Elife.* **2015**;4:e05828. doi:10.7554/eLife.05828.
16. Radchuk R, Radchuk V, Weschke W, Borisjuk L, Weber H. Repressing the expression of the SUCROSE NONFERMENTING-1-RELATED PROTEIN KINASE gene in pea embryo causes pleiotropic defects of maturation similar to an abscisic acid-insensitive phenotype. *Plant Physiol.* **2006**;140:263–78. doi:10.1104/pp.105.071167.
17. Gómez LD, Gilday A, Feil R, Lunn JE, Graham IA. AtTPS1-mediated trehalose 6-phosphate synthesis is essential for embryogenic and vegetative growth and responsiveness to ABA in germinating seeds and stomatal guard cells. *Plant J.* **2010**;64:1–13.
18. Shin J, Sánchez-Villarreal A, Davis AM, Du S-x, Berendzen KW, Koncz C, Ding Z, Li C, Davis SJ. The metabolic sensor AKIN10 modulates the Arabidopsis circadian clock in a light-dependent manner. *Plant Cell Environ.* **2017**;40:997–1008. doi:10.1111/pce.12903.
19. Jossier M, Bouly J-P, Meimoun P, Arjmand A, Lessard P, Hawley S, Grahame Hardie D, Thomas M. SnRK1 (SNF1-related kinase 1) has a central role in sugar and ABA signalling in Arabidopsis thaliana. *Plant J.* **2009**;59:316–28. doi:10.1111/j.1365-313X.2009.03871.x.

DOI: 10.1111/pce.12939





## References

- Aikawa, S., Kobayashi, M. J., Satake, A., Shimizu, K. K., and Kudoh, H. (2010). Robust control of the seasonal expression of the Arabidopsis *FLC* gene in a fluctuating environment. *Proceedings of the National Academy of Sciences*, 107:11632–11637.
- Alabadí, D., Oyama, T., Yanovsky, M. J., Harmon, F. G., Más, P., and Kay, S. A. (2001). Reciprocal regulation between *TOC1* and *LHY/CCA1* within the Arabidopsis circadian clock. *Science*, 293:880–883.
- Aldon, D., Mbengue, M., Mazars, C., and Galaud, J.-P. (2018). Calcium signalling in plant biotic interactions. *International Journal of Molecular Sciences*, 19:665.
- Allen, G. J., Chu, S. P., Harrington, C. L., Schumacher, K., Hoffmann, T., Tang, Y. Y., Grill, E., and Schroeder, J. I. (2001). A defined range of guard cell calcium oscillation parameters encodes stomatal movements. *Nature*, 411:1053–1057.
- Allen, G. J., Chu, S. P., Schumacher, K., Shimazaki, C. T., Vafeados, D., Kemper, A., Hawke, S. D., Tallman, G., Tsien, R. Y., Harper, J. F., Chory, J., and Schroeder, J. I. (2000). Alteration of stimulus-specific guard cell calcium oscillations in Arabidopsis *det3* mutant. *Science*, 289:2338–2342.
- Allen, G. J., Kuchitsu, K., Chu, S. P., Murata, Y., and Schroeder, J. I. (1999). Arabidopsis *abi1-1* and *abi2-1* phosphatase mutations reduce abscisic acid-induced cytoplasmic calcium rises in guard cells. *The Plant Cell*, 11:1785–1798.
- Alonso, J. M., Stepanova, A. N., Leisse, T. J., Kim, C. J., Chen, H., Shinn, P., Stevenson, D. K., Zimmerman, J., Pascual, B., Cheuk, R., Gadrinab, C., Heller, C., Jeske, A., Koesema, E., Meyers, C. C., Parker, H., Prednis, L., Ansari, Y., Choy, N., Deen, H., Geralt, M., Hazari, N., Hom, E., Karnes, M., Mulholland, C., Ndubaku, R., Schmidt, I., Guzman, P., Aguilar-Henonin, L., Schmid, M., Weigel, D., Carter, D. E., Marchand, T., Risseuw, E., Brogden, D., Zeko, A., Crosby, W. L., Berry, C. C., and Ecker, J. R. (2003).

- Genome-wide insertional mutagenesis of *Arabidopsis thaliana*. *Science*, 301:653–657.
- Alonso-Blanco, C. and Koornneef, M. (2000). Naturally occurring variation in *Arabidopsis*: An underexploited resource for plant genetics. *Trends in Plant Science*, 5:22–29.
- Amodeo, G., Talbott, L. D., and Zeiger, E. (1996). Use of potassium and sucrose by onion guard cells during a daily cycle of osmoregulation. *Plant & Cell Physiology*, 37:575–579.
- Araújo, W. L., Fernie, A. R., and Nunes-Nesi, A. (2011). Control of stomatal aperture: A renaissance of the old guard. *Plant Signaling & Behavior*, 6:1305–1311.
- Avonce, N., Leyman, B., Mascorro-Gallardo, J. O., Van Dijck, P., Thevelein, J. M., and Iturriaga, G. (2004). The *Arabidopsis* trehalose-6-P synthase *AtTPS1* gene is a regulator of glucose, abscisic acid, and stress signaling. *Plant Physiology*, 136:3649–3659.
- Azoulay-Shemer, T., Bagheri, A., Wang, C., Palomares, A., Stephan, A. B., Kunz, H. H., and Schroeder, J. I. (2016). Starch biosynthesis in guard cells but not in mesophyll cells is involved in CO<sub>2</sub>-induced stomatal closing. *Plant Physiology*, 171:788–798.
- Bacon, M. (2009). *Water use efficiency in plant biology*. John Wiley & Sons.
- Baena-González, E. (2010). Energy signaling in the regulation of gene expression during stress. *Molecular Plant*, 3:300–313.
- Baena-González, E., Rolland, F., Thevelein, J. M., and Sheen, J. (2007). A central integrator of transcription networks in plant stress and energy signalling. *Nature*, 448:938–943.
- Baudry, A., Ito, S., Song, Y. H., Strait, A. A., Kiba, T., Lu, S., Henriques, R., Pruneda-Paz, J. L., Chua, N.-H., Tobin, E. M., Kay, S. A., and Imaizumi, T. (2010). F-box proteins FKF1 and LKP2 act in concert with ZEITLUPE to control *Arabidopsis* clock progression. *The Plant Cell*, 22:606–622.
- Bauer, H., Ache, P., Lautner, S., Fromm, J., Hartung, W., Al-Rasheid, K. A. S., Sonnewald, S., Sonnewald, U., Kneitz, S., Lachmann, N., Mendel, R. R., Bittner, F., Hetherington, A. M., and Hedrich, R. (2013). The stomatal response to reduced relative humidity requires guard cell-autonomous ABA synthesis. *Current Biology*, 23:53–57.
- Bean, G. J., Marks, M. D., Hülskamp, M., Clayton, M., and Croxdale, J. L. (2002). Tissue patterning of *Arabidopsis* cotyledons. *New Phytologist*, 153:461–467.

- Bechtold, U., Lawson, T., Mejia-Carranza, J., Meyer, R. C., Brown, I. R., Altmann, T., Ton, J., and Mullineaux, P. M. (2010). Constitutive salicylic acid defences do not compromise seed yield, drought tolerance and water productivity in the Arabidopsis accession C24. *Plant, Cell & Environment*, 33:1959–1973.
- Belbin, F. E., Noordally, Z. B., Wetherill, S. J., Atkins, K. A., Franklin, K. A., and Dodd, A. N. (2017). Integration of light and circadian signals that regulate chloroplast transcription by a nuclear-encoded sigma factor. *New Phytologist*, 213:727–738.
- Bendix, C., Marshall, C. M., and Harmon, F. G. (2015). Circadian clock genes universally control key agricultural traits. *Molecular Plant*, 8:1135–1152.
- Benke, K. and Tomkins, B. (2017). Future food-production systems: Vertical farming and controlled-environment agriculture. *Sustainability: Science, Practice & Policy*, 13:13–26.
- Blum, A. (2009). Effective use of water (EUW) and not water-use efficiency (WUE) is the target of crop yield improvement under drought stress. *Field Crops Research*, 112:119–123.
- Bordage, S., Sullivan, S., Laird, J., Millar, A. J., and Nimmo, H. G. (2016). Organ specificity in the plant circadian system is explained by different light inputs to the shoot and root clocks. *New Phytologist*, 212:136–149.
- Borland, A. M., Hartwell, J., Weston, D. J., Schlauch, K. A., Tschaplinski, T. J., Tuskan, G. A., Yang, X., and Cushman, J. C. (2014). Engineering crassulacean acid metabolism to improve water-use efficiency. *Trends in Plant Science*, 19:327–338.
- Boxall, S. F., Dever, L. V., Knerova, J., Gould, P. D., and Hartwell, J. (2017). Phosphorylation of phosphoenolpyruvate carboxylase is essential for maximal and sustained dark CO<sub>2</sub> fixation and core circadian clock operation in the obligate crassulacean acid metabolism species *Kalanchoë fedtschenkoi*. *The Plant Cell*, 29:2519–2536.
- Boylan, M. T. and Quail, P. H. (1991). Phytochrome A overexpression inhibits hypocotyl elongation in transgenic Arabidopsis. *Proceedings of the National Academy of Sciences*, 88:10806–10810.
- Brandt, B., Munemasa, S., Wang, C., Nguyen, D., Yong, T., Yang, P. G., Poretsky, E., Belknap, T. F., Waadt, R., Alemán, F., and Schroeder, J. I. (2015). Calcium specificity signaling mechanisms in abscisic acid signal transduction in Arabidopsis guard cells. *eLife*, 4:e03599.



- Braun, D. M., Wang, L., and Ruan, Y. L. (2014). Understanding and manipulating sucrose phloem loading, unloading, metabolism, and signalling to enhance crop yield and food security. *Journal of Experimental Botany*, 65:1713–1735.
- Bunce, J. A. (2004). Carbon dioxide effects on stomatal responses to the environment and water use by crops under field conditions. *Oecologia*, 140:1–10.
- Busch, F. A. (2014). Opinion: The red-light response of stomatal movement is sensed by the redox state of the photosynthetic electron transport chain. *Photosynthesis Research*, 119:131–140.
- Caddick, M. X., Greenland, A. J., Jepson, I., Krause, K. P., Qu, N., Riddell, K. V., Salter, M. G., Schuch, W., Sonnewald, U., and Tomsett, A. B. (1998). An ethanol inducible gene switch for plants used to manipulate carbon metabolism. *Nature Biotechnology*, 16:177–180.
- Cao, D., Cheng, H., Wu, W., Soo, H. M., and Peng, J. (2006). Gibberellin mobilizes distinct DELLA-dependent transcriptomes to regulate seed germination and floral development in Arabidopsis. *Plant Physiology*, 142:509–525.
- Casal, J. J. (2013). Photoreceptor signaling networks in plant responses to shade. *Annual Review of Plant Biology*, 64:403–427.
- Chen, C., Xiao, Y. G., Li, X., and Ni, M. (2012). Light-regulated stomatal aperture in Arabidopsis. *Molecular Plant*, 5:566–572.
- Cheng, H., Qin, L., Lee, S., Fu, X., Richards, D. E., Cao, D., Luo, D., Harberd, N. P., and Peng, J. (2004). Gibberellin regulates Arabidopsis floral development via suppression of DELLA protein function. *Development*, 131:1055–1064.
- Cheng, W.-H., Endo, A., Zhou, L., Penney, J., Chen, H.-C., Arroyo, A., Leon, P., Nambara, E., Asami, T., Seo, M., Koshiba, T., and Sheen, J. (2002). A unique short-chain dehydrogenase/reductase in Arabidopsis glucose signaling and abscisic acid biosynthesis and functions. *The Plant Cell*, 14:2723–2743.
- Choudhary, M. K., Nomura, Y., Wang, L., Nakagami, H., and Somers, D. E. (2015). Quantitative circadian phosphoproteomic analysis of Arabidopsis reveals extensive clock control of key components in physiological, metabolic, and signaling pathways. *Molecular & Cellular Proteomics*, 14:2243–2260.

- Coello, P., Hey, S. J., and Halford, N. G. (2011). The sucrose non-fermenting-1-related (SnRK) family of protein kinases: Potential for manipulation to improve stress tolerance and increase yield. *Journal of Experimental Botany*, 62:883–893.
- Coello, P., Hirano, E., Hey, S. J., Muttucumar, N., Martinez-Barajas, E., Parry, M. A., and Halford, N. G. (2012). Evidence that abscisic acid promotes degradation of SNF1-related protein kinase (SnRK) 1 in wheat and activation of a putative calcium-dependent SnRK2. *Journal of Experimental Botany*, 63:913–924.
- Colbert, T., Till, B. J., Tompa, R., Reynolds, S., Steine, M. N., Yeung, A. T., McCallum, C. M., Comai, L., and Henikoff, S. (2001). High-throughput screening for induced point mutations. *Plant Physiology*, 126:480–484.
- Collett, C. E., Harberd, N. P., and Leyser, O. (2000). Hormonal interactions in the control of Arabidopsis hypocotyl elongation. *Plant Physiology*, 124:553–561.
- Cominelli, E., Galbiati, M., Albertini, A., Fornara, F., Conti, L., Coupland, G., and Tonelli, C. (2011). DOF-binding sites additively contribute to guard cell-specificity of *At-MYB60* promoter. *BioMed Central Plant Biology*, 11:162.
- Cominelli, E., Galbiati, M., Vavasseur, A., Conti, L., Sala, T., Vuylsteke, M., Leonhardt, N., Dellaporta, S. L., and Tonelli, C. (2005). A guard-cell-specific MYB transcription factor regulates stomatal movements and plant drought tolerance. *Current Biology*, 15:1196–200.
- Condon, A., Richards, R. A., Rebetzke, G. J., and Farquhar, G. D. (2002). Improving intrinsic water-use efficiency and crop yield. *Crop Science*, 42:122–131.
- Condon, A. G., Richards, R. A., Rebetzke, G. J., and Farquhar, G. D. (2004). Breeding for high water-use efficiency. *Journal of Experimental Botany*, 55:2447–2460.
- Correia, M., Rodrigues, M., Ferreira, M., and Pereira, J. (1997). Diurnal change in the relationship between stomatal conductance and abscisic acid in the xylem sap of field-grown peach trees. *Journal of Experimental Botany*, 48:1727–1736.
- Correia, M. J., Pereira, J. S., Chaves, M. M., Rodrigues, M. L., and Pacheco, C. A. (1995). ABA xylem concentrations determine maximum daily leaf conductance of field-grown *Vitis vinifera* L. plants. *Plant, Cell & Environment*, 18:511–521.
- Costa, J. M., Monnet, F., Jannaud, D., Leonhardt, N., Ksas, B., Reiter, I. M., Pantin, F., and Genty, B. (2015). *OPEN ALL NIGHT LONG* : The dark side of stomatal control. *Plant Physiology*, 167:289–294.

- Coupel-Ledru, A., Lebon, E., Christophe, A., Gallo, A., Gago, P., Pantin, F., Doligez, A., and Simonneau, T. (2016). Reduced nighttime transpiration is a relevant breeding target for high water-use efficiency in grapevine. *Proceedings of the National Academy of Sciences*, 113:8963–8968.
- Covington, M. F., Maloof, J. N., Straume, M., Kay, S. A., and Harmer, S. L. (2008). Global transcriptome analysis reveals circadian regulation of key pathways in plant growth and development. *Genome Biology*, 9:R130.
- Cowling, R. J. and Harberd, N. P. (1999). Gibberellins control Arabidopsis hypocotyl growth via regulation of cellular elongation. *Journal of Experimental Botany*, 50:1351–1357.
- Dakhiya, Y., Hussien, D., Fridman, E., Kiflawi, M., and Green, R. (2017). Correlations between circadian rhythms and growth in challenging environments. *Plant Physiology*, 173:1724–1734.
- Dalin, P., Ågren, J., Björkman, C., Huttunen, P., and Kärkkäinen, K. (2008). Leaf trichome formation and plant resistance to herbivory. In Schaller, A., editor, *Induced plant resistance to herbivory*, pages 89–105. Springer.
- Daloso, D. M., Antunes, W. C., Pinheiro, D. P., Waquim, J. P., Araújo, W. L., Loureiro, M. E., Fernie, A. R., and Williams, T. C. (2015). Tobacco guard cells fix CO<sub>2</sub> by both Rubisco and PEPcase while sucrose acts as a substrate during light-induced stomatal opening. *Plant, Cell & Environment*, 38:2353–2371.
- Daloso, D. M., dos Anjos, L., and Fernie, A. R. (2016). Roles of sucrose in guard cell regulation. *New Phytologist*, 211:809–818.
- Darwin, C. R. (1880). *The power of movement in plants*. Murray, J.
- Darwin, F. (1898). Observations on stomata. *Proceedings of the Royal Society of London*, 63:413–417.
- De Lucas, M., Davière, J. M., Rodríguez-Falcón, M., Pontin, M., Iglesias-Pedraz, J. M., Lorrain, S., Fankhauser, C., Blázquez, M. A., Titarenko, E., and Prat, S. (2008). A molecular framework for light and gibberellin control of cell elongation. *Nature*, 451:480–484.
- de Mairan, J.-J. (1729). Observation botanique. *Histoire de l'Académie Royale des Sciences*, page 35.

- Debast, S., Nunes-Nesi, A., Hajirezaei, M. R., Hofmann, J., Sonnewald, U., Fernie, A. R., and Börnke, F. (2011). Altering trehalose-6-phosphate content in transgenic potato tubers affects tuber growth and alters responsiveness to hormones during sprouting. *Plant Physiology*, 156:1754–71.
- Deng, X.-W., Caspar, T., and Quail, P. H. (1991). *cop1*: A regulatory locus involved in light-controlled development and gene expression in Arabidopsis. *Genes & Development*, 5:1172–1182.
- Deng, X.-W. and Quail, P. H. (1992). Genetic and phenotypic characterization of *cop1* mutants of *Arabidopsis thaliana*. *The Plant Journal*, 2:83–95.
- Des Marais, D. L., Auchincloss, L. C., Sukamtoh, E., McKay, J. K., Logan, T., Richards, J. H., and Juenger, T. E. (2014). Variation in *MPK12* affects water use efficiency in Arabidopsis and reveals a pleiotropic link between guard cell size and ABA response. *Proceedings of the National Academy of Sciences*, 111:2836–2841.
- Ding, Z., Doyle, M. R., Amasino, R. M., and Davis, S. J. (2007a). A complex genetic interaction between *Arabidopsis thaliana* *TOC1* and *CCA1/LHY* in driving the circadian clock and in output regulation. *Genetics*, 176:1501–1510.
- Ding, Z., Millar, A. J., Davis, A. M., and Davis, S. J. (2007b). *TIME FOR COFFEE* encodes a nuclear regulator in the *Arabidopsis thaliana* circadian clock. *The Plant Cell*, 19:1522–1536.
- Dixon, L. E., Knox, K., Kozma-Bognar, L., Southern, M. M., Pokhilko, A., and Millar, A. J. (2011). Temporal repression of core circadian genes is mediated through *EARLY FLOWERING 3* in Arabidopsis. *Current Biology*, 21:120–125.
- Dodd, A. N., Belbin, F. E., Frank, A., and Webb, A. A. R. (2015). Interactions between circadian clocks and photosynthesis for the temporal and spatial coordination of metabolism. *Frontiers in Plant Science*, 6:245.
- Dodd, A. N., Dalchau, N., Gardner, M. J., Baek, S. J., and Webb, A. A. (2014). The circadian clock has transient plasticity of period and is required for timing of nocturnal processes in Arabidopsis. *New Phytologist*, 201:168–179.
- Dodd, A. N., Gardner, M. J., Hotta, C. T., Hubbard, K. E., Dalchau, N., Love, J., Assie, J.-M., Robertson, F. C., Jakobsen, M. K., Goncalves, J., Sanders, D., and Webb, A. A. R. (2007). The Arabidopsis circadian clock incorporates a cADPR-based feedback loop. *Science*, 318:1789–1792.

- Dodd, A. N., Jakobsen, M. K., Baker, A. J., Telzerow, A., Hou, S.-W., Laplaze, L., Barrot, L., Poethig, S. R., Haseloff, J., and Webb, A. A. (2006). Time of day modulates low-temperature Ca<sup>2+</sup> signals in Arabidopsis. *The Plant Journal*, 48:962–973.
- Dodd, A. N., Parkinson, K., and Webb, A. A. R. (2004). Independent circadian regulation of assimilation and stomatal conductance in the *ztl-1* mutant of Arabidopsis. *New Phytologist*, 162:63–70.
- Dodd, A. N., Salathia, N., Hall, A., Kévei, E., Tóth, R., Nagy, F., Hibberd, J. M., Millar, A. J., and Webb, A. A. R. (2005). Plant circadian clocks increase photosynthesis, growth, survival, and competitive advantage. *Science*, 309:630–633.
- Doheny-Adams, T., Hunt, L., Franks, P. J., Beerling, D. J., and Gray, J. E. (2012). Genetic manipulation of stomatal density influences stomatal size, plant growth and tolerance to restricted water supply across a growth carbon dioxide gradient. *Philosophical Transactions of the Royal Society B: Biological Sciences*, 367:547–555.
- Doyle, M. R., Davis, S. J., Bastow, R. M., McWatters, H. G., Kozma-Bognár, L., Nagy, F., Millar, A. J., and Amasino, R. M. (2002). The *ELF4* gene controls circadian rhythms and flowering time in *Arabidopsis thaliana*. *Nature*, 419:74–77.
- Earley, E. J., Inghand, B., Winkler, J., and Tonsor, S. J. (2009). Inflorescences contribute more than rosettes to lifetime carbon gain in *Arabidopsis thaliana* (Brassicaceae). *American Journal of Botany*, 96:786–792.
- Easlon, H. M., Nemali, K. S., Richards, J. H., Hanson, D. T., Juenger, T. E., and McKay, J. K. (2014). The physiological basis for genetic variation in water use efficiency and carbon isotope composition in *Arabidopsis thaliana*. *Photosynthesis Research*, 119:119–129.
- Eastmond, P. J., Van Dijken, A. J. H., Spielman, M., Kerr, A., Tissier, A. F., Dickinson, H. G., Jones, J. D. G., Smeekens, S. C., and Graham, I. A. (2002). Trehalose-6-phosphate synthase 1, which catalyses the first step in trehalose synthesis, is essential for Arabidopsis embryo maturation. *The Plant Journal*, 29:225–235.
- Edwards, C. E., Ewers, B. E., McClung, C. R., Lou, P., and Weinig, C. (2012). Quantitative variation in water-use efficiency across water regimes and its relationship with circadian, vegetative, reproductive, and leaf gas-exchange traits. *Molecular Plant*, 5:653–668.

- Edwards, K., Johnstone, C., and Thompson, C. (1991). A simple and rapid method for the preparation of plant DNA for PCR analysis. *Nucleic Acids Research*, 19:1349.
- Efremova, N., Schreiber, L., Bar, S., Heidmann, I., Huijser, P., Wellesen, K., Schwarzsommer, Z., Saedler, H., and Yephremov, A. (2004). Functional conservation and maintenance of expression pattern of *FIDDLEHEAD*-like genes in *Arabidopsis* and *Antirrhinum*. *Plant Molecular Biology*, 56:821–837.
- Endo, M., Shimizu, H., Nohales, M. a., Araki, T., and Kay, S. A. (2014). Tissue-specific clocks in *Arabidopsis* show asymmetric coupling. *Nature*, 515:419–422.
- Erb, T. J. and Zarzycki, J. (2018). A short history of RubisCO: the rise and fall (?) of Nature’s predominant CO<sub>2</sub> fixing enzyme. *Current Opinion in Biotechnology*, 49:100–107.
- Eriksson, M. E., Hanano, S., Southern, M. M., Hall, A., and Millar, A. J. (2003). Response regulator homologues have complementary, light-dependent functions in the *Arabidopsis* circadian clock. *Planta*, 218:159–162.
- Esmon, C. A., Tinsley, A. G., Ljung, K., Sandberg, G., Hearne, L. B., and Liscum, E. (2006). A gradient of auxin and auxin-dependent transcription precedes tropic growth responses. *Proceedings of the National Academy of Sciences*, 103:236–241.
- Esquinas-Alcázar, J. (2005). Protecting crop genetic diversity for food security: Political, ethical and technical challenges. *Nature Reviews Genetics*, 6:946–953.
- Evans, N. H., McAinsh, M. R., and Hetherington, A. M. (2001). Calcium oscillations in higher plants. *Current Opinion in Biotechnology*, 4:415–420.
- Farquhar, G. and Richards, R. (1984). Isotopic composition of plant carbon correlates with water-use efficiency of wheat genotypes. *Australian Journal of Plant Physiology*, 11:539–552.
- Farré, E. M., Harmer, S. L., Harmon, F. G., Yanovsky, M. J., and Kay, S. A. (2005). Overlapping and distinct roles of *PRR7* and *PRR9* in the *Arabidopsis* circadian clock. *Current Biology*, 15:47–54.
- Feeney, K. A., Hansen, L. L., Putker, M., Olivares-Yañez, C., Jason, D., Eades, L. J., Larrondo, L. F., Hoyle, N. P., O’Neill, J. S., and van Ooijen, G. (2016). Daily magnesium fluxes regulate cellular timekeeping and energy balance. *Nature*, 532:375–379.

- Ferguson, J. N., Humphry, M., Lawson, T., Brendel, O., and Bechtold, U. (2018). Natural variation of life-history traits, water use, and drought responses in *Arabidopsis*. *Plant Direct*, 2:1–16.
- Fiene, J. G., Mallick, S., Mittal, A., Nansen, C., Kalns, L., Dever, J., Sword, G. A., and Rock, C. D. (2017). Characterization of transgenic cotton (*Gossypium hirsutum* L.) over-expressing *Arabidopsis thaliana* related to ABA-insensitive3(ABI3)/Viviparous1 (AtRAV1) and AtABI5 transcription factors: improved water use efficiency through altered guard cell physiology. *Plant Biotechnology Reports*, 11:339–353.
- Fowler, S., Lee, K., Onouchi, H., Samach, A., Richardson, K., Morris, B., Coupland, G., and Putterill, J. (1999). *GIGANTEA*: A circadian clock-controlled gene that regulates photoperiodic flowering in *Arabidopsis* and encodes a protein with several possible membrane-spanning domains. *EMBO Journal*, 18:4679–4688.
- Francia, P., Simoni, L., Cominelli, E., Tonelli, C., and Galbiati, M. (2008). Gene trap-based identification of a guard cell promoter in *Arabidopsis*. *Plant Signaling & Behavior*, 3:684–686.
- Frank, A., Matioli, C. C., Viana, A. J. C., Hearn, T. J., Kusakina, J., Belbin, F. E., Newman, D. W., Yochikawa, A., Cano-Ramirez, D. L., Chembath, A., Cragg-Barber, K., Haydon, M. J., Hotta, C. T., Vincentz, M., Webb, A. A., and Dodd, A. N. (2018). Circadian entrainment in *Arabidopsis* by the sugar-responsive transcription factor bZIP63. *Current Biology*.
- Franks, P. J., Doheny-Adams, T. W., Britton-Harper, Z. J., and Gray, J. E. (2015). Increasing water-use efficiency directly through genetic manipulation of stomatal density. *New Phytologist*, 207:188–195.
- Fu, X., Richards, D. E., Ait-Ali, T., Hynes, L. W., Ougham, H., Peng, J., and Harberd, N. P. (2002). Gibberellin-mediated proteasome-dependent degradation of the barley DELLA protein SLN1 repressor. *The Plant Cell*, 14:3191–3200.
- Fujita, T., Noguchi, K., and Terashima, I. (2013). Apoplastic mesophyll signals induce rapid stomatal responses to CO<sub>2</sub> in *Commelina communis*. *New Phytologist*, 199:395–406.
- Fujiwara, S., Wang, L., Han, L., Suh, S.-S., Salome, P. A., McClung, C. R., and Somers, D. E. (2008). Post-translational regulation of the *Arabidopsis* circadian clock through

- selective proteolysis and phosphorylation of pseudo-response regulator proteins. *The Journal of Biological Chemistry*, 283:23073–23083.
- Fukushima, E., Arata, Y., Endo, T., Sonnewald, U., and Sato, F. (2001). Improved salt tolerance of transgenic tobacco expressing apoplastic yeast-derived invertase. *Plant and Cell Physiology*, 42:245–249.
- Galbiati, M., Simoni, L., Pavesi, G., Cominelli, E., Francia, P., Vavasseur, A., Nelson, T., Bevan, M., and Tonelli, C. (2008). Gene trap lines identify Arabidopsis genes expressed in stomatal guard cells. *The Plant Journal*, 53:750–762.
- Gendreau, E., Traas, J., Demos, T., Grandjean, O., Caboche, M., and Hofte, H. (1997). Cellular basis of hypocotyl growth in *Arabidopsis thaliana*. *Plant Physiology*, 114:295–305.
- Gendron, J. M., Pruneda-Paz, J. L., Doherty, C. J., Gross, a. M., Kang, S. E., and Kay, S. A. (2012). Arabidopsis circadian clock protein, TOC1, is a DNA-binding transcription factor. *Proceedings of the National Academy of Sciences*, 109:3167–3172.
- Ghillebert, R., Swinnen, E., Wen, J., Vandesteene, L., Ramon, M., Norga, K., Rolland, F., and Winderickx, J. (2011). The AMPK/SNF1/SnRK1 fuel gauge and energy regulator: Structure, function and regulation. *Federation of European Biochemical Societies Journal*, 278:3978–3990.
- Glover, B. J. (2000). Differentiation in plant epidermal cells. *Journal of Experimental Botany*, 51:497–505.
- Glover, B. J., Perez-Rodriguez, M., and Martin, C. (1998). Development of several epidermal cell types can be specified by the same MYB-related plant transcription factor. *Development*, 125:3497–3508.
- Goda, H. (2004). Comprehensive comparison of auxin-regulated and brassinosteroid-regulated genes in Arabidopsis. *Plant Physiology*, 134:1555–1573.
- Gómez, L. D., Baud, S., Gilday, A., Li, Y., and Graham, I. A. (2006). Delayed embryo development in the *ARABIDOPSIS TREHALOSE-6-PHOSPHATE SYNTHASE 1* mutant is associated with altered cell wall structure, decreased cell division and starch accumulation. *The Plant Journal*, 46:69–84.
- Gomez, L. D., Gilday, A., Feil, R., Lunn, J. E., and Graham, I. A. (2010). *AtTPS1*-mediated trehalose 6-phosphate synthesis is essential for embryogenic and vegetative growth



- and responsiveness to ABA in germinating seeds and stomatal guard cells. *The Plant Journal*, 64:1–13.
- Gomez, L. D., Noctor, G., Knight, M. R., and Foyer, C. H. (2004). Regulation of calcium signalling and gene expression by glutathione. *Journal of Experimental Botany*, 55:1851–1859.
- Goodwin, S. M. and Jenks, M. A. (2005). Plant cuticle function as a barrier to water loss. In Jenks, M. A. and Hasegawa, P. M., editors, *Plant Abiotic Stress*, pages 14–36. Blackwell Publishing Ltd.
- Gorton, H. L., Williams, W. E., and Assmann, S. M. (1993). Circadian rhythms in stomatal responsiveness to red and blue light. *Plant Physiology*, 103:399–406.
- Gorton, H. L., Williams, W. E., Binns, M. E., Gemmell, C. N., Leheny, E. A., and Shepherd, A. C. (1989). Circadian stomatal rhythms in epidermal peels from *Vicia faba*. *Plant Physiology*, 90:1329–1334.
- Gould, P. D., Domijan, M., Greenwood, M., Tokuda, I. T., Rees, H., Kozma-Bognar, L., Hall, A. J., and Locke, J. C. W. (2018). Coordination of robust single cell rhythms in the Arabidopsis circadian clock via spatial waves of gene expression. *eLife*, 7:e31700.
- Graf, A., Schlereth, A., Stitt, M., and Smith, A. M. (2010). Circadian control of carbohydrate availability for growth in Arabidopsis plants at night. *Proceedings of the National Academy of Sciences*, 107:9458–9463.
- Gray, W. M., Ostin, A., Sandberg, G., Romano, C. P., and Estelle, M. (1998). High temperature promotes auxin-mediated hypocotyl elongation in Arabidopsis. *Proceedings of the National Academy of Sciences*, 95:7197–202.
- Green, R. M., Tingay, S., Wang, Z. Y., and Tobin, E. M. (2002). Circadian rhythms confer a higher level of fitness to Arabidopsis plants. *Plant Physiology*, 129:576–584.
- Greenham, K., Lou, P., Puzey, J. R., Kumar, G., Arnevik, C., Farid, H., Willis, J. H., and McClung, C. R. (2017). Geographic variation of plant circadian clock function in natural and agricultural settings. *Journal of Biological Rhythms*, 32:26–34.
- Greenham, K. and McClung, C. R. (2015). Integrating circadian dynamics with physiological processes in plants. *Nature Reviews Genetics*, 16:598–610.

- Griffiths, C. A., Sagar, R., Geng, Y., Primavesi, L. F., Patel, M. K., Passarelli, M. K., Gilmore, I. S., Steven, R. T., Bunch, J., Paul, M. J., and Davis, B. G. (2016). Chemical intervention in plant sugar signalling increases yield and resilience. *Nature*, 540:574–578.
- Grundy, J., Stoker, C., and Carré, I. A. (2015). Circadian regulation of abiotic stress tolerance in plants. *Frontiers in Plant Science*, 6:648.
- Halford, N. G., Hey, S., Jhurreea, D., Laurie, S., McKibbin, R. S., Paul, M., and Zhang, Y. (2003). Metabolic signalling and carbon partitioning: Role of Snf1-related (SnRK1) protein kinase. *Journal of Experimental Botany*, 54:467–475.
- Hall, A., Bastow, R. M., Davis, S. J., Hanano, S., Mcwatters, H. G., Hibberd, V., Doyle, M. R., Sung, S., Halliday, K. J., Amasino, R. M., and Millar, A. J. (2003). The *TIME FOR COFFEE* gene maintains the amplitude and timing of *Arabidopsis* circadian clocks. *The Plant Cell*, 15:2719–2729.
- Hall, A. and Brown, P. (2007). Monitoring circadian rhythms in *Arabidopsis thaliana* using luciferase reporter genes. *Methods in Molecular Biology*, 362:143–152.
- Hammond, J. P. and White, P. J. (2011). Sugar signaling in root responses to low phosphorus availability. *Plant Physiology*, 156:1033–1040.
- Hanano, S., Domagalska, M. A., Nagy, F., and Davis, S. J. (2006). Multiple phytohormones influence distinct parameters of the plant circadian clock. *Genes to Cells*, 11:1381–1392.
- Handley, R., Ekbom, B., and Ågren, J. (2005). Variation in trichome density and resistance against a specialist insect herbivore in natural populations of *Arabidopsis thaliana*. *Ecological Entomology*, 30:284–292.
- Hassidim, M., Dakhiya, Y., Turjeman, A., Hussien, D., Shor, E., Anidjar, A., Goldberg, K., and Green, R. M. (2017). *CIRCADIAN CLOCK ASSOCIATED 1 (CCA1)* and the circadian control of stomatal aperture. *Plant Physiology*, 175:1864–1877.
- Hayama, R. and Coupland, G. (2003). Shedding light on the circadian clock and the photoperiodic control of flowering. *Current Opinion in Plant Biology*, 6:13–19.
- Hayashi, Y., Takahashi, K., Inoue, S. I., and Kinoshita, T. (2014). Abscisic acid suppresses hypocotyl elongation by dephosphorylating plasma membrane H<sup>+</sup>-ATPase in *Arabidopsis thaliana*. *Plant and Cell Physiology*, 55:845–853.

- Haydon, M. J., Hearn, T. J., Bell, L. J., Hannah, M. a., and Webb, A. A. R. (2013a). Metabolic regulation of circadian clocks. *Seminars in Cell & Developmental Biology*, 24:414–421.
- Haydon, M. J., Mielczarek, O., Robertson, F. C., Hubbard, K. E., and Webb, A. A. R. (2013b). Photosynthetic entrainment of the *Arabidopsis thaliana* circadian clock. *Nature*, 502:689–692.
- Hayes, K. R., Beatty, M., Meng, X., Simmons, C. R., Habben, J. E., and Danilevskaya, O. N. (2010). Maize global transcriptomics reveals pervasive leaf diurnal rhythms but rhythms in developing ears are largely limited to the core oscillator. *Public Library of Science ONE*, 5:e12887.
- Hayes, S., Velanis, C. N., Jenkins, G. I., and Franklin, K. A. (2014). UV-B detected by the UVR8 photoreceptor antagonizes auxin signaling and plant shade avoidance. *Proceedings of the National Academy of Sciences*, 111:11894–11899.
- Hazen, S. P., Borevitz, J. O., Harmon, F. G., Pruneda-Paz, J. L., Schultz, T. F., Yanovsky, M. J., Liljegren, S. J., Ecker, J. R., and Kay, S. A. (2005a). Rapid array mapping of circadian clock and developmental mutations in Arabidopsis. *Plant Physiology*, 138:990–997.
- Hazen, S. P., Schultz, T. F., Pruneda-Paz, J. L., Borevitz, J. O., Ecker, J. R., and Kay, S. A. (2005b). *LUX ARRHYTHMO* encodes a Myb domain protein essential for circadian rhythms. *Proceedings of the National Academy of Sciences*, 102:10387–10392.
- Heintzen, C., Nater, M., Apel, K., and Staiger, D. (1997). AtGRP7, a nuclear RNA-binding protein as a component of a circadian-regulated negative feedback loop in *Arabidopsis thaliana*. *Proceedings of the National Academy of Sciences*, 94:8515–8520.
- Hellens, R. P., Edwards, E. A., Leyland, N. R., Bean, S., and Mullineaux, P. M. (2000). pGreen: a versatile and flexible binary Ti vector for Agrobacterium-mediated plant transformation. *Plant Molecular Biology*, 42:819–832.
- Hennessey, T. L. and Field, C. B. (1991). Circadian rhythms in photosynthesis: Oscillations in carbon assimilation and stomatal conductance under constant conditions. *Plant Physiology*, 96:831–836.
- Hennessey, T. L. and Field, C. B. (1992). Evidence of multiple circadian oscillators in bean plants. *Journal of Biological Rhythms*, 7:105–113.

- Herrero, E., Kolmos, E., Bujdoso, N., Yuan, Y., Wang, M., Berns, M. C., Uhlworm, H., Coupland, G., Saini, R., Jaskolski, M., Webb, A., Goncalves, J., and Davis, S. J. (2012). EARLY FLOWERING4 recruitment of EARLY FLOWERING3 in the nucleus sustains the Arabidopsis circadian clock. *The Plant Cell*, 24:428–443.
- Hetherington, A. M. and Woodward, F. I. (2003). The role of stomata in sensing and driving environmental change. *Nature*, 424:901–908.
- Hotta, C. T., Nishiyama Jr., M. Y., and Souza, G. M. (2013). Circadian rhythms of sense and antisense transcription in sugarcane, a highly polyploid crop. *Public Library of Science ONE*, 8:e71847.
- Hsu, P. Y., Devisetty, U. K., and Harmer, S. L. (2013). Accurate timekeeping is controlled by a cycling activator in Arabidopsis. *eLife*, 2:e00473.
- Hsu, P. Y. and Harmer, S. L. (2014). Wheels within wheels: the plant circadian system. *Trends in Plant Science*, 19:240–249.
- Hu, H., Dai, M., Yao, J., Xiao, B., Li, X., Zhang, Q., and Xiong, L. (2006). Overexpressing a NAM, ATAF, and CUC (NAC) transcription factor enhances drought resistance and salt tolerance in rice. *Proceedings of the National Academy of Sciences*, 103:12987–12992.
- Hu, H. and Xiong, L. (2014). Genetic engineering and breeding of drought-resistant crops. *Annual Review of Plant Biology*, 65:715–741.
- Huang, H. and Nusinow, D. A. (2016). Into the evening: Complex interactions in the Arabidopsis circadian clock. *Trends in Genetics*, 32:674–686.
- Huang, W., Perez-Garcia, P., Pokhilko, A., Millar, A. J., Antoshechkin, I., Riechmann, J. L., and Mas, P. (2012). Mapping the core of Arabidopsis circadian clock defines the network structure of the oscillator. *Science*, 336:75–80.
- Hubbard, K. and Dodd, A. (2016). Rhythms of life: The plant circadian clock. *The Plant Cell*, 28:tpc.116.tt0416.
- Hubbard, K. E., Siegel, R. S., Valerio, G., Brandt, B., and Schroeder, J. I. (2012). Abscisic acid and CO<sub>2</sub> signalling via calcium sensitivity priming in guard cells, new CDPK mutant phenotypes and a method for improved resolution of stomatal stimulus-response analyses. *Annals of Botany*, 109:5–17.

- Hubbard, K. E. and Webb, A. A. R. (2011). Circadian rhythms: *FLOWERING LOCUS T* extends opening hours. *Current Biology*, 21:636–638.
- Hugouvieux, V., Kwak, J. M., and Schroeder, J. I. (2001). An mRNA cap binding protein, ABH1, modulates early abscisic acid signal transduction in Arabidopsis. *Cell*, 106:477–487.
- Hülkamp, M. and Schnittger, A. (1998). Spatial regulation of trichome formation in *Arabidopsis thaliana*. *Seminars in Cell & Developmental Biology*, 9:213–220.
- Imaizumi, T., Schultz, T. F., Harmon, F. G., Ho, L. A., and Kay, S. A. (2005). FKF1 F-Box protein mediates cyclic degradation of a repressor of *CONSTANS* in Arabidopsis. *Science*, 309:293–297.
- Imaizumi, T., Tran, H. G., Swartz, T. E., Briggs, W. R., and Kay, S. A. (2003). FKF1 is essential for photoperiodic-specific light signalling in Arabidopsis. *Nature*, 426:302–306.
- Izawa, T., Mihara, M., Suzuki, Y., Gupta, M., Itoh, H., Nagano, A. J., Motoyama, R., Sawada, Y., Yano, M., Hirai, M. Y., Makino, A., and Nagamura, Y. (2011). *Os-GIGANTEA* confers robust diurnal rhythms on the global transcriptome of rice in the field. *The Plant Cell*, 23:1741–1755.
- Jakobson, L., Vaahtera, L., Töldsepp, K., Nuhkat, M., Wang, C., Wang, Y. S., Hõrak, H., Valk, E., Pechter, P., Sindarovska, Y., Tang, J., Xiao, C., Xu, Y., Gerst Talas, U., García-Sosa, A. T., Kangasjärvi, S., Maran, U., Remm, M., Roelfsema, M. R. G., Hu, H., Kangasjärvi, J., Loog, M., Schroeder, J. I., Kollist, H., and Brosché, M. (2016). Natural variation in Arabidopsis Cvi-0 accession reveals an important role of MPK12 in guard cell CO<sub>2</sub> signaling. *Public Library of Science Biology*, 14:e2000322.
- James, A. B., Monreal, J. A., Nimmo, G. A., Kelly, C. L., Herzyk, P., Jenkins, G. I., and Nimmo, H. G. (2008). The circadian clock in Arabidopsis roots is a simplified slave version of the clock in shoots. *Science*, 322:1832–1835.
- Jensen, P. J., Hangarter, R. P., and Estelle, M. (1998). Auxin transport is required for hypocotyl elongation in light-grown but not dark-grown Arabidopsis. *Plant Physiology*, 116:455–462.
- Johansson, M. and Staiger, D. (2015). Time to flower: Interplay between photoperiod and the circadian clock. *Journal of Experimental Botany*, 66:719–730.

- Johnson, C. H., Knight, M. R., Kondo, T., Masson, P., Sedbrook, J., Haley, A., and Tre-wavas, A. (1995). Circadian oscillations of cytosolic and chloroplastic free calcium in plants. *Science*, 269:1863–1865.
- Joo, Y., Fragoso, V., Yon, F., Baldwin, I. T., and Kim, S. G. (2017). Circadian clock component, LHY, tells a plant when to respond photosynthetically to light in nature. *Journal of Integrative Plant Biology*, 59:572–587.
- Jossier, M., Bouly, J. P., Meimoun, P., Arjmand, A., Lessard, P., Hawley, S., Grahame Hardie, D., and Thomas, M. (2009). SnRK1 (SNF1-related kinase 1) has a central role in sugar and ABA signalling in *Arabidopsis thaliana*. *The Plant Journal*, 59:316–328.
- Karaba, A., Dixit, S., Greco, R., Aharoni, A., Trijatmiko, K. R., Marsch-Martinez, N., Krishnan, A., Nataraja, K. N., Udayakumar, M., and Pereira, A. (2007). Improvement of water use efficiency in rice by expression of *HARDY*, an *Arabidopsis* drought and salt tolerance gene. *Proceedings of the National Academy of Sciences*, 104:15270–15275.
- Kataoka, T., Hayashi, N., Yamaya, T., and Takahashi, H. (2004). Root-to-shoot transport of sulfate in *Arabidopsis*. Evidence for the role of SULTR3;5 as a component of low-affinity sulfate transport system in the root vasculature. *Plant Physiology*, 136:4198–4204.
- Kawagoe, T. and Kudoh, H. (2010). Escape from floral herbivory by early flowering in *Arabidopsis halleri* subsp. *gemmifera*. *Oecologia*, 164:713–720.
- Kawagoe, T., Shimizu, K. K., Kakutani, T., and Kudoh, H. (2011). Coexistence of trichome variation in a natural plant population: A combined study using ecological and candidate gene approaches. *Public Library of Science ONE*, 6:e22184.
- Kay, S. A. and Remigereau, M.-S. (2016). Cultivated tomato clock runs slow. *Nature Genetics*, 48:8–9.
- Kell, D. B. (2011). Breeding crop plants with deep roots: Their role in sustainable carbon, nutrient and water sequestration. *Annals of Botany*, 108:407–418.
- Kelly, G., Lugassi, N., Belausov, E., Wolf, D., Khamaisi, B., Brandsma, D., Kottapalli, J., Fidel, L., Ben-Zvi, B., Egbaria, A., Acheampong, A. K., Zheng, C., Or, E., Distelfeld, A., David-Schwartz, R., Carmi, N., and Granot, D. (2017). The *Solanum tuberosum* *KST1* partial promoter as a tool for guard cell expression in multiple plant species. *Journal of Experimental Botany*, 68:2885 – 2897.

- Kelly, G., Moshelion, M., David-Schwartz, R., Halperin, O., Wallach, R., Attia, Z., Be-  
lausov, E., and Granot, D. (2013). Hexokinase mediates stomatal closure. *The Plant  
Journal*, 75:977–988.
- Kenney, A. M., McKay, J. K., Richards, J. H., and Juenger, T. E. (2014). Direct and indirect  
selection on flowering time, water-use efficiency (WUE,  $\delta^{13}\text{C}$ ), and WUE plasticity to  
drought in *Arabidopsis thaliana*. *Ecology and Evolution*, 4:4505–4521.
- Kerr, P. S., Rufty, T. W., and Huber, S. C. (1985). Endogenous rhythms in photosynthesis,  
sucrose phosphate synthase activity, and stomatal resistance in leaves of soybean  
(*Glycine max* [L.] Merr.). *Plant Physiology*, 77:275–280.
- Khan, S., Rowe, S. C., and Harmon, F. G. (2010). Coordination of the maize transcrip-  
tome by a conserved circadian clock. *BioMed Central Plant Biology*, 10:126.
- Khanna, R., Kikis, E. a., and Quail, P. H. (2003). *EARLY FLOWERING 4* functions in phy-  
tochrome B-regulated seedling de-etiolation. *Plant Physiology*, 133:1530–1538.
- Khoury, C. K., Bjorkman, A. D., Dempewolf, H., Ramirez-Villegas, J., Guarino, L., Jarvis,  
A., Rieseberg, L. H., and Struik, P. C. (2014). Increasing homogeneity in global food  
supplies and the implications for food security. *Proceedings of the National Academy  
of Sciences*, 111:4001–4006.
- Kiba, T., Henriques, R., Sakakibara, H., and Chua, N.-H. (2007). Targeted degradation of  
PSEUDO-RESPONSE REGULATOR5 by an SCF<sup>ZTL</sup> complex regulates clock function and  
photomorphogenesis in *Arabidopsis thaliana*. *The Plant Cell*, 19:2516–2530.
- Kiegle, E., Moore, C. A., Haseloff, J., Tester, M. A., and Knight, M. R. (2000). Cell-type-  
specific calcium responses to drought, salt and cold in the *Arabidopsis* root. *The  
Plant Journal*, 23:267–278.
- Kikis, E. A., Khanna, R., and Quail, P. H. (2005). ELF4 is a phytochrome-regulated compo-  
nent of a negative-feedback loop involving the central oscillator components CCA1  
and LHY. *The Plant Journal*, 44:300–313.
- Kim, H., Kim, Y., Yeom, M., Lim, J., and Nam, H. G. (2016). Age-associated circadian  
period changes in *Arabidopsis* leaves. *Journal of Experimental Botany*, 67:2665–  
2673.
- Kim, T.-H., Bohmer, M., Hu, H., Nishimura, N., and Schroeder, J. I. (2010). Guard cells  
signal transduction network: Advances in understanding abscisic acid CO<sub>2</sub>, and Ca<sup>2+</sup>  
signalling. *Annual Review of Plant Biology*, 61:561–591.

- Kim, W. Y., Ali, Z., Park, H. J., Park, S. J., Cha, J. Y., Perez-Hormaeche, J., Quintero, F. J., Shin, G., Kim, M. R., Qiang, Z., Ning, L., Park, H. C., Lee, S. Y., Bressan, R. A., Pardo, J. M., Bohnert, H. J., and Yun, D. J. (2013). Release of SOS2 kinase from sequestration with GIGANTEA determines salt tolerance in Arabidopsis. *Nature Communications*, 4:1352.
- Kim, W. Y., Fujiwara, S., Suh, S. S., Kim, J., Kim, Y., Han, L., David, K., Putterill, J., Nam, H. G., and Somers, D. E. (2007). ZEITLUPE is a circadian photoreceptor stabilized by GIGANTEA in blue light. *Nature*, 449:356–360.
- Kinoshita, T. and Hayashi, Y. (2011). New insights into the regulation of stomatal opening by blue light and plasma membrane H<sup>+</sup>-ATPase. *International Review of Cell and Molecular Biology*, 289:89–115.
- Kinoshita, T., Ono, N., Hayashi, Y., Morimoto, S., Nakamura, S., Soda, M., Kato, Y., Ohnishi, M., Nakano, T., Inoue, S.-i., and Shimazaki, K.-i. (2011). FLOWERING LOCUS T regulates stomatal opening. *Current Biology*, 21:1232–1238.
- Knight, H., Trewavas, A. J., and Knight, M. R. (1997). Calcium signalling in *Arabidopsis thaliana* responding to drought and salinity. *The Plant Journal*, 12:1067–1078.
- Ko, D. K., Rohozinski, D., Song, Q., Taylor, S. H., Juenger, T. E., Harmon, F. G., and Chen, Z. J. (2016). Temporal shift of circadian-mediated gene expression and carbon fixation contributes to biomass heterosis in maize hybrids. *Public Library of Science Genetics*, 12:e1006197.
- Koini, M. A., Alvey, L., Allen, T., Tilley, C. A., Harberd, N. P., Whitelam, G. C., and Franklin, K. A. (2009). High temperature-mediated adaptations in plant architecture require the bHLH transcription factor PIF4. *Current Biology*, 19:408–413.
- Kollist, H., Nuhkat, M., and Roelfsema, M. R. G. (2014). Closing gaps: Linking elements that control stomatal movement. *New Phytologist*, 203:44–62.
- Kolmos, E., Nowak, M., Werner, M., Fischer, K., Schwarz, G., Mathews, S., Schoof, H., Nagy, F., Bujnicki, J. M., and Davis, S. J. (2009). Integrating *ELF4* into the circadian system through combined structural and functional studies. *Human Frontier Science Program Journal*, 3:350–366.
- Koorneef, M., Elgersma, A., Hanhart, C. J., van Loenen-Martinet, E. P., van Rijn, L., and Zeevaart, J. A. (1985). A gibberellin insensitive mutant of *Arabidopsis thaliana*. *Physiologia Plantarum*, 65:33–39.



- Kudoh, H. (2016). Molecular phenology in plants: in natura systems biology for the comprehensive understanding of seasonal responses under natural environments. *New Phytologist*, 210:399–412.
- Kumar, K., Rao, K. P., Biswas, D. K., and Sinha, A. K. (2011). Rice WNK1 is regulated by abiotic stress and involved in internal circadian rhythm. *Plant Signaling & Behavior*, 6:316–320.
- Kurata, T. and Yamamoto, K. T. (1998). *petit1*, a conditional growth mutant of Arabidopsis defective in sucrose-dependent elongation growth. *Plant Physiology*, 118:793–801.
- Lai, A. G., Doherty, C. J., Mueller-Roeber, B., Kay, S. A., Schippers, J. H. M., and Dijkwel, P. P. (2012). *CIRCADIAN CLOCK-ASSOCIATED 1* regulates ROS homeostasis and oxidative stress responses. *Proceedings of the National Academy of Sciences*, 109:17129–17134.
- Larkin, J. C., Young, N., Prigge, M., and Marks, M. D. (1996). The control of trichome spacing and number in Arabidopsis. *Development*, 122:997–1005.
- Lastdrager, J., Hanson, J., and Smeekens, S. (2014). Sugar signals and the control of plant growth and development. *Journal of Experimental Botany*, 65:799–807.
- Lawlor, D. W. and Paul, M. J. (2014). Source/sink interactions underpin crop yield: The case for trehalose 6-phosphate/SnRK1 in improvement of wheat. *Frontiers in Plant Science*, 5:418.
- Lawson, T. and Blatt, M. R. (2014). Stomatal size, speed, and responsiveness impact on photosynthesis and water use efficiency. *Plant Physiology*, 164:1556–1570.
- Lawson, T., Kramer, D. M., and Raines, C. A. (2012). Improving yield by exploiting mechanisms underlying natural variation of photosynthesis. *Current Opinion in Biotechnology*, 23:215–220.
- Lawson, T., Oxborough, K., Morison, J. I. L., and Baker, N. R. (2002). Responses of photosynthetic electron transport in stomatal guard cells and mesophyll cells in intact leaves to light, CO<sub>2</sub>, and humidity. *Plant Physiology*, 128:52–62.
- Lawson, T., Simkin, A. J., Kelly, G., and Granot, D. (2014). Mesophyll photosynthesis and guard cell metabolism impacts on stomatal behaviour. *New Phytologist*, 203:1064–1081.

- Lebaudy, A., Vavasseur, A., Hosy, E., Dreyer, I., Leonhardt, N., Thibaud, J.-B., Véry, A.-A., Simonneau, T., and Sentenac, H. (2008). Plant adaptation to fluctuating environment and biomass production are strongly dependent on guard cell potassium channels. *Proceedings of the National Academy of Sciences*, 105:5271– 5276.
- Lee, D. J., Park, J. W., Lee, H. W., and Kim, J. (2009). Genome-wide analysis of the auxin-responsive transcriptome downstream of *iaa1* and its expression analysis reveal the diversity and complexity of auxin-regulated gene expression. *Journal of Experimental Botany*, 60:3935–3957.
- Lee, H. G., Seo, P. J., and Mas, P. (2016). MYB96 shapes the circadian gating of ABA signaling in Arabidopsis. *Nature Scientific Reports*, 6:17754.
- Lee, J. and Bowling, D. J. F. (1992). Effect of the mesophyll on stomatal opening in *Commelina communis*. *Journal of Experimental Botany*, 43:951–957.
- Legnaioli, T., Cuevas, J., and Mas, P. (2009). TOC1 functions as a molecular switch connecting the circadian clock with plant responses to drought. *The European Molecular Biology Organization Journal*, 28:3745–3757.
- Leivar, P. and Quail, P. H. (2011). PIFs: Pivotal components in a cellular signaling hub. *Trends in Plant Science*, 16:19–28.
- Levin, D. A. (1973). The role of trichomes in plant defense. *The Quarterly Review of Biology*, 48:3–15.
- Li, L. and Sheen, J. (2016). Dynamic and diverse sugar signaling. *Current Opinion in Plant Biology*, 33:116–125.
- Li, Y., Darley, C. P., Ongaro, V., Fleming, A. J., Schipper, O., Badauf, S. L., and McQueen-Mason, S. M. (2002). Plant expansins are a complex multigene family with an ancient evolutionary origin. *Plant Physiology*, 128:854– 864.
- Li, Y., Li, H., Li, Y., and Zhang, S. (2017). Improving water-use efficiency by decreasing stomatal conductance and transpiration rate to maintain higher ear photosynthetic rate in drought-resistant wheat. *Crop Journal*, 5:231–239.
- Li, Y., Van Den Ende, W., and Rolland, F. (2014). Sucrose induction of anthocyanin biosynthesis is mediated by DELLA. *Molecular Plant*, 7:570–572.

- Lilley, J. L. S., Gee, C. W., Sairanen, I., Ljung, K., and Nemhauser, J. L. (2012). An endogenous carbon-sensing pathway triggers increased auxin flux and hypocotyl elongation. *Plant Physiology*, 160:2261–2270.
- Liu, T., Carlsson, J., Takeuchi, T., Newton, L., and Farré, E. M. (2013). Direct regulation of abiotic responses by the *Arabidopsis* circadian clock component PRR7. *The Plant Journal*, 76:101–114.
- Liu, Z., Zhang, Y., Liu, R., Hao, H., Wang, Z., and Bi, Y. (2011). Phytochrome interacting factors (PIFs) are essential regulators for sucrose-induced hypocotyl elongation in *Arabidopsis*. *Journal of Plant Physiology*, 168:1771–1779.
- Lobell, D. B., Burke, M. B., Tebaldi, C., Mastrandrea, M. D., Falcon, W. P., and Naylor, R. L. (2008). Prioritizing climate change adaptation needs for food security in 2030. *Science*, 319:607–610.
- Løe, G., Toräng, P., Gaudeul, M., and Ågren, J. (2007). Trichome production and spatiotemporal variation in herbivory in the perennial herb *Arabidopsis lyrata*. *Oikos*, 116:134–142.
- Loreti, E., Poggi, A., Novi, G., Alpi, A., and Perata, P. (2005). A genome-wide analysis of the effects of sucrose on gene expression in *Arabidopsis* seedlings under anoxia. *Plant Physiology*, 137:1130–1138.
- Love, J., Dodd, A. N., and Webb, A. A. R. (2004). Circadian and diurnal calcium oscillations encode photoperiodic information in *Arabidopsis*. *The Plant Cell*, 16:956–966.
- MacGregor, D. R., Kendall, S. L., Florance, H., Fedi, F., Moore, K., Paszkiewicz, K., Smirnoff, N., and Penfield, S. (2015). Seed production temperature regulation of primary dormancy occurs through control of seed coat phenylpropanoid metabolism. *New Phytologist*, 205:642–652.
- Mair, A., Pedrotti, L., Wurzinger, B., Anrather, D., Simeunovic, A., Weiste, C., Valerio, C., Dietrich, K., Kirchler, T., Nägele, T., Vicente Carbajosa, J., Hanson, J., Baena-González, E., Chaban, C., Weckwerth, W., Dröge-Laser, W., and Teige, M. (2015). SnRK1-triggered switch of bZIP63 dimerization mediates the low-energy response in plants. *eLife*, 4:e05828.
- Makino, S., Matsushika, A., Kojima, M., Yamashino, T., and Mizuno, T. (2002). The APRR1/TOC1 quintet implicated in circadian rhythms of *Arabidopsis thaliana*: I.

- Characterization with APRR1-overexpressing plants. *Plant & Cell Physiology*, 43:118–122.
- Malyska, A., Bolla, R., and Twardowski, T. (2016). The role of public opinion in shaping trajectories of agricultural biotechnology. *Trends in Biotechnology*, 34:530–534.
- Martin, E. S. and Meidner, H. (1971). Endogenous stomatal movements in *Tradescantia virginiana*. *New Phytologist*, 70:923–928.
- Martins, M. C. M., Hejazi, M., Fettke, J., Steup, M., Feil, R., Krause, U., Arrivault, S., Vosloh, D., Figueroa, C. M., Ivakov, A., Yadav, U. P., Piques, M., Metzner, D., Stitt, M., and Lunn, J. E. (2013). Feedback inhibition of starch degradation in Arabidopsis leaves mediated by trehalose 6-phosphate. *Plant Physiology*, 163:1142–1163.
- Más, P., Alabadí, D., Yanovsky, M. J., Oyama, T., and Kay, S. A. (2003a). Dual role of TOC1 in the control of circadian and photomorphogenic responses in Arabidopsis. *The Plant Cell*, 15:223–236.
- Más, P., Kim, W.-Y., Somers, D. E., and Kay, S. A. (2003b). Targeted degradation of TOC1 by ZTL modulates circadian function in *Arabidopsis thaliana*. *Nature*, 426:567–570.
- Masle, J., Gilmore, S. R., and Farquhar, G. D. (2005). The *ERECTA* gene regulates plant transpiration efficiency in Arabidopsis. *Nature*, 436:866–870.
- Matsushika, A., Makino, S., Kojima, M., Yamashino, T., Mizuno, T., Matsushika, A., Kojima, M., Yamashino, T., and Mizuno, T. (2002). The APRR1/TOC1 quintet implicated in circadian rhythms of *Arabidopsis thaliana*: II. Characterization with CCA1-overexpressing plants. *Plant & Cell Physiology*, 43:118–122.
- Matsuzaki, J., Kawahara, Y., and Izawa, T. (2015). Punctual transcriptional regulation by the rice circadian clock under fluctuating field conditions. *The Plant Cell*, 27:633–648.
- Matthews, J. S., Violet-Chabrand, S. R., and Lawson, T. (2017). Diurnal variation in gas exchange: The balance between carbon fixation and water loss. *Plant Physiology*, 174:614–623.
- Matthews, J. S., Violet-Chabrand, S. R., and Lawson, T. (2018). Acclimation to fluctuating light impacts the rapidity and diurnal rhythm of stomatal conductance. *Plant Physiology*, 176(March):1939–1951.

- Mauricio, R. (1998). Costs of resistance to natural enemies in field populations of the annual plant *Arabidopsis thaliana*. *The American Naturalist*, 151:20–28.
- Mauricio, R. and Rausher, M. D. (1997). Experimental manipulation of putative selective agents provides evidence for the role of natural enemies in the evolution of plant defense. *Evolution*, 51:1435–1444.
- McAinsh, M. R., Evans, N. H., Montgomery, L. T., and North, K. A. (2002). Calcium signalling in stomatal responses to pollutants. *New Phytologist*, 153:441–447.
- McClung, C. R. (2013). Beyond Arabidopsis: The circadian clock in non-model plant species. *Seminars in Cell & Developmental Biology*, 24:430–436.
- McClung, R. C. (2006). Plant circadian rhythms. *The Plant Cell*, 18:792–803.
- McFadden, B. R. (2016). Examining the gap between science and public opinion about genetically modified food and global warming. *Public Library of Science ONE*, 11:e0166140.
- McLachlan, D. H., Lan, J., Geilfus, C. M., Dodd, A. N., Larson, T., Baker, A., Hörak, H., Kollist, H., He, Z., Graham, I., Mickelbart, M. V., and Hetherington, A. M. (2016). The breakdown of stored triacylglycerols is required during light-induced stomatal opening. *Current Biology*, 26:707–712.
- McWatters, H. G., Kolmos, E., Hall, A., Doyle, M. R., Amasino, R. M., Gyula, P., Nagy, F., Millar, A. J., and Davis, S. J. (2007). *ELF4* is required for oscillatory properties of the circadian clock. *Plant Physiology*, 144:391–401.
- Medlyn, B. E., De Kauwe, M. G., Lin, Y. S., Knauer, J., Duursma, R. A., Williams, C. A., Arneeth, A., Clement, R., Isaac, P., Limousin, J. M., Linderson, M. L., Meir, P., Martin-Stpaul, N., and Wingate, L. (2017). How do leaf and ecosystem measures of water-use efficiency compare? *New Phytologist*, 216:758–770.
- Medrano, H., Tomás, M., Martorell, S., Flexas, J., Hernández, E., Rosselló, J., Pou, A., Escalona, J. M., and Bota, J. (2015). From leaf to whole-plant water use efficiency (WUE) in complex canopies: Limitations of leaf WUE as a selection target. *The Crop Journal*, 3:220–228.
- Merlot, S., Mustilli, A.-C., Genty, B., North, H., Lefebvre, V., Sotta, B., Vavasseur, A., and Giraudat, J. (2002). Use of infrared thermal imaging to isolate *Arabidopsis* mutants defective in stomatal regulation. *The Plant Journal*, 30:601–609.

- Merquiol, E., Pnueli, L., Cohen, M., Simovitch, M., Rachmilevitch, S., Goloubinoff, P., Kaplan, A., and Mittler, R. (2002). Seasonal and diurnal variations in gene expression in the desert legume *Retama raetam*. *Plant, Cell & Environment*, 25:1627–1638.
- Meyer, S., Mumm, P., Imes, D., Endler, A., Weder, B., Al-Rasheid, K. A. S., Geiger, D., Marten, I., Martinoia, E., and Hedrich, R. (2010). *AtALMT12* represents an R-type anion channel required for stomatal movement in *Arabidopsis* guard cells. *The Plant Journal*, 63:1054–1062.
- Micallef, B. J., Haskins, K. A., Vanderveer, P. J., Roh, K.-S., Shewmaker, C. K., and Sharkey, T. D. (1995). Altered photosynthesis, flowering, and fruiting in transgenic tomato plants that have an increased capacity for sucrose synthesis. *Planta*, 196:327–334.
- Michael, T. P., Salome, P. A., Yu, H. J., Spencer, T. R., Sharp, E. L., McPeck, M. A., Alonso, J. M., Ecker, J. R., and McClung, R. C. (2003). Enhanced fitness conferred by naturally occurring variation in the circadian clock. *Science*, 302:1049–1053.
- Millar, A. J., Carré, I. A., Strayer, C. A., Chua, N. H., and Kay, S. A. (1995). Circadian clock mutants in *Arabidopsis* identified by luciferase imaging. *Science*, 267:1161–1163.
- Millar, A. J., Short, S. R., Chua, N. H., and Kay, S. A. (1992). A novel circadian phenotype based on firefly luciferase expression in transgenic plants. *The Plant Cell*, 4:1075–1087.
- Miyazaki, Y., Abe, H., Takase, T., Kobayashi, M., and Kiyosue, T. (2015). Overexpression of *LOV KELCH PROTEIN 2* confers dehydration tolerance and is associated with enhanced expression of dehydration-inducible genes in *Arabidopsis thaliana*. *Plant Cell Reports*, 34:843–852.
- Mizuno, T., Nomoto, Y., Oka, H., Kitayama, M., Takeuchi, A., Tsubouchi, M., and Yamashino, T. (2014). Ambient temperature signal feeds into the circadian clock transcriptional circuitry through the EC night-time repressor in *Arabidopsis thaliana*. *Plant & Cell Physiology*, 55:958–976.
- Mizuno, T. and Yamashino, T. (2008). Comparative transcriptome of diurnally oscillating genes and hormone-responsive genes in *Arabidopsis thaliana*: Insight into circadian clock-controlled daily responses to common ambient stresses in plants. *Plant & Cell Physiology*, 49:481–487.
- Mockler, T. C., Michael, T. P., Priest, H. D., Shen, R., Sullivan, C. M., Givan, S. A., McEntee, C., Kay, S. A., and Chory, J. (2007). The Diurnal Project: Diurnal and circadian

- expression profiling, model-based pattern matching, and promoter analysis. *Cold Spring Harbor Symposia on Quantitative Biology*, 72:353–363.
- Moghaddam, M. R. B. and Van Den Ende, W. (2013). Sweet immunity in the plant circadian regulatory network. *Journal of Experimental Botany*, 64:1439–1449.
- Mohawk, J. A., Green, C. B., and Takahashi, J. S. (2012). Central and peripheral circadian clocks in mammals. *Annual Review of Neuroscience*, 35:445–462.
- Moore, B., Zhou, L., Rolland, F., Hall, Q., Cheng, W.-H., Liu, Y.-X., Hwang, I., Jones, T., and Sheen, J. (2003). Role of the Arabidopsis glucose sensor HXK1 in nutrient, light, and hormonal signaling. *Science*, 300:332–336.
- Morison, J., Baker, N., Mullineaux, P., and Davies, W. (2008). Improving water use in crop production. *Philosophical Transactions of the Royal Society B: Biological Sciences*, 363:639–658.
- Mott, K. A., Berg, D. G., Hunt, S. M., and Peak, D. (2014). Is the signal from the mesophyll to the guard cells a vapour-phase ion? *Plant, Cell & Environment*, 37:1184–1191.
- Mott, K. A., Sibbersen, E. D., and Shope, J. C. (2008). The role of the mesophyll in stomatal responses to light and CO<sub>2</sub>. *Plant, Cell & Environment*, 31:1299–1306.
- Müller, N. A., Wijnen, C. L., Srinivasan, A., Ryngajllo, M., Ofner, I., Lin, T., Ranjan, A., West, D., Maloof, J. N., Sinha, N. R., Huang, S., Zamir, D., and Jiménez-Gómez, J. M. (2016). Domestication selected for deceleration of the circadian clock in cultivated tomato. *Nature Genetics*, 48:89–93.
- Müller, N. A., Zhang, L., Koornneef, M., and Jiménez-Gómez, J. M. (2018). Mutations in *EID1* and *LNK2* caused light-conditional clock deceleration during tomato domestication. *Proceedings of the National Academy of Sciences*, 115:7135–7140.
- Munemasa, S., Hauser, F., Park, J., Waadt, R., Brandt, B., and Schroeder, J. I. (2015). Mechanisms of abscisic acid-mediated control of stomatal aperture. *Current Opinion in Plant Biology*, 28:154–162.
- Murakami, M., Yamashino, T., and Mizuno, T. (2004). Characterization of circadian-associated APRR3 pseudo-response regulator belonging to the APRR1/TOC1 quintet in *Arabidopsis thaliana*. *Plant & Cell Physiology*, 45:645–650.
- Muranaka, T. and Oyama, T. (2016). Heterogeneity of cellular circadian clocks in intact plants and its correction under light-dark cycles. *Science Advances*, 2:e1600500.

- Murchie, E. H., Pinto, M., and Horton, P. (2009). Agriculture and the new challenges for photosynthesis research. *New Phytologist*, 181:532–552.
- Na, J.-K. and Metzger, J. D. (2014). Chimeric promoter mediates guard cell-specific gene expression in tobacco under water deficit. *Biotechnology Letters*, 36:1893–1899.
- Nadeau, J. A. and Sack, F. D. (2002). Stomatal development in Arabidopsis. *The Arabidopsis book*, 1:e0066.
- Nagel, D. H. and Kay, S. A. (2012). Complexity in the wiring and regulation of plant circadian networks. *Current Biology*, 22:R648–R657.
- Nagy, R., Grob, H., Weder, B., Green, P., Klein, M., Frelet-Barrand, A., Schjoerring, J. K., Brearley, C., and Martinoia, E. (2009). The Arabidopsis ATP-binding cassette protein AtMRP5/AtABCC5 is a high affinity inositol hexakisphosphate transporter involved in guard cell signaling and phytate storage. *Journal of Biological Chemistry*, 284:33614–33622.
- Nakamichi, N. (2015). Adaptation to the local environment by modifications of the photoperiod response in crops. *Plant & Cell Physiology*, 56:594–604.
- Nakamichi, N., Kiba, T., Henriques, R., Mizuno, T., Chua, N. H., and Sakakibara, H. (2010). PSEUDO-RESPONSE REGULATORS 9, 7, and 5 are transcriptional repressors in the Arabidopsis circadian clock. *The Plant Cell*, 22:594–605.
- Nakamichi, N., Kusano, M., Fukushima, A., Kita, M., Ito, S., Yamashino, T., Saito, K., Sakakibara, H., and Mizuno, T. (2009). Transcript profiling of an Arabidopsis *PSEUDO RESPONSE REGULATOR* arrhythmic triple mutant reveals a role for the circadian clock in cold stress response. *Plant & Cell Physiology*, 50:447–462.
- Nakamichi, N., Murakami-kojimo, M., Sato, E., Kishi, Y., Yamashino, T., and Mizuno, T. (2002). Compilation and characterization of a novel WNK family of protein kinases in *Arabidopsis thaliana* with reference to circadian rhythms. *Bioscience, Biotechnology, and Biochemistry*, 66:2429–2436.
- Nienhuis, J., Sills, G. R., Martin, B., and King, G. (1994). Variance for water-use efficiency among ecotypes and recombinant inbred lines of *Arabidopsis thaliana* (Brassicaceae). *American Journal of Botany*, 81:943–947.
- Nilson, S. E. and Assmann, S. M. (2007). The control of transpiration. Insights from Arabidopsis. *Plant Physiology*, 143:19–27.



- Nimmo, H. G. (2018). Entrainment of Arabidopsis roots to the light:dark cycle by light piping [Epub ahead of print]. *Plant Cell & Environment*.
- Niwa, Y., Yamashino, T., and Mizuno, T. (2009). The circadian clock regulates the photoperiodic response of hypocotyl elongation through a coincidence mechanism in *Arabidopsis thaliana*. *Plant & Cell Physiology*, 50:838–854.
- Noordally, Z. B., Ishii, K., Atkins, K. A., Wetherill, S. J., Kusakina, J., Walton, E. J., Kato, M., Azuma, M., Tanaka, K., Hanaoka, M., and Dodd, A. N. (2013). Circadian control of chloroplast transcription by a nuclear-encoded timing signal. *Science*, 339:1316–1319.
- Nozue, K., Covington, M. F., Duek, P. D., Lorrain, S., Fankhauser, C., Harmer, S. L., and Maloof, J. N. (2007). Rhythmic growth explained by coincidence between internal and external cues. *Nature*, 448:358–361.
- Nuccio, M. L., Wu, J., Mowers, R., Zhou, H. P., Meghji, M., Primavesi, L. F., Paul, M. J., Chen, X., Gao, Y., Haque, E., Basu, S. S., and Lagrimini, L. M. (2015). Expression of trehalose-6-phosphate phosphatase in maize ears improves yield in well-watered and drought conditions. *Nature Biotechnology*, 33:862–869.
- Nunes, C., O’Hara, L. E., Primavesi, L. F., Delatte, T., Schlupepmann, H., Somsen, G. W., Silva, A. B., Fevereiro, P. S., Wingler, A., and Paul, M. J. (2013). The trehalose 6-phosphate/SnRK1 signaling pathway primes growth recovery following relief of sink limitation. *Plant Physiology*, 162:1720–1732.
- Nusinow, D. A., Helfer, A., Hamilton, E. E., King, J. J., Imaizumi, T., Schultz, T. F., Farré, E. M., and Kay, S. A. (2011). The ELF4-ELF3-LUX complex links the circadian clock to diurnal control of hypocotyl growth. *Nature*, 475:398–404.
- Offringa, R. and Hooykaas, P. (1999). Molecular approaches to study plant hormone signalling. In Hooykaas, P. J. J., Hall, M. A., and Libbenga, K. R., editors, *New Comprehensive Biochemistry*, pages 391–410. Elsevier.
- Ogawa, M., Hanada, A., Yamauchi, Y., Kuwahara, A., Kamiya, Y., and Yamaguchi, S. (2003). Gibberellin biosynthesis and response during Arabidopsis seed germination. *The Plant Cell*, 15:1591–1604.
- Outlaw Jr., W. H. and De Vlieghere-He, X. (2001). Transpiration rate. An important factor controlling the sucrose content of the guard cell apoplast of broad bean. *Plant Physiology*, 126:1716–1724.

- Paez-Garcia, A., Motes, C., Scheible, W.-R., Chen, R., Blancaflor, E., and Monteros, M. (2015). Root traits and phenotyping strategies for plant improvement. *Plants*, 4:334–355.
- Panda, S., Poirier, G. G., and Kay, S. A. (2002). *tej* Defines a Role for Poly(ADP-ribose)ylation in establishing period length of the Arabidopsis circadian oscillator. *Developmental Cell*, 3:51–61.
- Pantin, F., Monnet, F., Jannaud, D., Costa, J. M., Renaud, J., Muller, B., and Genty, B. (2013). The dual effect of abscisic acid on stomata. *New Phytologist*, 197:65–72.
- Paparelli, E., Parlanti, S., Gonzali, S., Novi, G., Mariotti, L., Ceccarelli, N., van Dongen, J. T., Kölling, K., Zeeman, S. C., and Perata, P. (2013). Nighttime sugar starvation orchestrates gibberellin biosynthesis and plant growth in Arabidopsis. *The Plant Cell*, 25:3760–3769.
- Para, A., Farre, E. M., Imaizumi, T., Pruneda-Paz, J. L., Harmon, F. G., and Kay, S. A. (2007). PRR3 is a vascular regulator of TOC1 stability in the Arabidopsis circadian clock. *The Plant Cell*, 19:3462–3473.
- Park, J. Y., Canam, T., Kang, K.-Y., Ellis, D. D., and Mansfield, S. D. (2008). Overexpression of an Arabidopsis family A sucrose phosphate synthase (SPS) gene alters plant growth and fibre development. *Transgenic Research*, 17:181–192.
- Park, S.-Y., Fung, P., Nishimura, N., Jensen, D. R., Zhao, Y., Lumba, S., Santiago, J., Rodrigues, A., Alfred, S. E., Bonetta, D., Finkelstein, R., Provart, N. J., Rodriguez, P. L., McCourt, P., Zhu, J.-K., Schroeder, J. I., Volkman, B. F., and Cutler, S. R. (2009). Abscisic acid inhibits PP2Cs via the PYR/PYL family of ABA-binding START proteins. *Science*, 324:1068–1071.
- Patrick, J. W., Botha, F. C., and Birch, R. G. (2013). Metabolic engineering of sugars and simple sugar derivatives in plants. *Plant Biotechnology Journal*, 11:142–156.
- Paul, M., Pellny, T., and Goddijn, O. (2001). Enhancing photosynthesis with sugar signals. *Trends in Plant Science*, 6:197–200.
- Paul, M. J., Jhurreea, D., Zhang, Y., Primavesi, L. F., Delatte, T., Schlupepmann, H., and Winkler, A. (2010). Upregulation of biosynthetic processes associated with growth by trehalose 6-phosphate. *Plant Signaling & Behavior*, 5:386–392.

- Pei, Z.-M., Ghassemian, M., Kwak, C. M., McCourt, P., and Schroeder, J. I. (1998). Role of farnesyltransferase in ABA regulation of guard cell anion channels and plant water loss. *Science*, 282:287–290.
- Pei, Z.-M., Murata, Y., Benning, G., Thomine, S., Klusener, B., Allen, G. J., Grill, E., and Schroeder, J. I. (2000). Calcium channels activated by hydrogen peroxide mediate abscisic acid signalling in guard cells. *Nature*, 406:731–734.
- Peng, J., Carol, P., Richards, D. E., King, K. E., Cowling, R. J., Murphy, G. P., and Harberd, N. P. (1997). The Arabidopsis *GAI* gene defines a signalling pathway that negatively regulates gibberellin responses. *Genes & Development*, 11:3194–3205.
- Pérez-Pérez, J. M., Serrano-Cartagena, J., and Micol, J. L. (2002). Genetic analysis of natural variations in the architecture of *Arabidopsis thaliana* vegetative leaves. *Genetics*, 162:893–915.
- Persson, S., Wyatt, S. E., Love, J., Thompson, W. F., Robertson, D., and Boss, W. F. (2001). The Ca<sup>2+</sup> status of the endoplasmic reticulum is altered by induction of calreticulin expression in transgenic plants. *Plant Physiology*, 126:1092–1104.
- Pillitteri, L. J. and Dong, J. (2013). Stomatal development in Arabidopsis. *The Arabidopsis Book*, 11:e0162.
- Pittman, J. K. and Hirschi, K. D. (2003). Don't shoot the (second) messenger: Endomembrane transporters and binding proteins modulate cytosolic Ca<sup>2+</sup> levels. *Current Opinion in Plant Biology*, 6:257–262.
- Pokhilko, A., Mas, P., and Millar, A. J. (2013). Modelling the widespread effects of TOC1 signalling on the plant circadian clock and its outputs. *BioMed Central Systems Biology*, 7:23.
- Preuss, S. B., Meister, R., Xu, Q., Urwin, C. P., Tripodi, F. A., Screen, S. E., Anil, V. S., Zhu, S., Morrell, J. A., Liu, G., Ratcliffe, O. J., Reuber, T. L., Khanna, R., Goldman, B. S., Bell, E., Ziegler, T. E., McClerren, A. L., Ruff, T. G., and Petracek, M. E. (2012). Expression of the *Arabidopsis thaliana* *BBX32* gene in soybean increases grain yield. *Public Library of Science ONE*, 7:e30717.
- Pruneda-Paz, J. L., Breton, G., Para, A., and Kay, S. A. (2009). A functional genomics approach reveals CHE as a component of the Arabidopsis circadian clock. *Science*, 323:1481–1486.

- Ramon, M., Rolland, F., Thevelein, J. M., Van Dijck, P., and Leyman, B. (2007). ABI4 mediates the effects of exogenous trehalose on Arabidopsis growth and starch breakdown. *Plant Molecular Biology*, 63:195–206.
- Rawat, R., Takahashi, N., Hsu, P. Y., Jones, M. A., Schwartz, J., Salemi, M. R., Phinney, B. S., and Harmer, S. L. (2011). REVEILLE8 and PSEUDO-RESPONSE REGULATOR5 form a negative feedback loop within the Arabidopsis circadian clock. *Public Library of Science Genetics*, 7:e1001350.
- Rédei, G. P. (1962). Supervital mutants of Arabidopsis. *Genetics*, 47:443–460.
- Reichstein, M., Stoy, P. C., Desai, A. K., Lasslop, G., and Richardson, A. D. (2012). Partitioning of net fluxes. In Aubinet, M., Vesala, T., and Papale, D., editors, *Eddy covariance: A practical guide to measurement and data analysis*, pages 263–290. Springer.
- Resco de Dios, V. and Gessler, A. (2018). Circadian regulation of photosynthesis and transpiration from genes to ecosystems. *Environmental and Experimental Botany*, 152:37–48.
- Resco de Dios, V., Gessler, A., Ferrio, J. P., Alday, J., Bahn, M., del Castillo, J., Devidal, S., García-Muñoz, S., Kayler, Z., Landais, D., Martín-Gómez, P., Milcu, A., Piel, C., Pirhofer-Walzl, K., Ravel, O., Salekin, S., Tissue, D., Tjoelker, M., Voltas, J., and Roy, J. (2017). Circadian rhythms regulate the environmental responses of net CO<sub>2</sub> exchange in bean and cotton canopies. *Agricultural and Forest Meteorology*, 239:185–191.
- Resco de Dios, V., Gessler, A., Ferrio, J. P., Alday, J. G., Bahn, M., del Castillo, J., Devidal, S., García-Muñoz, S., Kayler, Z., Landais, D., Martín-Gómez, P., Milcu, A., Piel, C., Pirhofer-Walzl, K., Ravel, O., Salekin, S., Tissue, D. T., Tjoelker, M. G., Voltas, J., and Roy, J. (2016a). Circadian rhythms have significant effects on leaf-to-canopy scale gas exchange under field conditions. *GigaScience*, 5:43.
- Resco de Dios, V., Loik, M. E., Smith, R., Aspinwall, M. J., and Tissue, D. T. (2016b). Genetic variation in circadian regulation of nocturnal stomatal conductance enhances carbon assimilation and growth. *Plant, Cell & Environment*, 39:3–11.
- Riboni, M., Galbiati, M., Tonelli, C., and Conti, L. (2013). GIGANTEA enables drought escape response via abscisic acid-dependent activation of the florigens and SUPPRESSOR OF OVEREXPRESSION OF CONSTANS1. *Plant Physiology*, 162:1706–1719.

- Richards, D. E., King, K. E., Ait-ali, T., and Harberd, N. P. (2001). How gibberellin regulates plant growth and development: A molecular genetic analysis of gibberellin signaling. *Annual Review of Plant Physiology & Plant Molecular Biology*, 52:67–88.
- Riederer, M. and Schreiber, L. (2001). Protecting against water loss: Analysis of the barrier properties of plant cuticles. *Journal of Experimental Botany*, 52:2023–2032.
- Robertson, F. C., Skeffington, A. W., Gardner, M. J., and Webb, A. A. R. (2009). Interactions between circadian and hormonal signalling in plants. *Plant Molecular Biology*, 69:419–427.
- Rodrigues, A., Adamo, M., Crozet, P., Margalha, L., Confraria, A., Martinho, C., Elias, A., Rabissi, A., Lumbreras, V., Gonzalez-Guzman, M., Antoni, R., Rodriguez, P. L., and Baena-Gonzalez, E. (2013). ABI1 and PP2CA phosphatases are negative regulators of Snf1-related protein kinase1 signaling in Arabidopsis. *The Plant Cell*, 25:3871–3884.
- Roelfsema, M. R. G., Hanstein, S., Felle, H. H., and Hedrich, R. (2002). CO<sub>2</sub> provides an intermediate link in the red light response of guard cells. *The Plant Journal*, 32:65–75.
- Rosegrant, M. W. and Cline, S. A. (2003). Global food security: Challenges and policies. *Science*, 302:1917–1919.
- Rubery, P. H. (1990). Phytotropins: Receptors and endogenous ligands. *Symposia of the Society for Experimental Biology*, 44:119–146.
- Rubin, M. J., Brock, M. T., Baker, R. L., Wilcox, S., Anderson, K., Seth, J., and Weinig, C. (2018). Circadian rhythms are associated with shoot architecture in natural settings [Epub ahead of print]. *New Phytologist*.
- Ruggiero, A., Punzo, P., Landi, S., Costa, A., Oosten, M. J. V., and Grillo, S. (2017). Improving plant water use efficiency through molecular genetics. *Horticulturae*, 3:31.
- Rusconi, F., Simeoni, F., Francia, P., Cominelli, E., Conti, L., Riboni, M., Simoni, L., Martin, C. R., Tonelli, C., and Galbiati, M. (2013). The *Arabidopsis thaliana* MYB60 promoter provides a tool for the spatio-temporal control of gene expression in stomatal guard cells. *Journal of Experimental Botany*, 64:3361–3371.
- Ruts, T., Matsubara, S., Wiese-Klinkenberg, A., and Walter, A. (2012). Aberrant temporal growth pattern and morphology of root and shoot caused by a defective circadian clock in *Arabidopsis thaliana*. *The Plant Journal*, 72:154–161.

- Saad, A. S. I., Li, X., Li, H. P., Huang, T., Gao, C. S., Guo, M. W., Cheng, W., Zhao, G. Y., and Liao, Y. C. (2013). A rice stress-responsive *NAC* gene enhances tolerance of transgenic wheat to drought and salt stresses. *Plant Science*, 203-204:33–40.
- Saijo, Y., Hata, S., Kyojuka, J., Shimamoto, K., and Izui, K. (2000). Over-expression of a single  $\text{Ca}^{2+}$ -dependent protein kinase confers both cold and salt/drought tolerance on rice plants. *The Plant Journal*, 23:319–327.
- Saijo, Y., Kinoshita, N., Ishiyama, K., Hata, S., Kyojuka, J., Hayakawa, T., Nakamura, T., Shimamoto, K., Yamaya, T., and Izui, K. (2001). A  $\text{Ca}^{2+}$ -dependent protein kinase that endows rice plants with cold- and salt-stress tolerance functions in vascular bundles. *Plant & Cell Physiology*, 42:1228–1233.
- Sairanen, I., Novák, O., Pěňčík, A., Ikeda, Y., Jones, B., Sandberg, G., and Ljung, K. (2012). Soluble carbohydrates regulate auxin biosynthesis via PIF proteins in *Arabidopsis*. *The Plant Cell*, 24:4907–4916.
- Salomé, P., Michael, T., Kearns, E., Fett-Neto, A., Sharrock, R. A., and McClung, R. C. (2002). The *out of phase 1* mutant defines a role for PHYB in circadian phase control in *Arabidopsis*. *Plant Physiology*, 129:1674–1685.
- Sanchez, A., Shin, J., and Davis, S. J. (2011). Abiotic stress and the plant circadian clock. *Plant Signaling & Behavior*, 6:223–231.
- Sánchez-Villarreal, A., Davis, A. M., and Davis, S. J. (2018). AKIN10 activity as a cellular link between metabolism and circadian-clock entrainment in *Arabidopsis thaliana*. *Plant Signaling & Behavior*, 13:e1411448.
- Sánchez-Villarreal, A., Shin, J., Bujdoso, N., Obata, T., Neumann, U., Du, S. X., Ding, Z., Davis, A. M., Shindo, T., Schmelzer, E., Sulpice, R., Nunes-Nesi, A., Stitt, M., Fernie, A. R., and Davis, S. J. (2013). *TIME FOR COFFEE* is an essential component in the maintenance of metabolic homeostasis in *Arabidopsis thaliana*. *The Plant Journal*, 76:188–200.
- Sandoval, J. F., Yoo, C. Y., Gosney, M. J., and Mickelbart, M. V. (2016). Growth of *Arabidopsis thaliana* and *Eutrema salsugineum* in a closed growing system designed for quantification of plant water use. *Journal of Plant Physiology*, 193:110–118.
- Santelia, D. and Lawson, T. (2016). Rethinking guard cell metabolism. *Plant Physiology*, 172:1371–1392.

- Sato, Y. and Kudoh, H. (2016). Associational effects against a leaf beetle mediate a minority advantage in defense and growth between hairy and glabrous plants. *Evolutionary Ecology*, 30:137–154.
- Sato, Y. and Kudoh, H. (2017). Fine-scale frequency differentiation along a herbivory gradient in the trichome dimorphism of a wild *Arabidopsis*. *Ecology & Evolution*, 7:2133–2141.
- Schaffer, R., Ramsay, N., Samach, A., Corden, S., Putterill, J., Carré, I. A., and Coupland, G. (1998). The *late elongated hypocotyl* mutation of *Arabidopsis* disrupts circadian rhythms and the photoperiodic control of flowering. *Cell*, 93:1219–1229.
- Schepetilnikov, M. and Ryabova, L. A. (2018). Recent discoveries on the role of TOR (Target of Rapamycin) signaling in translation in plants. *Plant Physiology*, 176:1095–1105.
- Schindelin, J., Arganda-Carreras, I., Frise, E., Kaynig, V., Longair, M., Pietzsch, T., Preibisch, S., Rueden, C., Saalfeld, S., Schmid, B., Tinevez, J.-Y., White, D. J., Hartenstein, V., Eliceiri, K., Tomancak, P., and Cardona, A. (2012). Fiji: An open-source platform for biological-image analysis. *Nature Methods*, 9:676–682.
- Schindelin, J., Rueden, C. T., Hiner, M. C., and Eliceiri, K. W. (2015). The ImageJ ecosystem: An open platform for biomedical image analysis. *Molecular Reproduction & Development*, 82:518–529.
- Schluepmann, H., Berke, L., and Sanchez-Perez, G. F. (2012). Metabolism control over growth: A case for trehalose-6-phosphate in plants. *Journal of Experimental Botany*, 63:3379–3390.
- Schluepmann, H., Pellny, T., van Dijken, A., Smeekens, S., and Paul, M. (2003). Trehalose 6-phosphate is indispensable for carbohydrate utilization and growth in *Arabidopsis thaliana*. *Proceedings of the National Academy of Sciences*, 100:6849–6854.
- Schmidhuber, J. and Tubiello, F. N. (2007). Global food security under climate change. *Proceedings of the National Academy of Sciences*, 104:19703–19708.
- Schmittgen, T. D. and Livak, K. J. (2008). Analyzing real-time PCR data by the comparative  $C_T$  method. *Nature Protocols*, 3:1101–1108.
- Schöning, J. C., Streitner, C., Page, D. R., Hennig, S., Uchida, K., Wolf, E., Furuya, M., and Staiger, D. (2007). Auto-regulation of the circadian slave oscillator component

- AtGRP7* and regulation of its targets is impaired by a single RNA recognition motif point mutation. *The Plant Journal*, 52:1119–1130.
- Schroeder, J. I., Allen, G. J., Hugouvieux, V., Kwak, J. M., and Waner, D. (2001a). Guard cell signal transduction. *Annual Review of Plant Physiology & Plant Molecular Biology*, 52:627–658.
- Schroeder, J. I., Kwak, J. M., and Allen, G. J. (2001b). Guard cell abscisic acid signalling and engineering drought hardiness in plants. *Nature*, 410:327–330.
- Schultz, T. F., Kiyosue, T., Yanovsky, M., Wada, M., and Kay, S. A. (2001). A role for LKP2 in the circadian clock of Arabidopsis. *The Plant Cell*, 13:2659–2670.
- Seki, M., Ohara, T., Hearn, T. J., Frank, A., da Silva, V. C., Caldana, C., Webb, A. A., and Satake, A. (2017). Adjustment of the Arabidopsis circadian oscillator by sugar signalling dictates the regulation of starch metabolism. *Scientific Reports*, 7:e8305.
- Seo, P. J., Lee, S. B., Suh, M. C., Park, M.-J., Go, Y. S., and Park, C.-M. (2011). The MYB96 transcription factor regulates cuticular wax biosynthesis under drought conditions in Arabidopsis. *The Plant Cell*, 23:1138–1152.
- Seung, D., Risopatron, J. P. M., Jones, B. J., and Marc, J. (2012). Circadian clock-dependent gating in ABA signalling networks. *Protoplasma*, 249:445–457.
- Sharma, A., Wai, C. M., Ming, R., and Yu, Q. (2017). Diurnal cycling transcription factors of pineapple revealed by genome-wide annotation and global transcriptomic analysis. *Genome Biology & Evolution*, 9:2170–2190.
- Sheen, J. (2014). Master regulators in plant glucose signalling networks. *Journal of Plant Biology*, 57:67–79.
- Shimizu, H., Katayama, K., Koto, T., Torii, K., Araki, T., and Endo, M. (2015). Decentralized circadian clocks process thermal and photoperiodic cues in specific tissues. *Nature Plants*, 1:15163.
- Shin, J., Du, S., Bujdoso, N., Hu, Y., and Davis, S. J. (2013). Overexpression and loss-of-function at *TIME FOR COFFEE* results in similar phenotypes in diverse growth and physiological responses. *Journal of Plant Biology*, 56:152–159.



- Shin, J., Sánchez-Villarreal, A., Davis, A. M., Du, S.-x., Berendzen, K. W., Koncz, C., Ding, Z., Li, C., and Davis, S. J. (2017). The metabolic sensor AKIN10 modulates the *Arabidopsis* circadian clock in a light-dependent manner. *Plant, Cell & Environment*, 40:997–1008.
- Shor, E. and Green, R. M. (2016). The impact of domestication on the circadian clock. *Trends in Plant Science*, 21:281–283.
- Sibbernsen, E. and Mott, K. A. (2010). Stomatal responses to flooding of the intercellular air spaces suggest a vapor-phase signal between the mesophyll and the guard cells. *Plant Physiology*, 153:1435–1442.
- Siegel, R. S., Xue, S., Murata, Y., Yang, Y., Nishimura, N., Wang, A., and Schroeder, J. I. (2009). Calcium elevation-dependent and attenuated resting calcium-dependent abscisic acid induction of stomatal closure and abscisic acid-induced enhancement of calcium sensitivities of S-type anion and inward-rectifying K<sup>+</sup> channels in *Arabidopsis* guard cells. *The Plant Journal*, 59:207–220.
- Sievers, F., Wilm, A., Dineen, D., Gibson, T., Karplus, K., Li, W., Lopez, R., McWilliam, H., Remmert, M., Söding, J., Thompson, J., and Higgins, D. (2011). Fast, scalable generation of high-quality protein multiple sequence alignments using Clustal Omega. *Molecular Systems Biology*, 7:539.
- Simon, N. and Dodd, A. (2017). A new link between plant metabolism and circadian rhythms? *Plant, Cell & Environment*, 40:995–996.
- Simon, N., Kusakina, J., Fernández-López, Á., Chembath, A., Belbin, F., and Dodd, A. (2018a). The energy-signaling hub SnRK1 is important for sucrose-induced hypocotyl elongation. *Plant Physiology*, 176:1299–1310.
- Simon, N. M. L., Sawkins, E., and Dodd, A. N. (2018b). Involvement of the SnRK1 subunit KIN10 in sucrose-induced hypocotyl elongation [Epub ahead of print]. *Plant Signaling & Behavior*, page e1457913.
- Sirichandra, C., Wasilewska, A., Vlad, F., Valon, C., and Leung, J. (2009). The guard cell as a single-cell model towards understanding drought tolerance and abscisic acid action. *Journal of Experimental Botany*, 60:1439–1463.
- Sletvold, N. and Ågren, J. (2012). Variation in tolerance to drought among Scandinavian populations of *Arabidopsis lyrata*. *Evolutionary Ecology*, 26:559–577.

- Sletvold, N., Huttunen, P., Handley, R., Kärkkäinen, K., and Ågren, J. (2010). Cost of trichome production and resistance to a specialist insect herbivore in *Arabidopsis lyrata*. *Evolutionary Ecology*, 24:1307–1319.
- Snaith, P. J. and Mansfield, T. A. (1986). The circadian rhythm of stomatal opening: Evidence for the involvement of potassium and chloride fluxes. *Journal of Experimental Botany*, 37:188–199.
- Somers, D. E., Kim, W.-y., and Geng, R. (2004). The F-box protein ZEITLUPE confers dosage-dependent control on the circadian clock, photomorphogenesis, and flowering time. *The Plant Cell*, 16:769–782.
- Somers, D. E., Schultz, T. F., Milnamow, M., and Kay, S. A. (2000). ZEITLUPE encodes a novel clock-associated PAS protein from Arabidopsis. *Cell*, 101:319–329.
- Somers, D. E., Webb, A. A. R., Pearson, M., and Kay, S. A. (1998). The short-period mutant, *toc1-1*, alters circadian clock regulation of multiple outputs throughout development in *Arabidopsis thaliana*. *Development*, 125:485–494.
- Spreitzer, R. J. and Salvucci, M. E. (2002). RUBISCO: Structure, regulatory interactions, and possibilities for a better enzyme. *Annual Review of Plant Biology*, 53:449–475.
- Stadler, R., Buttner, M., Ache, P., Hedrich, R., Ivashikina, N., Melzer, M., Shearson, S. M., Smith, S. M., and Sauer, N. (2003). Diurnal and light-regulated expression of AtSTP1 in guard cells of Arabidopsis. *Plant Physiology*, 133:528–537.
- Staiger, D., Zecca, L., Wiczeorek Kirk, D. A., Apel, K., and Eckstein, L. (2003). The circadian clock regulated RNA-binding protein AtGRP7 autoregulates its expression by influencing alternative splicing of its own pre-mRNA. *The Plant Journal*, 33:361–371.
- Stewart, J. L., Maloof, J. N., and Nemhauser, J. L. (2011). PIF genes mediate the effect of sucrose on seedling growth dynamics. *Public Library of Science ONE*, 6:e19894.
- Stokes, M. E., Chattopadhyay, A., Wilkins, O., Nambara, E., and Campbell, M. M. (2013). Interplay between sucrose and folate modulates auxin signaling in Arabidopsis. *Plant Physiology*, 162:1552–1565.
- Strayer, C., Oyama, T., Schultz, T. F., Raman, R., Somers, D. E., Mas, P., Panda, S., Kreps, J. A., and Kay, S. A. (2000). Cloning of the Arabidopsis clock gene *TOC1*, an autoregulatory response regulator homolog. *Science*, 289:768–771.

- Streitner, C., Danisman, S., Wehrle, F., Schöning, J. C., Alfano, J. R., and Staiger, D. (2008). The small glycine-rich RNA binding protein *AtGRP7* promotes floral transition in *Arabidopsis thaliana*. *The Plant Journal*, 56:239–250.
- Suárez-López, P., Wheatley, K., Robson, F., Onouchi, H., Valverde, F., and Coupland, G. (2001). *CONSTANS* mediates between the circadian clock and the control of flowering in *Arabidopsis*. *Nature*, 410:1116–1120.
- Sulpice, R., Flis, A., Ivakov, A. A., Apelt, F., Krohn, N., Encke, B., Abel, C., Feil, R., Lunn, J. E., and Stitt, M. (2014). *Arabidopsis* coordinates the diurnal regulation of carbon allocation and growth across a wide range of photoperiods. *Molecular Plant*, 7:137–155.
- Takahashi, H., Watanabe-Takahashi, A., Smith, F. W., Blake-Kalff, M., Hawkesford, M. J., and Saito, K. (2000). The roles of three functional sulphate transporters involved in uptake and translocation of sulphate in *Arabidopsis thaliana*. *The Plant Journal*, 23:171–182.
- Takahashi, N., Hirata, Y., Aihara, K., and Mas, P. (2015). A hierarchical multi-oscillator network orchestrates the *Arabidopsis* circadian system. *Cell*, 163:148–159.
- Talbott, L. and Zeiger, E. (1998). The role of sucrose in guard cell osmoregulation. *Journal of Experimental Botany*, 49:329–337.
- Tallman, G. and Zeiger, E. (1988). Light quality and osmoregulation in *Vicia* guard cells: Evidence for involvement of three metabolic pathways. *Plant Physiology*, 88:887–895.
- Tanaka, Y., Sugano, S. S., Shimada, T., and Hara-Nishimura, I. (2013). Enhancement of leaf photosynthetic capacity through increased stomatal density in *Arabidopsis*. *New Phytologist*, 198:757–764.
- Thain, S. C., Hall, A., and Millar, A. J. (2000). Functional independence of circadian clocks that regulate plant gene expression. *Current Biology*, 10:951–956.
- The Royal Society (2009). Reaping the benefits: Science and the sustainable intensification of global agriculture. *Science Policy*, 797:60.
- Thines, B. and Harmon, F. G. (2010). Ambient temperature response establishes ELF3 as a required component of the core *Arabidopsis* circadian clock. *Proceedings of the National Academy of Sciences*, 107:3257–3262.

- Tomás, M., Medrano, H., Escalona, J. M., Martorell, S., Pou, A., Ribas-Carbó, M., and Flexas, J. (2014). Variability of water use efficiency in grapevines. *Environmental and Experimental Botany*, 103:148–157.
- Torii, K. U., Kanaoka, M. M., Pillitteri, L. J., and Bogenschutz, N. L. (2007). Stomatal development: Three steps for cell-type differentiation. *Plant Signaling & Behavior*, 2:311–313.
- Tunna, G. and Tunstad, S. (2017). Exploring the cost of trichomes in Arabidopsis [BSci Undergraduate Report, University of Bristol].
- Turner, A., Beales, J., Faure, S., Dunford, R. P., and Laurie, D. A. (2005). The pseudo-response regulator *Ppd-H1* provides adaptation to photoperiod in barley. *Science*, 310:1031–1034.
- Turner, N. C. (1973). Stomatal behavior and water status of maize, sorghum, and tobacco under field conditions. I: At high soil water potential. *Plant Physiology*, 51:31–36.
- Turner, N. C. (1974). Stomatal behavior and water status of maize, sorghum, and tobacco under field conditions. II: At low soil water potential. *Plant Physiology*, 53:360–365.
- Turner, N. C. (1991). Measurement and influence of environmental and plant factors on stomatal conductance in the field. *Agricultural and Forest Meteorology*, 54:137–154.
- Underwood, E. (2015). Models predict longer, deeper U.S. droughts. *Science*, 347:707.
- Valente, M. and Chaves, C. (2018). Perceptions and valuation of GM food: A study on the impact and importance of information provision. *Journal of Cleaner Production*, 172:4110–4118.
- Van Houtte, H., Vandesteene, L., López-Galvis, L., Lemmens, L., Kissel, E., Carpentier, S., Feil, R., Avonce, N., Beeckman, T., Lunn, J. E., and Van Dijck, P. (2013). Overexpression of the trehalase gene *AtTRE1* leads to increased drought stress tolerance in Arabidopsis and is involved in abscisic acid-induced stomatal closure. *Plant Physiology*, 161:1158–1171.
- Venuprasad, R., Lafitte, H. R., and Atlin, G. N. (2007). Response to direct selection for grain yield under drought stress in rice. *Crop Science*, 47:285–293.

- Verslues, P. E., Agarwal, M., Katiyar-Agarwal, S., Zhu, J., and Zhu, J. K. (2006). Methods and concepts in quantifying resistance to drought, salt and freezing, abiotic stresses that affect plant water status. *The Plant Journal*, 45:523–539.
- Violet-Chabrand, S., Matthews, J., Brendel, O., Blatt, M., Wang, Y., Hills, A., Griffiths, H., Rogers, S., and Lawson, T. (2016). Modelling water use efficiency in a dynamic environment: An example using *Arabidopsis thaliana*. *Plant Science*, 251:65–74.
- von Caemmerer, S. and Griffiths, H. (2009). Stomatal responses to  $\text{CO}_2$  during a diel crassulacean acid metabolism cycle in *Kalanchoe daigremontiana* and *Kalanchoe pinnata*. *Plant, Cell & Environment*, 32:567–576.
- Von Caemmerer, S., Lawson, T., Oxborough, K., Baker, N. R., Andrews, T. J., and Raines, C. A. (2004). Stomatal conductance does not correlate with photosynthetic capacity in transgenic tobacco with reduced amounts of Rubisco. *Journal of Experimental Botany*, 55:1157–1166.
- Wahl, V., Ponnu, J., Schlereth, A., Arrivault, S., Langenecker, T., Franke, A., Feil, R., Lunn, J. E., Stitt, M., and Schmid, M. (2013). Regulation of flowering by trehalose-6-phosphate signaling in *Arabidopsis thaliana*. *Science*, 339:704–708.
- Wang, Y., Beal, M., Chalifoux, M., Ying, J., Uchacz, T., Sarvas, C., Griffiths, R., Kuzma, M., Wan, J., and Huang, Y. (2009). Shoot-specific down-regulation of protein farnesyltransferase ( $\alpha$ -subunit) for yield protection against drought in canola. *Molecular Plant*, 2:191–200.
- Wang, Y., Liu, K., Liao, H., Zhuang, C., Ma, H., and Yan, X. (2008). The plant WNK gene family and regulation of flowering time in *Arabidopsis*. *Plant Biology*, 10:548–562.
- Wang, Y., Noguchi, K., Ono, N., Inoue, S.-i., Terashima, I., and Kinoshita, T. (2014). Over-expression of plasma membrane  $\text{H}^+$ -ATPase in guard cells promotes light-induced stomatal opening and enhances plant growth. *Proceedings of the National Academy of Sciences*, 111:533–538.
- Wang, Y., Wu, J.-F., Nakamichi, N., Sakakibara, H., Nam, H.-G., and Wu, S.-H. (2011). LIGHT-REGULATED WD1 and PSEUDO-RESPONSE REGULATOR9 form a positive feedback regulatory loop in the *Arabidopsis* circadian clock. *The Plant Cell*, 23:486–498.
- Wang, Z. Y. and Tobin, E. M. (1998). Constitutive expression of the *CIRCADIAN CLOCK ASSOCIATED 1 (CCA1)* gene disrupts circadian rhythms and suppresses its own expression. *Cell*, 93:1207–1217.

- Wasson, A. P., Richards, R. A., Chatrath, R., Misra, S. C., Sai Prasad, S. V., Rebetzke, G. J., Kirkegaard, J. A., Christopher, J., and Watt, M. (2012). Traits and selection strategies to improve root systems and water uptake in water-limited wheat crops. *Journal of Experimental Botany*, 63:3485–3498.
- Webb, A. A. (2003). The physiology of circadian rhythms in plants. *New Phytologist*, 160:281–303.
- Webb, A. A., McAinsh, M. R., Mansfield, T. A., and Hetherington, A. M. (1996). Carbon dioxide induces increases in guard cell cytosolic free calcium. *The Plant Journal*, 9:297–304.
- Webb, A. A. R. (1998). Stomatal rhythms. In Lumsden, P. J. and Millar, A. J., editors, *Biological rhythms and photoperiodism in plants.*, pages 69– 79. Bios Scientific Publishers.
- Wenden, B., Toner, D. L. K., Hodge, S. K., Grima, R., and Millar, A. J. (2012). Spontaneous spatiotemporal waves of gene expression from biological clocks in the leaf. *Proceedings of the National Academy of Sciences*, 109:6757–6762.
- Wilkins, M. B. (1992). Circadian rhythms: Their origin and control. *New Phytologist*, 121:347–375.
- Wilkins, O., Bräutigam, K., and Campbell, M. M. (2010). Time of day shapes Arabidopsis drought transcriptomes. *The Plant Journal*, 63:715–727.
- Wilkins, O., Waldron, L., Nahal, H., Provart, N. J., and Campbell, M. M. (2009). Genotype and time of day shape the *Populus* drought response. *The Plant Journal*, 60:703–715.
- Williams, W. E. and Gorton, H. L. (1998). Circadian rhythms have insignificant effects on plant gas exchange under field conditions. *Physiologia Plantarum*, 103:247– 256.
- Wituszynska, W., Slesak, I., Vanderauwera, S., Szechynska-Hebda, M., Kornas, A., Van Der Kelen, K., Muhlenbock, P., Karpinska, B., Mackowski, S., Van Breusegem, F., and Karpinski, S. (2013). LESION SIMULATING DISEASE1, ENHANCED DISEASE SUSCEPTIBILITY1, and PHYTOALEXIN DEFICIENT4 conditionally regulate cellular signaling homeostasis, photosynthesis, water use efficiency, and seed yield in Arabidopsis. *Plant Physiology*, 161:1795–1805.
- Wong, S. C., Cowan, I. R., and Farquhar, G. D. (1979). Stomatal conductance correlates with photosynthetic capacity. *Nature*, 282:424–426.

- Wood, N. T., Allan, A. C., Haley, A., Viry-Moussaïd, M., and Trewavas, A. J. (2000). The characterization of differential calcium signalling in tobacco guard cells. *The Plant Journal*, 24:335–344.
- Wyatt, S. E., Tsou, P. L., and Robertson, D. (2002). Expression of the high capacity calcium-binding domain of calreticulin increases bioavailable calcium stores in plants. *Transgenic Research*, 11:1–10.
- Xing, H. T., Guo, P., Xia, X. L., and Yin, W. L. (2011). PdERECTA, a leucine-rich repeat receptor-like kinase of poplar, confers enhanced water use efficiency in Arabidopsis. *Planta*, 234:229–241.
- Xiong, Y. and Sheen, J. (2012). Rapamycin and glucose-target of rapamycin (TOR) protein signaling in plants. *Journal of Biological Chemistry*, 287:2836–2842.
- Xoconostle-Cázares, B., Ramírez-Ortega, F. A., Flores-Elenes, L., and Ruiz-Medrano, R. (2010). Drought tolerance in crop plants. *American Journal of Plant Physiology*, 5:241–256.
- Xu, X., Hotta, C. T., Dodd, A. N., Love, J., Sharrock, R., Lee, Y. W., Xie, Q., Johnson, C. H., and Webb, A. A. (2007). Distinct light and clock modulation of cytosolic free  $Ca^{2+}$  oscillations and rhythmic *CHLOROPHYLL A/B BINDING PROTEIN2* promoter activity in Arabidopsis. *The Plant Cell*, 19:3474–3490.
- Yakir, E., Hassidim, M., Melamed-Book, N., Hilman, D., Kron, I., and Green, R. M. (2011). Cell autonomous and cell-type specific circadian rhythms in Arabidopsis. *The Plant Journal*, 68:520–531.
- Yamamoto, Y., Sato, E., Shimizu, T., Nakamich, N., Sato, S., Kato, T., Tabata, S., Nagatani, A., Yamashino, T., and Mizuno, T. (2003). Comparative genetic studies on the *APRR5* and *APRR7* genes belonging to the *APRR1/TOC1* quintet implicated in circadian rhythm, control of flowering time, and early photomorphogenesis. *Plant & Cell Physiology*, 44:1119–1130.
- Yang, Y., Costa, A., Leonhardt, N., Siegel, R. S., and Schroeder, J. I. (2008). Isolation of a strong Arabidopsis guard cell promoter and its potential as a research tool. *Plant Methods*, 4:6.
- Yanovsky, M. J. and Kay, S. A. (2002). Molecular basis of seasonal time measurement in Arabidopsis. *Nature*, 419:308–312.

- Yoo, C. Y., Pence, H. E., Jin, J. B., Miura, K., Gosney, M. J., Hasegawa, P. M., and Mickelbart, M. V. (2010). The Arabidopsis GTL1 transcription factor regulates water use efficiency and drought tolerance by modulating stomatal density via transrepression of *SDD1*. *The Plant Cell*, 22:4128–4141.
- Young, J. J., Mehta, S., Israelsson, M., Godoski, J., Grill, E., and Schroeder, J. I. (2006). CO<sub>2</sub> signaling in guard cells: Calcium sensitivity response modulation, a Ca<sup>2+</sup>-independent phase, and CO<sub>2</sub> insensitivity of the *gca2* mutant. *Proceedings of the National Academy of Sciences*, 103:7506–7511.
- Young, M. W. and Kay, S. A. (2001). Time zones: a comparative genetics of circadian clocks. *Nature Reviews Genetics*, 2:702–715.
- Zagotta, M., Shannon, S., Jacobs, C., and Meeks-Wagner, D. (1992). Early-flowering mutants of *Arabidopsis thaliana*. *Australian Journal of Plant Physiology*, 19:411–418.
- Zhang, J., Ren, W., An, P., Pan, Z., Wang, L., Dong, Z., He, D., Yang, J., Pan, S., and Tian, H. (2015a). Responses of crop water use efficiency to climate change and agronomic measures in the semiarid area of Northern China. *Public Library of Science ONE*, 10:e0137409.
- Zhang, Y., Andralojc, P. J., Hey, S. J., Primavesi, L. F., Specht, M., Koehler, J., Parry, M. A., and Halford, N. G. (2008). Arabidopsis sucrose non-fermenting-1-related protein kinase-1 and calcium-dependent protein kinase phosphorylate conserved target sites in ABA response element binding proteins. *Annals of Applied Biology*, 153:401–409.
- Zhang, Y., Liu, Z., Wang, J., Chen, Y., Bi, Y., and He, J. (2015b). Brassinosteroid is required for sugar promotion of hypocotyl elongation in Arabidopsis in darkness. *Planta*, 242:881–893.
- Zhang, Y., Liu, Z., Wang, L., Zheng, S., Xie, J., and Bi, Y. (2010). Sucrose-induced hypocotyl elongation of Arabidopsis seedlings in darkness depends on the presence of gibberellins. *Journal of Plant Physiology*, 167:1130–1136.
- Zhang, Y., Primavesi, L. F., Jhurrea, D., Andralojc, P. J., Mitchell, R. A. C., Powers, S. J., Schluepmann, H., Delatte, T., Wingler, A., and Paul, M. J. (2009). Inhibition of Snf1-related protein kinase (SnRK1) activity and regulation of metabolic pathways by trehalose 6-phosphate. *Plant Physiology*, 149:1860–1871.



- Zhang, Z., Zhu, J. Y., Roh, J., Marchive, C., Kim, S. K., Meyer, C., Sun, Y., Wang, W., and Wang, Z. Y. (2016). TOR signaling promotes accumulation of BZR1 to balance growth with carbon availability in *Arabidopsis*. *Current Biology*, 26:1854–1860.
- Zielinski, T., Moore, A. M., Troup, E., Halliday, K. J., and Millar, A. J. (2014). Strengths and limitations of period estimation methods for circadian data. *Public Library of Science ONE*, 9:e96462.